Tsunamis générés par des séismes au niveau de la zone de collision entre les plaques africaine et eurasienne : Etudes de cas pour l'évaluation du risque tsunami en Méditerranée occidentale et Atlantique nord

Jean Roger

▶ **To cite this version:**

Jean Roger. Tsunamis générés par des séismes au niveau de la zone de collision entre les plaques africaine et eurasienne : Etudes de cas pour l'évaluation du risque tsunami en Méditerranée occidentale et Atlantique nord. Géophysique [physics.geo-ph]. Université Pierre et Marie Curie - Paris VI, 2011. Français. NNT : . tel-00588880

HAL Id: tel-00588880

https://theses.hal.science/tel-00588880

Submitted on 26 Apr 2011

HAL is a multi-disciplinary open access archive for the deposit and dissemination of scientific research documents, whether they are published or not. The documents may come from teaching and research institutions in France or abroad, or from public or private research centers.

L'archive ouverte pluridisciplinaire **HAL**, est destinée au dépôt et à la diffusion de documents scientifiques de niveau recherche, publiés ou non, émanant des établissements d'enseignement et de recherche français ou étrangers, des laboratoires publics ou privés.

THESE DE DOCTORAT DE
L'UNIVERSITE PIERRE ET MARIE CURIE

Spécialité

Géosciences et Ressources Naturelles
(Ecole doctorale)

M. Jean ROGER

Pour l'obtention du grade de

DOCTEUR de l'UNIVERSITÉ PIERRE ET MARIE CURIE

Titre : Tsunamis générés par des séismes au niveau de la zone de collision entre les plaques africaine et eurasienne : Etudes de cas pour l'évaluation du risque tsunami en Méditerranée occidentale et Atlantique nord

soutenue le 11 février 2011

devant le jury composé de :

Dr Pierre Briole, **Directeur de thèse**,	ENS, Paris, France
Dr Hélène Hébert, **Co-directrice de thèse**,	CEA/DAM/DIF, Arpajon, France
Prof. Maria Ana Baptista, **Co-directrice de thèse**,	ISEL, Lisboa, Portugal
Prof. Narcisse Zahibo, **Rapporteur**,	Université Antilles-Guyane, Point-à Pitre, France
Prof. Ass. Mourad Bezzeghoud, **Rapporteur**,	Universidade de Evora, Evora, Portugal
Prof. Bertrand Meyer, **Examinateur**,	Université Pierre et Marie Curie, Paris, France
Dr. Louis Géli, **Examinateur**,	IFREMER, Brest, France
Prof. Ass. Hermann Fritz, **Examinateur**,	Georgia Institute of Technology, Savannah, USA

Université Pierre & Marie Curie - Paris 6
Bureau d'accueil, inscription des doctorants
Esc G, 2ème étage
15 rue de l'école de médecine
75270-PARIS CEDEX 06

Tél. Secrétariat : 01 44 27 28 10
Fax : 01 44 27 23 95
Tél. pour les étudiants de A à EL : 01 44 27 28 07
Tél. pour les étudiants de EM à MON : 01 44 27 28 05
Tél. pour les étudiants de MOO à Z : 01 44 27 28 02
E-mail : scolarite.doctorat@upmc.fr

Earthquake-generated tsunamis near the Africa-Eurasia collision zone: cases studies for tsunami hazard evaluation in the Mediterranean Sea and the northern Atlantic Ocean

Résumé

L'objectif principal de cette thèse est d'approfondir les connaissances en terme d'aléa tsunami en Méditerranée occidental et Atlantique nord. Elle se concentre sur des tsunamis d'origine sismique qui présentent l'avantage d'être précédés d'un précurseur utile pour déclencher l'alerte, car pouvant être ressenti par la population : le séisme. Deux types d'études sont présentés. Elles ont été effectuées sur la base de recherches de documents historiques et/ou de dépôts sédimentaires, en utilisant ensuite la modélisation numérique mettant en application une méthode de calcul de propagation de tsunami par différences finies. La modélisation permet de produire des cartes de hauteur de vagues maximum attendues pour chaque scénario, proposer des temps d'arrivée, des limites de zones d'inondation et l'étude des phénomènes de résonance. Les premières études concernent l'impact tsunami que peuvent avoir des sources sismiques (paramètres de rupture) préalablement proposées par des études antérieures (le tsunami de 1755 aux Antilles, à Terre-Neuve et celui de Zemmouri de 2003 dans le sud de la France). Et les secondes correspondent à des études approfondies sur les sources, proposant des scénarios de rupture et donc de génération/propagation de tsunami calant au mieux les données observations d'ordre géologique (sismicité, mécanismes au foyer, données GPS, ruptures de surface, etc.) et les données marégraphiques disponibles (hauteur de vagues, temps d'arrivée, périodes) et observations de terrains (limites et hauteur d'inondation, dégâts). Sur ce point les études ont porté sur les tsunamis de Jijel (1856), El Asnam (1580) et du détroit de Douvres (1580).

Mots-clés : tsunami, source sismique, modélisation numérique, risque, Méditerranée, Atlantique, Antilles, sismicité historique, bathymétrie, résonance

Abstract

The main objective of this thesis is to improve the knowledge of tsunami hazard in Western Mediterranean and Northern Atlantic. It focusses on earthquake-generated tsunamis which present the advantage to be preceded by a useful precursor for the warning, that can be felt by the population: the earthquake. Two types of studies are presented, using numerical modelling. It allows to built maximum wave height maps for each scenario, determine arrival times, inundation zones and study resonance phenomenon. The first studies concern the tsunami impact induced by seismic sources (rupture parameters) proposed by previous studies (the 1755 tsunami in the West Indies or in Newfoundland and the 2003 tsunami of Zemmouri in Southern France). The second studies concern the determination of rupture scenarios able to trigger tsunamis, with respect to the geology (seismicity, focal mechanisms, GPS measurements, surface fault ruptures, etc.) and the available maregraphic data (wave heights, arrival times, periods) and field surveys data (run-up distance and elevation, destructions). Concerning this last point, the studies considered the Jijel (1856), El Asnam (1980) and Dover Strait (1580) tsunamis. These studies have been done following historical documents and tsunami deposits search, using numerical modeling with a finite difference method for tsunami propagation calculations.

Keywords : tsunami, seismic source, numerical modelling, hazard, vulnerability, Mediterranean, Atlantic, Antilles, historical seismicity, bathymetry, resonance

Resumo

O principal objectivo desta tese é o de melhorar o conhecimento acerca do risco de tsunamis no Mediterrâneo Oeste e no Atlântico Norte. Está direccionada para os tsunamis gerados por sismos proporcionando assim a vantagem de se usar um precursor para o alerta, que pode ser sentido pela população: o sismo. São apresentados dois tipos de estudos, usando modelação numérica, permitindo assim obter gráficos da altura máxima das ondas para cada cenário, determinar o tempo de chegada, zonas de inundação e estudar zonas de ocorrência de ressonância. O primeiro estudo dedica-se ao impacto do tsunami induzido pelas fontes sísmicas (parâmetros de ruptura) proposto em estudos anteriores (o tsunami de 1755 Índias Ocidentais ou na Terra Nova e o tsunami de 2003 em Zemmouri no Sul da França). No segundo procura-se determinar os cenários de ruptura capazes de dar origem a um tsunami, tendo em conta a geologia (sismicidade, mecanismos focais, medidas GPS, rupturas de falhas de superfície, etc.), a disponibilidade de dados de maregráficos (altura das ondas, tempos de chegada, períodos) e os dados de campo (distância run-up e elevação, destruição). Relativamente a este último, os eventos considerados foram os tsunamis de Jijel (1856), El Asnam (1980), e Dover (1580). Estes estudos foram realizados com o apoio de documentos históricos e da investigação de depósitos de tsunamis, usando modelação numérica com o método das diferenças finitas para o cálculo da propagação dos tsunamis.

Palavras chave: tsunami, fonte sísmica, modelação numérica, risco, vulnerabilidade, Mediterrâneo, Atlântico, Antilhas, sismicidade histórica, batimetria, ressonância.

Remerciements

La première personne que je souhaite remercier pour avoir cru en moi et m'avoir poussé dans cette aventure est Hélène Hébert qui, même avec un agenda booké pour les 30 prochaines années, a toujours trouvé le temps de me conseiller (souvent), de me soutenir (parfois) et de lire (même la nuit) mes productions hautement philosophiques.

Je remercie Olivier Bour et Olivier Dauteuil (Géosciences Rennes) pour m'avoir informé sur la possibilité de faire une thèse sur publications et m'avoir motivé pour le faire. Je remercie François Baudin, directeur de l'école doctorale Géosciences et Ressources Naturelles de l'Université Pierre et Marie Curie de m'avoir aidé à réaliser ce projet, Pierre Briole (ENS) d'avoir accepté d'être mon directeur de thèse et Nicolas Chamot-Rooke de m'avoir accueilli au sein de son équipe à l'Ecole Normale Supérieure. De la même façon, je remercie Maria-Ana Baptista pour son accueil au Laboratoire de Géophysique de Lisbonne pour effectuer mes recherches sur le tsunami de 1755 principalement.

Je remercie les membres du jury d'avoir accepté de relire mon travail et d'être venus à Paris, certains de loin, pour m'évaluer.

Je remercie ma famille qui a toujours été là pour moi, avec un clin d'œil spécial à mam' (merci pour la correction des fautes de français par téléphone !), à mon père et à ma p'tite sœur (j'attends ton tour Laurence !!!). Mon frère, j'aurai aimé… Merci donc de m'avoir toujours motivé, soutenu et supporté tout ce temps passé loin de ma mer…

Merci à tous mes amis pour les bons moments passés au cours de ces dernières années avec une spéciale dédicace aux parisiens, Charlotte (bientôt ton tour !!!), Coraline (tu vois, c'était pas si dur ;>)), Alex (petit chinois, tu as un challenge pour la tienne maintenant…12…), Arthur (j'attends les pâtisseries !!),

Aux ENSsiens, Adeline, Alex An Dra, Eugénie (bientôt à vous les filles !!), Kenny, Dimitri, Flo, Alexis, Baptiste, Mathieu (Gnan), et bien sur, Sylvain (merci pour tout mec !),

A Cookies Monster l'australien, qui a eu bien raison de quitter Paris (les kangourous c'est mieux),

Aux malouins (et fiers de l'être !! SEMPER FIDELIS), Sven, Eru (tu sortiras un jour de ton village !!), Martine, Anne, Julien, Romain, Dédé, pour votre soutient, aux bons moments et aux nombreuses soirées retrouvailles à intra, à la Belle ou à la Cara…

A mes potes surfeurs, Davidzinho (salaam aleikhoum pequeno surfisto), Johnny, Jérôme, Fredo (badj… tu comprendras), Séb, RacFab' (prêt pour quand le format MP17 ?), Lionel (viva la Gwada !!), Karlito (bien sur que la planche suit toujours !),

Aux surfrideriens, de m'avoir soutenu dans ma guerre contre la destruction de la nature que j'ai menée en parallèle de ma thèse ; je pense à tous les bénévoles de l'antenne 35 (pour le meilleur et pour le pire !!), ceux des autres antennes, avec une spécial dédicace à Hugues-

Antoine et Didier, mais aussi à tous les peoples du siège à Biarritz, sans oublier Nat' à Marseille et surtout Marie-Amélie (et AK aussi bien sur !) à Brest !!! On y arrivera les mecs !!

A mes potes disséminés un peu partout dans la France et dans le monde (enfin c'est plutôt moi qui change beaucoup d'endroit… hé hé), les alsaciens, Lolo, Math (tu resteras un alsacien pour moi, quoi que tu en dises !), Jean DV, Régis, les bretons, Marco, Cheval, Sébi, Tonio, Jonathan (vivement le prochain voyage !!), la toulousaine Elisou, les orléanais, Jerem', Yanouuuuuuu (tu as eu raison de partir !), Ben (j'espère avoir un boulot en or comme le tien !), les djeun's à Arras Erwan et Laetitia, les portugais au Portugal, Koen, Adam et Antonio, les russes Pavel, Alice, Kate, les grecques Anna et Elena, le flamand-espagnol en Catalogne Ben, Anne la franco-écossaise (merci pour ta thèse !), Carole (c'est à mon tour de finir !!),

Un grand merci à Dr Rachid Omira, pour les bons moments à Lisbonne, à la fac et ailleurs,

A mes collègues de terrain et amis, Patrick Wassmer (dire que j'ai été ton élève à Stras!) et Raphaël Paris (calamité !),

Aux tsunamistes américains, Burak Uslu, Vasily Titov, Brian McAdoo, Galen Gisler, Hermann Fritz, Costas Synolakis, et les autres pour leurs conseils et leur sympathie,

A Narcisse Zahibo (Univ. AG, merci pour l'invitation au congrès en Guadeloupe) et Tiziana Rozetto (UCL, London) pour m'avoir remotivé sans le savoir à travailler sur les tsunamis lors de ma période de chômage en 2008,

Je ne m'arrêterai pas sans avoir remercié grandement Alain Rabaute, mon collègue de bureau pour ces longs mois (pour lui) passés en sa compagnie (Chuck Norris…), les discussions que nous avons pu avoir, et son aide précieuse pour l'accomplissement de mes travaux,

Pierpaolo Dubernet pour son aide technique en informatique, et les bons moments (une blague Pier ?),

Les bibliothécaires Dominique Gac (Géosciences Brest), Isabelle Jeannin (CEA) et Françoise Vivent (ENS) pour avoir toujours été super efficaces (même quand je m'y prenais à la bourre pour les articles…) et accueillantes,

Je remercie Dominique Gibert (Géosciences Rennes), sans qui tout ceci ne serait certainement pas arrivé s'il n'avait pas mentionné les tsunamis de manière passionnante lors d'un cours d'océanographie physique de DEUG 1ère année en 1999…,

Je ne remercierais pas la SNCF ni la RATP pour leurs retards en tout genre, mais en revanche, je remercierais Easyjet et les ADP pour leur efficacité quasi sans faille au cours de ces dernières années, avec toutefois quelques moments de stress…

Et enfin je remercie Delphine, pour tout, mais surtout pour son soutien et sa patience sans limite… <3

Aux victimes des catastrophes naturelles,

A ma famille pour qui la mer a toujours eu de l'importance,

Labor omnia vincit improbus

(Virgile, Les Géorgiques, 70-19 av. J.-C.)

Nous récoltons ce que nous semons…

Avant-propos

Le sujet traité dans cette thèse sur publications s'inscrit principalement dans le cadre de l'étude de l'aléa tsunami pour les territoires côtiers français en Méditerranée et Atlantique nord. Il s'agit d'un travail basé sur des documents d'observation concernant plusieurs évènements historiques, et sur des simulations numériques des tsunamis permettant de discuter des hypothèses de sources.

La thèse s'inscrit dans un cadre international de recherche, renforcé depuis le tsunami de 2004 dans l'Océan Indien. De multiples projets ont été initiés dans les mois et années qui ont suivi cette catastrophe. Le projet européen TRANSFER (Tsunami Risk And Strategies For European Regions) aborde les études d'aléa tsunami en Méditerranée occidentale, zone où, en 2003, le séisme de Zemmouri-Boumerdès avait produit un tsunami notable en Méditerranée occidentale et avait déjà rappelé la possibilité d'événements dans cette mer rarement touchée par les tsunamis. Depuis 2005, différents programmes de l'ANR (Agence Nationale de la Recherche) ont également soutenu des recherches dans le domaine des tsunamis. Ainsi, le projet ANR MAREMOTI (MAREgraphie, observation de tsunaMis, mOdélisation et éTudes de vulnérabIlité pour le nord-est Atlantique et la Méditerranée occidentale) vise à étudier l'aléa tsunami vis-à-vis des côtes métropolitaines, en Méditerranée comme sur les côtes atlantiques, où les conséquences du tsunami majeur de 1755 sont actuellement méconnues.

Les travaux de la thèse portent principalement sur une analyse des sources tsunamigéniques pour la Méditerranée occidentale, en retravaillant notamment sur les documents disponibles pour les événements historiques (1856, Jijel en Algérie) ou plus récents (1980, El Asnam), et également pour le tsunami de Lisbonne de 1755, pour lequel l'impact en champ lointain (Antilles, Amérique du Nord) est toujours discuté et mal documenté. Le cas du tsunami qui aurait été généré par le séisme de Douvres de 1580 est également traité. Un des objectifs est l'évaluation du risque tsunami pour des régions données (ou sites tests) en passant par la constitution de bases de données sur les sources sismiques potentiellement tsunamigéniques et la proposition de scénarios, la modélisation numérique de tsunamis historiques, la recherche de dépôts de paléotsunamis sur le terrain, des études de vulnérabilité, autant d'éléments qui participent à la mise en place des futurs systèmes d'alerte au niveau de tous les bassins selon la recommandation de l'UNESCO de janvier 2005, pour parvenir finalement à un système rapide d'alerte mondiale (SRAM).

Après un exposé présentant le contexte général et les différents outils utilisés au cours de la thèse, ces différents aspects de l'étude de l'aléa et du risque tsunami sont abordés de manière détaillée sous la forme d'études de cas réparties en deux grands axes : dans un premier temps nous avons décidé de tester des sources sismiques proposées dans la littérature et de regarder les effets des tsunamis qu'elles peuvent générer. Dans un second temps nous nous sommes concentrés plus en détail sur les sources en elles-mêmes afin de proposer des scénarios de rupture pouvant expliquer les observations.

Cette thèse a été réalisée en collaboration avec le Laboratoire de Détection et Géophysique du CEA (Bruyères-le-Châtel), le laboratoire de Géologie de l'Ecole Normale Supérieure (Ulm) et l'Instituto Dom Luiz de l'Université de Lisbonne, Portugal.

Table des matières

Résumé / Abstract 5

Remerciements 7

Avant-propos 11

Table des matières 13

1) Introduction 17

1.1 Contexte politico-géographique 19

1.2 Qu'est ce qu'un tsunami ? 23

1.2.1 Origine du mot et utilisation 23

1.2.2 Origine du phénomène 25

1.3 Les tsunamis en Europe 28

1.4 Contexte géologique et géodynamique 30

1.4.1 Méditerranée 33

1.4.2 Atlantique nord 35

2) Les outils pour étudier les tsunamis 37

2.1 Observations historiques 39

2.1.1 Enregistrements marégraphiques 39

2.1.1 Archives 41

2.1.2 Paléotsunamis – recherche de dépôts 45

2.1.2.1 Définition 45

2.1.2.2 Intérêt 48

2.2 Modélisation 53

2.2.1 La modélisation analogique 53

2.2.2 La modélisation numérique 55

2.2.2.1 Définition 55

2.2.2.2 Les différentes méthodes de modélisation numérique 56

2.2.2.2.1 Différences finies 57

2.2.2.2.1.1 Généralités 57

2.2.2.2.1.2 Exemples de codes aux différences finies 60

2.2.2.2.1.3 Le code CEA 61

2.2.2.2.2 Eléments finis 63

2.2.2.2.3 Comparaison entre les différences finies et les éléments finis 64

2.3 Données d'entrée 65

2.3.1 Données bathymétriques et topographiques 65

2.3.1.1 Données bathymétriques 65

2.3.1.2 Données topographiques 69

2.3.1.3 Réalisation d'une grille 70

2.3.2 Paramètres de faille 72

Transition 75

3) Etudes de cas 77

3.1 Impact des tsunamis 79

3.1.1 *The tsunami triggered by the 21 the 21 May 2003 Boumerdès-Zemmouri (Algeria) earthquake: field investigations on the Mediterranean coast and tsunami modeling* 83

3.1.2 *The 1755 Lisbon tsunami in Guadeloupe Archipelago : source sensitivity and investigation of resonance effects* 97

3.1.3 *The transoceanic 1755 Lisbon tsunami in the Martinique* 115

3.1.4 *Tsunami impact on Newfoundland, Canada, due to far-field generated tsunamis. Implications on hazard assessment* 121

3.1.5 *Holocene tsunamigenic sediments and tsunami modelling in the Thermaikos Gulf area (Northern Greece)* 133

3.1.6 *Tsunami catalog and vulnerability of Martinique (Lesser Antilles, France)* 161

3.2 Modèles de rupture 189

3.2.1 *The source of the Catania earthquake and tsunami (Southern Italy): New evidence from tsunami modeling of a locked subduction fault plane* 193

3.2.2 *The 1856 Djijelli (Algeria) earthquake and tsunami : source parameters and implications for tsunami hazard in the Balearic Islands* 197

3.2.3 *The 1856 Tsunami of Djidjelli (Eastern Algeria) : Seismotectonics, Modelling and Hazard Implications for the Algerian Coast* 209

3.2.4 *The El Asnam October 10th, 1980 inland earthquake : a new hypothesis of tsunami generation* 227

3.2.5 *Vulnerability of the Dover Strait to coseismic tsunami hazard : insights from numerical modeling* 239

4) Conclusions et perspectives 263

4.1 Conclusions générales 265

4.2 Perspectives 268

Bibliographie 271

Annexes 299

Annexe 1 *L'aléa tsunami en France métropolitaine* 301

Annexe 2 Rapport TSUNORD 317

Annexe 3 Procédure de réalisation des grilles bathymétriques 337

Partie 1

Introduction

1) Introduction

Cette thèse sur les tsunamis en Europe s'inscrit avant tout dans le continuum du tsunami de l'océan Indien du 26 décembre 2004 mais aussi dans un contexte politico-géographique dans lequel la mondialisation, la démographie, le changement climatique et bien d'autres raisons ont une part de responsabilité. Nous expliciterons ce contexte dit « extérieur » dans un premier temps, avant de nous intéresser au vif du sujet, c'est-à-dire les tsunamis. Nous rappellerons ce qu'est un tsunami, du mot à l'origine du phénomène, pour nous immerger ensuite dans l'histoire des tsunamis en Europe, puis au contexte géodynamique/géologique des deux grands bassins touchant l'Europe, à savoir, la mer Méditerranée et l'océan Atlantique.

La finalité générale de ce travail consiste en l'amélioration des connaissances de l'aléa tsunami en Europe et Atlantique Nord. Elle a été effectuée au sein des projets européens **TRANSFER** (**T**sunami **R**isk **AN**d **S**trategies **F**or the **E**uropean **R**egion, http://www.transferproject.eu/) et français **MAREMOTI** (**MARE**graphie, observations de tsuna**M**is, m**O**délisation et é**T**udes de vulnérab**I**Iité pour le nord-est Atlantique et la Méditerranée occidentale, ANR RiskNat 2008, http://www.maremoti.fr/).

1.1 Contexte politico-géographique

Le tsunami du 26 décembre 2004 généré par un séisme de subduction de magnitude 9.1 au large de Sumatra (Indonésie) et entraînant la mort de plus de 225000 personnes dans tous les pays adjacents de l'océan Indien (Indonésie, Sri Lanka, Inde et Thaïlande principalement) marque le début d'une « course » vers la connaissance des tsunamis, domaine jusque là globalement peu étudié par la communauté scientifique (excepté par certains pays comme le Japon, les Etats-Unis, la Norvège, l'Italie, la Turquie ou encore la France). Cette « euphorie » passe par le déblocage de fonds sans précédent à des niveaux aussi bien locaux (nationaux) qu'internationaux. Une multitude de projets de recherche voient ainsi le jour, même dans des pays avec de faibles ressources qui sont alors aidés par des nations plus riches : l'Allemagne se retrouve par exemple leader et unique financeur à hauteur de 50 millions d'euros d'un grand projet d'élaboration et d'installation d'un système d'alerte précoce aux tsunamis (GITEWS, ou German Indonesian Tsunami Early Warning System) en partenariat avec l'Indonésie (Rudloff et al., 2009). A noter que jusque là l'Allemagne ne se préoccupait pas vraiment des tsunamis de manière aussi assidue, exception faite d'un ou deux

chercheurs par-ci, par là, comme Anja Scheffers ou Dieter Kelletat de l'Université d'Essen qui s'intéressent aux paléotsunamis (Scheffers et Kelletat, 2003).

Suite à ce tsunami de l'océan Indien, la communauté internationale, par le biais de l'**UNESCO** qui gérait le système d'alerte de l'océan Pacifique depuis les années 1960, a décidé de doter chaque bassin océanique de système d'alerte aux tsunamis (Intergovernmental Oceanographic Commission, 2005). Cet objectif passe nécessairement par l'amélioration des connaissances sur l'aléa[1] tsunami dans tous les bassins océaniques, qui, elle, nécessite indéniablement une amélioration de la connaissance des sources tsunamigéniques et donc de la géologie et/ou de la tectonique des zones considérées.

Le problème majeur qui se pose actuellement à une échelle mondiale vient de la littoralisation[2] constante, avec une augmentation de la population côtière d'environ 8 % pour 10 ans qui est associée à une augmentation de la vulnérabilité[3] de ces populations face aux aléas naturels comme les tsunamis. En effet la population littorale, qui était estimée à 37 % de la population mondiale en 1994, représente aujourd'hui plus de 50 % de la population mondiale vivant dans la bande des 100 km, siège d'une activité économique importante (représentant par exemple 40% du produit intérieur brut (PIB) européen) (Amara, 2010) comme on peut le voir sur la Figure 1. Ajouté à l'attraction économique que représente le bord de mer, ces chiffres sont également la conséquence directe de l'accroissement rapide de la population mondiale (6,7 milliards actuellement) avec un taux d'accroissement estimé autour de 1,14 % (Figure 2). Ce chiffre signifie que la population actuelle aura été multipliée par 1,3 aux alentours de 2050, et avec elle, la population littorale, avec les conséquences que cela peut avoir en terme de vulnérabilité face aux aléas naturels, et donc de risque. La notion de risque étant définie par la relation de convolution (x) suivante :

(risque) = (aléa) x (vulnérabilité des enjeux)

Les enjeux peuvent être humains, économiques ou environnementaux.

[1] Aléa naturel : évènement à probabilité non nulle qui par opposition à un évènement provoqué par une activité humaine, a pour origine un phénomène naturel et se développe initialement dans un milieu naturel (air, eau, sol, …) (Dubois-Maury, 2005).

[2] Littoralisation : migration des populations vers les littoraux et maritimisation de l'économie (développement des transports maritimes intercontinentaux et des grands ports maritimes).

[3] Vulnérabilité : mesure les conséquences prévisibles d'un phénomène potentiellement catastrophique sur les enjeux (i.e. les personnes, les biens, les activités, etc.) (Dubois-Maury, 2005).

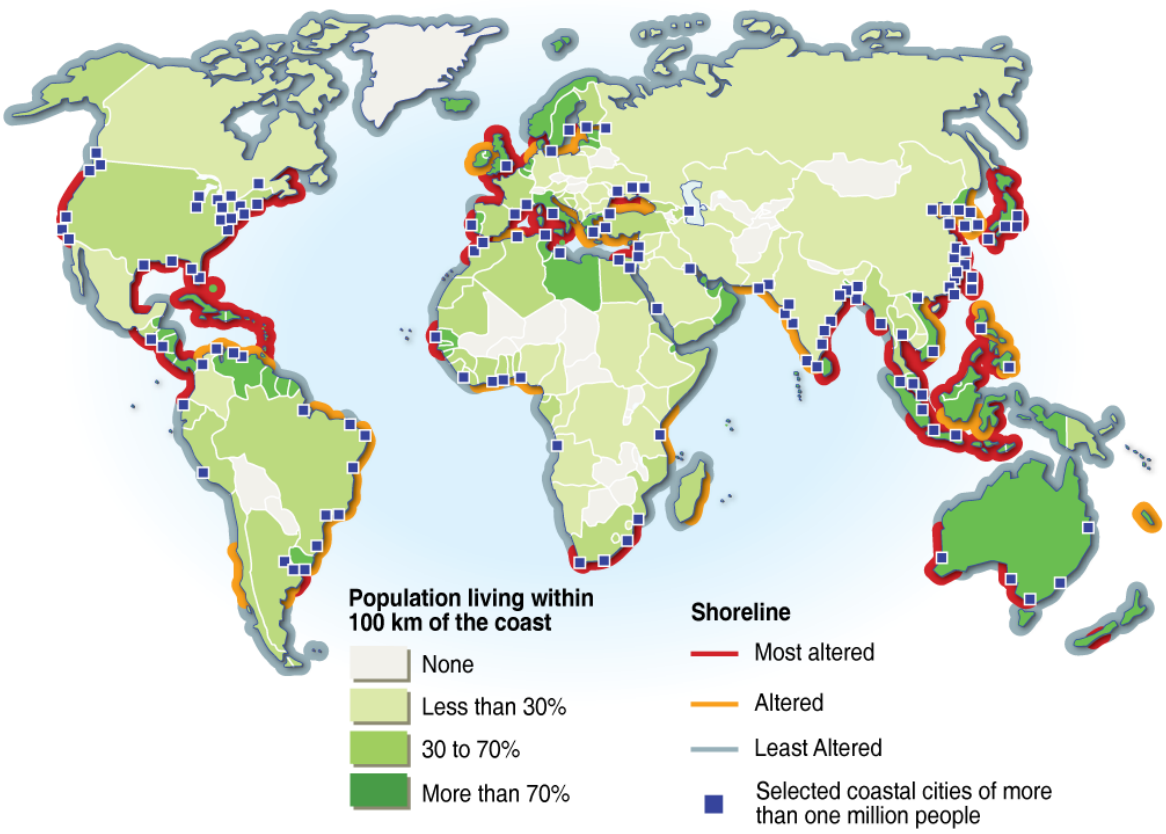

Figure 1 : Population côtière et zones côtières altérées (< 100 km). Les zones avec une population côtière dense sont les plus altérées (source : UNEP, 2007[4], d'après Burke et al. (2001)).

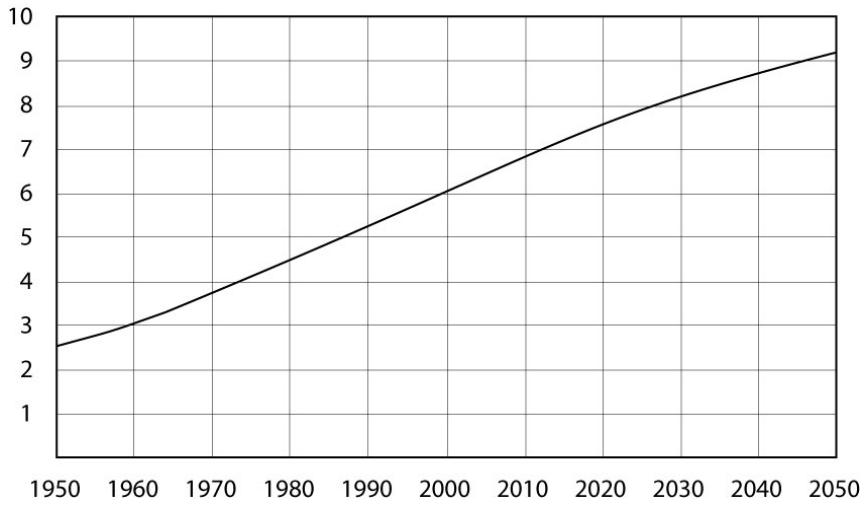

Figure 2 : Population mondiale (1950-2050) (source: U.S. Census Bureau, International Data Base, avril 2005).

[4] Lien : http://maps.grida.no/go/graphic/coastal-population-and-altered-land-cover-in-coastal-zones-100-km-of-coastline .

En définitive, quand on regarde la courbe des victimes des catastrophes naturelles, on en déduit que ce n'est effectivement pas la quantité de catastrophes naturelles qui augmente (comme le laisserait croire la tendance révélée par la Figure 3), pas plus que leur intensité en moyennant sur les dernières décennies, mais bien la population soumise à ces aléas (montée du niveau moyen des mers, inondations littorales, tempêtes, vagues de chaleur, destruction des barrières naturelles de protection – mangroves, récifs de corail – , etc.) (Bogardi, 2004). Bien sur, des études récentes montrent qu'une augmentation de ces derniers en termes de fréquence et d'intensité, associée à un réchauffement climatique planétaire désormais admis par la majorité de la communauté scientifique, est envisageable comme l'indique Szlafsztein (2005) ou encore McBean et Ajibade (2009). Les répercussions de ces évènements sur les populations et infrastructures côtières sont, à ce titre, catastrophiques car ils entraînent des changements massifs au niveau des côtes (érosion, destructions des digues, des routes, sécurité publique et économie affectée, etc.) (Stanchev et al., 2009) qui nécessitent une évolution/mise à jour constante des plans de prévention des risques pour les zones considérées. On voit même l'émergence de l'association des phénomènes extrêmes: par exemple, la montée du niveau de la mer due au réchauffement climatique peut rendre vulnérable à l'aléa tsunami à plus ou moins long terme (estimation du risque sur 100 ans et plus) une région qui ne l'était pas en augmentant les impacts côtiers des tsunamis ; certains groupes de travail ont décidé de prendre désormais en compte cette montée du niveau-marin dans les simulations de tsunami pour l'évaluation du risque tsunami à long terme (Tinti, 2005 ; Woods, 2008 ; Ministry of the Environment, 2008).

Pour information, au XXème siècle, les tsunamis se situent en 4ème position en terme d'occurrence à une échelle mondiale après les tornades, les inondations et les cyclones tropicaux avec un peu plus de 1000 évènements répertoriés, et en 4ème position également en terme de nombre de victimes, derrière les inondations, les séismes et les cyclones tropicaux (Bryant et al., 2005).

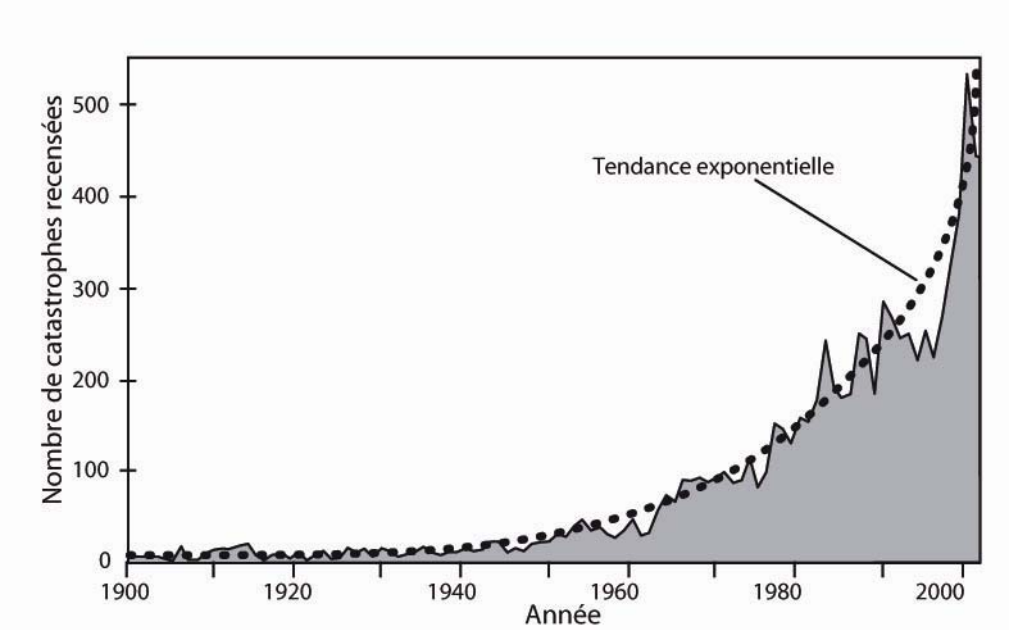

Figure 3 : Nombre de catastrophes naturelles recensées sur la période 1900-2001 (source: Bryant, 2005).

1.2 Qu'est ce qu'un tsunami ?

1.2.1 Origine du mot et utilisation

Le phénomène tsunami est connu dans la littérature depuis au moins 2000 ans. Le mot *tsunami* quant à lui voit son origine dans la littérature japonaise ou il signifie littéralement « vague de port » (*tsu*, port et *nami*, vague). Ce terme est employé pour la première fois dans un rapport daté du 2 décembre 1611 dans lequel un serviteur du seigneur japonais Tokugawa Ieyasu raconte l'arrivée de vagues géantes dans un port après le séisme de Sanriku (Cartwright et Nakamura, 2008). Les tsunamis sont très présents dans l'histoire japonaise ainsi que dans celle de pays d'Asie du sud-est comme la Russie, la Corée et même la Chine où on a retrouvé des témoignages d'une époque aussi lointaine que 47 av. J.C. Certaines personnes pensent même les voir en peinture puisque la fameuse 'Grande vague au large de Kanagawa' (on notera que la traduction littérale du cartouche de l'œuvre est : 'A l'intérieur de la vague au large de Kanagawa') du peintre Katsushika Hokusai publiée en 1831 devient le symbole des tsunamis à travers le monde (Figure 4); Cartwright et Nakamura (2009) démontre prudemment de manière très détaillée que cette vague est vraisemblablement une vague de tempête.

Figure 4 : Vague de Kanagawa, Hokusai (1831)

En occident les tsunamis sont plutôt connus sous la dénomination « raz de marée » (Maremoto, tidal wave, Flutwelle, etc.), le terme *tsunami* n'apparaît en occident qu'à la fin du 19ème siècle (Cartwright et Nakamura, 2008) et n'est utilisé par la communauté scientifique que depuis les années 1960. Pour clarifier la chose, ce phénomène n'a aucun lien de près comme de loin avec le phénomène de marée qui lui résulte du jeu des forces gravitationnelles exercées principalement par la lune et le soleil sur les océans terrestres. La marée peut néanmoins avoir des conséquences considérables sur l'impact d'un tsunami comme le montre Murty et Stronach (1989) au niveau de l'île de Vancouver (Canada) ou encore Weisz et Winter (2005), Kowalik et al. (2006) ou encore Kowalik et Proshutinsky (2010). En effet, un tsunami est une onde gravitaire de grande longueur d'onde λ très supérieure à la profondeur d'eau à l'endroit considéré (i.e. plusieurs dizaines à plusieurs centaines de kilomètres contre une profondeur d'eau maximum de seulement quelques kilomètres), avec une grande période T (en minutes voir dizaines de minutes) et présentant au large une amplitude A très faible de l'ordre de quelques dizaines de centimètres maximum en général (Tableau 1). A noter que cette amplitude au large est très peu perceptible par les marins du fait du très faible rapport entre A et λ (de l'ordre de quelques millièmes de pour cent), mais néanmoins on a découvert qu'elle pouvait être assez facilement suivie avec les satellites de mesure altimétrique[5] comme Topex-Poseidon, ERS-1, Jason-1, Envisat, etc. (Okal et al., 1999 ; Smith et al., 2005). A noter qu'il a été démontré (Occhipinti, 2006 ; Occhipinti et al., 2006, 2008a,b) que la propagation d'un tsunami affecte également l'atmosphère en faisant interagir les ondes électromagnétiques induites par le déplacement de ce tsunami avec les électrons présents dans l'atmosphère. Ceci

[5] L'altimétrie est la mesure de l'altitude d'un lieu ou d'une région donnée

peut être repéré par le biais de diverses méthodes comme les sondages radio ou l'utilisation des anomalies GPS (Occhipinti et al., 2006).

	Type d'onde	longueur d'onde	période	vitesse	amplitude
ondes courtes	vague générée par le vent	10 m	10 s	30 km/h ($c=1,25.(\lambda)1/2$)	1-20 m
ondes longues	tsunami	100 km	10-30 min	600 km/h* ($c=(g.h)1/2$)	10 cm - 1 m
	marée	1000 km	12 h**		quelques cm

* vitesse donnée pour une profondeur d'eau de 3000 m
** onde semi-diurne

Tableau 1 : Ordres de grandeur des paramètres principaux des différents types d'onde au large.

1.2.2 Origine du phénomène

Cette onde a une origine géologique résultant d'une déformation rapide (de quelques secondes à quelques minutes) du fond de la mer ou de sa surface directement. Elle peut être générée par plusieurs mécanismes différents :

La majorité des tsunamis ayant eu un impact plus ou moins fort et sur une grande région ont été générés par des séismes (Satake et Tanioka, 1999 ; Synolakis, 2004) comme ce fut le cas le 26 décembre 2004 à Sumatra en Indonésie avec des hauteurs de vagues atteignant 20 m et plus, des run-up atteignant parfois plus de 30 m et des inondations sur plusieurs kilomètres (Borrero et al., 2006 ; Tsuji et al., 2006 ; Paris et al., 2009), mais aussi plus récemment au Chili le 27 février 2010 avec des vagues atteignant 10 m ou de nouveau en Indonésie aux niveau des îles Mentawai le 26 octobre 2010.

Les glissements de terrain (aérien ou sous-marin) peuvent également générer des tsunamis (Ward, 2001 ; Harbitz et al., 2006) qui peuvent avoir des conséquences dramatiques en terme de hauteur de vagues, comme ce fut le cas le 18 novembre 1929 quand un séisme de magnitude 7.2 déstabilisa la couverture sédimentaire de la marge au sud de Terre-neuve (Canada) entraînant la génération d'un tsunami dévastateur qui fut même enregistré au Portugal, de l'autre côté de l'océan Atlantique (Fine et al., 2005). De la même façon, le 10 juillet 1958 à Lituya Bay en Alaska, un séisme de magnitude M_W 8.3 occasionna un glissement de terrain dans le fjord, générant à son tour une vague gigantesque dont le run-up maximum a été mesuré à 524 m (Fritz et al., 2009).

Une éruption volcanique peut également générer un tsunami consécutivement à l'explosion du dôme comme ce fut le cas dans le détroit de la Sonde (Indonésie) le 27 août 1883 lors de l'éruption du Krakatoa (Choi et al., 2003) ou par impact de coulées pyroclastiques en mer (Watts et Waythomas, 2003) comme ceux qui suivirent les coulées de Soufrière Hills à Montserrat en juillet 2003 (Mattioli et al., 2007).

Et pour finir, un tsunami peut être généré par une chute de corps (astéroïde, comète) (Hills et Mader, 1997 ; Paine, 1999 ; Ward et Asphaug, 2000) ou une explosion sous-marine nucléaire (Van Dorn et al., 1968), ou non, comme ce fut le cas le 6 décembre 1917 lorsque deux bateaux transportant des matières explosives entrèrent en collision dans le port d'Halifax (Canada) : il en résulta une énorme explosion qui généra un tsunami de plusieurs mètres de haut (Greenberg et al., 1993). Toutefois il semblerait que ce dernier mode de formation par explosion anthropique voulue (surtout nucléaire) soit prohibé par un traité international.

Le terme de « vague » est souvent utilisé pour nommé un tsunami, malheureusement à tort puisqu'un tsunami ne se comporte pas comme une vague classique (générée par le vent, de longueur d'onde de l'ordre de la dizaine à la centaine de mètres, et de période de quelques secondes) mais plutôt comme une marée très rapide, avec augmentation ou diminution rapide du niveau de la mer (quelques minutes), avec un déferlement observé seulement dans certains cas comme au niveau de la pointe de Koh Pu en Thaïlande en 2004 (Figure 5) où le tsunami s'est comporté comme un train de houle classique avec déferlement de type '*point break*'. Les caractéristiques des tsunamis générés par ces différents mécanismes sont résumées dans le tableau (Tableau 2). On y trouvera également une comparaison avec les vagues dites « classiques ».

Figure 5 Le tsunami du 26 décembre 2004 touchant la pointe de Koh Pu, Thaïlande

On notera que certaines ondes atmosphériques générées par des variations brusques de pression, des passages de fronts, des ondes gravitaires atmosphériques, ou toute autre perturbation atmosphérique, entraîneront des perturbations océaniques ayant les mêmes caractéristiques que les ondes précédemment citées ; on parlera alors de météotsunamis (Rabinovich et Monserrat, 1998 ; Vilibic, 2005 ; Vilibic et Beg Paklar, 2006 ; Monserrat et al., 2006 ; Sepic et al., 2009). Ce phénomène est assez bien connu et présent de manière récurrente dans certaines régions du monde (Baléares, Mer Adriatique, Japon, etc). Il est important de le connaître pour bien dissocier l'impact qu'il peut avoir sur les côtes avec celui d'un tsunami que l'on dira « classique » surtout en cas d'estimation de l'aléa tsunami d'origine sismique. Par exemple, en Méditerranée occidentale les *rissagas* (Jansa et al, 2007) posent un problème à la recherche d'évènements historiques dans les îles Baléares puisque les 2 types de tsunamis y sont vus de la même façon : ainsi lors d'enquêtes effectuées sur le terrain au cours de cette thèse pour évaluer l'impact du tsunami de mai 2003, il n'était pas rare d'être renvoyé directement vers ces fameuses *rissagas*, ceci étant un phénomène beaucoup plus connu et étudié aux Baléares que les tsunamis « classiques » (Paris et al., 2008).

Source	longueur d'onde	période	amplitude à la côte
séisme	100 km	20-30 min	0-30 m
glissement de terrain	100-200 m	< 8 min	0-200 m
explosion volcanique	quelques km	< 5 min	0-50 m

Tableau 2 : Comparaison des caractéristiques des tsunamis générés par 3 types de source.

Pour des raisons de standardisation des descriptions, les tsunamis pourront être classés en fonction de leur magnitude, avec par exemple l'échelle d'Imamura et Iida obtenue avec la relation suivante :

$m = \log_2 H_m$ (ou $H_m = 2^m$) avec la H_m la hauteur de vague maximale atteinte à la côte ou sur les enregistrements marégraphiques (Papadopoulos, 2003), ou avec un autre type de relation telle que celle de Murty et Loomis (1980).

Ils pourront également être classés en fonction de leur intensité $i_s = \log_2 \sqrt{2}(H)$ ou H représente cette fois la hauteur moyenne du tsunami à la côte (Soloviev, 1970), relation revue ensuite par Shuto (1993).

En fonction de l'étendue de la zone touchée on parlera de tsunamis locaux (à moins de 100 km de la source ou moins d'1h de propagation), régionaux (à moins de 1000 km de la source ou entre 1h et 3h de propagation) ou de télétsunamis ou tsunami transocéanique (impact à plus de 1000 km de la source et plus de 3h de propagation) (IOC, 2008).

1.3 Les tsunamis en Europe

Bien que leur occurrence soit nettement moins importante que dans l'océan Pacifique, et que leur amplitude moyenne soit généralement moins élevée, il existe toutefois un certain nombre de tsunamis recensés en Europe, pour la plupart générés en Méditerranée (ils représentent 10% des tsunamis à l'échelle mondiale), et plus particulièrement en Méditerranée orientale au niveau des zones de subductions grecque et italienne (par exemple, le catalogue de la NOAA en recense plus de 350, Roger et al., soumis, **Annexe 1**). Certains de ces tsunamis « européens » ont même marqué profondément l'histoire, que ce soit par exemple celui généré par l'éruption cataclysmique du Santorin (Grèce) en 1490 av. J.C. qui serait à l'origine de l'extinction de la civilisation Minoéenne (Pararas-Carayannis, 1973, 1992 ; Pareschi et al., 2006 ; Goodman-Tchernov et al., 2009) ou encore le « récent » tsunami, en terme de temps géologiques, associé au séisme de Lisbonne du 1er novembre 1755. Celui-ci fait l'objet de nombreuses études concernant la recherche de la zone de rupture (parmi ces études on trouvera celles de Udias et al., 1976 ; Johnston, 1996; Gjevik et al., 1997 ; Zitellini et al., 1999, 2001 ; Thiebot et al., 2006 ; Gutscher et al., 2006) à l'origine d'un télétsunami[6] dévastateur (Baptista et al., 1996, 1998(a,b), 2003) et l'impact de ce dernier sur les côtes européenne (Dawson et al., 2004 ; Haslett et Bryant, 2007), africaine (Levret, 1991 ; Kaabouben et al., 2009), mais aussi des îles de l'océan Atlantique (Andrade et al., 2006), les Caraïbes (Roger et al., 2010a,b) et les côtes américaines (Ruffman, 2006 ; Roger et al., 2010c) dans le cadre de l'évaluation du risque tsunamis dans ces régions : par exemple Lima et al. (2010) pour l'Espagne, Richardson et al. (2007) ou Horsburgh et al. (2008) pour les îles britanniques ; Barkan et al., 2009 ou Brink (2009) pour les Etats-Unis ; Zahibo et Pelinovsky (2001) ou Proenza et Maul (2010) pour les Caraïbes. Le méga-glissement Holocène (~8200 ans) du Storrega au niveau de la marge norvégienne fait également partie de ces évènements majeurs en Europe puisqu'il a affecté toutes les côtes de la mer du nord, de la Norvège à

[6] Tsunami généré par une source lointaine, généralement située à plus de 1000 km. Il cause des dégâts très importants en champ proche de la source, et a encore suffisamment d'énergie 1000 km plus loin, après avoir traversé un océan par exemple, pour en créer de nouveaux (UNESCO-IOC, 2006).

l'Islande en passant par l'Angleterre et l'Ecosse (Dawson et al., 1988 ; Smith et al., 2004 ; Bondevik et al., 2005 ; Weninger et al., 2008).

A ces tsunamis dévastateurs s'ajoutent de nombreux tsunamis de moindre amplitude mais pouvant toutefois avoir eu des conséquences non négligeables sur les communautés côtières. Pour ce qui concerne la Méditerranée, les tsunamis historiques répertoriés dans les bases de données sont localisés sur la Figure 6.

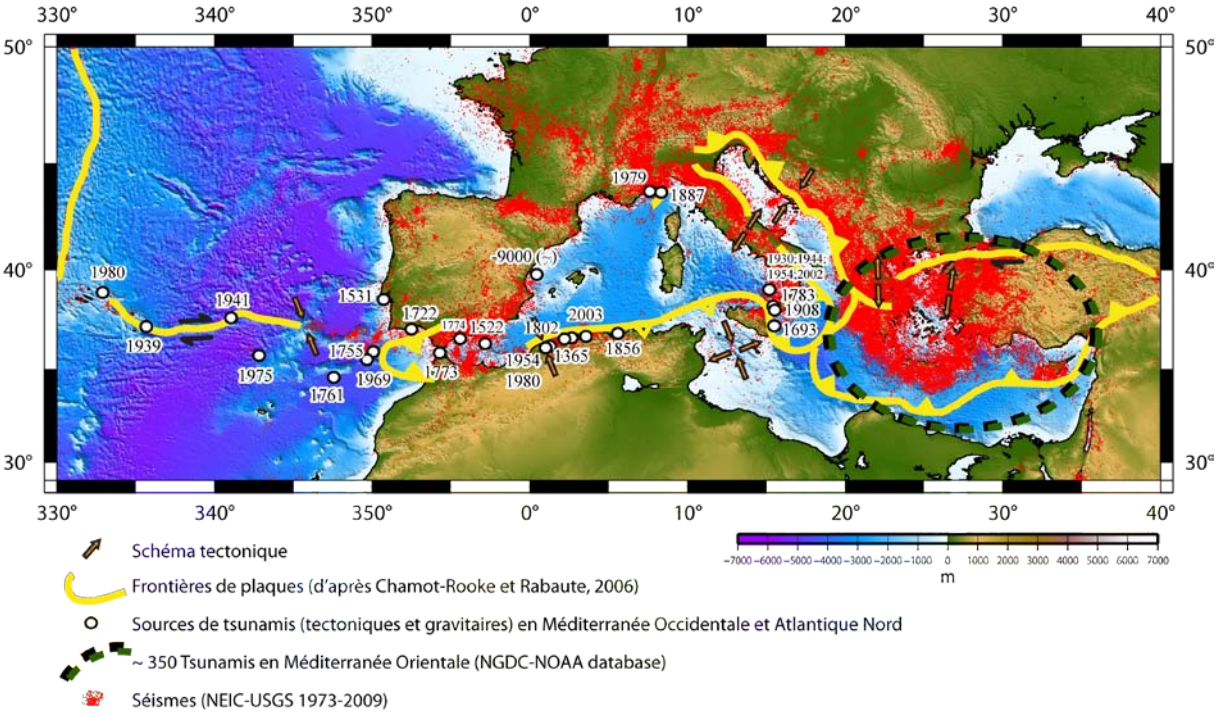

Figure 6 : Localisation des sources de tsunamis significatifs connus en Méditerranée et au large de la péninsule ibérique (Roger et al., soumis).

On notera que des ruptures de barrage associées à des glissements de terrains peuvent entraîner l'écoulement catastrophique des eaux dans une vallée sous la forme d'une vague gigantesque qui pourra parfois être assimilée à un tsunami comme ce fut le cas le 9 octobre 1963 à Vajont en Italie lorsqu'un glissement de terrain de 270 millions de m^3 chute dans un réservoir d'eau artificiel générant une vague gigantesque qui submergera la vallée située en dessous du barrage, tuant 1910 personnes (Mantovani et Vita-Finzi, 2003 ; Panizzo et al., 2005). Panizzo et al. (2005) indique que ce type de vague représente un cas particulier de tsunami.

Tous ces évènements et toutes ces sources tsunamigéniques sont répertoriés dans des catalogues dans lesquels on trouve des informations (événements, '*run-up*', dépôts, enregistrements marégraphiques, etc.) sur les tsunamis historiques et/ou contemporains

collectées dans le monde entier. Il existe des catalogues s'intéressant au monde entier comme celui de la NOAA (National Oceanic and Atmospheric Administration, USA) et du NGDC (National Geophysical Data Center, USA) (http://www.ngdc.noaa.gov/hazard/tsu.shtml), ou celui du Laboratoire des tsunamis de l'académie des sciences de Russie (http://tsun.sscc.ru/On_line_Cat.htm), à une échelle régionale comme le catalogue élaboré durant les projets européens GITEC (Genesis and Impact of Tsunamis on the European Coasts) et GITEC 2 pour la région Europe (Tinti et al., 1999 ; 2001) et à une échelle plus locale, ou à l'échelle d'un pays, comme le catalogue Italien (Tinti et al., 2004) ou le catalogue marocain (Kaabouben et al., 2009).

Ces catalogues représentent la première étape à l'étude des tsunamis dans une région. Ils permettent d'avoir une idée générale sur les sources potentiellement tsunamigéniques d'une région donnée, la récurrence temporelle du phénomène à un endroit donné, les amplitudes maximales auxquelles on peut s'attendre, et finalement l'aléa et le risque associé pour un segment de côte donné. Tout comme la recherche de documents historiques qui va les alimenter, les catalogues servent de base à toute étude sur les tsunamis, principalement celles qui traitent de l'évaluation du risque dans une région donnée, de la même façon que les catalogues de séismes servent de base à l'élaboration des plans de prévention du risque sismique.

Dans le cadre de cette thèse, je me suis principalement intéressé aux tsunamis générés par des séismes, d'une part parce que les groupes de travail des projets dans lesquels j'évoluais (TRANSFER et MAREMOTI) s'intéressaient à ce type de source, et d'autre part, parce qu'un séisme, beaucoup plus qu'un glissement de terrain ou une éruption volcanique, est capable de faire des dégâts considérables à distance comme nous avons pu le voir en décembre 2004 (tsunami de Sumatra) ou février 2010 (tsunami du Chili). Un tsunami généré par un séisme a aussi l' « avantage » d'avoir un précurseur, la secousse sismique, qui joue un rôle primordial dans le processus d'alerte.

1.4 Contexte géologique et géodynamique

Pour étudier les tsunamis correctement, il est nécessaire de commencer par comprendre pourquoi il y en a en déterminant quels sont les mécanismes à l'origine de leur formation dans la région qui nous intéresse.

1.4.1 Méditerranée

La Méditerranée est un des endroits du monde les plus complexes d'un point de vue géologique et géodynamique. En effet, la Méditerranée telle que nous la connaissons aujourd'hui est née il y a 30-35 Ma d'un isolement d'une portion de l'océan Téthys. Le jeu qui s'ensuit alors d'ouvertures et de fermetures de bassins contrôlé par la tectonique des plaques, avec des subductions, ouverture de bassins arrière-arcs, orogénèses alpines, lui confère une physiographie particulière (Jolivet et al., 2008).

A l'heure actuelle la Méditerranée est toujours une zone active d'un point de vue tectonique. Les limites de plaques actives sont très bien soulignées par une sismicité dite modérée en moyenne, avec une partie occidentale présentant une sismicité faible à modérée, et une partie orientale présentant une sismicité modérée à forte (Vannucci et al., 2004). Beaucoup plus présente et plus forte en Méditerranée orientale au niveau de l'Italie et de la Grèce avec, entre autres, de nombreux séismes de subduction de magnitude Mw > 6.0, comme les séismes de Calabre du 11 janvier 1693 (M_W 7.5), 5 février 1783 (M_W 6.9) et 28 décembre 1908 (M_W 7.1) (Gerardi et al., 2008) ou les séismes helléniques de 365 (Crète) et 1303 (Rhodes) de magnitudes estimées respectivement à 8.3 et 8.0 (Papazachos et Papazachou, 2003), on la trouve également en Méditerranée occidentale au niveau de la marge nord africaine avec des séismes comme ceux de Jijel ($M_S \geq 6.6$ les 21 et 22 aout 1856), Blida (M_W 7.3 le 2 janvier 1867), Ech Chelf (M_S 6.8 le 9 septembre 1954 et M_S 7.3 le 10 octobre 1980), Zemmouri-Boumerdès (M_W 6.8 le 21 mai 2003) en Algérie (Harbi et al, 2010 ; Hamdache et al., 2010), Almeria en Mer d'Alboran le 22 septembre 1522 (M_W estimée à 6.5 ; Gràcia et al., 2006) ou le séisme d'Al Hoceima du 24 février 2004 au Maroc (Cakir et al., 2006). Les mesures de déformation par GPS menées en Méditerranée pour la première fois dans la seconde partie des années 1990 (Anzidei et al., 1999) puis affinées ensuite dans les années 2000 ont permis d'estimer la direction NW-SE et le taux de convergence (ou collision) actuel des plaques africaines et eurasienne entre 3 et 10 mm/an (Nocquet et Calais, 2004, 2003), taux qui avait déjà été approché par les modèles Nuvel-1 et Nuvel-1A (DeMets et al., 1990). Enfin, en plus d'être sismiquement active, la marge algérienne serait actuellement réactivée en compression et serait une des zones les plus actives sismiquement parlant en Méditerranée occidentale (Cattaneo et al., 2010 ; Yelles-Chaouche et al., 2006).

On trouve en Méditerranée occidentale une sismicité ponctuée de séismes de magnitude supérieure à 6 (sismicité modérée à forte), présentant tous types de mécanismes au foyer (allant d'un régime compressif à l'est vers un régime décrochant à l'ouest en mer

d'Alboran), tout du long de la zone de collision entre les plaques africaine et eurasienne. Ces séismes sont localisés en milieu marin (Jijel, 1856 ; Zemmouri, 2003) ou à proximité (cas des séismes de El Asnam de 1954 et 1980) et sont donc capables de générer des tsunamis par simple transmission de la déformation cosismique à la masse d'eau sus-jacente ou voisine (Okal et Synolakis, 2003).

Dans le cadre de cette thèse, on se concentrera majoritairement sur la partie occidentale de la Méditerranée, de la Sicile à l'est, à la mer d'Alboran et le détroit de Gibraltar à l'ouest.

Afin d'évaluer le risque sismique de la zone et surtout le risque tsunami qui y est associé, il faut nécessairement s'intéresser aux structures potentiellement tsunamigéniques. Or ce n'est que très récemment, depuis les campagnes en mer MARADJA (« MARge Active DJAzaır ») 1 (2003) et 2 (2005), PRISMA (2004) et PRISME (2007) réalisant des mesures bathymétriques (multifaisceaux), de l'imagerie SAR (Side Scan Sonar) des fonds marins, de la gravimétrie, des mesures de réflectivité, du sondage de sédiments (CHIRP) et des profils de sismique réflexion haute résolution, que l'on a une idée de ce qui se passe au niveau de cette marge. En effet, avant 2003, la méconnaissance de la marge nord algérienne est marquée par l'absence de données morphologiques haute résolution. La thèse d'A. Domzig (2006) va alors permettre une avancée majeure dans ce domaine en permettant de caractériser la structure tectonique de la marge (expression morpho-structurale) en identifiant entre autres des loupes d'arrachement associées à des glissements de terrain sous-marins (instabilités gravitaires) et différents réseaux de failles en mer (dont un actif, Déverchère et al., 2005) et en évaluant la quantité de raccourcissement sur les structures actives ainsi identifiées.

Dès lors, la connaissance de la marge nord algérienne, et par extension, la connaissance de la tectonique en Méditerranée qui passe inévitablement par la connaissance des évènements historiques, vont permettre de proposer des scénarios de rupture cosismique et ainsi de quantifier le potentiel tsunamigénique de la zone. A première vue en Méditerranée occidentale, on se trouve face à un risque tsunami associé aux séismes avec une période de récurrence très grande et dont les sources, des failles inverses associées à des mécanismes compressifs, sont majoritairement localisées sur la marge nord algérienne. Des tsunamis d'origine sismique ont toutefois également été répertoriés en mer d'Alboran comme celui d'Almeria de 1522 qui serait à attribuer à la faille décrochante (avec une légère composante verticale) de Carboneras, potentiellement capable de générer des séismes de magnitude M_W ~7.2 (Gràcia et al., 2006 ; Reicherter et Hübscher, 2007), ou celui du 23 Février 1887 en mer

Ligure (Magnitude du séisme estimée à M ~6.2/6.5 et hauteur de *run-up* autour de 1-2 m, Eva et Rabinovich, 1997), mais leur impact est généralement plus localisé (Solovyev et al., 2000). A noter que pour la mer d'Alboran, l'origine des tsunamis est très controversée, entre une origine 100 % sismique et une origine gravitaire avec des glissements de terrain mis en évidence lors de campagnes marines récentes (Gràcia et al., 2006 ; Reicherter et Becker-Heidmann, 2009).

A ceci vient donc s'ajouter le fait que le pourtour de la Méditerranée, marge algérienne comprise, présente un talus continental très pentu avec une couverture sédimentaire très récente donc peu compactée, présentant les conditions idéales à l'occurence de glissements de terrain et de courants de turbidité[7] (Cattaneo et al., 2010 ; Camerlenghi et al., 2010) pouvant être à l'origine de tsunamis d'amplitudes et de zones d'impact directement liées aux paramètres physiques (taille, cohésion des matériaux, etc.) du volume mis en mouvement et de la pente (angle, hauteur, etc.) sur laquelle ils ont lieu. Parmi ces glissements on notera l'évènement de Nice (Côte d'Azur, France) du 16 octobre 1979 (Assier-Rzadkiewicz et al., 2000) et le Big'95 au large de Castellon (petite ville au nord de Valence) sur la côte espagnole méditerranéenne, daté aux alentours de 11000 ans et qui est à ce jour le plus gros évènement de ce type enregistré en Méditerranée occidentale avec un volume estimé supérieur à 26 km^3 (Lastras et al., 2002, 2004, 2007). Un séisme, même de moyenne magnitude (M_W > 4.0, Malamud et al., 2004), mais néanmoins bien placé et présentant une intensité épicentrale suffisante (Lee et al., 2008), est capable de déstabiliser la couverture sédimentaire de la marge et induire ainsi un ou plusieurs glissements de terrain sous-marins (Biscontin et al., 2001, 2004 ; Biscontin et Pestana, 2006) comme ce fut le cas en Algérie en 1954 avec le séisme d'Orléansville, actuelle Ech Chlef, qui engendra un courant de turbidité qui se propagea vers les îles Baléares, coupant au passage des câbles de liaison téléphoniques (El-Robrini et al., 1985 ; Solovyev et al., 1992).

1.4.2 Atlantique nord

La géologie de l'Atlantique nord est globalement moins complexe que celle de la Méditerranée mises à part deux zones bien spécifiques, les Caraïbes et la zone au sud/sud-ouest de la péninsule ibérique (Golfe de Cadix).

[7] Un courant de turbidité est un écoulement gravitaire lié à la différence de densité entre deux masses d'eau due principalement à la présence de sédiments dans l'un des deux fluides.

En effet, l'océan Atlantique est bordé de deux marges passives généralement asismiques. Toutefois certaines régions présentent une sismicité modérée comme la marge est-canadienne (Stein et al., 1979 ; Mazzotti et Adams, 2005) ou le golfe de Cadix (Grimison et Chen, 1986 ; Martin Davila et Pazos, 2003) ; cette sismicité est associée à la réactivation de failles sous le jeu de contraintes régionales dues dans le premier cas au rebond post-glaciaire sur l'Amérique du nord (Zoback et Grollimund, 2001 ; Mazzotti et Townend, 2010), et à la collision entre les plaques africaines et eurasienne dans le second cas (Terrinha et al., 2009 ; Zitellini et al., 2009). La zone de subduction active de la plaque Atlantique (plaque nord américaine) sous la plaque Caraïbes présente elle aussi une sismicité modérée. Cet océan, et donc ses marges, se sont mises en place il y a 185 millions d'années lorsque les plaques eurasienne et africaine d'un part, et américaine d'autre part, se sont séparées (Bird et al., 2007). Actuellement, il représente une surface de 82 millions de km² (il se trouve juste derrière l'océan Pacifique en terme de surface) qui s'élargit à un taux d'environ 2 cm/an.

Les seules zones actives sont la dorsale médio-Atlantique où la croûte océanique est créée, présentant une légère sismicité (Bergman et Solomon, 1990), la zone de subduction des Caraïbes (Russo et al., 1993), ainsi qu'une zone qui pose réellement problème aux scientifiques depuis de nombreuses décennies : la zone de contact entre les plaques africaine et eurasienne au large de la péninsule ibérique, de la mer d'Alboran à l'est, à la faille de Gloria reliant les Açores à l'ouest. On y trouve une sismicité diffuse avec une diversité de mécanismes au foyer (Udias et al., 1976 ; Kiratzi et Papazachos, 1995) et surtout, de très gros séismes comme ceux du 1er novembre 1755 (M_w=8.5/8.7, Ribeiro et al., 2006) ou du 28 février 1969 (M_w=7.8/8.0, Grandin et al., 2007), et de nombreuses structures sous-marines indiquant des contraintes compressives orientées NW-SE, dont le très mystérieux banc de Gorringe au large du Portugal (Johnston, 1996 ; Jiménez-Munt et al., 2010). La frontière de plaques y est alors très mal connue (Chamot-Rooke et Rabaute, 2006).

De la même façon qu'en Méditerranée, un certain nombre de tsunamis ont été recensés dans l'océan Atlantique avec des impacts locaux, régionaux ou à l'échelle de l'océan, provenant de sources sismiques ou gravitaires. Comme le souligne Murty (2005), les caractéristiques de l'océan Atlantique sont totalement différentes de celles de l'océan Pacifique dans lequel la majorité des tsunamis enregistrés à l'échelle du globe voient leur origine. Du fait de l'absence de zones de failles majeures telles que les zones de subduction circum-Pacifique, on ne peut pas y trouver de grands tsunamis trans-océaniques, exception faite du télétsunami associé au séisme de Lisbonne de 1755 (Roger et al., 2010c) ou de celui

généré par un gigantesque glissement de terrain sous-marin induit par un séisme de magnitude 7.2 le long de la marge sud de Terre-Neuve (Canada) le 18 novembre 1929 (Fine et al., 2005). Cette absence de grandes structures tectoniques potentiellement tsunamigéniques « facilite » en quelque sorte la tache d'évaluation de l'impact des tsunamis générés dans l'océan Atlantique en Europe de l'ouest, même si il faut tout de même rester prudent quand à la génération de tsunamis par des glissements de terrain au niveau des marges, induits ou non par de grands séismes intraplaques.

Partie 2

Les outils pour étudier les tsunamis

2) Les outils pour étudier les tsunamis

La connaissance des phénomènes naturels comme les tsunamis passe inévitablement par l'élaboration et l'utilisation d'outils, que ce soit pour les étudier directement sur le terrain, mais aussi en laboratoire. Les travaux sur le terrain concernent les recherches de documents historiques, les enquêtes post-évènement et les études de sols (marqueurs de tsunami récent et dépôts de paléotsunamis). Les travaux en laboratoire concernent tout ce qui touche à la modélisation (numérique ou analogique) ainsi que les études des échantillons de sédiments prélevés lors des investigations sur le terrain. Les outils et la méthodologie appliquée seront choisis en fonction de l'évènement et des objectifs prédéfinis.

2.1 Observations historiques

Les recherches historiques s'inscrivent dans un objectif général de compilation des données existantes sous forme de bases de données. Elles comprennent les prospections dans les archives, les centres de documentations, les bibliothèques privées et publiques, etc. Elles peuvent être complétées par des études de dépôts sédimentaires sur le terrain afin de mettre en évidence des évènements passés et ainsi élargir l'échelle de temps mise à notre disposition par la conservation des documents historiques et surtout par l'apparition de l'écriture. Des enquêtes auprès des usagers des ports, des capitaineries, etc., comme celle réalisée par Sahal et al. (2009) dans le cadre de la recherche d'information concernant le tsunami généré par le séisme de Zemmouri en Algérie (2003), permettent d'acquérir des informations supplémentaires sur des évènements récents qui sont parfois très peu connus. Les informations recherchées sont principalement les hauteurs de vagues, les distances d'inondation, les nombres de vagues, les périodes, les heures d'arrivée, les temps de parcours (si le tsunami est associé à un séisme ressenti par l'observateur), les dégâts occasionnés, la ou les zones touchées.

2.1.1 Enregistrements marégraphiques

La meilleure donnée actuellement mise à disposition des scientifiques modélisateurs de tsunamis afin de caler correctement les modèles est l'enregistrement marégraphique, ou enregistrement des variations du niveau de la mer en un point donné.

Ce type de donnée est la plus fiable et pose le moins de problème quant à son interprétation et la qualité de l'information qu'elle contient même s'il faut toutefois rester prudent sur le calibrage, l'échantillonnage et la position du capteur (localisation géographique, profondeur d'eau sous-jacente) qui enregistre les fluctuations du niveau marin. En effet, même si la tendance générale va petit à petit vers un remplacement des capteurs mécaniques, acoustiques ou à pression par des marégraphes radar (Martin Miguez et al., 2008), un échantillonnage trop espacé en temps risque de se faire au détriment de l'enregistrement des amplitudes minimales/maximales, voire même du temps exact d'arrivée, qui sont des informations très importantes pour calibrer les modèles. Par exemple, un signal échantillonné à 10 minutes (conçu pour enregistrer les marées la période du signal est de 6 h en moyenne) ne permettra pas d'enregistrer correctement une vague de période 20 minutes comme ce fut le cas en 2003 avec le tsunami de Zemmouri enregistré dans le sud de la France (Alasset et al., 2006 ; Sahal et al., 2009). Le taux d'échantillonnage peut être adaptatif, c'est-à-dire que le système peut automatiquement augmenter la fréquence dès lors qu'un séisme est enregistré par exemple, ce qui permet de ne pas devoir stocker d'énormes quantités de données. Concernant la localisation, le capteur peut se trouver dans une zone trop à l'abri, ou au contraire dans une zone où des phénomènes de résonance peuvent avoir lieu (Rabinovich, 2009), au risque de rendre le signal enregistré inexploitable.

Une instance internationale, **l'Intergovernmental Oceanographic Commission (IOC)**[8], met ce type de données à disposition sur internet (http://www.ioc-sealevelmonitoring.org/). Les données proviennent d'organismes partenaires comme le GLOSS[9], ou le PTWC[10].

Un autre type de données de niveau marin est disponible depuis quelques années et conçu spécifiquement pour l'enregistrement des tsunamis: il s'agit des données enregistrées par les DART (ou Deep-ocean Assessment and Reporting of Tsunamis), qui sont des capteurs de pression développés par la NOAA[11] positionnés au fond de la mer à des endroits stratégiques (à proximité des zones de subduction, loin des zones potentiellement instables d'un point de vue gravitaire, etc.) et reliés à une bouée équipée d'émetteur/récepteur pour la

[8] Organisme sous l'égide de l'UNESCO (http://ioc-unesco.org/)

[9] The Global Sea Level Observing System (http://www.gloss-sealevel.org/)

[10] Pacific Tsunami Warning Center (http://www.weather.gov/ptwc/)

[11] http://www.ndbc.noaa.gov/dart/dart.shtml

transmission des informations en temps réel (Gonzales et al., 1998) comme on peut le voir sur la Figure 7.

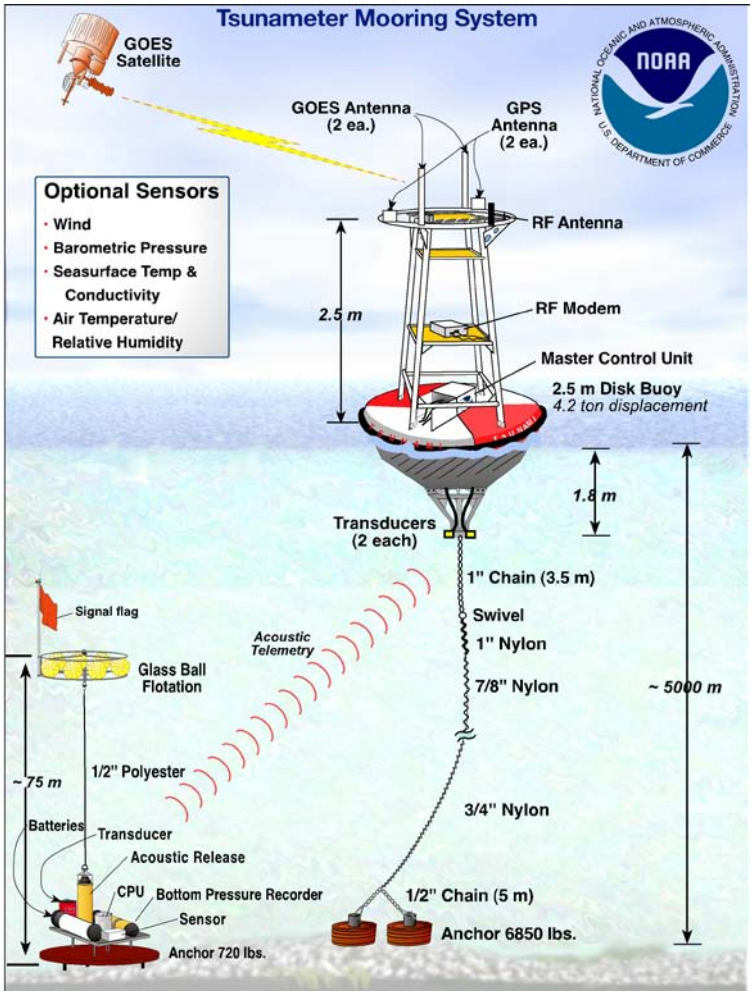

Figure 7 : Schéma explicatif du fonctionnement du système DART (source: NOAA, http://www.noaanews.noaa.gov/stories2005/images/tsunami-dart-system2.jpg).

2.1.1 Archives

Les évènements marins anormaux ou perturbations aquatiques (comme les seiches[12] dans les ports ou les surcotes associées aux tempêtes), associées ou non à des « tremblements de terre » ont souvent été répertoriés/mentionnés, de manière détaillée ou non, par les lettrés contemporains dans des lettres, des rapports périodiques soumis aux autorités supérieures, ou dans des documents d'église comme par exemple les nombreux documents disponibles contemporains aux séisme et tsunami de Lisbonne de 1755 (Baptista et al., 1998a). Aujourd'hui, les médias ont pris le relais de ces « rapporteurs », relatant de manière plus ou

[12] Les seiches sont des ondes stationnaires dans un bassin fermé ou semi-fermé (Ardhuin et al., 2010)

moins exacte, les faits observés ou ressentis, essayant de captiver au maximum leurs lecteurs comme l'indique B. David, président fondateur de **Communication Sans Frontières**, citant une « sur-médiatisation aiguë de l'évènement » de 2004 dans l'océan Indien, ainsi qu'une « mondialisation de l'information [confrontant] tout un chacun à des informations racoleuses et contradictoires issues de sources diverses et confuses » (Humacoop, 2005). L'avènement d'internet dans les dernières années a permis de faciliter et d'accroître considérablement les transferts de données, et la connaissance des phénomènes naturels tels que les tsunamis s'est globalisée. La moindre vague anormale fait maintenant le tour du monde des médias, principalement à cause ou grâce à l'évènement de décembre 2004, et tout le monde, chercheurs compris, peut désormais recevoir l'information quasiment en temps réel : bulletin **ITIC**[13] pour les tsunamis, alerte **USGS**[14] ou **CSEM**[15] pour les séismes, etc., et ces alertes sont même désormais disponibles sur les téléphones portables (par exemple voir http://www.emsc-csem.org/service/real_time/index.php pour l'alerte sismique ou http://www.tsunami-alarm-system.com/en/index.html pour l'alerte tsunami).

Mais revenons aux documents historiques : les archives sont très riches en informations concernant les séismes et les tsunamis bien qu'ayant souvent été délaissées par les chercheurs ou les ingénieurs du génie civil. Il est vrai qu'il faut du temps et des moyens humains et financiers pour effectuer des recherches historiques sérieuses, en recoupant les informations et en les (in-)validant. Par exemple, pour revenir au cas du tsunami de Lisbonne de 1755, les études cataloguaient, sans les discuter et sans les remettre en question, les observations concernant les effets, les temps d'arrivée, et surtout les tailles de vagues annoncés dans les documents historiques, ceux-ci n'étant parfois même pas contemporains de l'évènement. Dans des localités comme Cadix (Espagne) ou Tanger (Maroc), les tailles de vagues provenant des observations historiques (respectivement 18 m et 17 m en moyenne) étaient impossibles à reproduire avec les modèles numériques proposés. Ainsi, même lorsque le modèle était surestimé comme celui proposé par Gutscher et al. (2006) qui ne parvenait à obtenir que 6 m pour Cadix avec pourtant un rejet de 20 m sur la faille testée, il ne reproduisait que 30 à 50% de l'amplitude des vagues observées. Les travaux menés par Paul-

[13] International Tsunami Information Center : http://ioc3.unesco.org/itic/categories.php?category_no=146

[14] United States Geological Survey : https://sslearthquake.usgs.gov/ens/

[15] Centre Sismologique Euro-Méditerranéen : http://www.emsc-csem.org/service/register.php

Louis Blanc de l'**IRSN**[16] (Blanc, 2008, 2009) mettent fin à la controverse sur les amplitudes du tsunami à Cadix et au Maroc : les observations historiques ont été ré-analysées consciencieusement par l'auteur, s'obligeant à remonter systématiquement à la source des documents historiques, au rapport originel, qui aurait été ensuite repris dans diverses autres publications. Il en déduit qu'une amplitude maximale de 2,5 m aussi bien à Cadix que sur la côte marocaine est suffisante pour expliquer toutes les observations historiques (Blanc, 2009). Cela montre un bon exemple du fait qu'il faille considérer les données historiques avec précaution et prendre du recul quant aux différentes interprétations qui ont pu en être faites, quitte à les mettre de côté si on ne parvient pas à retrouver le document initial ou tout simplement à le déchiffrer ou l'interpréter.

Deux exemples 'européens' peuvent illustrer mes propos : le premier concerne le tsunami de Djijelli (Algérie) de 1856 qui aurait été enregistré au port de Mahon sur l'île de Minorque (Baléares) : plusieurs publications récentes utilisent une information concernant l'arrivée d'un tsunami à Mahon le 21 août 1856 sans jamais citer la référence historique ; seules les études menées par Harbi et al. (2003, 2010) indiquent les documents à l'origine de l'information, la publication de 2010 ne se référant étonnement pas à ceux cités dans celle de 2003. Cette donnée est par ailleurs discutable comme nous le verrons plus tard (dans Roger et Hébert, 2008, partie 3.2.1) puisque c'est la seule information de tsunami reportée ailleurs qu'en Algérie pour cet évènement de 1856 et que les tsunamis atmosphériques ainsi que les glissements de terrain sous-marins sont relativement fréquents à Minorque (A noter qu'une tempête sévit dans le nord de la Méditerranée occidentale à ce moment là, Sahal, 2007).

Le second exemple concerne le tsunami du 6 avril 1580 qui aurait suivi le fameux séisme destructeur de Calais-Douvres d'une magnitude estimée à M_L=5.8 (Neilson et al., 1984 ; Melville et al., 1996 ; Musson, 2004). De la même manière que le cas précédent, plusieurs études font référence à un ou plusieurs témoignages historiques faisant état d'inondations à Calais, Boulogne et Douvres, mais en menant une recherche approfondie sur cet évènement dans le cadre du projet MAREMOTI (mission TSUNORD 1, Roger et al., 2010d, **Annexe 2**), on se rend compte qu'aucun des auteurs ayant cité le(s) fameux document(s), que ce soit dans des catalogues de sismicité historique (Neilson et al., 1984 ; Musson, 1994) ou des études d'ingénierie pour la construction du tunnel sous la Manche (Varley, 1996), ne l'ont en leur possession et ne savent pas où il est disponible. Seule une

[16] Institut de Radioprotection et de Sûreté Nucléaire

personne finit par nous informer qu'il se trouve à la British Library de Londres, là où le service documentation nous avait dit que ce n'était pas le cas quelques semaines plus tôt. Or le problème de faire une nouvelle étude sans avoir le document historique, ou une copie, en sa possession, est le suivant : le document a pu être copié, puis repris, élagué, alourdi, cité et re-cité au fil du temps (430 ans) et on peut donc facilement affirmer que l'information originale a du être déformée, ce qui évidemment pose des problèmes en termes d'évaluation du risque sismique et du risque tsunami de la région pour lesquels nous avons besoin d'informations valides.

De plus, l'étude des documents historiques permet de découvrir des évènements là où personne ne s'y attendait : en effet, dans des régions où la culture du risque tsunami n'existe pas ou plus (typiquement comme à Sumatra en Indonésie avant 2004) (Inoue, 2005) et/ou où la période de récurrence de certains évènements comme les tsunamis est très large (Yamada et al., 2006 ; Jovanelly et Moore, 2009), les documents historiques tels que les archives du clergé, les carnets de bord des bateaux, etc., permettent de mettre à jour des évènements dans des régions où rien ne s'est passé depuis longtemps. Dans le détroit de Douvres par exemple, l'enquête de terrain de la mission TSUNORD 1 (Roger et al., 2010d) a révélé que les risques séisme et tsunami ne sont pas du tout connus et donc non ancrés dans la mémoire des habitants de la région, même de celle des historiens locaux, malgré une occurrence régulière de séismes de faibles magnitudes dans la région et de plusieurs évènements historiques dont un majeur le 6 avril 1580 (Roger et Gunnell, *soumis à Geology*, 2010 ; Roger et al., *in prep.*). Toutefois, des évènements plus récents ne sont pas forcément mieux connus : Dominey-Howes et Minos-Minopoulos (2004) montre que la population des jeunes (≤ 50 ans) des îles de Santorin (Grèce) ne possède pas la mémoire du risque 'éruption volcanique' comme les anciens (> 50 ans) qui en ont vécu une ; cette mémoire du risque n'a pas été transmise par la génération précédente, ou alors elle a été oubliée du fait du manque d'expérience d'une éruption de la part de cette population jeune. Ceci pose un problème puisque l'expérience d'un risque augmente la prudence et la perception face à ce risque.

A noter que de Vries (2010) indique que la vulnérabilité possède une forte composante temporelle, principalement reliée à l'appréhension du temps par les populations soumises à un aléa naturel, ce qui influence alors de manière significative leur vulnérabilité face à cet aléa.

A ces documents historiques « officiels » sont souvent associées les histoires, légendes et témoignages comme le démontre Dudley et al. (2009) dans leur étude sur l'intérêt des interviews vidéo des victimes de tsunami afin de sensibiliser les générations futures, ou Joku

et al. (2007) qui ont récolté les témoignages de tsunamis antérieurs à celui de 1998 en Indonésie et Papouasie Nouvelle-Guinée lors des études in situ pour quantifier l'impact du tsunami de Aitape du 17 juillet 1998 afin de faire un catalogue à jour des tsunamis dans la région et de voir si les gens avaient une connaissance de ce risque. En effet, les légendes relatent souvent une part de réalité, déformée au fil des siècles. La légende la plus connue relatant ce que l'on peut aisément attribuer à un tsunami revient au mythe de l'Atlantide (Platon, 360 J.C.) qui, d'après les interprétations qui en ont été faites, comme par exemple celles de Gutscher (2005), aurait disparu suite à un ou plusieurs forts séismes et un tsunami.

A noter que malgré une méconnaissance globale du risque tsunami en Indonésie en 2004, certaines populations, comme celles de Simeulue, avait conservé une culture du risque transmise par des histoires orales ce qui les sauva (McAdoo et al., 2006).

Une fois que des évènements sont connus et même localisés (source/impact/magnitude, etc), des recherches de dépôts de paléotsunamis sur le terrain peuvent être menées afin de corréler des évènements et de pouvoir remonter plus loin dans le temps pour un lieu donné.

2.1.2 Paléotsunamis – recherche de dépôts

2.1.2.1 Définition

Les dépôts de tsunamis, ou *tsunamites*, sont, comme leur nom l'indique, les dépôts sédimentaires laissés par les tsunamis lorsque l'eau se retire des zones terrestres inondées comme ceux que l'on peut observer à Dalaman (Turquie) dans les premières couches sédimentaires d'une plaine d'inondation séparée de la mer par un cordon dunaire (Figure 8). L'étude des dépôts de tsunamis a commencé à prendre de l'ampleur vers la fin des années 1980 (Dawson et al., 1991 ; Dawson et Shi, 2000) et s'est véritablement intensifiée suite au tsunami de 2004 dans l'océan indien qui a laissé d'importants dépôts quand la mer s'est retirée (Moore et al., 2006 ; Hori et al., 2007 ; Paris et al., 2007).

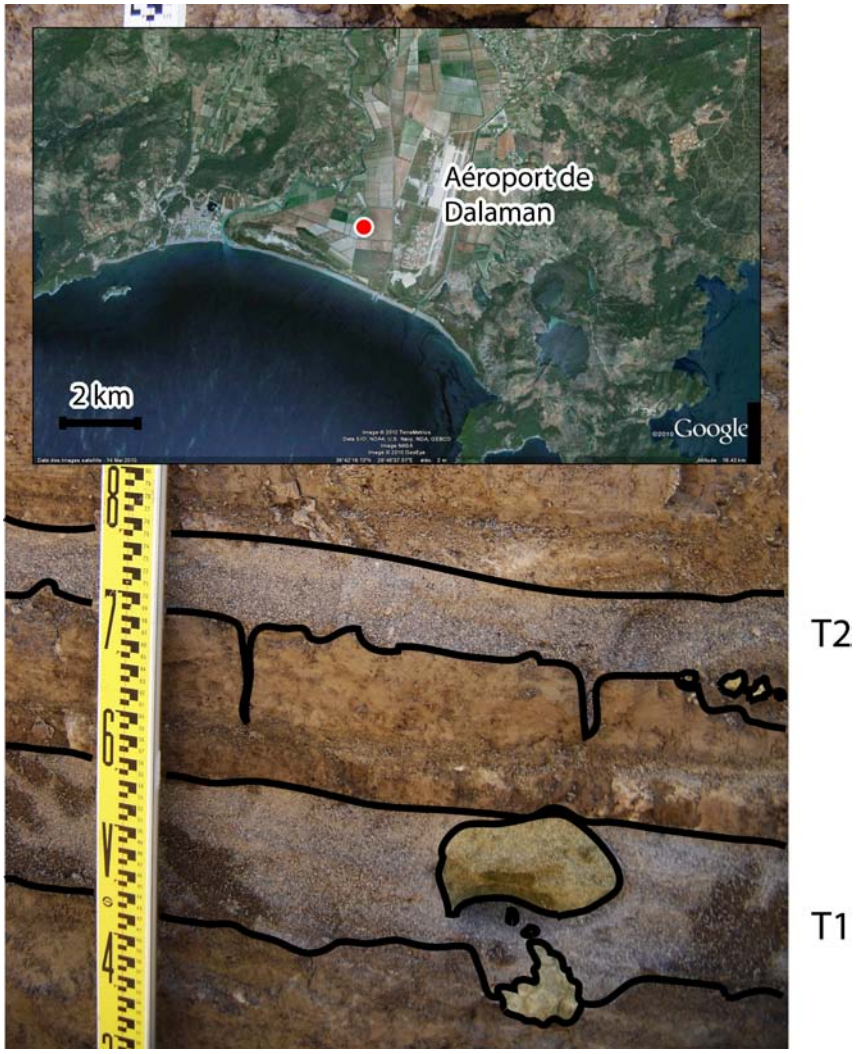

Figure 8 : Dépôts de tsunamis (T1 et T2) observés à Dalaman (Turquie) (photo : J. Roger, 2007). La localisation du site est indiquée par un point rouge.

Lorsqu'un tsunami se déplace, il a une tendance à éroder le fond de la mer et à mettre ainsi en suspension toutes sortes de particules sédimentaires allant de la plus fine ('*silts*') à des blocs rocheux ('*boulders*') de plusieurs dizaines de tonnes. Plusieurs types de dépôts sont alors identifiés lors des investigations sur le terrain et ensuite lors des analyses en laboratoire des échantillons de sédiments prélevés. On les reconnait de par la présence de planctons marins, de coquillages marins, de morceaux de coraux, mais aussi par un granoclassement (classement des grains de sédiment) caractéristique avec des particules de plus en plus fines à mesure que l'on va vers le haut de la couche et par un autre granoclassement relié à la direction du transport. On peut également y trouver des structures sédimentaires qui reflètent l'influence des courants sur le processus de dépôts, de la direction des flux (lamination croisée bi-directionnelle par exemple, Figure 9), par des *ripplemarks* (marques d'ondulation laissées par les vagues), etc. (Fujino et al., 2006 ; Scheffers, 2006).

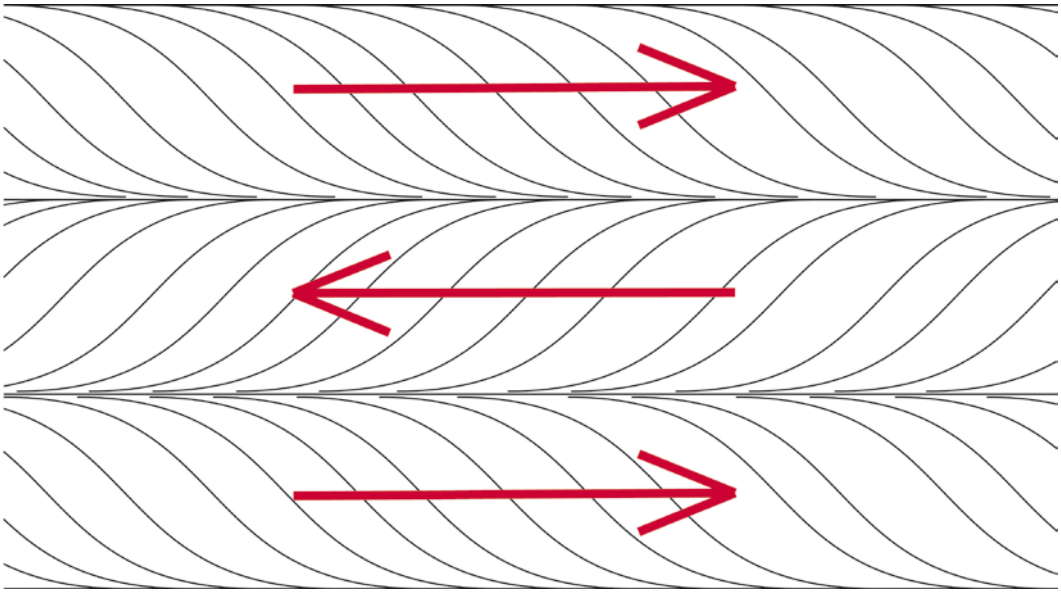

Figure 9 : Couches sédimentaires présentant une lamination croisée bi-directionnelle; les flèches indiquent le sens de l'écoulement associé à ces dépôts (‘*run-up*’ et ‘*run-down*’).

Mais une question fondamentale se pose : comment distinguer ces dépôts de tsunami des dépôts de tempête (ou *tempestites*)?

Les tempêtes font également partie des évènements hautement énergétiques capables d’éroder le fond de la mer et d’inonder ensuite les zones littorales de manière plus ou moins marquée. De la même façon que pour les tsunamis, l’eau apportée sur la terre par une tempête va ensuite se retirer et laisser en place des dépôts sédimentaires et des blocs arrachés au fond de la mer. Comment faire alors la distinction entre les dépôts de tempêtes et ceux de tsunamis ?

Pour les blocs, Nott (1997, 2003) a développé des modèles numériques permettant l’estimation de la hauteur de vague nécessaire pour les retourner et les déplacer. Goto et al. (2010) indiquent que cette méthode a été fréquemment utilisée pour décider si ces blocs avaient été apportés par une tempête ou un tsunami mais ils mentionnent aussi le fait que certaines personnes la remettent en question. En revanche l’analyse des périodes des vagues pourrait être la clé de cette distinction : en effet, les périodes des vagues, plus que les hauteurs, sont nettement plus importantes dans le cas d’un tsunami (facteur 100), ce qui leur permet de déplacer les blocs sur des distances plus importantes. Mais Goto et al. (2010) concluent que pour être vraiment précise, une telle étude doit prendre en compte à la fois les comportements locaux des vagues, la topographie et les paramètres initiaux des blocs, à savoir, si oui ou non ils sont fracturés, leur taille, etc.

Pour ce qui concerne les dépôts plus fins, différentes méthodologies ont également été élaborées même si elles sont encore aujourd'hui discutées. Par exemple, Morton et al. (2007) proposent une distinction par analyse du (grano-)classement des sédiments, expliquant que les conditions hydrodynamiques de transport et de dépôt étant différentes, elles mènent nécessairement à des faciès de dépôts différents, surtout pour les gros évènements. Le contraste le plus important entre ces deux types d'évènements est le suivant : un tsunami est un évènement qui est court dans le temps, qui peut être très épais (parfois 10 m et plus) et qui inonde une vaste étendue en une seule, voire deux ou trois fois, distribuant ainsi la matière en suspension quand le flux repart. Au contraire, une tempête est un évènement qui inonde graduellement pendant une période de temps beaucoup plus importante de l'ordre de plusieurs heures : l'inondation est souvent associée à une surcote comme ce fut le cas à la Nouvelle-Orléans, USA, en 2005, où le cyclone Katrina entraîna une montée des eaux atteignant un maximum de 4 m et plus en 12 h à certains endroits (Marshall, 2007 ; Fritz et al., 2007. A côté, Kortekaas et Dawson (2007) se concentrent plus sur la distance d'inondation et les '*rip-up clasts*' ou débris d'arrachement[17] et les blocs (*boulders*) contenus d'après eux, exclusivement dans ces dépôts de Martinhal (sud Portugal) pour le cas particulier du tsunami de Lisbonne de 1755.

2.1.2.2 Intérêt

Les dépôts de tsunamis permettent tout d'abord de remonter dans le temps encore plus loin que les archives humaines et d'avoir ainsi une vision à plus long terme de ce qui se passe dans une région donnée. Par exemple, Bussert et Aberhan (2004) mettent en évidence en Tanzanie des dépôts qu'ils associent aisément à des dépôts de tempêtes. En revanche, de par ses caractéristiques qui sont explicitées par les auteurs, une des couches de dépôts serait attribuable à un tsunami qu'ils datent au Jurassique supérieur.

Leur étude permet de connaître l'extension ou l'impact direct d'un tsunami (Paris et al., 2007) en tentant de corréler des dépôts de différents sites entre eux. Ils peuvent également être corrélés à des évènements historiques connus comme par exemple la crise Crétacé-Tertiaire avec la chute d'un astéroïde qui aurait généré un tsunami géant dont les dépôts ont été retrouvés un peu partout dans le golfe du Mexique (Tada et al., 2003 ; Goto et al., 2004, 2008), ou a des évènements plus récents de type inondation comme ceux indiqués dans les

[17] Débris arrachés à leur environnement de dépôt d'origine puis redéposés dans un environnement de dépôt différent.

travaux de Haslett et Bryant (2007) concernant des dépôts sédimentaires associés à des évènements hautement énergétiques (tempêtes, tsunamis) sur les côtes française et britanniques. Les dépôts de tsunamis sont contenus/conservés dans les archives naturelles de la Terre que sont les roches sédimentaires ou ce qui aspire à le devenir au cours des temps géologiques par recouvrement sédimentaire et compression. Les dépôts de tsunamis sont, pour faire simple, des dépôts marins dans des faciès terrigènes. Parfois difficiles à distinguer des dépôts associés aux tempêtes comme nous l'avons vu précédemment, leur identification autorise une datation de l'évènement qui leur est associé, de par leur position dans les couches géologiques, ou de par la présence d'éléments chimiques et de leurs isotopes (le carbone par exemple) (Vött et al., 2006 ; Haslett et Bryant, 2007) ou part thermoluminescence, luminescence stimulée par infrarouge (IRSL) ou encore luminescence stimulée optiquement (OSL[18]) (Bishop et al., 2005 ; Cunha et al., 2010). Si plusieurs niveaux de dépôts sont répertoriés dans un site donné, cela permet de proposer une période de récurrence de tsunami pour la région étudiée. Des études approfondies telles que celles menées par Wassmer et al. (2010) sur l'anisotropie de susceptibilité magnétique (ASM) des grains contenus dans les dépôts permettraient de connaître le nombre de vagues et leurs orientations : en effet, l'ASM permet de caractériser la fabrique des roches et donc aussi l'état de déformation d'un dépôt sédimentaire soumis aux contraintes imposées par les flux (ou courants) associés à un tsunami en fournissant une mesure moyenne de l'orientation préférentielle des grains (parallèle à la direction du flux) et en mettant en évidence des marqueurs de cette déformation quasi invisibles comme une imbrication spéciale des grains de chaque échantillon (pendage à contre-courant).

L'étude des dépôts permet même de reconstruire le processus de *run-up* via l'utilisation de modèles mathématiques comme l'ont montré Soulsby et al. (2007) pour le tsunami de Grand Banks de 1929 et de Storegga (6000 ans av. J.C.) ou Srisutam et Wagner (2010) pour le tsunami de 2004 en Thaïland (province de Phangnga) : les auteurs utilisent des méthodes d'inversion utilisant les propriétés hydrodynamiques des tsunamis ainsi que les dynamiques de sédimentation et proposent des relations permettant de calculer les hauteurs et distances de *run-up* en fonction des épaisseurs de dépôt et leur composition sédimentaire (en terme de taille de grains).

[18] La procédure de datation par luminescence stimulée optiquement est très bien explicitée par Lian et Huntley (2002) ou Cordier (2010).

Ils ont aussi le potentiel d'enregistrer l'épaisseur de la lame d'eau à terre (ou '*flow depth*') et la vitesse d'écoulement ou 'flow speed' (Jaffe et Gelfenbaum, 2007 ; Smith et al., 2007), qui sont des paramètres d'importance pour les ingénieurs côtiers.

Cela permet aussi de trouver les évènements les plus gros d'une région donnée (Pinegina et Bourgeois, 2001), ce qui sert ensuite essentiellement pour la proposition de scénarios maximisant pour les études de vulnérabilité. Ils représentent finalement des indicateurs paléosismologique pour une région donnée (Luque et al., 2001).

Il est important de noter ici que l'absence de dépôts dans un endroit donné, et plus particulièrement dans un endroit favorable à la conservation de ces dépôts, ne signifie en aucun cas qu'il n'y a pas eu de tsunami en ce lieu : le sol du site considéré peut avoir été remanié ou il se peut qu'il n'y avait rien à déposer aussi.

A noter que parfois, les recherches de paléotsunamis, que ce soit via les investigations dans les archives ou via les recherches in situ, sont initiées grâce aux résultats de modélisation ; en effet, ceux-ci peuvent révéler des régions qui sont particulièrement bien réceptives aux arrivées de ces ondes longues, ce qui pousse alors à mener des recherches approfondies pour valider ces résultats de calcul et les modèles associés. C'est dans cette optique que deux missions d'investigation sur le terrain on été menées dans les îles Baléares en juin 2008 (Majorque) et janvier 2010 (Minorque) : les résultats de modélisation obtenus dans le cadre du projet européen TRANSFER lors des tests de propagation de tsunami effectués pour les îles Baléares avec des sources sismiques tsunamigéniques localisées sur la marge nord africaine ont permis de souligner des zones particulièrement réceptives à l'arrivée d'ondes de tsunami. Une partie des résultats est présentée dans Roger et Hébert (2008). Ces zones côtières sont le plus souvent localisées dans le prolongement de canyons sous-marins comme le canyon de Minorque ou les nombreux canyons présents tout au long du promontoire des Baléares (Acosta et al., 2002), ou correspondent à des zones où peuvent avoir lieu des phénomènes de résonance. Les deux missions, en plus d'avoir pour but de collecter des données sur le tsunami de Zemmouri du 21 mai 2003 (revoir la date), visaient donc aussi des investigations in situ en terme de dépôts de tsunami dans des zones lagunaires (favorables au dépôt des sédiments et à leur conservation) préalablement identifiées grâce aux images satellites et en accord avec les résultats de modélisation (H_{max} ou hauteur de vague maximale obtenue en chaque point de la zone considérée) (Paris et al., 2008).

Les études sur les dépôts de tsunamis sont donc très intéressantes et riches en informations. Les dépôts de tsunamis apportent un enregistrement témoin pour de grands

séismes et représentent ainsi des outils paléosismologiques importants (Pinegina et Bourgeois, 2001). Associés aux documents historiques, ils permettent de proposer des périodes de récurrence de tsunami pour une région donnée ainsi que des scénarios plausibles.

Ces études de dépôts s'inscrivent dans une catégorie d'investigation plus vaste à savoir les enquêtes post-évènement ou '*survey post-event*'. Ces missions post-évènement, qui sont de plus en plus fréquentes depuis deux décennies, permettent de collecter une quantité considérable de données concernant le tsunami et les dégâts occasionnés, après le passage des secours et avant la reconstruction (Borrero et al., 2009), comme ce fut le cas lors des récentes campagnes aux Samoa américaines après le tsunami du 29 septembre 2009 (Donahue et al., 2009 ; Jaffe et al., 2010 ; EERI Special Earthquake Report, 2010 ; Okal et al., 2010), en Haïti après celui du 12 janvier 2010 (UNESCO, 2010), et dans le pacifique après le séisme du Chili du 27 février 2010 (Ramirez et al., 2010 ; Lagos et al., 2010). Des protocoles d'intervention ITST (International Post-Tsunami Survey) sur site sont même désormais proposés systématiquement et coordonnés par l'**UNESCO** depuis le tsunami des Samoa de 2009 et du Chili de 2010[19], comme celui diffusé récemment par l'**ITIC**[20] pour l'enquête de terrain aux Mentawai (Indonésie), ITSI-Mentawai[21] après le tsunami du 25 octobre 2010 (UNESCO/IOC, NOAA, ITIC, 2010).

[19] http://193.191.134.38/itic/index.php?option=com_content&view=section&id=6&Itemid=35

[20] International Tsunami Information Center

[21] http://193.191.134.38/itic/

2.2 Modélisation

La modélisation, qu'elle soit numérique aussi bien qu'analogique, est un outil qui permet de reproduire un phénomène physique, sur la base de principes fondamentaux et d'hypothèses formulées au préalable. Elle permet également d'estimer ce qui pourrait se produire dans une région donnée ; dans le cas des études de tsunamis, comme pour tout autre aléa naturel, la modélisation permet d'anticiper le comportement des vagues et les conséquences qu'elles pourraient avoir sur les communautés côtières. Menée intelligemment avec de solides bases géologiques, elle permet de proposer des scénarios crédibles dans des zones où trop peu ou même pas du tout d'évènements passés ont été répertoriés, du fait de l'absence ou de la mauvaise qualité des données historiques, ou tout simplement du fait de l'absence d'évènements.

La modélisation de tsunami consiste à reproduire des évènements passés ou à en imaginer de nouveaux ; elle se déroule en 3 phases distinctes : 1) la phase de génération du tsunami (rupture cosismique, glissement de terrain, impact, etc.) ; 2) la propagation du tsunami ; 3) l'interaction avec les côtes et l'inondation. Ces 3 phases seront détaillées dans la partie présentant le code **CEA** utilisé au cours de cette thèse (§2.2.2.2.1.3).

2.2.1 La modélisation analogique

La modélisation analogique est une tentative de reproduction/représentation d'un phénomène naturel (souvent appelé le système « cible ») par un autre, plus compréhensible et surtout plus analysable. On parlera aussi de modélisation dynamique.

Dans le cas des tsunamis, la modélisation analogique consiste à produire des vagues de même type (grande longueur d'onde par rapport à la profondeur d'eau du bassin considéré) à échelle réduite en laboratoire dans des « piscines à tsunami » (‘*wave pool*’, ‘*tsunami tank*’) équipées de capteurs en tout genre (capteurs à ultrasons, vélocimètres acoustiques Doppler, etc.) et autres caméras, comme par exemple le bassin à tsunamis du O.H. Hinsdale Wave Research Laboratory de l'Université de l'Oregon (USA)[22] (le lecteur pourra regarder l'étude menée dans ce laboratoire par Baldock et al. (2009) concernant la cinématique du front de tsunami au moment du déferlement ou ‘*breaking*’). Les vagues sont le plus souvent générées

[22] http://wave.oregonstate.edu/Facilities/Equipment/Tsunami_Wave_Basin/index.html . Construit dès 1972, le laboratoire a été désigné centre de recherche sur les tsunamis en 2001 par la National Science Foundation (USA).

par un piston actionné par un moteur dont les mouvements sont entièrement guidés par ordinateur, permettant ainsi d'avoir un contrôle (quasi-)total sur la forme de l'onde générée. Depuis quelques années, des chercheurs utilisent les vagues générées par des bateaux à grande vitesse comme modèle de tsunami (Parnell et al., 2008 ; Torsvik et al., 2009 ; Didenkulova et al., 2009). En effet, ils sont parvenus à démontrer par exemple que le run-up de ces vagues était similaire à celui des vagues de tsunami, similarité provenant du fait que les bateaux à grande vitesse produisent une zone de dépression étendue et perdurant dans le temps, au même titre que les déformations associées à des séismes ou à moindre mesure, à des glissements de terrain. Ces vagues posent régulièrement des problèmes de sécurité sur les plages (Figure 10).

Figure 10 : Vague générée par un bateau à grande vitesse à Malaga (Espagne): a) et b) amplification, c) d) et e) inondation, f) retrait, g) 2ème vague, h) déferlement (photos: J. Roger, 2010).

Elle représente aussi un moyen efficace pour valider les codes de modélisation numérique via l'élaboration de '*benchmarks*'. Des expériences sont menées dans les piscines à tsunami et les données acquises par les différents capteurs sont ensuite comparées aux résultats obtenus lors des simulations numériques comme font par exemple Grilli et al. (2005) qui se servent d'un générateur de glissements de terrain dans une cuve pour valider leur modèle numérique de génération de tsunami. Les '*benchmarks*' sont en quelque sorte des exercices qui vont également permettre de comparer les différents modèles numériques (§ 2.2.2) entre eux afin de les améliorer comme ceux que j'ai pu effectuer dans le cadre du projet européen TRANSFER : un de ces exercices consistait à reproduire avec les modèles numériques le déplacement et le run-up du tsunami de Okushiri (Japon) de 1993 modélisé en laboratoire dans un chenal expérimental (genre de bassin allongé) de 205 m de long, 3,4 m de large et 6 m de profondeur au maximum (Matsuyama et Tanaka, 2001). A noter que ce modèle analogique avait été élaboré afin de rechercher les mécanismes du run-up atteignant

un maximum de 31,7 m au niveau d'une petite plage que les modèles numériques ne parvenaient pas à expliquer. La Figure 11 montre un des résultats obtenu au cours de mes travaux pour TRANSFER ; on voit notamment que le modèle reproduit bien la première vague. Les arrivées suivantes sont moins bien reproduites du fait de problèmes de réflexion des ondes sur les bords de la cuve, de phénomènes de friction (non pris en compte dans le modèle utilisé), etc.

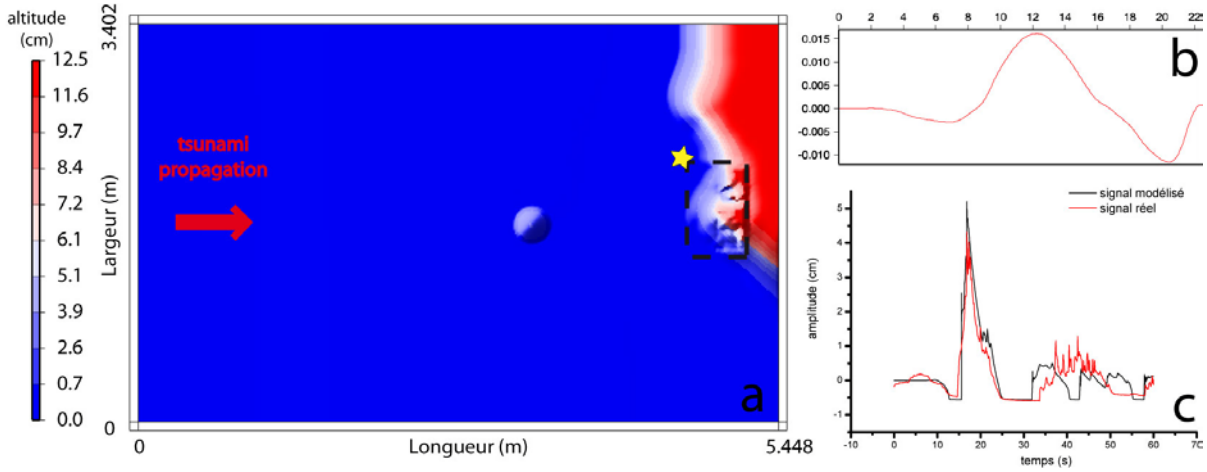

Figure 11 : a) Grille bathymétrique/topographique représentant la zone de Okushiri pour les simulations de tsunami. La zone de run-up maximum observé (tiretés noirs) a une meilleure résolution. b) Le signal est introduit par la gauche avec un piston contrôlé. c) Le signal modélisé est enregistré par un marégraphe synthétique (étoile jaune) et comparé avec les données expérimentales.

2.2.2 La modélisation numérique

2.2.2.1 Définition

La modélisation numérique s'est développée dans les années 1960. Elle propose la résolution d'équations (modèles mathématiques) décrivant un processus physique utilisant une approximation progressive (bien souvent des équations aux dérivées partielles), ou procédure de calcul par pas-de-temps, permettant d'obtenir le comportement du modèle considéré au cours du temps. On obtient ainsi une solution numérique approchée du comportement réel d'un phénomène physique.

Les avantages principaux de la modélisation numérique sont la possibilité de résolution de problèmes complexes d'une part, et d'autre part, une fois que le modèle fonctionne correctement, la possibilité de tester des quantités de scénarios sur des durées de plus en plus courtes et/ou d'avoir les nœuds des grilles de plus en plus nombreux (i.e. augmentation de la résolution). Ceci est en accord avec la loi empirique de Moore qui statue sur le fait que le

nombre de transistors constituant un processeur double tous les 1,5 ans (Voller et Porté-Agel, 2002), ce qui permet d'effectuer de plus en plus de calculs simultanément. Avec l'avènement des multiprocesseurs et des parallèlisations, qui sont basés sur le principe que les gros problèmes peuvent souvent être divisés en problèmes plus petits, que l'on peut ainsi effectuer simultanément, ou en parallèle, les résolutions désirées et les nombres de scénarios et de paramètres d'entrée dans un calcul ne sont plus un problème. En définitive, la modélisation numérique permet de s'affranchir de la construction d'expériences coûteuses, difficiles à réaliser, lentes (modélisation des changements climatiques par exemple opposée à leur observation en temps réel) et parfois même, dangereuses (pour les essais nucléaires par exemple, comme l'expliquent O'Nions et al. (2002)).

En amont de ces modèles que l'on appelle modèles numériques, il existe également des modèles analytiques qui sont des modèles mathématiques ayant une solution finie, comme par exemple celui utilisé dans le cadre des '*benchmarks*' du projet TRANSFER : cet exercice consistait cette fois à reproduire avec les modèles numériques des différents partenaires des solutions analytiques obtenues pour le *run-up* et le *run-down* d'un tsunami de forme connue (sinusoïdale) sur un plan incliné (Carrier et al., 2003). Les solutions analytiques permettent d'avoir une prévisualisation concise du comportement que peut avoir le modèle numérique, mais leur obtention peut vite devenir un véritable challenge.

Pour traiter des incertitudes pouvant exister, certains modèles seront basés, non plus sur des modèles mathématiques, mais sur des modèles statistiques. C'est par exemple le cas des modèles utilisés en météorologie ou climatologie pour prévoir le temps, qui nécessitent des estimations statistiques concernant entre autres les valeurs des paramètres entrés dans le modèle.

2.2.2.2 Les différentes méthodes de modélisation numérique

Il existe deux grandes familles de méthodes de modélisation numérique à savoir les méthodes statiques (on reproduit un phénomène naturel à un instant t donné en lui donnant tous les paramètres nécessaires) et les méthodes dynamiques (on reproduit un phénomène naturel sur un certain laps de temps, afin de suivre son évolution temporelle et spatiale).

Une méthode statique est une méthode qui met en application des équations dans lesquelles le temps est une constante introduite par l'opérateur. Elle permet d'obtenir une capture du système considéré à un instant t donné. Ce genre de méthode est par exemple utilisé pour les calculs de déformation initiale (t=0) dans le cadre d'une rupture sismique

donnée, en considérant toutefois que nous avons affaire à une rupture instantanée (non étalée dans le temps)[23], comme celle qui a été utilisée au cours de cette thèse comme nous le verrons par la suite (§2.2.2.3).

Les méthodes de modélisation numériques dynamiques principales sont représentées par les modèles par différences finies (Mitchell et Griffiths, 1980), volumes finis (Eymard et al., 2000) et par les modèles à éléments finis (Zienkiewicz et Cheung, 1967 ; Zienkiewicz et al., 2005). D'autres méthodes existent mais sont moins utilisées, comme par exemple les méthodes numériques spectrales (Patera et al., 1984), les méthodes aux éléments de frontière (Chen et Zhou, 1992), ou les méthodes variationnelles (des exemples d'application des méthodes variationnelles d'éléments finis sont décrits par Nedelec et Planchard (1973) ou encore Carlier et al. (2000)). Dans le domaine de la recherche sur les tsunamis, ce sont les deux méthodes principales de différences finies et éléments finis qui sont utilisées.

2.2.2.2.1 Différences finies

2.2.2.2.1.1 Généralités

Dans des problèmes avec conditions aux limites tels que les problèmes de propagation de tsunami, la méthode des différences finies est de loin la plus vieille[24], la plus utilisée et la moins complexe des méthodes numériques. Elle permet de résoudre des équations différentielles aux dérivées partielles, telles que les équations non-linéaires de Navier-Stokes utilisées en mécanique des fluides qui décrivent le mouvement des fluides, en respectant l'approximation des milieux continus (nous ne nous étendrons pas sur ce sujet dans le cadre de cette thèse), et qui donnent une description continue temporelle et spatiale des phénomènes étudiés. Pour information, ces équations (dont la formulation existe sous différentes formes) sont au nombre de trois :

- L'équation de continuité (ou équation de conservation de la masse) :

$$\frac{\partial \rho}{\partial t} + \vec{\nabla} \cdot (\rho \vec{v}) = 0 \qquad (1)$$

- L'équation de bilan (ou conservation) de la quantité de mouvement :

[23] Des ruptures dynamiques peuvent être également envisagées comme le rappellent Dutykh et Dias (2009).

[24] Euler, au 18ème siècle, semble être le premier à avoir utilisé des schémas de différences finies pour trouver des approximations de solutions à des équations différentielles ; cette méthode n'a cependant été développée considérablement qu'après la seconde guerre mondiale avec l'avénement des ordinateurs à calculs très rapides.

$$\frac{\partial(\rho\vec{v})}{\partial t} + \vec{\nabla}\cdot(\rho\vec{v}\otimes\vec{v}) = -\vec{\nabla}p + \vec{\nabla}\cdot\vec{\vec{\tau}} + \rho\vec{f} \qquad (2)$$

- L'équation de bilan de l'énergie :

$$\frac{\partial(\rho e)}{\partial t} + \vec{\nabla}\cdot((\rho e + p)\vec{v}) = \vec{\nabla}\cdot(\vec{\vec{\tau}}\cdot\vec{v}) + \rho\vec{f}\cdot\vec{v} - \vec{\nabla}\cdot\vec{q} + r \qquad (3)$$

avec

t le temps (s) ;

ρ la masse volumique du fluide (kg.m^{-3}) ;

$\vec{v}$ la vitesse d'une particule fluide (m.s^{-1}) ;

p la pression (Pa) ;

$\vec{\vec{\tau}} = (\tau_{i,j})_{i,j}$ le tenseur des contraintes visqueuses (Pa) ;

$\vec{f}$ résultante des forces s'exerçant sur le fluide (N.kg^{-1}), incluant à la fois les forces de volume, les accélérations d'entraînement et la force de Coriolis ;

e l'énergie totale par unité de masse (J.kg^{-1}) ;

$\vec{q}$ le flux de chaleur perdu par conduction thermique (J.m^{-2}.s^{-1}) ;

r la perte de chaleur volumique par rayonnement (J.m^{-3}.s^{-1}).

<u>Approximations :</u>

Dans le cas de la modélisation des tsunamis, seules les deux premières équations nous intéressent, à savoir la conservation de la masse (1) et de la quantité de mouvement (2).

La différence de grandeur entre la longueur d'onde λ et la profondeur d'eau h en tout point de la propagation ($\lambda >> h$) fait que l'approximation '*shallow water*' ou « eau peu profonde » (ou encore « couche mince ») des équations de Navier-Stokes est bien adaptée pour la propagation des tsunamis.

On considère que le fluide (l'eau) est incompressible ($\rho = cste$), homogène et non visqueux, l'équation (1) devient alors :

$$\vec{\nabla}\cdot\vec{v} = 0 \qquad (4)$$

et donc (2) se simplifie en :

$$\frac{\partial(\vec{v})}{\partial t} + (\vec{v} \cdot \vec{\nabla})\vec{v} = -\frac{1}{\rho}\vec{\nabla}p + \nu\nabla^2\vec{v} + \vec{f} \qquad (5)$$

avec $\nu = \frac{\mu}{\rho}$ la viscosité cinématique du fluide ($m^2.s^{-1}$).

Lorsque le fluide est au repos, on a $\vec{\nabla}p = \rho\vec{g}$ (avec g l'accélération de la pesanteur) ; on peut alors introduire l'élévation du niveau marin η, ce qui donne :

$$\frac{\partial(\vec{v})}{\partial t} + (\vec{v} \cdot \vec{\nabla})\vec{v} = -g\nabla\eta + \vec{f} \qquad (6)$$

Dans un premier temps cette méthode est basée sur la discrétisation des opérateurs de différenciation par différences finies : les différences finies sont des expressions du type $f(x+b) - f(x+a)$ dans laquelle on fait l'approximation de remplacer la variable continue x par une variable discrète[25] x_i , avec $x_i = (i-1)\delta_x, i \in [1,\ n]$ où i est un indice entier. Cette discrétisation n'est pas unique mais dépend des choix de l'opérateur.

Enfin cette méthode repose sur la convergence du schéma numérique obtenu vers la solution des équations différentielles aux dérivées partielles. Pour cela le schéma numérique utilisé doit présenter une certaine consistance et stabilité, qui seront déterminées par l'application du théorème de Lax-Richtmyer (Gary, 1966; Strikwerda, 2004). La consistance représente l'adéquation entre le système continu et le système discret : le système de départ ne doit pas être remplacé par un autre système. La stabilité permet, elle, de s'assurer que les approximations successives qui ont lieu au cours des calculs ne vont pas mener à des résultats aberrants et donc entraîner une divergence de ces résultats. Pour obtenir cette stabilité, les pas de discrétisation en temps et en espace doivent vérifier la condition CFL ou Courant-Friedrichs-Lewy du nom des 3 chercheurs qui la décrivirent en 1928 (Courant et al., 1928): le nombre de Courant C est limité par la relation $C \geq \frac{u \cdot \Delta t}{\Delta x}$, avec u la vitesse (L/T), Δt l'intervalle de temps et Δx le pas d'espace. La convergence implique la consistance et la stabilité (Peiro et Sherwin, 2005).

Il faut s'assurer que ces critères soient bien respectés à plus forte raison lorsque plusieurs grilles sont utilisées en imbrication dans le cas d'une étude multi-échelle (augmentation de la résolution à l'approche de la zone d'étude).

[25] Variable qui ne dépend pas d'une autre variable. Discrète = non continue.

2.2.2.2.1.2 Exemples de codes aux différences finies

Il existe un certain nombre de codes de modélisation de tsunami utilisant les différences finies, allant de modèles très simples à des versions plus compliquées permettant d'envisager tout type de scénario, aussi bien des tsunamis d'origine sismique que ceux générés par des glissements de terrain ou des impacts d'astéroïdes, prenant en compte ou non la friction, la dispersion des ondes, etc.

Je vais présenter brièvement ceux que j'ai eu l'occasion de découvrir un peu plus en détail que les autres au cours des cinq dernières années avant de présenter succintement le fonctionnement du code **CEA** qui a servi de pilier de base à cette thèse.

a- MOST :

Le code tsunami le plus connu et réputé utilisant les différences finies est le code MOST (Method Of Splitting Tsunami)[26] développé par V. Titov (**PMEL**[27]) et C. Synolakis (**UCL**[28]) dans le cadre du projet américain EDFT (Détection précoce et prévision de tsunami) qui est un assemblage de codes capables de simuler la generation d'un tsunami, sa propagation et son interaction à l'approche des côtes avec calcul du run-up (Titov et Gonzales, 1997) ; ce modèle est entièrement intégré dans le programme d'alerte aux tsunami de la **NOAA** (Meinig et al., 2005 ; Tang et al., 2009).

b- SWAN :

Un second code a montré ses capacités et a servi de base à plusieurs autres codes (dont celui réalisé par le **CEA** et utilisé dans le cadre des travaux présentés dans la partie suivante de cette thèse) : le code de modélisation SWAN de C. Mader (**JPL**[29]) qui se base sur la théorie de la propagation des ondes longues en eaux peu profondes ('*Shallow water Theory*') en coordonnées sphériques en resolvant les équations d'hydrodynamique de Navier-Stokes (Mader, 1988). Mader avait auparavant amélioré et utilisé un autre modèle, ZUNI, décrit par Amsden (1973) et utilisant aussi les différences finies (Mader, 1973).

[26] http://nctr.pmel.noaa.gov/time/background/models.html

[27] Pacific Marine Environmental Laboratory, hébergé par la NOAA.

[28] University of Southern California.

[29] Jet Propulsion Laboratory, USA.

c- COMCOT :

Un troisième code en différences finies est également bien connu dans la communauté scientifique : il s'agit de COMCOT (COrnell Multi-grid COupled Tsunami Model)[30]. Ce modèle est également basé sur la théorie de déplacement des ondes en eaux peu profondes en coordonnées sphériques ou cartésiennes. Le schéma numérique utilisé pour résoudre les équations est une méthode différentielle explicite de type « saute-mouton » (ou '*leap-frog*') comme celle utilisée dans le cadre de cette thèse (§ 2.2.2.3). Ce modèle a l'avantage d'avoir été concu pour être facile d'approche pour des gens non-spécialistes, sous la forme d'un logiciel presse-boutons dans lequel l'utilisateur entre ses paramètres. Tout comme la plupart des codes actuels, COMCOT gère le multi-grille avec des grilles imbriquées. Les tsunamis générés par des séismes tout comme ceux générés par des glissements de terrain sont modélisables (Liu et al., 1998).

2.2.2.2.1.3 Le code CEA

Les différentes modélisations de tsunami effectuées dans le cadre de cette thèse ont été réalisées avec le code de modélisation de tsunami du **Commissariat à l'Energie Atomique** (**CEA**). Ce modèle a été développé au sein du **Laboratoire de Géophysique et Télédétection** (**LDG**, Bruyères le Châtel, France) (Heinrich et al., 1996 ; 1998). Ce code est composé de deux parties principales : une première partie qui calcule la déformation initiale associée à une rupture (séisme) et qui est réalisée via le modèle de dislocation d'Okada (1985) que nous expliciterons directement dans la partie 2.3.2 traitant des paramètres de faille; et une seconde partie qui correspond à la modélisation du tsunami à partir de l'intégration de la déformation initiale calculée au préalable et que l'on considère identique à celle de la surface (transmission de la déformation à la colonne d'eau sus-jacente sans perte) quand le contenu en haute fréquence est faible. En effet, comme le précisent Geist et Dmowska (1999), la couche d'eau océanique agit comme un filtre atténuant les hautes fréquences (comparable à un filtre passe-bas) selon une loi proportionnelle à $\frac{1}{\cosh(kh)}$ ou $k = \frac{2\pi}{\lambda}$ est le nombre d'onde et h la profondeur d'eau. Il est alors important que le bord supérieur de la faille soit en dessous de la surface terrestre, à environ 2-3 km de profondeur (Figure 12). Le calcul de la propagation du tsunami se fait ensuite via l'utilisation d'un modèle qui résout les équations aux dérivées

[30] http://ceeserver.cee.cornell.edu/pll-group/comcot.htm

partielles par la méthode des différences finies. Il met en oeuvre une procédure itérative utilisant un pas de temps fixé par l'opérateur.

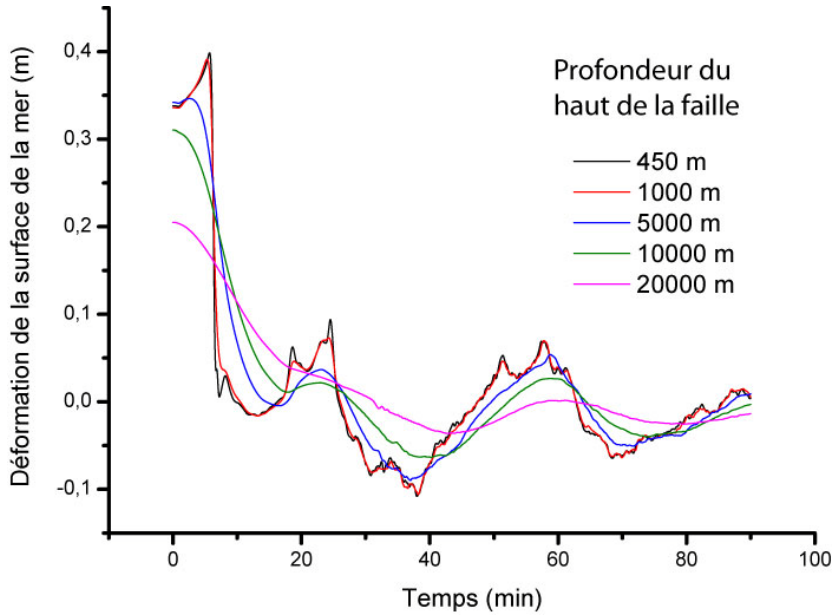

Figure 12 : Marégrammes synthétiques montrant la déformation de la surface de la mer au cours du temps pour une même source positionnée à différentes profondeurs. L'apparition des hautes fréquences est visible sur les signaux correspondant aux sources à 1000 et 450 m.

Les équations que nous avons vues précédemment (§2.2.2.2.1.1) sont discrétisées sur une grille constituée de mailles de type C ou « maille centrée » composée de 5 points de calcul comme sur le schéma ci-dessous (Figure 13) :

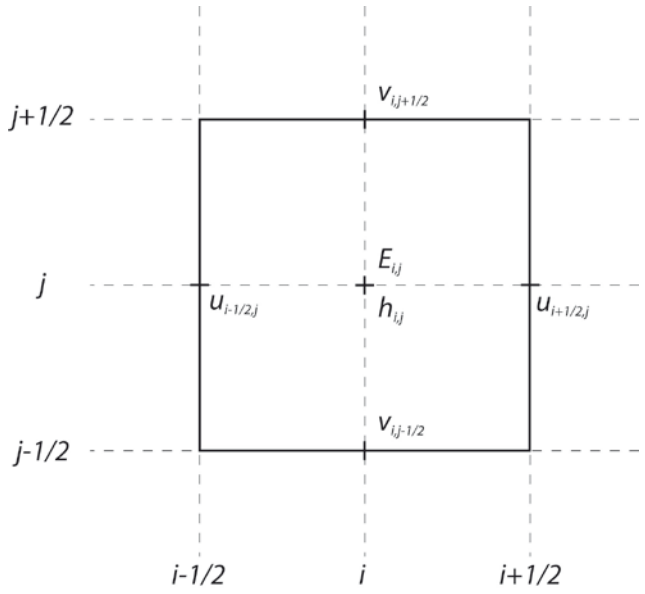

Figure 13 : Maille de type C. L'élévation de l'eau E en un point de profondeur h est calculée au centre de la maille; les vitesses u et v au centre des côtés des mailles (source: Piatanesi, 1999).

Le calcul de l'élévation de l'eau E en un point correspondant à la profondeur h se fait au centre des mailles ; le calcul des vitesses u et v se fait au centre des côtés des mailles. Le schéma numérique est centré en temps et décentré en espace et est implicite de type Crank-Nicolson (schéma d'ordre 2) ; ce dernier point signifie que l'on doit résoudre un système linéaire pour obtenir les $u_{i,j}^{n+1}$ et $v_{i,j}^{n+1}$ à partir des $u_{i,j}$ et $v_{i,j}$. Le détail du schéma utilisé dans le code **CEA** est présenté par Piatanesi (1999).

Le calcul de l'inondation se fait en extrapolant dans les mailles sèches les valeurs calculées dans les mailles voisines mouillées selon la méthode présentée par Kowalik et Murty (1993). La friction en mer ou à terre lors de l'inondation n'est pas prise en compte dans les calculs.

A noter que le schéma de discrétisation est en quelque sorte un substitut au système original (continu) donc il faut faire attention aux artefacts de discrétisation comme les phénomènes de dispersion ou les instabilités numériques que nous avons vus dans le paragraphe précédent (§2.2.2.2.1.1).

2.2.2.2.2 Eléments finis

De la même façon que la méthode des différences finies, elle a aussi pour objectif de résoudre les équations différentielles aux dérivées partielles, telles que les équations non-linéaires de Navier-Stokes, en passant par leur discrétisation.

La grande particularité de la méthode des éléments finis provient principalement du fait que les modèles de simulation de tsunami qui l'utilisent nécessitent des grilles non structurées (une grille non structurée est une grille irrégulière, c'est-à-dire que le pas d'espace est non constant). La maille de départ (qui peut être triangulaire, carrée, etc.) est définie par l'utilisateur et est subdivisée pour améliorer la précision des calculs dans les zones d'intérêt ; dans le cas de l'étude des tsunamis, cette subdivision des mailles a lieu à proximité des côtes, là où les interactions entre les vagues et la bathymétrie/topographie sont les plus importantes (ce point sera discuté dans la partie 2.3.1). Le grand intérêt de cette méthode vient de sa capacité à pouvoir résoudre proprement la géométrie côtière, ce qui n'est pas toujours le cas de la méthode à différences finies surtout si la résolution de la bathymétrie est mal choisie (Murty et al., 2006).

Au même titre qu'il existe plusieurs codes utilisant les éléments finis pour modéliser la propagation des tsunamis, il existe plusieurs codes utilisant les éléments finis mais ils sont

moins connus. Parmi les principaux, on trouvera le code de l'Université de Bologne (Italie) qui a fait ses preuves au cours des deux dernières décennies lors des simulations effectuées pour des projets italiens et européens (Tinti et al., 1994 ; Tinti et Gavagni, 1995 ; Tinti et Piatanesi, 1996a, 1996b ; etc.) ; le code TsunAWI (développé au Alfred Wegener Institute, Allemagne) et sa nouvelle adaptation TsunaFLASH (Pranowo et Behrens, 2009) ; et le code ADCIRC de l'US Army (qui servit à faire les cartes d'inondation de Walsh et al. (2000)), qui fut remplacé par le code MOST (§2.2.2.2.1.2) (Venturato et al., 2007). D'autres codes ont également été utilisés comme ceux de Myers et Baptista (1995) ou Guesmia et al. (1996) resolvant des équations de Boussinesq : l'approximation de Boussinesq des équations de Navier-Stokes est valide pour les ondes faiblement non-linéaire comme les tsunamis ; elle tient compte de la structure verticale (en supprimant la coordonnée verticale) des composantes verticales et horizontales du flux et du phénomène de dispersion des fréquences (Zeytounian, 2003). Ces propriétés sont particulièrement efficaces pour modéliser les vagues dans des eaux peu profondes et dans des ports. Ce type de modèle, dit modèle de Boussinesq, est notamment utilisé dans le cas de la génération de tsunamis par glissements de terrains comme celle qui est modélisée par le module FUNWAVE du programme GEOWAVE développé par P. Watts, S. Grilli et J. Kirby (voir par exemple Watts et al. (2003) pour le fonctionnement de GEOWAVE ou encore Kirby (2003) pour la théorie derrière FUNWAVE).

A noter qu'une méthode de génération automatique de mailles au cours de la simulation, ou méthode à maille adaptative, principalement utilisée jusque là en météorologie ou océanographie, est également appliquée à la modélisation des tsunamis depuis quelques années, aussi bien avec des éléments finis que des volumes finis (Mader et Gittings, 2002 ; George et Leveque, 2006 ; Pranowo et al., 2008); elle permet de réduire le nombre total de mailles des grilles utilisées dans les simulations tout en améliorant la résolution dans les zones d'intérêt et d'obtenir de bonnes solutions numériques (Behrens et Bader, 2009).

2.2.2.2.3 Comparaison entre les différences finies et les éléments finis

La différence entre les méthodes de différences finies et d'éléments finis vient dans un premier temps de la façon avec laquelle les variables d'écoulement sont approximées et ensuite des processus de discrétisations. Les éléments finis préservent les flux, ce qui n'est pas obligatoirement le cas des différences finies qui remplacent les dérivées par approximation en utilisant le développement au premier ordre des séries de Taylor de la fonction considérée (Peiro et Sherwin, 2005). La méthode des éléments finis a l'avantage de

permettre une prise en compte simple et systématique des conditions aux limites quelle que soit la forme du domaine, ce qui n'est pas le cas de la méthode aux différences finis néanmoins plus facile à mettre en œuvre sur des problèmes simples. Mais quand on regarde les modèles de tsunamis utilisés un peu partout dans le monde, on s'aperçoit qu'il n'y a pas de tendance à se dégager : les modèles à différences finies ou éléments finis sont tout autant utilisés aussi bien pour les simulations de tsunamis générés par des glissements de terrains que par des séismes. La méthode des éléments finis est de plus en plus utilisée pour regarder l'interaction des ondes longues (dont font partie les tsunamis) avec des géométries de type structure portuaire et les phénomènes de résonance (Thompson et Hadley, 1995 ; Bellotti, 2007).

2.3 Données d'entrée

Pour modéliser les tsunamis, deux types de données sont nécessaires : les données de bathymétrie/topographie qui se présenteront sous formes de grilles (ou MNT, modèle numériques de terrain) et les données concernant la source du tsunami (ou paramètres de sources).

2.3.1 Données bathymétriques et topographiques

2.3.1.1 Données bathymétriques

Les données de bathymétrie sont des données essentielles pour la modélisation d'un tsunami. De leur qualité dépendra la précision et la pertinence des résultats de simulation obtenus. En effet, un principe fondamental (approximation) de la propagation des ondes longues en milieu de faible profondeur relie la vitesse de déplacement d'un tsunami à la profondeur d'eau en un point donné : $C = \sqrt{g \cdot h} = \frac{\lambda}{T}$, avec C la vitesse de phase, g = 9,8 m.s^{-2} l'accélération de la pesanteur, h la profondeur d'eau, λ la longueur d'onde du tsunami et T sa période. D'après la théorie des vagues en faible profondeur ('*shallow water theory*'), $C = C_g$ dans une zone de faible prodondeur (i.e. $\lambda >> h$), avec C_g la vitesse de groupe, ou vitesse de transport de l'énergie ; celle-ci diminue donc aussi avec la réduction de la profondeur d'eau. C'est dans les zones côtières que la remontée des fonds marins est la plus importante, marquant ainsi la zone de ralentissement, de diminution de la longueur d'onde et d'amplification des vagues (ou '*wave shoaling*'), menant parfois à leur déferlement (Figure

14). A noter que même au large, l'influence de la géométrie des fonds océaniques sur les ondes de tsunami est importante : un tsunami se propagera beaucoup plus vite à l'aplomb des grandes plaines abyssales, qu'au dessus d'une dorsale.

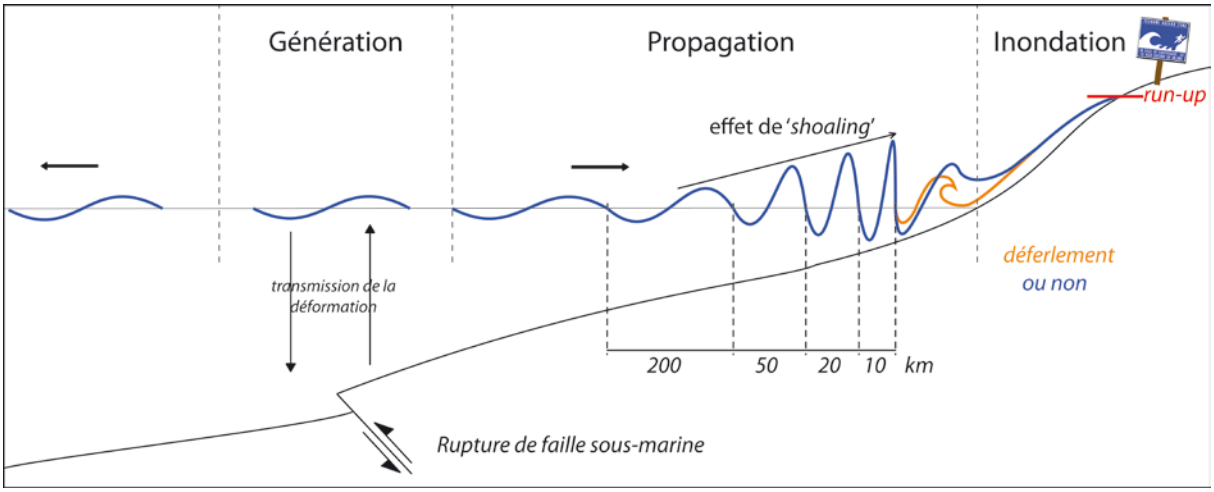

Figure 14 : Génération, propagation et interaction avec la côte pour un tsunami généré par un séisme. Deux types de comportement au rivage sont proposés, avec ou sans déferlement.

Une connaissance accrue de la géométrie du fond de la mer et de la côte (géomorphologie côtière prenant en compte la géométrie des baies ou des ports, la pente des plages, la présence de canyons sous-marins ou de récifs coralliens, etc.) permettra de s'approcher au mieux de la réalité et donc du comportement d'un tsunami réel dans la région considérée ; ainsi les processus de réfraction, réflexion, amplification des ondes qui seront reproduits permettront une meilleure estimation de l'impact d'un tsunami en terme de zone touchée, mais aussi de hauteur de vagues et de distance ou hauteur d'inondation ('*run-up*') (Chatenoux and Peduzzi, 2005, 2007 ; Cochard et al., 2008 ; Duong et al., 2008).

Par exemple, la forme de certaines baies peut les rendre propices à l'effet entonnoir ('*funelling effect*') comme nous le verrons plus tard pour la baie de la Trinité en Martinique (partie 3.1.3). De la même manière les canyons sous-marins vont entraîner une concentration de l'énergie des vagues sur leurs côtés (Figure 15) ; il se passe en définitive la même chose que pour les vagues longues classiques (houle) comme au niveau du canyon de Capbreton dans le sud-ouest de la France (Cirac et al., 2001 ; Abadie et al., 2006 ; Bourillet, 2007): c'est à l'extrémité côtière des deux côtés de ce canyon que l'on trouve parmi les plus grosses vagues d'Europe[31]. Pour expliquer ceci, Speranski et Calliari (2001) indiquent que les

[31] http://wwz.ifremer.fr/var/drogm/storage/images/media/drogm/cartographie/projets/plateau_continental/capbreton/vue_3d/297398-1-fre-FR/vue_3d.jpg

irrégularités de la topographie du fond de la mer agissent comme des « lentilles bathymétriques », entraînant une focalisation des vagues (‘*wave focusing*’) en certain endroits donnant lieu à des amplifications notables des ondes (Berry, 2007). Ce point peut poser des problèmes en terme de vulnérabilité quand la région focale inclue des sections de côte. C’est typiquement le cas des îles : lorsque le train d’onde incident contourne une île du fait de la réfraction, les deux fronts ainsi créés de part et d’autre se rejoignent en un point situé à l’opposée (‘*wrap around*’), dans une zone a priori à l’abri, entraînant une amplification notable des vagues, associée bien souvent à un flux destructif (Yeh et al., 1994 ; Lin et Liu, 2007).

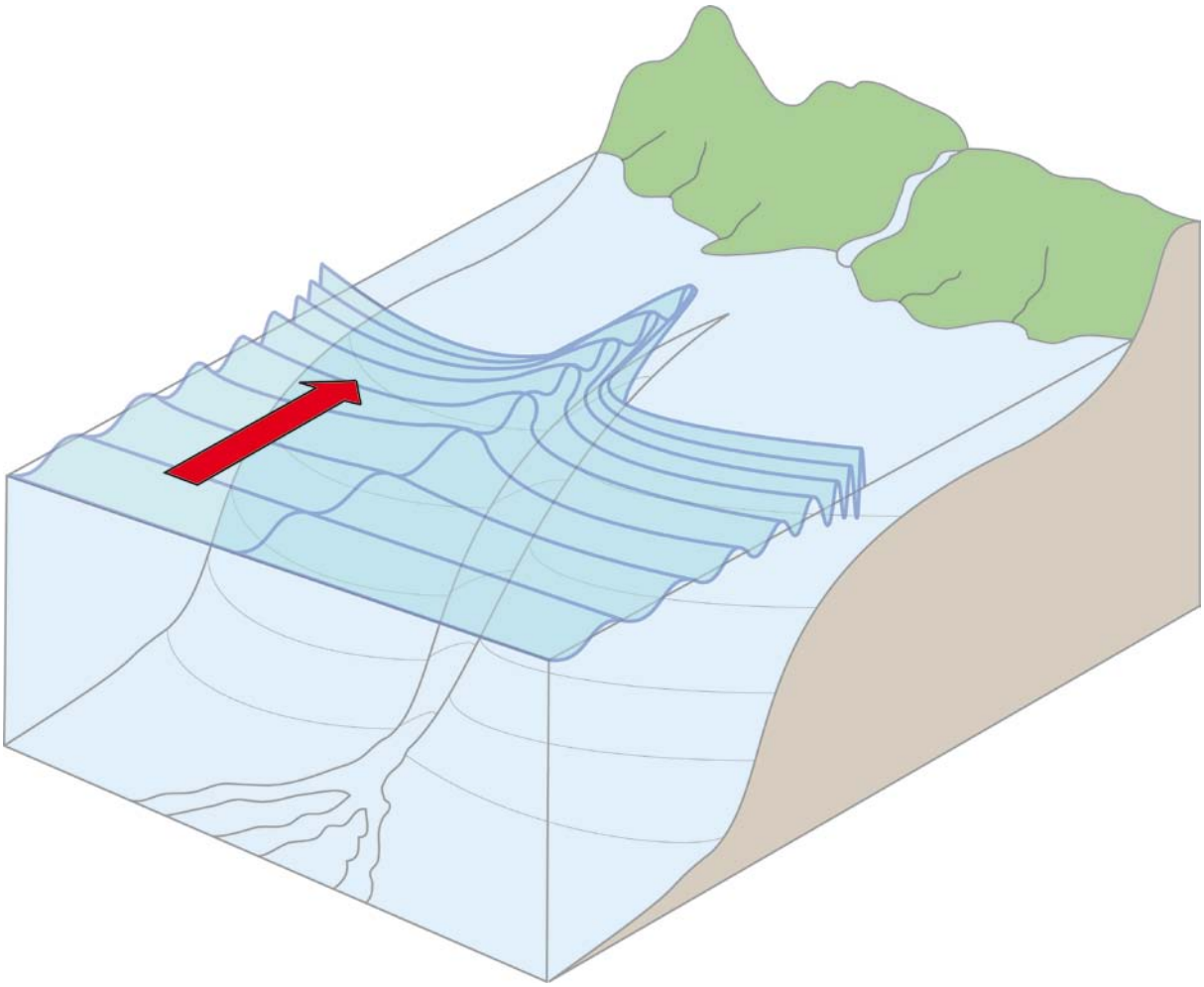

Figure 15 : Effet d'un canyon sous-marin sur la forme du tsunami; ralentissement et amplification des ondes beaucoup plus important sur les côtés du canyon. (La flèche indique le sens de propagation)

Satake (1988) met en évidence les mêmes phénomènes de ‘*wave trapping*’ ou ‘*wave focusing*’ pour les tsunamis trans-océaniques qui se voient focalisés et défocalisés par les grandes structures sous-marines (rides océaniques, plaines abyssales) de l’océan Pacifique.

Les barrières de corail peuvent jouer un rôle important quant à la propagation et l'impact d'un tsunami dans le sens où elles sont capable de retarder sa propagation (remontée de la bathymétrie induisant une diminution de la vitesse) et diminuer son amplitude (Baba et al., 2008). Il convient alors de les reproduire au mieux dans les grilles qui serviront aux simulations. A noter que Cochard et al. (2008) indiquent que, lorsque cette barrière de corail se trouve fragmentée, comme c'est le cas en Martinique, on aura alors une augmentation de la vitesse du tsunami (+ courants) dans les chenaux existants. Enfin, la présence d'une barrière de corail défini un bassin clos (lagon) qui peut réagir à l'arrivée des ondes longues si la période propre de ces vagues (période d'oscillations) est égale ou proche à la période propre du lagon ou d'une de ses harmoniques (Gourlay, 1996 ; Losada et al., 2008).

En accord avec la discussion sur les modèles numériques utilisés, et pour des raisons de temps de calcul, il sera possible d'utiliser des données bathymétriques dont la résolution croit à l'approche des côtes afin de reproduire au mieux les structures capables d'avoir une incidence majeure sur le comportement du tsunami.

Les données bathymétriques généralement utilisées proviennent de collections uniformisées de jeux de données telles que GEBCO[32] (IOC, IHO et BODC, 2003) ou SRTM30+[33] (Sandwell et Smith, 2009). Ces jeux de données sont fournis sous forme de grilles régulières. Les données GEBCO, publiées pour la première fois en 1905, sont maintenant disponibles avec une résolution de 30 secondes d'arc (~925 m à l'équateur), tout comme les données SRTM30+. A savoir que les données GEBCO proviennent principalement de campagnes de levés bathymétriques (par sondeurs multifaisceaux ou sonars latéraux bathymétriques par exemple) (Lurton, 2001) et de mesures gravimétriques par satellite (anomalie à l'air libre) qui permettent de déterminer la bathymétrie (Basu et Saxena, 1993). L'intérêt du couplage des deux méthodes permet d'une part d'améliorer la précision des données obtenues par méthode gravimétrique, dans les zones où des campagnes marines ont été réalisées, et d'autre part de pallier la limite d'exploitation des données gravimétriques près des côtes, dans des zones de variations rapides en temps et espace du niveau marin (zones littorales où les marées sont visibles), dans les zones de forte couverture sédimentaire et les zones avec des structures de type mont sous-marin montrant une compensation isostatique

[32] General Bathymetric Chart of the Oceans, http://www.gebco.net/

[33] Shuttle Radar Topography Mission, http://topex.ucsd.edu/marine_topo/mar_topo.html

importante, générant ainsi des incertitudes plus ou moins fortes (Vignudelli et al., 2005, 2008 ; Hwang et al., 2006 ; Lebedev et al., 2008). D'ailleurs dans ces zones de faibles profondeurs (lacs, côtes, plateau continental, etc.), c'est la méthode d'interférométrie sonar latérale qu'il convient d'utiliser (Llort-Pujol et al., 2009).

En fonction de l'étude réalisée, des données d'autres types pourront être ajoutées aux jeux de données précédents comme par exemple les données d'acquisition aéroportées LIDAR (Light Detection and Ranging) qui permettent de couvrir de vastes zones côtières en peu de temps (jusqu'à 50 km^2/h), ce qui représente un avantage dans des zones de fortes marées. De plus cette méthode technique permet de couvrir des zones aquatiques de faible profondeur (< 20 m) ce qui permet de compléter les données de sondage classiques. A noter que la fréquence du LIDAR topographique, n'utilisant pas les mêmes fréquences de signal et la même méthode de mesure, est 10 fois plus élevée que celle du LIDAR bathymétrique (Quadros et al., 2008). On peut également ajouter des données provenant de cartes marines (point de sondes, lignes de niveau) qui sont alors scannées, géoréférencées[34] et digitalisées. Elles sont essentiellement utilisées dans les ports ou les baies par exemple, afin de reproduire au mieux les structures portuaires ou encore la forme des récifs coralliens pour les études approfondies sur les phénomènes de résonance (Sahal et al., 2009 ; Roger et al., 2010a).

Pour les simulations de tsunami, la qualité des résultats dépendra donc fortement de la qualité des données bathymétriques. De la même façon, les données topographiques sont à prendre en considération prudemment dans l'interprétation des résultats de calcul d'inondation.

2.3.1.2 Données topographiques

Les données topographiques sont nécessaires pour les calculs d'inondation. Comme pour les données bathymétriques, la qualité des résultats de simulation d'inondation est directement reliée à la qualité des données topographiques. En effet, plus ces données seront précises et reproduiront au mieux le terrain considéré et plus l'inondation se rapprochera de la réalité (Yeh et al., 1994 ; Borrero et al., 2006), et plus l'évaluation de la distance maximum d'inondation et du *run-up* dans le cadre des études de risque seront crédibles.

[34] Géoréférencer des cartes ou toute sorte de données signifie positionner celles-ci dans un système de coodonnées géographiques connues (ex : World Geodetic System 1984) ou établir une relation entre elles et une projection géographiques donnée (une projection géographique, ou cartographique, est une transformation mathématique faisant correspondre un point de l'ellipsoïde géodésique à un point d'un plan ; par exemple, les projections Lambert sont des projections sur un cône tangent à l'ellipsoïde le long d'un parallèle origine).

Les données topographiques actuelles généralement utilisées sont les données SRTM[35] d'une résolution de 3s d'arc, soit environ 93 m à l'équateur et représentent une couverture quasi mondiale (entre 56° de latitude sud et 60° de latitude nord). Comme leur nom l'indique, elles ont été acquises via l'utilisation d'antennes radar doubles (interférométrie radar exactement) positionnées à bord de la navette spatiale en orbite autour de la Terre (Farr et al., 2007).

De la même façon que dans le cas des données bathymétrique, des données provenant de levés aériens LIDAR ou de la numérisation puis digitalisation de cartes topographiques peuvent être intégrées dans les modèles numériques de terrain (MNT ou '*Digital Elevation Model*') qui serviront ensuite aux simulations d'inondation.

2.3.1.3 Réalisation d'une grille

Etant donné le fait que cette étape représente une portion de temps non négligeable dans le processus de préparation des données et de modélisation numérique, il convient de la présenter un minimum dans le cadre de cette thèse.

La réalisation de la grille qui servira de support aux calculs de propagation de tsunami passe par la collecte de différents types de données (non obligatoires) présentées dans la Figure 16.

[35] Shuttle Radar Topography Mission, http://www2.jpl.nasa.gov/srtm/

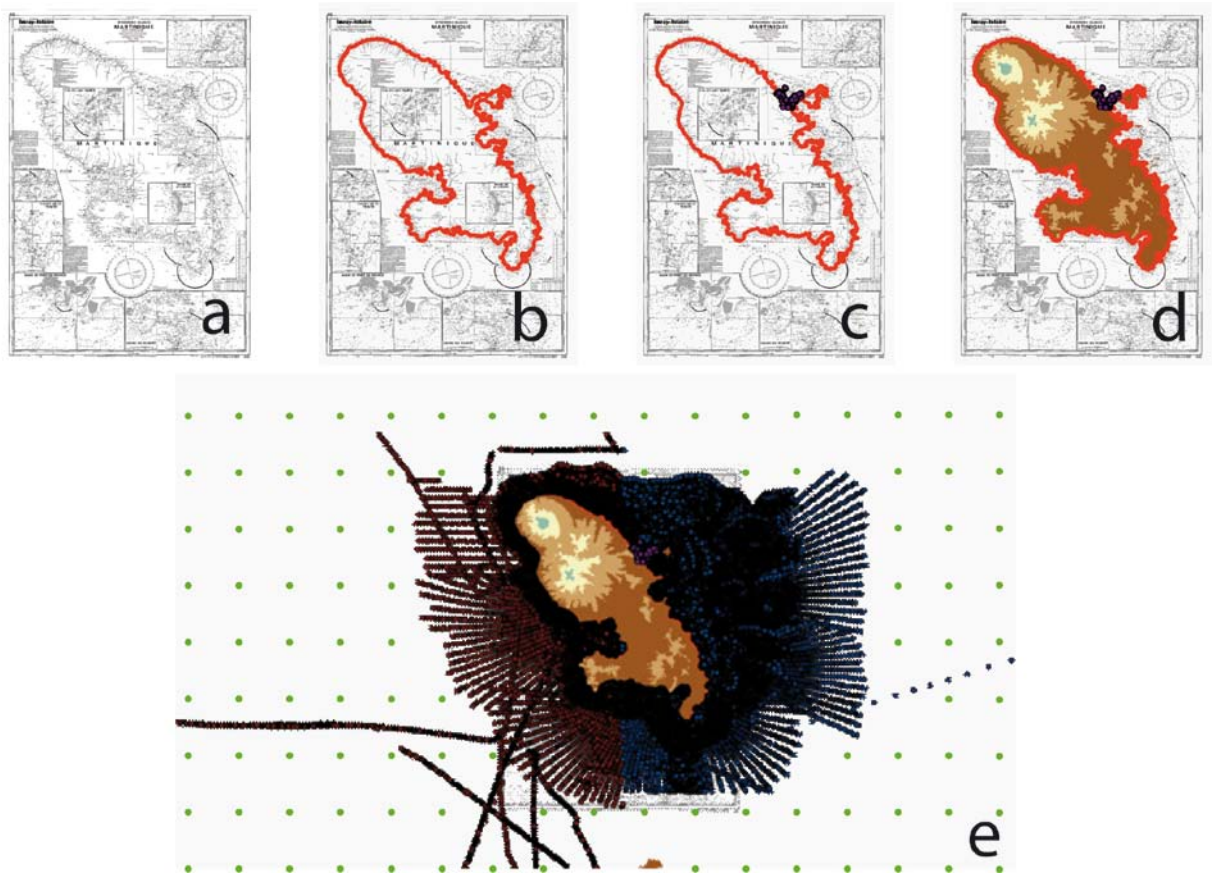

Figure 16 : Collecte des données bathymétriques/topographiques pour l'île de la Martinique: a) carte marine géoréférencée ; b) intégration du trait de côte ; c) digitalisation des zones d'intérêt ; d) insertion des données topographique de type SRTM ; c) insertion des données bathymétriques haute résolution et des données GEBCO (points verts).

Une fois que ces données sont toutes regroupées, il faut produire une grille uniforme en accord avec les besoins du modèle et de la résolution recherchée. Pour cela on utilise des méthodes d'interpolation ou d'extrapolation[36] afin de produire des grilles régulières, avec un pas de temps constant et sans trous. J'ai pu tester plusieurs méthodes de ce type au cours de ma thèse et j'ai retenu la méthode du krigeage pour ce type de jeu de données très irrégulier (zones de points très denses et zones de points très éparses). Gratton (2002) la définit comme étant la méthode optimale d'estimation de valeurs, aussi bien par interpolation qu'extrapolation, en se basant sur le principe que des objets rapprochés dans l'espace tendent à posséder des caractéristiques similaires (on parlera alors d'autocorrélation spatiale) ; c'est

[36] Méthodes mathématiques permettant de construire une courbe à partir de points existants au préalable. Dans notre cas, cette courbe permet alors de calculer les valeurs en des nœuds de grille inexistants. Plusieurs types d'interpolation/extrapolation existent : parmi eux, l'interpolation linéaire, polynomiale, par krigeage, par splines, etc.

donc une méthode locale, cette méthode ne regarde que les points voisins du point à définir. Elle permet en outre de calculer l'erreur d'estimation.

Une fois que les interpolations sont effectuées, nous avons à notre disposition une ou plusieurs grilles régulières (visible dans Roger et al. (2010b), partie 3.1.3 concernant cet exemple sur la Martinique), dont nous connaissons les paramètres (pas d'espace, nombre de points, etc.), utiles pour le bon fonctionnement des calculs.

Un document technique concernant la réalisation des grilles a été remis au **CEA** et est visible en **Annexe 3**.

2.3.2 Paramètres de faille

Dans le cadre de ma thèse, seuls les tsunamis générés par des séismes ont été modélisés. Nous ne nous attarderons donc pas sur les paramètres nécessaires à la modélisation des glissements de terrain sous-marins. En revanche, le lecteur intéressé par les mécanismes de génération de tsunami par glissement de terrain pourra se référer par exemple aux études de Ward (2001), Haugen et al. (2005) ou encore Harbitz et al. (2006). L'étude de Okal et Synolakis (2003) concerne quant à elle la comparaison theorique entre les tsunamis générés par des ruptures de type séisme et ceux induits par des glissements de terrain.

La rupture (co-)sismique (ou fracturation associée à un séisme) correspond à un relachement ou une chute des contraintes accumulées sur un plan de faille donné. En effet, sous le jeu de la tectonique des plaques, des rebonds post-glaciaires, des injections d'eau sous-pression dans les forages géothermiques, etc., le milieu dans lequel on se trouve (la roche) va être soumis à un certain nombre de contraintes. Dans un premier temps une déformation dîte élastique s'opérera, jusqu'à un certain point. Lorsque ce point, appelé seuil de contrainte (qui dépend de la résistance des roches) est franchi, il y a alors rupture, correspondant à une libération de l'énergie jusque là accumulée. Cette libération d'énergie se matérialise concrêtement par un mouvement relatif du mur et du toit de la faille. Elle est plus ou moins rapide et peut se faire sur un ou plusieurs segments de faille simultanément. Dans le cas du modèle utilisé pour réaliser mes travaux, nous considérons que la rupture est instantanée et uniforme.

La rupture en profondeur se traduit par une déformation du sol en surface dans la majeure partie des cas (sauf les séismes très profonds et les petites magnitudes). C'est cette déformation de surface qui va nous intéresser pour la modélisation des tsunamis puisque c'est

elle qui va entraîner une déformation de la colonne d'eau sus-jacente, générant ainsi un tsunami. Elle est modélisée via le modèle de dislocation d'Okada (1985) qui reproduit correctement les déplacements cosismiques observés (par exemple : Shen et al., 1996 ; Johanson et al., 2006 ; Tong et al., 2010). D'autres modèles permettant le calcul de la déformation comme ceux Mansinha et Smylie (1971) ou Dahlen (1971).

Ce modèle nous oblige à considérer un milieu (demi-espace) élastique, isotrope et homogène dans lequel la rupture s'exerce sur un plan de faille rectangulaire et dont les caractéristiques suivantes doivent être connues : position dans l'espace (longitude, latitude), longueur et largeur du plan de faille, profondeur de son centre, azimut de la projection en surface du haut du plan de faille, pendage du plan de faille. Les paramètres de rupture sont représentés par le glissement cosismique (en m) et l'angle de glissement sur le plan de faille. Ces paramètres géométriques sont reliés entre eux par des relations empiriques telles que celles présentées par Wells et Coppersmith (1994). Ils sont présentés sur la Figure 17. Une constante μ ($N.m^2$) correspondant à la rigidité du milieu considéré doit également être apportée dans le modèle ; elle sera principalement déterminée par des lois empiriques (Bilek et Lay, 1999 ; Geist et Bilek, 2001). Les déplacements ainsi calculés sont des fonctions non linéaires de ces paramètres (sauf longitude/latitude et glissement) et des fonctions linéaires du glissement cosismique.

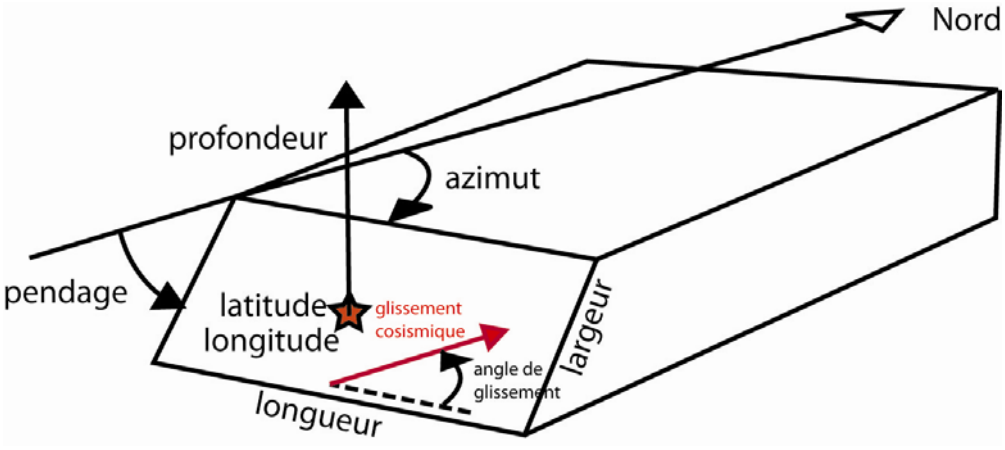

Figure 17 : Paramètres de rupture cosismique.

TRANSITION

Les travaux présentés par la suite représentent une mise en application de tout ce qui a été exposé précédemment, de la fouille d'archives à la réalisation d'un catalogue des tsunamis pour une région donnée, en passant par les recherches de dépôts sur le terrain, aux modélisations numériques permettant d'évaluer le risque tsunami pour des zones précises. Les zones étudiées dans le cadre de cette thèse constituent des sites tests pour le projet européen TRANSFER (Baléares, côte algérienne) et le projet national français MAREMOTI (impact du tsunami de 1755 en Atlantique, détroit de Calais). Je les ai classées par type d'étude et non par zone, proposant ainsi des cas de tsunami dont je n'ai étudié que l'impact, en acceptant une source préalablement déterminée par des études antérieures, et des cas pour lesquels je me suis avant tout penché sur la source afin de proposer des scénarios de rupture permettant d'expliquer des observations historiques ou des enregistrements marégraphiques. Les évènements étudiés se répartissent en deux groupes : ceux qui se sont produits en bassin fermé, à savoir la Méditerranée occidentale, et en bassin ouvert, à savoir l'Atlantique, avec l'unique cas du séisme et du tsunami de Lisbonne de 1755. Le cas du séisme du détroit de Calais de 1580 servira d'exemple à la démonstration de la difficulté de proposer des scénarios dans une zone de faible sismicité intraplaque.

TRANSITION

Les travaux présentés par la suite représentent une mise en application de tout ce qui a été exposé précédemment, de la fouille d'archives à la réalisation d'un catalogue des tsunamis pour une région donnée, en passant par les recherches de dépôts sur le terrain, aux modélisations numériques permettant d'évaluer le risque tsunami pour des zones précises. Les zones étudiées dans le cadre de cette thèse constituent des sites tests pour le projet européen TRANSFER (Baléares, côte algérienne) et le projet national français MAREMOTI (impact du tsunami de 1755 en Atlantique, détroit de Calais). Je les ai classées par type d'étude et non par zone, proposant ainsi des cas de tsunami dont je n'ai étudié que l'impact, en acceptant une source préalablement déterminée par des études antérieures, et des cas pour lesquels je me suis avant tout penché sur la source afin de proposer des scénarios de rupture permettant d'expliquer des observations historiques ou des enregistrements marégraphiques. Les évènements étudiés se répartissent en deux groupes : ceux qui se sont produits en bassin fermé, à savoir la Méditerranée occidentale, et en bassin ouvert, à savoir l'Atlantique, avec l'unique cas du séisme et du tsunami de Lisbonne de 1755. Le cas du séisme du détroit de Calais de 1580 servira d'exemple à la démonstration de la difficulté de proposer des scénarios dans une zone de faible sismicité intraplaque.

Partie 3

Etudes de cas

3) Etudes de cas

Au cours de cette thèse je me suis intéressé de près à plusieurs évènements historiques ayant principalement eu lieu en Méditerranée occidentale. Dans un premier temps, une partie de mon travail a consisté à tester des sources sismiques prédéfinies par des études antérieures afin de regarder l'adéquation des résultats de modélisation de tsunami (impact modélisé) avec les observations historiques (impact réel), avec pour objectif de valider ou non l'hypothèse de génération proposée et proposer des clés pour la réduction du risque tsunami dans les régions considérées.

Pour d'autres évènements, le travail a consisté à proposer des scénarios de rupture, en accord avec la géologie (déformation en surface, GPS, sismicité, mécanismes au foyer), et capables de reproduire les données historiques ou d'instrumentation (marégrammes).

3.1 Impact des tsunamis

La première étude concerne le tsunami de Zemmouri-Boumerdès de 2003 qui a été modélisé en utilisant plusieurs scénarios de rupture proposés dans la littérature afin de comparer l'impact sur les côtes françaises méditerranéennes, en terme de temps de trajet, de hauteurs de vagues et de phénomènes de résonance, avec les données récoltées sur le terrain par A. Sahal. Cette étude a fait l'objet du stage de Master 2 de B. Lemaire que j'ai supervisé avec H. Hébert. Titre du stage : *Modélisation du tsunami généré par le séisme de Zemmouri (Algérie) de 2003 et des effets de sites observés dans certains ports de la côte d'Azur.* Ayant obtenu de bons résultats, les travaux ont été approfondis et ont donné lieu à une publication :

3.1.1 Sahal, A., **Roger, J.**, Allgeyer, S., Lemaire, B., Hébert, H., Schindelé, F., Lavigne, F. (2009). ***The tsunami triggered by the 21 May 2003 Boumerdès-Zemmouri (Algeria) earthquake : field investigations on the Mediterranean coast and tsunami modeling***. Natural Hazards and Earth System Sciences, **9**, 1823-1834.

La deuxième étude concerne le tsunami de Lisbonne de 1755 dont les mécanismes de génération restent encore un mystère malgré les nombreuses études menées au cours des dernières décennies : afin de tenter de contraindre la source, j'ai testé différents scénarios de

génération de ce tsunami proposés jusque là (Baptista et al., 2003 ; Gutscher et al., 2006 ; Barkan et al., 2008) et regardé l'impact en champ lointain aux Antilles (Guadeloupe et Martinique, dans le cadre du projet MAREMOTI) et à Terre-Neuve (collaboration avec *Natural Resources Canada* et communication à l'International Tsunami Symposium, Toronto 2010), c'est-à-dire là où des documents historiques, préalablement archivés, indiquaient des arrivées de vagues de tsunami comparables avec les résultats des simulations numériques.

3.1.2 **Roger, J.**, Allgeyer, S., Hébert, H., Baptista, M.A., Loevenbruck, A., Schindelé, F. (2010). ***The 1755 Lisbon tsunami in Guadeloupe Archipelago : source sensitivity and investigation of resonance effects***. The Open Oceanography Journal, **4**, 58-70.

3.1.3 **Roger, J.**, Baptista, M.A., Sahal, A., Allgeyer, S., Hébert, H. (2010). ***The transoceanic 1755 Lisbon tsunami in the Martinique***. Pure and Applied Geophysics, Proceedings of the International Tsunami Symposium, Novosibirsk, Russia, July 2009, **168**(6-7), 1015-1031, doi: 10.1007/s00024-010-0216-8.

3.1.4 **Roger, J.**, Baptista, M.A., Mosher, D., Hébert, H., Sahal, A. (2010). ***Tsunami impact on Newfoundland, Canada, due to far-field generated tsunamis. Implications on hazard assessment***. Proceedings of the 9th U.S. National and 10th Canadian Conference on Earthquake Engineering, July 25-29, 2010, Toronto, Canada, n°1837.

La troisième étude concerne l'étude de dépôts de tsunami dans le golfe de Thermaikos (Thessaloniki, Grèce) et la validation par le biais de la modélisation numérique de la source proposée par Papanikolaou et Papanikolaou (2007) comme étant un candidat potentiel à l'origine du tsunami ayant apporté ces sédiments.

3.1.5 Reicherter, K., Papanikolaou, I., **Roger, J.**, Mathes-Schmidt, M., Papanikolaou, D., Rössler, S., Grützner, C., Stamatis, G. (2010). ***Holocene tsunamigenic sediments and tsunami modelling in the Thermaikos Gulf area (Northern Greece)***. Zeitschrift für Geomorphologie, **54**(3), 099-126.

Une étude supplémentaire a été menée en parallèle concernant la réalisation d'un catalogue des tsunamis en Martinique et une première étude de vulnérabilité face à cet aléa naturel. Ce catalogue a été réalisé par F. Accary sous ma responsabilité dans le cadre de son mémoire de Master 1.

3.1.6 Accary, F., **Roger, J.** (2010). ***Tsunami catalog and vulnerability of Martinique (Lesser Antilles, France)***. Science of Tsunami Hazards, **29**(3), 148-174.

Open Access

The 1755 Lisbon Tsunami in Guadeloupe Archipelago: Source Sensitivity and Investigation of Resonance Effects

J. Roger*[,1,2], S. Allgeyer[2,3], H. Hébert[2], M.A. Baptista[1], A. Loevenbruck[2], F. Schindelé[2]

[1]*Centro de Geofisica da Universidade de Lisboa, Rua Ernesto de Vasconcelos, Faculdade de Ciências Ed. C8, 6°, 1700 Lisboa, Portugal;* [2]*CEA, DAM, DIF, F-91297 Arpajon, France;* [3]*Ecole Normale Supérieure / Laboratoire de Géologie, 24, rue Lhomond, 75231 Paris CEDEX 5, France*

Abstract: On the 1st of November 1755, a major earthquake of estimated Mw=8.5/9.0 destroyed Lisbon (Portugal) and was felt in whole Western Europe. It generated a huge tsunami which reached coastlines from Morocco to Southwestern England with local run-up heights up to 15 m in some places as Cape St Vincent (Portugal). Important waves were reported in Madeira Islands and as far as in the West Indies where heights of 3 m and damages are reported. The present knowledge of the seismic source(s), presented by numerous studies, was not able to reproduce such wave heights on the other side of the Atlantic Ocean whatever the tested source. This could be due to the signal dispersion during the propagation or simply to the lack of simulations with high resolution grids. Here we present simulations using high resolution grids for Guadeloupe Archipelago for two different sources. Our results highlight important wave heights of the range of 1 m to more than 2 m whatever the source mechanism used, and whatever the strike angle in some particular coastal places.

A preliminary investigation of the resonance phenomenon in Guadeloupe is also presented. In fact, the studies of long wave impact in harbours as rissaga phenomenon in the Mediterranean Sea leads us to propose the hypothesis that the 1755 waves in the West Indies could have been amplified by resonance phenomenon.

Most of the places where amplification takes place are nowadays important touristic destinations.

Keywords: Tsunami, modelling of the wave propagation in Atlantics, 1755 Lisbon earthquake, Lesser Antilles, wave resonance. .

1. INTRODUCTION AND HISTORICAL SETTINGS

Strong magnitude tsunamis are relatively infrequent in the Atlantic Ocean. There are two different areas prone to tsunami generation: the western end of the Eurasia – Nubia (EN) plate boundary east of 19°W – in the North East Atlantic area and the Caribbean subduction zone in the West Central Atlantic area.

In this study we focus in the area corresponding to the western segment of the EN plate boundary east of 19ºW. This area is morphologically complex, characterized by seamounts (the Gorringe Bank, the Coral Patch and Ampère seamounts) that delimitate the abyssal plains: Horseshoe and Tagus (Fig. **1**). where discrete segments of plate boundary are hard to identify [1, 2]. The seismicity and the focal mechanisms computed for the main earthquakes do not solve clearly the problem of location of the interplate domain east of 19°W [3]. The focal mechanisms [4, 5] indicate right lateral and reverse faulting on roughly east - west oriented structures. This is usually interpreted as the result of the relatively low inter-plate motion (ca. 4 mm/y) given by kinematic plate models (e.g. [6-8]).

This slow convergence rate may be the explanation for the fact that strong tsunamis are infrequent events in this area. In fact large subduction zones with high convergence rates seem to be mainly responsible for the generation of huge tele-tsunamis [9].

However in the last 300 years there are several events reported with origin in the North Atlantic area. The most important submarine earthquakes are the events of the Gloria Fault-Azores (M 7.9, 1975.05.26), Horseshoe Abyssal Plain (M 7.9, 1969.02.28), Madeira-Azores (M 8.2, 1941.11.25), Grand Banks (M 7.2 + large submarine slump, 1929.11.18), North Atlantic-Azores (1761.03.31) and Lisbon (1755.11.1) [10], with variations of geodynamical context. Some of them are known to have generated an ocean-wide tsunami, principally the Lisbon event.

Another possible tsunami origin in the Atlantic ocean is the eventual collapse of volcanoes' flanks, like in the Canary Islands [11]. This could generate massive waves propagating towards the coasts despite the important dispersion phenomenon for such landslide's waves [12, 13].

The biggest event is represented by the 1st of November 1755 tsunami induced by a Mw=8.5/9.0 earthquake, commonly known as "Lisbon tsunami". In fact the earthquake was strongly felt in the Portuguese capital, Lisbon, where a lot of casualties and destructions have been reported. About 60 thousand people died during this catastrophic event [14]. Casualties and/or damages have been reported along the entire coast of Cadiz Gulf from Morocco [15] to Portugal, Spain, and even to England [16-18] (at mean 900 deaths due only to the tsunami in Lisbon according to [19]). The waves crossed the Atlantic Ocean, impacting Madeira and Azores

*Address correspondence to this author at the Ecole Normale Supérieure, Laboratoire de Géologie, UMR 8538, 24, rue Lhomond, bur. 359, 3ème étage, 75231 Paris CEDEX 5, France; E-mail: jeanrog@hotmail.fr

1874-2521/10 2010 Bentham Open

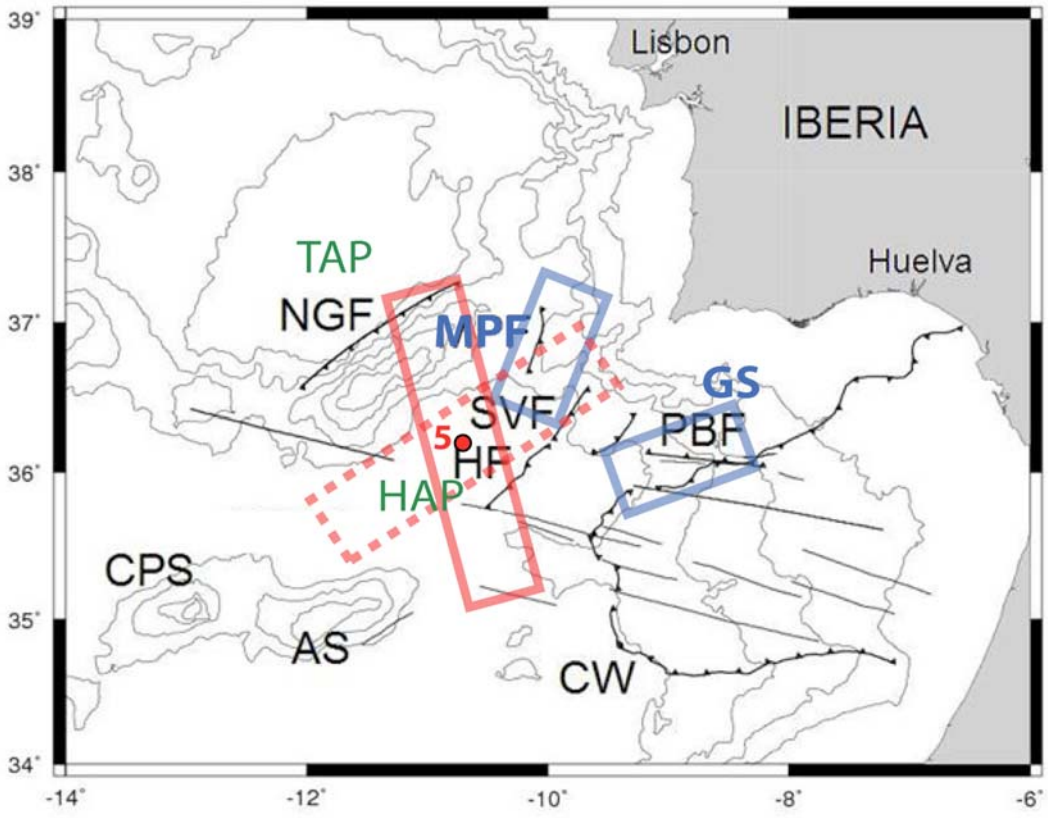

Fig. (1). Location of the tested sources associated to known faults over bathymetric map: [36]'s source n°5 in red solid rectangle and in dashed red for the strike variation of 57°; [42]'s combined source in blue rectangles. *CPS – Coral Patch seamount, AS – Ampere seamount; CW – Cadiz Wedge [40]; NGF - North Gorringe Fault; MPF - Marques de Pombal fault; HF- Horseshoe Fault; SVF - Sao Vicente fault; PBF – Portimao Bank Fault; TAP – Tagus Abyssal Plain; HAP – Horseshoe Abyssal Plain, adapted from* [3].

Archipelagos [20], and were reported possibly as far as Newfoundland coasts [21] and in the West Indies [21-26]. Further analysis of historical documents [27], geological investigations [28] and numerical modelling using backward ray tracing [29, 30] allowed to locate this submarine earthquake southwest of Cape St Vincent, South Portugal [31, 32]. In the last decade a significant effort was made in order to identify possible tsunamigenic sources in the area but until now the source of the 1755 event is still a matter of debate.

Different hypotheses have been proposed associated with different sources especially since the 28th February 1969 Horseshoe Abyssal Plain earthquake [33, 34]. Actually, one of the main problems is that none of these sources can be associated with tectonic structures (presented on Fig. **1**) long enough to account for a Mw 8.5 earthquake. Thus these are not able to explain the important wave arrival and run-up of several meters in different places all along the Atlantic shores and especially in the Caribbean area (Saba, Antigua, Dominica, Guadeloupe, Martinique, ...) mentioned in some historical reports [22-26] and field investigations by [35] as shown by [36]. In Guadeloupe, [35] indicate that the church in Ste Anne (located on Fig. **3**) was hit by the tsunami of 1755. An historical description of the phenomenon in Guadeloupe Island has been collected by [37]: " *Only, on November 1st, a very curious fact occurred and arrived to us by the tradition. On several points of the coast, there was a considerable withdrawal of the sea. At Saint-Anne, it withdrew up to the line of the cayes*[1] *which wrap the natural harbour, by leaving only two passages, and coming back with violence, invaded the earth. In the village, then considerable, of this municipality, the waves came and broke against the porch of the church. This curious phenomenon occurred throughout the Antilles, and it is so described in Ephemerides, noted day by day by an inhabitant of Sainte-Marie's parish (Martinique).*" (this text has been translated from the French original version [37]).

The line of the cayes corresponds to the coral reef barrier that enclosed Sainte-Anne's Bay. It is located about 600 m from the shoreline at its maximum distance. The maximum water depth in the so-formed lagoon is about 3 m. It reaches 6 m depth in the two mentioned passages in [37].

Recent field work, including topography measurements from the shoreline up to the aforementioned church (Fig. **5**) located it at a distance of 220 m in land, with a minimum elevation of the bottom of the church's main door of 3,2 m (Titov, 2008, pers. comm.). We consider that the shape of the bay and the elevation of the church with regard to the sea level 250 years ago have probably not changed significantly since 1755.

Two hypotheses could be proposed in order to explain that none of the proposed sources were able to generate important wave heights in the Antilles: the first concerns the

[1] Caye : French word signifying small rocky islet often composed by sand and/or coral

Table 1. The Fault Parameters from Source n°5 (a) from [36], and Marques de Pombal (MPTF) – Guadalquivir Segement (GS) Combined Source (b) from [42]

Source		Lon(°)	Lat(°)	Depth of Centre of Fault Plane	Average Slip (m)	Strile(°)	Dip (°)	Rake/slip Angle (°)	Length (km)	Width (km)	Rigidity (N.m²)
a) Barkanetal (2008)		-10.753	36.042	30.7	13.1	345	40	90	200	80	45.10
b) Baptista et al (2003)	**GS**	-8.7	36.1	20.5	20	250	45	90	105	55	30.10
	MPTF	-10	36.8	20.5	20	21.7	24	90	96	55	30.10

fact that trans-oceanic dispersion phenomenon could play a role in such far-field propagation of earthquake generated tsunamis [38] but much less than in the case of landslide generated tsunamis [39], if propagation numerical models take into account this dispersion. The second and more convincing hypothesis is based on the lack of high resolution data used in modellings when approaching the coasts. Thus, these data reproduce more accurately the underwater structures and the shape of the coasts, and allow to properly account for the non linear coastal amplification of tsunamis.

The objective of this study is not to discuss the previously proposed seismic sources [28, 32, 36, 40-42]; the goal is to investigate wave amplification phenomena in the Guadeloupe shield using high resolution datasets, underlining the probable important character of resonance phenomenon in the West Indies in harbours and in water bodies formed by coral reef barriers [43, 44]. We focus our study on Guadeloupe Island and more particularly on the previously mentioned bay of Ste Anne.

2. BATHYMETRIC GRIDS AND NUMERICAL MODELLING OF TSUNAMI GENERATION AND PROPAGATION.

The numerical model used in this study to compute tsunami generation and propagation associated with earthquake has been used for years in order to study tsunami hazard for various exposed regions, from French Polynesia [45] to the Mediterranean Sea [46-49].

The initial deformation calculus is based on elastic dislocation computed through Okada's formula [50]. Our method considers that the sea-bottom deformation is transmitted without losses to the entire water column, and solves the hydrodynamical equations of continuity (1) and momentum (2). Non linear terms are taken into account, and the resolution is carried out using a Crank Nicolson finite difference method centred in time and using an upwind scheme in space.

$$\frac{\partial(\eta + h)}{\partial t} + \nabla.[v(\eta + h)] = 0 \quad (1)$$

$$\frac{\partial v}{\partial t} + (v.\nabla).v = -g\nabla\eta \quad (2)$$

η corresponds to the water elevation; h to the water depth; v to the horizontal velocity vector; g to the gravity acceleration.

The wave propagation is calculated from the epicenter area in the Cadiz Gulf (Southern Portugal and Spain to the East) through the Atlantic Ocean (Fig. **2**) on 5 levels of imbricated grids of increasing resolution as approaching Guadeloupe Archipelago with a special focus on Ste Anne's Bay. The larger grid (0), corresponding to the geographical coordinates of Fig. (**2**), is built from GEBCO World Bathymetric Grid 1' [51] and is just a resampling of this grid at a space step of 5'. The grid resolution increases close to the studied site i.e. when the water depth h decreases along with the tsunami propagation celerity $c = \sqrt{gh}$ that depends only on h in shallow water non dispersive assumption. The time step used to solve the equations decreases when the grid step decreases, and respects for each grid level the CFL (Courant-Friedrichs-Lewy) criterion to ensure the numerical stability.

The grid (1) is a focus on Guadeloupe Archipelago with a resolution of 1'. It has been obtained by a combination of GEBCO 1' data and high resolution multi-beam, resampled bathymetric data from the French Hydrographic Service (SHOM). This grid has been included only for numerical stability reasons. The grid (2) has nearly the same geographical coordinates of grid (1) (Fig. **3**), including the whole Guadeloupe Archipelago with a spatial resolution of 500 m. The data used are the same as for grid (1).

The grid (3) represents a focus on Point-à-Pitre's Bay with a spatial resolution of 150 m and has been computed using re-sampled SHOM dataset only.

High resolution grid of Sainte-Anne's Bay, which is set up for the final grid level, is obtained from digitized, georeferenced and interpolated nautical bathymetric charts and multi-beam bathymetric data from the French Hydrographic Service (SHOM). This grid (4) has a resolution of 40 m and it is able to reproduce the coral reef barrier partially closing the bay and the shallow bathymetric features which could have a significant influence on wave trapping and amplification, potentially associated with resonance phenomenon.

Another grid of Ste Anne's Bay with a resolution of 10 m was computed in order to test these resonance effects. This grid (5) has not been included in the propagation calculations.

3. TESTED SOURCES

Several sources have been tested from the literature [28, 32, 36, 41, 42], and we decided to present the two sources that best fit the West Indies historical observations.

The first one is the source (n°5) with optimized parameters from [36]. In spite of the fact that this source is not very well constrained through morphological analysis (Fig. **1**) this is the first simulation that shows significant amplification in the West Indies, on a low resolution grid (ETOPO2, 2' resolution).

The second tested source concerns the Marques de Pombal – Guadalquivir combined source from [42]. Despite the fact that the proposed coseismic slip might to be too large regarding the geodynamical conditions (especially the plates convergence rate), this source has the advantage to be based on proved geological submarine features [28] visible on Fig. (**1**).

Concerning the first case, the used parameters are issued by [36]. They are presented in Table **1** and are consistent with a Mw=8.5±0.3 earthquake commonly accepted for this event [52] and associated with a seismic moment $5 < Mo < 10.10^{21}$ N.m. As the shear modulus μ indicated by [36] seems to be too large for this region (they use $\mu \sim 60.10^9$ N.m² associated with a seismic moment (Mo) of $1.26\ 10^{22}$ N.m), we decided to test $\mu = 30.10^9$ N.m²,value commonly used in this region, and $\mu = 45.10^9$ N.m², more currently used in compression zone in oceanic lithosphere context. This rigidity parameter (or shear modulus) is estimated from previous studies of [53] and [54], in accordance with relationships between all faults parameters presented by [55] and relevant with a compressionnal mechanism in this area. The lowest value gives a Mw=8.5 earthquake and the second one a Mw=8.6 earthquake. Then we test a variation of the strike angle for this source, all other parameters remaining equal; the two different azimuths are presented on Fig. (**1**).

The second tested source has been proposed by [28] and [42] as previously mentioned and corresponds to a Mw=8.5 earthquake ($Mo=6.63\ 10^{21}$ N.m). It is a combination of two fault segments located offshore Southern Portugal and Iberia: the Marques de Pombal Thrust Fault (MPTF) and the Guadalquivir Segment (GS). They are located on Fig. (**1**) and their parameters are described in Table **1**.

4. RESULTS OF MODELLING

The presented results are obtained after 9 hours of tsunami propagation in the Atlantic Ocean. The first wave reached the easternmost island of Guadeloupe Archipelago circa 7 hours (propagation) after the earthquake (synthetic gage 6 on Fig. **6**) which is in agreement with tsunami travel time indicated in historical reports presented in [56] or in [57].

The results of calculations with two different values for the shear modulus in the case of [36]'s source indicate no differences of far-field wave amplification between these two cases, all other parameter remaining equal. Thus we do not discuss more about the choice of this parameter in this study.

Fig. (**2a**) represents the maximum wave heights obtained on grid (0) (North-Atlantic Ocean) after 9 hours of tsunami propagation using the source n°5 from [36]. Maximum wave heights reached nearly 5 m above the rupture area. The results show that the tsunami energy is not radiated uniformly but seems to follow two major wave paths: the first one towards the Azores Islands and Northern America, especially Newfoundland. The second one oriented toward Southern America (French Guyana, Surinam) and the West Indies. [58] and [59] show that these paths are due firstly to the tsunami initial directivity associated to the fault azimuth and then to the refraction of tsunami waves in shallow regions as

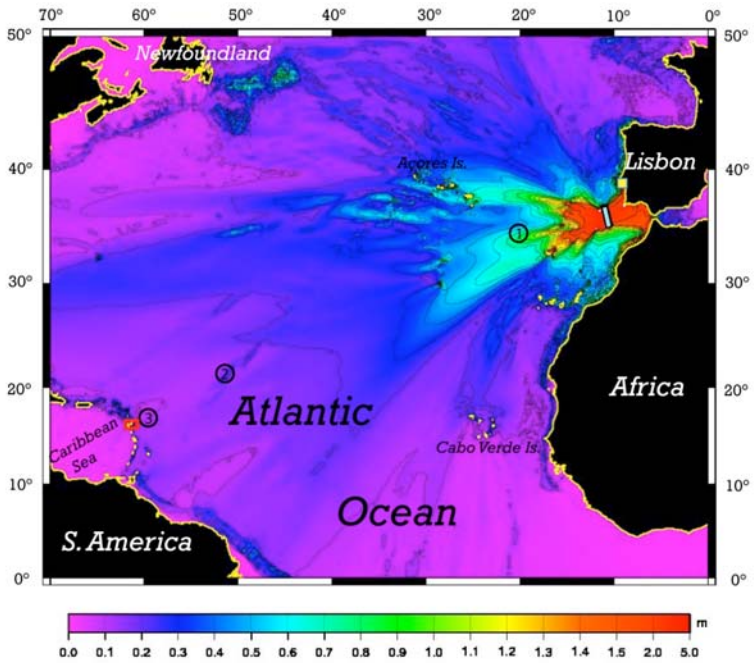

Fig. (2a). Maximum wave heights cumulated on 9 hours after the seismic rupture southwestern Lisbon and calculated on a 5' resolution grid (grid 0). The black and blue rectangle indicates [36]'s source n°5 and the red rectangle shows the location of grid (2). Numbers indicate synthetic tide gages location.

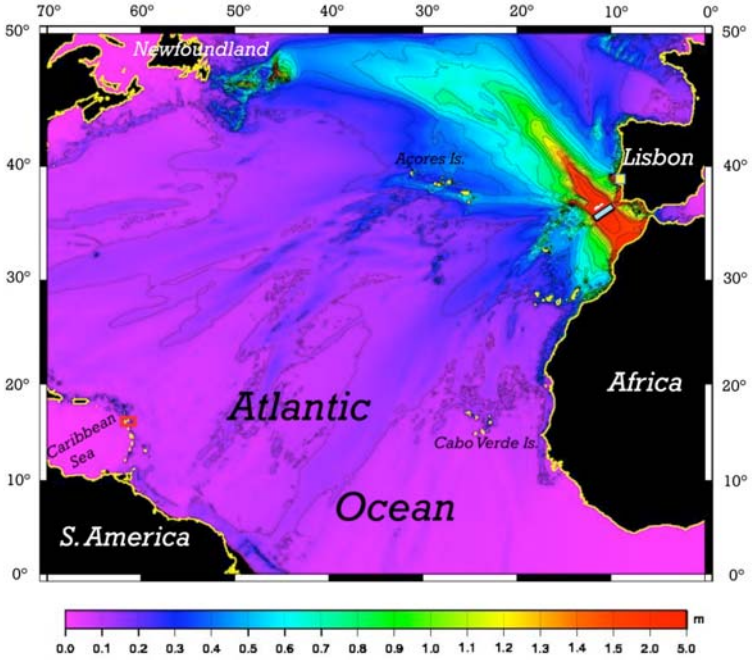

Fig. (2b). Maximum wave heights cumulated on 9 hours after the seismic rupture southwestern Lisbon and calculated on a 5' resolution grid (grid 0). The black and blue rectangle indicates [36]'s source n°5 with strike 57° and the red rectangle shows the location of grid (2).

mid-ocean ridges leading to a focusing and defocusing of these waves. Mid-ocean ridges and continental shelves can act as topographic waveguides which is known as trapping effect [58].

Fig. (**2b**) displays the maximum wave heights obtained on grid (0) (North-Atlantic Ocean) after 9 hours of tsunami propagation using the source n°5 from [36] with a modified strike angle of 57° instead of 345° for the previous test. This angle corresponds to the estimated strike of the Gorringe Bank (NGF in Fig. **1**). In this configuration, the major part of wave energy is radiated in a NW-SE direction toward Greenland and Newfoundland to the North-West and Morocco to the South-East.

Fig. (**2c**) represents the maximum wave heights obtained on grid (0) (North-Atlantic Ocean) after 9 hours of tsunami propagation using the combined source from [42]. The wave

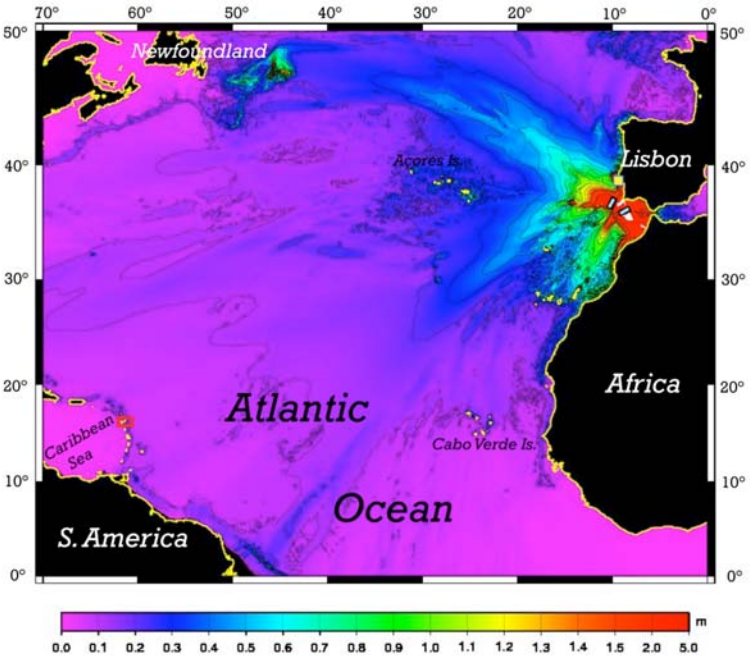

Fig. (2c). Maximum wave heights cumulated on 9 hours after the seismic rupture southwestern Lisbon and calculated on a 5' resolution grid (grid 0). The black and blue rectangles indicates [42]'s composed source.

energy is radiated mostly toward Greenland and Newfoundland to the North-West, Morocco and Canaries Islands to the South and toward Southern America to the South-West.

Fig. (**3a-3b-3c**) shows the maximum wave heights in Guadeloupe Archipelago always after 9 hours of propagation onto grid (2) in each of the 3 previously presented cases. The imbrication time between each grid has been cautiously estimated in order to be sure to catch the first sea surface deformation in the underneath grid. It reveals that wave amplification is not constantly distributed along the coastlines of the different islands. Only several locations are subject to wave heights of more than 0.5 m until 2.2 m. These locations are the same for each tested sources in the framework of that study with more or less amplifications, highlighting the local amplification processes only related to local bathymetry and coast locations. It is interesting to notice that these are the same places considering wind-generated waves amplification; for example: Sainte-Anne, Saint-François, Le Moule, Anse-Bertrand (located on Fig. **3a**, **3b** and **3c**) for Grande-Terre are good places for wave amplification due to local

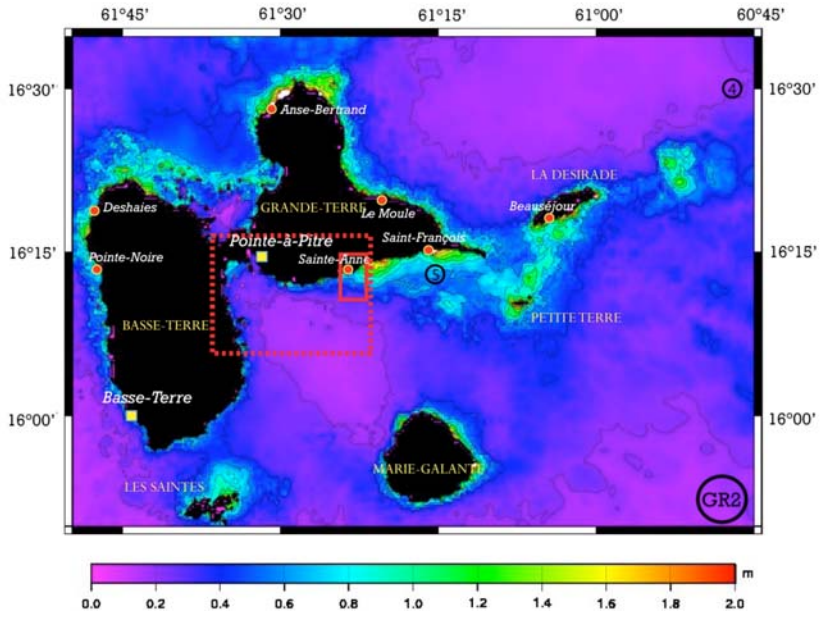

Fig. (3a). Maximum wave heights on Guadeloupe Archipelago (grid 2) using [36]'s source n°5. The red dashed rectangle indicates the location of grid (3) (150 m) and the red solid rectangle the location of grid (4) (40 m resolution) on Ste Anne's Bay (Fig. 4). Numbers indicate synthetic tide gages location.

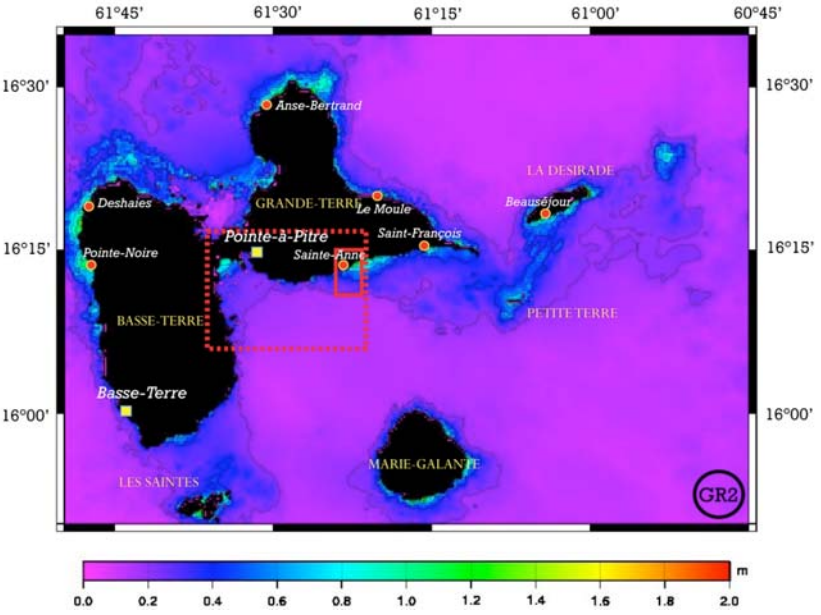

Fig. (3b). Maximum wave heights on Guadeloupe Archipelago (grid 2) using [36]'s source n°5 with strike 57°

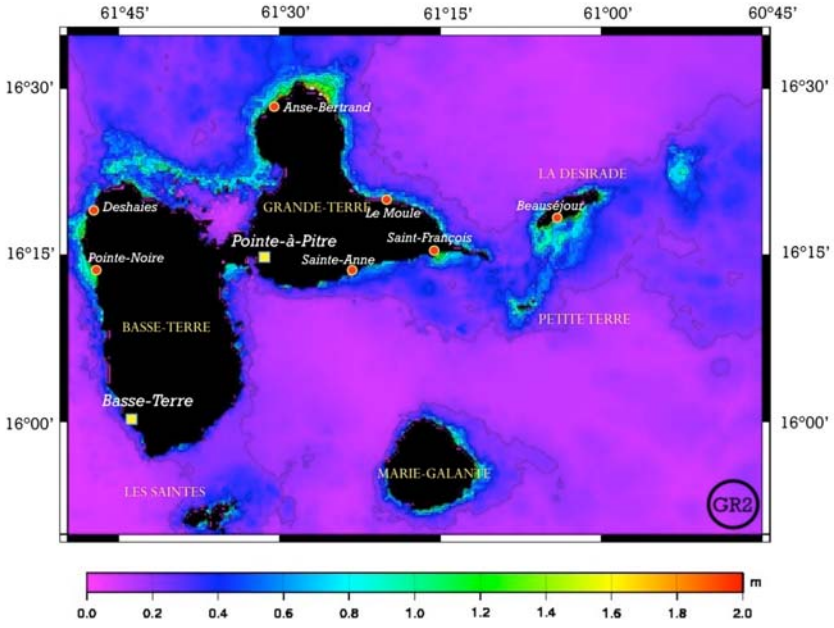

Fig. (3c). Maximum wave heights on Guadeloupe Archipelago (grid 2) using [42]'s source.

bathymetry with very low slope. A focus on these special areas shows that the characteristic wavelengths are approximately the same order of those of the bays where there is important wave amplification.

Other locations are highlighted on the other islands of the archipelago as on La Désirade or Les Saintes. There are some wave amplification on Petite-Terre Islands: despite these places are uninhabited, the fact that it is a game reserve, frequented daily by tens of tourists, forces us to consider these islands in hazard studies, mainly due to their poor elevation (peak at 8 m).

Fig. (**4**) shows a focus on maximum wave heights calculated in Point-à-Pitre's Bay and nearby areas (grid 3). It allows to see if wave amplifications are located near populated areas [60] as Le Gosier, Saint-Anne, Goyave, etc. Thus, there are some wave heights of more than 1 m in Saint-Anne's Bay and in the lagoon between Le Gosier and its little island called "îlet du Gosier", places which are highly

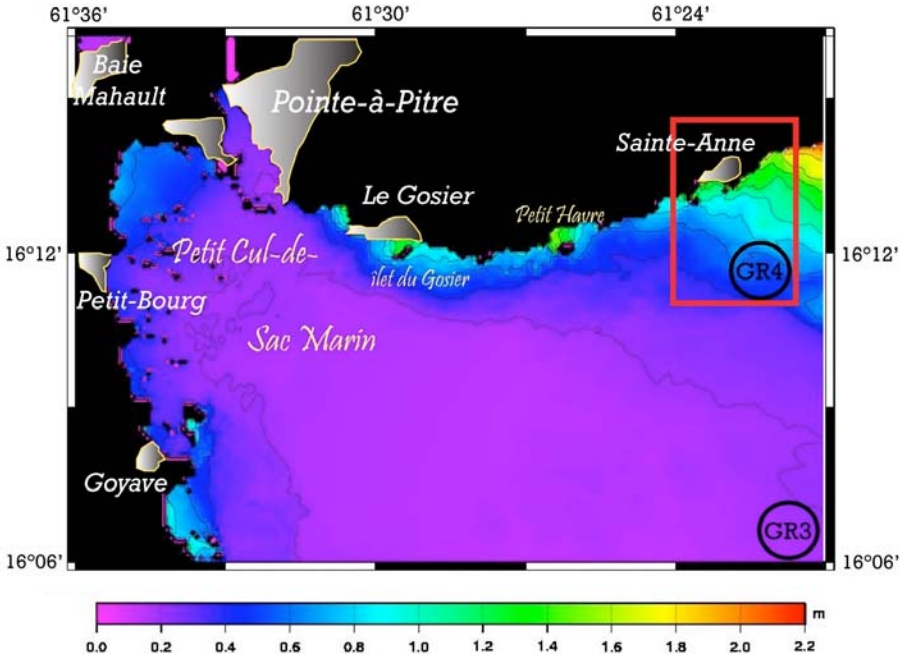

Fig. (4). Maximum wave heights on grid (3) using [36]'s source n°5. Populated areas are reported in grey; the red rectangle indicates location of grid (4).

frequented because of their famous white sand's beaches. There are significant heights in the "Petit Havre" lagoon between Le Gosier and Sainte-Anne, located outside urbanized areas but as commonly frequented by tourists, divers and surfers.

Fig. (**5**) shows a zoom on maximum wave heights calculated in Sainte-Anne's Bay (Grande-Terre) and nearby areas (grid 4). The calculation results cumulated on 9 hours have been associated with a satellite view [61] in order to have an idea of the potentially endangered coastal areas in the case of such a scenario. The maximum wave height recorded in this bay are usually not greater than 1.2 m. Belley's Bay, next bay to the East, shows wave heights reaching more than 2 m.

5. DISCUSSION

Fig. (**6**) shows the tsunami signal recorded on several synthetic tide gages located on its way from the Iberian Peninsula to the bay of Sainte-Anne, Guadeloupe. Firstly we can see that the signal (especially the first tsunami wavelength) is attenuated when crossing the Atlantic Ocean from tide gage 1, located near the rupture area, to gage 2 and then gage 3, near the Caribbean Sea, in what concerns grid (0) (synthetic tide gages 1, 2 and 3 are located on Fig. **2a**). As expected, the signal is the same between gage 3 and gage 4 (located on Fig. **3a**) because they are located in the same area on two different grids. Then it is interesting to mention an amplification of the signal as approaching the coastline (shoaling effect) and the progressive appearance of what seems to be a long-period oscillation with a period of about 15 minutes, about 30 minutes after the first arrival. This could be attributed to a resonance phenomenon due to the interaction of the long waves with the Guadeloupian shelf as shown by [62].

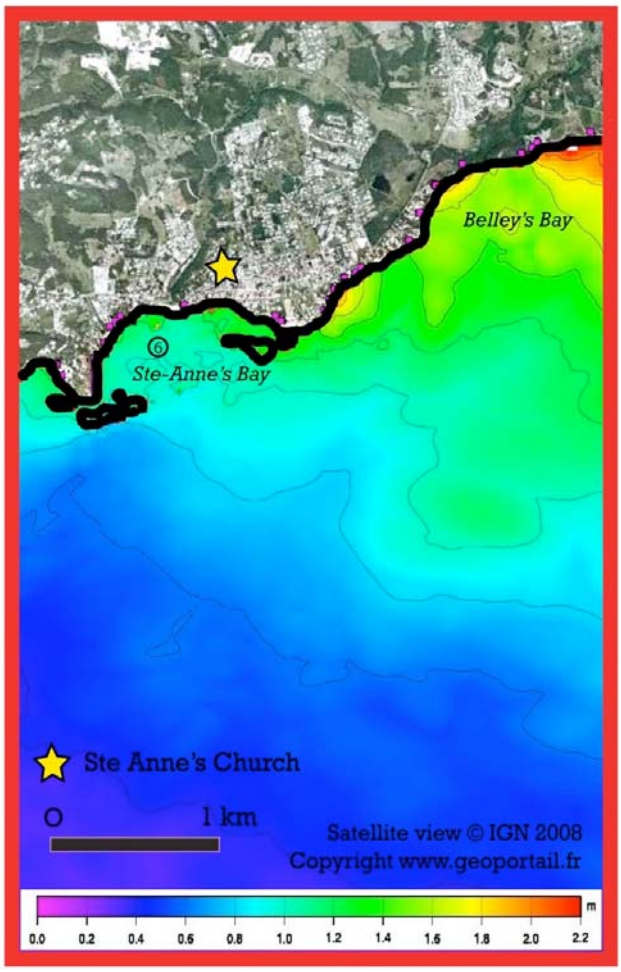

Fig. (5). Maximum wave heights on grid (4) using [36]'s source n°5. A satellite view is superimposed on it. The number in Saint-Anne's Bay indicates the synthetic tide gage (6) location.

According to the fact that every water body (including man-made harbors or bays) has a natural oscillation mode with eigenperiod depending on physical characteristics of the water body [63] i.e. its geometry and depth [64, 65], we calculate the resonance of the Saint-Anne's Bay using a method inspired from [66]. This study proposes the use of spectral analysis with an FFT algorithm from the evolution of an arbitrary initial surface (we use a Gaussian surface) at some gage points. One of the spectrum that we obtained is represented on Fig. (**7**). We can see several resonance periods which correspond to the natural eigenperiods of the bay. The largest is approximately at 890 seconds, while the others at 400, 305, 213, … seconds.

When we assume that the considered bay can be assimilated to an elongated channel of 1300 m length (longitudinal cross section) and 4 m depth, e.g. with a parabolic shape, we can use a simple analytic model [67] which predicts that the highest period is $T = \frac{2l}{\sqrt{gh}}$ (internal resonance of the bay). This corresponds in our case, to a period of 400 seconds. The first period, very large and also dissipative (890 s), can be explained with the non-closed structure of the bay. The period analysis of the synthetic signal recorded on gage 1 (grid 0), i.e. near the source, shows that in both cases of tested source [36, 42], we can observed period peaks at the resonance periods of the bay (Fig. **8A** and **8B**). These peaks are observed on the period spectrum of the signal of the synthetic tide gage located within the bay (Fig. **9A** and **9B**). A focus on the small periods range (< 500 s) shows that the signal coming from [42]'s source is more enclined to react at the resonance period of the bay (Fig. **9B**) than the one generated by [36]'s source.

CONCLUSION

Despite the lack of reported information concerning the tsunami arrival in 1755 in Guadeloupe Archipelago, numerical modelling indicates that these islands are not protected from an ocean-wide tsunami generated by a 1755-like earthquake offshore the Iberian Peninsula even if the rupture mechanism is not favourable. Indeed the fault's strike angle of these sources does not allow for major wave propagation towards the West Indies, as shown with the Gorringe Bank's strike angle attributed to [36]'s source. However, the sensitivity study of the strike of [36]'s source shows that the strike 345° has an important role on wave coastal amplification.

Thus, this study clearly shows that a seismic source [36, 42] located in the eastern part of North Atlantic Ocean is

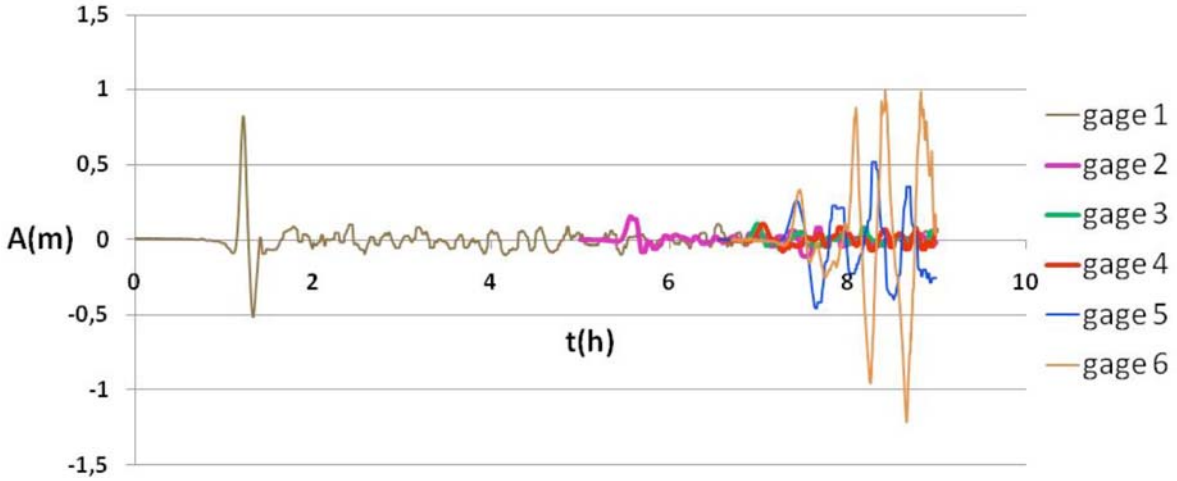

Fig. (6). Signal recorded on synthetic tide gages located on three different grids from the source area to the bay of Sainte-Anne (Guadeloupe). The position of each tide gages are reported on Fig. 2, 3 and 5.

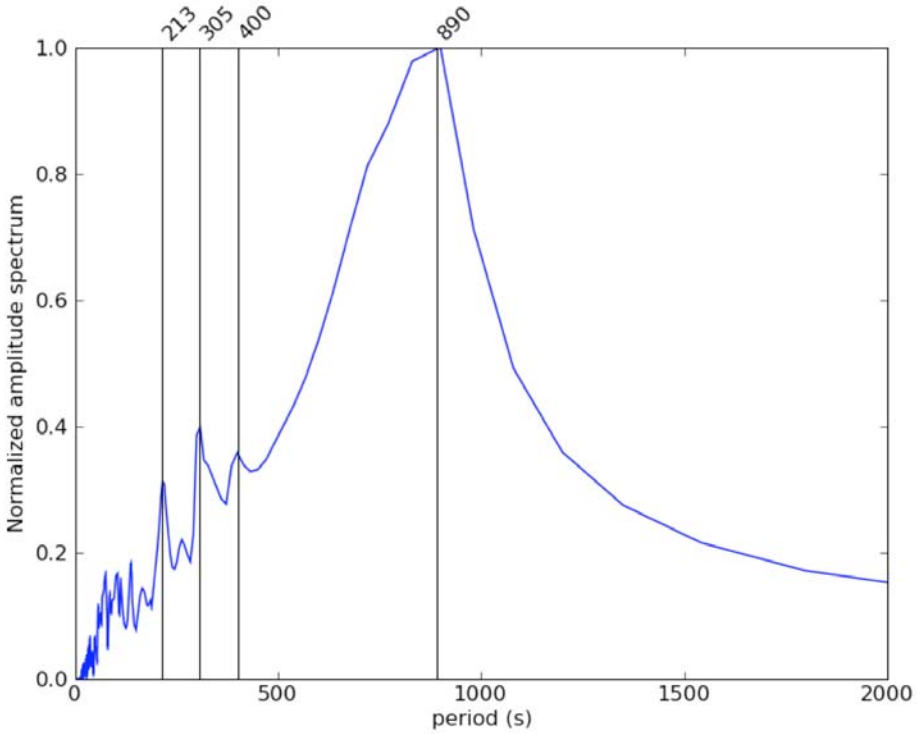

Fig. (7). Normalized amplitude spectrum of the bay of Saint-Anne.

able to produce important wave heights of more than 1 m in the Guadeloupian Archipelago, especially in some well-shaped bays or lagoon, whatever the rupture fault strike angle. But, the tested source from [36], with a well-oriented strike, leads to a major energy path towards the West Indies, producing wave heights of more than 2 m. This corresponds to wave amplification of a factor 20 in the case of [36]'s source. In the same way, [42]'s source leads to a wave amplification from 0.1 m offshore the island to more than 1 m in some particular coastal locations i.e. a factor 10. These observations are in good agreement with [68].

The second important thing that this study highlights, is that the Guadeloupian shelf seems to react to long-wave arrivals, leading to a low-frequency oscillation. The resonance study of such places allows to determine which particular range of period is able to amplify when entering these water bodies.

In summary, we conclude that it is not necessary to have a source radiating maximum wave energy towards the Caribbean Islands to produce significant waves in this area. This study does not allow for a distinction between proposed source mechanisms for the 1755 event, i.e. which source

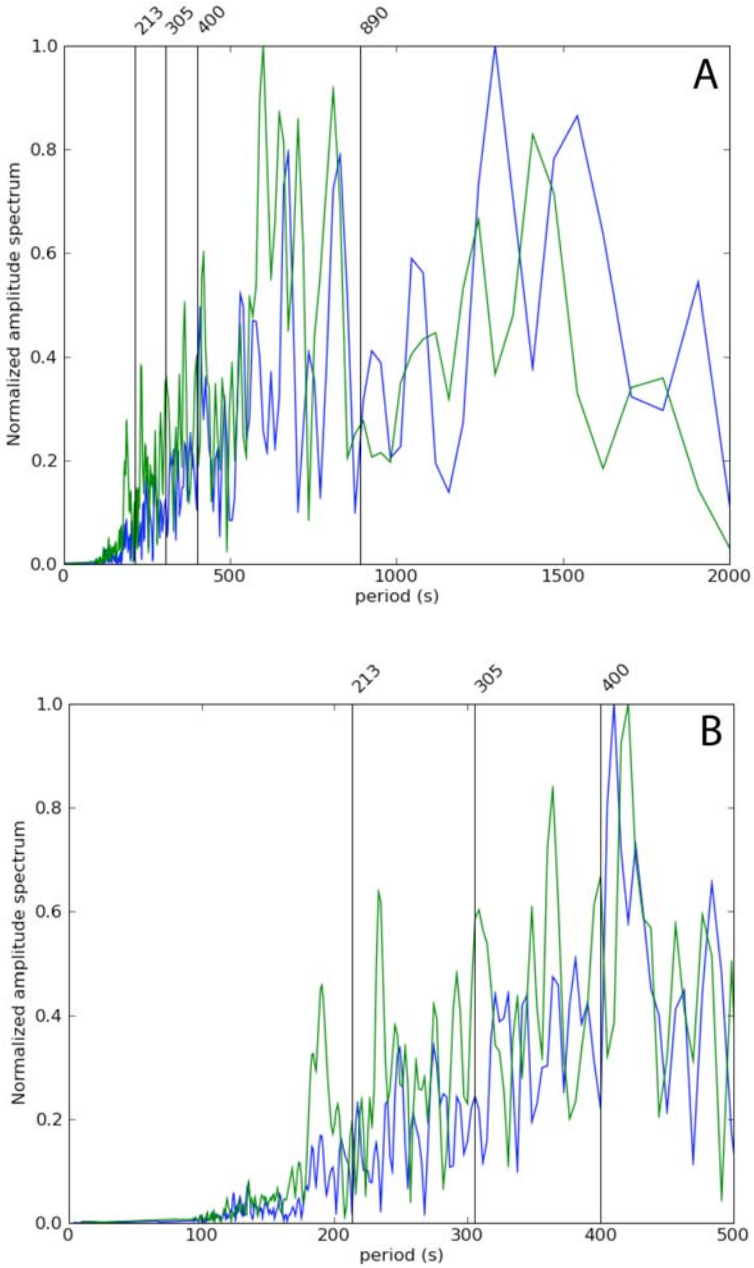

Fig. (8). Normalized amplitude spectrum of the synthetic signal computed near the source (grid 0, gage 1) in both tested cases [36, 42]; **A**) the full period spectrum, **B**) focus on low period modes. [36]'s source is represented in blue and [42]'s source is represented in green.

location and parameters gives the best match between simulations and observations. It clearly shows that different proposed sources for a 1755-like event produce significant amplifications in the Caribbean Islands as reported in historical documentations.

The important increase of coastal population and infrastructures since 1755, especially in the Caribbean Islands due to intensively developing tourism, coupled with the results presented in this study clearly show the importance of the implementation of a tsunami warning system in the Atlantic that can account for tele-tsunamis. Thus other far-field events as the 1761 tsunami should be considered further. All the more as, in such case of far field tsunamis, people do not locally feel the earthquake as a warning sign.

Future work on far-field impact should focus on Martinique Island (French territory), 150 km south to Guadeloupe, and/or other locations on the Western coasts of the Atlantic Ocean, in order to try to correlate November 1755 historical reports and numerical modelling results.

ACKNOWLEDGEMENTS

We would like to thank the SHOM (France) for providing us the high resolution bathymetric dataset for Guadeloupe; Eric Thauvin (CEA-DASE) for is precious help concerning grids making; Prof. Narcisse Zahibo for his invitation to the workshop "Caribbean Waves 1" and his availability for the field survey at Sainte Anne's; Dr Paul Louis Blanc

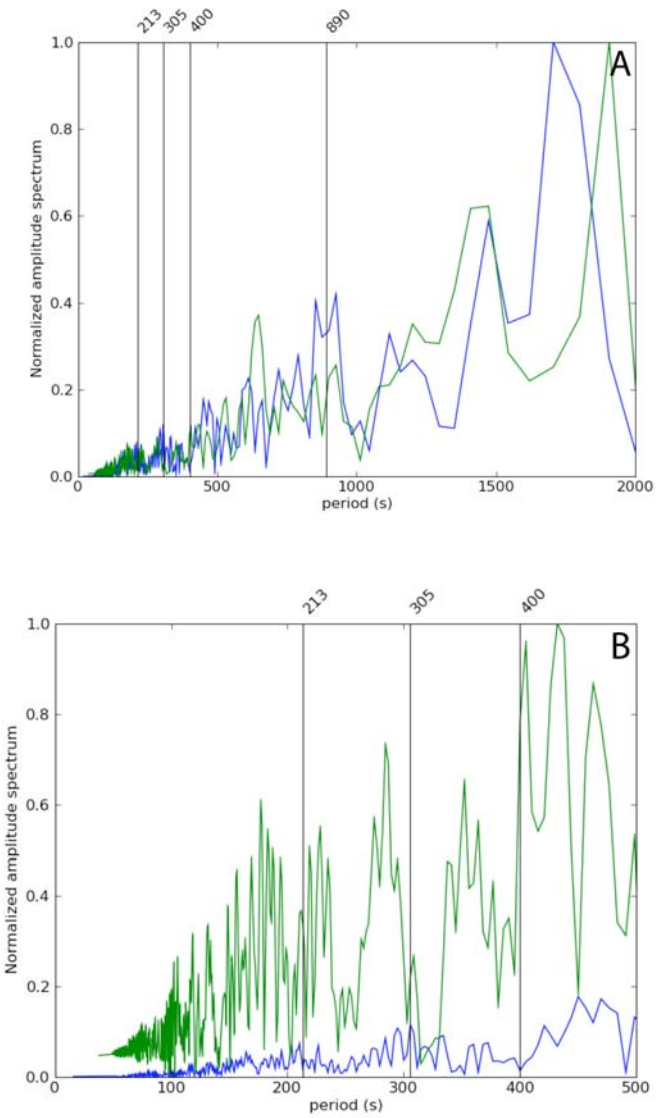

Fig. (9). Normalized amplitude spectrum of the synthetic signal computed in the bay (grid 0, gage 1) in both tested cases [36, 42]; **A**) the full period spectrum, **B**) focus on low period range. [36]'s source is represented in blue and [42]'s source is represented in green. An offset as been introduced between the two signals for a better visibility.

for sending some original reports from Martinique; and Laurence Roger for the translation of historical documents.

We would like to thank the two referees, Carl B. Harbitz and Ahmet C. Yalciner for their constructive comments concerning our manuscript.

This study has been funded by the project MAREMOTI from the French ANR (Agence Nationale de la Recherche), under the contract ANR-08-RISKNAT-05-01c.

REFERENCES

[1] Sartori R, Torelli L, Zitellini N, Peis D, Lodolo E. Eastern segment of the Azores-Gibraltar line (central-eastern Atlantic): an oceanic plate boundary with diffuse compressional deformation. Geology 1994; 22: 555-8.

[2] Tortella D, Torne M, Pérez-Estaún A. Geodynamic evolution of the eastern segment of the Azores-Gibraltar zone: the Gorringe Bank and the Gulf of Cadiz region. Mar Geophys Res 1997; 19: 211-30.

[3] Miranda JM, Baptista MA, Terrinha P, Matias L. Tsunamigenic Source Areas For Portugal Mainland, Iberia. 31 Gen. Ass. European Seismological Commission, 2008, Crete, Greece.

[4] Borges JF, Fitas AJS, Bezzeghoud M, Teves-Costa P. Seismotectonics of Portugal and its adjacent Atlantic area. Tectonophysics 2001; 337: 373-87.

[5] Buforn E, Bezzegoud M, Udias A, Pro C. Seismic sources on the iberia-african plate boundary and their tectonic implications. Pure Appl Geophys 2004; 161: 623-6.

[6] DeMets C, Gordon R, Argus D, Stein S. Effect of recent revisions to the geomagnetic reversal time scale on estimates of current plate motions. Geophys Res Lett 1994; 21: 2191-4.

[7] Sella GF, Dixon TH, Mao A. REVEL: a model for Recent plate velocities from space geodesy. J Geophys Res 2002; 107: 2081.

[8] Fernandes RMS, Ambrosius BAC, Noomen R, *et al.* The relative motion between Africa and Eurasia as derived from ITRF2000 and GPS data. Geophys Res Lett 2003; 30(16): 1828.

[9] Geist EL, Parsons T. Assessment of source probabilities for potential tsunamis affecting the U.S. Atlantic coast. Mar Geol 2008; doi:10.1016/j.margeo.2008.08.005.

[10] Baptista MA, Miranda JM. Revision of the Portugal catalog of tsunamis. Nat Hazards Earth Syst Sci 2009; 9: 25-42.

[11] Ward SN, Day SJ. Cumbre Vieja volcano – potential collapse and tsunami at La Palma, Canary Islands. Geophys Res Lett 2001; 28: 3397-400.
[12] Harbitz CB, Løvholt F, Pedersen G, Masson DG. Mechanisms of tsunami generation by submarine landslides: a short review. Norwegian J Geol 2006; 86: 255-64.
[13] Okal EA. Normal mode energetics for far-field tsunamis generated by dislocations and landslides. Pure Appl Geophys 2003; 150(10-11): 2189-221.
[14] Chester DK. The 1755 Lisbon earthquake. Prog Phys Geogr 2001; 25: 363-83.
[15] Levret A. The effects of the November 1, 1755 lisbon earthquake in morocco. Tectonophysics 1991; 193: 83-94.
[16] Borlase W. Letter to the Rev. Charles Lytteton. Philosophical Transactions of the Royal Society of London 1755; 49: 373-8.
[17] Borlase W. Observations on the Islands of Scilly. Frank Graham, Newcastle upon Tyne, 1758.
[18] Richardson D. DEFRA Report: Tsunamis – Assessing the Hazard for the UK and Irish Coasts. 2006. Available from: http//www.defra.gov.uk/environ/fcd .
[19] Baptista MA, Heitor S, Miranda JM, Miranda P, Mendes VL. The 1755 Lisbon tsunami; evaluation of the tsunami parameters. J Geodyn 1998a; 25(2): 143-57.
[20] Andrade C, Borges P, Freitas MC. Historical tsunami in the Açores archipelago (Portugal). J Volcanol Geothermal Res 2006; 156(1-2): 172-85.
[21] ten Brink U. Tsunami hazard along the U.S. Atlantic coast. Mar Geol 2009; doi:10.1016/j.margeo.2009.03.011.
[22] Affleck Captain, of the Advice Man of War, An account of the Agitation of the sea at Antigua, Nov. I, 1755., Communicated by Charles Gray, Esq; F.R.S. in a letter to William Watso, F.R.S. Philoso Trans, Vol. XLIX. Part II. for the Year 1756, London, 1757. pp 668-70.
[23] Lettée (Mr), Lettre de Martinique du 5 novembre 1755, lue par Réaumur le 28 janvier P.V. Séances Acad. Sci. Paris, 1756; 75, pp. 48-49.
[24] Anonymous. Lettre de Martinique du 15 décembre 1755, lue par Duhamel le 24 mars P.V. Séances Acad. Sci. Paris, 1756; 75: p.145.
[25] Daney S. Histoire de la Martinique depuis la colonisation jusqu'en 1815; Par M. Sidney Daney, Membre du conseil colonial de la Martinique, Tome III. Fort-Royal, E. Ruelle, Imprimeur du Gouvernement, 1846; pp. 237-8.
[26] Brunet P (attribué à -) "Journal d'un vieil habitant de Sainte-Marie (1745-1765)" ou "Ephémérides d'un vieil habitant de Sainte-Marie"). Annexe in Rufz de Lavison Etienne (Dr) Etudes historiques et Statistiques sur la Population de la Martinique. St. Pierre, 1850; p.394.
[27] Martinez Solares JM, Lopez Arroyo A, Mezcua J. Isoseismal map of the 1755 Lisbon earthquake obtained from Spanish data. Tectonophysics 1979; 56(3): 301-13.
[28] Zitellini N, Chierici F, Sartori R, Torelli L. The tectonic source of the 1755 Lisbon earthquake and tsunami. Ann di Geofisica 1999 ; 42: 49-55.
[29] Baptista MA, Miranda PMA, Miranda JM, Mendes VL. Constrains on the source of the 1755 Lisbon tsunami inferred from numerical modelling of historical data on the source of the 1755 Lisbon tsunami. J Geodyn 1998b; 25(1-2): 159-74.
[30] Baptista MA, Miranda PMA, Miranda JM, Mendes VL. Rupture extent of the 1755 Lisbon earthquake inferred from numerical modeling of tsunami data. Phys Chem Earth 1996; 21(12): 65-70.
[31] Udias A, Lopez AA, Mezcua J. Seismotectonics of the Azores-Alboran region. Tectonophysics 1976; 31: 259-89.
[32] Johnston A. Seismic moment assessment of earthquakes in stable continental regions - III. New Madrid, 1811-1812, Charleston 1886 and Lisbon 1755. Geophys J Int 1996; 126: 314-44.
[33] Fukao Y. Thrust faulting at a lithosphere plate boundary. The Portugal earthquake of 1969. Earth Planet Sci Lett 1973; 18: 205-16.
[34] Gjevik B, Pedersen G, Dybesland E, *et al*. Modelling tsunamis from earthquake sources near Gorringe Bank southwest of Portugal. J Geophys Res 1997; 102(C13): 27.931-27.949.
[35] Morton RA, Richmond BM, Jaffe BE, Gelfenbaum G. Reconnaissance investigations of Caribbean extreme wave deposits – preliminary observations, interpretations, and research directions. USGS Open-file Report 2006; pp. 2006-1293.
[36] Barkan R, ten Brink U, Lin J. Far field tsunami simulations of the 1755 Lisbon earthquake: implications for tsunami hazard to the U.S. East Coast and the Caribbean. Mar Geol 2008; doi:10.1016/j.margeo.2008.10.010.
[37] Ballet J. La Guadeloupe. Renseignements sur l'histoire, la flore, la faune, la géologie, la minéralogie, l'agriculture, le commerce, l'industrie, la législation, l'administration. Tome IIe – 1715-1774. Basse-Terre, Imprimerie du Gouvernement 1896; p.286.
[38] Glimsdal S, Pedersen GK, Atakan K, Harbitz CB, Langtangen HP, Løvholt F. Propagation of the Dec. 26 2004 Indian Ocean Tsunami: effects of dispersion and source characteristics. Int J Fluid Mech Res 2006; 33(1): 15-43.
[39] Løvholt F, Pedersen G, Gisler G. Oceanic propagation of a potential tsunami from the La Palma Island. J Geophys Res 2008; 113: C09026.
[40] Gutscher M-A, Malod J, Rehault J-P, *et al*. Evidence for active subduction beneath Gibraltar. Geology 2002; 30(12): 1071-4.
[41] Gutscher M-A, Baptista MA, Miranda JM. The gibraltar arc seismogenic zone (part 2): constraints on a shallow east dipping fault plane source for the 1755 Lisbon earthquake provided by tsunami modeling and seismic intensity. Tectonophysics 2006; 426 : 153-66.
[42] Baptista MA, Miranda JM, Chierici F, Zitellini N. New study of the 1755 earthquake source based on multi-channel seismic survey data and tsunami modeling. Nat Hazards Earth Syst Sci 2003; 3: 333-40.
[43] Gourlay MR. Wave set-up on coral reefs. 2: Set-up on reefs with various profiles. Coast Eng 1996; 28: 17-55.
[44] Losada IJ, Gonzalez-Ondina JM, Diaz-Hernandez G, Gonzalez EM. Numerical modeling of nonlinear resonance of semi-enclosed water bodies: description and experimental validation. Coast Eng 2008; 55: 21-34.
[45] Sladen A, Hébert H, Schindelé F, Reymond D. Evaluation of far-field tsunami hazard in French Polynesia based on historical data and numerical simulations. Nat Hazards Earth Syst Sci 2007; 7: 195-206.
[46] Alasset P-J, Hébert H, Maouche S, Calbini V, Meghraoui M. The tsunami induced by the 2003 Zemmouri earthquake (Mw=6.9, Algeria): modelling and results. Geophys J Int 2006; 166: 213-26.
[47] Roger J, Hébert H. The 1856 Djijelli (Algeria) earthquake: implications for tsunami hazard in Balearic Islands. Nat Hazards Earth Syst Sci 2008; 8: 721-31.
[48] Yelles-Chaouche AK, Roger J, Déverchère J, *et al*. The Tsunami of Djidjelli (eastern Algeria) of August 21-22nd, 1856: Seismotectonic context, Modelling and implications for the Algerian coast. Pure Appl Geo Top 2009; doi:10.1007/s00024-008-0433-6.
[49] Sahal A, Roger, J, Allgeyer, S, *et al.* The tsunami triggered by the 21 May 2003 Boumerdès-Zemmouri (Algeria) earthquake: field investigations on the French Mediterranean coast and tsunami modelling. Nat Hazards Earth Syst Sci 2009; 9: 1823-34.
[50] Okada Y. Surface deformation due to shear and tensile faults in a half-space. Bull Seismol Soc Am 1985; 75: 1135-54.
[51] British Oceanographic Data Centre - The Centenary Edition of the GEBCO Digital Atlas, Liverpool, UK, 1997.
[52] Solares JMM, Arroyo AL. The great historical 1755 earthquake. Effects and damage in Spain. J Seismol 2004; 8: p. 275.
[53] Bilek SL, Lay T. Rigidity variations with depth along interpolate megathrust faults in subduction zones. Nature 1999; 400: 443–6.
[54] Geist EL, Bilek SL. Effect of depth-dependent shear modulus on tsunami generation along subduction zones. Geophys Res Lett 2001; 28(7): 1315-8.
[55] Wells DL, Coppersmith KJ. New empirical relationships among magnitude, rupture length, rupture width, rupture area, and surface displacement. Bull Seismol Soc Am 1994; 84(4): 974-1002.
[56] Zahibo N, Pelinovsky EN. Evaluation of tsunami risk in the Lesser Antilles. Nat Hazards Earth Syst Sci 2001; 1: 221-31.
[57] Lander JF, Whiteside LS, Lockridge PA. A brief history of tsunami in the Caribbean Sea. Sci Tsunami Hazards 2002; 20: 57-94.
[58] Titov V, Rabinovich AB, Mofjeld HO, Thomson RE, Gonzalez FI. The global reach of the 26 December 2004 Sumatra Tsunami. Science 2005; 309: 2045.
[59] Satake K. Effects of bathymetry on tsunami propagation: application of ray tracing to tsunamis. Pure Appl Geophys 1988; 126(1): 27-36.
[60] IGN. Guadeloupe, carte touristique au 1 :100000. 1997; N°3615.
[61] Géoportail [homepage on the Internet]. IGN/BRGM, 2007-2009. Available from: http//www.geoportail.fr

[62] Monserrat S, Vilibic I, Rabinovich AB. Meteotsunamis: atmospherically induced destructive ocean waves in the tsunami frequency band. Nat Hazards Earth Syst Sci 2006; 6: 1035-51.

[63] Jansa A, Monserrat S, Gomis D. The rissaga of 15 June 2006 in Ciutadella (Menorca), a meteorological tsunami. Adv Geosci 2007; 12: 1-4.

[64] Monso de Prat JL, Escartin GJ. Long wave resonance effectsproduced by changes in the layout of the port of Ciutadella (Menorca, Spain). Bulletin of the Permanent International Association of Navigation Congresses 1994: vol. 83-84: pp. 209-16.

[65] Woo S-B, Hong S-Y, Han K-N. Numerical study of nonlinear resonance in narrow bay. OCEANS'04. MTTS/IEEE TECHNO-OCEAN'04 2004; 3: 1512-1518.

[66] Yalciner A, Pelinovsky E. A short cut numerical method for determination of periods of free oscillations for basins with irregular geometry and bathymetry. Ocean Eng 2007; 34(5-6): 747-57.

[67] Rabinovich AB. Seiches and harbor oscillations. handbook of coastal and ocean enginnering, London: Imperial College Press 2009; p. 1300.

[68] Hwang L-S, Lin A. Experimental investigation of wave run-up under the influence of local geometry. In Adams W, Ed. Tsunamis in the Pacific Ocean. Honolulu: East-West Center Press 1970; pp. 407-26.

Received: October 15, 2009 Revised: November 05, 2009 Accepted: December 07, 2009

© Roger *et al.;* Licensee *Bentham Open.*

This is an open access article licensed under the terms of the Creative Commons Attribution Non-Commercial License (http://creativecommons.org/licenses/by-nc/3.0/) which permits unrestricted, non-commercial use, distribution and reproduction in any medium, provided the work is properly cited.

Pure Appl. Geophys.
© 2010 Springer Basel AG
DOI 10.1007/s00024-010-0216-8

Pure and Applied Geophysics

The Transoceanic 1755 Lisbon Tsunami in Martinique

J. Roger,[1,2] M. A. Baptista,[1] A. Sahal,[3] F. Accary,[2,3] S. Allgeyer,[4] and H. Hébert[4]

Abstract—On 1 November 1755, a major earthquake of estimated M_w=8.5/9.0 destroyed Lisbon (Portugal) and was felt in the whole of western Europe. It generated a huge transoceanic tsunami that ravaged the coasts of Morocco, Portugal and Spain. Local extreme run-up heights were reported in some places such as Cape St Vincent (Portugal). Great waves were reported in the Madeira Islands, the Azores and as far as the Antilles (Caribbean Islands). An accurate search for historical data allowed us to find new (unpublished) information concerning the tsunami arrival and its consequences in several islands of the Lesser Antilles Arc. In some places, especially Martinique and the Guadeloupe islands, 3 m wave heights, inundation of low lands, and destruction of buildings and boats were reported (in some specific locations probably more enclined to wave amplification). In this study, we present the results of tsunami modeling for the 1755 event on the French island of Martinique, located in the Lesser Antilles Arc. High resolution bathymetric grids were prepared, including topographic data for the first tens of meters from the coastline, in order to model inundations on several sites of Martinique Island. In order to reproduce as well as possible the wave coastal propagation and amplification, the final grid was prepared taking into account the main coastal features and harbour structures. Model results are checked against historical data in terms of wave arrival, polarity, amplitude and period and they correlate well for Martinique. This study is a contribution to the evaluation of the tele-tsunami impact in the Caribbean Islands due to a source located offshore of Iberia and shows that an 8.5 magnitude earthquake located in the northeastern Atlantic is able to generate a tsunami that could impact the Caribbean Islands. This fact must be taken into account in hazard and risk studies for this area.

Key words: Tsunami, earthquake, Caribbean, far-field, wave amplification, run-up.

1. Introduction

Martinique Island is part of a subduction volcanic arc of 850 km length, resulting from the convergence of the Atlantic Plate under the Caribbean Plate at an average rate of 2 cm/year (Stein *et al.*, 1982) (Fig. 1). This subduction is the cause of shallow earthquakes, some of them with magnitude greater than 7, as was the case of the 5 April 1690, 8 February 1843 (Feuillet *et al.*, 2002) the 18 November 1867 Virgin Island $M_w = 7.5$ earthquake (Zahibo *et al.*, 2003a, b) and the 21 November 2004 $M_w = 6.3$ earthquake of Les Saintes (Zahibo *et al.*, 2005). Important seismic activity is also associated with magmatic activity. The volcanic activity itself can generate pyroclastic flows or lahars that are able to reach the sea and create tsunamis (De Lange *et al.*, 2001; Waythomas and Watts, 2003).

Tsunamis observed in the area result from strong magnitude earthquakes ($M \geq 7$), namely the 1867 Virgin Islands $M_w = 7.5$ earthquake (O'Loughlin and Lander, 2003; Zahibo *et al.*, 2003a, b), or from submarine mass failures (for example, see Lopez-Venegas *et al.*, 2008) as the 14 January 1907 Jamaica landslide (O'Loughlin and Lander, 2003), or the potential landslide on the flank of the Kick'em Jenny underwater volcano (Smith and Shepherd, 1996). Such a landslide could be very large in the Lesser Antilles (Deplus *et al.*, 2001; Le Friant *et al.*, 2009).

According to Pelinovsky *et al.* (2004), volcanic eruptions in the area may also cause tsunamis, as was the case of the July 2003 eruption in Montserrat. For Martinique Island, tsunami waves were observed at least in April 1767 following an earthquake SE of Barbados, and in 1902 due to the volcanic eruption and explosion of Mount Pelée (O'Loughlin and Lander, 2003). Lander *et al.* (2002) collected data from around 30 tsunamis for the Caribbean region

[1] Centro de Geofisica da Universidade de Lisboa, Rua Ernesto de Vasconcelos, Faculdade de Ciências, Ed. C8, 6°, 1700 Lisbon, Portugal. E-mail: jeanrog@hotmail.fr

[2] Ecole Normale Supérieure, Laboratoire de Géologie, UMR 8538, 24, rue Lhomond, 75231 Paris Cedex 5, France.

[3] Université Paris 1 Panthéon-Sorbonne, Laboratoire de Géographie Physique, UMR 8591, 1 place Aristide Briand, 92195 Meudon Cedex, France.

[4] CEA, DAM, DIF, 91297 Arpajon, France.

Published online: 13 November 2010

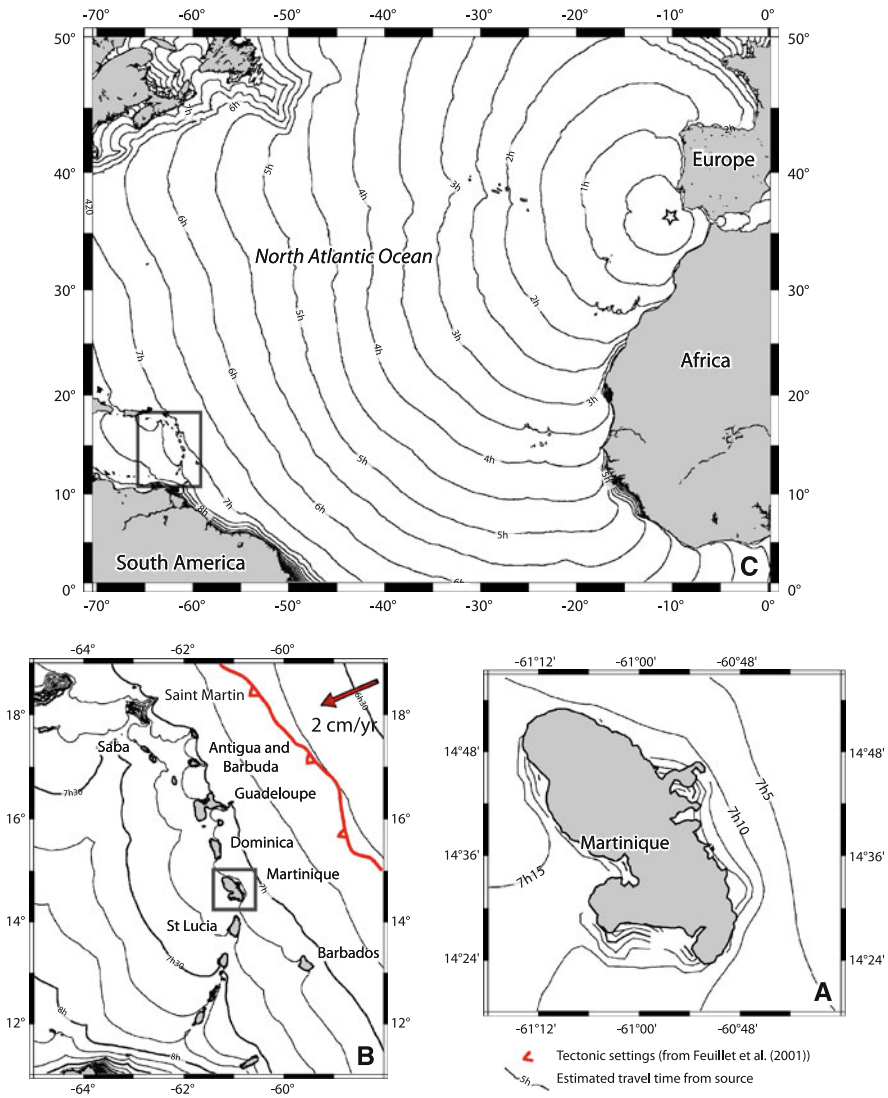

Figure 1
Geographic map locating Martinique Island (**a**) within the Lesser Antilles Arc (**b**) and in the North Atlantic Ocean (**c**). The tsunami travel times (*TTT*), based on a point source (*white star*) close to the source of Baptista *et al.* (2003), are represented by *continuous black curves*

including local sources (source distance <200 km), regional events (<1,000 km) and transoceanic events (>1,000 km). Among them, reliable sources report observations for the 1755 Lisbon tsunami.

The tsunami observed in the Antilles at that time has been associated with the great Lisbon earthquake of November 1, 1755. This event was observed all along the eastern Atlantic shores from Morocco to the United Kingdom, and caused many casualties and damage (Baptista *et al.*, 1998b, 2009a). In addition, numerous coeval reports indicate important abnormal waves in the Antilles.

Recent results of tsunami modeling show that an earthquake with magnitude up to 8.0/8.5 with an epicenter located offshore the Iberian Peninsula is indeed able to produce significant wave heights in the western Atlantic (Barkan *et al.*, 2009), and more particularly in the coastal areas of Guadeloupe Island (Roger *et al.*, 2010), 7 h 30 min of tsunami propagation after the main shock (see tsunami travel times on Fig. 1).

In order to shed some light on the event observed in the French Antilles on 1 November 1755, we made a detailed search for historical documents on these islands and we present here a compilation of those observations with focus on Martinique Island.

The main objective of this study is to test the impact of a tsunami generated by a seismic source proposed for the 1755 event using numerical modeling and high resolution bathymetric data near the coast. We investigate the tsunami far field propagation and the coastal wave amplification close to Martinique Island. The results of numerical modeling correlate well with the available historical data in some selected sites in Martinique Island.

2. *The 1755 Event*

On 1 November 1755, a great earthquake of estimated magnitude $M = 8.5 \pm 0.3$ (Solares and Arroyo, 2004) destroyed the town of Lisbon and was felt in the whole of western Europe, as far east as Hamburg (Germany). Compilations of historical data concerning the earthquake are presented by Sousa (1919), Machado (1966), Solares and Arroyo (2004), while compilations on tsunami data are presented in Romero (1992), Baptista *et al.*, (1998a, 2003), Kaabouben *et al.* (2009) and Barkan *et al.* (2009).

Several authors investigated the source of the Lisbon earthquake, using either macroseismic data (Machado, 1966; Martínez Solares *et al.*, 1979; Levret, 1991; Solares *et al.*, 2004), average tsunami amplitudes (Abe, 1979), or scale comparisons with the 28 February 1969 event (Johnston, 1996). A different approach was considered by Baptista (1998) and Baptista *et al.* (1998a, b) throughout the systematic study of the historical records of the 1755 tsunami wave heights observed along the Iberian and Morocco coasts. These authors proposed a source location, based on tsunami hydrodynamics modeling, located close to the southwest Portuguese continental margin. Zitellini *et al.* (1999) identified a very large active, compressive, tectonic structure located 100 km offshore SW Cape St Vincent (Marques de Pombal thrust fault) which was proposed as a good candidate for the generation of the 1755 event, although its dimensions cannot justify the seismic moment of the 1755 earthquake. Later, Baptista *et al.* (2003) used this structure to build a composite source and checked its reliability against the NE Atlantic tsunami data.

An alternative solution was proposed by Gutscher *et al.* (2002) as an active accretionary wedge overlying an eastward dipping basement and connected to a steep, east dipping slab of cold, oceanic lithosphere beneath Gibraltar. Tsunami simulation results, using this source geometry, are presented in Gutscher *et al.* (2006). Vilanova *et al.* (2003) considered an event triggered in the Lower Tagus Valley as the source of most of the damage observed close to Lisbon, and even of some "tsunami like" phenomena described in Oeiras and along the estuary of the Tagus River (Baptista and Miranda, 2009b). Recently, a new source based on historical data in the NW Atlantic and far-field tsunami modeling was proposed with an orientation perpendicular to previously suggested trending features (Barkan *et al.*, 2009).

2.1. *Historical Data*

2.1.1 *Data Sources and Descriptions*

The results of the research of historical data concerning the observation of the 1755 tsunami in the Caribbean are summarized in Table 1, showing that the tsunami was observed on several islands, including the French Antilles.

Most of these reports have been quoted in later documents such as the *Procès-Verbal des Séances de l'Académie des Sciences* of 1756 (Anonymous, 1755; Lettée, 1755), or the supplement to the Gentleman's Magazine (Urban, 1755). Most of the reports provide information on the location of historical observations (Table 1). Indeed, at this time, Martinique Island was among the most important trade center, especially Fort-de-France's Bay, attended by experienced sailors.

The accurate reading of these documents allows us to conclude that there are only three distinct sources of information: the first one is the letter read by Duhamel concerning an anonymous witness (Anonymous, 1755); the second one is the letter of Lettée (1755); and the third one is the document

Table 1

Historical observed tsunami data in the Lesser Antilles for 1 November 1755 event

Place	Lon. (°W)	Lat. (°N)	Run-up (m)	Maximum inundation distance (MID) (m)	Withdrawal depth (m)	Withdrawal distance (MWD) (m)	Source
Martinique							
La Trinité	60.96	14.74	0.6 (3), 0.9 (2), 1.2[a] (4, 5), 9.0 (1)	66 (2)	9.0 (1)	6[b] (2), 66 (4, 5)	(1) Anonymous (1755), (2) Lettée (1755), (3) Daney (1846), (4) Brunet (1850), (5) Ballet (1896)
Le Galion	60.92	14.73	Minor effects				Brunet (1850), Ballet (1896)
Le Robert	*60.94*	*14.68*	*Nothing observed*				*Brunet (1850), Ballet (1896)*
Sainte-Marie	*60.99*	*14.78*					*Brunet (1850), Ballet (1896)*
Saint-François (actual Le François)	60.89	14.62	Just mentioned				Anonymous (1755)
Lamentin's river	61.01	14.60	The sea rise up in the rivers				Brunet (1850), Ballet (1896)
Fort Royal's river (actual Fort-de-France)	61.06	14.60	circa 0.9 m more than normal				Brunet (1850), Ballet (1896)
Epinette's river	60.96	14.735					Daney (1846), Brunet (1850), Ballet (1896)
Martinique	61.00	14.60	Just mentioned				Affleck (1756)
Guadeloupe							
Saint-Anne	61.38	16.22	3.2*	220*		600*	Ballet (1896)
Barbados							
Carlisle Bay	59.01	13.08					Affleck (1756)
Barbados	59.55	13.16	3.8 (6)				(6) Affleck (1756), (7) Urban (1755), (8) Anonymous (1756)
Antigua	61.80	17.07	1.2 (7)–3.8 (6)		1.8		(6) Affleck (1756, (7) Urban (1755)
Sabia	63.23	17.63	6.3				Affleck (1756
St. Martin	63.05	18.05			4.5[c]		Affleck (1756

The italisized entries indicate the places where nothing was observed. The conversion between the historical measures French *Pas du Roy* and meters is 1 pas du Roy = 15/16 English foot = 0.324 m. The numbers within brackets refer to the information source

* Indicates values measured in situ and deduced on maps according to historical observations (this concerns only Guadeloupe)

[a] Value given above the high tides

[b] This value from Lettée, 1755 could be both the withdrawal distance or the withdrawal depth

[c] Report of a boat moored in 4.5 m of water that falls on the side: the withdrawal depth could be more or less important

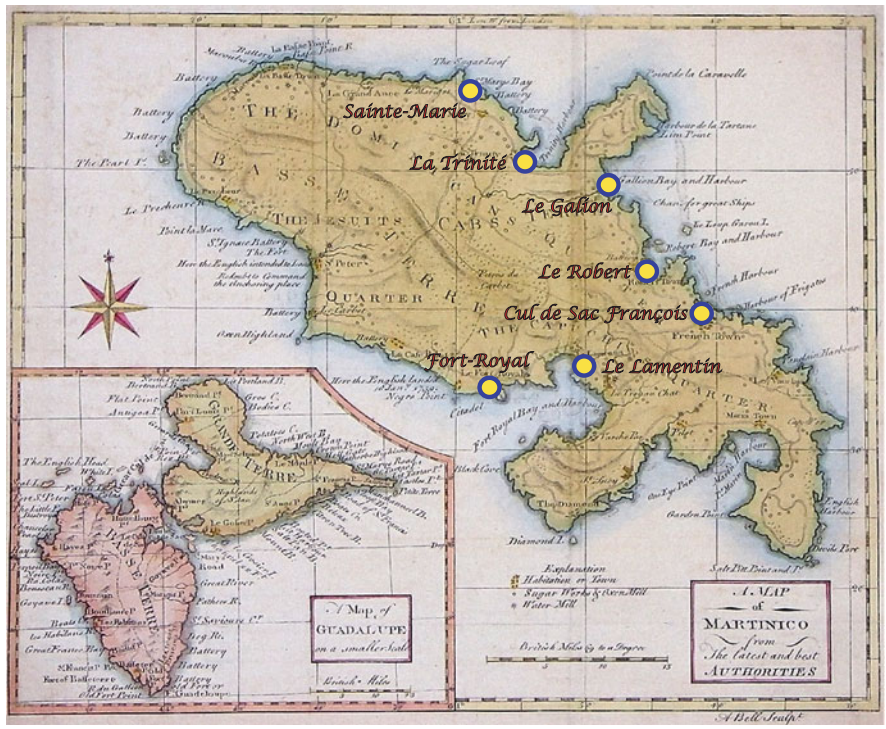

Figure 2
Geographical location of the historical observations and studied sites on Martinique Island on an historical map of Martinique and Guadeloupe Islands (BELL, 1759, *Courtesy of* J. Bodington.)

certainly used by Daney (1846), Brunet (1850) and Ballet (1896).

However, this third document is by far the richest one with respect to the tsunami. It is a very precise description of the hydrological phenomenon, focusing especially on La Trinité Bay, describing the various oscillations of the sea level: the succession of flows and withdrawals, amplitudes, periods, etc. In most records, the arrival of several waves is mentioned (actually flow and withdrawal), the first one not always being the strongest. The same document also informs us about the observation or the non-observation of these same wave-trains around the island: limited at Le Galion Bay, nothing at either Le Robert or in St Marie, an "unusual deposit" by the sea in the Epinette River, and specific responses of the Lamentin and the Fort-Royal Rivers (west coast) are also mentioned. These locations are indicated on a British marine map of this period (Fig. 2).

The letter read by Duhamel (Anonymous, 1755) indicates that the sea reached about 9 m (30 ft, in the original) above its usual level four times. The phenomenon was observed from La Trinité Bay to the François Cul-de-sac. Lettée (1755) indicates that the phenomenon started at 4 p.m. at La Trinité Bay, beginning with a 6-meter drop of the sea level (20 ft, in the original), flooding the shore 60 m inland (200 ft, in the original), damaging houses up to 1 m from the ground. It took 30 min for the sea level to return to normal.

Concerning the other islands of the Antilles (Barbados, Guadeloupe, Saba and St Martin, located on Fig. 1), we can find some information about the inundation of docks in harbors, streets, houses and other.

We tried to read/interpret all this information in terms of tsunami parameters. All details concerning the number of waves, the period, and the height are summarized in Table 1.

2.2. *Studied Sites in Martinique*

The studied sites are presented in Fig. 2. These are La Trinité Bay, located on the east coast of the

Table 2

Parameters of the two source segments used for tsunami modeling

Source		Lon. (°)	Lat. (°)	Depth of center of fault plane (km)	Average slip (m)	Strike (°)	Dip (°)	Rake/slip angle (°)	Length (km)	Width (km)	Rigidity (N m^2)	Mo (N m)
Baptista *et al.* (2003)	GB	−8.7	36.1	20.5	20	250	45	90	105	55	30.0 10^9	3.46 10^{21}
	MPTF	−10	36.8	20.5	20	21.7	24	90	96	55	30.0 10^9	3.17 10^{21}

island, and Fort-de-France Bay, on the west coast of the island, presenting a special focus on the harbor (already here in 1755) and the international airport of Le Lamentin.

A few other sites, mentioned in the historical reports, are also analyzed: Ste-Marie, Le Galion Bay, Le Robert, St-François. These sites are presented in Fig. 2.

3. Tsunami Modeling

3.1. The Model Earthquake

The model earthquake used in this study for the 1755 earthquake is the double segment source proposed by Baptista *et al.* (2003), that includes the Marques de Pombal thrust fault (MPTF) identified by Zitellini *et al.* (1999), and a second thrust fault oriented along the Guadalquivir Bank (GB).

They are included in Fig. 1 (as a point source) and their parameters, presented in Table 2, account for a M_w 8.5 earthquake with a seismic moment of $M_o = 6.63 \times 10^{21}$ N m.

The selection of this model earthquake was based upon two facts: (1) Gutscher *et al.* (2002)'s proposed source produces late tsunami arrivals in the near field (Gutscher *et al.*, 2006); (2) Barkan *et al.* (2009)'s source is not a tectonic based source and its direction cuts the most prominent structures in the area, although it is able to radiate energy towards the Caribbean.

3.2. Numerical Method

The numerical model used in this study is based on the non linear shallow water wave theory. It allows us to compute tsunami generation and propagation associated with an earthquake and has been used for years in order to study tsunami hazards for various exposed regions, from French Polynesia (Sladen *et al.*, 2007) to the Mediterranean Sea (Alasset *et al.*, 2006; Roger and Hébert, 2008; Yelles-Chaouche *et al.*, 2009; Sahal *et al.*, 2009).

Our method assumes instantaneous displacement of the sea surface, identical to the vertical sea-bottom deformation, transmitted without losses to the entire water column; the vertical sea-bottom deformation is computed using the elastic dislocation model of Okada (1985). Given the initial free surface elevation, the model solves the hydrodynamical equations of continuity (1) and momentum (2). Non linear terms are taken into account, and the resolution is carried out using a finite difference method centred in time and using an upwind scheme in space.

The inundation is calculated based on the methodology presented by Kowalik and Murty (1993), relying on an extrapolation of the fluxes calculated in wet cells and in dry meshes:

$$\frac{\partial(\eta + h)}{\partial t} + \nabla[v(\eta + h)] = 0 \quad (1)$$

$$\frac{\partial v}{\partial t} + (v\nabla)v = -g\nabla\eta \quad (2)$$

η corresponds to the water elevation, h to the water depth, v to the horizontal velocity vector, g to the gravity acceleration.

3.3. Bathymetric Grids

The wave propagation is calculated from the epicenter area offshore of the Iberian Peninsula (southern Portugal and Spain to the east) across the Atlantic Ocean on six levels of imbricated grids of increasing resolution, approaching the Lesser Antilles including Martinique Island with special focus on La Trinité Bay and Fort-de-France Bay. The largest grid (grid 0, level 1), corresponding to the geographical

coordinates of Fig. 1a, is built from GEBCO World Bathymetric Grid 1′ (IOC, IHO and BODC, 2003) and is just a resampling of this grid at a space step of 5′ (~9,250 m). The grid resolution increases close to the studied site in order to account for a correct description of shorter wavelengths. Indeed, the wave celerity is expressed by $c = \sqrt{gh}$ (in shallow water non dispersive assumption), and thus decreases when h decreases near the coast, implying wave shortening. The time step used to solve the equations decreases when the grid step decreases, and respects for each grid level the Courant-Friedrichs-Lewy (CFL) criterion to ensure the numerical stability. The resolution for the levels 2 (grid 1), 3 (grid 2), 4 (grid 3), 5 (grid 4) and 6 (grid 5 and 6) are, respectively, 1′ (1,850 m), 500, 150, 40 and 20 m. The highest resolution grids (levels 5 and 6), 40 and 20 m, correspond to the zooms on La Trinité Bay and the northern part of Fort-de-France Bay including the harbor and Lamentin International Airport. The bathymetric dataset was obtained through the merging of GEBCO 1′ data, high resolution multi-beam and resampled bathymetric data from the French Hydrographic Service (SHOM). The intermediate grids (1–4) have been included for numerical stability reasons and correct wavelength sampling during the imbrication. In order to compute tsunami propagation on land, topographic data were manually digitized from topographic maps published by IGN (2006a, b, c).

4. *Modeling Results and Comparison with Historical Data*

Figure 3 displays the maximum water heights computed across the Atlantic Ocean after 9 h 30 min of propagation. It shows three main energy paths: the strongest towards South America (Brazil), a second

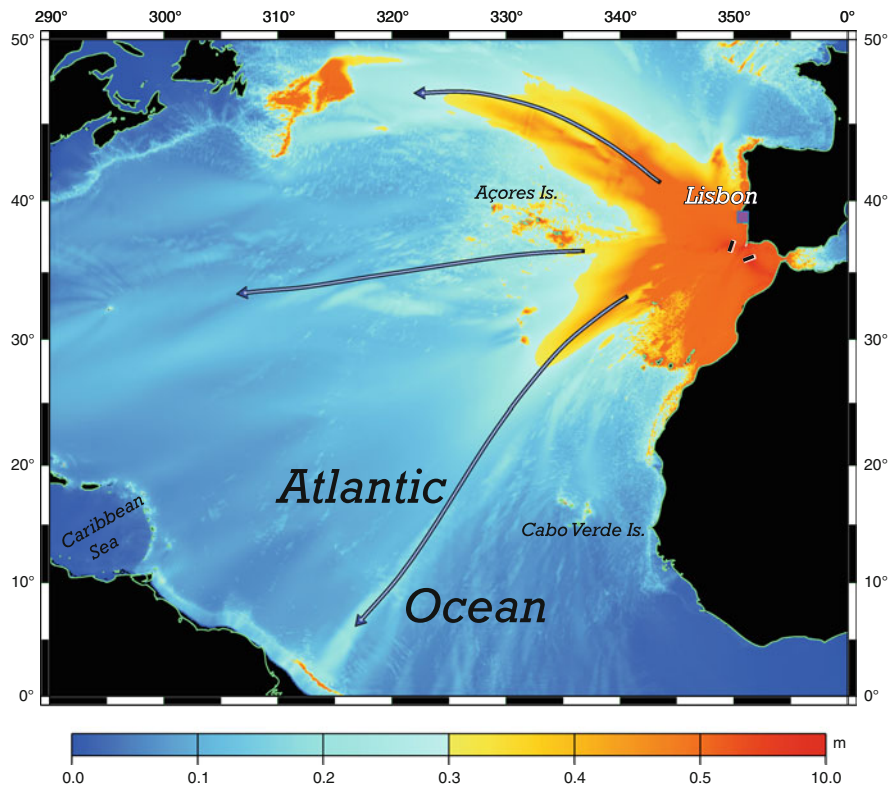

Figure 3
Maximum wave heights over the Atlantic Ocean after 9 h 30 min of tsunami propagation, calculated with the combined source of Baptista *et al.* (2003). The *arrows* highlight the three main tsunami energy paths. The two segments of the source are represented by the *black* and *white rectangles*

towards Newfoundland and the weakest towards the USA (Florida). This radiation pattern is due to the geometrical shape of the source and its azimuth, and to the most relevant submarine features (submarine basins, ridges and transform faults, for example) along the oceanic path that will act as waveguides during tsunami propagation as noted by SATAKE (1988), HÉBERT *et al.* (2001) and TITOV *et al.* (2005). It is worth noting that the Caribbean area is not among the most impacted areas for this computed tele-tsunami on this large-scale grid.

In Fig. 4, we present the maximum wave heights along Martinique Island (grid 2, resolution 500 m and grid 3, resolution 150 m) obtained after 9 h 30 min of tsunami propagation. It clearly shows that only a few sites are prone to wave amplification around the island. This corresponds to sites either directly exposed to long wave arrival coming from the Iberian Peninsula or also located on the other side of the island, in the Caribbean Sea. The wave heights observed along the coast of Martinique vary between 1 and 2 m. The coastal segment from the bay of La Trinité and the north coast of the neighboring *Presqu'île de la Caravelle* to the north of the island near Le Lorrain exhibits maximum values of more than 2 m. Along the southeast coast, the bays of Le Galion, Le Robert and Le François, the wave heights are generally less significant. Then the southeastern coast of the island, offshore of Le Vauclun, shows again significant wave heights of more than 1.5 m.

The potential protective role of the fragmented coral reef barrier from Le Vauclun to Le Galion (shown in Fig. 4) against long wave arrivals has to be stressed. The display of the maximum tsunami height with a shaded bathymetric gradient shows a relative protection of the coastal sites by the coral reef, on the southeastern part of the island. This residual coral reef (appearing as a line on the right) leads to an attenuation of the tsunami effect for the thus-protected bays of Le Galion, Le Robert and Le François. The northeastern (La Trinité, Ste Marie, Le Lorrain) and southern part of the island, which are probably not protected enough by the coral reef which is too deep (5–10 m under sea level), shows again some significant wave heights, at the northern part of the island, from La Trinité to Le Lorrain and farther north.

The surfing spots indicated in Fig. 4 highlight the coastal areas not protected by a sufficient coral reef barrier against classic wind long waves.

Figure 5 (grid 5 and 6) present a focus on the specific site of La Trinité Bay and Fort-de-France Bay and neighboring areas after 9 h 30 min of tsunami propagation. It shows the maximum water height reached by the sea level and the flow depth (maximum wave height minus topography) on land.

The high resolution (20 and 40 m) grids of La Trinité and Fort-de-France Bays (Fig. 5) are able to reproduce the segments of this coral reef barrier, the harbour morphology and coastal shapes as well as the shallow bathymetric features that could affect significantly tsunami propagation near the coast and might contribute to wave trapping and amplifications, potentially associated with resonance phenomena (ROGER *et al.*, 2010).

We can clearly see that several places are inundated in both grids, sometimes until several hundreds of meters from the shore: until 100 m in La Trinité and 250 m in La Moïse, on the east side of La Trinité Bay; and until more than 1 km in Fort-de France Bay (near the airport). This inundation is especially significant all around La Trinité Bay where we can find flow depth values of more than 2 m in the town but also in other urban areas such as La Clique and Anse Cosmy (north of La Trinité) and La Moïse, on the eastern side of the bay (Fig. 5). The 9 m (30 ft) wave height value indicated in ANONYMOUS (1755) (Table 1) is probably a mistake; it is likely between 3 and 30 ft if we refer to the other descriptions at La Trinité (LETTÉE, 1755; DANEY, 1846; BRUNET, 1850; BALLET, 1896). The presented results show a maximum inundation distance (MID) of about 100 m in the southern part of the bay (the town of La Trinité), and 250 m in the northeastern area (Anse Cosmy); thus, longer than the historical observations. However, this computed inundation limit may be overestimated due to the fact that friction is not considered and this may be important in urban areas.

Concerning Fort-de-France Bay (grid 6), the wave heights are smaller than in La Trinité (by about a factor of 3), but they can reach 1.5 m offshore of Fort St-Louis and in the inlet of Château Lézards, deep inside of the bay, south of the airport of Le Lamentin. In addition, several places exhibit inundation, in the

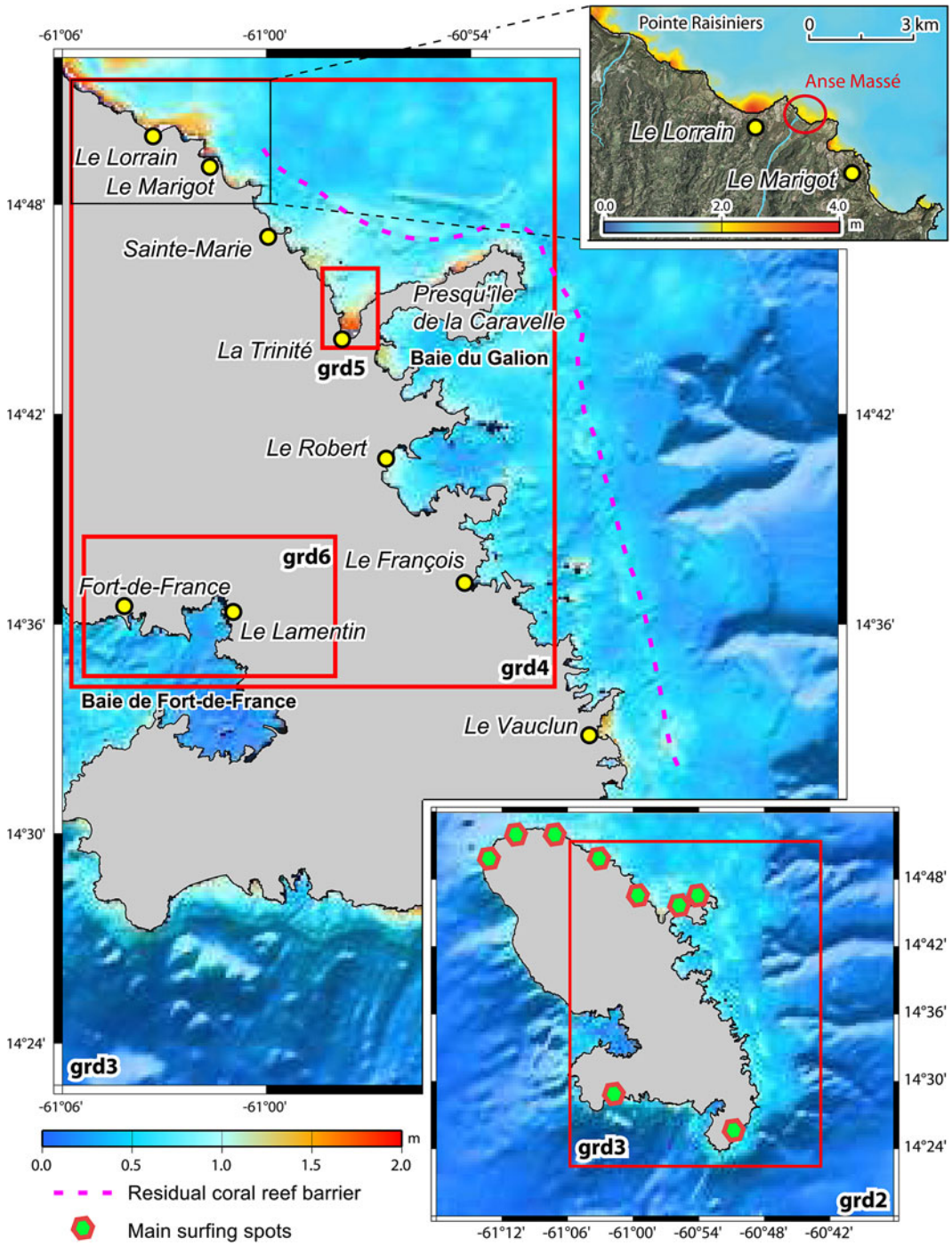

Figure 4

Maximum wave heights illuminated by a bathymetric gradient on Martinique Island on grid 2 and 3 after 9 h 30 min of tsunami propagation using Baptista *et al.* (2003)'s seismic source. The *yellow dots* are the places mentioned in the text. The *red rectangles* show the location of the different imbricated grids. A focus (*black rectangle* on grid 3) shows evidence of wave amplification offshore of a lagoon domain (Anse Massé) southwestward to Le Lorrain. The residual coral reef barrier is indicated with dashed pink curve (from Battistini, 1978). The main *surfing spots* are indicated by *green hexagons* (from http://www.wannasurf.com)

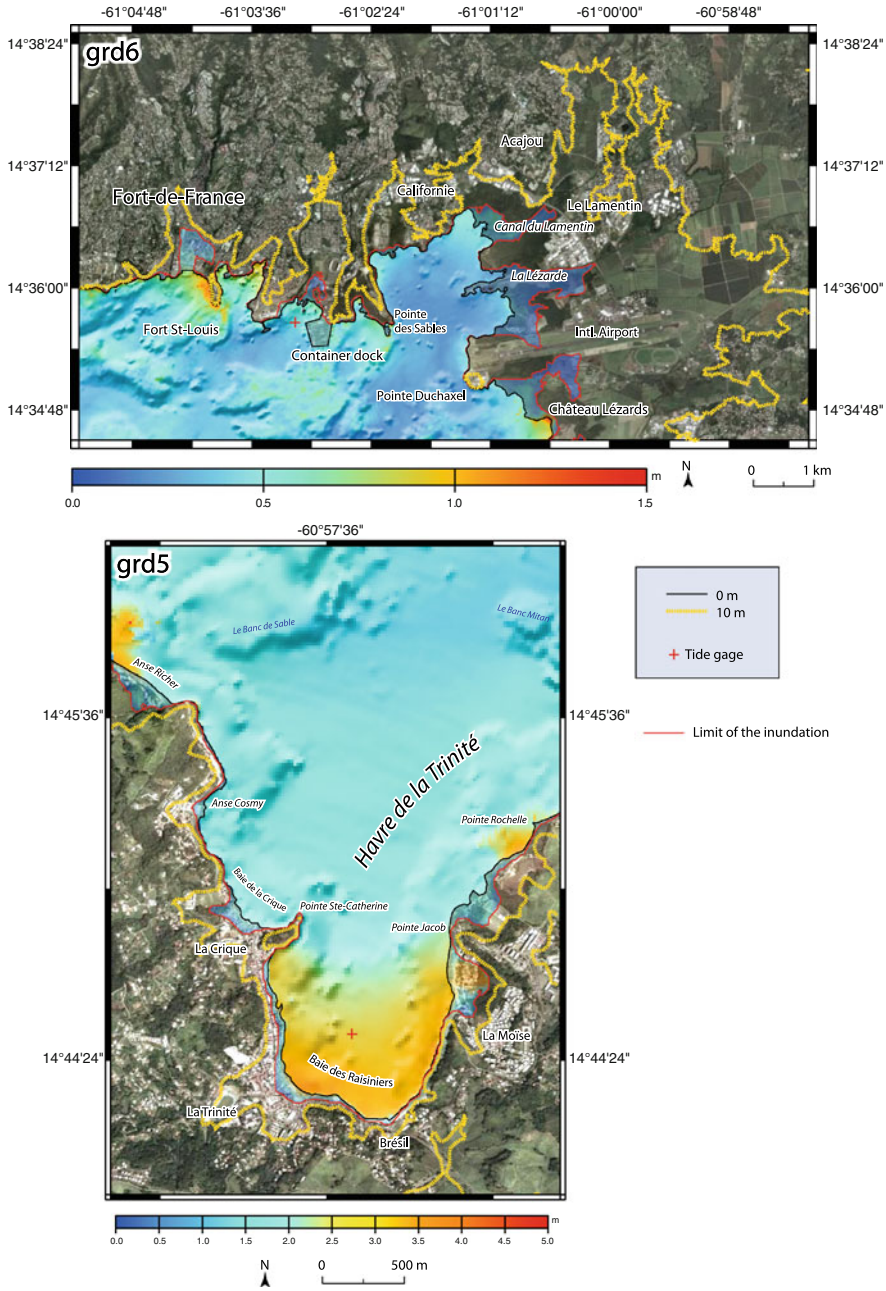

Figure 5

Maximum wave heights illuminated by a bathymetric gradient at sea and maximum water depth on land in high resolution grids 5 and 6 after 9 h 30 min of *tsunami* propagation. The *red line* underlines the inundation limit. The *red crosses* represent the synthetic tide gauges location. The altitude limits of 0 and 10 m are indicated, respectively, by *black* and *yellow lines*

Fort-de-France town center, which is very low and in the area of the container dock, but also the areas close to the canal of Le Lamentin and the Lézarde River, close to the airport, which are partially inundated. All these inundations in Fort-de-France Bay happen in low lands and mostly in swamps with maximum wave heights of no more than 50 cm. This is in good agreement with the historical data indicating that the Lamentin River, located north of the Airport, was subject to an abnormal phenomenon on 1 November

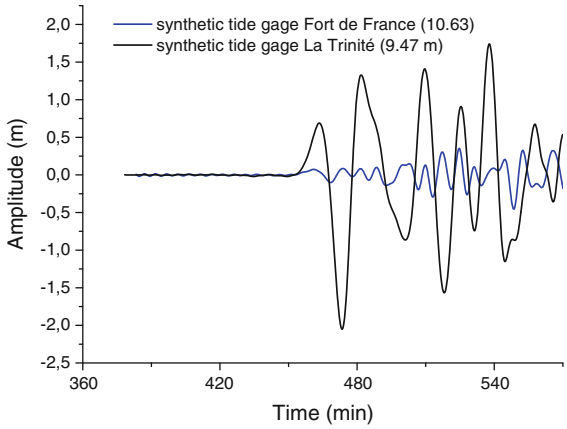

Figure 6
Synthetic maregrams obtained after 9 h 30 min of tsunami propagation for two synthetic tide gauges located in the bays of La Trinité and Fort-de-France. Their positions are given in Fig. 4. The water depth at the gauge location is indicated

1755 with the sea rising up in the rivers 3 feet (∼90 cm) more than normal (Ballet, 1896).

Synthetic tide gauges have been positioned (Fig. 5) in order to obtain information concerning principally tsunami arrival, wave polarities, amplitude and periods at specific locations in both bays.

Figure 6 represents the synthetic signal recorded by two synthetic tide gauges located on both sides of the island, one in La Trinité Bay and one in Fort-de-France Bay. It shows that the effects of the tsunami would be less dramatic in Fort-de-France Bay than they would be in La Trinité Bay at approximately the same water depth (∼10 m). Then it indicates that the first tsunami wave arrives in La Trinité Bay within a travel time of about 7 h 30 min. This is in agreement with the time announced in the available historical documents.

Concerning La Trinité, the computed polarity and the relative amplitudes are in agreement with the reported historical facts: there is a small sea elevation of 70 cm (reported to be 60 cm above the maximum tide level) followed by an significant withdrawal in about 10 min (reported to occur in 4 min) and then a significant inundation of the docks and the streets. The time between the first two waves has been estimated to be 15 min. The computed time between these two waves is around 20 min. According to Ballet (1896)'s accurate description of the phenomenon in La Trinité, we are globally in good agreement concerning periods and relative amplitude between each wave, except for the position of the most significant and destructive wave: it is reported to be the fourth one (Ballet, 1896) but the results of computation show that it is the fifth (Fig. 6).

5. Discussion

The effects of the tide and friction have not been considered in this study.

The historical tide prediction (done using the actual mean sea level with data from 1980–1985 for Le Robert and data from 2005–2008 for Fort-de-France) on 1 November 1755 for Le Robert indicate that, despite the fact that the amplitude of tide was only of about 40 cm crest to trough, the sea was up or at the beginning of withdrawal at 2 p.m., the hour of arrival of the tsunami according to the historical documents. For data concerning Fort-de-France, the amplitude of tide has been estimated to be less than 20 cm crest to trough. In both cases, this tide amplitude certainly could have had an additional effect on the tsunami coastal amplification and inundation, even a negligible effect regarding the tsunami height of more than 3 m in La Trinité Bay.

The simulations have been done without taking into account the friction effects. Even though Dotsenko (1998) shows that the dissipation due to friction effects is negligible offshore (open-sea and shelf areas), Dao and Tkalich (2007) show that the roughness parameter is important in wave-shore interaction including shallow water and inundation friction. This is something important to be noted because it means that, in our case, the friction term is equal to 0 and, thus, the run-up limits presented in the following are certainly overestimated regarding the computed scenarios. In fact, if the friction is important due to the presence of lots of buildings or dense vegetation, for example, so the propagation on land will be slowed down more quickly than without buildings (Yanagasiwa *et al.*, 2009). According to Hébert *et al.* (2009) the non consideration of friction could correspond to an overestimation of wave heights of about 30%.

5.1. Role of Coastal Features

It is important to try to reproduce as well as possible the coastal and bathymetric features in low water depth, i.e. in the area of wave shoaling and refraction processes around seafloor topographic highs, because the particular characteristics of the coastline (coastal geo-morphology, e.g. the geometry of bays, harbours, slope of beaches), or the presence of submarine canyons or coral reef barriers, will have direct consequences on the wave behavior and amplification factor and on the inundation or run-up (Chatenoux and Peduzzi, 2005, 2007; Cochard *et al.*, 2008; Duong *et al.*, 2008).

In the same way, as underlined by Roger and Hébert (2008) for the Balearic Islands in the Mediterranean Sea, the knowledge of the location of submarine canyons is important to assess the tsunami hazard along the coasts because of the focusing role they can play on long wavelengths. Thus, the impact on long waves of the submarine canyons located a few kilometers from the shore in the southeastern part of the island (Fig. 3) should be determined in the future, especially if the coral reef, actually acting as a shield, is going to disappear.

Thus, La Trinité is a U-shaped bay (or funnel-shaped bay), with a maximum length of about 1.2 km and a maximum width of about 1.0 km, oriented N–S and opened northward with a mean depth of 4 m and a very low bathymetric slope (0.33°). This shape is particularly interesting to consider in the case of tsunami wave amplification studies and hazard assessment. In fact, this apparently protected bay with a narrow inlet can amplify the tsunami, and thus its destructive power, presenting a funnel-shape for the arrival waves to travel through (Monserrat *et al.*, 2006). This could explain the observed and modeled wave amplification at this specific location. In addition, it is important to mention that the coral reef barrier in front of this bay could be qualified as residual, i.e. not able to protect the bay against long wave arrival because it is too deep and cut. This situation is emphasized by the high touristic frequentation all year long, especially for this location.

Fort-de-France is located eastward of swamplands, lowlands bordering the Lamentin River, and is constantly inundated with a mean altitude of less than 1 m above sea level. In spite of the fact that the historical reports do not mention any catastrophic wave arrival in Fort-de-France Bay in these places in 1755, the present vulnerability of the area should be taken into account because of its economical central role, located in lowland areas. This omega-shaped (Ω) bay (9 km length and 3 km width in the narrowest place) is oriented E–W and opened westward. Its maximum water depth is about 30 m in the boats channel to the harbor but elsewhere it is only about 10 m deep at most. The general bathymetric slope of the bay from the east (Lamentin Airport) to the west (entrance of the bay) is less than 0.1°.

Several authors have referred to the effects of the presence of coral reef barriers close to the coast, such as the increase in the propagation time, and the reduction of the amplitude (Baba *et al.*, 2009). But on the other side, Cochard *et al.* (2008) indicate that when fragmented, waves are able to accelerate through so-created channels.

For Martinique Island, Fig. 4 shows that the coral reef barrier could be qualified as residual; only a line of 25 km length between the *presqu'île de la Caravelle* and Le Vauclin is visible. The progressive disappearance of the coral reef in Martinique is due to geological reasons such as fast subsidence or volcanic eruptions (Battistini, 1978), and to human stresses such as the pollution or the overfishing in these rich areas (Bouchon *et al.*, 2008; Legrand *et al.*, 2008).

This happens in particular offshore of the north-east coast where the reef does not protect from the assault of normal waves because it is generally underwater at 5–10 m depth (Battistini, 1978) as shown in Fig. 4 with the location of surfing spots. In fact, only the southeastern part of the reef remains, partially protecting the coast from classical waves, with a width sprawl of about 1–2 km; three of the sites discussed in this paper are affected: the bays of Le Galion, Le Robert and Le François. In 1755, according to the historical documents, we know that nothing was observed in Le Robert and just a little in Le Galion (Ballet, 1896). Despite the fact that we have not tested the real effect of this coral barrier, the general results obtained with maximum wave heights in the case of the 1755 event are in favor of this.

Le François is only mentioned in one document (Anonymous, 1755), but in view of this supposed important protection by the different coral reef parts at this time, we could easily suppose that it was too protected to receive anything or that there was simply nobody able to report something there, or was at mean significant damage/impact in 1755. Thus, numerical modeling results of maximum wave heights of about 0.5–1.0 m inside this bay (Fig. 4) could mean that the used bathymetry on the coral reef has changed in 250 years in agreement with the previous remark concerning the coral disappearance.

On the contrary, Sainte-Marie, located north of La Trinité, shows a good exposure to long wave arrival and thus the tsunami modeling (Fig. 3) indicates significant wave heights (more than 1.5 m) in this location in spite of the fact that historical reports clearly mention that nothing was observed here on 1 November 1755 (Ballet, 1896).

The lack of historical information concerning wave arrival near the urban coastal areas of Sainte-Marie, Le Marigot or Le Lorrain in the north and Le Vauclain in the south, where numerical modeling indicates wave heights of more than 2 m (Fig. 4), could be explained by the lack of population here in 1755, according to the available historical maps of 1753 (Le Rouge, 1753) and 1759 (Bell, 1759), or simply the lack of educated people able to write a report of the phenomenon. A search for tsunami deposits in some typical lagoon areas on La Martinique Coast as behind the Anse Massé with the Lorrain River or the Capot River at the Pointe des Raisiniers (Fig. 4) could provide additional information about this tsunami of 1755.

5.2. *Discussion on Vulnerability and Hazard Map Purposes*

The results shown in Fig. 5 could be considered as a contribution to the tsunami (hazard) vulnerability map of La Martinique Island. The use of satellite views reveals the location of populated areas and economic interests in general, correlated with a water elevation map (sea and land) on these high resolution grids (Fig. 5).

The maximum wave heights are well correlated with the surfing spots as in the case of Guadeloupe Island (Roger *et al.*, 2010), i.e. the places of high touristic frequentation (Fig. 4).

At the time of the 1755 tsunami, the population of the French Antilles is not known exactly, but in Martinique, it corresponds to about 100,000 inhabitants, including 84,000 slaves. The shore inhabitants were mainly fishermen and sailors. Although it was populated, the vast majority of the population lived quite far from the shore working in sugar cane activity. Historical synthesis reports that most of them were illiterates (about 95% of the whole population of the French Antilles).

Nowadays, the situation is quite different; the French Antilles count 810,000 inhabitants, including about 400,000 inhabitants for Martinique, with an important influx of tourists estimated to reach about 1 million people per year, resulting in highly frequented beaches, especially during high season. Also, the main economic activities are located along the shore with an estimated income of about 278 million euros in 2007 (Comité Martiniquais du Tourisme, 2008): the development of the tourism industry and the lack of a coastal management policy has furthermore increased this exposure, leading to a concentration of 90% of the population along the shores, in places less than 20 m high (Schleupner, 2007), which is to say 343,000 inhabitants in 1999 (INSEE, 1999). This population is highly exposed to coastal inundation hazards.

In addition, our study also clearly shows that some vital exchange areas (economic, touristic, and above all, for emergency aid) such as Lamentin International Airport or the container's dock (Fort-de-France harbor) are prone to tsunami inundation due to the wave arrival from the eastern Atlantic Margin, despite its orientation towards the west (especially the low lands of no more than one meter altitude (and particularly the airport runway).

6. *Final Conclusion and Perspectives*

This study shows that the historical observations of 1 November 1755 tsunami in Martinique Island can be reproduced using a tsunami source located offshore of Iberia. The predicted inundation parameters are in

agreement with the historical reports at La Trinité and Fort-de-France Bay.

It also indicates that some places along the coast seem to be partially protected from tsunami impact by the residual coral reef barrier. This point deserves further in situ investigations.

Martinique is presently a highly populated island offering some of the most popular tourist beaches in the Caribbean. There could be considerable human casualties in the case of a tsunami event. In fact, this part of the world is well-prepared for hurricane hazards, but is relatively unprepared for the suddenness of a tsunami-like event, especially coming from the eastern part of the Atlantic Ocean.

The tsunami risk in Martinique is not quite existent in people's minds, as meteorological events (storms, cyclones) occur more frequently. Local administrations are not much prepared for tsunamis and rescue units vulnerable to earthquakes and inundations from the sea. For example, they would be destroyed if a like earthquake like the one in 1839 (which destroyed Fort-de-France) occurred (Courteau, 2007). The increasing exposure of the Martinique population to tsunami hazards, combined with a functional and economic vulnerability, including tourism pressure, makes Martinique highly exposed to tsunami risks. The occurrence of an event comparable to the one of 1755 would, nowadays, have a much more important impact on the life in the island.

This study represents the initial stage for the production of a vulnerability map concerning the tsunami hazard, using far-field sources. Further investigation of tsunami hazards in the area should consider the impact of potential local sources.

Another aspect that should be further investigated concerns the tsunami deposits. For example, a special focus on the region of Le Lorrain is presented in Fig. 4; it allows us to indicate that the wave amplification could have been sufficient here to inundate the lowlands of the river of Le Lorrain. The estuary of this river presents a kind of lagoon system, with lowlands potentially floodplain protected partially by a rocky dune; this could have stopped some of the water from the tsunami in 1755. Thus, it is a potential site to look for tsunami deposits. A second site qualified for tsunami deposits is located north of Le Lorrain and corresponds to the alluvial fan of the Capot River (Pointe des Raisiniers), presenting a lagoon profile too. Further study should model the tsunami inundation capabilities in this area, depending mainly on the dune height.

Acknowledgments

The authors would like to thank the SHOM (France) for providing the high resolution bathymetric dataset for Guadeloupe; Paul Louis Blanc (IRSN) for sending some original reports from Martinique and for discussions; João Catalão (University of Lisbon) for bathymetry digitizing and preparation of the bathymetric grid; Ronan Créach (SHOM) for his expertise on oceanic tides; Suzanne Débardat (Paris Observatory) for the understanding of historical time zones; Alain Rabaute (GeoSubSight company) for technical advices. They would like to thank Uri ten Brink (USGS) and an anonymous referee for their constructive comments for the improvement of the manuscript. This study has been funded by the project MAREMOTI from the French ANR (Agence Nationale de la Recherche), under the contract ANR-08-RISKNAT-05-01c.

References

Abe, K. (1979), *Size of great earthquakes of 1873–1974 inferred from tsunami data.* J. Geophys. Res. 84, 1561–1568.

Affleck, B. (1755), *An account of the agitation of the sea at Antigua, Nov. 1, 1755. By Capt. Affleck of the Advice Man of War. Communicated by Charles Gray, E/q; F.R.S in a Letter to William Watson, F.R.S.*

Alasset, P.-J., Hébert, H., Maouche, S., Calbini, V., Meghraoui, M. (2006), *The tsunami induced by the 2003 Zemmouri earthquake* ($M_w = 6.9$, *Algeria)*: *modelling and results*. Geophys. J. Int. 166, 213–226.

Anonymous (1755), *Lettre de Martinique du 15 décembre 1755, lue par Duhamel le 24 mars 1756*. P.V. Séances Acad. Sci. Paris, 75, p. 145.

Anonymous (1756), Journal Historique sur les Matières du tems, juin 1756. Suite des Tremblements de Terre. pp. 462–464.

Baba, T., Mleczko, R., Burbidge, D., Cummins, P.R., Thio, H.K. (2009), *The Effect of the Great Barrier Reef on the Propagation of the 2007 Solomon Islands Tsunami Recorded in Northeastern Australia*. Pure Appl. Geophys. 165, 2003–2018.

Ballet, J. (1896), *La Guadeloupe. Renseignements sur l'histoire, la flore, la faune, la géologie, la minéralogie, l'agriculture, le commerce, l'industrie, la législation, l'administration*. Tome II^e – 1715–1774. Basse-Terre, Imprimerie du Gouvernement.

Baptista, M.A. (1998), *Génese propagação e impacte de tsunamis nas costas portuguesas*. PHD Thesis, University of Lisbon, Portugal (in Portuguese).

Baptista, M.A., Miranda, J.M. (2009a), *Revision of the Portuguese catalog of tsunamis*, Nat. Hazards Earth Syst. Sci. 9, 25–42. http://www.nat-hazards-earth-syst-sci.net/9/25/2009/nhess-9-25-2009.html

Baptista, M.A., Miranda, J.M. (2009b), *Evaluation of the 1755 Earthquake Source Using Tsunami Modeling,* in Geotechnical, Geological and Earthquake Engineering, Book Series, Vol. 7, 425–423: The 1755 Lisbon Earthquake Revisited. Springer, Netherlands. ISBN:978-1-4020-8608-3.

Baptista, M.A., Heitor, S., Miranda, J.M., Miranda, P., and Mendes-Victor, L. (1998a), *The 1755 Lisbon tsunami; evaluation of the tsunami parameters*, J. Geodyn. 25, 143–157.

Baptista, M.A., Miranda, P.M.A., Miranda, J.M., Mendes-Victor, L. (1998b), *Constrains on the source of the 1755 Lisbon tsunami inferred from numerical modelling of historical data on the source of the 1755 Lisbon tsunami.* J. Geodyn. 25(1–2), 159–174.

Baptista, M.A., Miranda, J.M., Chiericci, F., Zitellini, N. (2003), *New Study of the 1755 Earthquake Source Based on Multi-channel Seismic Survey Data and Tsunami Modeling*, Nat. Hazards and Earth Syst. Sci. 3, 333–340.

Barkan, R., Brink, T. U., Lin, J. (2009), *Far field tsunami simulations of the 1755 Lisbon earthquake: implications for tsunami hazard to the U.S. East Coast and the Caribbean*. Mar. Geol. 264, 109–122.

Battistini, R. (1978), *Les récifs coralliens de la Martinique. Comparaison avec ceux au sud-ouest de l'Océan Indien*. Cah. O.R.S.T.O.M., sér. Océanogr. Vol. XVI (2), 157–177.

Bell, A. (1759), *Map of Martinico for the latest and best authorities. Map of Guadalupe on a smaller scale*. Scots Magazine. Available at http://evo.bio.psu.edu/caribmap/lesser/bodington.htm

Bouchon, C., Portillo, P., Bouchon-Navaro, Y., Louis, M., Hoetjes, P., De Meyer, K., Macrae, D., Armstrong, H., Datadin, V., Harding, S., Mallela, J., Parkinson, R., Van Bochove, J.-W., Wynne, S., Lirman, D., Herlan, J., Baker, A., Collado, L., Nimrod, S., Mitchell, J., Morrall, C., Isaac, C. (2008), *Status of Coral Reefs of the Lesser Antilles: The French West Indies, The Netherlands Antilles, Anguilla, Antigua, Grenada, Trinidad and Tobago*. In: Wilkinson, C et al. (eds) Status of coral reefs of the world. Vol. 3, 265–280. Australian Institute of Marine Sciences, Australia.

Brunet, P. (attribué à -) (1850), *"Journal d'un vieil habitant de Sainte-Marie (1745–1765)" ou "Ephémérides d'un vieil habitant de Sainte-Marie")*. Annexe *in* Rufz de Lavison, Etienne (Dr), 1850. Etudes historiques et Statistiques sur la Population de la Martinique. St. Pierre. p. 394.

Chatenoux, B., Peduzzi, P. (2005), *Analysis on the role of bathymetry and other environmental parameters in the impacts from the 2004 Indian Ocean Tsunami*. A Scientific Report for the UNEP Asian Tsunami Disaster Task Force. UNEP/GRID-Europe. http://www.grid.unep.ch/product/publication/download/environment_impacts_tsunami.pdf.

Chatenoux, B., Peduzzi, P. (2007), *Impacts from the 2004 Indian Ocean Tsunami: analyzing the potential protecting role of environmental features*. Nat. Hazards. 40, 289–304. doi:10.1007/s11069-006-0015-9.

Cochard, R., Ranamukhaarachchi, S.L., Shivakoti, G.P., Shipin, O.V., Edwards, P.J., Seeland, K.T., (2008), *The 2004 tsunami in Aceh and Southern Thailand: A review on coastal ecosystems, wave hazards and vulnerability*. Perspectives in Plant Ecology, Evolution and Systematics. 10, 3–40.

Comité Martiniquais du Tourisme (2008), *Bilan Grand Public*. 9 p.

Courteau, R. (2007), *Rapport sur l'évaluation et la prévention du risque du tsunami sur les côtes françaises en métropole et outre-mer*. Office parlementaire d'évaluation des choix scientifiques et technologiques, 168 p.

Daney, S. (1846), *Histoire de la Martinique depuis la colonisation jusqu'en 1815*; Par M. Sidney Daney, Membre du conseil colonial de la Martinique, Tome III. Fort-Royal, E. Ruelle, Imprimeur du Gouvernement. pp. 237–238.

Dao, M.H., Tkalich, P., (2007), *Tsunami propagation modelling—a sensitivity study*. Nat. Hazards Earth Syst. Sci. 7, 741–754.

De Lange, W.P., Prasetya, G.S., Healy, T.R. (2001), *Modelling of tsunamis generated by pyroclastic flows* (*ignimbrites*). Natural Hazards, 24(3), 251–266. doi:10.1023/A:1012056920155.

Deplus, C., Le Friant, A., Boudon, G., Komorowski, J.-C., Villemant, B., Harford, C., Ségoufin, J., Cheminée, J.-L. (2001), *Submarine evidence for large-scale debris avalanches in the Lesser Antilles Arc*. Earth Planet. Sci. Lett. 192, 145–157.

Dotsenko, S.F. (1998), *Numerical modelling of the propagation of tsunami waves in the Crimean Peninsula shelf zone*. Phys. Oceanogr. 9(5), 323–331.

Duong, N.A., Kimata, F., Meilano, I. (2008), *Assessment of Bathymetry Effects on Tsunami Propagation in Viet Nam*. Adv. Nat. Sci. 9(6).

Feuillet, N., Manighetti, I., Tapponnier, P., Jacques, E. (2002), *Arc parallel extension and localization of volcanic complexes in Guadeloupe, Lesser Antilles*. J. Geophys. Res. 107(B12), 2331. doi:10.1029/2001JB000308.

Gutscher, M.A., Malod, J., Rehault, J.P., Contrucci, I., Klingelhoefer, F., Mendes-Victor, L.A., Spakman, W. (2002), *Evidence for active subduction beneath Gibraltar*. Geology 30, 1071–1074.

Gutscher, M.-A., Baptista, M.A., Miranda, J.M. (2006), *The Gibraltar Arc seismogenic zone (part 2): Constraints on a shallow east dipping fault plane source for the 1755 Lisbon earthquake provided by tsunami modeling and seismic intensity*. Tectonophysics 426, 153–166.

Hébert, H., Schindelé, F., Heinrich, P. (2001), *Tsunami risk assessment in the Marquesas Islands* (*French Polynesia*) *through numerical modeling of generic far-field events*. Nat. Hazards Earth Syst. Sci. 1, 233–242.

Hébert, H., Reymond, D., Krien, Y., Vergoz, J., Schindelé, F., Roger J., Loevenbruck, A. (2009), *The 15 August 2007 Peru earthquake and tsunami: influence of the source characteristics on the tsunami heights*. Pure Appl. Geophys. 166, 1–22.

INSEE (2009), *Population et logements par commune depuis le recensement de 1962* (*1961 pour les Dom*). Available on http://www.insee.fr/fr/themes/detail.asp?reg_id=99&ref_id=poplog-com.

Institut Géographique National (2006a), *Fort-de-France, Montagne Pelée, PNR de la Martinique*. Carte de Randonnée, 4501 MT, édition 2, 1: 25000.

Institut Géographique National (2006b), *Le Lamentin, presqu'île de la Caravelle, PNR de la Martinique*. Carte de Randonnée, 4502 MT, édition 2, 1: 25000.

Institut Géographique National (2006c), *Le Marin, presqu'île des trois îlets, PNR de la Martinique*. Carte de Randonnée, 4503 MT, édition 2, 1: 25000.

IOC, IHO and BODC (2003), *Centenary Edition of the GEBCO Digital Atlas, published on CD-ROM on behalf of the Intergovernmental Oceanographic Commission and the International Hydrographic Organization as part of the General Bathymetric Chart of the Oceans*. British Oceanographic Data Centre, Liverpool, UK.

Johnston, A. (1996), *Seismic moment assessment of earthquakes in stable continental regions. III. New Madrid, 1811–1812, Charleston 1886 and Lisbon 1755*. Geophys. J. Int. 126, 314–344.

Kaabouben, F., Baptista, M.A., Iben Brahim, A., El Mouraouah, A., Toto, A. (2009), *On the moroccan tsunami catalogue*, Nat. Hazards Earth Syst. Sci. 9, 1227–1236.

Kowalik, Z., Murty, T.S. (1993), *Numerical simulation of two-dimensional tsunami run-up*. Marine Geodesy. 16, 87–100.

Lander, J.F., Whiteside, L.S., Lockridge, P.A. (2002), *A brief history of tsunami in the Caribbean Sea*. Sci Tsunami Hazards 20, 57–94.

Le Friant, A., Boudon, G., Arnulf, A., Robertson, R.E.A. (2009), *Debris avalanche deposits offshore St. Vincent* (*West Indies*): *Impact of flank-collapse events on the morphological evolution of the island*. J. V. Geotherm. Res. 179(1–2), 1–10.

Le Rouge, G.-L. (1753), *La Martinique une des Antilles Françoises de l'Amérique*. Available at http://evo.bio.psu.edu/caribmap/lesser/bodington.htm.

Legrand H., Rousseau Y., Pérès C., and Maréchal J.-P. (2008), *Suivi écologique des récifs coralliens des stations IFRECOR en Martinique de 2001 à 2006*. Revue d'Ecologie. 63(1–2), 67–84.

Lettée (Mr) (1755), *Lettre de Martinique du 5 novembre 1755, lue par Réaumur le 28 janvier 1756*. P.V. Séances Acad. Sci. Paris, 75, pp. 48–49.

Levret, A. (1991), *The effects of the November 1, 1755 "Lisbon" earthquake in Morocco*. Tectonophysics 193, 83–94.

Lopez-Venegas, A.M., ten Brink, U.S., Geist, E.L. (2008), *Submarine landslide as the source for the October 11, 1918 Mona Passage tsunami: observations and modeling*. Marine Geol. 254(1–2), 35–46.

Machado, F. (1966), *Contribuiçao para o estudo do terramoto de 1 de Novembro de 1755*, Rev. Fac. Ciencias de Lisboa, 2ª Serie-C, 14(1), 19–31.

Martínez Solares, J. M., López Arroyo, A., Mezcua, J. (1979), *Isoseismal map of the 1755 Lisbon earthquake obtained from Spanish data*. Tectonophysics 53, 301–313.

Monserrat, S., Vilibic, I. and Rabinovich, A.B. (2006), *Meteotsunamis: atmospherically induced destructive ocean waves in the tsunami frequency band*. Nat. Hazards Earth Syst. Sci. 6, 1035–1051.

O'Loughlin, K.F., Lander, J.F. (2003), *Caribbean tsunamis: a 500-year history from 1498–1998*. Advances in Natural and Technological Hazards Research, Kluwer Academic Pulishers, Boston, 263 pp.

Okada, Y. (1985), *Surface deformation due to shear and tensile faults in a half-space*. Bull. Seismol. Soc. Am. 75, 1135–1154.

Pelinovsky, E., Zahibo, N., Dunkley, P., Edmonds, M., Herd, R., Talipova, T., Kozelkov, A., Nikolkina, I. (2004), *Tsunami generated by the volcano eruption on July 12-13, 2003 at Montserrat, Lesser Antilles*. Sci. Tsunami Hazards, 22(1), 44–57.

Roger, J., Hébert, H. (2008), *The 1856 Djijelli (Algeria) earthquake: implications for tsunami hazard in Balearic Islands*. Nat. Hazards Earth Syst. Sci. 8, 721–731.

Roger, J., Allgeyer, S., Hébert, H., Baptista, M.A., Loevenbruck, A., Schindelé, F. (2010), *The 1755 Lisbon tsunami in Guadeloupe Archipelago: contribution of numerical modelling*. Open Oceanogr. J. 4, 58–70.

Romero, M.L.C. (1992), *El riesgo de Tsunamis en España. Analisis y valoracion geográfica.* 209 pp, Insituto Geografico Nacional, Madrid. ISBN:84-7819-041-4, in Spanish

Sahal, A., Roger, J., Allgeyer, S., Lemaire, B., Hébert, H., Schindelé, F., Lavigne, F. (2009), *The tsunami triggered by the 21 May 2003 Boumerdes-Zemmouri* (*Algeria*) *earthquake: field investigations on the French Mediterranean coast and tsunami modeling*. Nat. Hazards Earth Syst. Sci. 9, 1823–1834.

Satake, K. (1988), *Effects of bathymetry on tsunami propagation: application of ray tracing to tsunamis*. Pure Appl. Geophys. 126(1), 27–36.

Schleupner, C. (2007), *Spatial assessment of sea level rise on Martinique's coastal zone and analysis of planning frameworks for adaptation*. J. Coast. Conserv. 11, 91–103.

Sladen, A., Hébert, H., Schindelé, F., Reymond, D. (2007), *Evaluation of far-field tsunami hazard in French Polynesia based on historical data and numerical simulations*. Nat. Hazards Earth Syst. Sci. 7, 195–206.

Smith, M.S., Shepherd, J.B. (1996), *Tsunami waves generated by volcanic landslides: an assessment of the hazard associated with Kick'em Jenny*. Geological Society, London, Special Publications, 110, 115–123.

Solares, J.M.M., Arroyo, A.L. (2004), *The great historical 1755 earthquake. Effects and damage in Spain*. J. Seismol. 8, 275–294.

Sousa, F.L.P. (1919), *O Terremoto do 1° de Novembro de 1755 em Portugal*. In: Um estudo demográfico Vol. I, Serviços Geológicos de Portugal e II.

Stein, S., J.F. Engeln, D.A. Wiens, K. Fujita, R.C. (1982), *Speed, Subduction seismicity and tectonics in the Lesser Antilles arc*. J. Geophys. Res. 87, B10, 8642–8644.

Titov, V., Rabinovich, A.B., Mofjeld, H.O., Thomson, R.E., Gonzalez, F.I. (2005), *The global reach of the 26 December 2004 Sumatra Tsunami*. Science. 309, 2045. doi:10.1126/science.1114576.

Urban, S. (1755), Supplement to the Gentleman's Magazine for the year 1755, printed by: Henry, D. and Cave, R., St. John' Gate, London, 587–591.

Vilanova, S.P., Nunes, C.F., Fonseca, J.F.B.D. (2003), *Lisbon 1755: a case of triggered onshore rupture?* Bull. Seismol. Soc. Am. 93(5), 2056–2068.

Waythomas, C.F., Watts, P. (2003), *Numerical simulation of tsunami generation by pyroclastic flow at Aniakchak Volcano*, Alaska. Geophysical Res. Lett. 30(14), 51–54.

Yanagasiwa, H., Koshimura, S., Goto, K., Miyagi, T., Imamura, F., Ruangrassamee, A., Tanavud, C. (2009), *The reduction effects of mangrove forest on a tsunami based on field surveys at Pakarang Cape, Thailand and numerical analysis*. Estuar. Coastal Shelf Sci. 81, 27–37.

Yelles-Chaouche, A.K., Roger, J., Déverchère, J., Bracene, R., Domzig, A., Hebert, H., Kherroubi, A. (2009), *The Tsunami of Djidjelli (eastern Algeria) of August 21-22nd, 1856: Seismotectonic context, Modelling and implications for the Algerian coast*. Pure Appl. Geophys. Topical Volume. doi:10.1007/s00024-008-0433-6.

Zahibo, N., Pelinovsky, E., Yalçiner, A., Kurkin, A., Koselkov, A., Zaitsev, A. (2003a), *The 1867 Virgin Island tsunami: observations and modeling*. Oceanol. Acta 26(5–6), 609–621.

ZAHIBO, N., PELINOVSKY, E., YALÇINER, A., KURKIN, A., KOSELKOV, A., ZAITSEV, A. (2003b), *The 1867 Virgin Island tsunami*. Nat. Hazards Earth Syst. Sci. 3, 367–376.

ZAHIBO, N., PLINOVSKY, E., OKAL, E., YALÇINER, A., KHARIF, C., TALIPOVA, T., KOZELKOV, A. (2005), *The earthquake and tsunami of November 21, 2004 at Les Saintes, Guadeloupe, Lesser Antilles*. Sci. Tsunami Hazards 23(1), 25–39.

ZITELLINI, N., CHIERICI, F., SARTORI, R., TORELLI, L. (1999), *The tectonic source of the 1755 Lisbon earthquake and tsunami*. Annali di Geofisica. 42, 49–55.

(Received December 31, 2009, revised May 3, 2010, accepted June 7, 2010)

Proceedings of the 9th U.S. National and 10th Canadian Conference on Earthquake Engineering
Compte Rendu de la 9ième Conférence Nationale Américaine et 10ième Conférence Canadienne de Génie Parasismique
July 25-29, 2010, Vancouver, Canada ♦ Paper No. 1837

TSUNAMI IMPACT ON NEWFOUNDLAND, CANADA, DUE TO FAR-FIELD GENERATED TSUNAMIS. IMPLICATIONS ON HAZARD ASSESSMENT.

J. Roger[1,2], M.A. Baptista[2,3], D. Mosher[4], H. Hébert[5], A. Sahal[6]

ABSTRACT

In Canada, tsunamis associated with submarine earthquakes have been considered in terms of hazard assessment for many years; mainly due to the Pacific tsunami threat and to gravitational instabilities on continental slopes. This latter instance refers to the case of a submarine landslide and consequent tsunami generated by the Mw=7.2 earthquake of 18th November 1929 on the Grand Banks of Newfoundland.

In this study, we investigate the impact on Newfoundland of far field generated tsunamis in the Atlantic Ocean and consideration of such tsunami hazards for the Canadian Atlantic Coast.

In the framework of the study of the 1755 Lisbon tele-tsunami, we show that a 1755 tsunami like event, with the source located offshore the Iberian Peninsula, can impact Newfoundland. The coastal amplification is also studied in detail using high resolution bathymetric grids. Finally the results of tsunami propagation modeling are compared to historical data of the 1st November 1755 concerning at least two places in Newfoundland.

Objectives

It is the intent of this paper to investigate the feasibility of trans-Atlantic tsunamis impacting the opposing continental margin by simulating the Lisbon 1755 tsunami arrival in Newfoundland, Canada.

[1] Ecole Normale Supérieure / Laboratoire de Géologie, 24, rue Lhomond, 75231 Paris CEDEX 5, France
[2] Centro de Geofisica da Universidade de Lisboa, Rua Ernesto de Vasconcelos, Faculdade de Ciências Ed. C8, 6°, 1700 Lisboa, Portugal
[3] ISEL, Instituto Superior de Engenharia de Lisboa
[4] Natural Resources Canada / Geological Survey of Canada – Atlantic / 1 Challenger Drive (P.O. Box 1006) / Dartmouth, Nova Scotia, Canada B2Y 4A2
[5] CEA, DAM, DIF, F-91297 Arpajon, France
[6] Université Paris 1 Panthéon-Sorbonne, Laboratoire de Géographie Physique, UMR 8591, 1 place Aristide Briand, 92195 Meudon Cedex, France

Introduction

On the 1st November 1755, an earthquake of estimated magnitude Mw=8.5/9.0 occurred offshore the Iberian Peninsula. This destructive event, known as the Lisbon earthquake because of its devastating effect on Lisbon, Portugal, was felt in the whole of Western Europe as far north as Hamburg (Germany). As a direct consequence of the earthquake, a destructive and widespread tsunami was generated which reached the coasts of Portugal, Spain, Morocco, and even those of southern England and the Atlantic archipelago of Madeira and the Azores. Recent studies highlighted coeval reports of tsunami arrivals in the West Indies on the 1st of November 1755, with noticeable wave amplitudes and significant flooding of low coastal areas on the French Island of Martinique (Roger et al. subm.).

In this study, we investigate the possible impact of this transoceanic event in the North Atlantic area of Canada. Additional historical data from Newfoundland is analyzed. These documents demonstrated the occurrence of an uncommon phenomenon in Bonavista, Newfoundland. Tocque (1846) and Batterson et al. (1999) indicated that the sea emptied the harbour; after ten minutes the water returned and inundated low parts of the town.

A separate report concerns observations at St. John's, on the east coast of Newfoundland (Batterson et al. 1999). This report indicates that on the 11/01/1775 in St. John's, the "sea suddenly rose 10 m". This could be linked to a storm. But the 11/01 may well refer to the first of November, as this is the notation order convention for the United States. The USA uses month/day/year, as opposed to the European convention, which is day/month/year. The year, 1775 could easily have been written in error for 1755; the year of the Lisbon earthquake.

Numerical modelling

Coseismic tsunami generation is modeled using available seismic source parameters from Zitellini et al. (1999) for the 1755 tsunami source located offshore the Iberian Peninsula. The double segment source used in this model includes a segment based on geological features oriented toward North America. Tsunami propagation on measured bathymetric grids is modeled taking into account shallow water theory and the hydrodynamic equations of continuity (Eq. 1) and momentum conservation (Eq. 2).

$$\frac{\partial(\eta + h)}{\partial t} + \nabla.[v(\eta + h)] = 0 \qquad (1)$$

$$\frac{\partial v}{\partial t} + (v.\nabla).v = -g\nabla\eta \qquad (2)$$

Different model results based on low resolution (5') bathymetric grids (Roger et al. 2009; Roger et al. subm.) demonstrate two main tsunami pathways containing most of the energy and thus maximum wave heights (Fig. 1). One pathway is directed towards South America and another one towards Canada, and more specifically towards Newfoundland (Fig. 1, GR00).

The use of high resolution bathymetric grids for Newfoundland is necessary to investigate detailed propagation near the coast. The bathymetric data used are a combination of Gebco 1' dataset (British Oceanographic Data Centre, 1997) and bathymetric data of the Canadian Hydrographic Service. The grids include 4 different resolution levels with special focus on the regions of Bonavista and St. John's with a spatial resolution of 150 m. This resolution is able to

reproduce correctly the shape of the coast (Roger et al. 2009 ; Sahal et al. 2009). Topographic data were included to produce a continuous (ocean-land) digital elevation model in order to compute inundation.

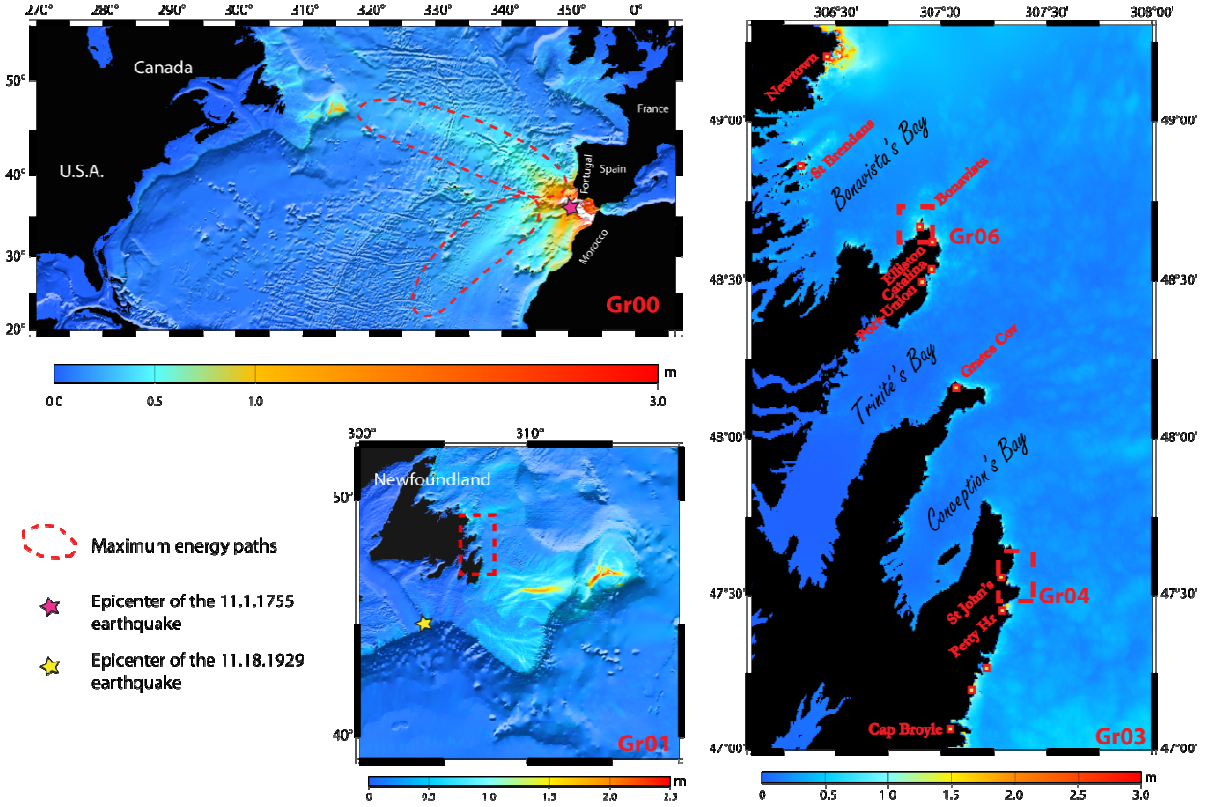

Figure 1. Maximum wave heights illuminated by bathymetric gradient after 9h of tsunami propagation using Baptista et al. (2003)'s combined seismic source.

Modeling Results and Discussion

The results presented in Figure 1 (GR01 and GR03) show that some areas are prone to tsunami amplification due to shoaling effects. Wave heights of more than 2 m are modeled on the shallow banks of the Newfoundland continental shelf. At several locales along the coast, such as Newton/Torbay, Bonavista (and area), Grates Cove, Freshwater Bay (Blackhead) and St. John's, significant wave heights of more than 1.5 m are modeled.

Figure 2 shows that the peninsula of Bonavista could be affected by tsunami waves sourced from the Iberian Peninsula. Wave heights reach 2.5 m and more in some locations, with inundation of low-lying lands, particularly the town centre, around the harbour, and the swamp areas north to the town.

Concerning St. John's, first results obtained on the 150 m resolution grid indicate that the waves do not enter the bay (the lack of accurate bathymetric data inside the bay (Fig. 3) should be considered cautiously). Even modeling with a finer grid (40 m), the waves do not enter the harbour. The narrow restriction (300 m) at the mouth of the harbour provides significant protection. Nevertheless, models indicate 1 m tsunami wave heights reach the entrance of the harbour.

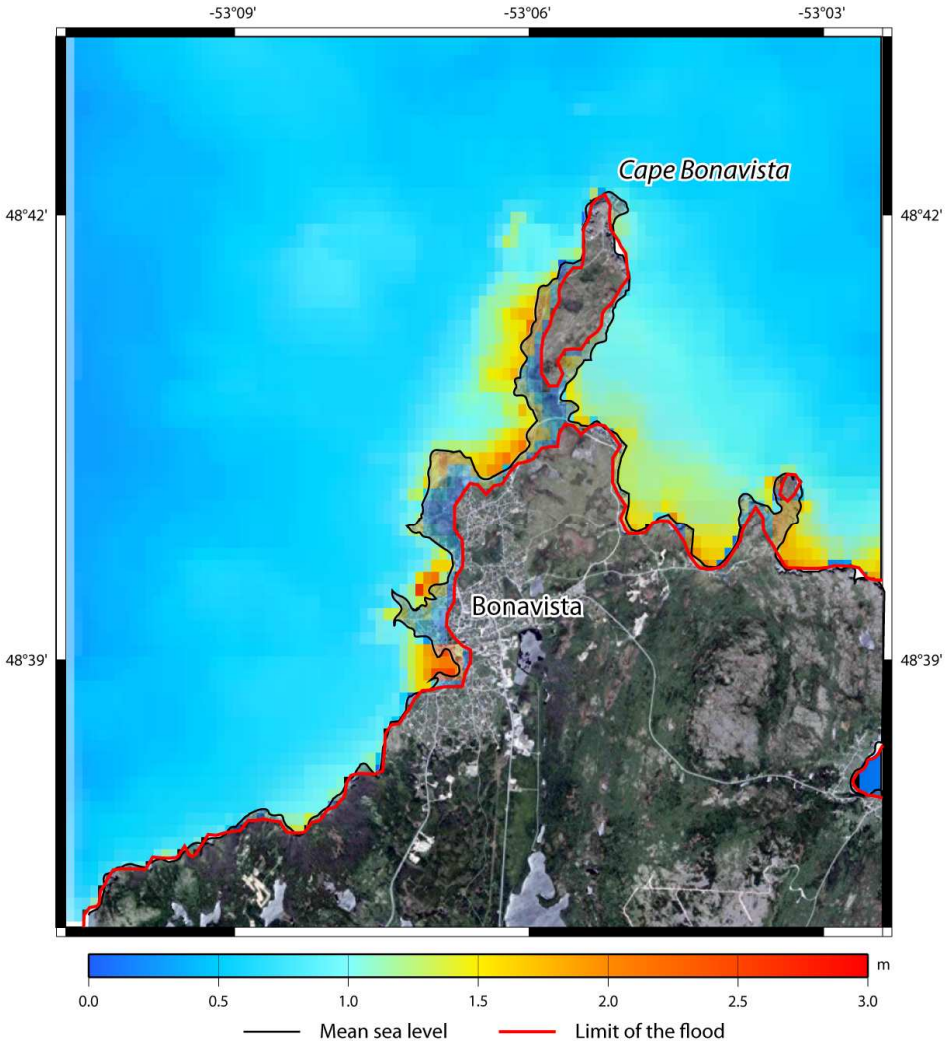

Figure 2. Sea surface elevation and maximum flow depth on the 150 m resolution grid (GR06) showing the Cape of Bonavista after 9 h of tsunami propagation. A satellite view (Google Earth ™) allows the correlation between populated areas and wave amplification.

Wave height reaches a maximum of about 2 m in Freshwater Bay, just south of St. John's Harbour and west of Cape Spear, North America's easternmost point. Freshwater Bay is a funnel-shaped embayment with a shoaling barrier beach and back-beach lagoon. Its morphology and orientation seems to be particularly receptive to long waves (Fig. 3) such as those modeled in this study. The back-bay lagoon area and estuary would be a likely locale to search for tsunami deposits.

1755 Lisbon tsunami simulation results for Bonavista Harbour, Newfoundland are in good agreement with brief historical accounts of inundation of the town at that time. Today, this town is well developed (1 km radius from the central harbour) and so it is not totally inundated in the numerical simulation. In 1755, however, the town was likely much smaller and focused around the harbour, since fishing was the sole source of livelihood. The entire settlement could have been impacted from the tsunami, therefore.

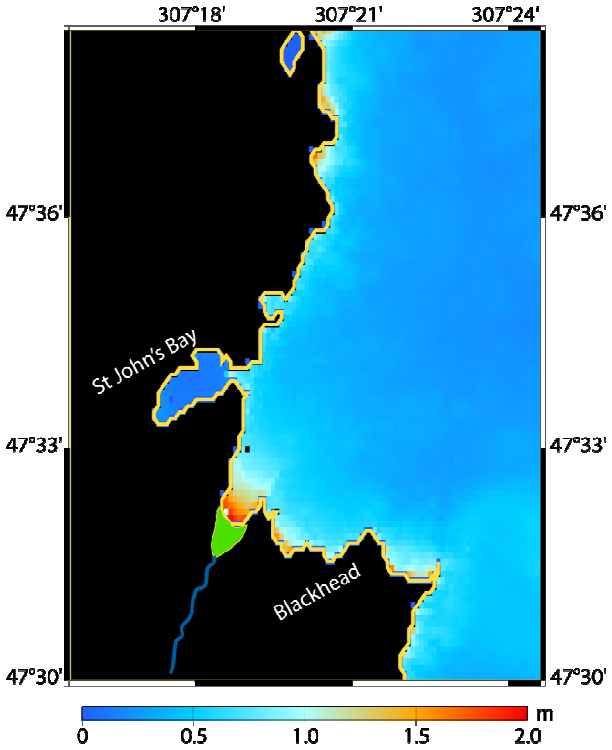

Figure 3. Maximum wave heights on St John's Bay and neighborhood (GR04) after 9 h of tsunami propagation. The green area symbolizes a laguna system alimented by a small river and protected by a dune row.

Conclusion

Numerical modeling confirms the possibility that reporting of wave arrival and inundation of the town of Bonavista in 1755 can be associated to the Lisbon tsunami. Concerning controversial reports of St. John's, it would seem that the harbour is well protected by the Narrows at the mouth of the harbour. The harbour mouth is eastward facing, however. With appropriate wave propagation direction and a more detailed bathymetic grid, tsunami impact is possible. These reports cannot be ruled out entirely, therefore. Lack of reporting in the rest of Newfoundland of the 1755 event can be readily explained by sparseness of population, community isolation, and general illiteracy amongst the outport population during that epoch (Batterson pers. comm.; Rowe 1980). Even in 1929, news of the Grand Banks tsunami impact on the Burin Peninsula of Newfoundland's south coast took two days to reach St. John's.

This study has shown that trans-Atlantic tsunami propagation is possible. In addition to tsunami hazards associated with the submarine slope instability, such as the 1929 tsunami (Grand Banks), Canada's East Coast must consider the hazard associated with tsunamis from far-field sources therefore.

Acknowledgements

The authors would like to thank *the Canadian Hydrographic Service* for providing the high resolution bathymetric data for Newfoundland. They would like to thank Garry Rogers, Kelin Wang, Brian Hill, John Adams and Roy Hyndman from *Natural Resources Canada*, Melissa Kane de *Natural Resources Canada Library*, Martin Batterson of the *Geological Survey*

of Newfoundland and Labrador and Alan Ruffman of *Geomarine Associates Ltd* for their discussions and willingness to share information.

This study has been funded by the French ANR project MAREMOTI under contract ANR-08-RISKNAT-05-01c.

References

Baptista, M.A., Miranda, J.M., Chierici, F., Zitellini, N., 2003. New Study of the 1755 Earthquake Source Based on Multi-channel Seismic Survey Data and Tsunami Modeling, Natural Hazards and Earth System Sciences, 3, 333-340.

Batterson, M., Liverman, D.G.E., Ryan, J., Taylor, D., 1999. The assessment of geological hazards and disasters in Newfoundland: an update. Current Research (1999) Newfoundland Department of Mines and Energy Geological Survey, Report 99-1, pages 95-123.

Roger, J., Allgeyer, S., Hébert, H., Baptista, M.A., Loevenbruck, A., Schindelé, F., 2009. The 1755 Lisbon tsunami in Guadeloupe Archipelago: contribution of numerical modelling. Accepted for publication in The Open Oceanography Journal.

Roger, J., Baptista, M.A., Sahal, A., Allgeyer, S., Hébert, H. The transoceanic 1755 Lisbon tsunami in the Martinique. Submitted to Pure and Applied Geophysics, Proceeding Edition of the 20th International Tsunami Symposium, Novosibirsk, July 2009.

Rowe, F.W., 1980. A History of Newfoundland and Labrador. McGraw-Hill Ryerson, 563 pages.

Sahal, A., Roger, J., Lemaire, B., Hébert, H., Schindelé, F., Lavigne, F., 2009. The tsunami triggered by the 21 May 2003 Boumerdes-Zemmouri (Algeria) earthquake: field investigations on the French Mediterranean coast and tsunami modelling. Natural Hazards and Earth System Sciences. 9, 1823-1834.

Tocque, P., 1846. Wandering Thoughts, or Solitary Hours. Thomas Richardson and son, London, 387 pp.

Zitellini, N., Chierici, F., Sartori, R., Torelli, L. (1999), The tectonic source of the 1755 Lisbon earthquake and tsunami. Annali di Geofisica. 42, 49–55.

Nat. Hazards Earth Syst. Sci., 9, 1823–1834, 2009
www.nat-hazards-earth-syst-sci.net/9/1823/2009/
© Author(s) 2009. This work is distributed under
the Creative Commons Attribution 3.0 License.

Natural Hazards and Earth System Sciences

The tsunami triggered by the 21 May 2003 Boumerdès-Zemmouri (Algeria) earthquake: field investigations on the French Mediterranean coast and tsunami modelling

A. Sahal[1], **J. Roger**[2,3], **S. Allgeyer**[2], **B. Lemaire**[2], **H. Hébert**[2], **F. Schindelé**[2], **and F. Lavigne**[1]

[1]Université Paris 1 Panthéon-Sorbonne, Laboratoire de Géographie Physique, UMR 8591, 1 place Aristide Briand, 92195 Meudon Cedex, France
[2]CEA, DAM, DIF, Bruyères le Châtel, 91297 Arpajon Cedex, France
[3]Centro de Geofisica da Universidade de Lisboa, Rua Ernesto de Vasconcelos, Faculdade de Ciências Ed. C8, 6°, 1700 Lisboa, Portugal

Received: 2 April 2009 – Revised: 27 August 2009 – Accepted: 2 October 2009 – Published: 10 November 2009

Abstract. A field survey was organized on the French Mediterranean coasts to investigate the effects of the tsunami induced by the 21 May 2003 Boumerdès-Zemmouri (Algeria) earthquake (M_w=6.9). The results show that eight harbours were affected by important sea level disturbances that caused material loss. Unfortunately, the low sampling rate of the French tide gage records (10 min) does not allow for a proper evaluation of the tsunami wave amplitudes since these amplitudes were probably underestimated in the harbours where these sensors are installed. The survey brings to light regional and local contrasts among the harbours' hydrological responses to the tsunami.

To better understand these contrasts, a numerical simulation of the sea level elevations induced by the tsunami was conducted. The simulation showed a certain correlation between the field results and the wave amplification along the coast; however it underestimated the observed phenomena. Another simulation was then conducted using high resolution bathymetric grids (space step of 3 m) centred more specifically on 3 neighbouring harbours, however, again the simulation results did not match the amplitudes recorded through the observations. In order to better understand the wave amplification mechanisms inside each grid, a Gaussian signal was virtually broadcasted from the source to the harbours. Virtual sensors identified the periods which are stimulated – or not – by the arrival of the signal in each grid. Comparing these periods with those previously recorded emphasizes the proper period of each waterbody.

This paper evaluates the limitations of such a study, focusing specifically on (1) the importance of having accurate and precise data about the source (the lack of information about the signal amplitude leads to an underestimation of the tsunami, thus reproducing only a fourth to a third of the observed phenomenon), (2) the need for networked tide gages with high resolution records and short sampling rates, and (3) the importance of conducting field studies immediately after a tsunami occurs.

Correspondence to: A. Sahal
(alexandre@sahal.fr)

1 Introduction

The Western Mediterranean coasts have suffered from tsunamis in the past, and their present exposure to future tsunami hazard is undeniable. In this geographical location, three main regions are identifiable sources (seismic, as well as submarine landslide sources) for tsunamis:(1) the region of the Ligurian sea from Sanremo to Livorno (Italy) where seismic activities have triggered many devastating tsunamis, such as the earthquake-induced tsunami of 1887 (Eva and Rabinovich, 1997); (2) Sicily and the Aeolian Islands (Italy) which were the sources of numerous tsunamis triggered by eruption-induced submarine landslides (Tinti et al., 2004; Maramai et al., 2005; Gerardi et al., 2008), or triggered by earthquakes, as was the case of Catania in 1693 (Gutscher et al., 2006); and (3) the North-African margin which was a source that triggered several noticeable tsunamis, such as in 1365 and in 1856 (Roger and Hébert, 2008), as well as in 1980 when the El Asnam earthquake triggered a small tsunami that moderately impacted the Spanish shoreline (as shown by tide gauge observations) (Soloviev, 2000).

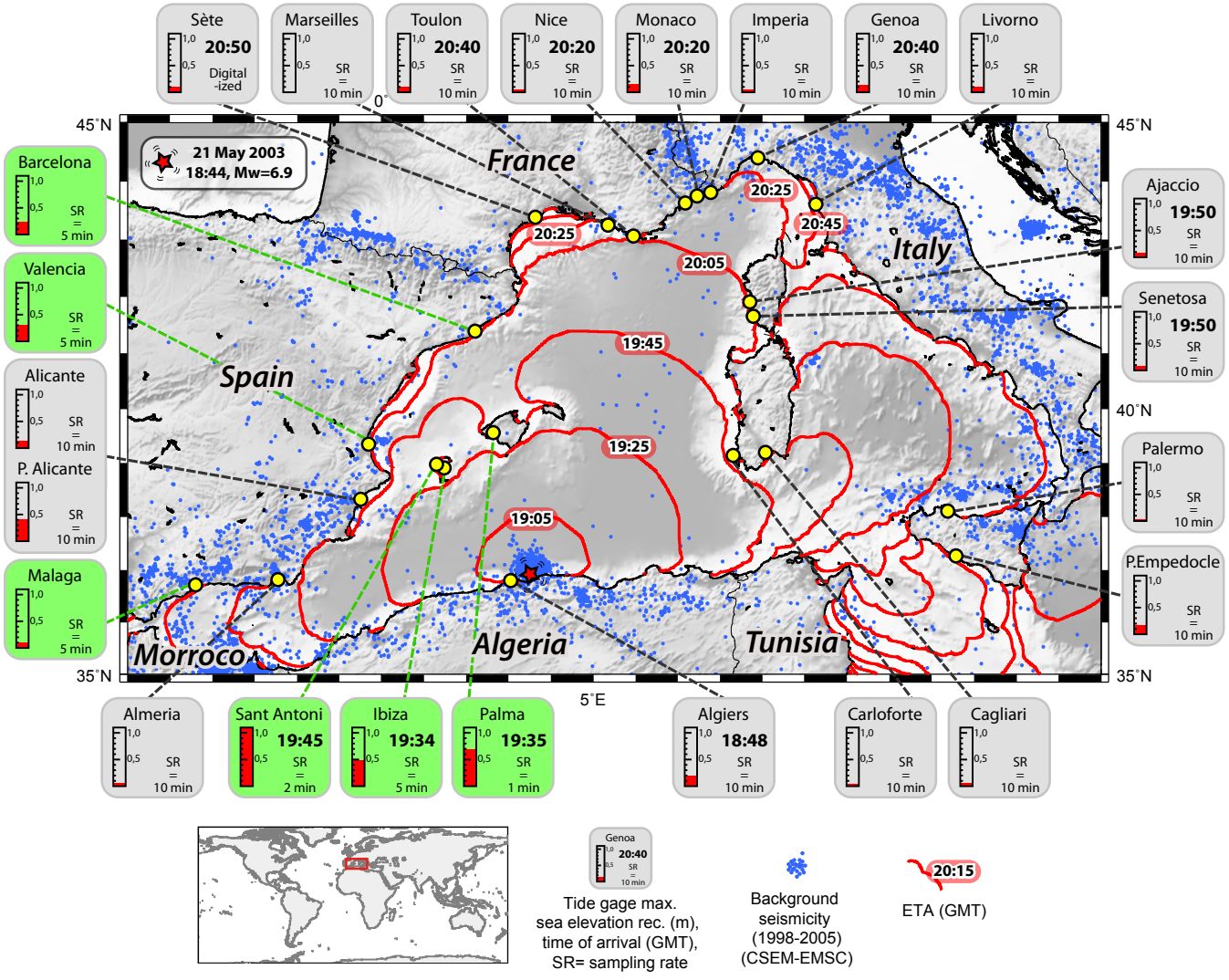

Fig. 1. The 21 May 2003 tsunami in the Western Mediterranean Sea: estimated travel time and tide gage records. The background seismicity depicts the 2003 seismic crisis. The tsunami travel times (red lines) were computed using the TTT SDK v 3.2 (http://www.geoware-online.com/). The colour code for the tide gage stations indicates the various sampling rates for the data acquisition (see text for details).

The French Mediterranean coast was affected by some of these tsunamis, and additionally has suffered from the impact of local submarine landslides, such as in 1979, when the Nice airport embankment collapsed and triggered a tsunami affecting the Baie des Anges, and more specifically, Antibes (Assier-Rzadkiewicz et al., 2000).

More recently, on 21 May 2003 at 18:44 UTC, an earthquake of moment magnitude M_W=6.9 occurred in the region of Boumerdès-Zemmouri, Algeria, generating a tsunami which reached the Western Mediterranean coasts in a time span of a few minutes to several hours (Alasset et al., 2006). Figure 1 shows the maximal sea level elevations recorded by the tide gages of the Western Mediterranean Sea.

The tide gages in operation in 2003 recorded sea level elevations ranging from a few centimetres in Sardinia (Italy) to a meter in the Balearic Islands (Spain). The sampling rates from the tide gages vary from 1 to 10 min. Figure 1 shows that the tide gages with precise sampling rates (less than 5 min, coloured in green) were the only ones to record significant sea level variations (with the exception of Puerto Alicante). In fact, tide gages with sampling rates equal to or larger than 10 min (coloured in grey) are ineffective in recording all the amplitudes of tsunami-induced sea level oscillations because such oscillations happen to have too short main periods (between 15 and 20 min) compared to the sampling interval.

Therefore, the French and Italian tide gage records are not sufficient to evaluate the local impact of the 21 May 2003 Boumerdès-Zemmouri tsunami on the French Mediterranean coast. Consequently, a witness-based investigation along the

shoreline was required to assess the actual impact of this tsunami. In May 2007, a three month field investigation began on the French Riviera and in Corsica to assess if anyone had noticed sea level variations during the evening and the night of 21–22 May 2003, and to build an observation database.

The aim of this article is to: (1) expose the methodology and the results of this field investigation, (2) determine if the simulation can reproduce the same effects using different approaches, (3) improve the understanding of the resonance effects along a tsunami path through frequency analysis, and (4) identify what can be improved concerning data collection in the Western Mediterranean Sea, and more specifically on the French coast, to better understand and mitigate the tsunami hazard.

2 Building a database based on harbour observations

2.1 Field investigation methodology

Figure 1 shows that the tsunami triggered at 18:44 UTC in Algeria should have begun impacting the French coasts around 20:10 UTC (21:10 LT). Since the tsunami occurred at night and during the holiday off-season, the field investigation methodology had to be adapted to account for a potential lack of witnesses, as no one may have been present on the beaches. Therefore, potential witnesses would have been people living on their boats or working in the harbours at night. Consequently, the investigation concentrated mostly on harbours: a total of 135 harbours were contacted and almost all of the harbours accepted to consult their surveillance logs – if one existed – for the night of 21–22 May 2003. During three months, a widely diffused "call for witnesses" was posted in each harbour office next to the meteorological forecasts which are consulted daily by people who sail and fish offshore. The poster asked those who had noticed any hydrological phenomena during the night of 21–22 May 2003 to call a dedicated phone number.

Coast guards, semaphores, the Maritime Rescue Coordination (CROSS) and commercial harbour pilots were also contacted. They agreed to verify their logs for anomalies during the evening and night of 21–22 May 2003. Figure 2 shows the location of investigated harbours and semaphores.

It should be noted that harbours and semaphores cover most of the French seashore, and for the purpose of this study, they represent a comprehensive view of the studied terrain.

Eye-witnesses participated in a semi-directed interview. These interviews were adapted to the specific context of observation: direct observation from a wharf, from a boat alongside the quay, from a boat offshore, or from a specific location (observation tower, semaphore, for example). Details about hydrological phenomena were collected concerning unusual currents, siphons, sea-level variations and/or the corresponding consequences (for example boats moving and making specific noises, boats touching the sea-bottom, etc.). Noticeable impacts were also noted: broken mooring lines, sunken boats, displaced two-ton moorings, etc. The chronological timeline and the physical measurements of these hydrological phenomena, as well as their impacts, were collected as precisely and as often as possible. Written information from the harbour offices' logs was collected and studied when it described unusual phenomena.

Every local, regional and national newspaper archive was also reviewed. The review focused on the week following the earthquake.

2.2 Results and discussion

Of the 135 harbours that were investigated, only 66 had the capacity to observe any unusual hydrological phenomenon through their nocturnal surveillance structure. Of the 66, only 8 harbours noticed hydrological anomalies which could be attributed to the 21 May 2003 earthquake-induced tsunami. The other 69 harbours did not have the nocturnal structures needed and were therefore unable to notice if anything had happened during the night. Also, the following day, they did not notice any consequences of any hydrological anomaly. This is not to say that nothing happened, rather it could mean the phenomenon did not leave any noticeable damage. Figure 3 focuses on the Eastern part of the French Riviera (yellow frame on Fig. 2), which appears to be the only affected area.

Table 1 illustrates the characteristics of each harbour, the number of direct witnesses and the corresponding phenomena. It also shows the chronological timeline of the sea level variation as reported by the witnesses.

Not all harbours were affected by the tsunami in this area. The affected harbours are quite different from each other: various sizes, azimuths of the entrance and of the coast, etc. Most of them were affected by sea elevation variations and boiling phenomena. Of the 8 affected harbours, 6 suffered material loss. La Figueirette and Mouré-Rouge harbours were the most affected: they both suffered from a high amplitude drop of the sea level (0.9 to 1.5 m and 1.5 m, respectively). At the same time, Cannes – Vieux-Port was less affected by sea-level variations. To better understand these differences at a local level, modelling was focused on this area (Fig. 4).

These results have practical limitations. On the one hand, it is quite difficult for witnesses to remember the precise time the event occurred, especially several years after the event. On the other hand, some witnesses are sailors who know their boat and the bathymetry of the harbours quite well. They can easily estimate the sea level variations since they need to adjust their moorings according to the sea level. Other witnesses were working as harbour guards during the night of 21–22 May 2003 and were able to take note of anomalies at precise hours.

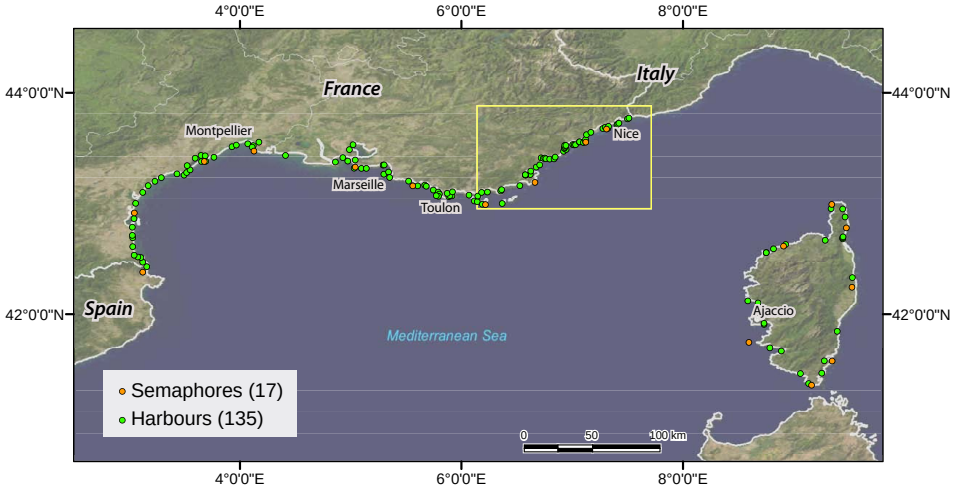

Fig. 2. Location of the investigated harbours and semaphores on the French seashore (background ESRI).

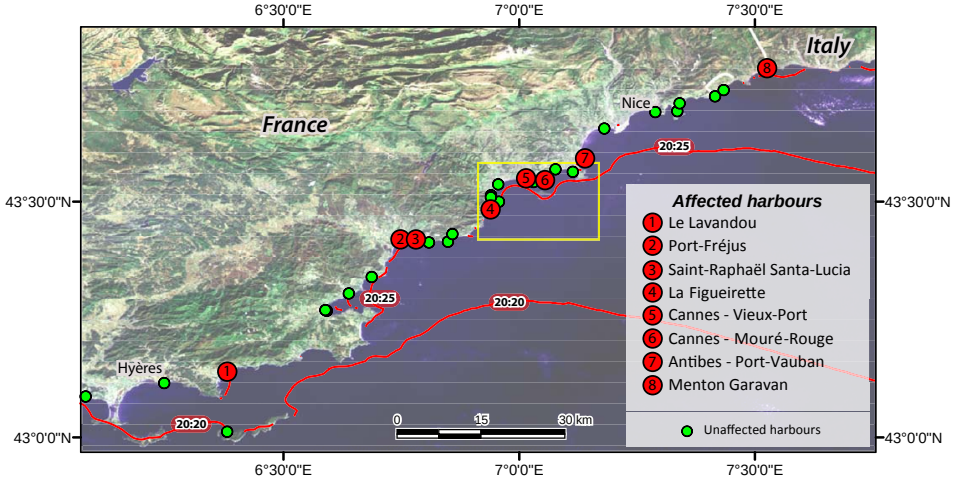

Fig. 3. Location of the harbours affected or supposedly unaffected by the 21 May 2003 earthquake-induced tsunami (background ESRI).

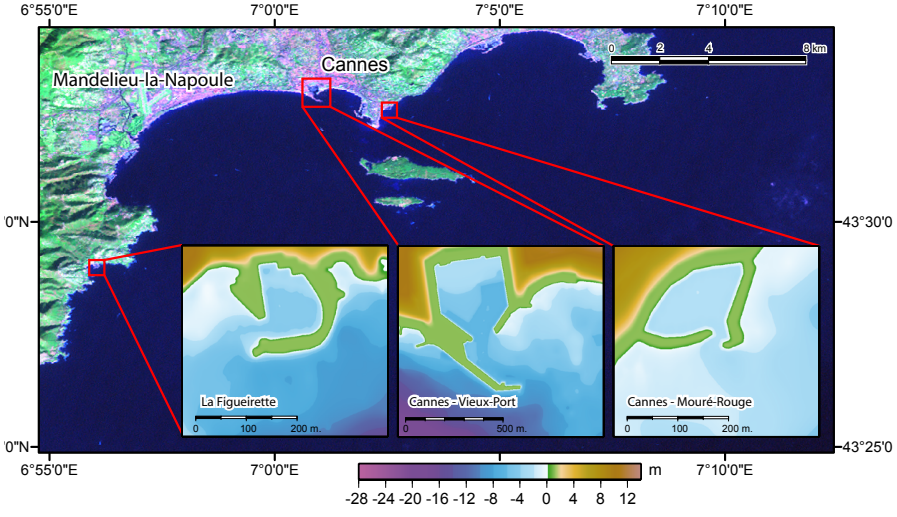

Fig. 4. The three harbours selected for the modelling (background Landsat TM).

Table 1. French harbours affected by the 21 May 2003 tsunami: characteristics and observed hydrological phenomena according to witnesses.

	Basin/harbour characteristics						Observations											
								Time interval				Minimal trough (m)		Maximal crest (m)				
	Major lenght	Minor lenght	Mean depth	Entrance level	Entrance azimuth	Global azimut	Direct witnesses	min	max	min	max	min	max	min	max	max. currents	Other hydrologic phenomena	Noticed impacts
	(m)	(m)	(m)	(m)												(nds)		
Le Lavandou	400	140	4.5	145	S	S	1		22:30									boats sank
Port-Fréjus	650	210	3	68	E	S	1	20:00	21:00			−0.15	−0.2		0			none
Saint-Rahaël Santa-Lucia	380	125	4.5	47	N and S	S	1		21:30		04:00							keels touched the sea bed in the harbour
La Figueirette	146	140	3.6	23	W	SE	4	20:00	20:30		02:00	−0.9	−1.5	0.7	0.9	15	strong current; eddies; boiling phenomena	keels touched the sea bed in the harbour; a 5 m long vessel sank; 2-ton mooring moved; mooring disrupted
Cannes – Vieux-Port	480	335	5.7	236	E	S	1	21:30			00:00					12	strong currents; boiling phenomena	numerous 2-ton moorings moved
Cannes – Mouré Rouge	200	100	1.9	26	S	SE	3	20:30	21:00	00:30	00:45	−1.5		0.3			fishes jumping out of the water; eddies; siphon and "water step" at the antry of the harbour	a vessel was grounded on the dam; moorings disrupted; numerous 2-ton mooring moved
Antibes – Port-Vauban	1000	520	5.5	180	N	E	3		21:00			−0.6			0.2			keels touched the sea bed in the harbour
Menton Garavan	550	160	2.5	57	ENE	S	2		21:00		23:00	−4.0			0		big eddies at the the harbour entry of	none

Nevertheless, in order to build observation databases a large number of testimonies are needed. Unfortunately, only a few could be recorded. The lack of witnesses can be explained by the phenomenon's arrival late at night on the French coasts (after 21:00 LT). Video surveillance tapes could have been more objective witnesses, but they are not kept longer than a month. Therefore it is essential that such field investigations be processed as soon as an event occurs since time is a crucial factor.

To better understand these observations, the tsunami was modelled in the Western Mediterranean Sea and the effects on the three selected harbours of the French Riviera were simulated.

3 Tsunami modelling

3.1 Generalities

The method applied to model tsunami initiation, propagation and coastal impact has been in development for several years with the objective of studying tsunami hazards in regions such as French Polynesia (Sladen et al., 2007) and the Mediterranean Sea (Alasset et al., 2006; Roger and Hébert, 2008), and to better understand the source characteristics of tsunamigenic earthquakes (Hébert et al., 2005; Sladen and Hébert, 2008). The initial sea surface elevation is obtained from the sea bottom co-seismic deformation (computed using the Okada formula, 1985), and considers a full and instantaneous deformation from the bottom to the surface of the sea. Then, to calculate the propagation, the hydrodynamical equations are solved, under the non-linear shallow water approximation, with a finite difference Crank Nicolson scheme applied to a series of nested bathymetric grids to account for the shoaling effect that occurs close to shores. It is worth noting that for this type of shallow water propagation, the tsunami propagation is non-dispersive, and the celerity equation depends only on water depth.

In the present case, different authors attempted to describe the seismic event, proposing different sources and deformation scenarios, based either on seismic or GPS data (Delouis et al., 2004; Mourad Bezzeghoud, University of Evora, Portugal, personal communication in 2006; Meghraoui et al., 2004; Semmane et al., 2005; Yelles et al., 2004; parameters are described in Table 2).

All of these scenarios have been tested and the results indicate that several sources match the tide gage records in the Balearic Islands fairly well, especially Delouis'. However, even though the phases were properly modelled, the

Table 2. Sources and characteristics of the 21 May 2003 earthquake according to various authors.

	Delouis	Bezzeghoud	Meghraoui	Semmane	Yelles
Longitude	36.83° N	36.83° N	36.83° N	36.83° N	36.91° N
Latitude	3.65° E	3.65° E	3.65° E	3.65° E	3.65° E
Depth of the fault centre (km)	∼6	∼8	∼8	∼16	∼9
Strike (°)	70	64	54	54	60
Dip (°)	45	50	50	47	42
Rake (°)	95	111	90	90	84
Length (km)	60	50	54	64	32
Width (km)	24	16	15	32	14

computed amplitudes proved to be too low to fit the data (Alasset et al., 2006). Thus, given that all of the seismic sources yielded nearly similar results in terms of tsunamis, the source proposed by Delouis et al. (2004) was the one chosen in this study for the purpose of modelling.

The main bathymetric grid used for tsunami modelling includes the entire Western Mediterranean Sea. It was built from GEBCO data (GEneral Bathymetric Chart of the Oceans, British Oceanographic Data Centre, 1997, resolution 1') and interpolated at a space step of 1000 m. The grid was used to model the co-seismic deformation derived from the model proposed by Delouis et al. (2004), and then to compute the maximal sea elevation reached in each cell of the grid in the Western Mediterranean Sea during the first 4 hours after the earthquake (Fig. 5).

3.2 Results

3.2.1 General results

Figure 5 clearly shows that the maximal energy wave is directed mostly towards the Balearic Islands, as aforementioned by Alasset et al. (2006). In fact, this pattern is very dependent on the fault azimuth used, but all models showed that the Balearic Islands were the most impacted. At the same time, various acceptable azimuths only changed which island was impacted the most, either Ibiza or Majorca (Alasset et al., 2006). This kind of pattern is also noticeable for the 1856 Jijel (Algeria) earthquake and associated tsunami, which is assumed to have struck mostly Menorca and the eastern part of Mallorca (Roger and Hébert, 2008). Whatever the case, the role that submarine canyons appear to play in wave amplification should be mentioned.

Figure 5 also reveals amplifications in several places along the Spanish, Sardinian, Corsican and South-eastern French shorelines. However, these amplifications are still less than 10 cm high on this large grid (grid 0). On the large scale, modelling clearly shows that for the French shoreline, amplified values coincide well with the areas that the field investigation determined to be affected, e.g. the Eastern French Riviera. In contrast, the Western Mediterranean French shoreline (Gulf of Lion) shows less important sea level elevations.

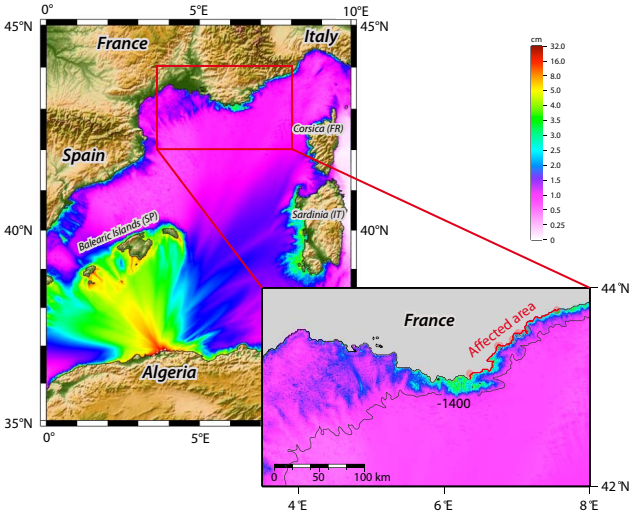

Fig. 5. Modelling of the maximal sea elevation reached during the first 4 h after the earthquake, based on Delouis' source (grid 0).

Such low elevations could be mostly explained by the shield effect of the Balearic Islands, by the loss of energy of the phenomenon when reaching the continental margin of the Gulf of Lion, and by the wide extent of the corresponding submarine shallow shelf. However, more generally, in South-eastern France, the simulated amplifications (a few centimetres of wave amplitude) are less than those witnessed during the event, but could be in agreement with the recorded signal from the tide gages in Nice (43.695° N, 7.285° E). However, the results obtained using a large scale grid of 1000 m of resolution are not expected to account for the shoaling effect which mostly contributes to the tsunami amplification when the water depth decreases in the last few tens of meters, especially along Mediterranean French coasts which are associated with steep slopes. Areas of major amplification may also match bathymetric features such as submarine canyons or particular shelf shapes that are not well mapped on the GEBCO grid.

Therefore, in order to more accurately estimate the amplification associated with the shoaling effect, the model was processed on a more precise scale on the coasts, using multi-scale grids. Coastal and harbour bathymetric grids were built to gradually enhance the precision of bathymetric data from the source to the studied harbours. As mentioned previously, the Figueirette and Mouré-Rouge harbours seem to be the locations where the most important amplifications were reported in 2003. However, nothing was reported by witnesses for the Vieux-Port of Cannes located between these 2 harbours. Thus, these 3 harbours represent good candidates to more accurately study wave amplification in Southern France during the 2003 event and to understand the observed differences.

The high resolution grids of the 3 studied harbours were built with data from GEBCO and from the French SHOM

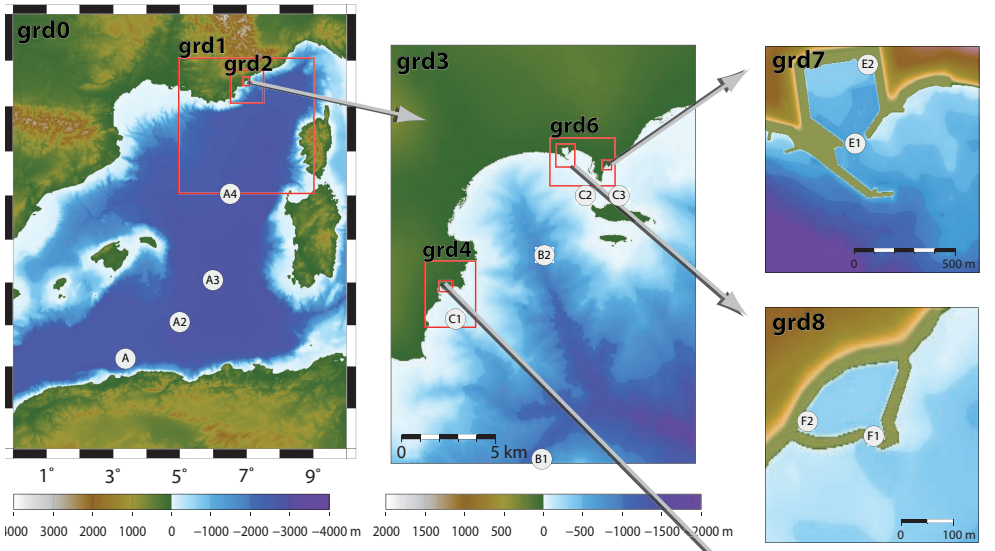

Grid (grd) n°	Boundaries		Space step (m.)
0	0°/10°E	35°N/45°N	1000
1	5°E/9°E	41°N/44°N	500
2	6.5°E/7.5°E	43°N/43.75°N	150
3	6.9°E/7.1°E	43.4°N/43.6°N	40
4	6.924°E/6.955°E	43.47°N/43.49°N	13
5 (Figueirette)	6.9316°E/6.9366°E	43.4816°N/43.485°N	3
6	7.005°E/7.05°E	43.528°N/43.552°N	13
7 (Vieux-Port)	7.01°E/7.023°E	43.5416°N/43.5516°N	3
8 (Mouré-Rouge)	7.04°E/7.945°E	43.54°N/43.544°N	3

Fig. 6. Grids and sensors used to model the maximal sea elevation reached in the three studied harbours after the 21 May 2003 earthquake.

(Service Hydrographique et Océanographique de la Marine) with a 3 m space step and completed using navigation maps (Escales, 2007). Interpolation/extrapolation was used in parts of the harbours with no available data, by using pictures, satellite views, etc., in order to obtain a better representation of the harbours' geometry. Finally, a total of 9 imbricated grids were built on 6 levels of resolution (Fig. 6).

3.2.2 Results in harbours

The modelling results (Fig. 7) show the greatest amplification inside the La Figueirette harbour, which is the smallest studied harbour (maximum wave height reaching over 22 cm).

This result is clearly less than the observations, as the observations reveal a maximum wave height reaching more than 70 cm in La Figueirette harbour. Even if the modelled propagation time was matched to the observed time of arrival (one hour after the earthquake, taking into account potential inaccuracies in witness accounts), the simulated elevation would still be less than the reported observation. As in previous studies on the impact of this event on the Balearic Islands (Alasset et al., 2006), the model reproduces only a fourth to a third of the recorded or observed maximal amplitudes.

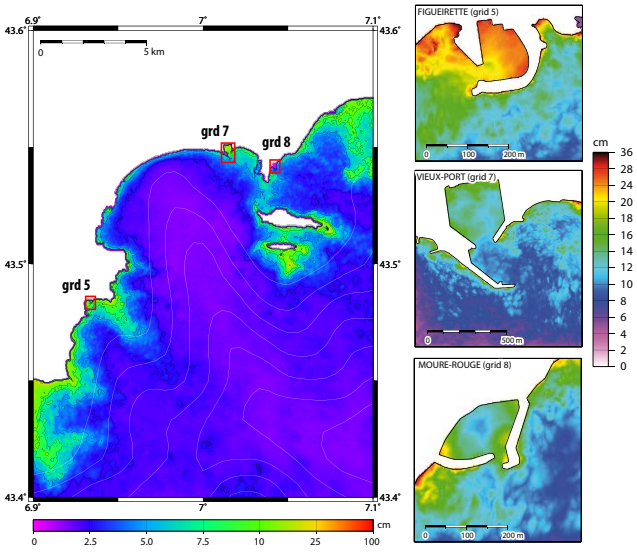

Fig. 7. Maximal sea level elevation during the first 4 h after the earthquake in the three studied harbours and the bay of Cannes.

Concerning the Vieux-Port, the largest studied harbour (located between the 2 harbours where the maximum amplitudes were observed), a very small sea level variation is obtained, with a maximum of about 15 cm. The Mouré-Rouge harbour is hardly larger than La Figueirette, and seems to be much less affected. Perhaps the presence of the Lérins Islands to the south of the Mouré-Rouge harbour shielded it (Fig. 7), but this has to be demonstrated further.

Globally, the detailed modelling does not allow for a reproduction of the observations in terms of amplitude. It is important to mention here that the accounts given by witnesses four years after an event need to be considered with caution. However, these modelling results confirm that the La Figueirette harbour was the most affected site, at least in relation to the two other ones studied.

One idea proposed in this study is that additional amplifications, due to resonances outside or inside the considered harbours, may have also occurred. The modelling method already accounts for these phenomena, as in French Polynesia (e.g. Hébert et al., 2009) where long lasting resonance periods observed were efficiently accounted for by the tide gages in Taiohae Bay. Therefore, since the seismic source seems to produce amplitudes that are too low, a frequency analysis of the signal from the source (Algerian Margin) to the French coasts is conducted. Additionally, the responses are tested in the bay and in the harbours and then discussed using synthetic modelling.

3.2.3 Frequency analysis in harbours

Numerous studies have shown that submarine features or sudden bathymetric changes could have consequences on incident wave amplitudes, inducing, for example, the shelf resonance (Monserrat et al, 2006; Horillo et al., 2008; Munger and Cheung, 2008). Carrier et al. (1971) showed that seismic-generated tsunamis, like atmospheric pressure disturbances, are possible causes of harbour resonance. Changes in the geometry of a harbour modify its natural period of oscillation (Monso de Prat and Escartin Garcia, 1994; Bellotti, 2007). This is an important aspect to consider in order to protect a harbour against the arrival of long waves.

In the realm of this study, the objective is to understand why, in the same area, some harbours like the La Figueirette harbour were affected in 2003, while others such as the Vieux-Port and Mouré-Rouge harbours were not affected or were only affected a little. Therefore, the study focused on the evolution of periodic components of the tsunami during its propagation from its origin (the Algerian margin) to its arrival on the continental shelf and onwards to the coast.

The aim is to use parallel synthetic tsunami modelling in order to avoid relying on the seismic source and in order to consider only the harbours. To define the periods which need to be studied, the results of the modelling are integrated with data about the seismic source and are analysed. The attention is then focused on the most precise grids (the harbours): synthetic tide gages are placed over the different grids (a few are located on Fig. 6), particularly in harbours, in locations which do not correspond to nodes (minimal sea level amplitude for the standing wave), i.e. near the structures of the harbours in question (breakwaters, piers, etc.), where the anti-nodes occur. This is an important aspect to take into account for resonance investigations. Spectral analysis of each recorded synthetic signal is performed using FFT (Fig. 8).

On the scale of the Western Mediterranean sea, the frequency analysis of the signal recorded by the synthetic sensors from the Algerian shore to the French coasts reveals the appearance and disappearance of main periods. Except for a global diminution of the main amplitude during the propagation from A1 to A2 (loss of energy due to depth and geometrical spreading), the sensors recorded a decrease in the low frequency peak (20–25 min) as time passes from sensor A1 to sensor A4. A second peak (16–17 min) remains during the entire propagation process. These two peaks can be linked to the geometry of the rupture. Nothing particular about the high frequencies (less than 10 min) can be deduced.

Similarly, given that every water body (including man-made harbours or bays) has natural oscillation modes with eigenperiods that depend on its physical characteristics (Jansa et al., 2007), i.e. its geometry and depth (Monso de Prat and Escartin Garcia, 1994; Woo et al, 2004), a spectral analysis in the different grids was conducted, especially on the 3 harbours' grids, using a method inspired by Yalciner and Pelinovsky (2006) which these authors used in the Marmara Sea. This methodology consists in comparing the evolution of a signal modelled with the available information about its source all along its path to the evolution of a well known synthetic signal along the same path. Through modelling, the synthetic signal is altered by the environment of the basin. By comparing these two signals, this methodology enables one to highlight the main frequencies (peaks) of each grid: if a peak is invisible on the synthetic signal analysis but visible on the source based signal analysis, it can be deduced that this peak is attributable to the source. It is to be noted that unlike in the case of the Marmara Sea, the studied basin is open. Several tests on open basins which resonance periods were known have been conducted in the bay of Sainte-Anne (Guadeloupe, eastern Caribbean Sea) and validated this methodology for such basins (Roger et al., 2009). Following this methodology, a FFT algorithm is used to analyse the evolution of an arbitrary initial surface with virtual gage points (Fig. 9). In this case, the known synthetic signal is a Gaussian.

A manual correlation between the main frequency peaks of the different spectra is conducted. The main period peak (low frequencies), which corresponds to a very large and also dissipative period (the more the harbour is open, the more it is large; the resonance is not well auto-maintained), can be explained by the non-closed structure of the harbour (confirmed by additional calculations not presented here in this study).

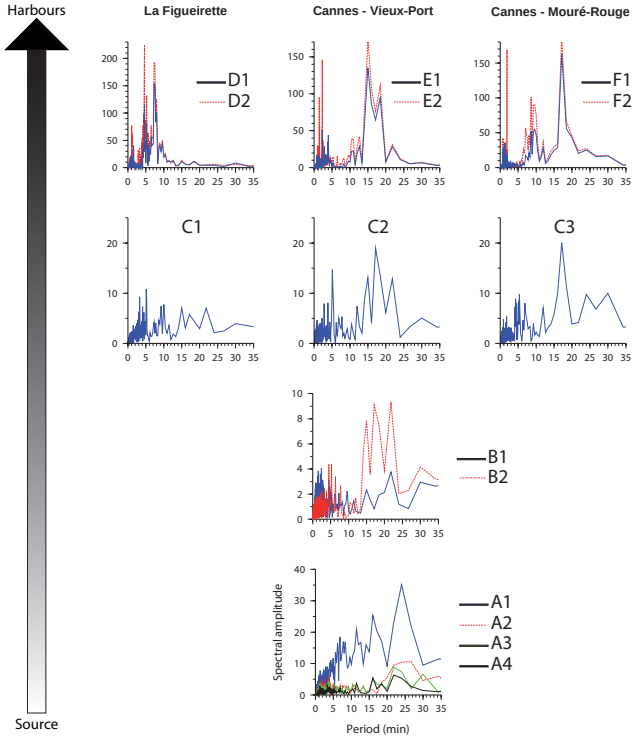

Fig. 8. Signal evolution from the source (Delouis et al., 2004) to the harbours in the Gulf of La Napoule (A1 to F2 are the sensors located on Fig. 6).

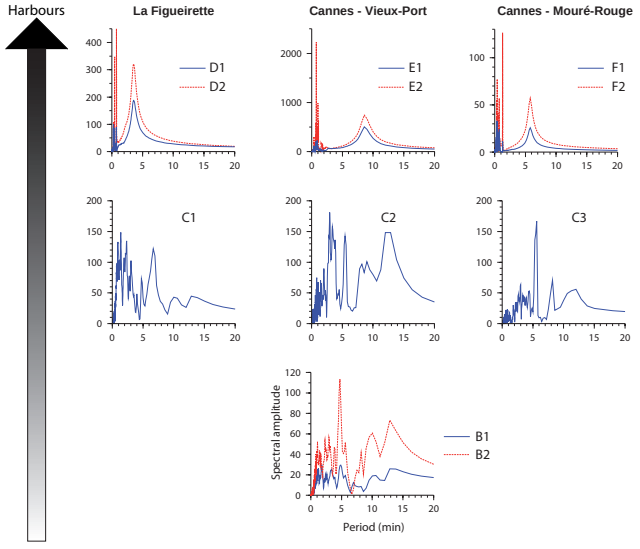

Fig. 9. Responses of the virtual sensors to a synthetic signal.

The comparison of the signals recorded by five synthetic sensors located in the La Napoule Bay (B1, B2, C1, C2 and C3, Fig. 8) shows that the previously described 16–17 min peak is still present and even amplified offshore from the Vieux-Port and the Mouré-Rouge harbours (respectively C2 and C3). As this peak is not on the signal spectrum for the area where the Gaussian is applied (Fig. 9), the peak is consequently linked to the source, and not to a local resonance phenomenon. The amplification of this peak is limited offshore from the La Figueirette's harbour (C1), probably due to the presence of a submarine canyon (Fig. 6, grd3) which diminishes the spectral amplitudes (important dissipation). Similarly, a 7–8 min peak appears in front of the La Figueirette harbour (Fig. 8) which is not reproduced by the synthetic signal (Fig. 9). Can this peak be linked to the source? All the other peaks present in Fig. 8 are in phase with the calculated synthetic signals (Fig. 9).

Regarding the signal in the La Figueirette harbour, the D1 and D2 synthetic signal graphs (Fig. 9) show that the 16–17 min peak is still present on Fig. 8, but its amplitude is clearly diminished. The signals recorded from the application of the Gaussian (Fig. 9) indicate that the 5 min peak could be generated by a resonance effect caused by the entrance of the harbour since it disappears when the harbour is closed. The 1 min peak is also attributable to the harbour's entrance, while the 7–8 min peak (which is the same on D1 and D2, Fig. 8) could correspond to a resonance outside the harbour.

In comparison to the signal in the Vieux-Port harbour, the 16–17 min peak is visible at the arrival of the signal in the harbour (Fig. 8) and could be attributed to the source as it is not reproduced by the synthetic signal (Fig. 9). No peak is attributable to the harbour's entrance. On the other hand, the 1 min peak is still visible, associated with the 2 and 4 min peaks (Fig. 8). These three peaks are amplified from the entrance (E1) to the far end of the harbour (E2). The 2 and 4 min peaks are not attributable to the Gaussian signal and are therefore probably due to a local interference (resonance before the harbour's entrance).

In the Mouré-Rouge harbour, the peaks which are due to the resonance of the harbour (less than 2 min) are well reproduced by the Gaussian and are amplified from F1 to F2. The peak associated with the entrance of the harbour (around 6 min) is still visible, but partially masked by a larger peak of a 10 min period which is not reproduced by the synthetic signal. This peak could be generated by the semi-enclosed water body between the Lérins Islands and the continental shore.

3.3 Discussion about the modelling

The amplifications observed by the witnesses are neither reproduced by a realistic earthquake source (Delouis et al., 2004), nor by any source available (Yelles et al., 2004; Meghraoui et al., 2004). Consequently, the study attempted to determine the characteristics which would have produced the actual observations. The detailed frequency analysis allows one to distinguish the imputable spectral component of

the source from the spectral characteristics due to harbour structures. The additional synthetic analysis using a Gaussian signal indicates which type of signal is able to stimulate the harbours or bays in question, leading to important wave amplifications. As in the Balearic Islands where the modelled amplitudes also fit poorly to the actual observations, this issue remains unexplained. Numerical dispersion exists in the modelling method, but results obtained in French Polynesia with much longer propagation paths never suffered from this poor fit when using realistic seismic sources.

When comparing the spectrums obtained with the signal coming from the seismic source to the spectrums obtained with the signal coming from the synthetic Gaussian signal, one can clearly see that some of the peaks present on the second spectrum (synthetic) do not appear on the first one (seismic source signal). This indicates that the modelled source does not stimulate all the proper modes (fundamental and/or harmonics) of the harbours. The eigenperiod of the source's signal is probably not correct, whether or not what was observed in the La Figueirette and Mouré-Rouge harbours is actually a resonance phenomenon.

The lack of physical dispersion in the propagation model could be a primary reason for the mismatch between the models and the observations, after taking into consideration the validity of eyewitness reports, as previously mentioned. Indeed, for such a moderate event, shorter tsunami wavelengths could have also been generated. A more rigorous model should take into account the dispersion of wavetrains (Boussinesq model). In addition, the very late observations reported in the harbours could be in agreement with late arrivals of dispersed wavetrains, characterized by shorter periods, which could have caused the La Figueirette's harbour to resonate. Another reason, not completely independent from the former, stands that some places along the coast could be receptive to some waves arriving from Algeria that exhibit resonance phenomena, as it was shown by Roger and Hébert (2008) in the Balearic Islands for the 1856 event. Once again, late and dispersed wavetrains could induce resonances at specific arrival times. A proper physical dispersion would allow shorter wavelengths to get amplified, stimulating short eigenperiods in some harbours. However, using a Boussinesq model would also diminish the final amplitudes, yet, it would not be required for this study as the earthquake source seems to be too low with respect to tsunami observed amplitudes.

Another weakness in the modelling could be the lack of data concerning the exact bathymetry of the harbours. Bathymetric data is not currently dense enough on the coasts (shallow water) and practically non-existent in harbours. However the data from SHOM are well resolved close to the shores, except in the harbours where the constructed grids may be not precise enough, as previously mentioned (see Sect. 3.2). However, an error of 15% on the mean water depth should not shift the main spectral values by more than 10%.

Nevertheless, the models presented in this study have helped determine the resonance periods in the studied sites, and these periods appear to be important parameters for sea level variation amplifications. By integrating data from witnessed observations into the model, the identification of the signal's periodic components in proximity to the harbours, and even at the tsunami's source, is possible. This approach displays the relationship between the resonance period (or the harmonics) of a basin – such as a harbour – and its exposure to wave amplification (Bellotti, 2007).

Harbour resonance is probably not the only parameter which has an influence on the harbours' response to the signal. A statistical study comparing the harbours' entrance orientation, geometry, etc. to the witnessed impacts could bring forward other explanations.

4 Conclusions

Four years after the tsunami triggered by the 21 May 2003 Boumerdès-Zemmouri (Algeria) earthquake, a long and careful survey was conducted along the French Mediterranean coast. The maritime authorities and 135 harbours were contacted and interviewed about the observations they noticed in the hours following the earthquake.

Assessing the impacts of such a relatively small tsunami was quite challenging, as it had not been identified as a tsunami by the harbour authorities, and therefore no official national report was made concerning its impact. The conducted survey enlightened and summarized the effects of the 2003 Mediterranean Sea tsunami on the French coasts, which had not previously been studied. The results of this study showed that the effects of the tsunami was underestimated by the French tide gage records, as it had consequent effects in many French harbours.

Compared to the field observations, the various modelling approaches showed an underestimation of about a fourth to a third of the actual effects of the 21 May 2003 tsunami. Such a gap could be linked to an underestimation of the initial deformation amplitude at the source. The role of the resonance phenomenon has been underlined as an important factor of wave amplification in bays and harbours. This phenomenon needs to be refined in a detailed tsunami modelling, especially for small magnitude events. Knowing the period of resonance for each harbour allows one to deduce which wave frequency falls into resonance inside that particular water body, and thus helps one to more accurately predict and prevent the effects of the hazard for specific tsunami wavelengths. A more detailed analysis of a harbour's resonance would nevertheless be improved using continuous tide gage data whose spectral analysis provides the main eigenperiods of the basins (Monserrat et al., 1998).

Finally, the Western Mediterranean shores are not the most exposed to the tsunami hazard. The hazard level is quite low, with low recurrence and low intensities. However, the shores

are very vulnerable, as they are highly urbanized and populated, especially during summer. The 2003 phenomenon would have caused more damage due to the 15-knot currents (7 m/s) that were observed if it had occurred in the middle of the day when traffic is increased in harbours.

This study underlines the need for post-tsunami surveys to be organized as soon as a tsunami occurs, covering all the potentially affected shores. It would be interesting to organize such surveys for the 2003 event in all the Western Mediterranean basin, and more particularly in Spain, Algeria, Tunisia and Italy, where modelling shows an important amplification of the sea level elevation along these shores.

Acknowledgements. The authors would like to thank the CEA (French atomic energy commission) who financed the field investigation along the French shore. The work was funded within the FP6 European project TRANSFER under contract 037058 and within the RiskNat program under contract ANR-08-RISKNAT-005-01/MAREMOTI. The paper benefited from constructive reviews by Alexander B. Rabinovich and an anonymous referee.

The authors would also like to thank all the administrations who provided them with the records of the tide gages:

J. P. Alasset, from the "Institut de Physique du Globe de Strasbourg", who collected several records of the Italian tide gages through the "Istituto Superiore per la Protezione e la Ricerca Ambientale" (ISPRA).

The Italian ISPRA, and more specifically the technical services provided by S. Corsini, for the tide gage in Genova.

The French "Service Hydrologique de la Marine Nationale" (SHOM), and more specifically R. Jehan who provided the records of the tide gage in Nice (France); R. Creach and P. Bonnefond from the SHOM's RONIM project for the other French tide gages.

The French "Service de Navigation Maritime Languedoc Roussillon" (SNMLR), who provided the records of the tide gage in Sète.

The Spanish "Instituto Español de Oceanografía de Madrid" (IEO, Spanish Oceanographic Institute), and more specifically M. J. Garcia who provided the records of the tide gage in Palma de Mallorca.

The Spanish "IGN Madrid", and the "Puertos del Estado Madrid" administrations, for the records of the other Spanish gages.

The CROSS, for searching their database for interventions during the evening of 21 and the night of 21–22 May.

All the harbours' staff which participated in, or facilitated, the field investigation.

All of the witnesses who accepted to share their experience of the 2003 Boumerdès-Zemmouri tsunami with us.

Finally, Christa Teplicky who kindly corrected this article.

Edited by: S. Tinti
Reviewed by: A. Rabinovich and another anonymous referee

References

Alasset, P.-J., Hébert, H., Maouche, S., Calbini, V., and Meghraoui, M.: The tsunami induced by the 2003 Zemmouri earthquake (Mw=6.9, Algeria): modelling and results, Geophys. J. Int., 166, 213–226, 2006.

Assier-Rzadkieaicz, S., Heinrich, P., Sabatier, P. C., Savoye, B., and Bourillet, J. F.: Numerical Modelling of a Landslide-generated Tsunami: The 1979 Nice Event, Pure Appl. Geophys., 157(10), 1707–1727, 2000.

Bellotti, G.: Transient response of harbours to long waves under resonance conditions, Coast. Eng., 54, 680–693, 2007.

Carrier, G. F., Shaw, R. P., and Miyata, M.: The response of narrow mouthed harbours in a straight coastline to periodic incident waves, J. Appl. Mech., 38E-2, 335–344, 1971.

Delouis, B., Vallee, M., Meghraoui, M., Calais, E., Maouche, S., Lammali, K., Mahsas, A., Briole, P., Benhamouda, F., and Yelles, K.: Slip distribution of the 2003 Boumerdès-Zemmouri earthquake, Algeria, from teleseismic, GPS, and coastal uplift data, Geophys. Res. Lett., 31, L18607, doi:10.1029/2004GL020687, 2004.

Eva, C. and Rabinovich, A. B.: The February 23, 1887 tsunami recorded on the Ligurian coast, western Mediterranean, Geophys. Res. Lett., 24(4), 2211–2214, 1997.

Escales: Guide de Bord, edited by: "Editions de Chabassol", Bussy-St-Georges, France, 592 pp., 2007.

Gerardi, F., Barbano, M. S., De Martini, P. M., and Pantosti, D.: Discrimination of Tsunami Sources (Earthquake versus Landslide) on the Basis of Historical Data in Eastern Sicily and Southern Calabria, B. Seismol. Soc. Am., 98(6), 2795–2805, 2008.

Gutscher, M. A., Roger, J., Baptista, M.-A., Miranda, J. M., and Tinti, S.: Source of the 1693 Catania earthquake and tsunami (southern Italy): New evidence from tsunami modelling of a locked subduction fault plane, Geophys. Res. Lett., 33, L08309, doi:10.1029/2005GL025442, 2006.

Hébert, H., Schindelé, F., Altinok, Y., Alpar, B., and Gazioglu, C.: Tsunami hazard in the Marmara Sea (Turkey): a numerical approach to discuss active faulting and impact on the Istanbul coastal areas, Mar. Geol., 215, 23–43, 2005.

Hébert, H., Reymond, D.,, Krien, Y., Vergoz, J., Schindelé, F., Roger J., and Loevenbruck , A.: The 15 August 2007 Peru earthquake and tsunami: influence of the source characteristics on the tsunami heights, Pure Appl. Geophys., 166, 1–22, 2009.

Jansa, A., Monserrat, S., and Gomis, D.: The rissaga of June 2006 in Ciutadella (Menorca), a meteorological tsunami, Adv. Geosci., 12, 1–4, 2007, http://www.adv-geosci.net/12/1/2007/.

Maramai, A., Graziani, L., and Tinti, S.: Tsunamis in the Aeolian Islands (southern Italy): a review, Mar. Geol., 215(1–2), 11–21, 2005.

Meghraoui, M., Maouche, S., Chemaa, B., Cakir, Z., Aoudia, A., Harbi, A., Alasset, J.-P., Ayadi, A., Bouhadad, Y., and Benhamoud, F.: Coastal uplift and thrust faulting associated with the Mw=6.8 Zemmouri (Algeria) earthquake of 21 May, Geophys. Res. Lett., 31, L19605, doi:10.1029/2004GL020466, 2003.

Monserrat, S., Rabinovich, A. B., and Casas, B.: On the Reconstruction of the Transfer Function for Atmospherically Generated Seiches, Geophys. Res. Lett., 25(12), 2197–2200, 1998.

Monserrat, S., Vilibić, I., and Rabinovich, A. B.: Meteotsunamis: atmospherically induced destructive ocean waves in the tsunami frequency band, Nat. Hazards Earth Syst. Sci., 6, 1035–1051,

2006, http://www.nat-hazards-earth-syst-sci.net/6/1035/2006/.

Monso de Prat, J. L. and Escartin Garcia, F. J.: Long wave resonance effects produced by changes in the layout of the port of Ciutadella (Menorca, Spain), Bulletin of the Permanent International Association of Navigation Congresses, 83/84, 209–216, 1994.

Munger, S. and Cheung, K. F.: Resonance in Hawaii waters from the 2006 Kuril Islands tsunami, Geophys. Res. Lett., 35, L07605, doi:10.1029/2007GL032843, 2008.

Roger, J. and Hébert, H.: The 1856 Djijelli (Algeria) earthquake and tsunami: source parameters and implications for tsunami hazard in the Balearic Islands, Nat. Hazards Earth Syst. Sci., 8, 721–731, 2008,
http://www.nat-hazards-earth-syst-sci.net/8/721/2008/.

Roger, J., Allgeyer, S., Hébert, H., Baptista, M. A., Loevenbruck, A., and Schindelé, F.: The 1755 Lisbon tsunami in Guadeloupe Archipelago: contribution of numerical modelling, The Open Oceanography Journal, accepted, 2009.

Semmane, F., Campillo, M., and Cotton, F.: Fault location and source process of the 2003 Boumerdès, Algeria, earthquake inferred from geodetic and strong motion data, Geophys. Res. Lett., 32, L01305 1–4, 2005.

Sladen, A., Hébert, H., Schindelé, F., and Reymond, D.: Evaluation of far-field tsunami hazard in French Polynesia based on historical data and numerical simulations, Nat. Hazards Earth Syst. Sci., 7, 195–206, 2007,
http://www.nat-hazards-earth-syst-sci.net/7/195/2007/.

Sladen, A. and Hébert, H.: On the use of satellite altimetry to infer the earthquake rupture characteristics: application to the 2004 Sumatra event, Geophys. J. Int., 172, 707–714, 2008.

Soloviev, S., Solovieva, O. N., Go, C. N., Kim, K. S., and Shchetnikov, N. A.: Tsunamis in the Mediterranean Sea 2000 B.C. – 2000 A.D. Advances in Natural and Technological Hazards Research, Kluwer Academic Publishers, 237 pp., 2000.

Tinti, S., Maramai, A., and Graziani, L.: The new catalogue of the Italian tsunamis, Nat. Hazards, 33, 439–465, 2004.

Woo, S.-B., Hong, S.-Y., and Han, K.-N.: Numerical study of nonlinear resonance in narrow bay, OCEANS '04, MTTS/IEEE TECHNO-OCEAN '04, 3, 1512–1518, ISBN: 0-7803-8669-8, 2004.

Yalciner, A. C. and Pelinovsky, E. N.: A short cut numerical method for determination of periods of free oscillations for basins with irregular geometry and bathymetry, Ocean. Eng., 34(5–6), 747–757, 2007.

Yelles, K., Lammali, K., and Mahsas, A.: Coseismic deformation of the May 21st, 2003, Mw=6.8 Boumerdes earthquake, Algeria, from GPS measurements, Geophys. Res. Lett., 31, L13610, doi:10.1029/2004GL019884, 2004.

Zeitschrift für Geomorphologie Vol. 54, Suppl. 3, 099-126
Stuttgart, Juli 2010

Article

Holocene tsunamigenic sediments and tsunami modelling in the Thermaikos Gulf area (northern Greece)

Klaus Reicherter, Ioannis Papanikolaou, Jean Roger, Margret Mathes-Schmidt, Dimitrios Papanikolaou, Stefan Rössler, Christoph Grützner and Georgios Stamatis

with 10 figures and 1 table

Abstract. Shallow drill cores in flat and southerly exposed coastal areas around the Thermaikos Gulf (Thessaloniki, northern Greece) provided evidence for past high energy sedimentary events, which are interpreted as tsunamites. A tsunamigenic source is located along the western tip of the North Anatolian Fault Zone (NAFZ) in the North Aegean Basin, where water depths ranging between 1.200 and 1.650 m are sufficiently deep to generate tsunamis. However, the event layers up to now cannot be assigned to individual seismic or landslide sources, but the potential of a tsunami threat in the Thermaikos Gulf area can now be tested, following both sedimentological and modelling processes. Such potential threat regarding the Thermaikos Gulf has only recently been notified, but never tested and studied in depth.

As a result, several Holocene coarse clastic marine layers have been found intercalated in clayey or gypsiferous lagoonal deposits. These layers have erosive bases, show fining-up and thinning-up sequences, and include shell debris, foraminifera and rip-up clasts of lagoonal sediments. A widely observed significant feature of these layers involves mud-coated beach clasts, clasts that rework the high-plasticity clays of lagoons. Such features that indicate highly disturbed sedimentological processes (hyperpycnal flows) are rarely described elsewhere. Multiple intercalations of these layers with all the mentioned indicative features downhole are interpreted as paleotsunami deposits from tsunamis generated by earthquakes or earthquake-triggered submarine landslides in the Thermaikos Gulf.

Modelling of the tsunami potential of the basin-bounding fault southwards of the Thermaikos Gulf provides an example for possible tsunami generation at only one segment of NAFZ along an approx. 55 km normal fault at the southern fault-bound margin of the North Aegean Basin.

Keywords: Aegean Sea, tsunamites, tsunami modelling, Greece, Thermaikos Gulf

1 *Introduction*

During the last 20 years, several tsunamigenic sedimentary layers or tsunamites have been described – mainly in the circum-Pacific region (e.g. Atwater 1992; Atwater & Yamaguchi 1991; Atwater & Moore 1992; Atwater et al. 2005; Kelsey et al. 2005; Minoura & Nakaya 1991; Nanayama et al. 2003). Generally, coarse-grained or blocky deposits known from the Caribbean, Alaska or Australia are distinguished from fine-grained sandy layers, which are distributed spatially (e.g. Minoura & Nakaya 1991; Gianfreda et al. 2001; Luque et al. 2002; Pinegina et al. 2003; Tuttle et al. 2004). The origin of those layers or block accumulations around the coasts of the large open oceans is still highly debated and vividly discussed (Tuttle et al. 2004; Kortekaas & Dawson 2007; Switzer & Jones 2008).

©2010 Gebrüder Borntraeger Verlagsbuchhandlung, Stuttgart, Germany
www.borntraeger-cramer.de
DOI: 10.1127/0372-8854/2010/0054S3-0021
0372-8854/10/5403-0021 $ 7.00

On the other hand, regarding smaller and highly shaped coastal domains (with bays, gulfs, deltas and estuaries), like portions of the eastern Mediterranean Sea, one can expect rarely storm deposits of exceptionally large storms, simply because of meteorological and hydrographical reasons (out of the tropical-subtropical hurricane/typhoon area). The very rare occurrence and very long return period of storms, the shallow bathymetry of the Mediterranean (partly larger shallow shelves, storm wave base around 25 m, short wave periods), and, the exposition of the coastlines, together with the rare occurrence and preservation of storm deposits favor other depositional mechanisms. In the study area of the Thermaikos Gulf (northern Greece, Fig. 1), winter storms seldom reach more than 8 on the Beaufort scale and winds are directed towards the SW or S (Hofrichter 2002; mean max. wind speed in January is 30 km/h, with peaks around 70 km/h). Winds during the summer are weaker, they are directed mostly towards the S or SW (as during the winter), but a few times (usually 1/10 or 1/15) are directed towards the N. During these days the weather is relatively bad, linked with heavy rainfall. During the summertime storms, the wind is usually

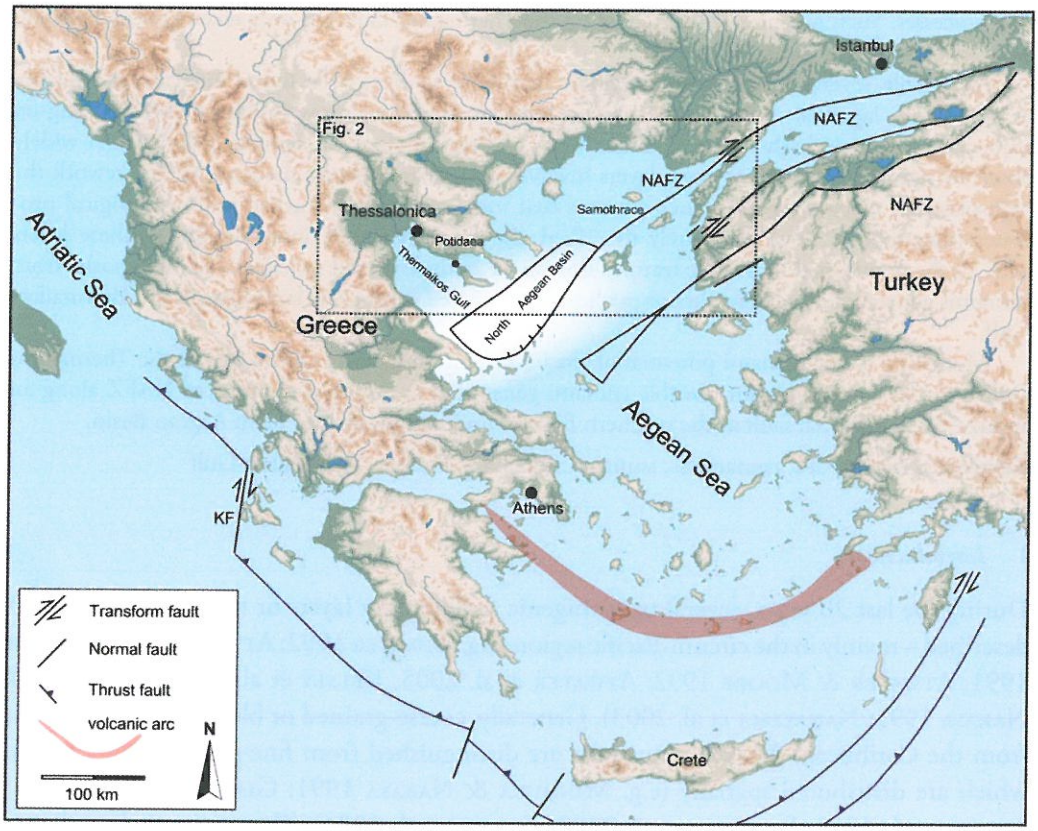

Fig. 1. Geodynamic setting of the Eastern Mediterranean and tectonic framework of the North Aegean Basin (NAFZ, North Anatolian Fault Zone; KF, Kefalonia Transform Fault). Square indicates study area in the northern Aegean realm (Fig. 2).

N directed. Minor tides, e.g. in Thessaloniki port, have a mean amplitude of 22 cm, based on the Hellenic Hydrographic Service (1991).

Along the coasts of the Eastern Mediterranean Sea (Adria, Aegean), also sedimentary remains of tsunami waves have been described (e.g., Italy: Mastronuzzi & Sanso 2000; Pantosti et al. 2008; Greece: Dominey-Howes 1996; Dominey-Howes et al. 1999, 2000, 2006; Vött et al. 2008; Cyprus: Kelletat & Schellmann 2002). The potential sources for the generation of tsunamis in the Mediterranean involve volcanic explosions, strong earthquakes (M_W > 6.5) or big landslides and sufficient water depth (i.e. volume of water to move). Then, a suitable environment to host and preserve the high-energy sedimentary layers is needed, because of the bi-directional flow and the erosive power of the backwash. Spit bars and lagoons protected from the open sea by beach ridges serve as archives for tsunamites as their topography allows the conservation of a tsunami record.

1.1 *Geodynamic framework, causative fault and historical seismicity*

The North Aegean Basin (NAB or North Aegean Trough) is one of the areas with the highest seismicity in Europe and the Mediterranean in general and characterized by the western continuation of the North Anatolian Fault Zone (NAFZ, Fig. 1). GPS values between the islands of Thassos and Limnos indicate that the northern branch accommodates approximately 16 mm/yr (McClusky et al. 2000). The NAFZ separates into a northern branch, which crosses the Marmara Sea and the Saros basin and forms the transtensional southern margin of the NAB, and into a southern one, passing Lesbos island. The NAB reaches widths of 30–40 km and depths from 900–1,650 m (Papanikolaou et al. 2002). The basin-bounding fault has a total length of 160 km, and can be divided into three major segments, each of 50–55 km length, each one forming a seismogenic source capable of hosting an M 7 earthquake event (Papanikolaou & Papanikolaou 2007).

Historical and instrumental seismicity in the NAB and NAFZ area include at least three major events (M 7.5 in 1905; M 7.0 in 1982; and M 6.8 in 1983; data from Papazachos & Papazachou 1989). The hypothetical seismogenic source in the NAB, we have taken into our tsunami modelling, represents the westernmost approx. 55 km long oblique normal fault segment, accommodating a vertical and horizontal displacement that might generate a M=7.1 event, producing a maximum vertical offset of up to 3–4 m, posing also a tsunami threat apart from submarine landslides (Papanikolaou & Papanikolaou 2007).

Historical reports on past tsunami events generated from fault activity along within the NAB (data from: Papadopoulos & Chalkis 1984; Soloviev 1990) include the 1893 Samothrace event (Feb. 09, 1893; M 6.5; Alexandropoulis: vertical run-up 0.8 m, landward incursion 40 m reported); the 1902 Thessaloniki event (Jan. 22, 1902; M 6.6); the 1928 Strimonikos Bay events (Apr. 22, 1928; M 6.3; Alexandropoulis: vertical run-up 0.6 m reported); the 1932 Chalkidiki event (M 7.0); the 1959 Salamina/Thessaloniki event (cause unknown, Thessaloniki: vertical run-up 0.9 m reported). The last major event occurred in 1978 close to the Strimonikos Bay (M 6.5; Soloviev 1990). The catalogue also has some questionable events like the 330 BC Lemnos event (M 7.0), which is not evidenced by data yet.

The oldest interpreted as a possible tsunami event in the NAB area probably occurred in 479 BC, the rest of the reported tsunamis cover the last 120 years whereas all recent events report small vertical run-ups below or not exceeding 1 m (Papazachos & Papazachou 1989). So, we observe a time gap of no reports of almost 2,400 years, implying that the historical records for tsunamis are incomplete before the end of the 19th century. This is in agreement with the historical earthquake record that is considered as complete for events > M=6.5 only since 1845 AD (Papazachos et al. 2000). The Herodotus Histories (Urania, Book 8, 129) report on a series of large waves and sea withdrawals occurring in winter 479 BC during the Persian-Greek war. Large portions of the Persian troops perished by drowning near Potidaea, western Chalkidiki peninsula (Fig. 1), while sieging the Greek village. Therefore, Herodotus's report is regarded as the first description of a historical tsunami (e.g. Bolt 1978).

Our Greek-German project involves the extraction and study of sediment cores from coastal deposits of the Thermaikos Gulf in Northern Greece, in order to identify paleotsunami deposits and to correlate them to the activity of faults from the North Aegean Basin. We collected almost 300 m of long core samples from several localities along the coasts of the Thermaikos Gulf both eastwards and westwards of Thessaloniki (Fig. 2). In this paper, we focus on the sedimentary record in lagoons and spit bars between Katerini and Thessaloniki (Fig. 3a) and, Thessaloniki and Kassandra (westernmost peninsula of Chalkidiki), in three areas: Angelochori (Fig. 3b), Cape Epanomi (Fig. 3c) and Sozopoli (Fig. 3d).

2 *Working area and drilling locations in the Thermaikos Gulf*

The Thermaikos Gulf is a relatively shallow marine area in northern Greece (Figs.1 and 2). Spit bars and lagoons developed since the last major sea level rise after the Late Glacial Maximum. Lagoons are typically developed along the coast, which are protected from the open sea by small, approx. 1–2 m high beach ridges. These lagoons, partly salines (salt works), serve as archives for tsunamites as their topography allows the conservation of a tsunami record. The study area is subject to extensive fluvial sedimentary input in the Thessaloniki plain by major rivers Gallikos, Axios, Loudias, and Aliakmon since approximately 4000 BC (Psimoulis et al. 2006; Ghilardi et al. 2008a). Such sedimentation process has modified significantly the coastline so that the delta moved approx. 35 km eastward since the last 2,500 years. If additionally high-energy marine events, i.e. tsunami or sea currents, contributed to the migration and coastal modification is not clear. However, large portions of the sediment load are transported coast-parallel towards the south, forming spits and spit bars, in the back of which lagoons are established. Three of such lagoonal areas have been chosen for percussion drilling. These areas are exposed towards the South, where the possible tsunami source is situated. Furthermore, we probed several sites on the western shore of the bay, north of Katerini near Korinos within the Alikes lagoon (Fig. 2). All eastern sites are located south of Thessaloniki.

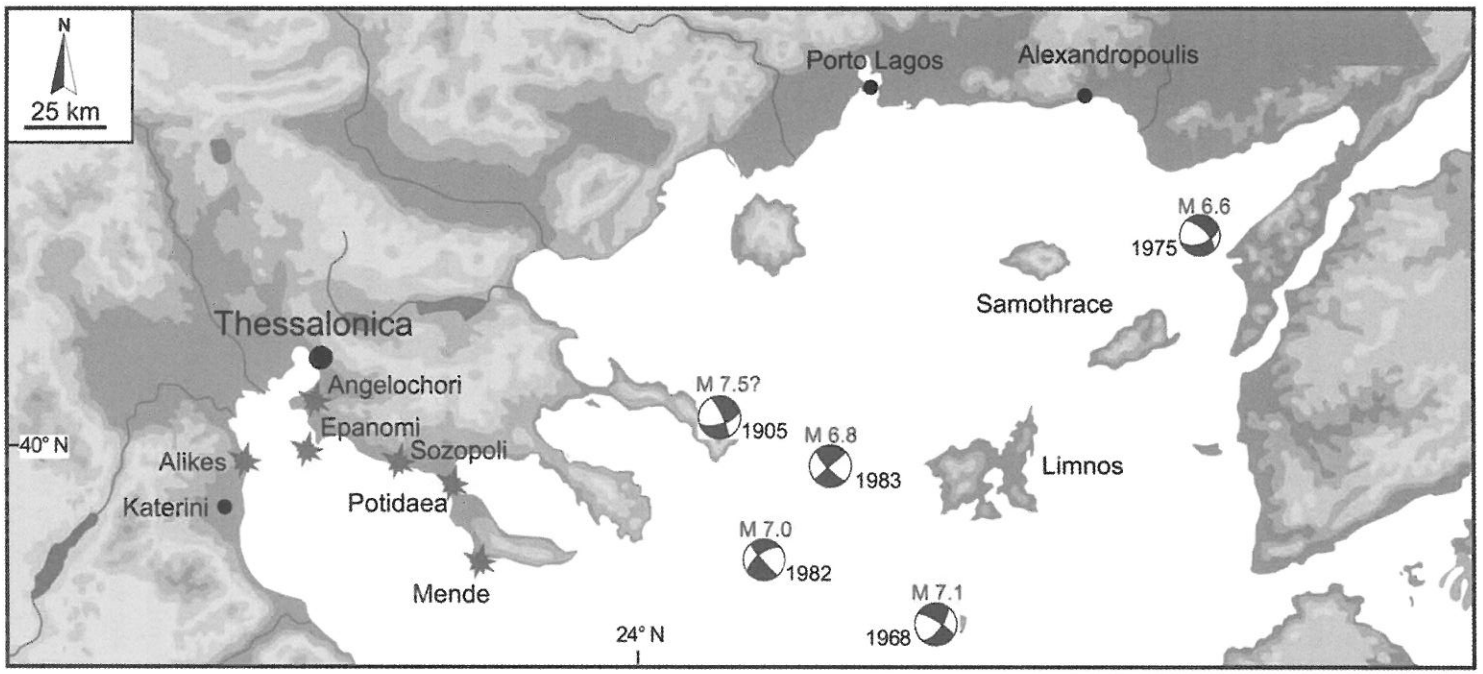

Fig. 2. Working and drilling area in the Thermaikos Gulf in the northernmost part of the Aegean Sea. Stars indicate study areas, see detailed maps of Fig. 3. Included are locality, date, magnitude and focal solutions of all major events (M≥6.5) that have been recorded in the instrumental catalogue.

The Alikes lagoon north of Katerini and close to the Korinos village (Fig. 3a) is characterized by a large alluvial and lagoonal plain. In the northern part an extensive salina is located (Fig. 3a). Miocene and Pliocene bedrocks are outcropping approximately 3 km away from the coast. No river or creek drainage was developed in the Holocene. At eight locations we obtained more than 30 m of sediment cores (4 m long cores from all sites). Drill holes B 28 to B 30 were drilled along a 1,000 m long profile perpendicular to the coastline. The distance of the drill holes to the sea varies from 50 to 1,000 m. The beach is characterized by a small dune belt and by a small beach ridge of maximum 1 m in height.

Angelochori is located on a large spit bar approx. 20 km south of Thessaloniki. The saline is situated directly north of the drilling area (Fig. 3b). The coastline stretches E–W. The Angelochori area is made up geologically mainly by Neogene sandy sediments (Messinian, Lalechos 1969), where in a bay a closed lagoon developed. In total 12.65 m of core material was obtained from five different locations (2–4 m long cores from all sites), whose distance to the sea varies from 50 to 900 m. The present-day beach berm is only 0.5–1 m high, probably generated during winter storms.

The Cape Epanomi is located further south than Angelochori; the beach is exposed to the south (Fig. 3c). Here, a large spit bar with lagoon and chevron-like features (Bourgeois & Weiss 2009) are developed. The lagoon is drained, but no saline was established. The geological setting is comparable to the Angelochori site; however, at Cape Epanomi the lagoon receives fresh-water input from a small river. The present-day beach berm is 1 m high, and several dunes have been developed close to the beach. In total, about 20 m of sediment cores were obtained from four localities at Cape Epanomi (2–7 m long cores from all sites).

The little village of Sozopoli is located only 20 km northwest of the channel of Potidaea forming the nearest site to the historical tsunami reports (Fig. 3d). Here, also, the Neogene sands dominate the geology, expressed in huge cliffs. There is an Upper Miocene/Lower Pliocene succession of alternating beds of sands, clayey marls and clays that in Sozopoli dip towards the SW (Mollat & Antoniades 1978). However, Quaternary sands and sandy clays are also developed. Besides a coastal dune belt, a small lagoon is developed, which at present day has dried out. The beach is again exposed to the south; a small beach ridge of 0.5–1 m forms a small barrier. At Sozopoli beach approximately 30 m of sedimentary cores were obtained from four locations (2–5 m long cores from all sites).

3 *Methodology*

During fieldwork in 2007 and 2008, we applied percussion drilling with an open window sampler and reached depths of maximum 10 m (Cape Epanomi, B 16, Fig. 3c). After core description, the same site was drilled with a sampler with 1 m long PVC liners step-by-step for laboratory research and sampling. In total, 100 m of cores in liners were obtained. Sampling was carried out both in the field and lab. In the laboratory, cores were split lengthwise, logged and sub-sampled for grain size, organic content, micro- and macrofossils,

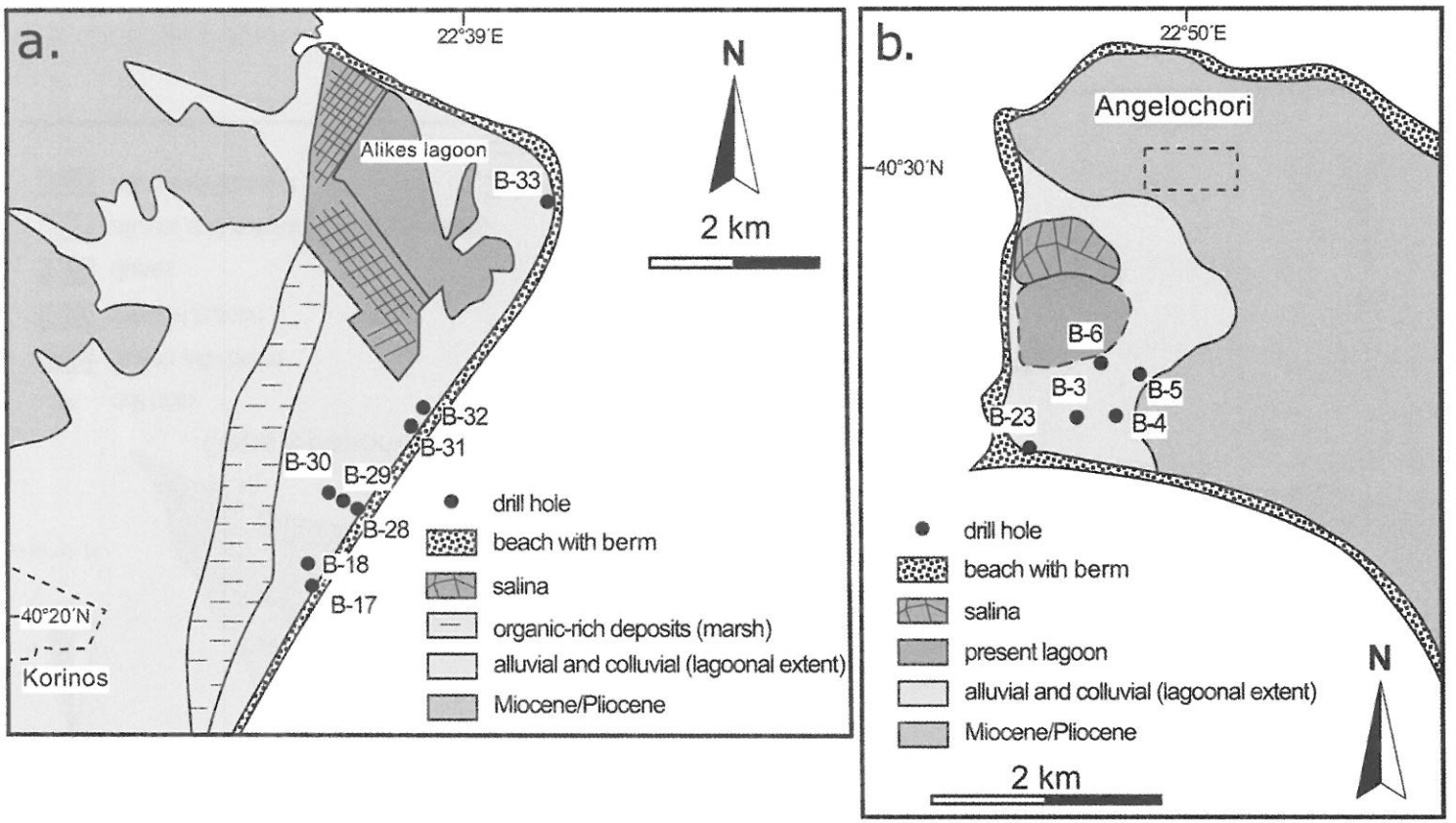

Fig. 3. A. Geological sketch map of the Korinos/Alikes area and location of drill holes. B. Geological sketch map of the Angelchori area and location of drill holes.

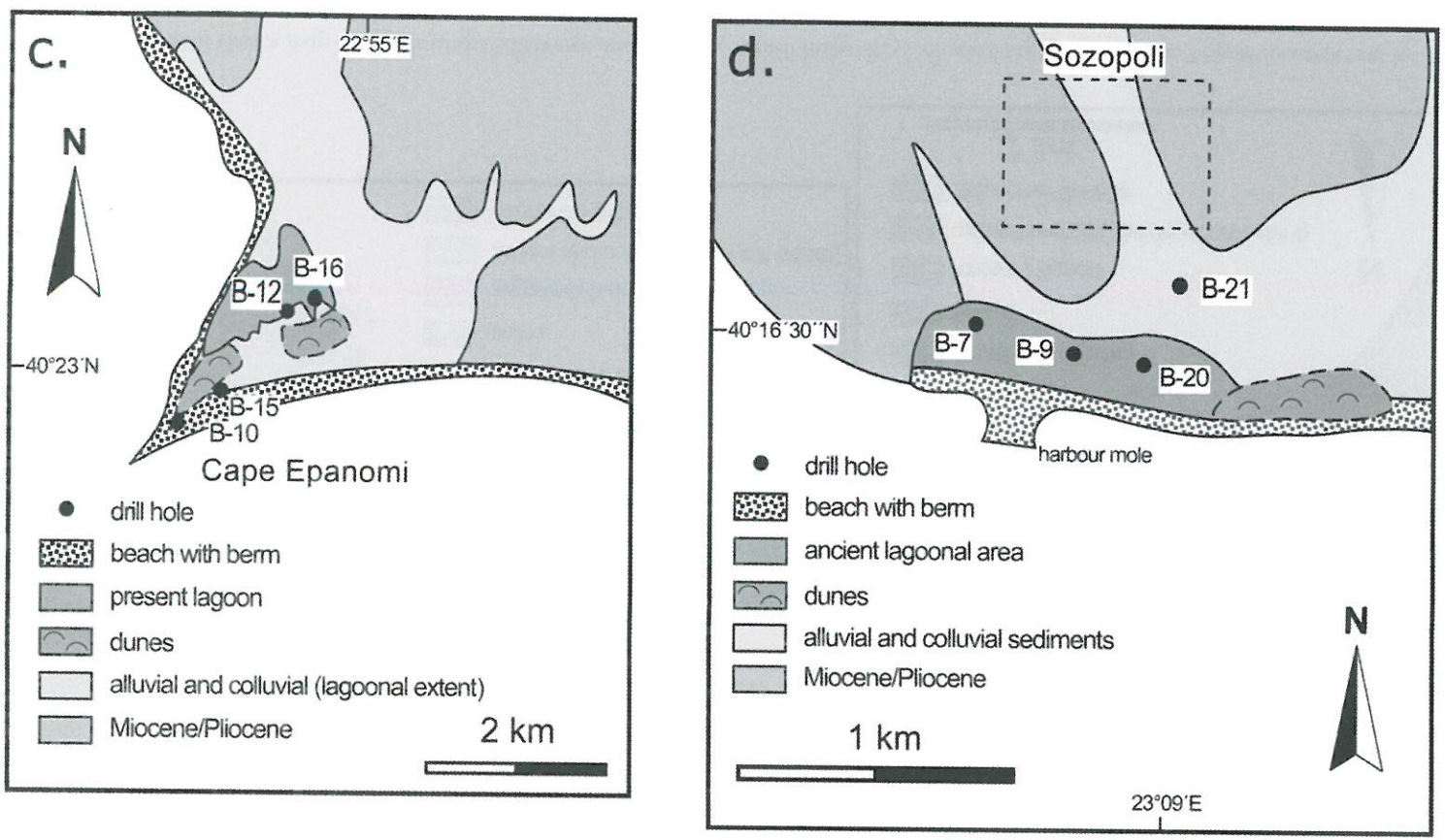

Fig. 3. C. Geological sketch map of the Cape Epanomi area and location of the drill holes. D. Geological sketch map of the Sozopoli area and location of the drill holes.

geophysical, and radiocarbon analyses (AMS dating in progress). Sedimentological analyses include sieving, washing, and laboratory core description. Magnetic susceptibility on cores has been measured and micropaleontological samples have been picked (foraminifera, shells, ostracodes, echinoid spines and remains).

4 *Sedimentary evidence for tsunamites*

The Korinos/Alikes lagoon site on the western shore of the Thermaikos Gulf was investigated in eight sites. The sedimentary history of the lagoon is best mirrored in core B 29 (Fig. 4a), a site located approximately 600 m W of the present-day coastline (N 40°19'46.34,

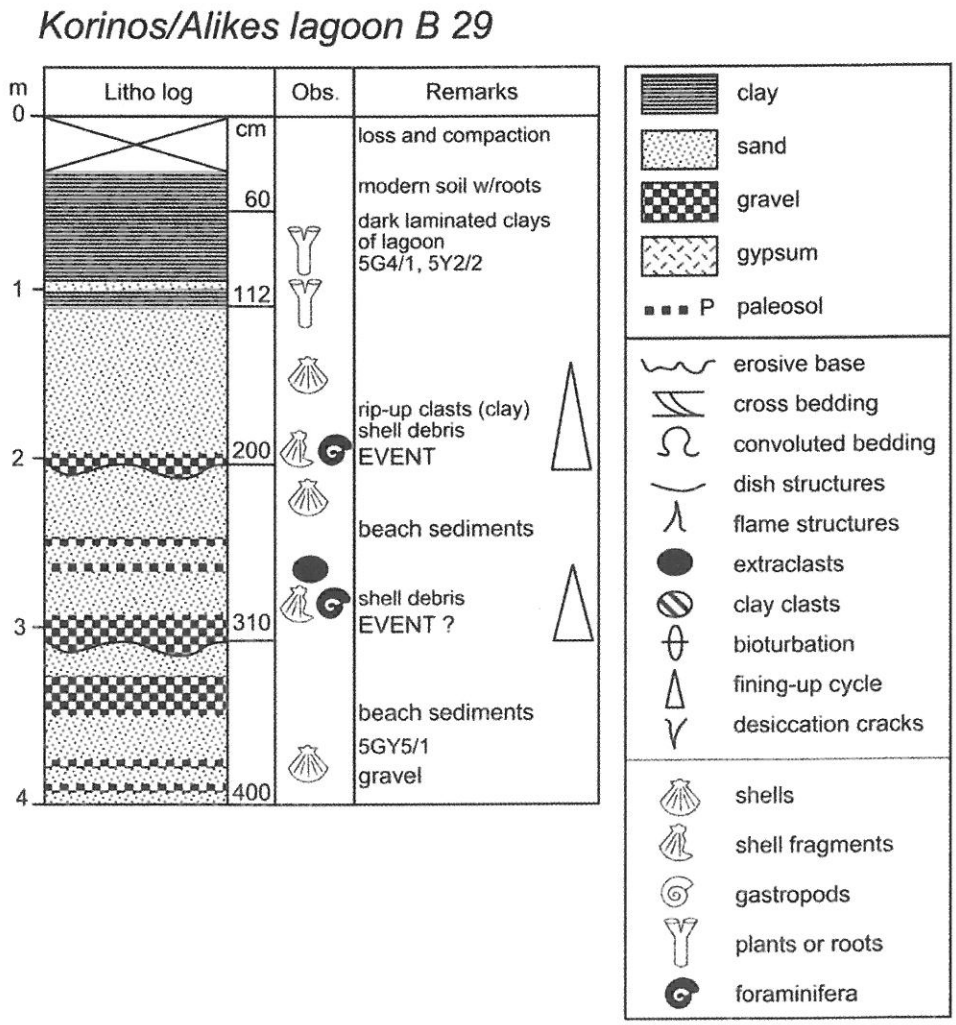

Fig. 4. A. Core-log of Korinos/Alikes lagoon B29.

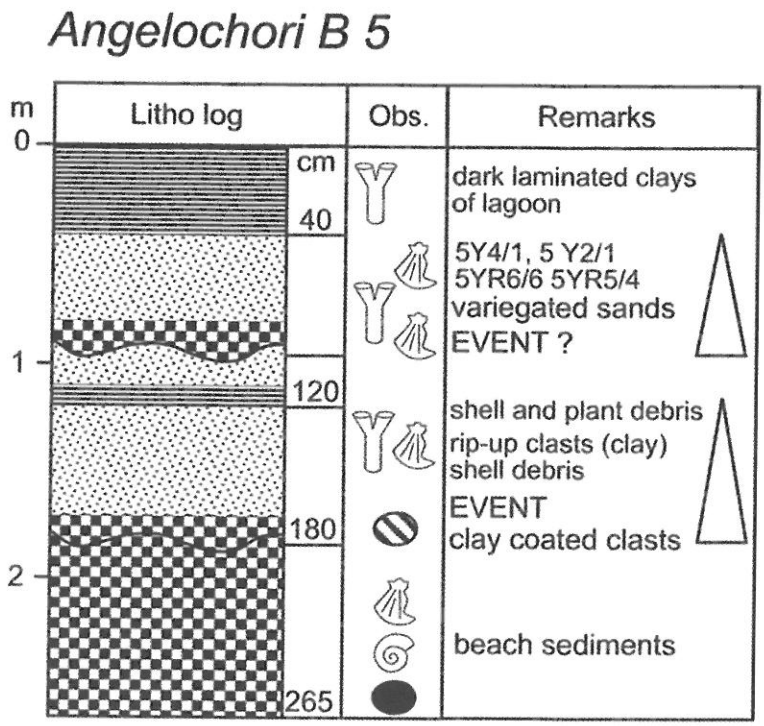

Fig. 4. B. Core-log of B5 (see Fig. 4a for legend).

E 22°37'35.98). A maximum depth of 4 m was reached, the lower portion up to 3.10 m yields typical beach sediments, as marine gravels and medium-grained sands with the faunal content (lamellibranches, gastropods). At 3.10 m above an erosive surface a thick gravel layer is intercalated forming a fining-up cycle of approx. 50 cm thickness. This layer contains broken shells, foraminifera and extra-clasts. Fine-grained beach sands follow upsection. These are overlain by another fining-up sequence with an erosive base. Again, extra-clasts, shell debris and foraminifera have been encountered in the washing residues, also frequent are clayey rip-up clasts. The subsequent interval to 1.12 m below surface is made up of variegated sands, which grade into dark laminated lagoonal clays with plant remains, and are occasionally intercalated by eolian sands.

The Angelochori site revealed several individual stages of the lagoonal development. Here we describe the sedimentary findings of core B5 (N 40°28'53.28, E 22°49'40.38, for location see Fig. 3b). Below approx. 2 m depth, the core consists of open-marine beach gravel and sands with typical faunal elements (gastropods, lamellibranchs, echinoid spines) (Fig. 4b). Upsection two fining-up cycles of 80 cm and 60 cm thickness follow. These have erosive bases (e.g., Fig. 5), show two fining-up and thinning-up sequences (a bundle of layers that get thinner upsection, but yielding the same depositional process), and include shell debris, plant remains and rip-up clasts of lagoonal sediments. Interestingly, at the bases

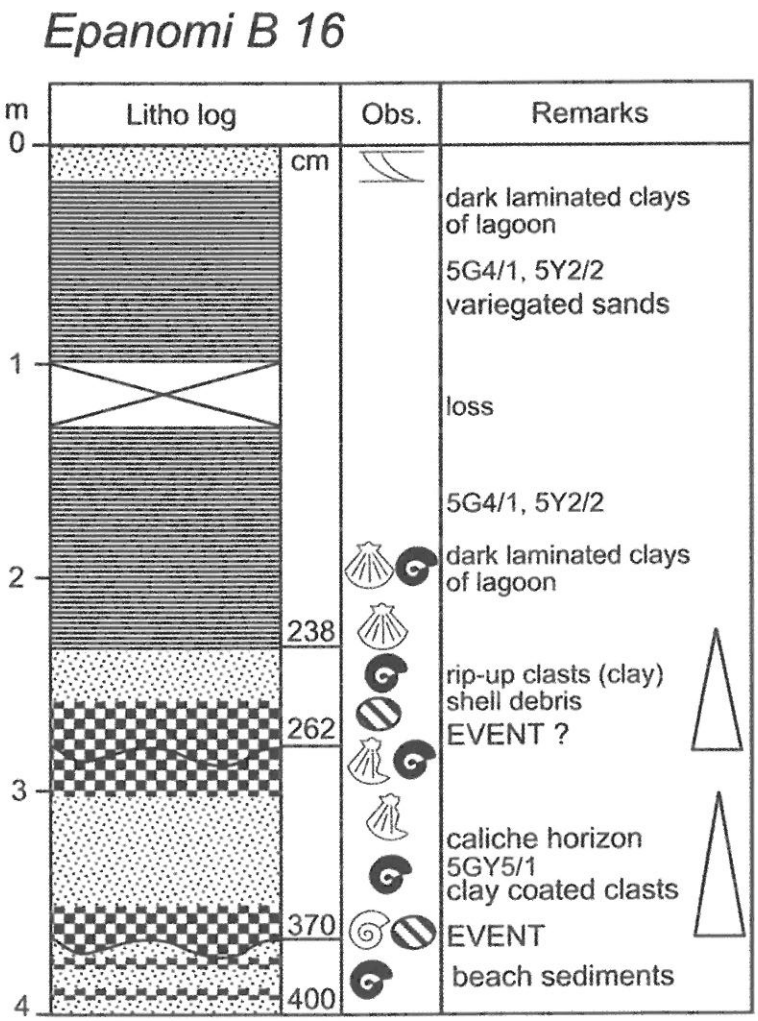

Fig. 4. C. Core-log of Cape Epanomi B16 (see Fig. 4a for legend).

of the two layers, some clasts (hard rock) have a clay coating of 0.5 to 1 cm thickness. We interpret these "mud-coated" clasts as beach gravel, which gathered a clay coating while being transported into the fine-grained clayey, semi-lithified lagoonal sediments during an erosional event. This can be regarded as a new indicative sedimentary feature of tsunamites, we call those findings "mud-coated clasts". In contrast to the rip-up clasts in the sandy portion of the event layer (e.g., Fig. 5), mud-coated clasts have a core of hard rock. We do not consider these coated clasts as artificially produced by drilling or extraction of the cores. They have been found always in sandy or gravel layers, also at sites Cape Epanomi and Sozopoli. The topmost layer is made up of 0.4 m of dark laminated clays with plant rests typical for a lagoon (Fig. 4b).

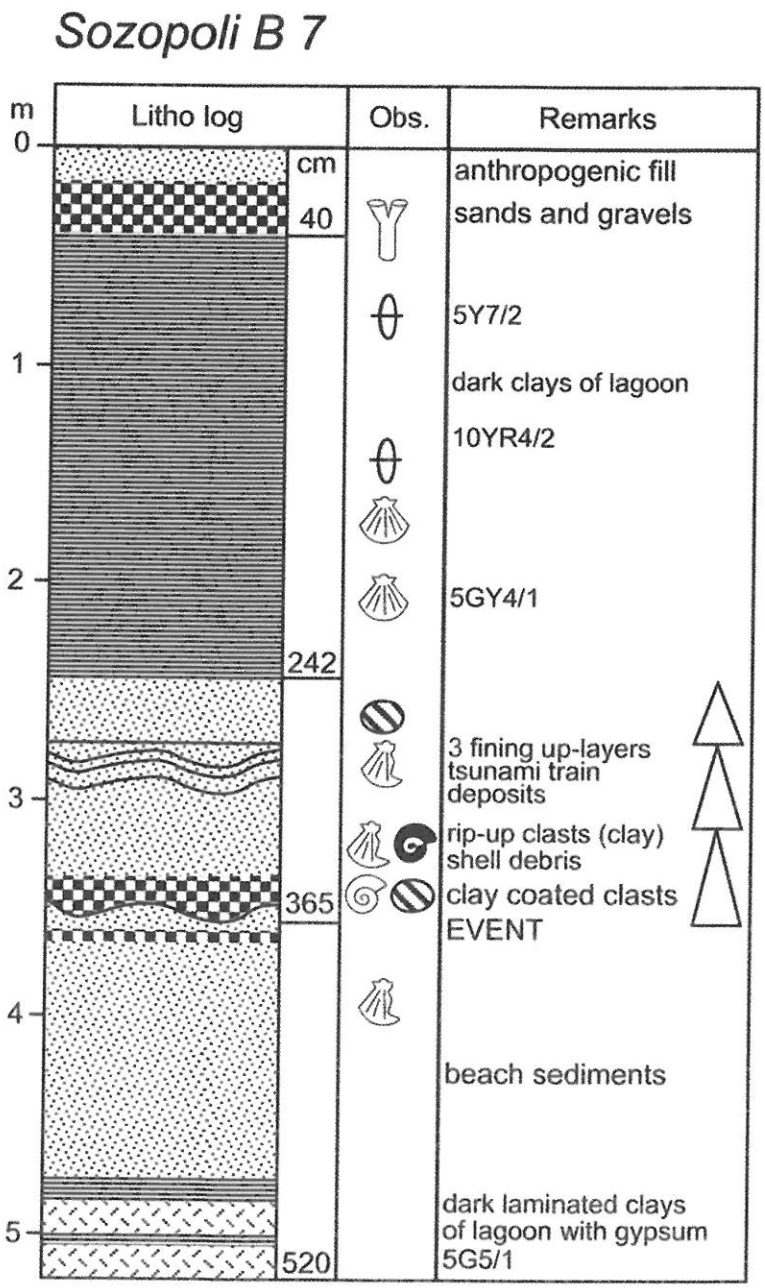

Fig. 4. D. Core-log of B7 in Sozopoli (see Fig. 4a for legend).

The cores of the Cape Epanomi show at around 4 m depth interbedded open marine beach gravel and sands (N 40°23'17.04, E 22°54'37.50, location in Fig. 3c). After an erosive event two fining- and thinning-up cycles do follow (Fig. 4c). Typical sedimentary features involve rip-up clasts, mud-coated clasts and shell debris (partly articulated *Acanthocardia tuberculata and A. aculeata.*, which indicates a sudden death of the animal). Other faunal elements are echinoid spines and gastropods. The lowest layer of the two events yields a carbonate crust (caliche) in the upper sandy portion. Ostracods and foraminifera are found in all samples throughout the core, and consist mainly of *Cibicides* sp. and *Ammonia* sp. Upsection 2.1 m of lagoonal clayey sediments, partly laminated, partly burrowed, follow. Relatively uniform grain-size distribution of sandy intervals at the top of the core are interpreted as wind-blown sands from the nearby dunes. The topmost layer is made up of dune sands, partly cross-bedded.

The Sozopoli location (N 40°16'30.18, E 23° 8'42.78, Fig. 3d) yielded almost comparable sedimentary sequences as already encountered in the previously described sites. However, in contrast to the other drill sites, below open marine beach sediments, gypsum has been found in > 5 m deep drill holes (Fig. 4d). The drilling ended in gypsiferous sediments, gypsum and laminated dark clays. This sequence is interpreted as typical ephemeral lagoonal, which dries out temporarily. Then the core evolves to shell-rich open marine sands and gravel, including a paleosol horizon. Between 3.65 and 2.42 m an interval with erosive base, shell debris, rip-up and coated clasts (Figs. 5 and 6). Looking in detail at the interval, three fining- and thinning-up cycles can be distinguished. Up to now, these cycles have not been observed and described in storm sediments. This typical tsunamite-feature has previously been described from tsunamites in southern Spain and interpreted by Reicherter & Becker-Heidmann (2009) as tsunami train deposits. In particular, at least three major waves entered the lagoon, and left three sedimentary packages with erosive bases. Mainly gastropods, lamellibranchs, echinoid spines, some ostracodes and rare foraminifera make up the faunal components in these layers. Foraminifers do not allow a bathymetric estimate of water depth of their original habitat.

On the basis of several aligned drillings it is possible to trace the event layers in the study region of Sozopoli (Fig. 7a). The cross section is situated at 100 m distance from the beach towards the eastern part of Sozopoli (Fig. 3d). The upper event layer was found and correlated in all three cores, allowing the layer to be interpreted as tsunami deposit affecting the entire area. Comparable parallel sections have also been constructed for the Angelochori and Cape Epanomi sites (Rössler 2008).

The profile perpendicular to the coast at location Korinos/Alikes lagoon (Fig. 3a) stretches over 800 m and yielded evidence for event layers (Fig. 7b) preserved on the western part of the Thermaikos Gulf. The lower event layer was found in all three cores, suggesting a tsunami event affecting the Korinos/Alikes lagoonal area. A thinning and pinching-out of the layer can be observed in core B 30. The upper event layer is only present in core B 29.

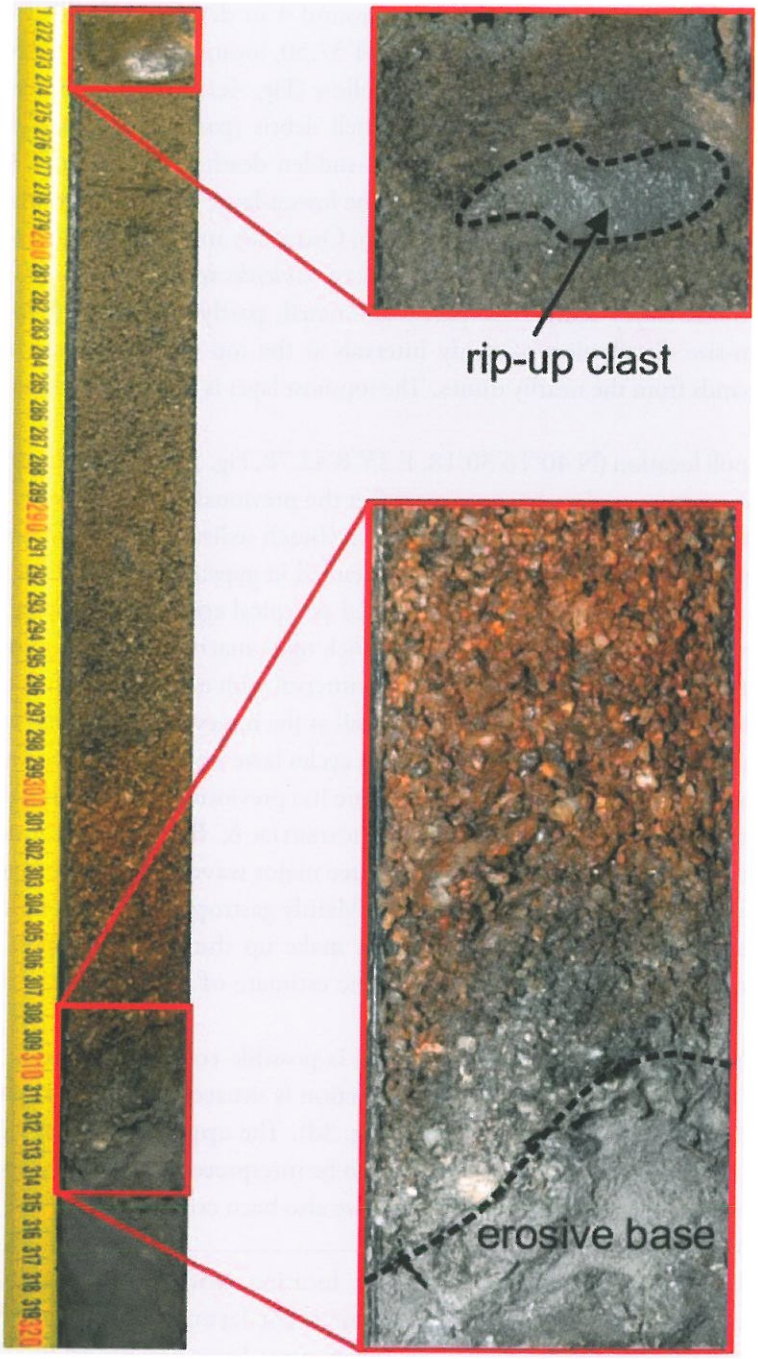

Fig. 5. Close-up of core B 20 (core-log in Fig. 7a) from locality Sozopoli, showing two cycles of the tsunami train. The lower layer has an erosive base at 3.15 m depth, and is fining-up. The second layer starts with rip-up clasts at 2.74 m depth, and is generally finer-grained (section in Fig. 7).

Fig. 6. A. Coated clast, core Sozopoli B9, 284–288 cm, stippled line indicates clay smear around the quartzitic clast. B. Coated clast, core Sozopoli B9, 284–288 cm, clast was taken out of the core to show greenish-grey clay drape of the clast in a sandy matrix (see Fig. 7 for litholog).

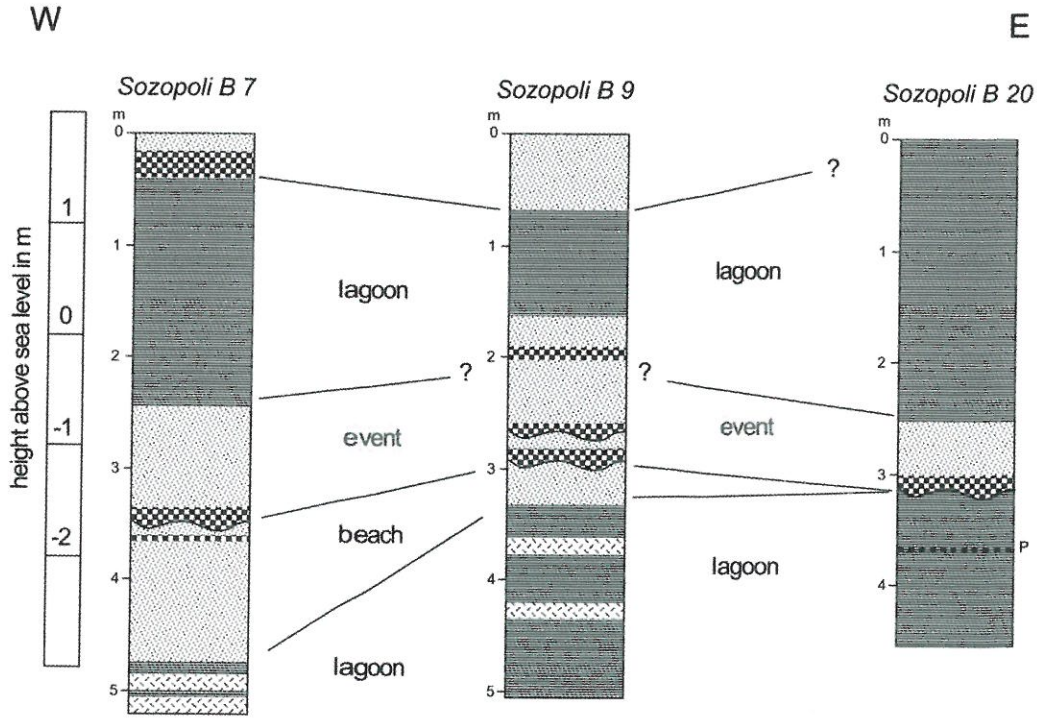

Fig. 7. A. Lithologs of Sozopoli cores. The section is located approximately 100 m from the coast and parallel to the beach. The tsunamigenic event has been found in all cores (see Fig. 4a for legend).

5 *Tsunami simulation and modelling in the Thermaikos Gulf*

Recent offshore studies have underpinned the possibility of a tsunami generation that could affect the Thermaikos Gulf, caused by an activation of an oblique normal fault located in the western part of the North Aegean Basin. The geodynamic framework in the study area is dominated by the western termination of the North Anatolian Fault Zone with major steep normal, oblique and strike-slip faults, separated in several segments. Depending on the hazard scenario implied, whether involving single segment or multisegment ruptures, these structures can host earthquakes of magnitude M 7 up to M 7.7, whereas the westernmost segment can produce an earthquake associated with a maximum vertical displacement of approx. 3 m (Papanikolaou & Papanikolaou 2007).

5.1 *Seismic source parameters for a tsunami in the Thermaikos Gulf*

The southern marginal fault of the North Aegean Basin is divided in four major segments (Papanikolaou et al. 2002; Papanikolaou & Papanikolaou 2007). In this study we consider only the approx. 55 km oblique normal fault segment towards the southwestern end of the basin (located on Fig. 8) named "source 1" by Papanikolaou & Papanikolaou (2007).

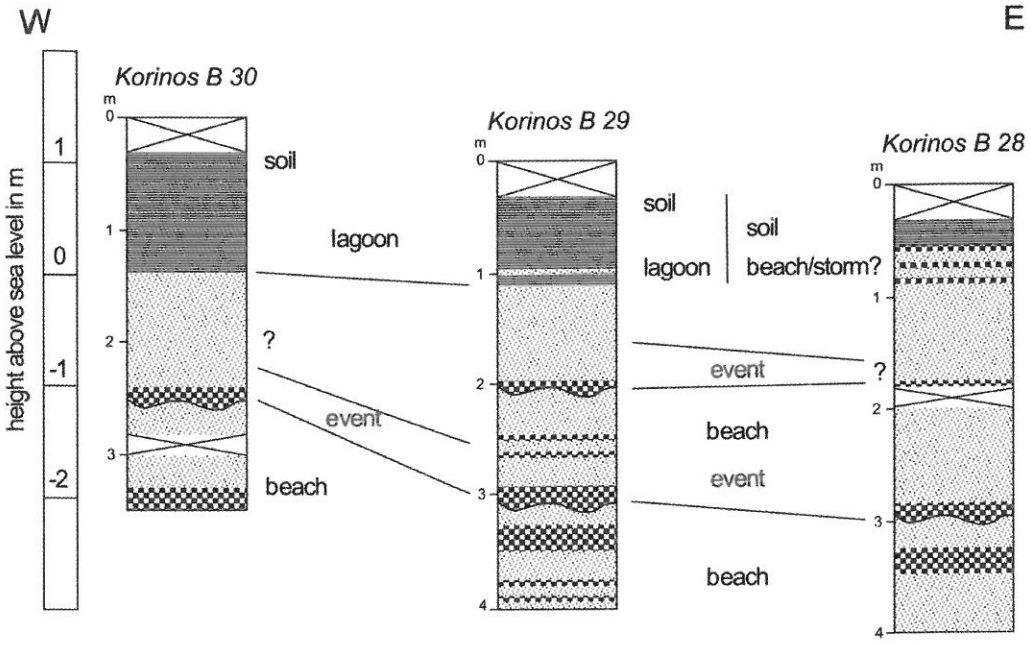

Fig. 7. B. Lithologs of the Korinos/Alikes lagoon. The sections are located approximately 100–800 m from the coast and perpendicular to the beach (see Fig. 4a for legend). The lower major tsunamigenic event is found in all three sections. Whereas the upper event is not present in cores B 30, and B 28, which is mainly due to the fact that B 30 is located too far from the coast and B 28 may be affected by coastal erosion during former storms.

This source can accommodate a M_W 7.0 event. According to Wells & Coppersmith (1994), such an event could produce a maximum vertical displacement up to 3–4 m, on the fault plane, corresponding to a maximum vertical offset of more than 2 m, which could induce a destructive tsunami. The other possible seismic source in the area represents a sub-vertical 70 km long, E–W trending shear zone northwards the previous source. This strike-slip fault has been revealed only by lithoseismic profiles, since it produces no vertical displacement (Papanikolaou et al. 2006).

The seismic source parameters have been determined from the previously mentioned study, in agreement with bathymetric features and geological context and empirical observations by Wells & Coppersmith (1994) and Stock & Smith (2000). They are summed up in Table 1.

5.2 *Initial deformation and tsunami modelling*

The calculation code has been developed by the CEA (France) and it is based on the same model of waves propagation in shallow water under non-linearity assumption than the SWAN code (Mader 2004).

Table 1. Seismic source parameters for tsunami modeling.

Longitude of the center of the fault plane (°)	Latitude of the center of the fault plane (°)	depth to top of the fault (km)	Coseimic slip (m)	Strike (azimuth) (°)	Dip (°)	Rake (slip angle on rupture plane; =0 if strike slip; 90° if reverse and -90° if normal) (°)	Length of the fault plane (km)	Width of the fault plane (km)	shear modulus (Pa)
23.89	39.34	1.2	2	220	45	-70	55	5	45×10^9

The initial sea-bottom deformation (Fig. 8) is based on elastic dislocation computed through OKADA formula (1985). Our method solves the hydrodynamic equations of continuity (1) and motion (2) conservation considering within a good approximation that this deformation is transmitted without losses to the entire water column. Non-linear terms are taken into account, and the resolution is carried out using a CRANK NICOLSON finite difference method centered in time and using an upwind scheme in space. This method has been widely used in the Pacific Ocean and Mediterranean Sea and contributed to tsunami hazard studies in several locations (HÉBERT et al. 2001, 2007; ROGER & HÉBERT 2008; YELLES-CHAOUCHE et al. 2009).

$$\frac{\partial(\eta + h)}{\partial t} + \nabla \cdot [v(\eta + h)] = 0 \tag{1}$$

$$\frac{\partial v}{\partial t} + (v \cdot \nabla) \cdot v = -g \nabla \eta \tag{2}$$

η corresponds to the water elevation; h to the depth; v to the horizontal speed vector; g to the gravity.

Wave propagation is calculated on one grid, whose geographical coordinates correspond to those of Fig. 1. This grid is built from GEBCO World Bathymetric Grid 1' (BRITISH OCEANOGRAPHIC DATA CENTER 1997) and is just an interpolation of this grid at a space step of 20" (≈ 500 m). Due to the lack of more accurate data in the studied area, the grid resolution is invariant from the source toward the studied sites: the water depth h decreases along with the tsunami propagation speed equation $c=\sqrt{gh}$ that depends only on h in non dispersive assumption (this can be explained by the fact that the interesting sites are located close to the tested source and thus the dispersion cannot have an important impact on wave

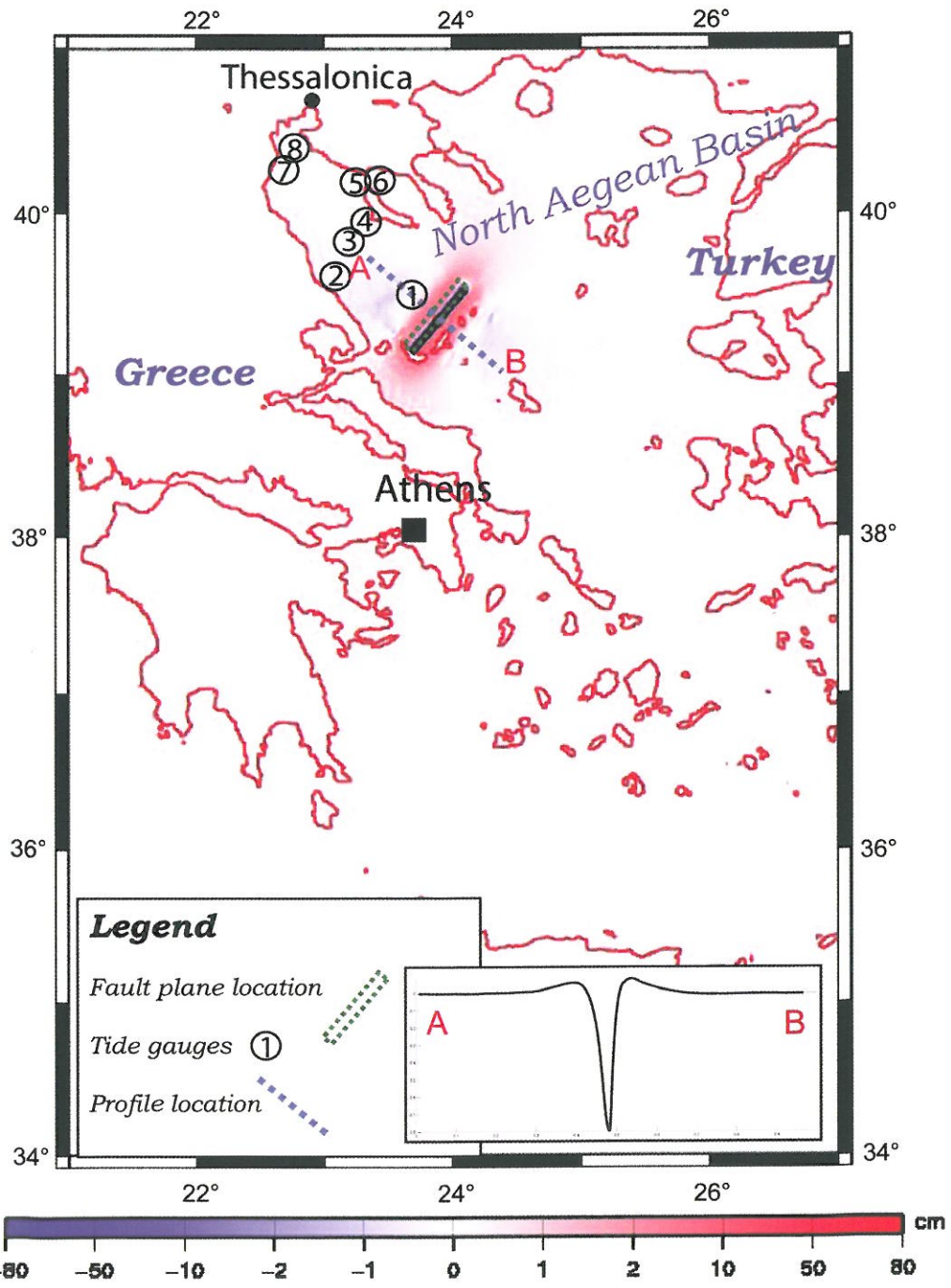

Fig. 8. Tsunami simulation. Location of initial sea-bottom deformation along the southern boundary of the North Aegean Basin and profile cut of the initial wave (A–B). Locations of synthetic tide gauges are indicated.

energy reduction). A profile cut perpendicular to the fault direction shows an initial wave shape characteristic for normal rupture with a small peak following a trough and an initial peak to trough amplitude of about 0.9 m.

Eight synthetic tide gauges have been located in the south of Thessaloniki (Fig. 8) in order to look at the variations of the sea level due to tsunami propagation in some particular places as time passes.

5.3 *Results of modelling*

Despite the lack of accurate bathymetric data, we can underline several important outcomes. Firstly, we can mention that the maximum wave heights[1] after three hours of tsunami propagation presented on Fig. 9A, is clearly oriented in the major direction of deformation as indicated by Okal (1988). Several particular coastal places show a maximum wave height of more than 40 cm (after three hours of tsunami propagation). This indicates possible important wave amplification as approaching the coast in these areas, especially in the last

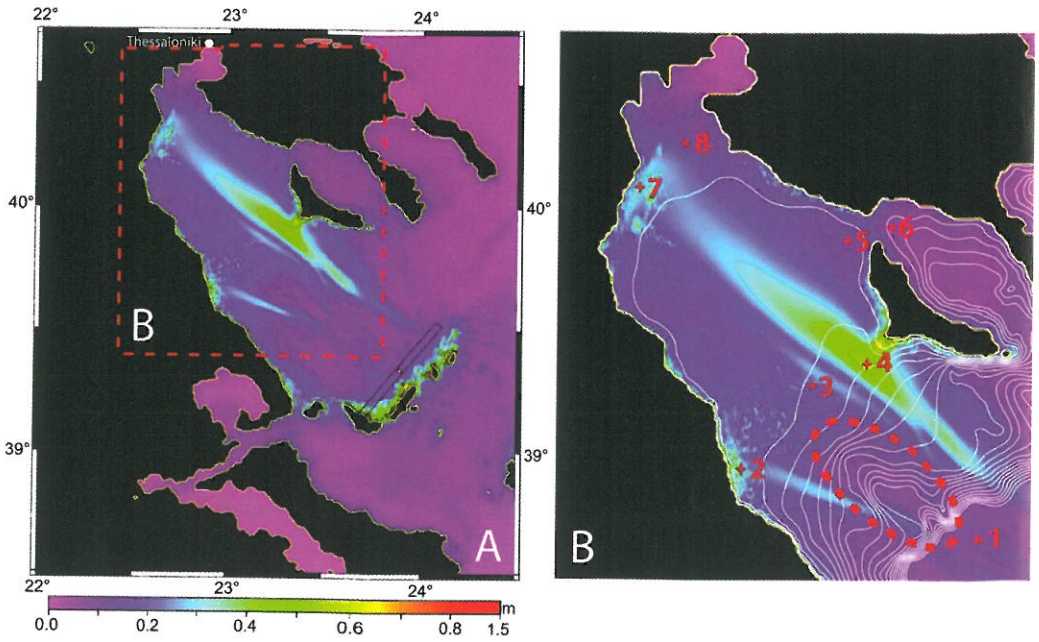

Fig. 9. A. Modelled maximum wave heights cumulated on 3 hours of tsunami propagation south of Thessaloniki. B. Distribution of two wave paths on both sides of a submarine canyon (red dashed line) revealed by bathymetric contours. Red numbers refer to tide gauge locations in Fig. 10.

[1] The maximum wave height represents the maximum (in term of height) reached by the sea at a considered point during a period t. Thus, if we look at all the points of a map, and take for each the altitude of the highest wave reached during a period t (3 hours in our case), we can obtain maximum wave heights in the Thermaikos Gulf.

tens of meter (shoaling effect and resonance phenomenons). One of these points (22.9° E / 39.6° N) is associated to a major tsunami propagation way, which seems clearly linked to a submarine canyon (Fig. 9B) as shown by Roger & Hébert (2008). Such submarine feature leads to a kind of particular repartition of wave energy: the amplitude is more important on both sides when approaching the coast. This can be explained by the principle that wave go faster in deep water, i.e. in the canyon, and that waves move slowly in shallower water, i.e. on its sides, added to the fact that wave amplitude increases when it slows.

Recorded tide gauge signals (Fig. 10) show the evolution of the tsunami signal as it moves from the source area towards the coastline. Due to the location of these tide gauges on the 500 m resolution bathymetric grid, the recorded signals only give an idea of wave evolution in the considered water body. We can notice that there is clearly an amplification of the signal with a factor 5 as waves move far from the source (gauges 1, 4 and 2 or 7). This amplification is less important at gauges 5 and 8, not linked with maximum tsunami energy lobes. Gauges 1 and 4 show the same first wave arrival, but the gauge 4 reveals something which looks like an oscillation in the basin probably due to reflection: its elongated shape allows energy to concentrate in the centre of the semi-enclosed water body. This is supported by the lack of shallow bathymetric features in the corresponding area, which could be linked to wave amplification as discussed previously. The synthetic signal of gauges 5 and 6 have to be taken into account cautiously because GEBCO data in this area do not represent correctly the coastline. Synthetic tide gauge 3 has been added in order to check the evolution of the signal outside the main tsunami energy lobe.

In our case, the resolution of the map is unfortunately too low to represent correctly what could happen near the shore (wave amplification known as the shoaling effect). The 30 to 80 cm approaching the coast can only give us an idea of wave amplification in the last hundreds of meters. Taking into account resonance effects that could play a major role in the last tens of meters and even before, due to the shape of the coast, the bathymetric features as submarine canyons, and empirical laws, we could expect wave heights of more than 2 m at the coast.

6 *Discussion*

As a preliminary result, we have found several coarse clastic layers intercalated in fine-grained lagoonal deposits along the coast. Multiple intercalations of these layers downhole are interpreted as either paleotsunamis of repeated earthquake activity or tsunami-like waves induced by submarine slides triggered by seismic shaking in the Thermaikos Gulf. Spit bars and lagoons serve as archives for tsunamites as their topography allows the conservation of a tsunami record. These areas are exposed towards the South, where the possible tsunami source is situated. Comparable tsunamigenic layers have also been found on the western margin of the Thermaikos Gulf in the Korinos lagoon and saline (Fig. 2).

The tsunamigenic sedimentary packages have erosive bases, show fining-up and thinning up sequences, and include shell debris and rip-up clasts of clayey lagoonal sediments. Addi-

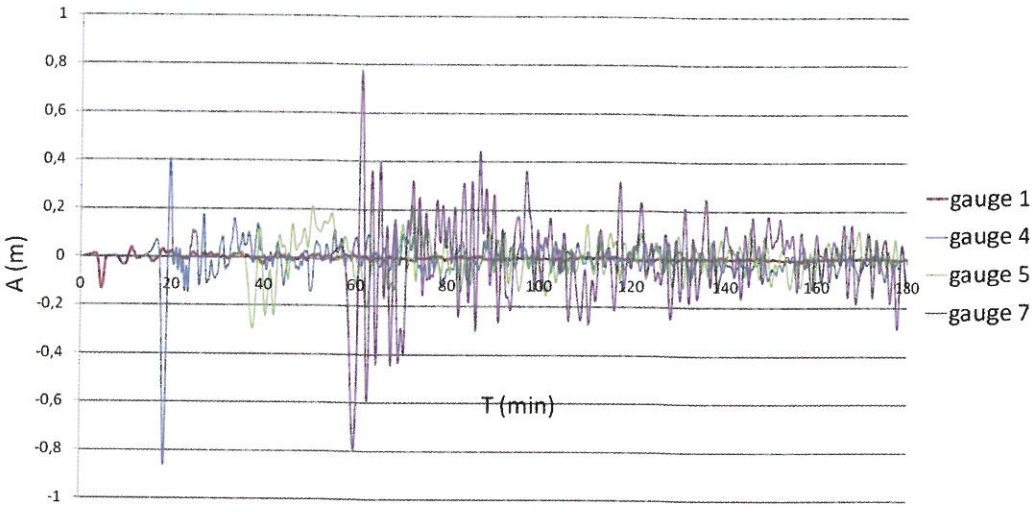

Fig. 10. Recorded signal on four synthetic tide gauges located in the south of Thessaloniki during three hours of tsunami propagation. For tide gauges locations see Fig. 9b.

tionally, we introduce a new type of tsunami indicator: the coated clast, a mud-coated hard rock clast. Mud-coasted clasts are rarely described in marine environments (KREISA 1981; DASHTGARD et al. 2006); their origin is highly disputed, but may be also storm-related (KREISA 1981).

Dating of the sediments (radiocarbon, mainly charcoal and shells) of samples in the near future will help us to establish a robust time frame, a) for the sedimentary history, b) the sedimentation rates, c) for the coastal evolution during the Holocene, d) to date precisely the event layers or tsunamites in order to correlate those to seismic events, and e) in order to obtain or extract recurrence intervals for the seismic source. However, based on radioncarbon datings by GHILARDI et al. (2008a), we can tentatively delineate sedimentation rates for at least the Holocene in the Thermaikos area. GHILARDI et al. (2008a and b) documented sedimentation rates of approximately 1 m per 1,000 years. Taking this into account and that all of our tsunamgenic layers are found at a maximum depth of 3.70 m, we suggest a Holocene age for the event layers.

Recent offshore studies have underpinned the possibility of a tsunami generation that could affect the Thermaikos Gulf, caused by an activation of an oblique normal fault located in the western part of the North Aegean basin. The geodynamic framework in the study area is dominated by the western termination of the North Anatolian Fault Zone with oblique normal and strike slip faults, separated in several segments, the westernmost of which can host an M 7 earthquake associated with a maximum vertical displacement of approx. 3 m (PAPANIKOLAOU & PAPANIKOLAOU 2007).

First results of tsunami modelling in Thessaloniki zone in the North Aegean Basin show that some sites seem to be more inclined to tsunami amplification particularly for coastal

areas. The "source 1" proposed by Papanikolaou and Papanikolaou (2007) could be a good candidate for tsunami hazard estimation and mitigation in this area. Then it reveals a wave focus of long waves on two coastal points due principally to the presence of a submarine canyon. The use of more accurate bathymetric data, particularly for coastal areas where wave amplification has been highlighted, would help to define what could be the wave amplification in the last tens of meter as approaching the coastline.

7 *Conclusions*

Tsunamigenic events in the Thermaikos Gulf in northern Greece occur, however, their recurrence periods are relatively long. The tsunami hazard in Greece was generally considered low in comparison to e.g. the circum-Pacific regions by Papadopoulos & Chalkis (1984). Regarding our study area, the Thermaikos Gulf was not included in the ten "tsunami" regions of Greece, where Northern Crete and Gulf of Corinth are considered to be of the highest hazard. However, data presented in this paper both sedimentological and modelling, clearly shows that the Thermaikos Gulf should be included in the areas of tsunami hazards. The seismic source is of medium capacity/volume compared to other worldwide sources, mostly large thrusts, therefore the expected tsunami wave would be of low to medium height. However, this is a densely populated area, where the second biggest city of Greece and several holiday resorts do exist. Therefore, even if the tsunami danger is regarded as small or medium, it can pose a high risk. Moreover, the absence of such events over the last centuries increases the probability of experiencing one in the near future. More studies and dating would help us clarifying the above.

The future project aims a) to verify whether a tsunami occurred in 479 BC, b) to identify whether other unknown tsunami deposits can be traced in the Thermaikos Gulf coastal sediments, c) to assess the tsunami hazard, d) to assess the seismic hazard by calculating the recurrence interval of the oblique normal fault located in the southwestern part of the North Aegean Basin, indirectly through the tsunami recordings.

Evidence for a slightly lower sea level around 500 BC in NW Greece was provided (Vött et al. 2006a). However, it is questionable whether the 500 BC sea level of 1.9–2.2 m below present sea level can be projected towards the Thermaikos Gulf, because the investigations in the study area of Vött et al. (2006a) may have been influenced by an active tectonic graben and subsidence. On the other side, it has to be mentioned that Pirazzoli & Pluet (1992) were able to distinguish at least five elevated Holocene shorelines between 1.6 and 3.75 m above present sea level. This contrasts findings of Pavlopoulos et al. (2007) on Skyros Island, who have observed a sea-level rise of approximately 3 m since 3,750 years PB. In conclusion, future paleogeographic reconstructions of the coastline in the Thermaikos Gulf have to consider the high mobility of the coast. And, furthermore, the impact of tsunamis on the low land coastal system around the Thermaikos Gulf has to be evaluated carefully.

Acknowledgements

We would like to thank the bilateral Greek-German IKYDA project (daad.de) and the RWTH Aachen University for financial support. Thanks are extended to our students Simon Virgo, Fabian Syberberg, Carlo Schneider, Marc Froewis and Sarah Dreßen who formed an excellent drilling team during the field campaigns. Thanks are extended to J. Bourgeois and an anonymous reviewer, their thoughtful comments helped to improve the quality of our manuscript.

References

Atwater, B.F. (1992): Geologic evidence for earthquakes during the past 2000 years along the Copalis River, Southern Coastal Washington. – J. Geophys. Res. **97** (B2): 1901–1919.

Atwater, B.F. & Moore, A.L. (1992): A tsunami about 1000 years ago in Opuget Sound, Washington. – Science **258:** 1614–1623.

Atwater, B.F. & Yamaguchi, D.K. (1991): Sudden, probably coseismic submergence of Holocene trees and grass in coastal Washington state. – Geology **19:** 706–709.

Atwater, B.F., Musumi-Rokkaku, S., Satake, K., Tsuji, Y., Ueda, K. & Yamaguchi, D.K. (2005): The orphan tsunami of 1700: Japanese clues to a parent earthquake in North America. – US Geol. Surv. Prof. Pap. **1707:** 133 pp.

Bolt, B.A. (1978): Earthquakes. – 241 pp., Freeman and Company, San Francisco.

Bourgeois, J. & Weiss, R. (2009): "Chevrons" are not mega-tsunami deposits – A sedimentologic assessment. – Geology **37:** 403–406.

British Oceanographic Data Centre (1997): The Centenary Edition of the GEBCO Digital Atlas, Liverpool, U.K.

Dashtgard, S.E., Gingras, M.K. & Butler, K.E. (2006): Sedimentology and stratigraphy of a transgressive, muddy gravel beach: Waterside Beach, Bay of Fundy, Canada. – Sedimentology **53:** 279–296.

Dominey-Howes, D. (1996): The Geomorphology and Sedimentation of Five Tsunamis in the Aegean Sea Region, Greece. – Ph.D. thesis: 272 pp., Coventry University.

Dominey-Howes, D., Dawson, A.G. & Smith, D.E. (1999): Late Holocene coastal tectonics at Falasarna, western Crete (Greece): a sedimentary contribution. – Geol. Soc. London Spec. Publ. **146:** 343–352.

Dominey-Howes, D., Cundry, A. & Crudace, I. (2000): High energy flood deposits on Astypalaea Island, Greece: possible evidence for the AD 1956 southern Aegean tsunami. – Mar. Geol. **163:** 303–315.

Dominey-Howes, D., Humphreys, G.S. & Hesse, P.P. (2006): Tsunami and palaeotsunami depositional signatures and their potential value in understanding the late-Holocene tsunami record. – The Holocene **16:** 1095–1107.

Fouache, E., Ghilardi, M., Vouvalidis, K., Syrides, G., Styllas, M., Kunesch, S. & Stiros, S. (2008): Contribution on the Holocene Reconstruction of Thessaloniki coastal Plain, North Central Greece. – J. Coast. Res. **134** (5): 1161–1173.

Ghilardi, M., Kunesch, S., Styllas, M. & Fouache, E. (2008): Reconstruction of Mid-Holocene sedimentary environments in the central part of the Thessaloniki Plain (Greece), based on microfaunal identification, magnetic susceptibility and grain-size analyses. – Geomorphology **97:** 617–630.

Ghilardi, M., Fouache, E., Queyrel, F., Syrides, G., Voulalidis, K., Kuneshc, S., Styllas, M. & Stiros, S. (2008b): Human occupation and geomorphological evolution of the Thessaloniki plain (Greece) since Mid Holocene. – J. Archaeol. Sci. **35:** 111–125.

Ghilardi, M. & Desruelles, S. (2009 in press): Geoarchaeology, where human, social and earth sciences meet with archaeology. – Surveys and Perspectives Integrating Environment and Society **1** (2); http://sapiens.revues.org/index422.html.

Gianfreda, F., Mastronuzzi, G. & Sansó, P. (2001): Impact of historical tsunamis on a sandy coastal barrier: an example from the northern Gargano coast, southern Italy. – Nat. Haz. and Earth Sys. Sci. **1:** 213–219.

Hébert, H., Heinrich, P., Schindelé, F. & Piatanesi, A. (2001): Far-field simulation of tsunami propagation in the Pacific Ocean: impact on the Marquesas Islands (French Polynesia). – J. Geophys. Res. **106:** 9161–9177.

Hébert, H., Sladen, A. & Schindelé, F. (2007): The great 2004 Indian Ocean tsunami: numerical modelling of the impact in the Mascarene Islands. – B. Seismol. Soc. Amer. **97:** 208–222.

Hellenic Hydrographic Service (1991): Tide data of Greek Ports. – 73 pp.

Hofrichter, R. (ed.) (2002): Das Mittelmeer. – Band **1:** 184–195, Spektrum Akademischer Verlag, Heidelberg, Berlin.

Kelletat, D. & Schellmann, G. (2002): Tsunamis on Cyprus: Field Evidences and ^{14}C Dating Results. – Z. Geomorph. NF **46** (1): 19–34.

Kelsey, H.M., Nelson, A.R., Hemphill-Haley, E. & Witter, R.C. (2005): Tsunami history of an Oregon coastal lake reveals a 4600 yr record of great earthquakes on the Cascadia subduction zone. – Geol. Soc. Amer. Bull. **177:** 1009–1032.

Kortekaas, S. & Dawson, A.G. (2007): Distinguishing tsunami and storm deposits: An example from Martinhal, SW Portugal. – Sedimentology **200** (3–4): 208–221.

Kreisa, R.D. (1981): Storm-Generated Sedimentary Structures in Subtidal Marine Facies With Examples from the Middle and Upper Ordovician of Southwestern Virginia. – J. Sediment. Res. **51:** 823–848.

Lalechos, N. (1969): 1:50,000 Geological map of Greece, Sheet "Epanomi". – Institute of Geological and Mining Research.

Luque, L., Lario, J., Civis, J., Silva, P.G., Zazo, C., Goy, J.L. & Dabrio, C.J. (2002): Sedimentary record of a tsunami during Roman times, Bay of Cádiz, Spain. – J. Quatern. Sci. **17** (5–6): 623–631.

Mader, C. (2004): Numerical modeling of water waves. – Sec. ed. CRC Press, 286 pp.

Mastronuzzi, G. & Sansó, P. (2000): Boulders transport by catastrophic waves along the Ionian coast of Apulia (southern Italy). – Mar. Geol. **170:** 93–103.

McClusky, S., Balassanian, S., Barka, A., Demir, C., Ergintav, S., Georgiev, I., Gurkan, O., Hamburger, M., Hurst, K., Kahle, H., Kastens, K., Kekelidze, G., King, R., Kotzev, V., Lenk, O., Mahmoud, S., Mishin, A., Nadariya, M., Ouzounis, A., Paradissis, D., Peter, Y., Prilepin, M., Reilinger, R., Sanli, I., Seeger, H., Tealeb, A., Toksoz, M.N. & Veis, G. (2000): Global Positioning System constraints on plate kinematics and dynamics in the Eastern Mediterranean and Caucasus. – J. Geophys. Res. **105:** 5695–5719.

Minoura, K. & Nakaya, S. (1991): Traces of tsunami preserved in inter-tidal lacustrine and marsh-deposits – Some examples from northeast Japan. – J. Geol. **99:** 265–287.

Mollat, H. & Antoniades, P. (1978): 1:50,000 scale Geological Map of Greece, Sheet "Vasilika". – Institute of Geological and Mining Research.

Nanayama, F.K., Satake, K., Furukawa, R., Shimokawa, K., Atwater, B., Shigeno, K. & Yamaki, S. (2003): Unusually large earthquakes inferred from tsunami deposits along the Kuril Trench. – Nature **424:** 660–663.

Okada, Y. (1985): Surface deformation due to shear and tensile faults in a half-space. – Bull. Seismol. Soc. Amer. **75:** 1135–1154.

Okal, E. (1988): Seismic parameters controlling far-field tsunami amplitudes: a review. – Nat. Haz. **1:** 67–96.

Pantosti, D., Barbano, M.S., Smedile, A., De Martini, P.M. & Tigano, G. (2008): Geological evidence of paleotsunamis at Torre degli Inglesi (northeast Sicily). – Geophys. Res. Lett. **35**, L05311; doi: 10.1029/2007/GL032935.

Papadopoulos, G.A. & Chalkis, B.J. (1984): Tsunamis observed in Greece and the surrounding area from antiquity up to the present times. – Mar. Geol. **56:** 309–317.

Papanikolaou, D., Alexandri, M., Nomikou, P. & Ballas, D. (2002): Morphotectonic structure of the western part of the North Aegean Basin based on swath bathymetry. – Mar. Geol. **190:** 465–492.

Papanikolaou, D., Alexandri, M. & Nomikou, P. (2006): Active faulting in the North Aegean basin. – In: Dilek, Y. & Pavlides, S. (eds.): Postcollisional tectonics and magmatism in the Mediterranean region and Asia. – Geol. Soc. Amer. Spec. Pap. **409:** 189–209; doi:10.1130/2006.2409 (11).

Papanikolaou, I.D. & Papanikolaou, D.I. (2007): Seismic hazard scenarios from the longest geologically constrained active fault of the Aegean. – Quatern. Int. **171–172:** 31–44.

Papazachos, B.C. & Papazachou, C.B. (1989): The Earthquakes of Greece. – Ziti Publ. Thessalonica: 356 pp. (in Greek).

Papazachos, B.C., Comninakis, P.E., Karakaisis, G.F., Karakostas, B.G., Papaioannou, C.A., Papazachos, C.B. & Scordilis, E.M. (2000): A catalogue of earthquakes in Greece and surrounding area for the period 550BC-1999. – Publ. Geoph. Lab. Univ. Thessaloniki.

Pavlopoulos, K., Triantaphyllou, M., Karymbalis, E., Karkanas, P., Kouli, K. & Tsourou, T. (2007): Landscape evolution recorded in the embayment of Palamari (Skyros Island, Greece) from the beginning of the Bronze Age until recent times. – Géomorph. relief, processus, environment **1/2007:** 37–48.

Pinegina, T., Bourgeois, J., Bazanova, L., Melekesetev, I. & Braitseva, O. (2003): A millennial-scale record of Holocene tsunamis on the Kronotskiy Bay coast, Kamchatka, Russia. – Quatern. Res. **59:** 36–47.

Pirazzoli, P. & Pluet, J. (1992): World Atlas of Holocene Sea-Level Changes. – 300 pp., Elsevier Science Ltd..

Psimoulis, P., Ghilardi, M., Fouache, E. & Stiros, S. (2006): Subsidence and evolution of the Thessaloniki plain, Greece, based on historical levelling and GPS data. – Eng. Geol. **90:** 55–70.

Reicherter, K. & Becker-Heidmann, P. (2009): Tsunami Deposits in the Western Mediterranean: Remains of the 1522 Almería Earthquake? – In: Reicherter, K., Michetti, A.M. & Silva, P.G. (eds.) (2009): Palaeoseismology: Historical and prehistorical records of earthquake ground effects for seismic hazard assessment. – J. Geol. Soc. London Spec. Publ. **316**.

Roger, J. & Hébert, H. (2009): The 1856 Djijelli (Algeria) earthquake and tsunami: source parameters and implications for tsunami hazard in the Balearic Islands. – Nat. Haz. and Earth Sys. Sci. **8:** 721–731.

Rössler, S. (2008): Geologische Erkundung und geomorphologische Charakterisierung von küstennahen, geeigneten Ablagerungsräumen für tsunamigene Sedimenten im Golf von Saloniki (Thermaikos Golf). – Unpubl Diploma thesis: 118 pp., Geol. Inst., Univ. Leipzig.

Soloviev, S.L. (1990): Tsunamigenic Zones in the Mediterranean Sea. – Nat. Haz. **3:** 183–202.

Stock, C. & Smith, E.G.C. (2000): Evidence for different scaling of earthquake source parameters for large earthquakes depending on faulting mechanism. – Geophys. J. Int. **143:** 157–162.

Switzer, A.D. & Jones, B.G. (2008): Large-scale washover sedimentation in a freshwater lagoon from the southeast Australian coast: sea-level change, tsunami or exceptionally large storm? – The Holocene **18:** 787–803.

Tappin, D.R. (2007): Sedimentary features of tsunami deposits. Their origin, recognition and discrimination: An introduction. – Sed. Geol. **200:** 151–154 (and articles therein).

Tuttle, M.P., Ruffman, A., Anderson, T. & Jeter, H. (2004): Distinguishing tsunami deposits from storm deposits along the coast of northeastern North America: Lessons learned from the 1929 Grand Banks tsunami and the 1991 Halloween storm. – Seismol. Res. Lett. **75:** 117–131.

Vött, A., Brückner, H., Handl, M. & Schriever, A. (2006a): Holocene palaeogeographies of the Astakos coastal plain (Akarnania, NW Greece). – Palaeogeogr., Palaeoclimatol., Palaeoecol. **239:** 126–146, Amsterdam.

Vött, A., May, M., Brückner, H. & Brockmüller, S. (2006b): Sedimentary evidence of late Holocene tsunami events near Lefkada Island (NW Greece). – Z. Geomorph. N.F. Suppl. **146:** 139–172, Berlin, Stuttgart.

Vött, A., Brückner, H., May, M., Lang, F., Herd, R. & Brockmüller, S. (2008): Strong tsunami impact on the Bay of Aghios Nikolaos and it environs (NW Greece) during Classical-Hellenistic times. – Quat. Int. **181:** 105–122.

Wells, D.L. & Coppersmith, K.J. (1994): New empirical relationships among magnitude, rupture length, rupture width, rupture area, and surface displacement. – Bull. Seismol. Soc. Amer. **84:** 974–1002.

Yelles-Chaouche, A.K., Roger, J., Deverchere, J., Bracene, R., Domzig, A., Hebert, H. & Kherroubi, A. (2009): The Tsunami of Djidjelli (eastern Algeria) of August 21–22nd, 1856: Seismotectonic context, Modelling and implications for the Algerian coast. – Pageoph, Topical Volume; doi: 10.1007/s00024-008-0433-6.

Addresses of the authors:
Klaus Reicherter (corresponding author), Margret Mathes-Schmidt, Stefan Rössler and Christoph Grützner, Institute of Neotectonics and Natural Hazards, RWTH Aachen University, Lochnerstrasse 4–20, 52056 Aachen, Germany; k.reicherter@nug.rwth-aachen.de.
Ioannis Papanikolaou and Georgois Stamatis, Laboratory of Mineralogy & Geology, Department of Geological Sciences and Atmospheric Environment, Agricultural University of Athens, 75 Iera Odos Str., 118 55 Athens, Greece.
Dimitrios Papanikolaou, Laboratory of Natural Hazards, Department of Geology and Geoenvironment, University of Athens, Panepistimioupoli Zografou, 157 84 Athens, Greece.
Ioannis Papanikolaou, Benfield-UCL Hazard Research Centre, University College London, UK, i.papanikolaou@ucl.ac.uk.
Jean Roger, CEA, DAM, DIF, F-91297 Arpajon, France, now at: Ecole normale supérieure, Paris.

ISSN 8755-6839

SCIENCE OF TSUNAMI HAZARDS

Journal of Tsunami Society International

Volume 29 Number 3 2010

TSUNAMI CATALOG AND VULNERABILITY OF MARTINIQUE (LESSER ANTILLES, FRANCE)

Accary, F.[1,2], Roger, J.[2]*

[1] Université Paris 1 Panthéon-Sorbonne, Laboratoire de Géographie Physique, UMR 8591, 1 place Aristide Briand, 92195 Meudon Cedex, France.

[2] Ecole Normale Supérieure, Laboratoire de Géologie, UMR 8538, 24, rue Lhomond, 75231 Paris cedex 5, France
*e-mail: jeanrog@hotmail.fr

ABSTRACT

In addition to meteorological hazards (hurricanes, heavy rainfalls, long-period swells, etc.), the Caribbean Islands are vulnerable to geological hazards such as earthquakes, landslides and volcanic eruptions caused by the complex tectonic activity and interactions in the region. Such events have generated frequently local or regional tsunamis, which often have affected the island of Martinique in the French West Indies. Over the past centuries, the island has been struck by destructive waves associated with local or regional events - such as those associated with the eruption of the Saint-Vincent volcano in 1902 and by tsunamis of distant origin as that generated by the 1755 Lisbon earthquake.

The present study includes a classification of tsunamis that have affected Martinique since its discovery in 1502. It is based on international tsunami catalogs, historical accounts, and previous scientific studies and identifies tsunamigenic areas that could potentially generate destructive waves that could impact specific coastal areas of Martinique Island. The potential threat from tsunamis has been greatly increasing because of rapid urban expansion of coastal areas and development of tourism on the island.

Key- words: Tsunami, earthquakes, landslides, volcanic eruptions, Martinique, Caribbean, risk, hazards, vulnerability.

Science of Tsunami Hazards, Vol. 29, No. 3, page 148 (2010)

1. INTRODUCTION

1.1 Generalities

The Caribbean region, with its complex geodynamic and climatic context, is particularly prone to tsunami generation (O'Loughlin and Lander, 2003). The Caribbean tectonic plate is bordered to the north and south by numerous strike-slip faults where major earthquakes can occur. The magnitude Mw 7.0 Haiti earthquake of 12 January 2010 (Leroy et al, 2010) is a recent example of a destructive seismic event - similar to others that has occurred in the past along the Northern Caribbean margin (Pararas-Carayannis, 2010). Also, destructive earthquakes occur along the eastern boundary of the Caribbean plate (Germa, 2008) where there is active subduction with the North American plate at a rate of 2 cm/year, as well as along the western boundary – particularly along the Pacific coast - which is characterized by a higher rate of subduction of 9 cm/year (Grindlay et al, 2005).

Martinique is located within the Lesser Antilles islands group along the Atlantic subduction zone. This group is distinguished from the Greater Antilles (to the North), which is separated by the Anegada Strait between Puerto-Rico and the Virgin Islands (Fig. 1). The volcanic arc, which constitutes the Lesser Antilles, is over 850 km long and 450 km wide (Zahibo and Pelinovsky, 2001). Its formation results from tectonic processes associated to the subduction of the Atlantic plate beneath the Caribbean plate in two distinct phases: the first from the Eocene to the Oligocene (50 to 20 Myr BP), and the second during the Miocene (10 Myr BP) (OVSG-IPGP, 2005). Martinique and the neighbouring island of Sainte Lucie are located near the center of the volcanic arc and were created by the volcanic activity of these two phases (MacDonald et al, 2000). Numerous volcanoes are still active in the Lesser Antilles and some of them had eruptions and associated collateral events which generated tsunamis: Montserrat (Herd et al, 2005), Guadeloupe (Feuillard et al, 1983), Saint-Vincent (Le Friant et al, 2009), Mount Pelée on Martinique (Pararas-Carayannis, 2006; Leone and Lesales, 2008), Kitts in Saba, Liamiuga in St Kitts and Nevis and the Kick'em Jenny submarine volcano (Smith and Shepherd, 1993, Pararas-Carayannis, 2006) (Fig. 1).

Associated with such geological activity, the tropical climate of the archipelago results in violent storms, frequently causing coastal landslides that can generate local tsunamis. Also, along with the geological hazards associated with earthquakes, volcanic eruptions represent a real tsunamigenic threat. The mechanisms of tsunami generation from volcanic eruptions, debris avalanches, pyroclastic flows and collateral flank failure mechanisms in the Lesser Antilles - and Martinique in particular - have been examined and evaluated (Pararas-Carayannis, 2006). Also several historical catalogs have been compiled for tsunamis and tsunami-like events that have occurred in the region (Lander, 1997; Lander et al, 2002; O'Loughlin and Lander, 2003; Lander et al, 2003), with a special focus on the Lesser Antilles (Zahibo and Pelinovsky, 2001, Saffache, 2005b). However, there seems to have been no specific study of the tsunami hazard in Martinique itself. Thus, the primary objective of the present study is to review the pre-existing databases on events that impacted Martinique and to propose a new catalog, composed only of the well-known and documented tsunamis. Furthermore, the present study reviews briefly the island's vulnerability, with a special emphasis on La Trinité Bay. However, in order to understand the historical accounts of tsunamis that have affected Martinique in the past, we need to review its geographical and geo-tectonic setting.

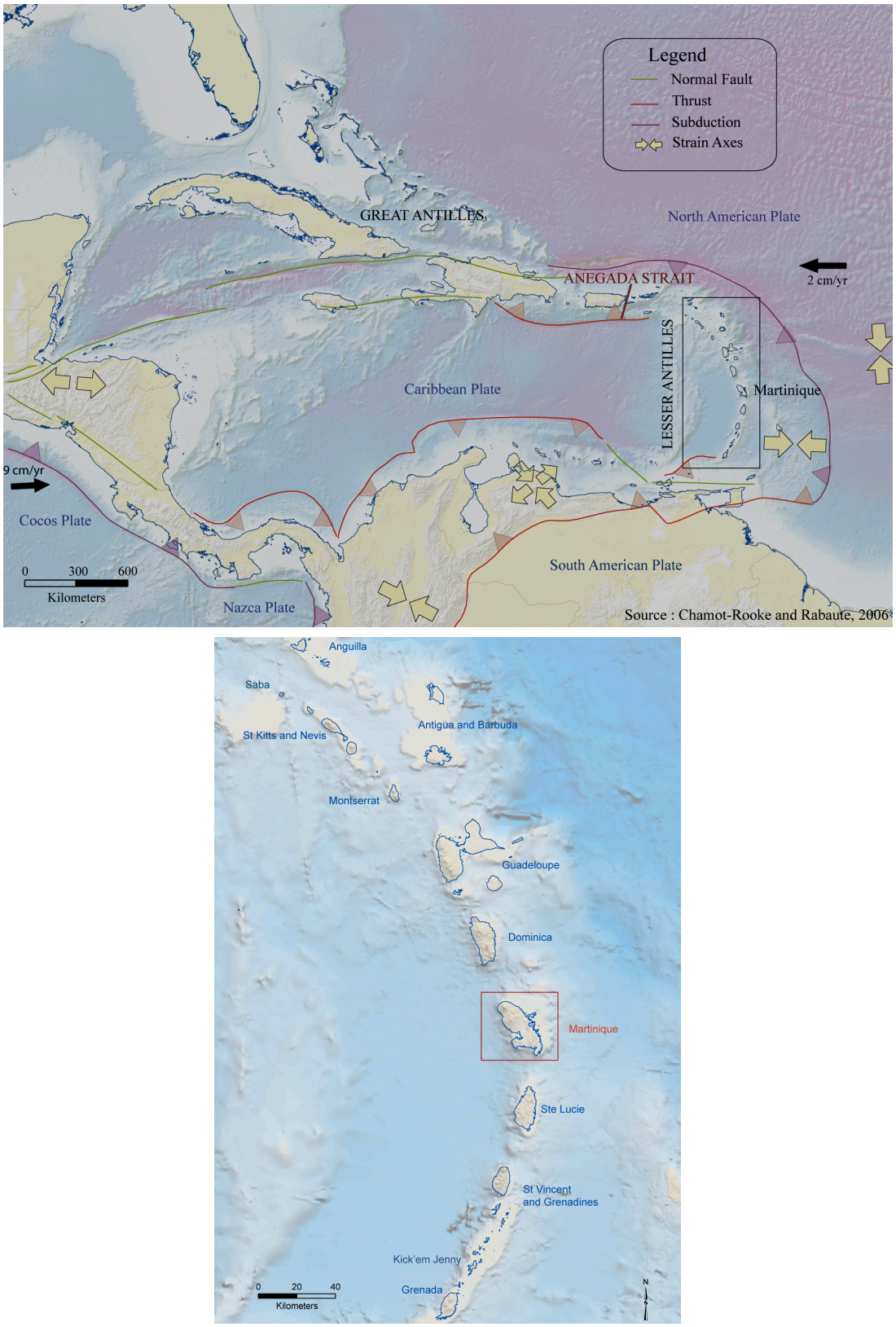

Fig. 1: Geodynamical context of the Antilles (tectonic scheme from Chamot-Rooke and Rabaute, 2006; bathymetric data from GEBCO (IOC, IHO and BODC, 2003) and geographic location of Martinique Island within the Lesser Antilles.

1.2 Martinique

1.2.1 Geography

Martinique is a volcanic island located upon a subduction zone and which has Mount Pelée, an active volcano (Westercamp and Tazzieff, 1980; MacDonald et al, 2000, Pararas-Carayannis, 2006). The island exhibits various reliefs ranging from swamplands near the sea to volcanoes. Mount Pelée reaches 1398 m in height and three other peaks exceed 1000 m. If we draw a line between Fort-de-France (west coast) and La Trinité (east coast) The highest reliefs are found in the northern part of the island (Fig. 2). The southern part of the island is mainly constituted of low hills and swamplands. The littoral exhibits alternation between steep cliffs in the north and sand beaches (Les Anses d'Arlet, la Caravelle, St Anne, etc.) and mangrove forests (Le Lamentin for example) in the south (Saffache, 2005a).

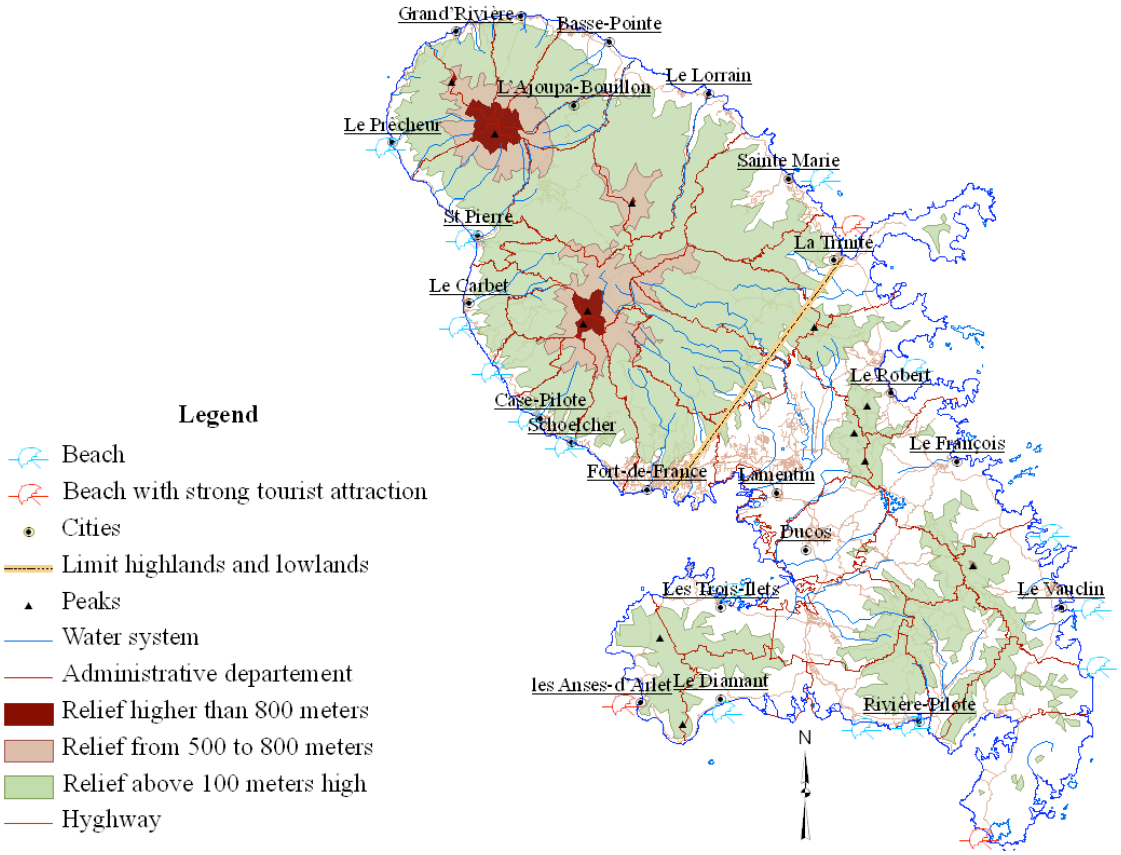

Fig. 2: Geography of Martinique Island. The yellow line indicates the limit between the hilly landscape (northern part) and the plain (southern part).

The great 2004 Sumatra event demonstrated that a steep continental slope and coastal features such as coral reefs, mangrove forests and lagoons help reduce the degree of a tsunami's impact by slowing down its propagation and absorbing or reflecting part of its energy (Kathiresan and Rajendran, 2005, Kunkel et al, 2006). However other coastal features can increase a tsunami's adverse impact by resonance amplification or by inducing strong currents generation usually in bays or harbours (Sahal et al, 2009, Roger et al, 2010a). Beaches with gentler slopes also tend to amplify the wave heights due to a shoaling effect.

1.2.2 Historical Development of Martinique

In pre-colonial times, the island of Martinique was subjected to two successive waves of human settlement, first in the 4th century BC (with the arrival of the Arrawak people) and then in the 13th century AD (with the Caribbean people) (Lalung, 1948). Following the arrival of the Europeans in 1502 and the settlement of French colonists in 1635 (Lambolez, 1905; Chauleau, 1993; Charbit, 2006), the island was integrated into the French colonial empire and its population increased tenfold thanks to triangular trade (Charbit, 2006; Clément, 2009). Nowadays, Martinique has a population of over 400.000 (INSEE, 2009), which is mostly concentrated in the conurbation of Fort-de-France, Schoelcher and Le Lamentin (Calmont and Vassoigne, 1999), as well as in a few other towns deemed attractive, such as Sainte Marie and Le Robert. These five agglomerations concentrate nearly fifty percent of the population of the island (INSEE, 2009).

The bay of Fort-de-France concentrates poles of economic activity, political and decision-making centres and luxury commuter towns (Schoelcher) (Calmont and Vassoigne, 1999). Some southern cities benefit from the attractiveness of heliotropical tourism, which attracts about 700.000 visitors every year (Schleupner, 2007). The increase in tourist influx along the coastal zones and the popularity of seaside activities require that a study of the tsunami hazard has a high priority and must be undertaken, thus we begun by documenting historical tsunami data into the following catalogue.

2. TSUNAMI CATALOG

2.1 Data

The conclusions of the present study rely mainly on the historical database of tsunamis that have been recorded in Martinique and the neighbouring islands. Material used for this database includes original historical documents (testimonies, letters, etc.), which are considered as primary sources, whereas secondary sources are derived from recent studies, tsunami catalogues, simulation results, etc.

2.1.1 The Catalog

Existing historical tsunami catalogs provide a general idea of the tsunami hazard in the Antilles. These catalogs are archived and updated by different government organizations such as NOAA (U.S. National Oceanic and Atmospheric Administration) and the Tsunami Laboratory at Novosibirsk (Russia), or compiled by research of historical records (Lander et al, 2002; O'Loughlin and Lander, 2003; Saffache et al, 2003). Although derived from the same original historical data – which includes dates, source areas, wave heights or other miscellaneous information - these catalogs produce different results because of differences in the methodology of compilation. In our study, all of these existing catalogs have been analysed and inter-correlated in order to produce a single, better-documented tsunami catalog.

The worldwide tsunami catalog from NOAA provided at the following internet site (http://www.ngdc.noaa.gov/hazard/tsu_db.shtml) and that of the Tsunami Laboratory of Novosibirsk (http://tsun.sscc.ru/proj.htm) do not index all the tsunamis that have occurred but only the most significant.

Catalogs by O'Loughlin and Lander (2003) and Lander et al. (1997, 2002, 2003) list tsunamis for the entire Caribbean. The catalog by Saffache et al. (2003) includes earthquakes and abnormal sea level rises that have occurred in the French Antilles (Guadeloupe and Martinique Islands). Although helpful, these catalogs have a broader regional focus and do not provide sufficient information on specific events to be adequate for a risk assessment study of Martinique. To properly assess the risk, it is necessary to review carefully local historical archives as indicated subsequently.

2.1.2 Historical Documents

Analysis of historical documents (Du Tertre, 1668, Boyer-Peyreleau, 1823; Hess, 1902; Lacroix, 1904; Lambolez, 1905), and particularly of various testimonies recorded in Martinique archives (http://www.manioc.org; http://gallica.bnf.fr), highlights details that were omitted from earlier catalogs and scientific papers. Most of these documents report on the 1902 catastrophe on the island (Hess, 1902, Lacroix, 1904) and some provide useful information on its historical development since 1635 (Royer-Peybeleau, 1826; Du Tertre, 1668, Lambolez, 1905). Review of these accounts is helpful in documented the destructive impact of tsunamis on the local population, on the resulting losses and on reactions (Hess, 1902; Lambolez, 1905). Moreover, these accounts provide an important amount of information for specific locations, as for example the impact of the May 5, 1902 tsunami in the vicinity of the Guérin factory (Hess, 1902), as well as on records of false alarms and the lack of proper warning by public authorities during the eruption of the Mount Pelée volcano (Lambolez, 1905). However, in spite of the wealth of details that can be found in these historical sources, many more historical documents pertaining to the Martinique's maritime trade were lost due to the destruction of archives (by the 1902 eruption of Mount Pelée). Hopefully, research studies may help compensate for these gaps in knowledge.

2.1.3 Scientific Studies

Some tsunamis have been investigated in detail through scientific research. Such research provides details, which can complement the data already gathered through historical analysis. Events that have been researched include the 1755 Lisbon earthquake and tsunami (Baptista et al, 1998; Chester, 2001; Baptista et al, 2003; Barkan et al, 2009; Roger and Baptista, 2009; Roger et al., 2010a, 2010b), the 1761 earthquake (Baptista et al, 2006), and those associated with recurring eruptions of the submarine volcano Kick'em Jenny (Smith and Shepherd, 1993, Pararas-Carayannis, 2006). These studies help visualise what could happen in an areas where information is lacking and help assess the generating sources and impacts of potential tsunamis.

2.2 Data Selection

2.2.1 Storm Surges

In reviewing the data in existing catalogs attention was paid in identifying and excluding storm surges that may have been wrongly listed as tsunamis. It appeared that numerous phenomena recorded as tsunamis in Martinique were in fact storm surges generated by storms and hurricanes, which are frequent in the Antilles region (Royer-Peybeleau, 1826; Lambolez, 1905; Saffache et al, 2003; O'Loughlin and Lander, 2003). Thus, seventeen events (in 1642, 1694, 09/12/1756, 08/24/1757, 08/14/1766, 09/05/1776, 10/12/1780, 08/14/1788, 09/06/1816, 10/21/1817, 09/21/1818, 07/26/1825, 09/20/1834, 09/09/1872, 09/04/1883, 08/18/1891 and 08/08/1903) had to be taken away from our catalogue because they had been generated by hurricanes. For example, Revert's account (1949) lists a total of 34 hurricanes between 1633 and 1903. Among hurricane generated storm surges, seven events (in 1642, 1694, 1756, 1757, 1766, 1780 and 1883) were particularly destructive to crops and ships. The worse of these storm surges appears to have been that of August 18, 1891, which wrecked the city of Le Lamentin (Lambolez, 1905) and caused severe damages (Revert, 1949).

2.2.2 Uncertain Tsunamis

After cross-matching data gathered from different scientific studies, some tsunamis had to be left out of the catalogue, since no evidence indicates that they actually reached Martinique. Among these, many are of volcanic origin, whether at the global scale associated with the 1883 eruption of the Kratatau volcano in Indonesian (Choi et al, 2003; Pararas-Carayannis, 2003), or at the scale of the Lesser Antilles with the low intensity eruptions of the Kick'em Jenny (Smith and Shepherd, 1993) and of the Souffrière Hills in Montserrat (1824, 1897, 1997), 320 kms away from Martinique. Finally, this selective process also excludes the formation of an 'ephemeral mud island' as the one off the coasts of Trinidad at various points in time, specifically in 1853, 1874, 1911, 1928, 1934) (O'Loughlin and Lander, 2003).

2.3 Criterion of Validity

The criterion of validity used in the present study is different from that which was used in the catalog compiled by the Laboratory of Tsunamis of Novosibirsk (www.tsun.sscc.ru/) and that used by O'Loughlin and Lander (2003). The scale of validity used for the Martinique catalog adhered to factual information as specifically as possible (Table 1). Thus, events reported as 'abnormal oscillations' by some observers (with degree 1 on the tsunami scale), were separated from tsunamis that appear more frequently in different sources (with degree 4), or from those to which all sources systematically refer (degree 5). Degree 2 corresponds both to known tsunamis, but about which it is not certain whether they impacted Martinique or not (degree 2a) and to tsunamis that may have occurred but were not recorded in Martinique, in spite of a violent earthquake or a landslide recorded by observers (2b). In other words, such events may be known to have occurred, but none of the sources available either suggests that the event in question caused a tsunami or that it affected Martinique. However, it was decided to include them in the study because it is possible that such events were not recorded on the island simply because there were no observers on site, or for other reasons (occurring at night, micro tsunami, etc.).

3. RESULTS AND DISCUSSION

3.1 Results

Overall, the present study included at least thirty-three tsunamis, of which only five did not reach Martinique according to original references. These included the 1831 Granada tsunami, the 1874 and 1880 Dominica tsunamis and the 1985 and 2004 Guadeloupe tsunamis (Table 2). In addition to date and localisation, the catalog indexes the origin, the degree of validity associated to some tsunamis, as well as some parameters such as amplitude and run up. Also, the catalog lists various other notes and information, regarding contradictions that were found in the researched sources (as for example, the 1751 tsunami). The catalog stands out due to the heterogeneity of the level of information available for each event. Thus, some tsunamis, such as those of 1755 or 1902, benefit from the abundance of details in well-documented sources and additionally conducted research. However, other events such as the 1657 and 1874 tsunamis are very poorly documented, since they occurred a long time ago (1657 was the year of the first earthquake ever perceived by the colonists, who had only just settled on the island in 1635), or because of the sparseness of damage caused by the reported 'abnormal oscillations' (as for the 1874 event).

3.1.1 Detailed Analysis

A more detailed review of the various tsunamis reported in the database has allowed the present study to group some events in accordance to their origin characteristics (seismic, volcanic), or in accordance to the propagation characteristics (local, regional, or far-field tsunamis). Of all the events indexed in the catalog, only four are absent from Figure 3 (the Hispaniola earthquake of 1751; the Lisbon earthquake of 1755; the Surinam earthquake of 1767 and the Costa Rica earthquake of 1991).

Figure 3 shows the origin of twenty-six tsunamis generated near the Lesser Antilles, of which twenty-one were observed on Martinique. These include the tsunamis which occurred on the following dates: 6 April 1690; September 1702; 6 March 1718; 30 November 1823 and 1824; 30 November 1827; 26 October 1829; 26 July 1837; 11 January 1839; 8 February 1843; 18 November 1867; 8 November 1876; 5 May 1902; 7 May 1902; 8 May 1902; 9 May 1902; 20 May 1902; 30 August 1902; 16 February 1906; 24 July 1939; 25 December 1969; 22 April 1991 and 21 November 2004.

Of the thirty-three tsunamis listed in the catalog, half are of seismic origin generated mainly around the Virgin Islands (as the 18 November 1867 event) and Guadaloupe (as the 1843, 1969, 1985 and 2004 events). Tsunamis in the region are also generated from volcanic sources and more than ten of those recorded were associated with the volcanoes of the Caribbean archipelago (i.e. Kick'em Jenny, Souffrière Saint-Vincent, Mount Pelée and the 'Souffrière' of Montserrat). Tsunamis generated by landslides in the region seem to be under-represented in the diagram – with only one event being included. However, it should be noted that landslides could be triggered by both seismic and volcanic events. It is therefore necessary to take into account that 13% of all tsunamis are of multiple origins (Fig. 4).

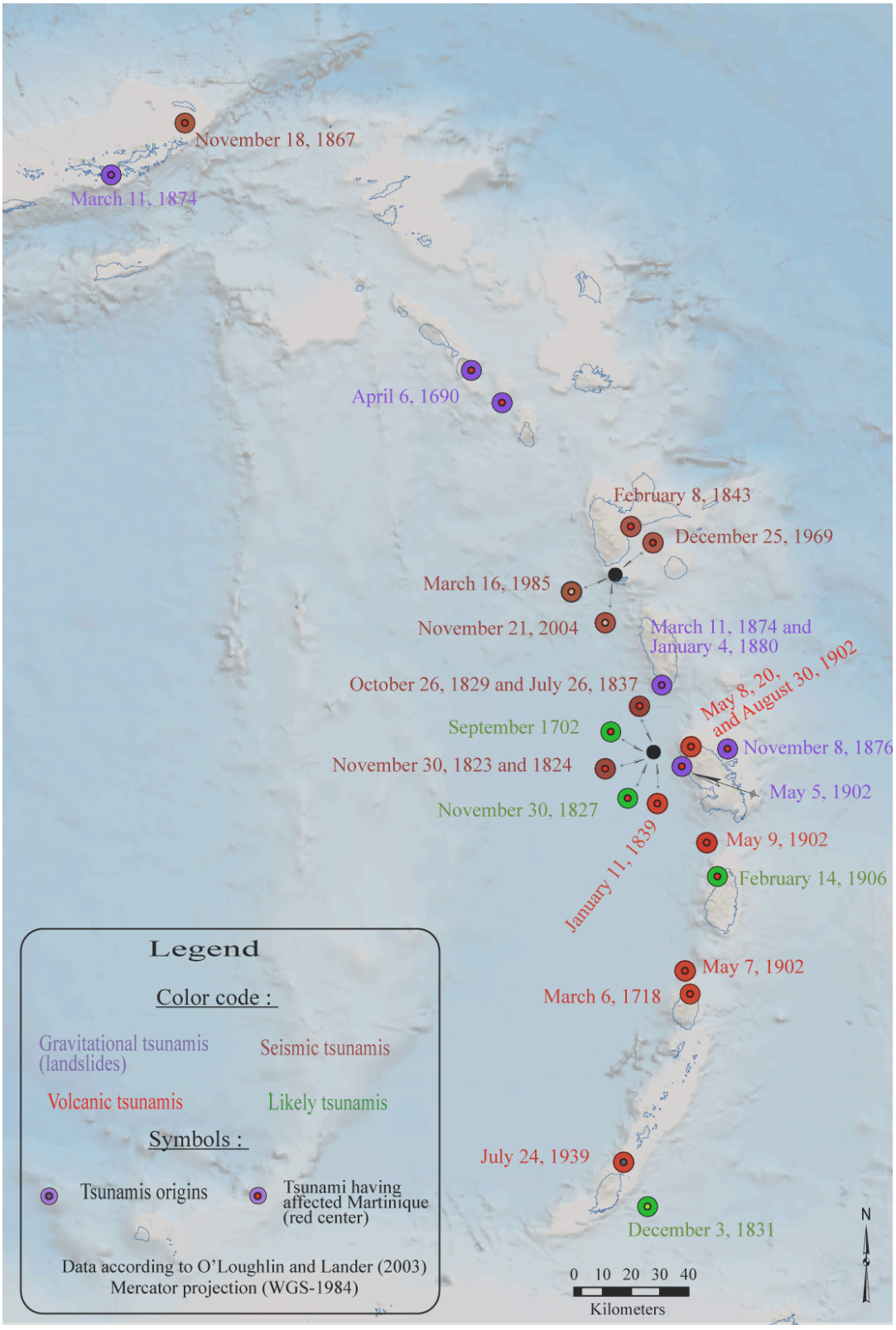

Fig. 3: Sources of tsunamis in the arc of the Lesser Antilles.

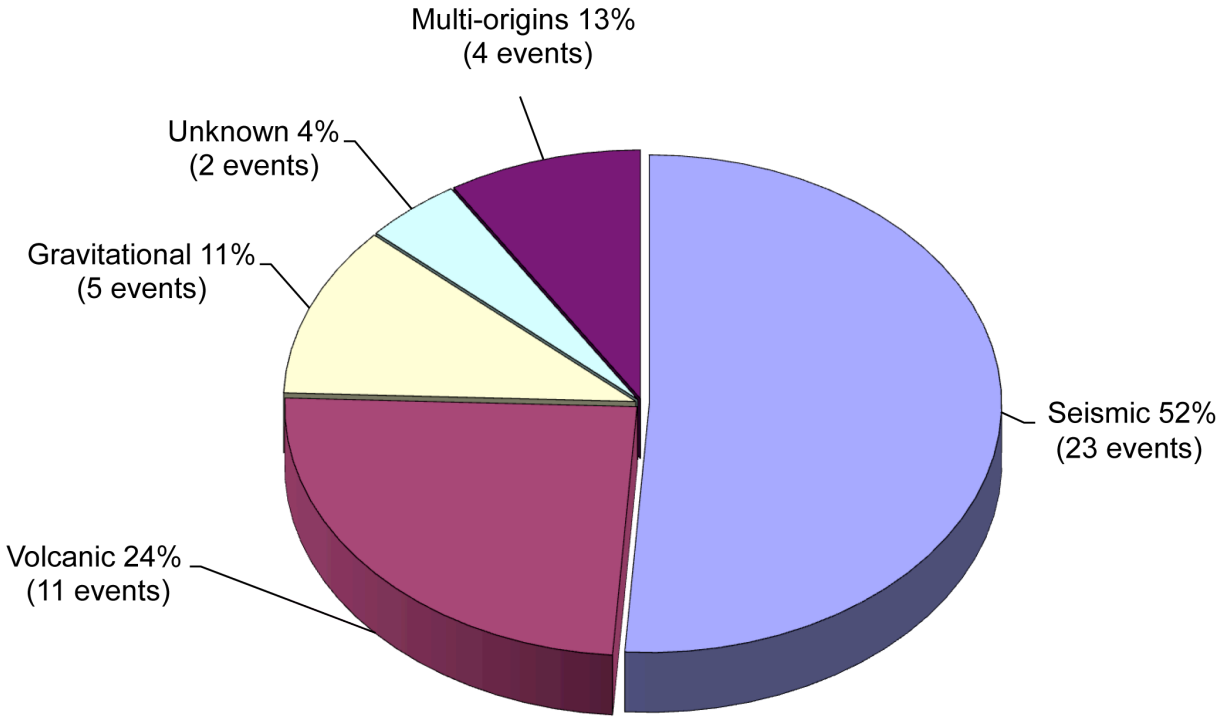

Fig. 4. Distribution of tsunamis according to origin.

Lastly, two events (1829 and 1837) are of unknown origin. This lack of information is attributed to the inadequacy of historical accounts and the inability to determine the tsunami source mechanism. Thus, these two events may have been caused either by a passing hurricane or by an earthquake. It should be noted that in those times, the violence of hurricanes could foster 'jolts' that were thought to be earthquakes. However, this confusion regarding the origin of tsunamis only affects 6% of the total number (i.e. the two events).

The second diagram (Fig. 5) illustrates the prevalence of local tsunamis (comprising of 49% of the total) over regional tsunamis (comprising of 36%). Martinique is therefore mostly subjected to tsunamis originating near neighbouring islands such as Saint Vincent, or Guadaloupe. The only tsunami of distant origin is represented by the single Lisbon tsunami of 1755.

Although many tsunamis have been observed on the coasts of Martinique, few have been located with geographic accuracy. Thus, in the majority of cases, the original references mention Martinique without attempting to classify the coasts on the island that were affected by tsunami wave action.

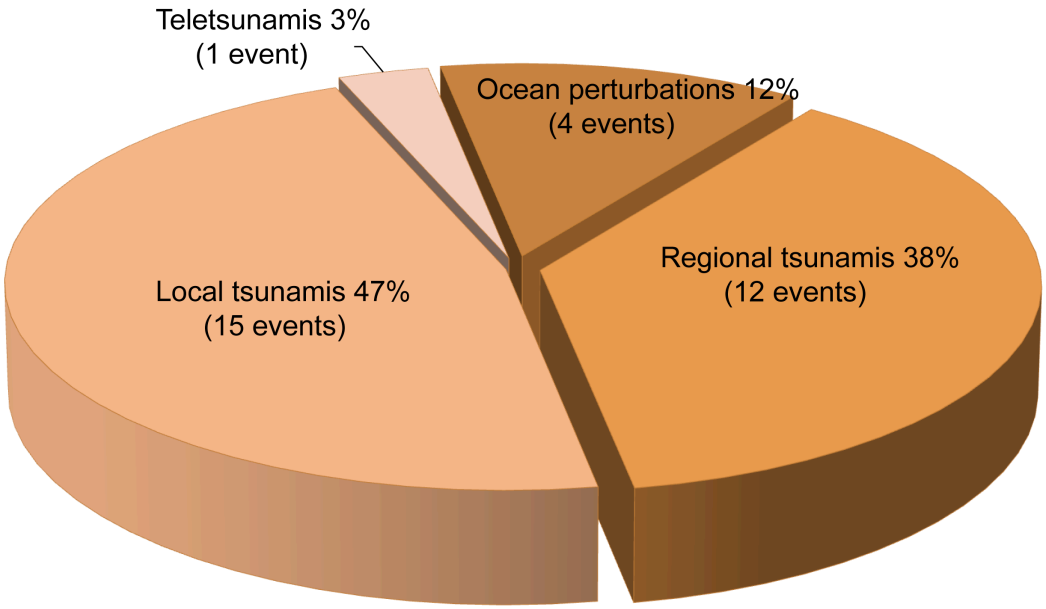

Fig. 5. Classification of tsunamis according to impacted zone.

The map (Fig. 6) shows towns in Martinique that were affected by tsunamis, according to observations found in different reference sources. These indicate which of the coastal areas are particularly vulnerable to tsunami impact. Among them, is the coastal area along the flanks of the volcano stretching from Macouba to The Carbet via Le Précheur (Northwest), but also the coast stretching from Case-Pilote to Trois-Ilets, along the bay of Fort-de-France and, finally, the tourist area stretching from Sainte Marie to the Robert, near the presqu'isle of the Caravelle (La Trinité). Other sites could have been impacted but lack of educated population to document what happened limited most of the observations in major towns.

Figure 7 helps visualise the cities that are most vulnerable to the tsunami hazard in Martinique. Saint Pierre (27%) and La Trinité (26%) are the towns that would be most affected. The 27% mentioned for St Pierre indicate that 27% of the listed tsunamis in the catalog affected St Pierre. The destruction of the capital city of Saint Pierre during the cataclysmic eruption of 1902 was a definitive blow since it resulted in the deaths of the city's population (28.000 people), but also its status as capital at the benefit of Fort-de-France. La Trinité presents an original profile in so far as it is affected to locally produced tsunamis (such as those of 1876, 1902, etc.), but also to tsunamis of distant origin (such as that of 1755), which makes this location as the most sensitive on the island in terms of exposure to the tsunami hazard. Some towns in the North of the island (Basse-Pointe, Macouba, le Précheur) are also exposed to 'oscillations', as it was shown in 1902, when Mount Pelée was particularly active.

However, it should be noted that an overwhelming majority of the population on Martinique is concentrated in coastal towns and areas, which are particularly vulnerable to tsunamis (Goiffon, 2003).

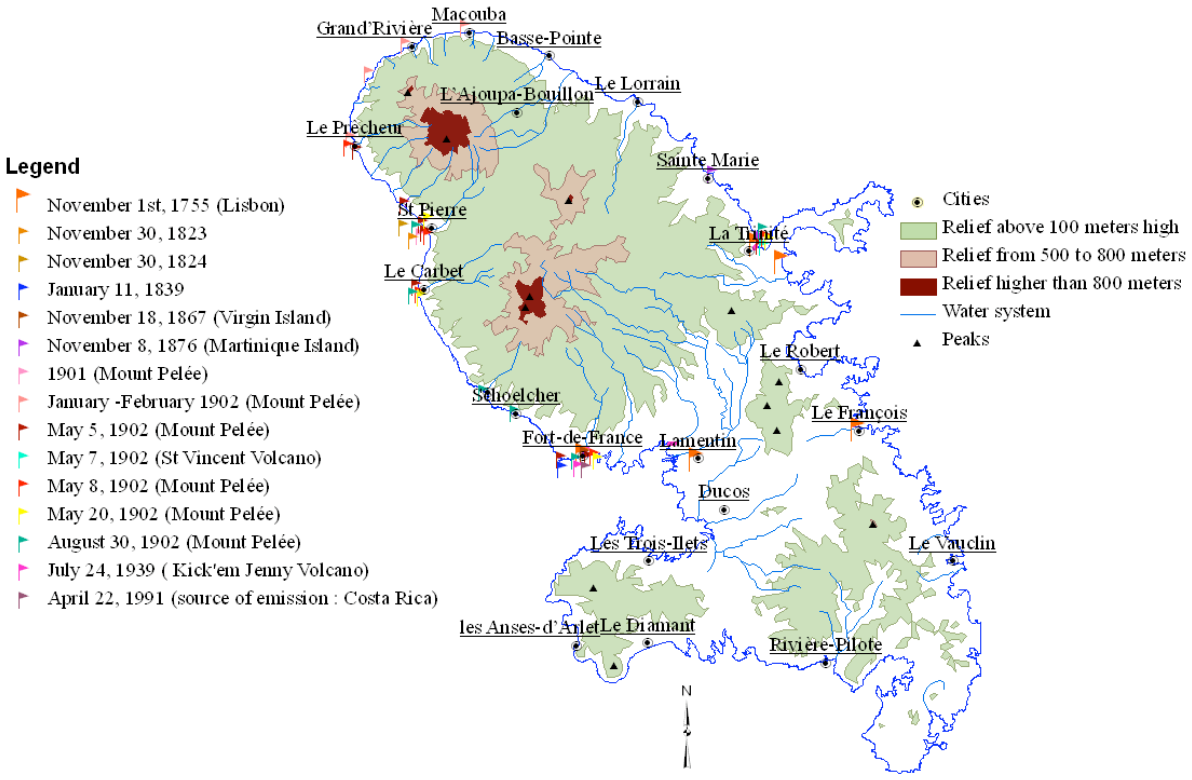

Fig. 6. Cities in Martinique impacted by past tsunamis.

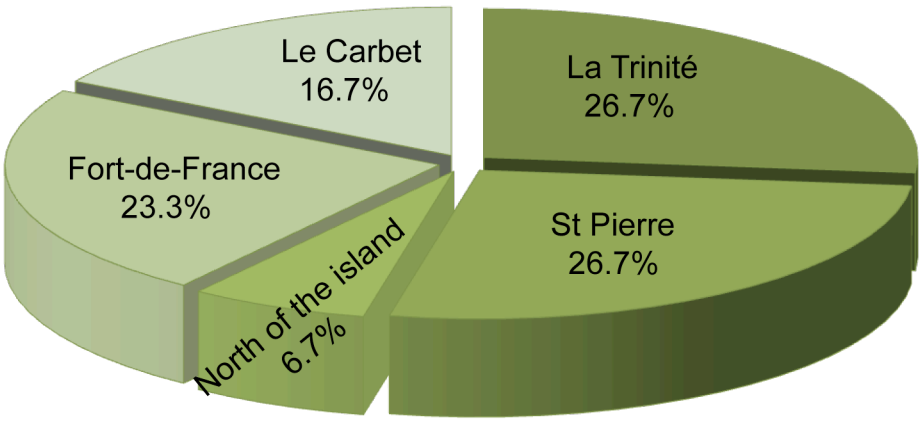

Fig. 7. Towns in Martinique affected by tsunami hazard.

3.1.2 Major Events

1755 November 1

The tsunami of 1 November 1755 is the only event of distant origin ever recorded in Martinique. The 1755 earthquake and tsunami were extremely destructive in Lisbon. The tsunami was recorded in Madera and in Morocco (Barkan et al, 2009) and reached the American continent and the Caribbean region (Roger et al, 2010a, 2010b, 2010c). The first of its waves reached the Island of Martinique in the afternoon and its subsequent effects lasted for about four hours (from 14:00 hrs to 18:00 hrs). This gap is consistent with the results obtained by numerical simulations, since the tsunami's origin time was at about 09:30 on November 1 and took over 7 hours to reach the coasts of Martinique (Roger et al, 2010). The Presqu'isle of Caravelle and the small town of La Trinité (west coast) were the first ones affected. Subsequent tsunami wave refraction around the island was observed as in the Baleares during the tsunami of Zemmouri in 2003 (Alasset et al, 2006) - and the bay of Fort-de-France was flooded. This phenomenon of wrap around is well described by Yeh et al. (1994). At the same time there was a rise in sea level along the coasts, the level of some rivers. There was sharp increase in sea level at Lamentin (Fort Royal) and Epinette (La Trinité), leading to further inland inundation (Lambolez, 1905; Baptista et al, 1998; Baptista et al, 2003; Lander et al, 2003; Roger et al, 2010b).

The Tsunamis of 1902

Various tsunamis that occurred in 1902 (on May 5th, 7th, 8th, 20th and 30th) affected extensive areas stretching from Grand-Rivière, in the North of the island, to La Trinité, via the area of Le Prêcheur, le Carbet–Case Pilote and the Trois Ilets. Fig 6 shows the various areas that were flooded. Inspite of the diversity of tsunami origins, the waves exhibited high concentrations at the same localities. Thus, the tsunami generated by the May 5th lahar flow impacted St-Pierre, the Carbet, Fort-de-France and La Trinité, as was the tsunami generated by the eruption of La Souffrière on the Island of St-Vincent, although with lesser intensity.

3.2 Discussion

Documenting through a regional study - within the framework of the Caribbean - the tsunamis that affected the island of Martinique allows to identify as well coastlines vulnerable to the tsunami hazard. However, the list of events described above, just like the catalog and the maps, show that tsunamis are potentially destructive in this area of the Caribbean, where high-magnitude earthquakes (in 1690, 1751, 1831, 1843, 1867, 1969 and 1991) and volcanic eruptions (in 1718, 1880, 1902 and 1939) are frequent and can also result in landslides (as in 1690, 1718, 1876, 1880, 1902 and 1985). Tsunamis that can affect Martinique can be generated from diverse local as well as distant sources. Mainly tsunamis that can affect Martinique tend to be of local origin, thus there is not sufficient time to issue a tsunami warning. Earthquakes generate the majority of tsunamis, although many are caused by gravitational flank collapses as well as lahars and landslides. Although the sources of many tsunamis have been identified as located in many of the islands of the Caribbean arc, Martinique on its own, principally because of the re-awakening of the Mount Pelée volcano has generated over eight local tsunamis within a year (1902), of which two were registered as 'abnormal oscillations'.

From a spatial point of view, according to Figure 8, we can say that three towns are particularly vulnerable: Fort-de-France (the political and economical capital of the island), La Trinité and Saint-Pierre. Presently, a tsunami generated by a new eruption of Mount Pelée would potentially affect the towns of Le Précheur, Grand-Rivière, Macouba, and Saint-Pierre, which have a total population of 8,360 inhabitants (plus the tourists), i.e. 2% of the population of the island (INSEE, 2009). On the contrary, a tsunami like that of 1755 would affect the towns of Fort-de-France, Le Lamentin, La Trinité and Le François, i.e., where over 40% of the population (162,131 inhabitants) are located (INSEE, 2009). Relatively, only the southern and the west coasts of the island seems to be protected from tsunamis because of the presence of natural and residual coral reef barriers.

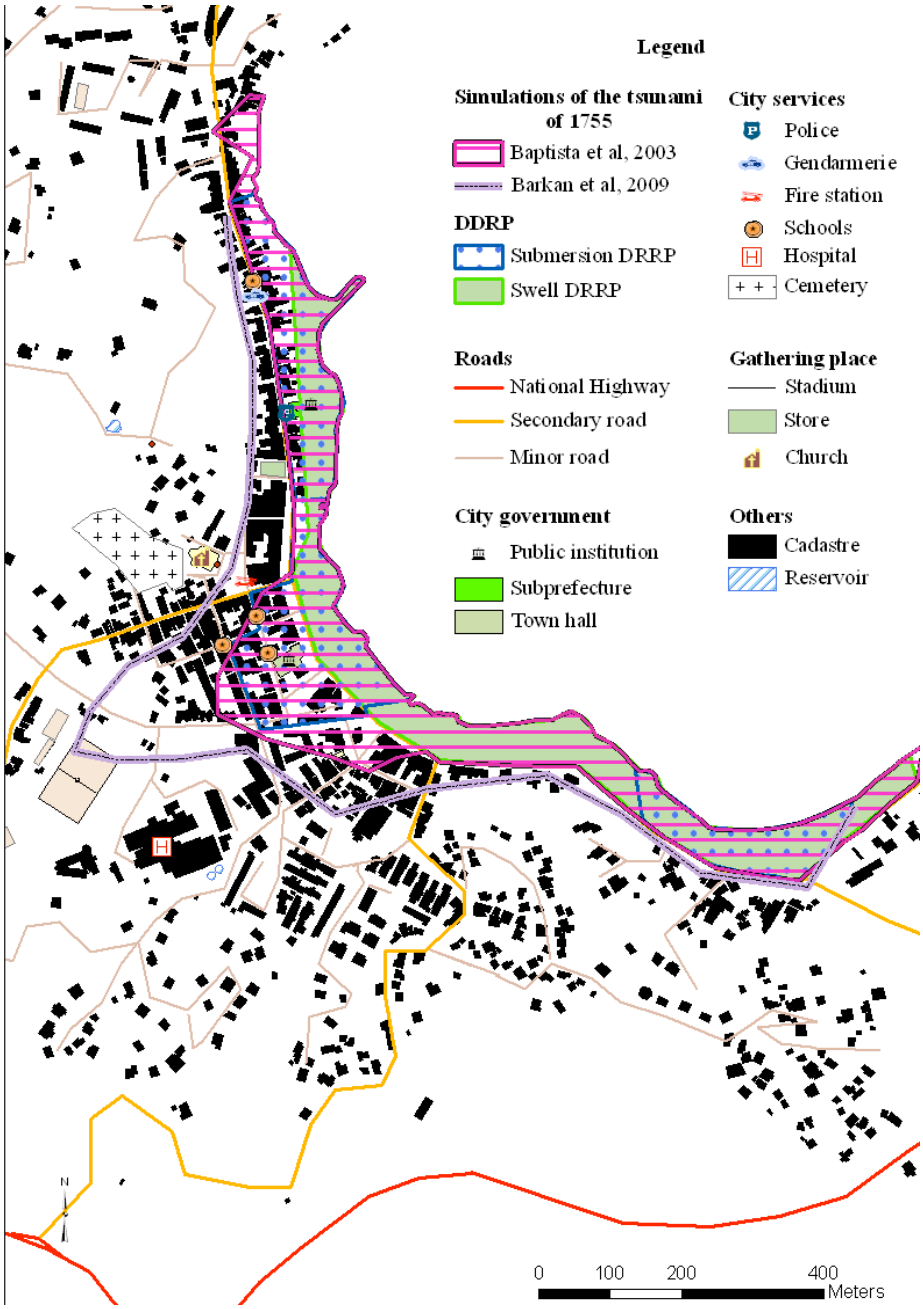

Fig. 8: Vulnerability of La Trinité: local submersion hazard limit and proposition of extension according to tsunami simulation. All the strategic sites and roads are indicated.

3.2.1 Uncertain Tsunamis

The detailed catalog (chart) also lists tsunamis, which cannot be documented with certainty. The following is a discussion of seven such events.

The first is a set of two tsunamis that appear in all written testimonies with only date, time and origin. Archived exactly one year apart, respectively on 30 November 1823 and 30 November1824, both of these events purportedly caused 'damages in the harbour' on those two dates - seemingly the Saint-Pierre harbour. Moreover, both events appear to have occurred following periods of high temperatures that were accompanied by torrential rains (Mallet, 1852, 1853, 1854). These similarities lead to two distinct hypotheses. It is entirely possible that these two purported tsunamis were in fact one single event, wrongly reported as separate events due to transcription of calendar mistakes. Alternatively, it is somewhat possible that the two events resulted from earthquakes that occurred exactly one-year apart. However it is highly unlikely that such coincidence in the day and month actually occurred. Finally, it is also entirely possible that the reported tsunamis were storm surges generated by hurricanes.

The tsunami of 8 November 1876 is reported in a letter that is referred in Lambolez (1905). This letter recollects 'waves' and 'bellowing swell' between the Presqu'isle of the Caravelle and Sainte Marie, stating that 'often to occur here'. This purported tsunami seems to have originated from a submarine landslide if we take its description into account. However, there is a significant margin of error when dealing with historical sources that contain vague descriptions. Significantly, this event is not listed in any of the other reference sources.

Finally, insufficient information is provided regarding the remaining uncertain tsunamis as to their geographic origin location, so that these cannot be really considered as real events by the present study. In fact, many of these events are referred to in an unspecific way and may have been induced by landslides, earthquakes, and storms - as was the case for the 3 June 1718 or 2 August 1837 events. Other tsunami events listed as 'abnormal oscillations' (i.e. the 1657 event) make it even harder to assess the validity of their tsunamigenic nature. All of these tsunami events, because of vagueness of the information, are associated with a degree of validity (see Table 1) that allows us to visualise them quickly and dissociate them from those that are better documented as certain.

Overall, only the tsunamis that caused serious and significant damages, both in material and in human lives, are verifiable with any kind of factual certainty in assessing Martinique's potential tsunami hazard. These major events have become the subject of numerous studies, which further permit the assessment of tsunami risk for other coastal areas of the island. Unfortunately some tsunamis, although destructive, are harder to document adequately because of lack of interest. For example the 1761 tele-tsunami, associated through its origin with the Lisbon earthquake of 1761, illustrates the difficulties in the compiling of historical catalogs, since good registration of events depends on the validity of historical reports and of various documents. In the case of 1761, only a few specialists (Zahibo and Pelinovski, 2001; Baptista et al, 2006) have studied this tele-tsunami, and the results do not allow us to integrate this event in the study of tsunamis in Martinique, due to the lack of proper historical accounts, regarding the impact on the island.

3.2.2 Uncertainty of Sources

In view of the above listed uncertainties, the results need to be evaluated critically, since they rely partly on sources that may depend on author's subjectivity.

Historical sources must be used with caution as they may introduce erroneous data, due to inadequate understanding by the reporting past scientists and observers. Thus, of the many recorded 'raz-de-marées' (common French for tsunami), only a few are actually tsunamis. Let us note that the observation and localisation of tsunamis depends mainly on human presence along impacted areas and that at coastal areas with low population density significant tsunami impact may not have been properly reported. Furthermore many of the names of localities on the island have changed through centuries, so it is not always easy to locate precisely the extent of the flooded zones (i.e. 'as far as the stone bridge on river Roxelane', (Lambolez, 1905)). The use of secondary sources is also a factor of uncertainty, as the problem raised by O'Loughlin and Lander (2003) shows, when they explain the existence of different dates for a single event due to calendar mistakes. Finally, the absence of information in the archives does not necessarily mean an absence of an actual tsunami, since literate men – who were scarce in this colonial island, only transcribed these events.

Additionally, the results of tsunami modelling depend on the data gathered by the research specialists; therefore, as with any other scientific endeavour, they come with a margin of error or uncertainty. These models can overestimate or underestimate tsunami amplitudes. Only a study of sedimentary deposits (as in Morton et al, 2006) can confirm whether the listed tsunamis actually occurred. However, subsequent development of the heavily populated coastal areas makes such investigations almost impossible, unless construction works expose accidentally tsunami deposits (Nicolae-Lerma, pers. comm., 2010).

Lastly, the data gathered by the mareographs of SHOM may have been useful, but no access was possible. Moreover, most of the mareographic equipment has only been installed recently (October 2005) on Martinique (Créach, pers. Comm., 2010).

Up to now the present study concentrated on the tsunami hazard in Martinique but without including a social-economic dimension: the vulnerability. Only the coastal town of La Trinité was chosen for further assessment of the tsunami hazard.

3.2.3 Vulnerability of La Trinité

The town of La Trinité is located on the Atlantic coast of the island. It has a population of 13,582, distributed over an area of 45.8 km². Although the town concentrates only 3.5% of the Martinique's total population, it is the designated local administrative centre ('sous-préfecture' - district level) and is host to the only hospital on this part of the coast. Moreover, La Trinité has been affected in the past by eight tsunamis of various origins (seismic, volcanic, landslides) and generating sources (Lisbon, Saint-Vincent, Martinique). Of those recorded in La Trinité, which seem to be the largest, only the 1755 tsunami provides sufficient data to conduct a vulnerability study of the town nowadays. Moreover, La Trinité is located at very low elevation (< 5 m) and concentrates its public offices in a narrow area very close to the sea, which increases the town's tsunami vulnerability. Thus, Figure 8 shows

the strategic sites of the town (schools, administrative centres, firehouses, hospitals, etc.) as well as the simulation results that were produced using the source of Barkan et al. (2009), maximising a scenario for the Caribbean, located in the Iberian peninsula but not based on existing submarine or geological structures (Roger et al, 2010a). The results of modelling, however, have not been yet published for Martinique.

As a matter of fact, no Disaster Risk Reduction Plan (DRRP) seems to be interested in indexing the vulnerability of the coastal areas with regards to the tsunami risk, whereas the Swell and Submersion DRRP are already taken into account in urbanization planning. The use of maximising the scenarios with tsunamis generated either by earthquakes affecting the Caribbean and/or based on already-existing geological structures (Baptista et al, 1998; Baptista et al, 2003; Barkan et al., 2009; Roger et al, 2010a,b) on the locality of La Trinité, allowed the present study to compare the modelled inundation of the 1755 event (the models are consistent with the historical accounts and observations, Roger et al., 2010a,b) with those modelled by the two DRRP. The studies indicate that the tsunami inundation similar to that of 1755 would flood the town and all its strategic sites (district offices, mayor's house, schools, police stations, firehouse and emergency centres, etc.), with a maximum flow depth much more significant than that indicated by DRPP, and that serious material and human damage is possible, if prevention measures are not properly implemented (education, works, buildings displacements, etc.) (Leone et al., 2010). Moreover, the present study indicates that the road network will be directly impacted by a potential sea-level rise associated with a similar tsunami. For example, the main coastal road, which separates the town from the sea, would be inundated, thus causing serious problems with the evacuation of people and the transportation of supplies. Additionally, all the buildings within the first 200 m from the coastline will be inundated according to the simulation of the maximum potential scenario for the Caribbean (Barkan et al., 2009). Of all the buildings in La Trinité, only the hospital s is located outside this inundation zone. It should also be noted that the 1755 tele-tsunami flooded the bay of Fort-de-France and of Lamentin, which nowadays is the center of the island's political and economic activity and of the island's main airport and harbor (Lamentin) as mentioned by Roger et al. (2010b).

The DEM (Digital Elevation model) used for tsunami simulations (propagation and inundation) in La Trinité Bay has been constructed using high resolution bathymetry (obtained from high resolution multi-beam and re-sampled bathymetric data of the French Hydrographic Service, SHOM; Roger et al. 2010b) and from topographic data (IGN, 2006); The model reproduces submarine features, coastal configuration and the aerial landscape.

4. CONCLUSION

The compilation of the present tsunami catalog for Martinique Island leads to the following conclusions:

After an accurate comparison of the different available historical catalogs, only twenty-eight events have been classified as tsunamis that reached Martinique since its discovery. Among them, twenty-three tsunamis – corresponding to 50% of the total - have been generated by earthquakes, directly or indirectly (induced landslides). For the majority of cases it was not possible to discriminate between a direct or indirect cause due to the lack of adequate historical data. In the same way, 28% of those tsunami events have occurred

following volcanic eruptions but again, it is very difficult to make the distinction between a direct origin associated with a lahar entering the sea, or a volcano's flank instability, or else a combination of an earthquake and an eruption. 49% of the events (16/33) have had a local impact.

The present study allowed the conduct of a preliminary vulnerability study of the tsunami hazard. In fact, tsunamis have affected several localities along the coast of Martinique, but some of them, due mainly to the geographical location, coastal configuration and mainly because of lack of proper observations, may show a lack of impact. Thus, the town of La Trinité was the perfect example for this study of tsunami risk and vulnerability, since this is the area of increased tourist activity and coastal urbanization, indicative of similarly exponential vulnerability of other coastal towns. The choice of the 1755 Lisbon tsunami as the worse possible scenario for tsunami impact on Martinique highlights the need to improve the current anti-flood DRR plan for the island.

ACKNOWLEDGEMENTS

The present research was funded by the MAREMOTI project from the French ANR (Agence Nationale de la Recherche) under contract ANR-08-RISKNAT-05-01c and by the LRC Yves Rocard (Laboratoire de Recherche Conventionné CEA-ENS). We are grateful to Alain Rabaute (GeoSubSight company) and Pierpaolo Dubernet (ENS Paris) for their technical support, as well as to Irina Nikolkina (LaRGe, Université Antilles-Guyane), Yanni Gunnell (CNRS, Université Lumière-Lyon 2) and Pascal Saffache (CEREGMIA, Université Antilles-Guyane) for constructive discussions about tsunamis in the Caribbean, and to Manuel Pubellier (ENS Paris) for discussions concerning the geodynamic context in the Antilles and surrounding areas. We also thank Lola Wilhelm for improving the English version of the manuscript and George Pararas-Carayannis for his help in improving the quality of the paper and for editing it.

REFERENCES

Alasset P.J, H. Hébert, S. Maouche, V. Calbini, M. Meghraoui (2006). The tsunami induced by the 2003 Zemmouri earthquake (MW = 6.9, Algeria): modelling and results, Geophys. J. Int, 166**,** 213–226.

Baptista M. A., S. Heitor and L. Mendes Victor (1998). The 1755 Lisbon tsunami; Evaluation of the tsunami parameters, J. of Geodynamics, 25(2), 143–157.

Baptista M.A., J. M. Miranda, F. Chierici and N. Zitellini (2003). New study of the 1755 earthquake source based on multi-channel seismic survey data and tsunami modeling, Natural Hazards and Earth System Sciences, 3, 333–340.

Baptista M.A., J.M. Miranda and J.F. Luis (2006). In Search of the 31 March 1761 Earthquake and Tsunami Source, Bulletin of the Seismological Society of America, 96(2), 713–721.

Barkan R, U. Brink, J. Lin (2009). Far field tsunami simulations of the 1755 Lisbon earthquake: Implications for tsunami hazard to the U.S. East Coast and the Caribbean, Marine Geology, n°264, 109–122.

Boyer-Peyreleau, E.E. (1823). Les Antilles Françaises, particulièrement la Guadeloupe, depuis leur découverte jusqu'au 1er Novembre 1823, 3 volumes, Brissot-Thivars, Paris.

Calmont A. and C. De Vassoigne (1999). Guadeloupe, Martinique, Guyane: Des espaces tropicaux entre insularité et continentalité, Mappemonde n°54 (1999.2).

Charbit Y. (2006). Les colonies françaises au xviie siècle : mercantilisme et enjeux impérialistes européens, Revue européenne des migrations internationales.

Chauleau Y. (1993). Dans les iles du vent, la Martinique XVIIe-XIXe siècle, l'Harmattan.

Chester D-K. (2001). The 1755 Lisbon earthquake, Progress in Physical Geography, 25, 363–383.

Choi B. H., E. Pelinovski, K.O. Kim and K.O. Lee (2003). Simulation of the trans-oceanic tsunami propagation due to the 1883 Krakatau volcanic eruption, Natural Hazards and Earth System Sciences,3, 321–332.

Clément A. (2009). "Du bon et du mauvais usage des colonies" : politique coloniale et pensée économique française au XVIIIe siècle, Cahiers d'économie politique, N°56, pp. 101-127.

Du Tertre J.-B. (1668-1671). Histoire générale des Antilles habitées par les Français.

Feuillard M., C.J. Allegre, G. Brandeis, R.Gaulon, J.L. Le Mouel, J.C. Mercier, J.P .Pozzi and M.P. Semet (1983). The 1975–1977 crisis of la Soufriere de Guadeloupe (F.W.I): A still-born magmatic eruption, Journal of Volcanology and Geothermal Research**,** 16(3-4), 317-334.

Germa A. (2008). Evolution volcano-tectonique de l'île de la Martinique (Arc insulaire des petites Antilles): Nouvelles contraintes géochronologiques et géomorphologiques, Thèse de Doctorat, Université d'Orsay.

Goiffon M. (2003). Pression foncière et littoralisation à la Martinique: Pression anthropique et environnement en Amérique latine, Les Cahiers d'Outre-Mer, N° 223.

Grindlay N. R., M. Hearne and P. Mann (2005). High Risk of Tsunami in the Northern Caribbean, Eos, 86,(12).

Herd R.A., M. Edmonds, V-A Bass (2005). Catastrophic lava dome failure at Soufriere Hills Volcano, Montserrat, 12–13 July 2003, Journal of Volcanology and Geothermal Research, 148, 234– 252.

Hess J. (1902). La Catastrophe de la Martinique, Note d'un reporter, Ed. Eugène Fasquelle, Paris.

Institut Géographique National (2006). Le Lamentin, presqu'île de la Caravelle, PNR de la Martinique. Carte de Randonnée, 4502 MT, édition 2, 1 : 25000.

INSEE (2009). Enquête de recensement sur la population en Martinique, le 1er Janvier 2006, INSEE Antilles-Guyane, N°39, Janvier 2009.

Kathiresan K. and N Rajendran (2005). Coastal mangrove forests mitigated tsunami, Estuarine, Coastal and Shelf Science, 65, 601-606.

Kunkel C.M., R.W. Hallberg and M. Oppenheimer (2006). Coral reefs reduce tsunami impact in model simulations, Geophysical Research letters, 33, L23612, doi:10.1029/2006GL027892.

Lacroix A. (1904). La Montagne Pelée et ses éruptions, Editions Masson. 663 pp.

Lambolez C.L. (1905). Saint-Pierre – Martinique, Annales des Antilles françaises, Journal et album de la Martinique : Naissance, vie et mort de la cité créole (1635 – 1902), Livre d'or de la Charité, Ed : Berger-Levrault et Cie, Paris.

Lander F. (1997). Caribbean tsunami, an Initial History, Naturals Hazards and Hazards Management in the Greater Caribbean and Latin America, 3, 1–18.

Lander F., L.S. Whiteside and P.A. Lockridge (2002). A Brief history of tsunamis in the Caribbean Sea, The International Journal of The Tsunami Society, 20(2), 57–94.

Lander F., L.S. Whiteside and P.A. Lockridge (2003). Two Decades of global tsunamis (1982-2002), Science of Tsunami Hazards, 21(1), 3-88.

Lalung H. (1948). Les Caraïbes, peuple étrange, aujourd'hui disparu, Bourrelier et Cie, Paris.

Le Friant A., G. Boudon, A. Arnulf, R. Robertson (2009). Debris avalanche deposits offshore St. Vincent (West Indies): Impact of flank-collapse events on the morphological evolution of the island, Journal of Volcanology and Geothermal Research, 179, 1–10.

Leone F. and T. Lesales (2008). L'évaluation intégrée du risque volcanique. Application à la montagne Pelée (Martinique), in Pagney Benito-Espinal (Ed) - Les interfaces ruptures, transitions et mutations, coll. Espaces tropicaux. Presses Universitaires de Bordeaux.

Leone F., F. Lavigne, R. Paris, J-C Denain and F. Vinet (2010). A spatial analysis of the December 26th, 2004 tsunami-induced damages: Lessons learned for a better risk assessment integrating buildings vulnerability, Applied Geography, in press.

Macdonald R., C.J. Hawkesworth, E. Heath (2000). The Lesser Antilles volcanic chain: a study in arc magmatism, Earth-Science Reviews,49, 1–76.

Mallet, R. (1853). Catalogue of Recorded Earthquakes from 1606 B.C. to A.D. 1850, Part I, 1606 B.C. to 1755 A.D. Report of the 22nd Meeting of the British Association for the Advancement of Science, held in Belfast, Sept. 1852, John Murray, London, 177 pp.

Mallet R. (1854). Catalogue of Recorded Earthquakes from 1606 B.C. to A.D. 1850, Part II, 1755 A.D. to 1784 A.D., Report of the 23Td meeting of the British Association for the Advancement of Science, held in Hull, Sept. 1853, John Murray, London, 118-212.

Mallet R. (1855). Catalogue of Recorded Earthquakes from 1606 B.C. to A.D. 1850, Part III, 1784 A.D. to 1842 A.D., Report of the 24" Meeting of the British Association for the Advancement of Science, John Murray, London, 326 pp.

Morton R., B. Richmond, B. Jaffe, G. Gelfenbaum (2006). Reconnaissance Investigation of Caribbean extreme wave deposits – preliminary observations, interpretations, and research directions, Open-File Report 2006-1293, USGS.

O'Loughlin K. and F. Lander (2003). Caribbean Tsunamis, A 500 year History from 1498 – 1998, Kluwer Academic Publishers.

Pararas-Carayannis, G., 2003. Near and Far-Field Effects of Tsunamis Generated by the Paroxysmal Eruptions, Explosions, Caldera Collapses and Slope Failures of the Krakatau Volcano in Indonesia, on August 26-27, 1883, Presentation for the International Seminar/Workshop on Tsunami "In Memoriam 120 Years Of Krakatau Eruption Tsunami And Lesson Learned From Large Tsunami" August 26th 29th 2003, Jakarta and Anyer, Indonesia. Also published in the Journal of Tsunami Hazards, Volume 21, Number 4. 2003

Pararas-Carayannis, G., 2006. Risk Assessment of Tsunami Generation from Active Volcanic Sources in the Eastern Caribbean Region - In "CARIBBEAN TSUNAMI HAZARDS"- Proceedings of National Science Foundation Caribbean Tsunami Workshop, March 30-31, 2004, Puerto Rico, Aurelio Mercado-Irizarry - Philip Liu, Editors. ISBN 981-256-545-3, 341 pp. 2006, Hard Cover Book. World Scientific Publishing Co. Pte.Ltd., Singapore.

Pararas-Carayannis G., (2010). Assessment of Tsunamigenic Potential along the Northern Caribbean Margin – Case Study: Earthquake and Tsunamis of 12 January 2010 in Haiti. Science of Tsunami Hazards, Vol 29, No. 3 (Review of draft report).

Revert E. (1949). La Martinique : Etude géographique et humaine, Paris : Nouvelles Éditions latines, 559 pp. Collection : Bibliothèque de l'Union française.

Roger J. and M.A. Baptista (2009). Synthèse des informations historiques relatives au tsunami associé au séisme de Lisbonne de 1755 dans les Antilles, Programme ANR RISKNAT, projet MAREMOTI**,** Rapport d'activité n°2.1

Roger J., M-A Baptista, A. Sahal, F. Accary, S. Allgeyer, H. Hébert (2010b). The transoceanic 1755 Lisbon tsunami in Martinique, Pure and Applied Geophysics, proceedings of the International Tsunami Symposium, Novosibirsk, Russia. (in press).

Roger, J., S. Allgeyer, H. Hébert, M.A. Baptista, A. Loevenbruck, F. Schindelé (2010a). The 1755 Lisbon tsunami in Guadeloupe Archipelago : sourve sensitivity and investigation of resonance effects, The Open Oceanography Journal, 4, 58-70.

Roger, J., M.A. Baptista, D. Mosher, H. Hébert, A. Sahal (2010c). Tsunami impact on Newfoundland, Canada, due to far-field generated tsunamis. Implications on hazard assessment. Proceedings of the 9th U.S. National and 10th Canadian Conference on Earthquake Engineering, July 25-29, 2010, Toronto, Canada, n°1837.

Saffache P. (2005a). Petit manuel de géographie de la mer et des littoraux : essai de compréhension du milieu littoral martiniquais, Matoury : Ibis Rouge Editions, Presses Universitaires Créoles, Collection Géographie & Aménagement des Espaces Insulaires, 53 pp.

Saffache P. (2005b). The vulnerability of the island of Martinique to the risk of a tsunami, Études caribéennes, n°3. http://etudescaribeennes.revues.org/653

Saffache P., J.V Marc, J. Mavoungo, V. Huyghues-Belrose , O. Cospar (2003), Tremblements de terre et raz de marée dans les Départements Français d'Amérique (1643-2002) : éléments pour un aménagement raisonné et une prise de conscience de la vulnérabilité du milieu. Éditions Publibook Université, Collection Sciences Humaines et Sociales, Série Géographie, Paris.

Sahal A., J. Roger, S. Allgeyer, B. Lemaire, H. Hébert, F. Schindelée, F. Lavigne (2009). The tsunami triggered by the 21 May 2003 Boumerdès-Zemmouri (Algeria) earthquake: field investigations on the French Mediterranean coast and tsunami modeling, Natural Hazards and Earth System Sciences,9, 1823–1834.

Schleupner C. (2007). Spatial assessment of sea level rise on Martinique's coastal zone and analysis of planning frameworks for adaptation, J Coast Conserv, 11, 91–103.

Smith M. and J. Shepherd (1993). Preliminary Investigations of the Tsunami Hazard of Kick'em Jenny Submarine Volcano, Natural Hazards, 7, 257-277.

Yeh, H., Liu, P., Briggs, M., Synolakis, C. (1994). Propagation and amplification of tsunamis at coastal boundaries. Nature, 372, 353-355.

Westercamp D. and H. Tazieff (1980). Martinique, Guadeloupe Saint-Martin, La Désirade, Guides Géologiques Régionaux, Masson, Paris.

Zahibo N. and E. Pelinovsky (2001). Evaluation of tsunami risk in the Lesser Antilles, Natural Hazards and Earth System Sciences, 1, 221–231.

Zahibo N., E. Pelinovsky, A. Yalciner, A. Kurkin, A. Koselkov, A. Zaitsev (2003). Le tsunami de 1867 aux ÎlesVierges : observations et modélisation, Oceanologica Acta, 26, 609–621.

Zahibo N., E. Pelinovski, E. Okal, A.Yalçiner, Ch.Kharif, T. Talipova, A. Kozelkov (2005). The earthquake and tsunami of november 21, 2004 at Les Saintes, Guadeloupe, Lesser Antilles. Science of Tsunami Hazards, 23(1), 25-39.

Table 1: Criterion of validity

Degree of validity	Meaning
1	'Abnormal oscillations'
2 a	Tsunamis generated but not observed in Martinique
2 b	Known earthquake or landslides which did not lead to a tsunami, according to the available sources
3	Events sometimes recorded as tsunamis, but about which sources disagree and/or give contradictory accounts
4	Tsunamis regularly referred to by a significant proportion of sources
5	Tsunamis systematically and unanimously recorded as such

DATE				Localisation of tsunamis			Parameters							Validity coefficient	Consequences	sources	Additional information
Year	Month	Day	Hours	Origin of the tsunami		Affected towns and rivers in Martinique	Type	Cause (Intensity, Magnitude)	Period	Range	run-up	Nb waves	Withdrawal		Damages		
1657				Martinique	Martinique		Abnormal sea oscillations	S						1	Houses (seism)	Lambolez, 1905	First earthquake since 1635
1690	April	6	16h LT	Antigua and Guadeloupe (S) + Redonda (L)	Charlestown, Charlotte-Amalie, Guadeloupe, Martinique, Barbade/Barbuda (?), Ste Lucie, Montserrat, Antigua, St Christopher		Regional tsunami	S (XI, 8,1), L					201 m (Charlestown), 16,5 to 18,5 m à St Thomas	4		Lander, 1997 ; Lander et al, 2002 ; O'Loughlin and Lander, 2003	Similar event in 1843, 1985, 2004
1702	Septem ber			Martinique, Guadeloupe	Martinique, Guadeloupe, Antigua		Regional tsunami	S (VIII, 6,5)						2 a	-	Saffache et al, 2003 ; O'Loughlin and Lander, 2003	Excited animals
1718	March	6	night	Martinique, St Vincent	Martinique, St Vincent		Local tsunami	S + L (Mart) + V (St-Vincent)						4		Lambolez, 1905 ; O'Loughlin and Lander, 2003	
1751	Novem ber	21	7h50 LT	Hispaniola	Antilles (including Martinique)		Regional tsunami	S (XI, 8)						3		O'Loughlin and Lander, 2003 ; [www.tsun.sscc.ru]	
1755	Novem ber	1st	2h à 6 h	Lisbonne	Martinique	Trinité, Galion, Fort-Royal, Lamentin, Cul-de-sac François	Télétsunami	S (Ms : XII, 8,75 - 9)	15 min (Trinité)		12 pieds (Trinité)	3	200 "pas" (= 124 m)	5	Damaged houses, docks, shops, and boats	Lambolez, 1905 ; Saffache et al, 2003	No tsunami referenced in Ste Marie and Le Robert. No awareness of tsunami event by slaves (slaves collected fishes on the beach during the sea withdrawal caused by the tsunami).
				Lisbonne	Martinique	Epinette River (Trinité), Lamentin River and Fort-Royal River	Télétsunami	S (Ms : XII, 8,75 - 9)			3 pieds (Lam)	3		5	Damaged houses, docks, shops, and boats	Lambolez, 1905 ; Saffache et al, 2003	
				Lisbonne	Martinique		Télétsunami	S (Ms : XII, 8,75 - 9)		4,6 (VII) to 1,8 m		3	1,6 km	5	Damaged houses, docks, shops, and boats	Zahibo and Pelinovski, 2001 ; O'Loughlin and Lander, 2003	
1767	April	24	6h30 LT	Surinam	Martinique, Barbade		Regional tsunami	S						4		O'Loughlin and Lander, 2003	
1823	Novem ber	30	3h10 LT	Martinique	Martinique	St Pierre (Harbour)	Local tsunami	S (4,8)						4	Damaged boats	O'Loughlin and Lander, 2003 ; Saffache et al, 2003	Similar events on a 1 year interval

1824	November	30	3h30 LT	Martinique	Martinique	St Pierre (Harbour)	Local tsunami	S (4,8)						4	Damaged boats	O'Loughlin and Lander, 2003 ; Saffache et al, 2003	
1827	November	30	3h LT	Martinique, Guadeloupe, Antigua			Regional tsunami	S (VIII, 6,5)						2 a		O'Loughlin and Lander, 2003	
1829	October	26		Martinique	Martinique		Local tsunami	S ou Storm						4		O'Loughlin and Lander, 2003	
1831	December	3	19h40LT	Grenada	St Kitts, St Vincent, Guyana, Trinidad		Regional tsunami	S (IX, 7)						2ab		O'Loughlin and Lander, 2003	Effect of the tsunami reported at St Kitts and Trinidad
1837	July	26	12h51 UT	Martinique	Martinique		Local tsunami	S ou Storm						2ab	Numerous casualties	Lander, 1997 ; Lander et al, 2002 ; O'Loughlin and Lander, 2003	
1839	January	11	6h LT	Martinique	Martinique	harbour	Local tsunami	S (IX, 6,9) : id Seaquakes						4	Boats damaged by the tsunami, 400 houses destroyed in Fort Royal (S), 400 deads	Lambolez, 1905 ; O'Loughlin and Lander, 2003	
1843	February	8	10h35 LT	Guadeloupe	Antilles (including Martinique)		Regional tsunami	S (XII, 8,3)		1,2 m				2 b		Lander, 1997 ; Lander et al, 2002 ; O'Loughlin and Lander, 2003	Similar event in 1690, 1985, 2004
1867	November	18	14h50 LT	Iles Vierges	Antilles (including Martinique)	Fort-de-France	Regional tsunami	S (X, 7,3)		0,7 m				5		Zahibo and Pelinovski, 2001; Zahibo et al, 2003 ;; O'Loughlin and Lander, 2003	
1874	March	11	4H30 LT	Dominique and St Thomas	Dominique and St Thomas		Regional tsunami	L						1		O'Loughlin and Lander, 2003	
1876	November	8	15h	Martinique	Martinique	between Ste Marie and the Presqu'île de la Caravelle (Trinité)	Local tsunami	L ?						4	No damages	Lambolez, 1905	
1880	January	4	11 h LT	Dominique	Dominique		Local tsunami	V + L						2 b		O'Loughlin and Lander, 2003	River level rised by 3,7 m (Roseau)
1901				Martinique	Martinique	Rade de St Pierre	Abnormal sea oscillations, violent currents	V				3 or 4		4	No damages	Saffache et al, 2003	
1902	February-March			Martinique	Martinique	North of the island : Macouba - Le Prêcheur	Abnormal sea oscillations, violent currents	V						4	No damages	Saffache et al, 2003	

1902	May	5	13h LT	Martinique (Factory Guerin)	Martinique	La Guérite - Bellevue (between Fort de France and the Pointe des nègres)	Local tsunami	V (3rd lahar)					100 m	5	Flooded houses and roads (Fonds Core). Flooded shops, boats moved towards coast, destroyed docks	Hess, 1902 ; Lambolez, 1905 ; Saffache et al, 2003	
			13h LT	Martinique (Factory Guerin)	Martinique	Blanche River, Roxelane River(St Pierre)	Rising of rivers level	V (3rd lahar)	2 min (Blanche)	8 mètres (Rox)	"Pont de Pierre" (Rox)	1	10 m to 300 feet (Blanche)	5		Hess, 1902 ; Lambolez, 1905 ; Saffache et al, 2003	
			13h LT	Martinique (Factory Guerin)	Martinique	St Pierre (Port :Company Girard, Square Bertin, Fonds-Coré, le Mouillage) + Carbet	Local tsunami	V (3rd lahar)	1 to 2 min	3 to 4 m for the first wave to 20 m	20 m (with the fontain of the square Bertin)	2 to 15 vagues	From 60 to 70 m (Mr Sully) and to 1m20 (person resqued). About 20 to 30 m	5		Hess, 1902 ; Lambolez, 1905 ; Saffache et al, 2003	
			13h LT	Martinique (Factory Guerin)	Martinique	Trinité	Local tsunami	V (3rd lahar)		80 cm		3		5		Hess, 1902 ; Lambolez, 1905 ; Saffache et al, 2003	
1902	May	7	19h LT	St Vincent	Martinique	Trinité	Local tsunami	V				3	80 cm	5		Lander, 1997 ; Lander et al, 2002 ; O'Loughlin and Lander, 2003	
1902	May	7	14 - 15h LT	St Vincent	Martinique	Madame River (Fort de France), Des Pères River (St Pierre)	Local tsunami	V			25 cm			5		Saffache et al, 2003	
1902	May	8	19H - 20h LT	Martinique (Mount Pelée)	Martinique	St Pierre, le Précheur, Carbet, Trinité, Fort-de-France	Local tsunami	V (Nuées ardentes)		3 m (St Pierre), 2m (Carbet)	40 cm (Fort). 200 m (Carbet)	3	1,50 to 2 m (Fort de France)	5	Destruction of all boats in the harbour, except Roddam. 52 km2 destroyed, 38,000 deads, 1 survivor (prisonnier)	O'Loughlin and Lander, 2003	
1902	May	9		Martinique, Ste Lucie	Martinique		Anormal perturbations	V (vent volcanique)						5		O'Loughlin and Lander, 2003	
1902	May	20		Martinique (Mount Pelée, Souffrière St Vincent)	Martinique	Saint Pierre, Carbet, Petite Anse to St Pierre, Fort de France, Trinité	Local tsunami	V		3,50 m (wave hight) : Carbet	50 m at the Petite Anse, 40 cm to St Pierre Fortification			5	Destroyed houses, boats, docks	Saffache et al, 2003	

1902	August	30	21h25 LT	Martinique (Mount Pelée)	Martinique	Saint Pierre, Carbet, Fort de France, Schoelcher, Case Pilote, Trinité	Local tsunami	V		3 m (St Pierre), 1 m at Fort-de-France and Trinité	100 m at Case Pilote, 30 m at Schloecher			5	Flooded docks in Fort de France, including La Savanne square	Saffache et al, 2003 ; O'Loughlin and Lander, 2003	
1906	February	16	1h25 LT	Ste Lucie	Martinique, St Vincent, Guadeloupe, Grenade, Dominique, Barbade		Local tsunami	S (VIII)						2 a		Lander et al, 2002	Tsunamigenic seism reported the same year, Dec. 31, in Venezuela.
1939	July	24	12h LT	Kick'em Jenny	Antilles (including Martinique)	Fort-de-France, Le Vauclin	Regional tsunami	V (VEI: 1)						4		Smith and Shepherd, 1993 ; O'Loughlin and Lander, 2003	
1969	December	25		Guadeloupe	Antilles (including Martinique)		Regional tsunami	S (X - XI, 7,7)						2 b		O'Loughlin and Lander, 2003 ; Zahibo et al, 2005	Barbade, Antigua, Dominique
1985	March	16	14h54 UT	Guadeloupe	Guadeloupe		Local tsunami	S (VI, 6,3) + L						2 b		O'Loughlin and Lander, 2003	Similar event in 1690, 1843, 2004
1991	April	22	21h56 UT	Costa Rica	Antilles (including Martinique)	Fort-de-France Bay	Regional tsunami	S (X - XI; 7,6)						4		Lander et al, 2002 ; O'Loughlin and Lander, 2003	
2004	November	21	11h40 UT	Guadeloupe (Les Saintes)	Guadeloupe		Local tsunami	S (6,3)						2 b		Zahibo et al, 2005	Similar events in 1690, 1843, 1985

3.2 Modèles de rupture

Dans cette partie je présente les travaux menés sur les sources sismiques : les données de géologie/géophysique (déformation en surface, GPS, sismicité, mécanismes au foyer) permettent de proposer des scénarios de rupture qui sont validés par les données de tsunami (enregistrements marégraphiques, observations historiques).

La première étude menée (pendant mon Master 2 Recherche à Brest) concerne les séisme et tsunami de Calabre de 1693. L'objectif de cette étude et son originalité étaient de proposer un scénario de rupture cosismique en relation avec la subduction sous la Calabre, considérée jusque là comme inactive, tout en restant en accord avec les connaissances géologiques de la région.

3.2.1 Gutscher, M.-A., **Roger, J.**, Baptista, M.A., Miranda, J.M., Tinti, S. (2006). *The source of the Catania earthquake and tsunami (Southern Italy) : New evidence from tsunami modeling of a locked subduction fault plane*. Geophysical Research Letter, **33**, L08309, doi:10.1029/2005GL025442

La seconde étude menée concerne les séismes et le tsunami de 1856 à Jijel en Algérie : une première partie a été réalisée dans le cadre du projet TRANSFER avec l'étude d'impact des tsunamis générés par des sources sismiques localisées en Méditerranée occidentale sur les îles Baléares, et plus particulièrement sur le port de Palma (Majorque). Des scénarios de rupture cosismique ont été proposés basés principalement sur la thèse d'A. Domzig et les récentes campagnes géophysique au niveau de la marge nord-algérienne. Nous avons également profité de cette étude pour regarder de manière plus en détail l'influence des canyons sous-marins sur le comportement du tsunami à l'approche des côtes.

3.2.2 **Roger, J.**, Hébert, H. (2008). *The 1856 Djijelli (Algeria) earthquake and tsunami : source parameters and implications for tsunami hazard in the Balearic Islands*. Natural Hazards and Earth System Sciences, **8**(4), 721-731.

Une seconde partie a considéré cette fois-ci uniquement la côte algérienne pour le même évènement de 1856 ; l'objectif étant cette fois de tester la reproductibilité des observations historiques de tsunami en justifiant le choix de la source. L'importance de l'évaluation des sources potentiellement tsunamigéniques au niveau de la marge algérienne est soulignée.

3.2.3 Yelles-Chaouche, A.K., **Roger, J.**, Déverchère, J., Bracène, R., Domzig, A., Hébert H., Kherroubi, A. (2009). *The 1856 Tsunami of Djidjelli (Eastern Algeria) : Seismotectonics, Modelling and Hazard Implications for the Algerian Coast*. Pageoph Topical Volume, doi: 10.1007/s00024-008-0433-6.

Parallèlement à ces études, je me suis intéressé de près au séisme d'El Asnam (Algérie) de 1980, connu pour avoir fait de nombreuses victimes et des dégâts importants dans la région d'El Asnam, mais moins connu pour avoir été suivi par un mini-tsunami ayant été enregistré par 6 marégrammes de la côte sud espagnole. Ce séisme, dont l'épicentre a été localisé à plus de 40 km de la côte à proximité de l'épicentre du séisme d'Orléansville de 1954, a aussi été suivi par au moins une rupture de câble de liaison téléphonique sous-marine au large d'Alger, tout comme ce fut le cas en 1954. Ces ruptures de câble ont été associées à des courants de turbidité induits par les secousses que certaines études rendent coupables de la génération du tsunami. Dans l'étude présentée ici, je montre que le tsunami de 1980 n'a pas pu être généré par un glissement de terrain du fait de sa période trop courte et de son aire d'impact trop grande et que le séisme lui-même est capable de l'avoir généré.

3.2.4 **Roger, J.**, Hébert, H., Ruegg, J.-C., Briole, P. (en revision). *The El Asnam October 10th, 1980 inland earthquake : a new hypothesis of tsunami generation*. Geophysical Journal International, doi: 10.1111/j.1365-246X.2011.05003.x.

Récemment une étude annexe au projet MAREMOTI a été menée pour l'évaluation du potentiel tsunamigénique du détroit de Calais-Douvres : en effet, c'est suite à la découverte de nombreux documents sur le séisme et le tsunami de 1580 que je me suis lancé dans des modélisations de tsunami en proposant des scénarios de rupture en utilisant les nombreuses

études géophysique disponibles dans la région. L'originalité de cette étude soumise à la revue *Geology* provient du fait que je propose la génération de tsunamis par des failles du détroit de Calais-Douvres réactivées par le rebond post-glaciaire (Scandinave), ne se limitant donc pas à la génération des tsunamis par des séismes localisés aux frontières des plaques, ou intraplaques mais localisés dans le panneau plongeant comme ceux étudiés par Satake et Tanioka (1999), Saito et Furumura (2009). Des études récentes présentées dans l'article ont montré que de telles failles, sous le jeu des différents champs de contraintes dus par exemple au rebond post-glaciaire mais aussi à l'ouverture océanique ou l'orogénèse alpine, peuvent accommoder des séismes de magnitude MW 6.0 et plus, ainsi potentiellement capables de générer des tsunamis (Mazzotti et Townend, 2010).

3.2.5 **Roger, J.**, Gunnell, Y. (soumis). *Vulnerability of the Dover Strait to coseismic tsunami hazard : insights from numerical modeling*. Soumis à Geophysical Journal International.

Source of the 1693 Catania earthquake and tsunami (southern Italy): New evidence from tsunami modeling of a locked subduction fault plane

M.-A. Gutscher,[1] J. Roger,[1] M.-A. Baptista,[2] J. M. Miranda,[2] and S. Tinti[3]

Received 9 December 2005; revised 20 February 2006; accepted 1 March 2006; published 29 April 2006.

[1] The 1693 Catania earthquake, which caused 60000 deaths in eastern Sicily and generated a 5–10 m high tsunami, is investigated. GPS data indicate ESE-WNW convergence in the Calabrian arc at 4–5 mm/yr. New high-resolution seismic data image active compression at the toe of the accretionary wedge. The lack of instrumentally recorded thrust earthquakes suggests the presence of a locked subduction fault plane. Thermal modeling is applied to calculate the limits of the seismogenic zone. Tsunami modeling is performed to test the hypothesis that the 1693 earthquake occurred on the subduction fault plane (160 × 120 km in size) with 2 m of mean co-seismic slip. This source successfully reproduces historical observations with regard to polarity and predicts 1–3 m high amplitudes. It is likely that only the SW segment of the subduction fault plane ruptured in 1693 and 1169, implying a recurrence interval of roughly 500 years for similar events. **Citation:** Gutscher, M.-A., J. Roger, M.-A. Baptista, J. M. Miranda, and S. Tinti (2006), Source of the 1693 Catania earthquake and tsunami (southern Italy): New evidence from tsunami modeling of a locked subduction fault plane, *Geophys. Res. Lett.*, *33*, L08309, doi:10.1029/2005GL025442.

1. Introduction

[2] Southern Italy has been struck repeatedly by very strong historical earthquakes (Mercalli intensity IX or greater), in 1169, 1542, 1624, 1693, 1783, 1905, 1908, often associated with destructive tsunami [*Piatanesi and Tinti*, 1998; *Jacques et al.*, 2001]. While several of these events, like the 1908 Messina, 1905 or 1783 Calabria earthquakes occurred along mapped, crustal, normal faults [*Tinti and Piatanesi*, 1996; *Monaco and Tortorici*, 2000; *Jacques et al.*, 2001] the source of some of the older events remains enigmatic. Since no strong (M6) earthquakes have occurred in the past 50 years, it is difficult to identify the main active faults. The 1693 event, with maximum intensities of X to XI, caused 60,000 casualties [*Piatanesi and Tinti*, 1998]. Because it generated an Ambraseys-Sieberg intensity V tsunami [*Tinti et al.*, 2004], and the isoseismals are open to the sea (Figure 1), it appears that the source region is offshore. Although its exact position remains unknown, it is of major importance for the assessment of seismic and tsunami risk in the region.

[3] Calabria is located above a 300 km wide, NW dipping subduction zone which is associated with an active volcanic arc, the Aeolian Islands (Figure 1) and a well defined Wadati-Benioff zone, with earthquakes descending to nearly 500 km depth (Figure 2). A continuous, high P-wave velocity anomaly (slab of cold dense lithosphere) is imaged by travel-time tomography down to 660 km depth, where the slab flattens and underlies the western Mediterranean below Sardinia [*Lucente et al.*, 1999; *Wortel and Spakman*, 2000]. It is widely accepted that Calabria has migrated SE to its current position due to a rapid roll-back of the Ionian-Tyrrhenian slab [*Malinverno and Ryan*, 1986; *Gvirtzman and Nur*, 1999; *Faccenna et al.*, 2001] and that the high heat flow and young oceanic lithosphere in the Tyrrhenian Sea are the result of the associated back-arc extension [*Zito et al.*, 2003].

[4] One major question, however, remains unanswered, "is the Calabria subduction zone still active"? The lack of seismicity along the subduction fault plane (with a characteristic shallow dipping thrust-type focal mechanism) implies one of three possibilities; 1) subduction has ceased, 2) subduction is active but aseismic, or 3) subduction is active and there is a large locked seismogenic zone. High-resolution seismic profiles image compressive deformation at the toe of the wedge [*Hieke et al.*, 2005] (Figure 3). The folding of the 10 m thick transparent layer identified as the 3500 BP Augias Turbidite [*Cita et al.*, 1984], indicates active shortening. Deep penetration multi-channel seismic profiles image SE vergent ramp thrusts, soling out to a regional NE dipping decollement [*Cernobori et al.*, 1996] and offer proof that compression at the toe is tectonic in origin and not gravitational. The recent discovery of a province of mud volcanoes, indicates active dewatering in the Calabrian prism [*Ceramicola et al.*, 2005]. If the third hypothesis is true, then Calabria may exhibit a similar behavior as the Nankai or Cascadia subduction zones, marked by long repeat times between great earthquakes on the order of hundreds of years [*Hyndman and Wang*, 1995; *Oleskevich et al.*, 1999]. The purpose of this paper is to test the hypothesis of a subduction fault plane source for the 1693 Catania earthquake, using tsunami modeling.

2. Fault Plane Geometry and Thermal Modeling

[5] The shallow (<20 km depth) geometry of the subduction fault plane is constrained by multi-channel seismic profiles, imaging a shallow NW dipping decollement (<2°), steepening somewhat (>5°) at greater depth [*Cernobori et al.*, 1996]. The deeper geometry is obtained from the distribution of earthquake hypocenters (Figure 2).

[6] In order to determine the updip and downdip limits of the potentially seismogenic portion of the fault plane, 2-D numerical modeling of forearc thermal structure was per-

[1]UMR6538 Domaines Oceaniques, Institut Universitaire European De La Mer, Plouzane, France.
[2]Center for Geophysics, University of Lisbon, Lisbon, Portugal.
[3]Department of Physics and Geophysics, University of Bologna, Bologna, Italy.

Copyright 2006 by the American Geophysical Union.
0094-8276/06/2005GL025442$05.00

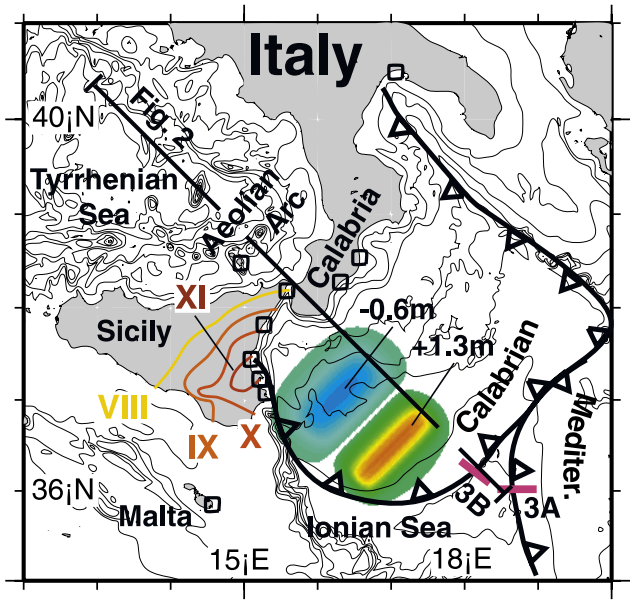

Figure 1. Location map, with proposed tsunami source. The initial vertical elastic displacement, ranging from +1.3 m to −0.6 m, was calculated for a rectangular fault plane with dimensions of 120 × 160 km and 2 m mean (but non-uniform) co-seismic slip. Also shown are bathymetric contours (500 m interval) from the Gebco 1 min grid [*BODC*, 2003], isoseismals (contours of equal shaking intensity) of the 1693 earthquake, position of virtual mareograph stations (squares - see text for geographic names), and the position of the thermal and seismic profiles (see Figures 2 and 3).

formed [*Peacock and Wang*, 1999; *Gutscher and Peacock*, 2003]. The updip limit is commonly considered to correspond to the 100–150°C isotherms and the downdip limit to the 350–450°C isotherms [*Scholz*, 1990; *Oleskevich et al.*, 1999]. The age of the subducting oceanic lithosphere is not well known, but the Ionian Sea is believed to be a remnant of the Tethys ocean and thus likely Jurassic in age [*Faccenna et al.*, 2001]. An age of 130 Ma was taken. Available heat-flow data from the region show a typical forearc pattern, with low values of 50 mW/m2 in the Ionian Sea and very high values reaching 150–200 mW/m2 in the SE Tyrrhenian Sea, where very young oceanic lithosphere is present in the Marsili basin [*Zito et al.*, 2003].

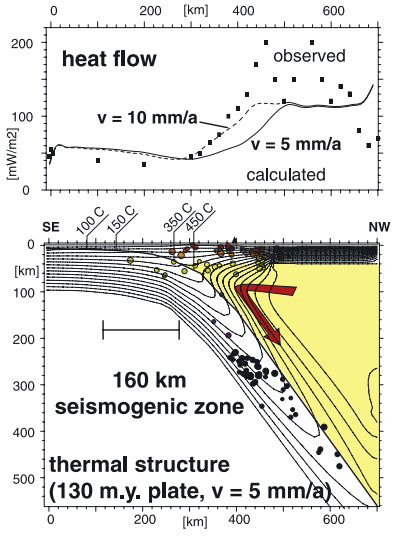

Figure 2. Thermal structure of the Calabrian arc, with the projected position of earthquakes from the relocated hypocenter catalog 1964–1995 [*Engdahl et al.*, 1998]. The observed heat flow [*Zito et al.*, 2003] is shown (squares) together with the calculated heat flow for two subduction velocities.

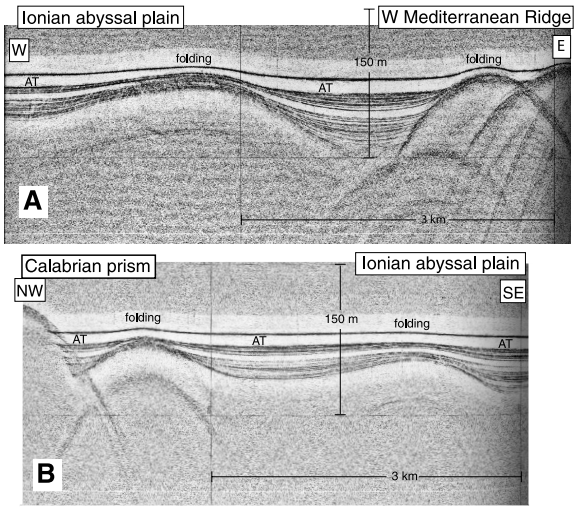

Figure 3. High-resolution (3.5 kHz) seismic profiles from the Ionian Sea. (a) across the toe of the Western Mediterranean Ridge, (b) across the toe of the Calabrian prism. Both profiles reveal active compressional deformation and syn-tectonic sedimentation. Folding affects the uppermost turbdite layers and even disturbs the sea-floor. The 10–15 m thick transparent layer labelled AT represents the Augias Turbidite deposited as a result of the Santorini collapse of 1500 BC [*Cita et al.*, 1984; *Hieke et al.*, 2005].

[7] Recent GPS measurements of the South Italian region confirm the overall NW motion of Africa with respect to Eurasia at a velocity of 5 mm/yr, as well as the SE motion of an intermediate Calabria block at 4–5 mm/yr (in a Nubia fixed reference frame), suggesting that subduction has not ceased [*D'Agostino and Selvaggi*, 2004]. We calculated the thermal structure of the Calabrian arc for subduction velocities of 0–20 mm/yr. Although 10 mm/yr provides the best fit to the observed heat-flow pattern (Figure 2), we retain the thermal structure for a velocity of 5 mm/yr as observed by GPS. The thermally predicted downdip width of the seismogenic zone is 160 km, spanning 120 km to 280 km from the deformation front.

3. Fault Parameters

[8] Very high intensities (X and XI) and a strong tsunami were reported in eastern Sicily in 1693. However, no available historical records indicate widespread damage in Calabria, or Central Italy. Thus, it seems unlikely that the entire 300 km long subduction fault plane ruptured, as this would have produced a magnitude Mw = 8.3 felt over a greater distance. This is calculated, for a mean co-seismic slip of 2 m, from the relationship Mo = μSD, where rigidity $\mu = 3 \times 10^{10}$ Pa, the rupture area S = 300 km × 160 km = 48000 km^2, and the slip

D = 2 m. This yields Mo = 2.88 × 10^{21} Nm and then using Mw = 2/3 log Mo − 6.03, the resulting magnitude is Mw = 8.28. Therefore, we consider only a 120 km long segment, which yields a smaller magnitude of Mw = 8.0. The fault plane dips 5° to the NW, extending from 5 km depth (shallowest) to 20 km depth (deepest).

[9] The mean co-seismic slip of 2 m is obtained by considering the recurrence interval and the subduction velocity (4 mm/yr). In 1169 a strong earthquake with similar intensities (X and XI) struck eastern Sicily, producing almost exactly the same isoseismal pattern [*Barbano et al.*, 1984]. If the two earthquakes occurred along the same fault, then a recurrence time of about 500 years is implied.

4. Tsunami Modeling

[10] The fault parameters above were used to perform tsunami wave form modeling of a shallow NW dipping subduction source. The initial displacement of the seafloor, considered to be similar to the initial displacement of the water surface, is calculated using the elastic half-space approach [*Okada*, 1985]. The vertical seafloor displacement (for a pure thrust mechanism) is shown in map view and ranges from 1.3 m uplift to the SE, to 0.6 m subsidence to the NW (Figure 1). To account for non-uniform slip within the fault plane [*Geist and Dmowska*, 1999], we used the smooth closure condition [*Freund and Barnett*, 1976] applying a skewness parameter of 0.3 and a discretization of 8 km. For the tsunami wave propagation, finite difference software SWAN Code [*Mader*, 2004] was applied, using a shallow water non-linear wave model and a cell size of 0.025 degrees. The Gebco 1 min bathymetric grid was used [*British Oceanographic Data Centre (BODC)*, 2003].

[11] Synthetic mareograms were calculated for ten stations in the southern Italy region (Figure 4). These stations were selected for the most part on the availability of historical records.

[12] They are situated along the eastern coast of Sicily (from S to N: Syracuse, Augusta, Catania, Taormina and Messina), one in the Aeolian islands (Vulcano), one on Malta, two on the SE coast of Calabria and one in the Gulf of Taranto.

[13] Synthetic mareograms provide information on wave phase, amplitude and arrival time of the tsunami wave (Figure 4). One of the most crucial observations concerning the 1693 tsunami was a strong withdrawal of the sea at all port towns of the eastern coast of Sicily which was so sudden and violent that many ships were damaged [*Piatanesi and Tinti*, 1998].

5. Discussion

[14] Previous source models for the 1693 earthquake tested primarily NE-SW trending normal faults on-land in eastern Sicily, as well as NNW-SSE trending steeply dipping normal faults offshore along the Malta escarpment [*Piatanesi and Tinti*, 1998; *Bianca et al.*, 1999; *Tinti et al.*, 2001]. None of the on-land faults tested succeeds in reproducing the observed initial withdrawal of the sea at all eastern Sicily port towns, and these must therefore be rejected as potential sources [*Piatanesi and Tinti*, 1998]. Along the Malta escarpment south of Syracuse, marine seismic profiles reveal no evidence of Quaternary deformation [*Argnani and Bonazzi*, 2005].

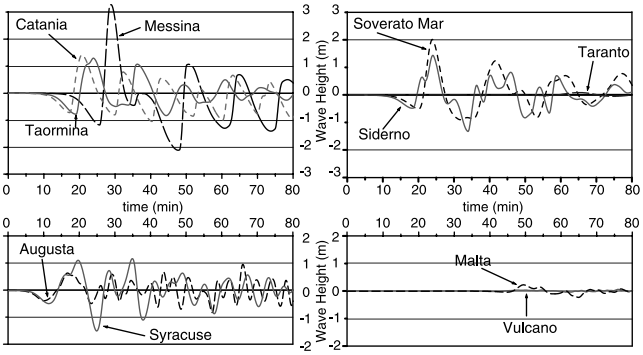

Figure 4. Synthetic mareograms calculated for the ten virtual tide gauge stations in the SE Italy region.

But the main drawback of all of these proposed sources is that unreasonably large slip values (6–8 m) are required [*Piatanesi and Tinti*, 1998; *Tinti et al.*, 2001] to generate an earthquake of magnitude 7–7.5, with respect to the length of the fault, violating established earthquake scaling laws [*Wells and Coppersmith*, 1994]. The large surface area of the subduction fault generates a very strong earthquake M8.0 for only 2 m of co-seismic slip and is consistent with relative plate velocities (4–5 mm/yr) and the available evidence on the recurrence interval (500 yrs). For the non-uniform slip model tested, the maximum slip is 4 m and thus requires portions of the fault to have accumulated a significant slip deficit during the previous seismic cycle.

[15] The subduction fault plane generates a tsunami with an initial withdrawal of the sea for all stations in eastern Sicily. Wave heights obtained, range from 1–1.3 m for the east coast of Sicily, with the highest amplitude (3.3 m) in Messina. Although this may appear small with respect to the 5–10 m high wave reported, these simulations do not reproduce the amplification effects from the run-up, which may increase wave heights by a factor of 2 to 5. For instance, following the 26 December 2004 M9.3 earthquake, the tsunami amplitudes observed at tidal gauge stations in SE India (Vishakapatnam, and Tuticorin) were only 1.4 m (http://www.nio.org/jsp/tsunami.jsp). Likewise in Colombo (Sri Lanka) and NW Sumatra (Sibolga, Belawan) recorded wave heights were 2.1 m and 0.5 m, respectively [*Merrifield et al.*, 2005]. Yet eye-witness accounts and the physical damage in these areas indicate wave heights ranging from 5–10 m.

[16] Calculated amplitudes for more distant stations (Vulcano, Malta or Taranto) are small (0.1–0.25 m). But depending on the amplification through run-up, this wave may have been noticeable. Travel-times are shortest for the east Sicily coast. The initial withdrawal would have occurred most rapidly in Syracuse and Augusta (10 min), and 15–20 min after the earthquake for Catania, and Taormina (Figure 4). The ensuing positive wave would have flooded the ports 5–10 min later. Unfortunately, no historical observations are available with regard to travel time and thus this key piece of information cannot be used to support or disprove a particular source model.

6. Conclusion

[17] High-resolution seismic images from the toe of the Calabrian accretionary wedge as well as recent GPS data

indicate ongoing ESE-WNW convergence in the Calabrian arc at rates of roughly 4–5 mm/yr. The lack of instrumentally recorded thrust earthquakes supports the hypothesis of a locked subduction fault plane. For the periodicity of 500 years suggested by historical records, a mean co-seismic slip of about 2 m can be expected. Tsunami modeling of a subduction fault plane (160 × 120 km in size) successfully reproduces the available historical observations with regard to polarity and predicts 1–3 m amplitudes. If this hypothesis is true, then it is likely that only the SW segment of the subduction plane ruptured in 1693 and 1169. It is unknown when the remainder of the subduction fault plane may have ruptured, yet this knowledge is crucial for estimating the seismic and tsunami hazard in the Southern Italian region.

[18] **Acknowledgments.** We thank the captain and crew of R/V *Atalante* and I. Lefevre for acquisition of the seismic data during a transit between Istanbul and Toulon in Oct. 2002. We acknowledge financial support from INSU. This article is IUEM contribution 991.

References

Argnani, A., and C. Bonazzi (2005), Malta Escarpment fault zone offshore eastern Sicily: Pliocene–Quaternary tectonic evolution based on new multichannel seismic data, *Tectonics*, *24*,TC4009, doi:10.1029/2004TC001656.

Barbano, M. S., M. T. Carrozzo, A. Chirenti, M. Cosentino, G. Lombardo, and M. Riuscetti (1984), Seismic zoning of Calabria and Sicily (south Italy), *Boll. Geofis. Teor. Appl.*, *XXVI*, 39–58.

Bianca, M., C. Monaco, L. Tortorici, and L. Cernobori (1999), Quaternary normal faulting in southeastern Sicily (Italy): A seismic source for the 1693 large earthquake, *Geophys. J. Int.*, *139*, 370–394.

British Oceanographic Data Centre (BODC) (2003), Centenary Edition of the GEBCO Digital Atlas [CD-ROM], Liverpool, UK.

Ceramicola, S., D. Praeg, A. Cova, X. Monteys, V. Unnithan, S. Garziglia, and the OGS Explora Scientific Party (2005), Newly imaged mud volcanic province on the Calabrian Arc in the central Mediterranean Sea: Preliminary results from cruise HERMES-HYDRAMED IONIO 2005, *Eos Trans. AGU*, *85*(47), Fall Meet. Suppl., Abstract T13B-0455.

Cernobori, L., A. Hirn, J. H. McBride, R. Nicolich, L. Petronio, M. Romanelli, and STREAMERS/PROFILES Working Groups (1996), Crustal image of the Ionian basin and its Calabrian margins, *Tectonophysics*, *264*, 175–189.

Cita, M. B., A. Camerlinghi, K. A. Kastens, and F. W. McCoy (1984), New findings of Bronze Age homogenites in the Ionian Sea: Geodynamic implications for the Mediterranean, *Mar. Geol.*, *55*, 47–62.

D'Agostino, N., and G. Selvaggi (2004), Crustal motion along the Eurasia-Nubia plate boundary in the Calabrian Arc and Sicily and active extension in the Messina Straits from GPS measurements, *J. Geophys. Res.*, *109*, B11402, doi:10.1029/2004JB002998.

Engdahl, E. R., R. D. van der Hilst, and R. Buland (1998), Global teleseismic earthquake relocation with improved travel times and procedures for depth relocation, *Bull. Seismol. Soc. Am.*, *88*, 722–743.

Faccenna, C., T. W. Becker, F. Pio Lucente, L. Jolivet, and F. Rosetti (2001), History of subduction and back-arc extension in the central Mediterranean, *Geophys. J. Int.*, *145*, 809–820.

Freund, L. B., and D. M. Barnett (1976), A two-dimensional analysis of surface deformation due to dip-slip faulting, *Bull. Seismol. Soc. Am.*, *66*, 667–675.

Geist, E. L., and R. Dmowska (1999), Local tsunamis and distributed slip at the source, *Pure Appl. Geophys.*, *154*, 485–512.

Gutscher, M.-A., and S. M. Peacock (2003), Thermal models of flat subduction and the rupture zone of great subduction earthquakes, *J. Geophys. Res.*, *108*(B1), 2009, doi:10.1029/2001JB000787.

Gvirtzman, Z., and A. Nur (1999), The formation of Mount Etna as the consequence of slab rollback, *Nature*, *401*, 782–785.

Hieke, W., H. B. Hirschleber, and G. A. Deghani (2005), The Ionian Abyssal Plain (central Mediterranean Sea): Morphology, subbottom structures and geodynamic history—An inventory, *Mar. Geophys. Res.*, *24*, 279–310.

Hyndman, R. D., and K. Wang (1995), The rupture zone of Cascadia great earthquakes from current deformation and the thermal regime, *J. Geophys. Res.*, *100*, 22,133–22,154.

Jacques, E., C. Monaco, P. Tapponnier, L. Tortorici, and T. Winter (2001), Faulting and earthquake triggering during the 1783 Calabria seismic sequence, *Geophys. J. Int.*, *145*, 809–820.

Lucente, F. P., C. Chiarabba, G. B. Cimini, and D. Giardini (1999), Tomographic constraints on the geodynamic evolution of the Italian region, *J. Geophys. Res.*, *104*, 20,307–20,327.

Mader, C. (2004), Numerical Modeling of Water Waves, 2nd ed., CRC Press, Boca Raton, Fla.

Malinverno, A., and W. B. Ryan (1986), Extension in the Tyrrhenian Sea and shortening in the Appenines as a result of arc migration driven by sinking of the lithosphere, *Tectonics*, *5*, 227–245.

Merrifield, M. A., et al. (2005), Tide gauge observations of the Indian Ocean tsunami, December 26, 2004, *Geophys. Res. Lett.*, *32*, L09603, doi:10.1029/2005GL022610.

Monaco, C., and L. Tortorici (2000), Active faulting in the Calabrian arc and eastern Sicily, *J. Geodyn.*, *29*, 407–424.

Okada, Y. (1985), Surface deformation due to shear and tensile faults in a half-space, *Bull. Seismol. Soc. Am.*, *75*, 1135–1154.

Oleskevich, D. A., R. D. Hyndman, and K. Wang (1999), The updip and downdip limits to great subduction earthquakes: Thermal and structural models of Cascadia, south Alaska, SW Japan, and Chile, *J. Geophys. Res.*, *104*, 14,965–14,991.

Peacock, S. M., and K. Wang (1999), Seismic consequences of warm versus cool subduction zone metamorphism: Examples from northeast and southwest Japan, *Science*, *286*, 937–939.

Piatanesi, A., and S. Tinti (1998), A revision of the 1693 eastern Sicily earthquake and tsunami, *J. Geophys. Res.*, *103*, 2749–2758.

Scholz, C. H. (1990), *The Mechanics of Earthquakes and Faulting*, 439 pp., Cambridge Univ. Press, New York.

Tinti, S., and A. Piatenesi (1996), Finite-element simulations of the 5 February 1783 Calabrian tsunami, *Phys. Chem. Earth*, *21*, 39–43.

Tinti, S., A. Armigliato, and E. Bortolucci (2001), Contribution of tsunami data analysis to constrain the seismic source: The case of the 1693 eastern Sicily earthquake, *J. Seismol.*, *5*, 41–61.

Tinti, S., A. Maramai, and L. Graziani (2004), The new catalogue of the Italian tsunamis, *Nat. Hazards*, *33*, 439–465.

Wells, D. L., and K. J. Coppersmith (1994), New empirical relationships among magnitude, rupture length, rupture width, rupture area, and surface displacement, *Bull. Seismol. Soc. Am.*, *84*, 974–1002.

Wortel, M. J. R., and W. Spakman (2000), Subduction and slab detachment in the Mediterranean—Carpathian region, *Science*, *290*, 1910–1917.

Zito, G., F. Mongelli, S. de Lorenzo, and C. Doglioni (2003), Heat flow and geodynamics in the Tyrrhenian Sea, *Terra Nova*, *15*, 425–432.

M.-A. Baptista and J. M. Miranda, Center for Geophysics, University of Lisbon, 1250 Lisboa, Portugal.

M.-A. Gutscher and J. Roger, UMR6538 Domaines Oceaniques, IUEM, F-29280 Plouzané, France. (gutscher@univ-brest.fr)

S. Tinti, Department of Physics and Geophysics, University of Bologna, I-40127 Bologna, Italy.

Nat. Hazards Earth Syst. Sci., 8, 721–731, 2008
www.nat-hazards-earth-syst-sci.net/8/721/2008/
© Author(s) 2008. This work is distributed under
the Creative Commons Attribution 3.0 License.

Natural Hazards and Earth System Sciences

The 1856 Djijelli (Algeria) earthquake and tsunami: source parameters and implications for tsunami hazard in the Balearic Islands

J. Roger and H. Hébert

Département Analyse, Surveillance, Environnement, Commissariat à l'Energie Atomique, 91297 Arpajon Cedex, France

Received: 18 February 2008 – Revised: 3 June 2008 – Accepted: 10 June 2008 – Published: 17 July 2008

Abstract. In 1856, one (or two) destructive earthquake(s) occurred off Djijelli (Algeria) and probably triggered a tsunami in the western Mediterranean Sea. Following recently published results of marine campaigns along the North-Algerian margin, a new source hypothesis for the earthquake has been proposed, and is constituted with a set of three "en échelon" fault segments positioned in agreement with previous studies of this earthquake and with macroseismic data available. The geometrical parameters for this source, in agreement with a Mw = 7.2 earthquake, display an average 40° NW dip, a 80° strike and mean dimensions of 80 km (length) × 20 km (width). A coseismic slip of 1.5 m is consistent with an average convergence rate of about 5–6 mm/yr and a recurrence period of 300–400 years. They are then introduced in the tsunami modelling code to study the propagation across the Mediterranean Sea with a special attention towards the Balearic Islands. A focus on the two major towns, Palma (Majorca) and Mahon (Minorca) Harbours shows that these places are not the most exposed (maximum water heights less than 1 m) by tsunami waves coming from this part of the African margin. Specific amplifications revealed by modelling occur off the southern coast of Minorca and the southeastern coast of Majorca, mostly related to submarine bathymetric features, and are able to produce coastal wave heights larger than 1 to 2 m as offshore Alcalfar (Minorca). A deep submarine canyon southward Minorca leads to the amplification of waves up to two times on both sides of the canyon. However these modellings could not be compared to any historical observations, non-existent for these sites. This work is a contribution to the study of tsunami hazard in western Mediterranean based on modelling, and offers a first assessment of the tsunami exposure in the Balearic Islands.

Correspondence to: J. Roger
(jean.roger@cea.fr)

1 Introduction and objectives

On 21 May 2003, a M_w 6.8 earthquake located about 50 km east of Algiers (Algeria) triggered a moderate tsunami in the western Mediterranean Sea that provoked significant seiches, leading to local floodings and damage essentially on boats, in several harbours in the Balearic Islands (Ayadi et al., 2003; Alasset et al., 2006) (see http://www.elmundo.es/elmundo/2003/05/22/sociedad/1053590416.html for example). This event reminded us that areas apparently (and recently) poorly prone to tsunami hazard, but with a significant tectonic activity, likely already experienced tsunami events, even though probably rare and moderate (Meghraoui et al., 2006).

The 2003 event benefited from modern seismological and geodetic records, thus the earthquake source has been debated to describe the fault rupture (Yelles et al., 2004; Delouis et al., 2004; Semmane et al., 2005; Braunmiller and Bernardi, 2005), the slip distribution (Delouis et al., 2004; Yelles et al., 2004) and the surrection observed along the coast (Delouis et al., 2004; Meghraoui et al., 2004). The tsunami observations at tide gauges were quite sparse and of poor quality, except in the Balearic Islands where the records allowed to discuss the earthquake source (Alasset et al., 2006).

By contrast, historical events in the northern Algerian margin that could have triggered tsunamis in the western Mediterranean Sea are not well known, but the sequence of events at least goes back to the Algiers earthquake in 1365 (Yelles, 1991). Among the historical events, one of the most significant and recent tsunami originating from northern Algeria was provoked by the 21–22 August 1856 seismic sequence that struck the area of Djijelli. In the following we discuss this earthquake sequence and the tsunami that it triggered, especially in the Balearic Islands where no observation is available except one reported in Mahon Harbour (Rothé, 1950) whose robustness is questionable. We first recall the general tectonic setting and the historical data

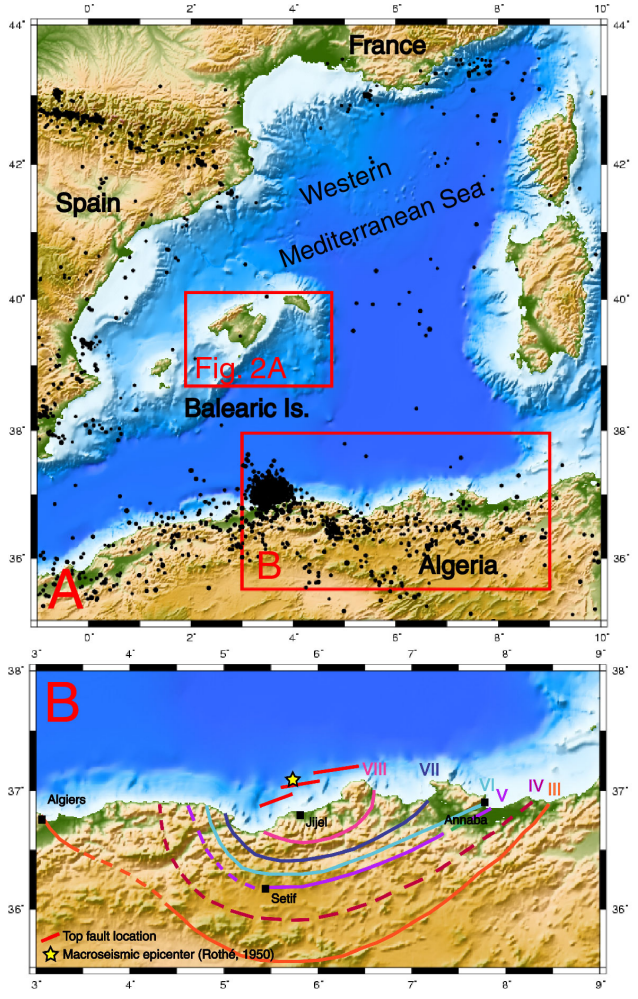

Fig. 1. **(A)** Geographical location of the study area in Western Mediterranean Sea and local seismicity from EMSC indicating the location of the plate boundaries. The zoom **(B)** shows the location of the 3 fault segments (in red) over GEBCO 1' shaded bathymetry and topography map of Djijelli area and isoseismal curves (MSK intensity scale) from Harbi et al. (2003). Location of Fig. 2A is reported. A represents the domain of the computational grid 0.

describing the event. Then we use tsunami numerical modelling to test different hypotheses allowing to discuss the earthquake source, and finally draw several conclusions regarding tsunami hazard in the Balearic Islands.

2 General settings

2.1 Geological context

The Mediterranean Sea is located at the boundary of two main tectonic plates, Europe and Africa. Their collision gives rise to a high seismicity level which is, in its western domain, essentially expressed in a moderate diffused seismic area, in northern Africa (Fig. 1A). Northern Algeria is part of this collision zone, where recent geodetic studies indicate an actual plate convergence rate of about 5.0 ±1mm/yr in a N 60° W direction (Calais et al., 2003; Nocquet and Calais, 2003, 2004; Serpelloni et al., 2007).

Earthquakes with magnitude Mw>5 frequently occur in the area (Harbi et al., 1999; Aoudia et al., 2000; Peláez Montilla et al., 2003), sometimes inducing important destructions and casualties (Adams and Barazangi, 1984). Well studied thrusting earthquakes essentially occur onshore, as for instance the largest recorded Ms7.3 1980 El Asnam earthquake (Ruegg et al., 1982; Deschamps et al., 1982; Meghraoui et al., 1988; Bezzehgoud et al., 1995).

According to available catalogues, tsunamis are frequent in Mediterranean and associated with both earthquakes and/or underwater landslides occurring on margins with steep slopes (Maramai et al., 2003; Papadopoulos and Fokaefs, 2005). Although North Algerian margin is not positioned above a subduction zone, many earthquakes and landslides along the margin are recorded each year and some destructive tsunamis have been reported over the past 700 years, 3 coming from great earthquakes in 1365, 1856 and 2003 (Yelles, 1991; Mokrane et al., 1994; Soloviev et al., 2000; Tinti et al., 2001; Alasset et al., 2006).

Recent studies along the Algerian margin have greatly improved the knowledge of the active structures (Domzig, 2006; Domzig et al., 2006; Yelles et al., submitted[1]). They bring to light the presence of compressional deformation features during the Quaternary period with inverse faults (pure compressive deformation) and strike slip faults leading to a clear seismogenic zone along the margin (Domzig, 2006).

The tsunamis generated during contemporary offshore earthquakes could have huge consequences on the Algerian coast which is considered as "near field" (less than 100 km) (Yelles et al., submitted[2]). But it could also have consequences in the Balearic Islands especially in harbours/bays where site effects are commonly frequent and where paper reports (see http://www.elmundo-eldia.com/2003/05/22/illes_balears/1053611977.html for example) mention non negligible wave arrivals up to 1 m high in 2003. And it is also worth mentioning here that some harbours in Balearic Islands located all along the southern coastline of Minorca and Majorca, as well as Mahon, Ciutadella or Palma, have been damaged in 2003, and that they are also prone to rissaga phenomenon i.e. meteorological tsunamis. In particular they can exhibit special behaviour to tsunami arrival, directly due

[1] Yelles, K., Domzig, A., Déverchère, J., Bracène, R., Mercier de Lépinay, B., Bertrand, G., Boudiaf, A., Winter, T., Kherroubi, A., Le Roy, P., and Djellit, H.: Evidence for a large active fault offshore West Algiers, Algeria, and seismotectonic implications, Geophys. J. Int., submitted.

[2] Yelles, K., Roger, J., Déverchère, J., Bracène, R., Domzig, A., Hébert, H., and Kherroubi, A.: The tsunami of Djijelli (Eastern Algeria) of 21–22nd August 1856: seismotectonic context, modelling, and implications for the Algerian coast, submitted to Pure and Applied Geophysics, Topical Issue on Tsunamis, submitted.

to their natural oscillation mode or to the resonant oscillation of the water body, inducing the so-called seiche (Monserrat et al., 1991; Gomis et al., 1993; Rabinovich and Monserrat, 1996 and 1998; Liu et al., 2003; Jansa et al., 2007).

It probably also could have consequences in southern France in the Golfe du Lion area where the slope of the continental shelf is rather low, or in the Côte d'Azur harbours too, where several witness accounts report oscillations and eddies in several harbours consecutive to the 2003 Zemmouri earthquake and associated tsunami (A. Sahal, pers. comm., 2007).

2.2 Historical facts

On the 21st and 22nd of August 1856 two earthquakes occurred near the Algerian coastal town of Djijelli about 300 km east to Algiers (Fig. 1B). The second one has an estimated magnitude Ms=5.7 (±0.17) and an intensity I_0=VIII MSK according to Harbi et al. (2003). It constitutes the best documented earthquake of North-East Algeria, described in many historical scientific reports and press articles. The quake was felt up to Nice (FR) and Genoa (IT). This couple of events has generated one (or two) tsunami wavetrains, which consequences added to earthquake damage and casualties along the Algerian coast and which are reported in bibliography (Gaultier de Claubry, 1856; Aucapitaine, 1856; De Senarmont, 1856; Ambraseys, 1982; Harbi et al., 1999; Harbi, 2001; Antonopoulos, 1990; Yelles Chaouche, 1991).

Unfortunately, as previously mentioned, no detailed reports are available concerning a potential Mediterranean Sea-wide tsunami. Only one possible effect is mentioned in Mahon Harbour in the Balearic Islands, but it cannot be ruled out that it may be related to a storm observed these days in the Western Mediterranean (reported in historical papers as La Gazette du Midi, n°7272, 22nd August 1856 or Le Moniteur Universel, 25th August 1856). Also, as usual for offshore earthquakes, and especially for historical events, the location and size of the source are difficult to assess from macroseismic data as mentioned by Harbi et al. (2003).

The main characteristics of the tsunami related to the two events of 1856 are summarized in Table 1. Firstly we observe from these data that there was an important flooding and a sea withdrawal following the earthquakes, which induced more or less damage along the Algerian coast and in the Balearic Islands. Secondly it is also worth noting that there is no reported information concerning tsunami estimated arrival times in historical data.

3 Numerical modelling

3.1 Sources definition

Firstly potential sources able to have generated the 1856 earthquake(s) and associated tsunami must be investigated. According to the fact mentioned by Harbi et al. (2003) that damage became more and more important and numerous as

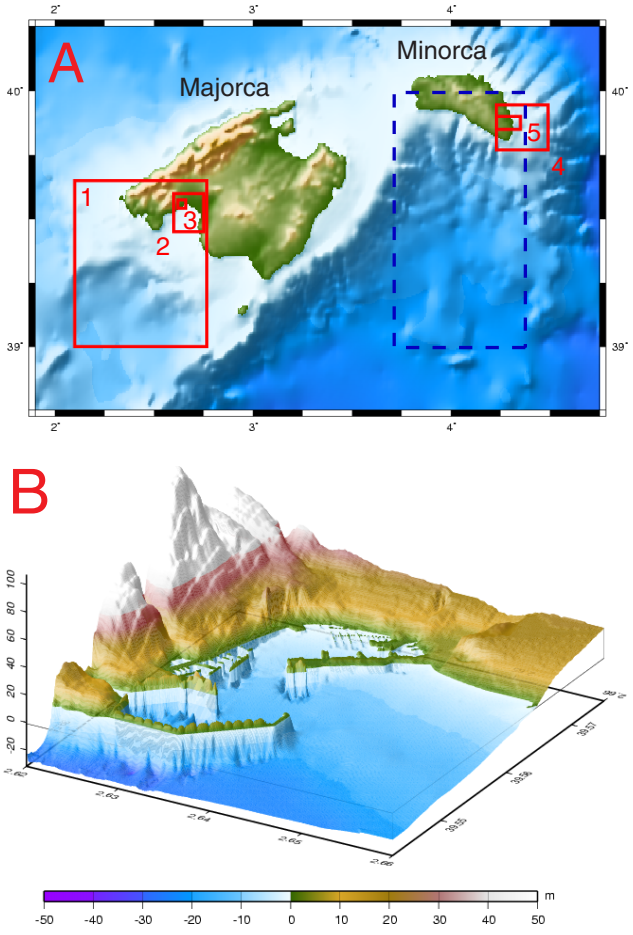

Fig. 2. **(A)** (localized in Fig. 1) shows the different levels of grid used in modelling (in red) and a special focus on a submarine canyon (in dashed blue); **(B)** represents the 3-D visualization of the high resolution grid (10 m) of Palma harbour (grid 3).

approaching the coastline, and confirmed by the isoseismal maps issued from historical reports for the 1856 event, a sea-located source offshore Djijelli has constantly been proposed (Harbi et al., 2003; Harbi et al., 1999) (Fig. 1B).

In addition, according to Ambraseys (1982) and Harbi et al. (2003), the main shock has been felt over a wide area well-oriented towards French Riviera and north-western Italia (esp. Nice and Genoa) as mentioned above. The lack of observations in the inner part of Algeria is mostly due to the low population density in desert areas, and put some uncertainties to the southernmost extent of macroseismic effects. Nevertheless the coastal extent of these effects is not influenced by these missing observations to the south, and the sum of all the information gathered from intensity map, isoseismal curves geometry, earthquake felt area, tsunami generation, etc., allow us to propose a source of about 100 km length. This, according to Stock and Smith (2000), corresponds to an Mw = 7.0–7.2 earthquake, i.e. the required magnitude to generate such a destructive tsunami, significantly larger than the 2003 event.

Table 1. Historical data set compiled from Gaultier de Claubry (1856), Aucapitaine (1856), De Senarmont (1856), Ambraseys (1982), Harbi et al. (1999), Harbi (2001), Antonopoulos (1990), Yelles Chaouche (1991).

Mentioned Town in reports	1st earthquake	2nd earthquake	remarks
Djijelli (Jijel, Algeria) 5.75° E, 36.81° N	A little harbour is severely damaged at the western extremity of the bay; water came back suddenly after a first sea withdrawal flooding low parts of the coast	2–3 m high wave; several back and forth; sea stays troubled during 3 days; the town is destroyed by the earthquake	*Concerning the 1st earthquake, it is unclear whether it is the shock or the tsunami which caused reported destructions*
Mahon (Minorca) 4.26° E, 36.88° N	Rapid flooding of the harbour; a lot of boats break their moorings		*Witnesses probably do not make the distinction between the 2 different waves arrivals*
Philippeville (ancient name for Skikda) 6.90° E, 36.87° N		Sea level draw down suddenly and rise up gradually of about 0.6 m	
Bougie (actual Bejaia) 5.07° E, 36.74° N		Several series of waves have flooded the coast; sea level has increased of about 5 m (3.75 m for some authors); coast has been flooded (5–6 times only 3 times for Aucapitaine, 1856) with a withdrawal of 35 m	
Bone (actual Annaba) 7.75° E, 36.90° N		Sea level rose for 1 m; flood and agitated sea during 12 h; a little isle seems to have disappeared under sea.	*Witnesses probably do not make the distinction between the 2 different waves arrivals*
15 mi N 7° E from Jijel on the boat "Tartare"			Extreme violence quake
Coasts of Sardinia, Nice, Malta, Mahon, Carloforte, Iglesias and San Petro Sardinia			Additional locations where the quake could have been felt (Rothé, 1950)

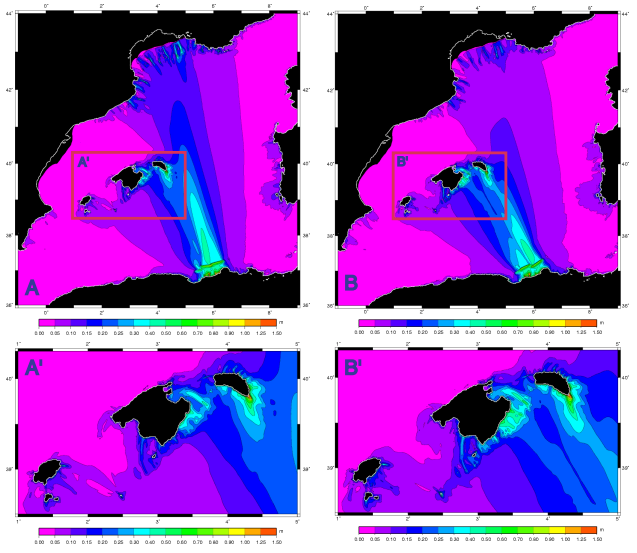

Fig. 3. Maximum wave heights cumulated on 1.5 h after the rupture involving the 3 segments simultaneously, with a mean strike of 80° (left, A and A') or 60° (right, B and B').

As said before, recent results from bathymetric and seismic MARADJA survey (Domzig, 2006) allowed us to propose potential sources (earthquake fault plane location) for the Djijelli tsunami of 21–22 August 1856. In fact Domzig (2006) indicates a fault system "en echelon" offshore Djijelli composed of at least three faults parallel to the coast dipping south-eastward (Fig. 1B). This source system seems to be in good agreement with the isoseismal map of Harbi et al. (2003) and with the earthquakes localization (37.10° N–5.70° E) from Rothé (1950, USGS/NEIC earthquakes catalogue). The mean strike of these three faults is well-oriented: Okal (1988) recalls that in the case of a tsunami generated by an earthquake, the maximum wave amplitudes are always localized in the major direction of deformation, i.e. an inverse fault with a 90° rake angle should generate a tsunami with maximum height in the direction perpendicular to the fault direction.

3.2 Modelling parameters of the 3 sources

In order to model the tsunami, we propose parameters for three segments (Table 2), able to generate an M_w = 7.2 earthquake, if they ruptured together. We have to put minimum conditions to fit the inferred seismic moment M_0, related to fault geometry through the law $M_0 = \mu SLW$ (where μ is the rigidity, S the average slip, L the fault length and W the fault width). In order to explain the observations in Northern Algeria we also tested our solution for local sites (Yelles-Chaouche et al., 2007).

An M_w7.2 earthquake corresponds to a M_o=1*10^{10} N.m (Aki, 1966), and, according to Stock and Smith (2000) and Wells and Coppersmith (1994), to a fault rupture length of 70–80 km and to a surface displacement of about 1–1.5 m. But they show that normally, in a subduction zone, length and

width must be in a ratio of 1 to 3. However fault widths larger than 20 km and longer than 40 km are not consistent with the structures identified here (Domzig, 2006), thus a source involving several segments has to be considered. The fault strike is chosen in accordance with the geomorphologic interpretation of the region by Domzig (2006): we use a mean strike of 80°. However the real geological strike in depth may differ from the seismological strike by 20° (Déverchère, pers. comm.), thus a 60° strike angle was also tested.

The recent seismic studies presented by Domzig et al. (2006) and Harbi et al. (1999) allow us to propose a depth of fault centre of about 10 km, and a dip of 40° in this study.

According to historical reports and to actual deformation measurements (Calais et al., 2003; Nocquet and Calais, 2003, 2004) indicating an average convergence rate of about 5–6 mm/yr in this region, we are able to propose a coseismic slip of 1.5–2 m which could be reached after 300–400 years (Hébert et al., 2007a). As for the rigidity, we assume a standard rigidity of $4.5*10^{10}$ N.m^2 (compression mechanism) in agreement with Bilek and Lay (1999) and Geist and Bilek (2001) for conventional earthquakes.

3.3 Deformation and Tsunami Modelling

The initial deformation calculus is based on elastic dislocation computed through Okada formula (1985). Our method considers that the sea-bottom deformation is transmitted without losses to the entire water column, and solves the hydrodynamical equations of continuity (1) and motion (2) conservation. Non linear terms are taken into account, and the resolution is carried out using a Crank Nicolson finite difference method centred in time and using an upwind scheme in space. This method has been widely used in the Pacific Ocean and contributed to tsunami hazard studies in several locations (Hébert et al., 2001, 2007b).

$$\frac{\partial(\eta+h)}{\partial t} + \nabla.[v(\eta+h)] = 0$$

$$\frac{\partial v}{\partial t} + (v.\nabla).v = -g\nabla\eta$$

η corresponds to the water elevation; h to the depth; v to the horizontal speed vector; g to the gravity.

The wave propagation is calculated on 4 levels of imbricated grids of increasing resolution for Majorca (allowing to focus on Palma harbour) and 3 levels for Minorca (allowing to focus on Mahon inlet) (Figs. 1 and 2). The larger grid (0), corresponding to geographical coordinates of Fig. 1A, is built from GEBCO World Bathymetric Grid 1' (British Oceanographic Data Center, 1997) and is just an interpolation of this grid at a space step of 500 m. The grid resolution increases close to the studied site i.e. when the water depth h decreases along with the tsunami propagation speed equation $c=\sqrt{gh}$ that depends only on h in non dispersive assumption.

High resolution grids, which are set up for the final grid level, are made from digitized, georeferenced and interpolated nautical bathymetric charts and/or multi-beam bathymetric data. For Palma harbour (Majorca), the grid has a resolution of 10 m (grid 3) able to reproduce harbour major infrastructures as docks or piers (Fig. 2B) which could have a significant influence on wave arrival times and amplitudes. In order to reproduce these structures at best, and not to put a low slope where there is a vertical wall, we have digitized the bathymetric map of the harbour in agreement with available harbour pictures to complete the lack of bathymetric values near these structures. Intermediate grids 1 and 2 are made with both datasets from grid 0 and 3 and data coming from

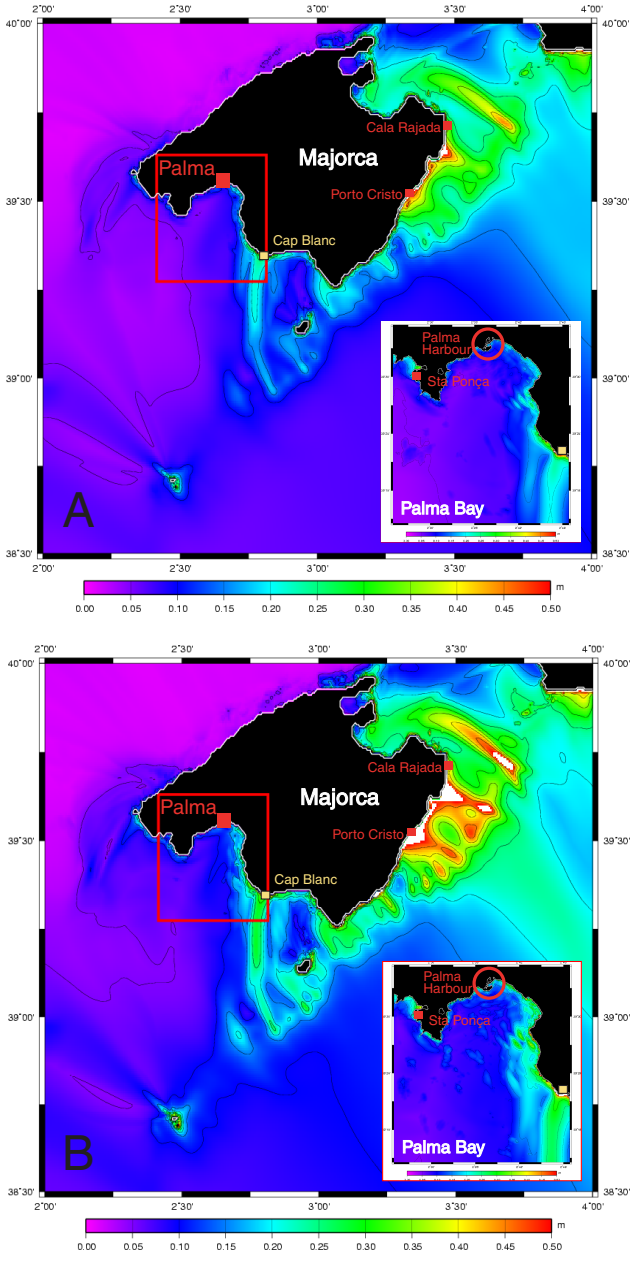

Fig. 4. Majorca Island and zoom on Palma Bay and neighbourhood for a 80° strike source (A) and a 60° strike source (B).

Table 2. Geographical and geometrical parameters of the 3 fault segments used for the modelling of the initial deformations of seafloor. The two values of strike angle are those tested in the study.

	Longitude (°)	Latitude (°)	Depth of the fault center (km)	Slip (m)	Strike (°)	Dip (°)	Rake (°)	Length (km)	Width (km) modulus (Pa)	Shear	M_w	M_0 (Nm)
west	5476	36 950	10	1.0	75 (55)	40	90	25	20	$4{,}5*10^{10}$	6.8	$2.2*10^{19}$
center	5736	37 080	10	1.5	85 (65)	40	90	37	20	$4{,}5*10^{10}$	7.1	$5*10^{19}$
east	6.150	37.178	10	1.5	75 (55)	40	90	44	20	$4{,}5*10^{10}$	7.1	$5.9*10^{19}$

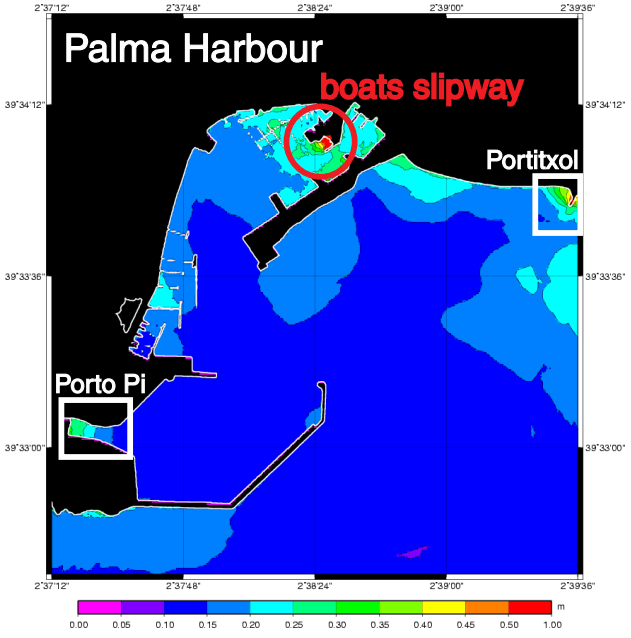

Fig. 5. Maximum wave heights for a 60° strike source: zoom on Palma Harbour.

multi-beam Spanish campaigns (de Mol, personal communication). Grid 1 has been chosen to be 120 m resolution and grid 2 to be 30 m resolution in order to never have more than a factor of 4–5 between imbricated grids, so that the shoaling effect is well reproduced and the wavelengths properly sampled. The process for Mahon is similar, leading to grids 4 (resolution 120 m) and 5 (resolution 30 m) imbricated in grid 0.

3.4 Results

3.4.1 Overview

The first results of numerical modelling of the 1856 tsunami propagation towards the Balearic Islands exhibit several interesting features (Fig. 3). Firstly, the value of the fault strike, all other parameters being equal, is clearly discriminatory as regards the areas impacted. With a 80° angle (Fig. 3A) the tsunami propagation is more oriented towards Southern France (Golfe du Lion) whereas a 60° oriented fault system (Fig. 3B) leads to a propagation principally towards the Balearic Islands, excluding Ibiza and Formentera which seem poorly threatened by a tsunami coming from this part of North-African margin (Roger and Hebert, 2007). This results contrasts with the 2003 event, which led to destructions along the coasts of these two islands (Perez, pers. comm.), and for which numerical modellings clearly confirmed the exposure of Ibiza and Formentera for this source area. Hereafter, detailed modellings for these two islands are thus discarded.

The results also indicate that some sites, principally along the eastern coast of Majorca and the South-East peninsula of Minorca, are particularly more reactive to tsunami wave arrivals and to their amplification, whatever the strike angle (60° or 80°): maximum wave height reaches 1 m and much more at some points (especially in Minorca) (Fig. 3A and B), and are on average are slightly larger with a 60° strike (Fig. 3B') than with a 80° (Fig. 3A).

3.4.2 Majorca

The result of modelling on Majorca shows non negligible heights (more than 40 cm) along the South-East to North-East coast of Palma Bay (Fig. 4). The waves seem to be amplified along particular ways where they may be guided and more amplified, in the South-East of Palma Bay in front of Cap Blanc and also in the North-Eastern part of the island (Fig. 4). A detailed study of the results in the higher resolution grids reveals that some particular points as in the small bay of Santa Ponça, westward to Palma (Fig. 4) are reached by large wave heights, all the more as the grid resolution is increased. It is to note that this bay is part of the bays which are inclined to the rissaga phenomenon frequent in the Balearic Islands (Monserrat et al., 2006).

Concerning Palma Harbour, actually located in the north-western part of the bay (Fig. 4), the modelling results for the 10 m resolution grid (for a 60° strike angle) show that wave amplification higher than 1 m takes place at the far end of the harbour (Fig. 5). The run-up computation of this last level of imbricated grid shows that only one inundation is modelled in the harbour, on a boat slipway in the very inner part of the harbour and that the little dock of Porto Pi shows local amplification as the little Marina of Portitxol outside Palma Harbour (Fig. 5).

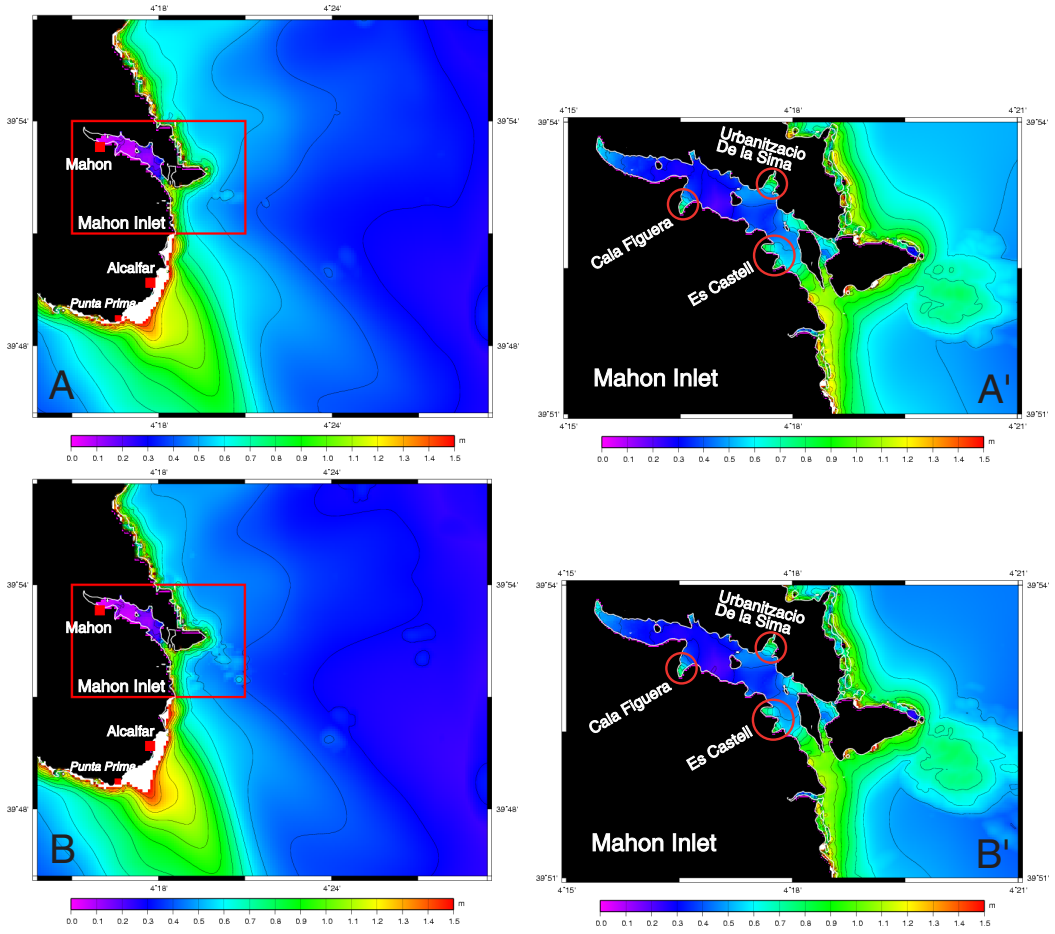

Fig. 6. Maximum wave heights along the South-eastern coast of Minorca Island for a 80° strike source **(A)** and a 60° strike source **(B)**. In both cases there is a zoom on Mahon Inlet pointing out some particular areas (**A'** and **B'**). Be careful that there is no calculated inundation, the white colour indicates only maximum wave heights above 1.5 m.

3.4.3 Minorca

As previously seen for Majorca, we notice that the waves seem to be amplified along particular ways approaching Minorca (Fig. 3). In addition, the results in the finer grids clearly show that maximum wave heights of more than 1.5 m are reached off the South-East extremity of Minorca.

Mahon Inlet seems to be rather protected from the modelled tsunami arrivals (Fig. 6A and B). The modellings performed on higher resolution (30 m) grids (grid 5) enhance wave amplification in the inlet but restricted to smaller bays included in the inlet as Cala Figuera, Es Castell or Urbanitzacio De la Sima (Fig. 6A' and 6B'). Thus the computation on this higher resolution grid allows us to make a more detailed analysis of this site certainly closer to the reality: the entrance of the inlet is better modelled with a 30-m pixel than with a 120-m pixel, allowing to better image this 500-m wide entrance and so to let long waves penetrate it.

4 Discussion

The paucity of observations on remote coastal sites precludes us to discuss the source based on tsunami data, but we can propose the following scenario for the 1856 event. Two main shocks have been reported, the second being the strongest according to historical reports. Firstly the western proposed segment ruptured on 21st August, with a cautious interpretation of historical data which indicates that the magnitude of the first earthquake was certainly low. Then both eastern segments proposed here, based on recent geological investigations (Domzig, 2006), could have broken on 22nd August and generated an earthquake with magnitude sufficient to have important consequences over a wide area in agreement with isoseismal maps from Harbi et al. (2003) and to generate a sea-wide tsunami (explaining the observation in Mahon inlet, Balearic Islands). The modelling results at the Mediterranean scale (Fig. 3) confirm that Minorca is mostly impacted by the two eastern segments, and indeed the modelling of the

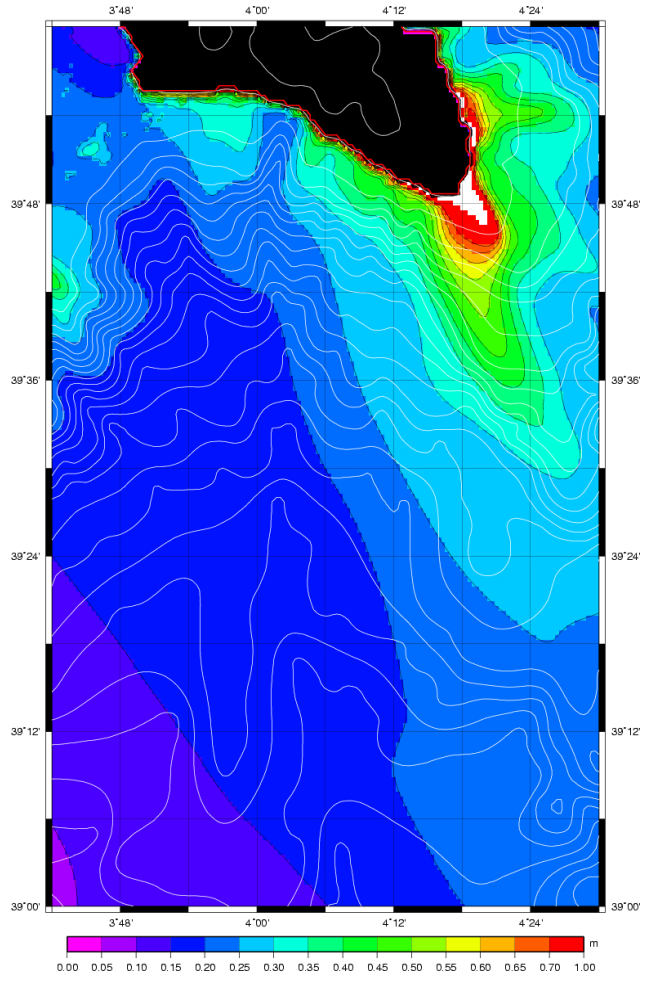

Fig. 7 Maximum wave heights for a 80° strike source onto bathymetric map southward Minorca (isocontour 100 m) that reveals the importance of the role of a submarine canyon (Minorca Canyon system) on the wave amplification.

western segment alone did not produce waves able to reach Minorca (Yelles-Chaouche et al., 2007).

Concerning the tsunami impact, first important differences are noted for Majorca, depending on the strike of the source, leading to sites more impacted along the coast of Palma Bay for a 60° strike than for a 80° strike (Fig. 3). Palma Harbour and Town are situated at the extreme North-West of the bay, and are the economical and touristy centre of the Balearic Islands. Our results indicate that these places are not much affected by tsunamis generated in the 1856 epicentral area (Figs. 4 and 5). On one hand the lack of historical reports concerning a tsunami in Palma in 1856 is consistent with our results. However the shape of the harbour including the location of piers was probably different from now and then our model may probably not represent exactly the resonant effect of the Palma Bay at that time, and especially the harbour resonance put in evidence after studying rissaga phenomenon (Monserrat et al., 2006 for example) or more simply the long wave arrival effects (Bellotti, 2007). A site as Palma Bay which can easily respond to atmospheric variations with non negligible oscillations is supposed to have a particular reaction like strong amplification (resonance) to long wave such as earthquake-induced tsunami (Jansa et al., 2007); concerning "classic" seismic long-waves, the work done on coastal structures studies indicates that this phenomenon can be reduced today taking into account the position and shape of the harbours entrance (Bellotti, 2007; Nakamura and Takayuki, 2003; Nakamura et al., 2000).

Regarding Minorca, whatever the strike, the modelling results of wave amplifications, and location of these amplifications, are rather the same (Figs. 3 and 6). A more detailed analysis reveals that the southernmost area offshore Minorca (offshore Alcalfar and Punta Prima) seems to considerably amplify wave heights, probably due to the shape of the bathymetry (Fig. 6A and 6B). In both cases we have almost the same results considering locations and amplitudes. According to modelling, Mahon inlet is not particularly receptive to long waves except in some little bays within the inlet (Fig. 6A' and 6B'), despite the fact that this places is frequently prone to rissaga phenomenon which waves direction and propagation speed are conducive to produce a resonant response and so naturally amplify them. Since the Balearic Islands and particularly inlets as Cuitadella (Western coast of Minorca) and Mahon or bays as Palma Bay are frequently inclined to rissaga phenomenon (meteorological tsunami that could be generated by strong jump in atmospheric pressure, gravity waves or other atmospheric sources) (Monserrat et al., 1991, 2006; Liu et al., 2003; Rabinovich and Monserrat, 1998; Gomis et al., 1993) we have to underline the important probability of site effects in these specific Balearic sites.

The site effects are thus very important to be mentioned in case of such a tsunami, which is among the strongest hazards expected in the area. We can observe a sea level variation of 2 m in a bay and nothing due to resonance/amplification phenomenon in the surrounding areas.

A particularly impressive phenomenon of long wave trapping shown on Fig. 3 is underlined in both tested cases in Minorca Island southward of Mahon Inlet (Fig. 6A and 6B). A less impressive phenomenon is also visible on the southeastern coast of Majorca (Fig. 4A and 4B). Actually additional tested seismic sources generating tsunamis in a zone from eastern Algeria to southern Sardinia (Roger and Hébert, 2007) induced such an amplification which is due to the particular V-shape of the bathymetry in this area, with slowly increasing depths. Concerning the inlet case no important amplifications occur in the modelling (Fig.6 A' and B'), although there are some reports of rissaga phenomenon in this place. Then we can suppose that either the resonant frequency of the inlet is probably not completely taken into account by our method, at least at this scale or that the tsunami frequency is different from the rissaga's one. However similarities of wavelengths and periods between seismic tsunami and atmospheric tsunami (Monserrat et al., 2006) allow to assume that a harbour or a bay frequently affected by the

rissaga phenomenon should react the same in the case of a seismic tsunami arrival.

In 1856, the density of populated areas in coastal Balearic locations, such as in the southern part of Minorca, is not well known. Available older historical cartographic documents (Seutter, 1741) only indicate a few settlements. Even though this population may have very locally increased in the 19th century, this rather low density did not favour numerous reports of possible observations. However modelling results indicate that this part of the islands is one of the more stricken ones by long waves. We can also easily see, considering the Balearic Promontory South to Minorca, that there is a clear influence on the waves amplitudes of a submarine canyon (Minorca Canyon system described by Acosta et al., 2002) (Fig. 7): in fact, in front of the canyon, the amplification is very low while it is important on both sides of the canyon. This is mostly due to the shoaling effect which slows down and amplifies the waves around the canyon, and is rather different from results obtained in a yet similar configuration off Myanmar during the 2004 Indian Ocean tsunami (Ioualalen et al., 2007). A similar phenomenon is observed offshore the Cap Blanc and offshore the coastline between Porto Cristo and Cala Rajada in Majorca (Figs. 4A and B).

5 Conclusions

The evaluation of the Djijelli 1856 earthquake macroseismic intensity is biased due to the offshore location of the main shock. The seismogenic potential and the faults system geometry offshore Djijelli is poorly documented, and events of such magnitude in the area are very rare. The lack of historical data of tsunami observations in the Balearic Islands in 1856 do not allow us to completely compare and validate our results based on tsunami modellings and thus our new source hypothesis. But we can mention here that the wave arrivals in the Balearic Islands concerning the 2003 tsunami are reported with highest values/damage in the same areas (except Ibiza) than for the modelled 1856 results, highlighting the highest exposure of the southeastern coast of Majorca to tsunamis coming from central and eastern Algeria.

On another hand, could the waves reported in Mahon be related to any submarine landslide? Indeed, submarine landslides can occur along the Algerian coast (Dan et al., in press; Domzig et al., submitted), mostly due to the very steep slopes of the area. Some of them can occur after seismic shaking (such as turbidites after the 1980 and 2003 earthquakes). The so-generated waves could reach levels consistent with the observations reported in Algeria. But these waves possibly generated by such landslides are probably not able to reach the Balearic Islands area: the shorter waves involved are unable to propagate at long distances without a significant dispersion that reduces the wave heights. Thus the reported flooding and destruction in Mahon could be explained by this kind of waves only if they are generated in short field (slopes of the Balearic Promontory).

Another possible interpretation could be the fact that there was a storm in Western Mediterranean at this time which could have led to destruction in Mahon harbour due to sea level rise correlate with atmospheric depression move. Thus the reports of floodings/destructions along the Algerian coast could be due to a local tsunami generated by a submarine landslide.

A perspective to this study would be to increase the resolution of our grids in test sites as Mahon and Palma and probably to choose other test sites more inclined to wave amplification on the East coast of Majorca and/or on the South coast of Minorca, in accordance with the actual inhabited areas, particularly those which present special reactions to rissaga phenomenon in order to calculate run-up. Then additional sources should be tested with various locations and strikes in order to constrain more precisely the hazardous areas in the Balearic, maybe with a systematic approach (Roger and Hébert, 2008). Finally, an on-field study concerning the possibility of existence of tsunami deposits in Western Mediterranean has to be taken into account with a special focus onto the Balearic Islands, in order to identify paleotsunamis, distinguishing them from storm events and propose recurrence period.

Acknowledgements. This work was performed within the framework of and funded by the European project TRANSFER under the contract 037058. We thank A. Domzig and J. Déverchère for their supply of information concerning the geodynamical interpretation of the Algerian offshore margin. Seismicity plotted on Fig. 1 was provided by EMSC-CSEM (www.emsc-csem.org). We are indebted to two anonymous reviewers and to A. B. Rabinovich who gave precious advices to improve the paper. Remarks made by F. Schindelé were also taken into account, and we acknowledge support from CEA.

Edited by: S. Tinti
Reviewed by: A. Rabinovich and two other anonymous referees

References

Acosta, J., Canals, M., Lopez-Martinez, J., Munoz, A., Herranz, P., Urgeles, R., Palomo, C., and Casamor, J. L.: The Balearic Promontory geomorphology (western Mediterranean): morphostructure and active processes, Geomorphology, 49, 177–204, 2002.

Adams, R. D. and Barazangi, M.: Seismotectonics and seismology in the Arab region: a brief summary and future plans, Bull. Seism. Soc. Am., 74(3), 1011–1030, 1984.

Aki, K.: Generation and propagation of G-waves from the Niigata earthquake of 16 June 1964 – 2. Estimation of earthquake movement, released energy and stress-strain drop from G spectrum, Bull. Earthq. Res. Inst., 44, 23–88, 1966.

Alasset, P. J., Hébert, H., Maouche, S., Calbini, V., and Meghraoui, M.: The tsunami induced by the 2003 Zemmouri earthquake

(Mw = 6.9, Algeria): modelling and results, Geophys. J. Int., 166, 213–226, 2006.

Ambraseys, N. N.: The seismicity of North Africa: the earthquake of 1856 at Jijeli. Bollettino Di Geofisica a Teorica ed Applicata. Vol. XXIV, No.93, 31–37, 1982.

Antonopoulos, J.: Data for investigating tsunami activity in the Mediterranean sea, Science of Tsunami Hazards, 8(1), 39–52, 1990.

Aoudia, A., Vaccari, F., Suhadolc, P., and Meghraoui, M.: Seismogenic potential and earthquake hazard assessment in the Tell Atlas of Algeria. Journal of Seismology, 4, 79–98, 2000.

Aucapitaine, M.: Note sur le tremblement de terre ressenti en Algérie du 21 au 25 août 1856. C. R. Acad. Sc. Paris, 2ème semestre, T. XLIII, 16, p. 765, 1856.

Ayadi, A., Maouche, S., Harbi, A., et al.: Strong Algerian earthquake strikes near capital city, EOS, 84(50), 5068, 561 pp. , 2003.

Bellotti, G.: Transient response of harboursto long waves under resonance conditions, Coast. Eng., 54, 680–693, 2007.

Bezzeghoud, M., Dimitrov, D., Ruegg, J. C., and Lammali, K.: Faulting mechanism of the El Asnamn (Algeria) 1954 and 1980 earthquakes from modelling of vertical movements, Tectonophysics, 249, 249–266, 1995.

Bilek, S. L. and Lay, T.: Rigidity variations with depth along interpolate megathrust faults in subduction zones, Nature, 400, 443–446, 1999.

Braunmiller, J. and Bernardi, F.: The 2003 Boumerdes Algeria earthquake: regional moment tensor analysis, Geophys. Res. Lett., 32, L06305, doi:10.1029/2004GL022038, 2005.

British Oceanographic Data Centre – The Centenary Edition of the GEBCO Digital Atlas, http://www.gebco.net/data_and_products/gebco_digital_atlas/, Liverpool, UK, 1997.

Calais, E., DeMets, C., and Nocquet, J.-M.: Evidence for a post-3.16 Ma change in Nubia-Eurasia plate motion, Earth Planet. Sci. Lett., 216, 81–92, 2003.

Dan, G., Savoye, B., Cattaneo, A., Gaullier, V., Déverchère, J., Yelles, K., and Maradja 2003 team: Recent sedimentary patterns on the Algerian margin (Algiers area, southwestern Mediterranean), AAPG/SEPM (Society for Sedimentary Geology) Special Vol. 93, Geological Society of America, in press, 2008.

Delouis, B., Vallée, M., Meghraoui, M., Calais, E., Maouche, S., Lammali, K., Mahsas, A., Briole, P., Benhamouda, F., and Yelles, K.: Slip distribution of the 2003 Boumerdes-Zemmouri earthquake, Algeria, from teleseismic, GPS, and coastal uplift data, Geophys. Res. Lett., 31, L18607, doi:10.1029/2004GL020687, 2004.

Deschamps, A., Gaudemer, Y., and Cisternas, A.: The El Asnam, Algeria, earthquake of 10 October 1980: multiple-source mechanism determined from long-period records. Bull. of the Seism. Soc. of Am., 72(4), 1111–1128, 1982.

Domzig, A.: Déformation active et récente, et structuration tectono-sédimentaire de la marge sous-marine algérienne. Thèse de Doctorat de l'Université de Bretagne Occidentale, 332 p., 2006.

Domzig A., Yelles K., Le Roy C., Déverchère, J., Bouillin, J-P., Bracène, R., Mercier De Lépinay, B., Le Roy, P., Calais, E., Kherroubi, A., Gaullier, V., Savoye, B., and Pauc, H.: Searching for the Africa–Eurasia Miocene boundary offshore western Algeria (MARADJA'03 cruise). C. R., Géoscience, 338, 80–91, doi:10.1016/j.crte.2005.11.009, 2006.

Domzig, A., Gaullier, V., Giresse, P., Pauc, H., Déverchère, J., and Yelles, K.: Deposition processes from echo-character mapping along the western Algerian margin (Oran-Tenes), Western Mediterranean, submitted, Marine and Petroleum Geology, special volume on Slope Instabilities, in press, 2008.

Gaultier de Claubry, M.: Sur les effets du tremblement de terre du 21 et 22 août 1856 dans certaines parties de l'Algérie, C. R. Acad. Sc. Paris, T. XLIII, 589–590, 1856.

Geist, E. L. and Bilek, S. L.: Effect of depth-dependent shear modulus on tsunami generation along subduction zones, Geophys. Res. Lett., 28(7), 1315–1318, 2001.

Gomis, D., Monserrat, S., and Tintoré, J.: Pressure-forced seiches of large amplitude in inlets of the Balearic islands, J. Geophys. Res., 98(C8), 14 437–14 445, 1993.

Harbi, A.: Analyse de la sismicité et mise en évidence d'accidents actifs dans le nord-est algérien, Thèse de Magister, 196 pp., USTBH Alger, 2001.

Harbi, A., Benouar, D., and Benhallou, H.: Re-appraisal of seismicity and seismotectonics in the north-eastern Algeria. Part I: Review of historical seismicity, J. Seismol., 7, 115–136, 2003.

Harbi, A., Benouar, D., and Benhallou, H.: Re-appraisal of seismicity and seismotectonics in the north-eastern Algeria. Part I: Review of historical seismicity, J. Seismol., 7, 115–136, 2003.

Harbi, A., Maouche, S., and Ayadi, A.: Neotectonics and associate seismicity in the Eastern Tellian Atlas of Algeria, J. Seismol., 3, 95–104, 1999.

Hébert, H., Heinrich P., Schindelé F., and Piatanesi A.: Far-field simulation of tsunami propagation in the Pacific Ocean: impact on the Marquesas Islands (French Polynesia), J. Geophys. Res., 106, 9161–9177, 2001.

Hébert, H., Roger, J., and Schindelé, F.: Advances in tsunami hazard assessment in the western Mediterranean Sea, Geophys. Res. Abstracts, 9, 06341, SRef-ID: 1670-7962/gra/EGU2007-A-06341, EGU Vienna, 2007a.

Hébert, H., Sladen, A., and Schindelé, F.: The great 2004 Indian Ocean tsunami: numerical modeling of the impact in the Mascarene Islands, B. Seismol. Soc. Am., 97, 1A, 208–222, 2007b.

Ioualalen, M., Pelinovsky, E., Asavanant, J., Lipikorn, R., and Deschamps, A.: On the weak impact of the 26 December Indian ocean tsunami on the Bangladesh coast, Nat. Hazard. Earth Syst. Sci., 7, 141–147, 2007.

Jansa, A., Monserrat, S., and Gomis, D.: The rissaga of 15 June 2006 in Ciutadella (Menorca), a meteorological tsunami, Adv. Geosci., 12, 1–4, 2007, http://www.adv-geosci.net/12/1/2007/.

Liu, P. L.-F., Monserrat, S., Marcos, M., and Rabinovich, A. B.: Coupling between two inlets: Observations and modelling, J. Geophys. Res., 108(C3), 3069, doi:10.1029/2002JC001478, 2003.

Maramai A., Graziani L., and Tinti S.: Updating and revision of the European Tsunami Catalogue, NATO Sciences Series: Submarine Landslides and Tsunamis, edited by: Yalciner, A. C., Pelinovsky, E., Okal, E., and Synolakis, C., Kluwer Academic Publishers, 25–32, 2003.

Meghraoui, M., Alasset, P.-J., and Hébert, H.: Potential tsunamigenic earthquake sources along the Algerian coast: lessons learned from recent earthquakes and implications for the western Mediterranean Sea, Geophys. Res. Abstracts, 8, 10009, SRef-ID: 1607-7962/gra/EGU06-A-10009, 2006.

Meghraoui, M., Maouche, S., Chemaa, B., Cakir, Z., Aoudia, A.,

Harbi, A., Alasset, P.-J., Ayadi, A., Bouhadad, Y., and Benhamouda, F.: Coastal uplift and thrust faulting associated with the Mw = 6.8 Zemmouri (Algeria) earthquake of 21 May 2003, Geophys. Res. Lett., 31, L19605, doi:10.1029/2004GL020466, 2004.

Meghraoui, M., Philip, H., Albarede, F., and Cisternas, A.: Trench investigations through the trace of the 1980 El Asnam thrust fault : evidence for paleoseismicity. B. Seism. Soc. Am., 78(2), 979–999, 1988.

Mokrane, A., Ait Messaoud, A., Sebai, A., Ayadi, A., Bezzeghoud, M., and Benhallou, H.: Les séismes en Algérie de 1365 à 1992, Publication du Centre de Recherche en Astronomie, Astrophysique et Géophysique, Département Etudes et Surveillance Sismique, ESS, C. R. A. A. G., Alger-Bouzaréah, 277 pp., 1994.

Monserrat, S., Ibbetson, A., and Thorpe, A. J.: Atmospheric gravity waves and the 'Rissaga' phenomenon, Q. J. R., Meteorol. Soc., 117, 553–570, 1991.

Monserrat, S., Vilibic, I., and Rabinovich, A. B.: Meteotsunamis: atmospherically induced destructive ocean waves in the tsunami frequency band, Nat. Hazard. Earth Sys. Sci., 6, 1035–1051, 2006.

Morita, S. and Nakamura, T.: A optimum design of wave resonators for coastal and harbour structures, Proceedings of Japan Society of Civil Engineers (JSCE), 740, 143–155, 2003.

Nakamura, T., Morita, S., and Takemoto, T.: Effectiveness of a large resonator installed at the harbour entrance for mitigating long-period wave, Memoirs of the Faculty of Engineering, Ehime Univ., 19, 269–277, 2000.

Nocquet, J.-M. and Calais, E.: Crustal velocity field of western Europe from permanent GPS array solutions, 1996–2001, Geophys. J. Int., 154, 72–88, 2003.

Nocquet, J.-M. and Calais, E.: Geodetic measurements of crustal deformation in the western Mediterranean and Europe, Pure Appl. Geophys., 161, 000-0000033-4553/04/000000-00, doi:10.1007/s00024-003-2468-z, 2004.

Okada, Y.: Surface deformation due to shear and tensile faults in a half-space, Bull. Seismol. Soc. Am., 75, 1135–1154, 1985.

Okal, E.: Seismic parameters controlling far-field tsunami amplitudes: a review, Nat. Hazard. Earth Sys. Sci., 1, 67–96, 1988.

Papadopoulos, G. A. and Fokaefs, A.: Strong tsunamis in the Mediterranean Sea: a re-evaluation, ISET Journal of Earthquake Technology, 463(42 #4), 159–170, 2005.

Peláez Montilla, J. A., Hamdache, M., and López Casado, C.: Seismic hazard in northern Algeria using spatially smoothed sesismicity. Results for peak ground acceleration, Tectonophysics, 372, 105–119, 2003.

Rabinovitch, A. B. and Monserrat, S.: Meteorological tsunamis near the Balearic and Kuril Islands: descriptive and statistical analysis, Nat. Hazard. Earth Sys. Sci., 13, 55–90, 1996.

Rabinovich, A. B. and Monserrat, S.: Generation of Meteorological Tsunamis (Large Amplitude Seiches) Near the Balearic and Kuril Islands, Nat. Hazard. Earth Sys. Sci., 18, 27–55, 1998.

Roger, J. and Hébert, H.: Tsunami hazard in Western Mediterranean: preliminary study of scenarios for the Balearic, Eos Trans. AGU, 88(52), Fall Meet. Suppl., Abstract S53A-1009, 2007.

Roger, J. and Hébert, H.: Systematic approach of tsunami modelling in Western Mediterranean, Geophys. Res. Abstracts, 10, EGU2008-A-02141, 2008.

Rothé, J.-P.: Les séismes de Kerrata et la sismicité de l'Algérie, Bulletin du service de la carte géologique de l'Algérie, 4ème série, Géophysique, 3, 40 pp., 1950.

Ruegg, J. C., Kasser, M., Tarantola, A., Lepine, J. C., and Chouikrat, B.: Deformations associated with the El Asnam earthquake of 10 October 1980: geodetic determination of vertical and horizontal movements, Bull. Seism. Soc. Am., 72(6), 2227–2244, 1982.

Semmane, F., Campillo, M., and Cotton, F.: Fault location and source process of the Boumerdes, Algeria, earthquake inferred from geodetic and strong motion data, Geophys. Res. Lett., 32, L01305, doi:10.1029/2004GL021268, 2005.

Senarmont (De), M. H.: Analyse des documents recueillis sur les tremblements de terre ressentis en Afrique du 21 août au 15 octobre 1856, C. R. Acad. Sc., Paris, T. XLIV, 586–594, 1856.

Serpelloni, E., Vannucci, G., Pondrelli, S., Argnani, A., Casula, G., Anzidei, M., Baldi, P., and Gasperini, P.: Kinematics of the western Africa-Eurasia plate boundary from focal mechanisms and GPS data, Geophys. J. Int., 169, 1180–1200, 2007.

Seutter, M.: Carte des ïles de Maiorque, Minorque et d'Yvice gravée par Matthieu Seutter, Graveur de S.M. Imper. et Cathol., Augsbourg, 1741.

Soloviev, S. L., Solovieva, O. N., Go, Ch. N., Kim, Kh. S., and Shchetnikov, N. A.: Tsunamis in the Mediterranean Sea, 2000 B.C.–2000 A.D., Advances in Natural and Technological Hazards Research, Kluwer Academic Publishers, 260 p., 2000.

Stock, C. and Smith, E. G. C.: Evidence for different scaling of earthquake source parameters for large earthquakes depending on faulting mechanism, Geophys. J. Int., 143, 157–162, 2000.

Tinti, S., Maramai, A., and Graziani, L.: A new version of the European tsunami catalogue: updating and revision, Nat. Hazard. Earth Sys. Sci., 1, 255–262, 2001.

Wells, D. L. and Coppersmith, K. J.: New empirical relationships among magnitude, rupture length, rupture width, rupture area, and surface displacement, B. Seismol. Soc. Am., 84(4), 974–1002, 1994.

Yelles-Chaouche, A. K.: Coastal Algerian Earthquakes: a potential risk of tsunamis in western Mediterranean? Preliminary investigation, Science of Tsunami Hazards, 9(1), special issue, 47–54, 1991.

Yelles-Chaouche, A. K., Déverchère, J., Domzig, A., Mercier de Lepinay, B., Babonneau, N., Hébert, H., Roger, J., Kherroubi, A., Graindorge, D., Bracene, R., Cattaneo, A., Gaullier, V., Savoye, B., Leroy, P., and Ait Ouali, R.: The tsunami of Djijelli (Eastern Algeria) of 21–22nd August 1856: the seismotectonic context an dits modelling, XXIV Assembly of IUGG, Perugia, Italy, JSS002, 2007.

Yelles, A. K., Lammali, K., Mahsas, A., Calais, E., and Briole, P.: Coseismic deformation of the 21st May 2003, Mw = 6.8 Boumerdes earthquake, Algeria, from GPS measurements, Geophys. Res. Lett., 31, L13610, doi:10.1029/2004GL019884, 2004.

Pure appl. geophys.
DOI 10.1007/s00024-008-0433-6

© Birkhäuser Verlag, Basel, 2009

Pure and Applied Geophysics

The 1856 Tsunami of Djidjelli (Eastern Algeria): Seismotectonics, Modelling and Hazard Implications for the Algerian Coast

ABDELKARIM YELLES-CHAOUCHE,[1] JEAN ROGER,[2] JACQUES DÉVERCHÈRE,[3,4] RABAH BRACÈNE,[5] ANNE DOMZIG,[6] HELENE HÉBERT,[2] and ABDELAZIZ KHERROUBI[1]

Abstract—On August 21st and 22nd 1856, two strong earthquakes occurred off the seaport of Djidjelli, a small city of 1000 inhabitants, located 300 km east of Algiers (capital of Algeria). In relation to these two earthquakes, an important tsunami (at least one) affected the western Mediterranean region and the eastern Algerian coastline between Algiers and La Calle (Algero-Tunisian border). Based on historical information as well as on data recently collected during the Maradja 2 survey conducted in 2005 over the Algerian margin, we show that the tsunami could have been generated by the simultaneous rupture of a set of three *en echelon* faults evidenced off Djidjelli. From synthetic models, we point out that the area affected along the Algerian coast extended from Bejaia to Annaba. The maximum height of waves reached 1.5 m near the harbor of Djidjelli.

Key words: Djidjelli, Algeria, 1856 tsunami, Faults, Wave modelling, Runup.

1. Introduction

Although the Algerian margin demonstrated its ability to potentially generate hazardous tsunamis (e.g., YELLES *et al.*, 1991; SOLOVIEV *et al.*, 2000; LORITO *et al.*, 2008, and references therein) as for instance during the recent May 21, 2003 Boumerdes earthquake, little is known about the size and impact of past or future tsunami events on the western Mediterranean coasts and mainly on the Algerian coast. This could be attributed mostly to the lack of historical informations and the fact that tsunamigenic events are rare (YELLES-CHAOUCHE, 1991). Historically, although some reports mention a tsunami related to the destructive earthquake of Algiers in 1365 (IBN KHALDOUN, 1369) or to the moderate event of Gouraya of January 15, 1891 (SOLOVIEV *et al.*, 2000), the first

[1] CRAAG, Route de l'Observatoire, B.P.63, Algiers, Algeria. E-mail: a.yelles@craag.dz
[2] CEA-DASE, Bruyères-le-Châtel, 91297 Arpajon, France.
[3] Université Européenne de Bretagne, France.
[4] CNRS, UMR 6538, Domaines Océaniques, Institut Universitaire Européen de la Mer, Université de Brest, Place Copernic, 29280 Plouzané, France.
[5] Division Exploration, Sonatrach, Boumerdès, Algeria.
[6] Laboratoire de Planétologie et Géodynamique, UMR 6112, Université de Nantes, France. Now at Midland Valley Exploration, 144 West George Street, Glasgow G2 2HG.

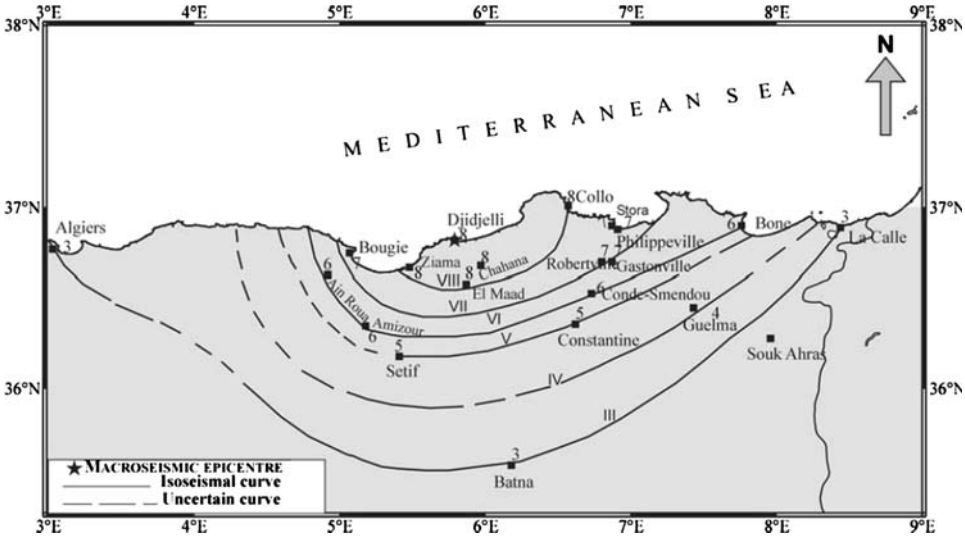

Figure 1
Isoseismal map of the Djidjelli earthquake of August 22, 1856 (I: VIII) after Harbi *et al.* (2003).

well documented event remains the Djidjelli tsunami associated with the seismic crisis of August 21–22, 1856 (Rothé, 1950; Ambraseys, 1982; Benhallou, 1985; Fig. 1).

During the instrumental period, two tsunamigenic events are evidenced as they were the first recorded by geophysical instruments. The first one occurred after the destructive El Asnam event of October 10, 1980 (M_s: 7.3; Ouyed *et al.*, 1981). Although located at a distance of about 60 km from the coast, the earthquake triggered a submarine landslide inducing a weak tsunami recorded by several tide gauge stations of southeastern Spain (Soloviev *et al.*, 1992; Papadopoulos and Fokaefs, 2005). The second tsunami, the more recent one, is the tsunami of Boumerdes of May, 21, 2003. This event, one of the most important in the western Mediterranean region within the last century, was generated by an earthquake of magnitude M_w 6.8 that occurred on the offshore reverse fault of Zemmouri (Yelles *et al.*, 2003; Alasset *et al.*, 2006). This thrust fault, with a length of about 50–55 km, is assumed to outcrop near the seafloor at about 10–15 km from the shoreline (Déverchère *et al.*, 2005). Effects of this tsunami were felt in the entire western Mediterranean region and especially along the Balearic coasts (Alasset *et al.*, 2006). The Boumerdes tsunami demonstrated for the first time the high potential of the Algerian margin for tsunami generation.

If the Algerian tsunamis are mainly related to strong earthquakes that could happen along the coastal region, landslides along the margin could also be another potential source of tsunamigenic events as discussed by some authors for the Orleansville and the El Asnam earthquakes (Ambraseys, 1982; Yelles, 1991).

The recent swath bathymetry survey, Maradja 2 survey, conducted along the eastern Algerian margin in November 2005 allowed us to map the seafloor of the region between

Dellys and Annaba by using a high resolution swath bathymetric system (Domzig, 2006) (Fig. 2a). These new bathymetric data, together with seismic sections recently carried out in the area, offer the opportunity through seafloor mapping and densification of the seismic sources, to revisit and discuss on a new basis the origin of the important historical Djidjelli tsunami event. Using numerical modelling of the tsunami waves triggered by the earthquake only, the aim of this study is to estimate and to discuss the effects of the tsunami due to the source inferred, and to compare this modelling to the available historical observations along the Algerian coast, and more particularly in the Djidjelli harbor area.

2. *The Djidjelli Earthquake of August 21 and 22, 1856*

The tsunami occurred during the French occupation of Algeria. Based on several historical archives available (newspapers, reports, etc) the seismic crisis of Djidjelli was well described by authors like Rothé (1950) and Ambraseys (1982) who reported many details on its effects on the Algerian and western Mediterranean coasts.

The Djidjelli sequence was marked by the occurrence of two main shocks, one on the night of August 21, and the second**,** more violent, on the night of August 22, 1856. The first shock, considered as a foreshock, happened at 21 h 45 mn (local time). It destroyed the old Genoese tower of the city and claimed the lives of a few people. Following the shock, Rothé (1950) and Ambraseys (1982) indicated that the sea receded for some distance and suddenly flooded the low-lying parts of the coast. Damage was equally serious in the region between Djidjelli and Collo (Fig. 1). The earthquake was felt over a large area from Algiers in the West to La Calle in the East and from Batna in the South to Nice (France) to the North. At Mahon in Minorca (Balearic Islands), the shock was followed by a rapid flooding of the harbor. As a result of it, many boats broke their moorings (Ambraseys, 1982, Soloviev, 2000).

The second shock occurred on August 22, at 11 h 40 min (local time). It was more violent than the first one and it is generally considered as the main shock. It destroyed what remained of local houses and killed few people, as the population was evacuated the day before. The shock triggered a sea wave of 2 to 3 meters high (observed at Djidjelli) that flooded the eastern Algerian coast several times. At Bougie (Bejaia) and Philippeville (Skikda), small towns located eighty kilometers west and east of Djidjelli, Ambraseys (1982) and Soloviev (2000) reported that the sea rose from about 5 meters, flooding the shore five to six times. In Bone, the sea rose by about one meter, flooding the parade grounds in a succession of waves that continued for twelve hours. These authors also reported that the shock was felt at Cagliari (Island of Sardinia) and Caloforte (Island of S. Pietro) as well as at Mahon in Spain. There the shock was less intense than that of the previous day but it was stronger in Nice and in Genoa in Italy.

Considering all these pieces of information and on the basis of the isoseismal map (Fig. 1), the earthquake was located a few kilometers offshore of Djidjelli, with an

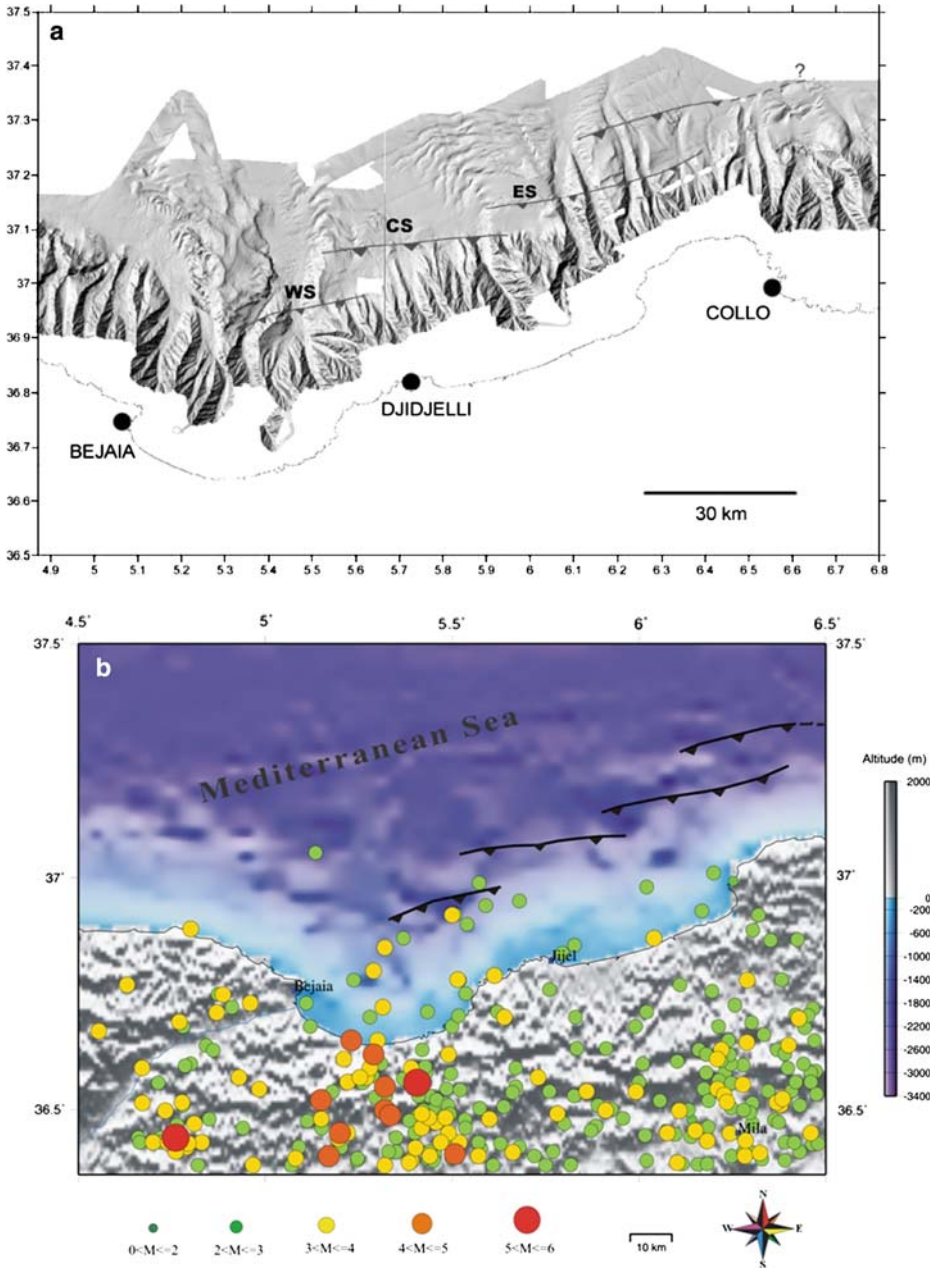

Figure 2

(a) Bathymetry offshore of Djidjelli with the four overlapping structures assumed active (Domzig, 2006). The three faults named WS (West Segment), CS (Central Segment), and ES (East Segment) are used in this study because they are thought to be at the origin of the 21 and 22 August, 1856 earthquakes and associated tsunamis (see text for details). (b) Recent seismic activity off Djidjelli (1980–2007 period, from CRAAG seismic catalogues).

estimated maximum intensity of VIII. Papadopoulos and Foakefs (2005) estimate that the tsunami intensity of 21 August 1856 was equal to 3 on the 6-point tsunami intensity scale and 5 on the 12-point scale. This places this particular tsunami among the significant ones observed in the Mediterranean Sea in the last two centuries.

3. *Physiography of the Margin off Djidjelli*

Off the coast of Djidjelli, the bathymetric map has been obtained from the Maradja 2 survey data (Fig. 2a). This survey was conducted in November 2005 on the French R/V Suroit and aimed firstly at obtaining a precise bathymetric map of the structures between Dellys and Annaba (eastern Algeria). For this purpose, a Kongsberg EM300 Simrad multibeam echosounder (EM 1000 for the continental shelf) for bathymetry and reflectivity was used. Simrad EM300 is a 32-kHz multibeam system which allows for an overall swath coverage up to 5 times water depth, increasing with depth to a maximum width of 5000 m at 1000 m depth. The reached resolution was of 15 $\times$ 35 m at 1000 m depth with a vertical accuracy from 2 m (central beam) to 10 m (lateral beam).

The survey was limited to the continental slope and part of the deep basin (Domzig, 2006). Between Bejaia and Collo, the margin is marked by a narrow shelf and a steep slope in front of the massif of Lesser Kabylia. The continental shelf disappears totally near Collo. In the bay of Bejaia, the slope is outlined by two main canyons with a N-S direction (Fig. 2a). They correspond to the marine extension of the Soummam River (Domzig, 2006). Further east, between Djidjelli and Collo, the slope of the margin is incised by several canyons. Off Djidjelli, these canyons are short whereas off Collo they extend down to the abyssal plain. According to the bathymetric map (Fig. 2a), the deep basin depicts a series of elongated ridges that can be interpreted as sediment waves or contourites developing at the foot of the slope. However, several linear topographic anomalies that can hardly be due to sedimentary processes only are also observed at the foot of the slope and upslope. They present a general NE-SW to E-W strike as presented in Figure 2a.

4. *Seismotectonics of the Djidjelli Margin*

Northern Algeria lies along the Eurasian-African plate boundary. With an average rate of about 5 mm/yr in a N 60°W, the convergence between the two main plates is responsible for the seismic activity which affects Algeria. Seismicity on land is generated by active faults oriented mostly NE-SW, located along the Atlasic mountains and the Neogene basins. Strong earthquakes could occur in the northern region, as the last one of Boumerdes of May 21, 2003. For a long time, offshore seismicity remained poorly known due to the lack of investigations along the margin.

In the Djidjelli region, the seismic activity deduced from historical catalogs (Mokrane *et al.*, 1994; Benouar, 1994) seems to be low with an activity mostly focused

along the southern suture between the internal and external domains. Nevertheless, since the recent installation of the Algerian Digital Seismic Network by the CRAAG (Centre de Recherche en Astronomie, Astrophysique et Géophysique), many seismic events were recorded recently along the coastline between Bejaia and Djidjelli. An updated seismic map of the region of Djidjelli (Fig. 2b) shows activity in proximity to the four scarp segments reported hereafter, which favors possible activity of these faults, and therefore, their ability to generate tsunamis.

From the analysis of the seismic lines carried out during the Maradja survey and of Sonatrach (Algerian Oil Company) commercial seismic lines (see location on Fig. 3a), cross sections along the margin in the region of Djidjelli were obtained. We observe that the central part of the margin is uplifted (Figs. 3b and c), whereas the lower slope is dominated by low-angle normal faults and slides rooted at the base of the Messinian salt layer (Fig. 3c). By correlating the bathymetry and the seismic lines, we find that uplifts are related to reverse faulting near the slope break or below the lower slope, although the geometry of thrusts is hardly visible (Figs. 3b and c). Thereafter, we could identify four *en echelon* segments, widely overlapping, which can be followed near the foot of the slope or in the lower slope (Fig. 2a). In front of Djidjelli, a first segment (named west segment) oriented NE-SW (N 75°E) has a surface extent of $\sim$25 km. This is a thrust fault related to an asymmetrical fold which produces the growth of a basin on its backlimb that is tilted towards the continent (Fig. 3b). The second one (named central segment) is observed north of the City of Djidjelli. This segment, about 30 km far from the coast is apparently slightly longer than the previous one ($\sim$35 km). This reverse fault striking N85°E is also related to another asymmetrical fold. Finally, two other scarps, with apparent lengths of $\sim$40–45 km and $\sim$30 km, are found northwest of Collo City. Among these two segments, the one located in the deep basin and striking N 80° is not clearly related to a deeper fault activity and could only result from salt tectonics; a process quite well identified in the eastern part of the studied area (Fig. 3c). We will therefore consider in the following only the segment located upslope and designate it east segment. Note that this segmentation pattern of the fault zone with similar lengths has also been observed during the May 21, 2003 Boumerdes earthquake rupture: Indeed, two main slip zones have been identified from a joint inversion of seismological waveforms and ground displacement observations (Delouis *et al.*, 2004) which are interpreted as being related to the two main cumulative scarps evidenced at the sea floor (Déverchère *et al.*, 2005).

Then, from bathymetric maps and seismic lines, the main characteristics of these three fault segments (length, width, depth) are determined (Table 1). It is worth to note that these parameters are only mean values deduced from the combination of observations made on bathymetry, seismic sections, and assumptions deduced from literature. Uncertainties remain, especially for strike and dip of faults that cannot be accurately determined from the available data set, since there is no means to directly describe the geometry of faults at depth and their spatial continuity.

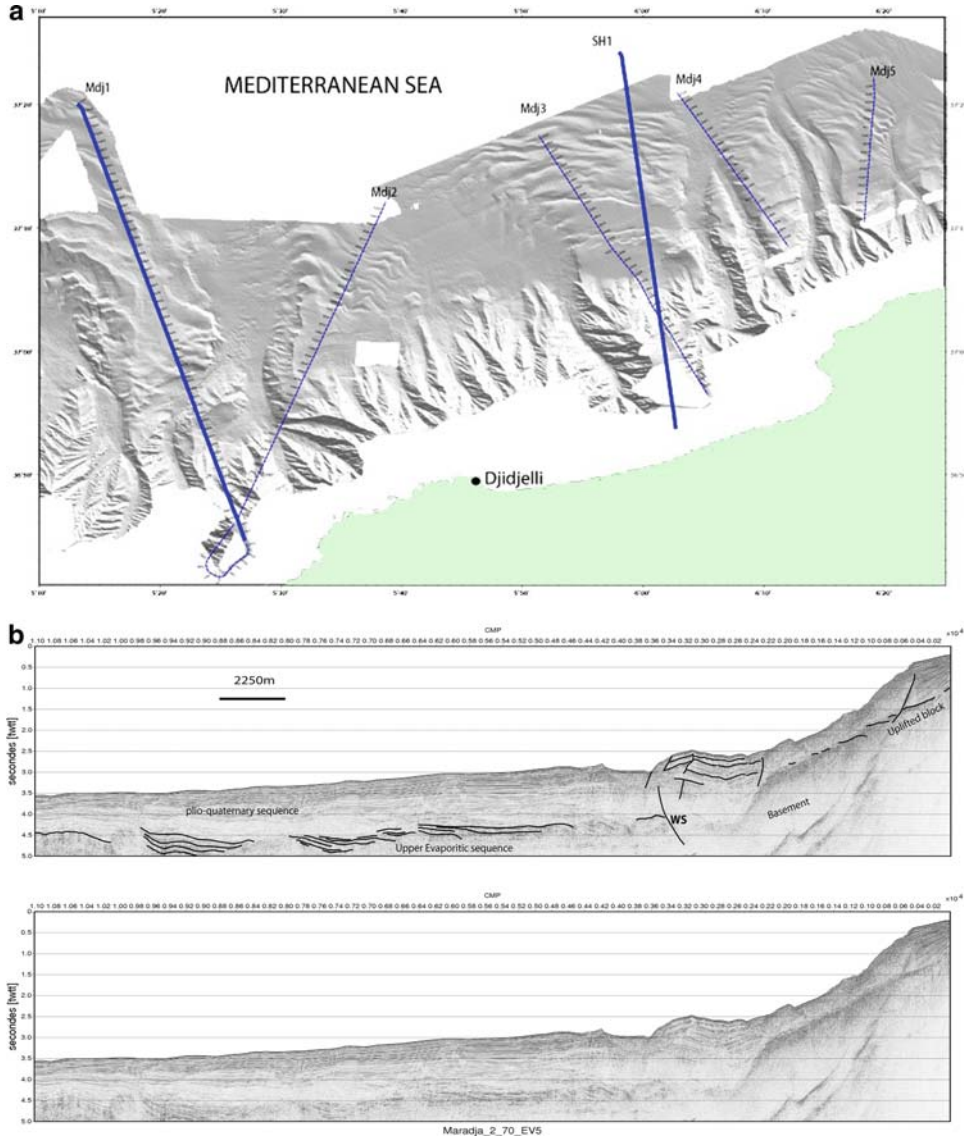

Figure 3

(a) Location map of the bathymetry with seismic lines shot during the Maradja 2 survey. Bold lines are the location of the seismic lines shown. One line from the industry (SH1) (dark line) is also plotted; (b): Seismic profile MDJ1 (in two-way travel time, TwT) across the West Segment WS (Fig. 2a) – Black line depicts the inferred position of WS according to the deposition pattern (growth strata) near the surface; (c): Processed commercial seismic section SH1 (480-channel, stacked and migrated) across the margin off Djidjelli and crosscutting the Eastern Segment ES (see location Fig. 2a). For (b) and (c) the upper one is the interpreted line, the lower one is the raw data.

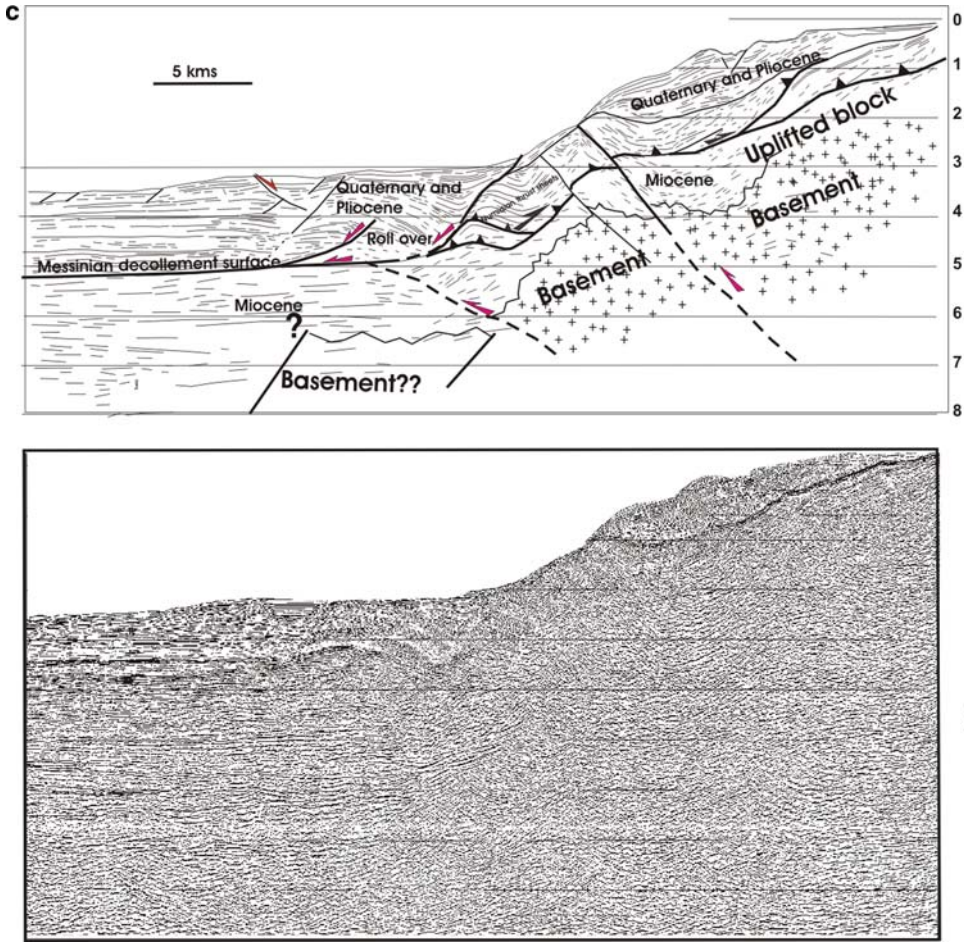

Figure 3
contd.

Table 1

	Longitude (°)	Latitude (°)	Center of fault plane deep (km)	Slip (m)	Strike (°)	Dip (°)	Rake (°)	Half length (m)	Width (m)	Shear modulus (Pa) = rigidity
West	5.4764	36.95	10	1.0	75	40	90	12500	20000	$4{,}5*10^{10}$
Center	5.736	37.0791	10	1.5	85	40	90	18500	20000	$4{,}5*10^{10}$
East	6.15	37.1784	10	1.5	75	40	90	22000	20000	$4{,}5*10^{10}$

Finally, we note that the overall length of the three segments considered here is about 100–105 km. According to Wells and Coppersmith law (1994), this value is consistent with the approximate magnitude inferred for the 1856 earthquake sequence from the isoseismal map, i.e., $7^{1/2}$ (Fig. 1; Harbi *et al.*, 2003, and references therein). Therefore, considering their effects at the surface, their apparent connection to deformed areas at depth (see e.g., Figs. 3b and c) and the consistency of cumulative length with the magnitude hypothesized, we assume that these segments, which are distributed as *en échelon* faults, could be (for at least two of them) responsible for the Djidjelli events of August 1856 (Yelles *et al.*, 2007; Roger and Hébert, 2008). Subsequently we propose to take into account these three western segments in order to model the tsunami of August 21–22, 1856, and we combine them in order to determine a range of possible triggering effects.

5. *Modelling of the Tsunami*

5.1. *Method*

For the generation of the tsunami wave, the coseismic deformation corresponds to an elastic dislocation model which involves the vertical deformation of the seafloor in the epicentral area as a function of the ground elastic parameters and the fault plane geometry (Okada, 1985). The different parameters used are also related to each other by the seismic moment relation: $\mathbf{M_0 = \mu ULW}$ (Aki, 1966), where $\boldsymbol{\mu}$ is the rigidity constant, $\mathbf{U}$ the average slip in the fault, and $\mathbf{L}$ and $\mathbf{W}$ the length and width of the fault plane, respectively.

In order to model the propagation of the sea waves, we use the depth averaged, nonlinear hydrodynamical equations of continuity (1) and motion (2) conservation describing the conservation of mass and momentum:

$$\frac{\partial(\acute{\eta} \pm h)}{\partial t} + \nabla \cdot [v(\acute{\eta} + h)] = 0 \tag{1}$$

$$\frac{\partial v}{\partial t,} + (v \cdot \nabla)v = -g\nabla\acute{\eta} + \Sigma f \tag{2}$$

where $\mathbf{h}$ is the water depth, $\acute{\boldsymbol{\eta}}$ the water elevation above mean sea level, $\mathbf{v}$ the depth-averaged horizontal velocity vector, $\mathbf{g}$ the acceleration of gravity and $\mathbf{f}$ the bottom friction and Coriolis forces. Thus nonlinear terms are taken into account, and the resolution is carried out using a Crank Nicolson finite-difference method centered in time and using an upwind scheme in space.

Amplification of the sea waves from the seafloor are based on the use of the available bathymetric data. In this study we use the GEBCO world bathymetric dataset (British Oceanographic Data Centre, 1997) mixed with the Maradja 2 data (200 m resolution)

along the eastern Algerian margin. Near the coast and due to the lack of swath bathymetry coverage of the continental shelf where the depth is less than 200 meters (a band of about 5 miles wide) digitized bathymetric maps from LECLAIRE (1972) were used.

On the other hand and in order to be complementary from other studies related to tsunamis in the western Mediterranean region (LORITO *et al.*, 2008; ROGER and HÉBERT, 2008), we choose to focus our study on the impact of the tsunami along the Algerian coastline and more specifically in Djidjelli. Figure 4 depicts the topography of the region of Djidjelli. The city is located along the coastline, at the foot of the Lesser Kabylian massif. This particular location could influence the runup on land, by stopping invasion of the water on the continent. One can also note that the present-day configuration of the lower part of the city with the old and new port of Djendjen (suburb of Djidjelli) is very different from the one of August 1856. Indeed, the harbor of the city, situated in the western part of the Djidjelli bay, depicts structures that directly develop over the seafloor

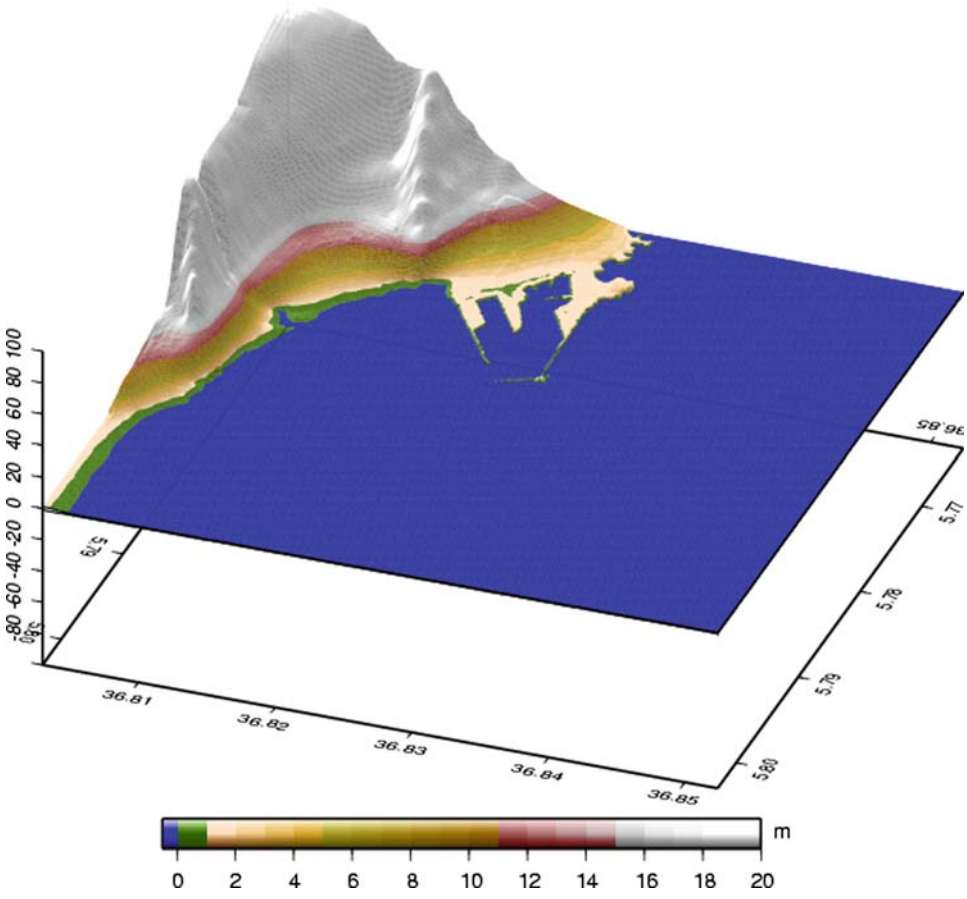

Figure 4
Topographic map on land in the region of Djidjelli.

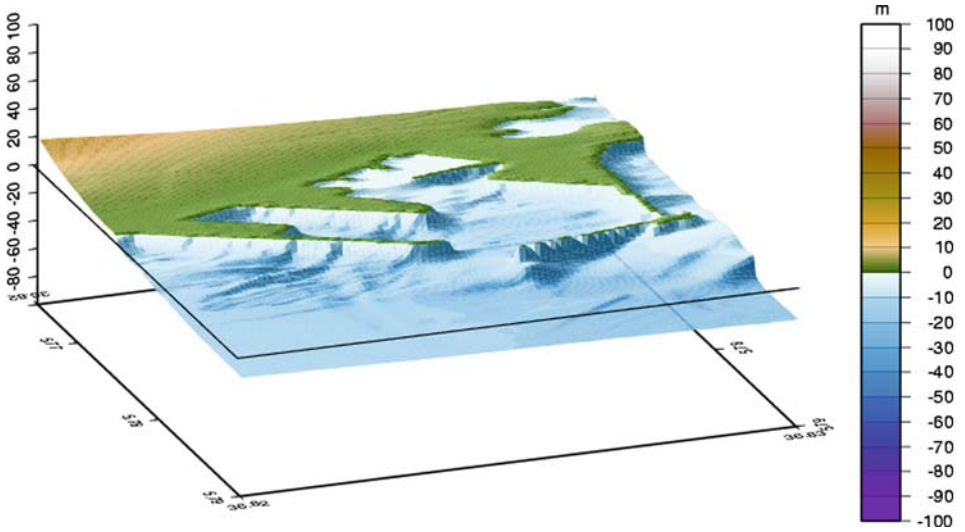

Figure 5
Submarine topography off the Djidjelli harbor.

(Fig. 5). Unfortunately, it was not possible to obtain topographic data of the new Djendjen harbor built in the 1990s. These structures could therefore play a role in the sea-wave propagation and amplification and seem to constitute a protection for the City of Djidjelli thanks to its long piers.

To set up our modelling, we created a set of three imbricated grids, the first one containing the sources with a resolution of 200 m; the second one being a zoom on the Djidjelli bay area with a resolution of 50 m; and the last one a zoom on the Djidjelli harbor with a resolution of 10 m (Figs. 4 and 5). Each grid has been built using krigging interpolation in order to unify the data coming from different origins. The last grid has been created from a combination of the previous cited data and from georeferencing and manual digitizing of a nautical bathymetric chart of the Djidjelli harbour with the same method as proposed by ROGER and HÉBERT (2008). Finally, the resolution of the bathymetric data increases from the abyssal region to the coast from a grid to another one, which is in direct relation with the slowdown of the waves and their amplification as they approach the coastline.

5.2. *Tested Seismic Sources*

In order to reproduce the tsunamis inferred by the two earthquakes, we tested several seismic sources in relation with the *en echelon* fault system evidenced by DOMZIG (2006) and further detailed in this study (Fig. 3). Different combinations of one fault, two or three faults (Fig. 6) were introduced in the model. As explained above, the fourth segment (the most eastern one) is apparently not related to an active fault and was not considered.

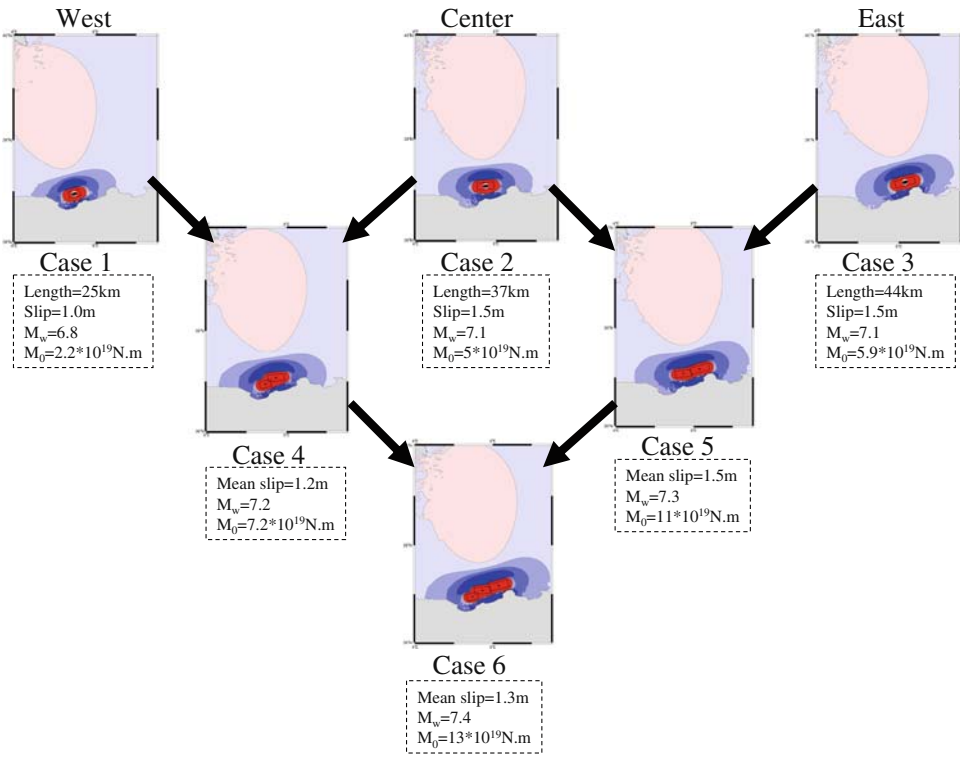

Figure 6
Initial deformation and location or assumed fault planes (black rectangle). Six models are proposed due to the complexity of the rupture and due to the presence of three active faults. The upper line is for each segment. The middle one corresponds to the combination of two segments. The lower model is the combination of the effects of the three segments.

Each hypothesis leads to a maximum earthquake magnitude (Fig. 6). In Table 1, we summarize the parameters chosen for the three main fault segments (West, Central and East) possibly involved in the rupture and the tsunami process. From the bathymetry and seismic lines, the strike, length, and width of the faults are estimated. The existence of some uncertainties discussed above on the different parameters (strike and length essentially) of these segments makes these tests only indicative. The main magnitude range expected is from 6.8 for the western segment to 7.4 for the combination of the three segments. This latter value is in agreement with the magnitude that can be assumed from the damage reported after the two earthquakes of 1856 (Rothé, 1950; Ambraseys, 1982).

5.3. Maximum Amplitude of the Sea Waves for Historical Sites

Based on a selection of several sites on the Algerian coastline and the Balearic Islands, we plot on Figure 7 the maximum sea-wave amplitudes in several places affected

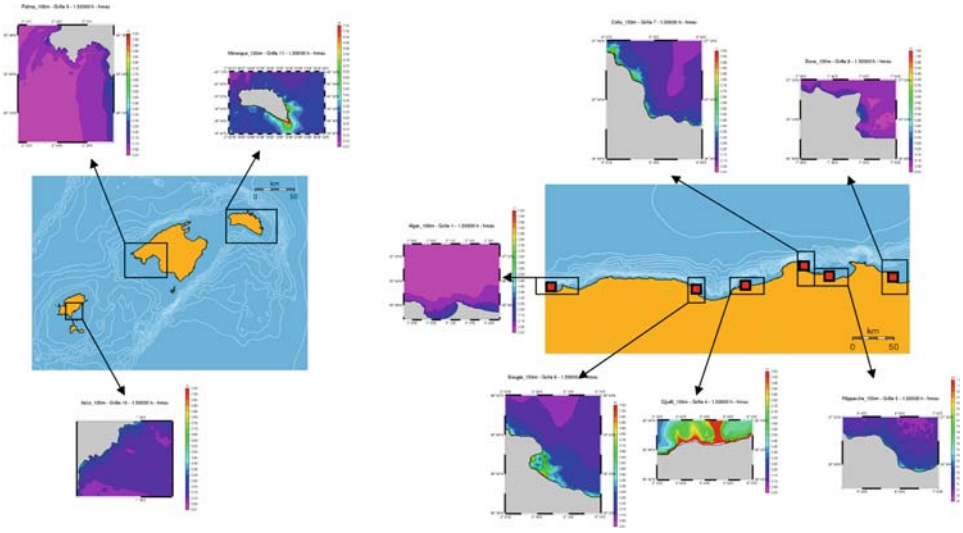

Figure 7
Maximum wave calculated amplitude for historical observations sites. This result is obtained from the combination of the three segments (case 6) and after a time propagation of 5400 s.

by the tsunami. We observe first, that in the Balearic Islands, some sites where the waves arrived an hour after the earthquake are more affected than others (ROGER and HÉBERT, 2008). The maximum is observed in the Minorca Island where the height reached 1.5 m at the southeastern point of the Island. This could be explained by the exposure of the sites to the sea wave propagation and also by the seafloor topography (HÉBERT *et al.*, 2007; ROGER and HÉBERT, 2007, 2008).

Secondly six sites were selected between Algiers in the west and Annaba in the east along the Algerian coastline. The maximum amplitude of the sea waves is measured near Djidjelli and Bejaia. Thus, in this region the maximum sea wave amplitude reaches respectively 1.5 m between 5° 42 E and 6° E. In Bejaia City the height does not exceed one meter. From Figure 7, one can see that on the Algerian coastline, the influence of the tsunami does not extend further than Algiers to the West and Annaba to the East. From our model, one can consider that the maximum energy of the tsunami dissipates more easily towards the North than laterally, indicating that the majority of exposed areas are located southward and northward of the seismic sources.

In order to measure the flooding of the lower part of the city of Djidjelli, a map of the zones invaded by the sea is proposed. Figure 8 shows a first attempt to quantify the maximum wave height and flooding limits in the Djidjelli coastline area. It is obtained by using the model of the three seismic sources with a maximum magnitude of $M_w = 7.4$. On this map we can see that the eastern part of the city is the most affected area, and that the runup may reach a height of 1.5 m. However, the use of our model does not allow us to reach runup values higher than two meters, whereas historical observations locally

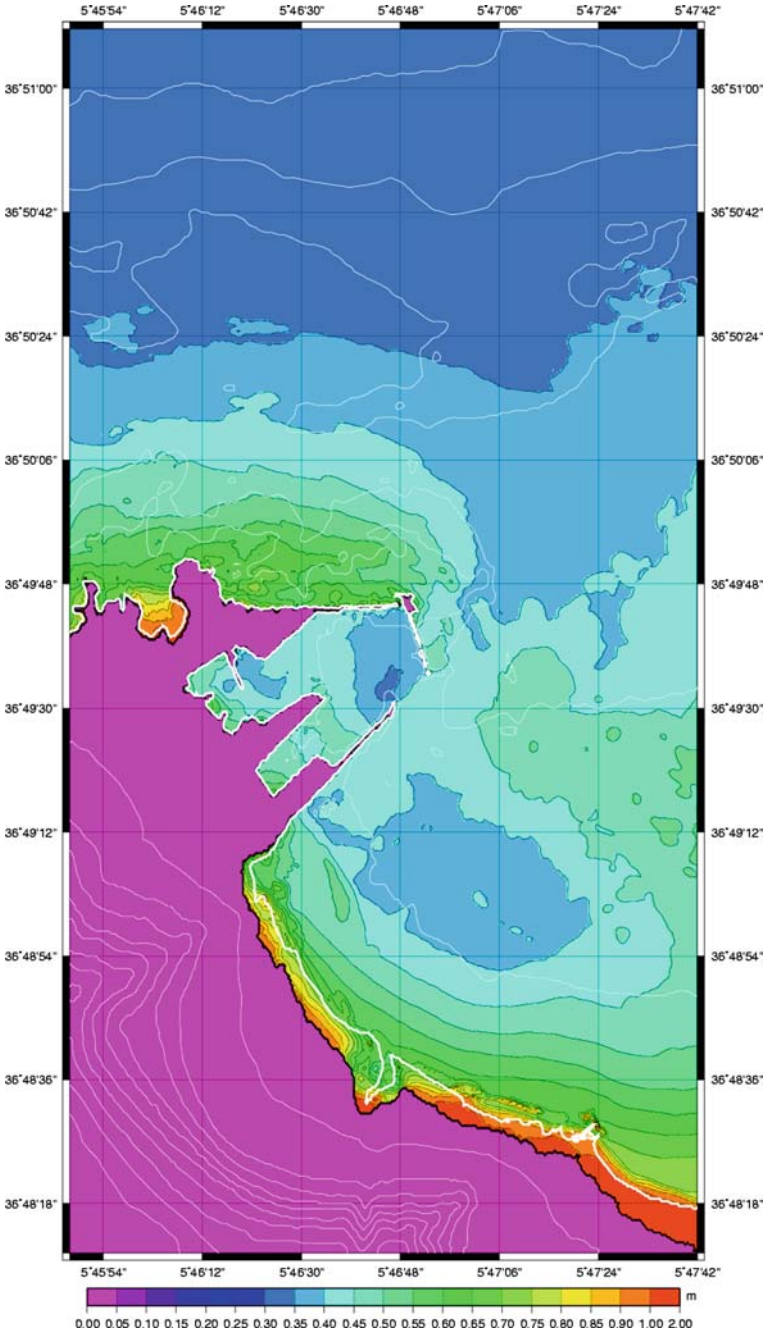

Figure 8

Maximum wave heights for a propagation of 30 minutes for the three segments source over bathy/topo grid (10 m each line). The blank line is the actual coastline of the city of Djidjelli. The dark line corresponds to the flooding limit area (runup).

provide values of more than 4 meters. This discrepancy could be attributed to the inaccuracy of the values reported by the observers at that time or to the poor bathymetric coverage near the shoreline, preventing us from predicting local wave amplifications. We also note that no flooding is evidenced in the western part of the city near the harbor, therefore the harbor with its present-day structure could play the role of a barrier to protect the old city.

6. *Discussion and Concluding Remarks*

The Djidjelli tsunami of August 1856 could be considered as one of the significant events in the Mediterranean region. Indeed, this is one of the well described tsunamigenic events which took place in the western Mediterranean region during the 19th century. Numerous observations on the impact of this event are available in literature, newspapers or reports. However, no attempt was made until now to explore the possible range of coastal impact of such an event, mainly because of the lack of knowledge related to the source of the event and regarding the bathymetry of the area. The Maradja 2 cruise conducted in 2005 is the first modern bathymetric survey carried out along the eastern margin and offers the opportunity to make a first approach of the implications of this active faulting occurring offshore. Based on the data collected during this survey and on a deep seismic section from the industry, the possible seismic sources of the Djidjelli tsunami (Algeria) of August 21 and 22 are hypothesized, and the possible triggered tsunami is presented. The *en echelon* pattern of the faults (3 segments) that have been identified for the first time near the foot of the margin expresses the deformation process of the margin as observed in other regions of the margin recently studied as Boumerdes or Annaba (Déverchère *et al.*, 2005; Domzig, 2006; Kherroubi *et al.*, in press). This set of faults with an NE-SW or E-W direction is in agreement with the deformation pattern on land (Meghraoui, 1988) which results from the slow convergence of the African and Eurasian plates with an estimate rate of about 0.5–0.7 cm/yr (De Mets, 1990). In accordance with literature, which mentioned two main shocks and many series of waves, we propose that the western fault segment (WS, Fig. 2) may have ruptured first, followed by the rupture of one or two other fault segments (CS and/or ES, Fig. 2) located further east. Despite the complexity of the rupture process, we propose that the use of the model with the involvement of the three segments is the more realistic scenario.

Based on the historical information on the area affected by the tsunami, our work proposes several sea-wave propagation scenarios, trying to reach the best fit to the historical observations. The tsunami affected mainly the eastern Algerian coast and the coast of the Balearic Islands. We would like to emphasize that, because of the proximity of the epicenter from the shoreline, all the tested sources gave the same effects in the harbor area. The discrepancy of sea-wave predictions with the historical observations could be explained by several factors, such the poor bathymetry coverage near the shore, which do not allow the creation of a very realistic bathymetric map for modelling.

Furthermore, we must mention the lack of precise temporal information on the arrival times of the tsunami on the Algerian and Balearic coasts. Indeed, the available archives do not report any approximate time delay between the earthquake and the sea-wave arrival on the coast. This could be related to the time occurrence of the first earthquake which struck in the evening and to the induced panic. Therefore, more temporal investigations of these data will be necessary to precisely determine the propagation of the tsunami.

In spite of our effort to build a realistic grid for the harbor with respect to the structures as piers, docks, etc. for the Algerian coast, the lack of very precise bathymetry as approaching the coast and especially in harbors prevents us from better knowing the role of the bathymetric structures, as submarine canyons for example, near the shore, on the wave amplification. Future bathymetric surveys on the Algerian continental shelf will allow to refine the runup model. Whatsoever, the occurrence of the Djidjelli tsunami indicates that waves of some meters could reach the different coastlines of the western Mediterranean region. Lorito *et al.* (2008) also demonstrate that the coastal area of Djidjelli could be affected by tsunamis triggered in the Sicily channel.

The tsunami hazard in Algeria became more obvious by the occurrence of the last Boumerdes tsunami of May 2003, also evidencing that the Algerian margin hosts several important active tsunamigenic faults that can cause damage on both parts of the western Mediterranean Sea. The acquisition of the recent data through the Maradja 1 and 2 surveys along the margin will allow us to re-assess the tsunamigenic hazard in Algeria, poorly constrained in the past owing to the lack of accurate and up-to-date surveys in this region.

Acknowledgments

We thank reviewers G.A. Papadopoulos and A.C. Yalciner for useful advice which enhanced clarification and improve the content and presentation of this paper. This work is a contribution to ANR (Agence Nationale de la Recherche) Projects ISIS and DANACOR (CATTELL: « Catastrophes telluriques et tsunamis » Programme, France). We have benefited from exchanges in the frame of the TASSILI CMEP (Comité Mixte d'Evaluation et de Prospective de la coopération scientifique franco-algérienne) Programme number 014MDU619.

References

Aki, K. (1966), *Generation and propagation of G-waves from the Nigata earthquake of June 16, 1964, Part 2: Estimation of earthquake moment, released energy, and stress-strain drop from the G wave spectrum*, Bull. Earthquake Res. Inst. Tokyo, Univ. *44*, 73–88.

Alasset, J.P., Hébert, H., Maouche, S., Calbini, V., and Meghraoui, M. (2006), *The tsunami induced by the 2003 Zemmouri earthquake (M_w: 6.9, Algeria): Modelling and results,* Geophys, J. Int., doi:10.111/j.1365-246X.

Ambraseys, N.N. (1982), *The seismicity of North Africa: the earthquake of 1856 at Jijelli, Algeria*, Bollettino Di Geofisica a Teoritica ed Applicata, XXIV, *93*, 31–17.

Benhallou, H. (1985), *Les catastrophes sismiques de la région d'Echelif dans le contexte de la sismicité historique de l'Algèrie*. Thèse d'Etat. USTHB. Alger, 294 p.

Benouar, D. (1994), *The seismicity of Algeria and the Maghreb during the twentieth century*, Ph.D. dissertation, Imperial College London, U.K.

British Oceanographic Data Centre (1997) *The Centenary Edition of the Gebco Digital Atlas,* Liverpool, U. K.

Delouis, B., Vallee, M., Meghraoui, M., Calais, E., Maouche, S., Lammali, K., Mahsas, A., Briole, P., Benhamouda, F. and Yelles, K. (2004), *Slip distribution of the 2003 Boumerdes Zemmouri earthquake Algeria from teleseismic, GPS and coastal uplift data*, Geophys. Res. Lett. *31*, L18607, doi 10 1029/2004 GL020687.

De Mets, C., Gordon, R., Argus, D.F., and Stein, S.(1990), *Current plate motions*, Geophys. J. Int. *101*, 425–478.

Déverchère, J., Yelles, K., Domzig, A., Mercier De Lépinay, B., Bouillin, J.-P., Gaullier, V., Bracène, R., Calais, E., Savoye, B., Kherroubi, A., Le Roy, P., Pauc, H., and Dan, G. (2005), *Active thrust faulting offshore Boumerdes, Algeria, and its relations to the 2003 M_w 6.9 earthquake*, Geophys. Res. Lett. *32*:L04311, doi:10.1029/2004GL021646.

Domzig, A. (2006), *Déformation active et récente et structuration tectono-sédimentaire de la marge sous marine algérienne*, Ph.D. Thesis, UBO-IUEM, Brest, France, 332 pp.

Harbi, A., Benouar, D., and Benhallou, H. (2003), *Re-appraisal of seismicity and seismotectonics in the north-eastern Algeria. Part I: Review of historical seismicity*, J. Seismol. *7*, 115–136.

Hebert, H., Roger, J., and Schindele, F. (2007), *Advances in tsunami hazard assessment in the western Mediterranean sea,* Geophys. Res. Abstracts, *9*, 06341, EGU Vienna, 15–20 April 2007.

Ibn Khaldoun, A.Z.Y. (1369), *Kitab al-Ibar*, edited in 1959, Maison du Livre Libanais, Beyrut.

Kherroubi, A., Deverchere, J., Yelles, K., Mercier Lepinay, B., Domzig, A., Cattaneo, A., Bracene, R., Gaullier, V. and Graindorge, D., *Recent and active deformation pattern off the easternmost Algerian margin: New evidence for tectonic reactivation*, Marine Geology, in press.

Leclaire, L. (1972), *La sédimentation holocène sur le versant méridional du bassin algéro-baléare (précontinent algérien)*, Mém. Mus. Nat. Hist. Nat. Paris, Nouv. Serv., C.24, 391 p.

Lorito, S., Tiberti, M.M., Basili, R., Piatanesi, A., and Valensise, G. (2008), *Earthquake-generated tsunamis in the Mediterranean Sea: Scenarios of potential threats to Southern Italy*, J. Geophys. Res., *113*, B01301, doi:10.1029/2007JB004943.

Meghraoui, M. (1988), *Géologie des zones sismiques du nord de l'Algérie: Paléosismologie, Tectonique active et Synthèse Sismotectonique*, Thèse de Doctorat es Science, U. de Paris XI, France, 356 pp.

Mokrane, A., Ait Messaoud, A., Sebai, A., Menia, N., Ayadi, A., and Bezzeghoud, M. (1994), *Les seîsmes en Algérie de 1365 à 1992*, Publication CRAAG.

Ouyed, M., Meghraoui, M., Cisternas, A., Deschamps, A., Dorel, J., Frechet J., Gaulon, R., Hatzfeld, D., and Phillip, H. (1981), *Seismotectonics of the El Asnam earthquake*, Nature *292*, 26–31.

Okada, E.A. (1985), *Surface deformation due to shear and tensile faults in a half-space*, Bull. Seismol. Soc. Am. *75*, 1135–1154.

Papadopoulos, G.A. and Fokaefs, A. (2005), *Strong tsunamis in the Mediterranean Sea: A re-evaluation,* ISET J. of Earthq. Technol. *42*, 159–170.

Roger, J. and Hebert, H. (2007), *Tsunami hazard in western Mediterranean: Preliminary study of scenarios for the Balearic*, EOS Trans. AGU, *88*(52), Fall Meet. Suppl., Abstract S53A–1009.

Roger, J. and Hebert, H. (2008), *The 1856 Djidjelli (Algeria) earthquake and tsunami: Source parameters and implications for tsunami hazard in the Balearic Islands*, Natural. Hazards Earth Syst. Sci., *8*, 721–731.

Rothe, J.P. (1950), *Les seîsmes de Kerrata et la seîsmicité de l'Algérie*, Bull. Serv. Carte Geol. Algérie, Série *4*, 3.

Soloviev, S.L., Campos-romero, M.L., and Plink, N.L. (1992), *Orleansville tsunami of 1954 and El Asnam tsunami of 1980 in the Alboran Sea (Southwestern Mediterranean Sea)*, Izvestiya, Earth Phys. *28*(9), 739–760.

Soloviev, S.L., Solovieva, O.N., Go, C.N., Kim, K.S., and Shchetnikov, N.A., *Tsunamis in the Mediterranean Sea 2000 B.C.-2000 A.D: Advances in Natural and Technological Hazards Research* (Kluwer Publications 2007). Vol. 13, 237 pp.

WELLS, D.L. and COPPERSMITH, K.J. (1994), *New empirical relationships among magnitude, rupture length, rupture width, rupture area, and surface displacement,* Bull. the Seismol. Soci. Am. *84*(4), 974–1002.

YELLES-CHAOUCHE, A.K. (1991), *Coastal Algerian earthquakes. A potential risk of tsunamis in Western Mediterranean? Preliminary investigations*, Science Tsunami Hazards, *9*(1), 47–54.

YELLES-CHAOUCHE, A.K., DJELLIT, H., and HAMDACHE, M. (2003), *The Boumerdes Algiers (Algeria) earthquake of May, 21, 2003 (M_w: 6.8)*, CSEM Lett., *20*, 1–3.

YELLES-CHAOUCHE, A.K., DEVERCHERE, J., DOMZIG, A., MERCIER DE LEPINAY, B., BABONNEAU, N., HEBERT, H., ROGER, J., KHERROUBI, A., GRAINDORGE, D., BRACENE, R., CATTANEO, A., GAULLIER, V., SAVOYE, B., LEROY, P., and AIT OUALI, R. (2007), *The tsunami of Djidjelli (eastern Algeria) of August 21–22, 1856: The seismotectonic context and its modelling*, IUGG Meeting, Perugia, Italy, 2–13 July 2007.

(Received February 2, 2008, revised September 17, 2008)

To access this journal online:
www.birkhauser.ch/pageoph

Geophysical Journal International

Geophys. J. Int. (2011) doi: 10.1111/j.1365-246X.2011.05003.x

The El Asnam 1980 October 10 inland earthquake: a new hypothesis of tsunami generation

J. Roger,[1,2] H. Hébert,[2] J.-C. Ruegg[3] and P. Briole[1]

[1] *Ecole Normale Supérieure, Laboratoire de Géologie, UMR* 8538, 24, *rue Lhomond,* 75231 *Paris, CEDEX* 5, *France. E-mail: jeanrog@hotmail.fr*
[2] *CEA, DAM, DIF,* F-91297 *Arpajon, France*
[3] *Institut de Physique du Globe de Paris, laboratoire de Sismologie,* 4 *place Jussieu,* 75252 *Paris, CEDEX* 5, *France*

Accepted 2011 February 25. Received 2011 February 25; in original form 2010 August 5

SUMMARY

The Western Mediterranean Sea is not considered as a high seismic region. Only several earthquakes with magnitude above five occur each year and only a handful have consequences on human beings and infrastructure.

The El Asnam (Algeria) earthquake of 1980 October 10 with an estimated magnitude $M_s = 7.3$ is one of the most destructive earthquakes recorded in northern Africa and more largely in the Western Mediterranean Basin. Although it is located inland, it is known to have been followed by a small tsunami recorded on several tide gauges along the southeastern Spanish Coast. In 1954, a similar earthquake having occurred at the same location induced a turbidity current associated to a submarine landslide, which is widely known to have cut submarine phone cables far from the coast. This event was followed by a small tsunami attributed to the landslide. Thus the origin of the tsunami of 1980 was promptly attributed to the same kind of submarine slide. As no evidence of such mass movement was highlighted, and because the tsunami wave periods does not match with a landslide origin in both cases (1954 and 1980), this study considers two rupture scenarios, that the coseismic deformation itself (of about 10 cm off the Algerian coast near Ténès) is sufficient to produce a low amplitude (several centimetres) tsunami able to reach the Spanish southeastern coast from Alicante to Algeciras (Gibraltar strait to the west).

After a discussion concerning the proposed rupture scenarios and their respective parameters, numerical tsunami modelling is performed on a set of bathymetric grids. Then the results of wave propagation and amplification (maximum wave height maps) are discussed, with a special attention to Alicante (Spain) Harbour where the location of two historical tide gauges allows the comparison between synthetic mareograms and historical records showing sufficient signal amplitude.

This study is part of the active tsunami hazard assessment in Mediterranean Sea especially concerning its occidental part, that is, the Algerian, Spanish and French coasts.

Keywords: Tsunamis; Seismicity and tectonics; Continental margins: convergent; Fractures and faults; Africa; Europe.

1 INTRODUCTION

1.1 Generalities

Although the Western Mediterranean Sea does not have such active margins as the Eastern Mediterranean Sea (subduction under southern Italy and Greece), it is subject to low to moderate seismicity ($M_w < 7.3$) mainly located in northern Africa, along the Algerian Margin and in the Alboran Sea. There is no general trend concerning the rupture mechanisms along this margin as it goes from pure compressive movement at the east (northern Italy/Tunisia/Algeria to a pure strike-slip trend in Alboran Sea to the west.

We present a study of the tsunami associated with the 1980 October 10 El Asnam earthquake ($M_s = 7.3$), which is the largest shallow event in the Western Mediterranean area during the 20th century. The epicentre has been estimated 45 km to the south of the Algerian shores of the Mediterranean Sea (Solovyev *et al.* 1992) in the same region of the 1954 Orléansville (renamed afterwards El Asnam) earthquake ($M_s = 6.7$, Rothé 1955). It is historically known that these two earthquakes have been followed by some sea level variations recorded on tide gauges located along the Spanish southeastern coast from Alicante to Algeciras (Gibraltar Strait). There are at least six tide gauge records available concerning the 1980 event. The tsunami was supposed to be generated by a

© 2011 The Authors
Geophysical Journal International © 2011 RAS

submarine turbidity current in both 1980 and 1954. The originality of this paper is that we propose that the tsunami may have been directly induced by the coseismic deformation of the earthquake without the need of submarine slide (not revealed yet by bathymetric surveys) as currently assumed for the 1980 event.

With the help of the numerous studies led after the earthquake (due particularly to the fact that this earthquake is associated with important vertical and horizontal movements) we propose a source composed of one or three segments and their associated parameters is able to generate a tsunami which can be recorded on Spanish coastal tide gauges and be compared to historical data.

1.2 Historical settings

1.2.1 The earthquake

On 1980 October 10 at 12h25 UTC, a magnitude $M_s = 7.3$ earthquake occurred at El Asnam (actual Ech Cheliff) at 36.159°N and 1.396°E (USGS location – Dewey 1990; Fig. 1), causing thousands of casualties (Ambraseys 1981) and accompanied by an important coseismic deformation (Ruegg *et al*. 1982; Lammali *et al*. 1997). It is the largest instrumentally recorded earthquake in northern Africa (Cisternas *et al*. 1982). This event occurred nearly at the same location as the earthquake of 1954 (epicentre located at 36.285°N–1.566°E, i.e. in the locality of Beni-Rached) and is supposed to correspond to the release of accumulated strain either on the same fault segment or on two nearby distinct ones (Dewey 1990; Lammali *et al*. 1997).

On 1928 August 24 and 1934 September 7, two other less important fault ruptures ($m_b = 5.4$ and 5.0, respectively) occurred on the same fault system of the 1954 and 1980 events; their epicentres have been located in Oued Rhiou, westward from El Asnam, and El Abadia, eastward of Beni-Rached (Fig. 1; Shah & Bertero 1980).

1.2.2 The tsunami

The two earthquakes of 1954 and 1980 were both followed by low amplitude tsunamis that reached the Spanish coast and were recorded by sea-level gauges located in some harbours (Solovyev *et al*. 1992). The event of 1980 has been recorded on six tide gauges located at Alicante (one on the outer breakwater and one on the inner breakwater), Cartagena, Almeria, Malaga and Algeciras (see locations on Fig. 1). Both in 1954 and in 1980, the best signal with the highest amplitude has been recorded on the Alicante instruments. Nevertheless there is no strong difference between the signal recorded at Algeciras, that is, the furthest in the Alboran Sea, and the signal recorded in Almeria in terms of maximum wave amplitude and period. The recorded signals with their respective frequency spectra are shown in Fig. 2. Arrival times identified by Solovyev *et al*. (1992) are also indicated: they are in good agreement with the theoretical tsunami traveltime (TTT) calculation shown on Fig. 2. The record in Cartagena has not been published because of its poor quality (Solovyev *et al*. 1992). Only three gauges have recorded both signals: Alicante (outer gauge), Malaga and Algeciras; at the three locations the maximum wave heights are reached for the 1954 event with a factor of 2 between 1954 and 1980.

It is generally accepted that the tsunami observed in 1980 was related to turbidity currents (Solovyev *et al*. 1992, 2000;

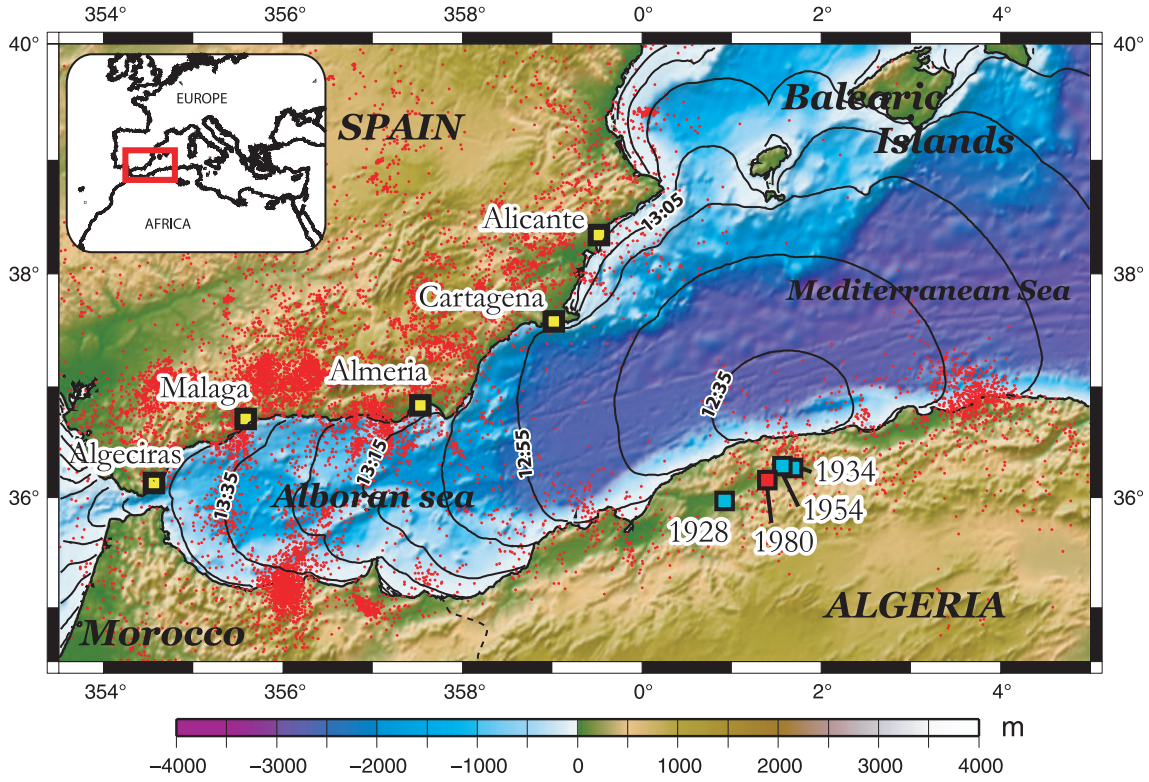

Figure 1. Location of the epicentres of the El Asnam earthquake of 1980 October 10, the 1954 Orléansville earthquake and the 1928 and 1934 events. The six tide gauges (two at Alicante) that recorded the tsunami are also indicated by yellow-black boxes. The red dots represent the local seismicity (data USGS, from 1973 to present). The black solid curves represent the theoretical tsunami traveltimes for a source located offshore El Asnam area and computed using the TTT SDK v 3.2 (http://www.geoware-online.com).

© 2011 The Authors, *GJI*
Geophysical Journal International © 2011 RAS

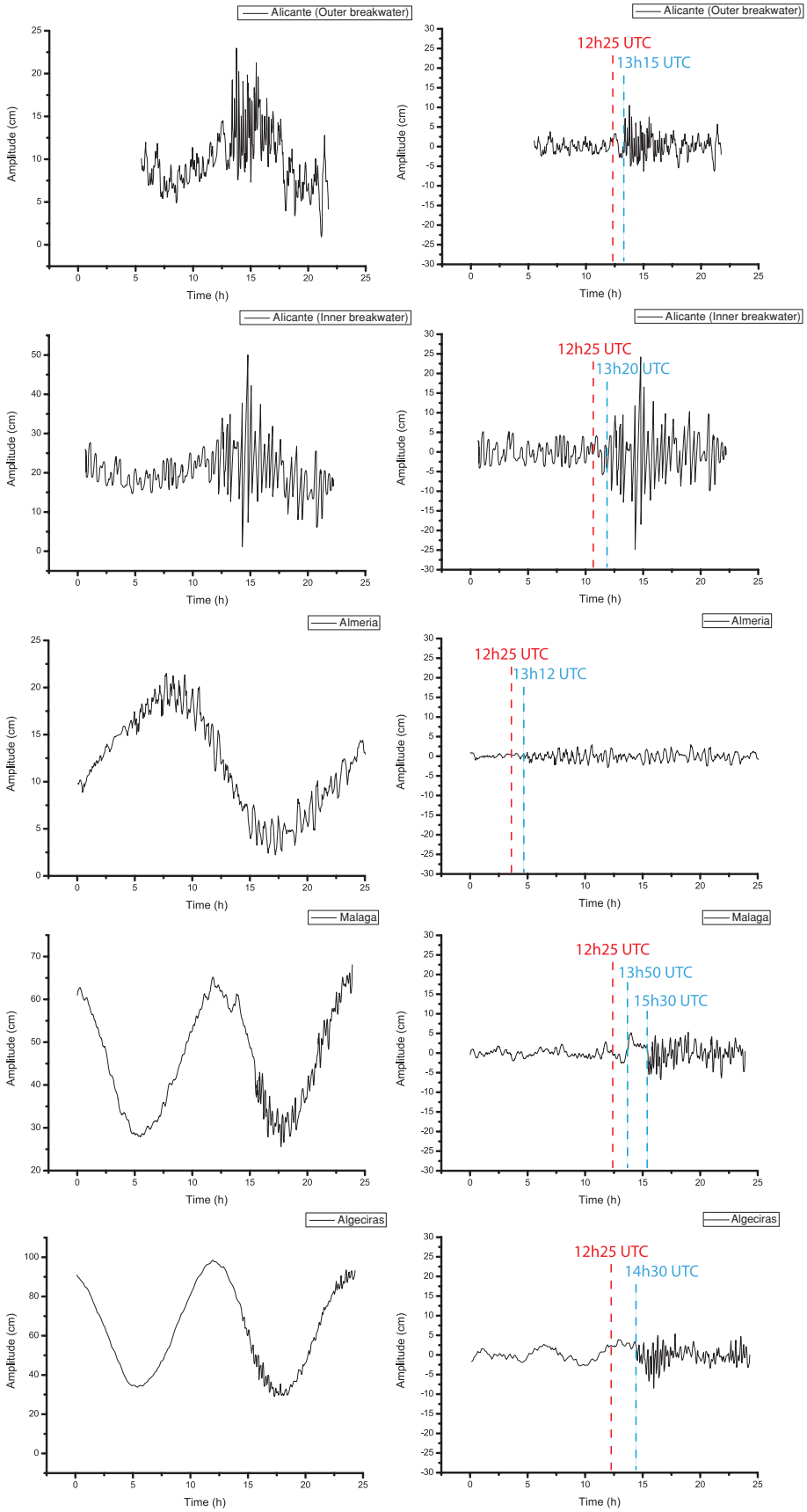

Figure 2. Historical tide gauge records at the locations indicated on Fig. 1: original (left-hand panels) and residual (detided) (right-hand panels). The time of the earthquake is pointed in red and the tsunami arrival as pointed in blue as indicated by Solovyev *et al*. (1992).

© 2011 The Authors, *GJI*
Geophysical Journal International © 2011 RAS

Papadopoulos *et al*. 2007), which have been reported for several earthquakes along the north Algerian Margin. The reason is found during the 1954 earthquake, when some submarine phone cables (five of the eight actives at that time exactly) offshore of Algeria were seriously damaged (as far as 100 km from the coast): this phenomenon has been associated with the motion of one or several turbidity currents generated by seismic shaking and/or submarine landslides (Heezen & Ewing 1955; Bourcart & Glangeaud 1956; Solovyev *et al*. 1992). Events where damage has occurred to three of these cables are described in Heezen & Ewing (1955): the first cable, located less than 40 km from the shore, ruptured 40 min after the earthquake; the last one, located 110 km from the Algerian shore, ruptured 5 hr after the earthquake. This is in opposition to the fast recorded TTT of about 50 min for Alicante Harbour, 250 km away from the Ténès shore. In addition, it is reported that those cables were dashed-damaged, that is, that some segments were damaged and others not, revealing several different turbidity currents and/or landslides. Concerning the 1980 event, there were fewer cables in activity near the Algerian Margin than in 1954 and only one cable rupture, linked to a small turbidity current near the bay of Algiers (200 km from epicentre), has been reported (El-Robrini *et al*. 1985). According to the recent marine surveys on the Algerian Margin, no recent scarp and/or important mass transport deposits have been highlighted offshore of the Ténès region (Cattaneo *et al*. 2010). In addition, Bourcart & Glangeaud (1956) indicate that a single turbidity current generated by the main shock in 1954 is not able to explain, alone, the rupture of all cables, some of them were located too far away from the slide location; some secondary slides generated by aftershocks may have generated turbidity currents too.

Nevertheless, the destabilization of the sedimentary cover on the continental slope of the Algerian margin spawning turbidity currents is currently associated with strong earthquakes (Yelles Chaouche 1991; Cattaneo *et al*. 2010).

If related to any submarine landslide, the signal recorded along the Spanish coast requires an adequate period of several minutes, typically around 2–10 min at most (Kulikov *et al*. 1996; Assier-Rzadkiewicz *et al*. 2000; Ioualalen *et al*. 2010). Thus the measured period of the oscillations of about 15–25 min for both 1954 and 1980 events on each available record (Solovyev *et al*. 1992) are not consistent with a landslide source.

In addition it requires a very important submarine mass movement to produce some sea level disturbances of still several centimetres as distant as in the harbour of Algeciras (Fig. 2) located 500 km away from the source area (see location on Fig. 1). In fact the reason is that since short tsunami wavelengths related to a small extent of the source (typically landslide sources) are dispersed during the propagation, they are unable to retain their energetic content at distances. Even if several turbidity currents have been reported, they should have simultaneously occurred to produce sufficient tsunami amplitude. However, such coherent submarine landslides have not been highlighted during recent Maradja bathymetric and seismic studies (Domzig *et al*. 2009).

Correlated to the previous point, tsunamis generated by submarine landslides often exhibit very large, or at least significant, run-up heights close to the source area (Tappin *et al*. 2001; Okal & Synolakis 2004; Harbitz *et al*. 2006; Tappin *et al*. 2008), an occurrence not mentioned by eyewitnesses to the 1980 earthquake along the Algerian coast.

These considerations allow us to propose a pure earthquake origin for the 1954 and 1980 tsunamis. In the following, we provide additional constraints from numerical modelling that confirm this hypothesis.

2 NUMERICAL MODELLING

2.1 Sources parameters

The detailed analysis of the El Asnam 1980 earthquake reveals a predominant thrusting mechanism on a fault plane split into three main segments (Fig. 3)—called southwestern, central and northeastern in the following—(Yielding *et al*. 1981; King & Yielding 1984), linked to each other by some smaller segments, with an average strike N45°E and with a mean dip angle of 54° to the northwest (Ambraseys 1981; Cisternas *et al*. 1982; Deschamps *et al*. 1982) combined with a small left-lateral displacement (Philip & Meghraoui 1983; Solovyev *et al*. 1992) which is apparently not significant (Nabelek 1985). This mechanism is well revealed by the field analysis that shows an important uplift of several metres all along the surface rupture, with a maximum of about 5–6 m in the area located northwest of the junction of the southern and central fault segments associated with a depression of about 1 m southeast of it (Kasser *et al*. 1987; Ruegg *et al*. 1982; Shah & Bertero 1980). This overall rupture pattern is directly related to the compressional regional setting associated with the active convergence between the European and African plates (Ouyed *et al*. 1981; Boudiaf *et al*. 1998).

The magnitude of the El Asnam earthquake has been estimated as $M_s = 7.3$ from surface waves (Cisternas *et al*. 1982; Deschamps *et al*. 1982). The energy magnitude is estimated to $M_w = 7.1$ by the Global Centroid-Moment-Tensor (CMT) Project (http://www.globalcmt.org/cgi-bin/globalcmt-cgi-bin/CMT4/), with a seismic moment of about $M_0 = 5.07\text{e}{+19}$ N-m. Because the well-accepted relationship between M_w and M_s allows us to estimate that $M_w \approx M_s$ in the range of magnitude 5.5–7.5 (Hanks & Kanamori 1979; Wells & Coppersmith 1994), and because the energy magnitude released during the main shock is not constrained very well due to the lack of nearby stations at the time of the earthquake (the first stations were deployed only two days after the main shock), we decided to propose scenarios for a $M_w = 7.3$ earthquake.

According to Wells & Coppersmith (1994), the surface and subsurface rupture lengths are not necessarily different: they indicate that the ratio between those lengths could be equal to 1 for a $M_w = 7.3$ earthquake. In addition, rupture plan length and width must be in a ratio of about 1:3.

Geodetic measurements help to partially constrain the average slip and the rake angle on the different fault plane (Ruegg *et al*. 1982; Yielding 1985; Bezzeghoud *et al*. 1995). We look at the geodetic measurements to choose the fault parameters with respect to the geological post-seismic surveys.

The rigidity coefficient μ has been chosen assuming a standard rigidity of 3.0×10^{10} N m^2 (compression mechanism) in agreement with Bilek & Lay (1999) and Geist & Bilek (2001) for conventional earthquakes.

The dip angle is obtained with regard to the aftershock depth distribution (for example Yielding *et al*. 1989).

These analyses allow the proposal of several rupture scenarios. Only two will be presented in the following.

2.2 Rupture models

2.2.1 First model: one-segment rupture

In order to simplify the problem we have considered for our calculation models that the rupture zone was made of only one fault plane (Fig. 3) encompassing the three identified segments (presented by

© 2011 The Authors, *GJI*
Geophysical Journal International © 2011 RAS

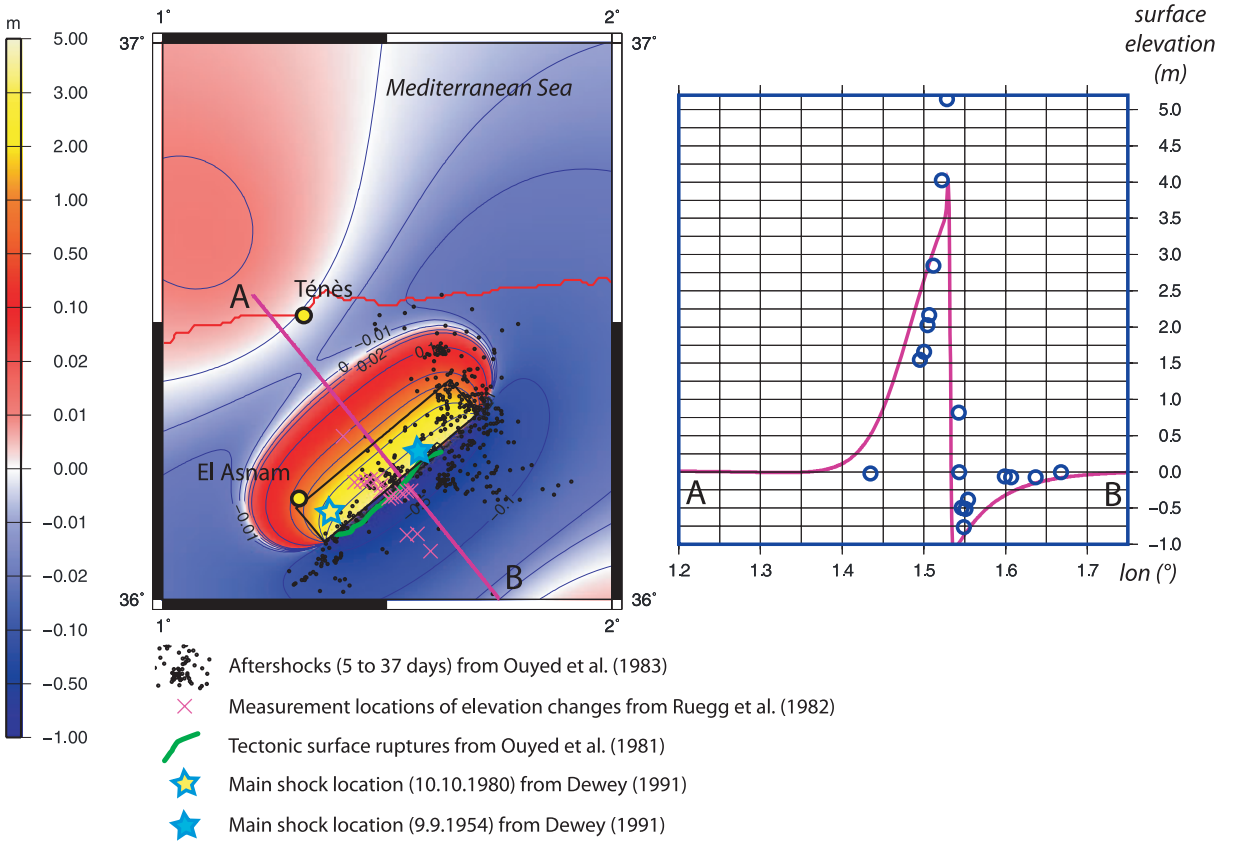

Figure 3. Coseismic deformation for a model composed of a single fault plane (black rectangle) corresponding to a M_w 7.3 earthquake in the area of El Asnam. The locations of the surface breaks, main shocks of 1954 and 1980, and aftershocks' epicentre from Ouyed *et al*. (1983) are indicated. A cross-section (A–B) in the middle of the rupture zone showing surface vertical displacement is represented (purple curve) and superimposed to on-field post-seismic measurements of elevation changes projected on a profile from Ruegg *et al*. (1982) (blue dots).

Table 1. Parameters for the two different scenarios of $M_w = 7.3$ rupture for the 1980 earthquake discussed in this study.

	Longitude of fault plane centre (°)	Latitude of fault plane centre (°)	Depth of fault plane centre (km)	Coseismic slip (m)	Strike (°)	Dip (°)	Rake (°)	Length (km)	Width (km)	Rigidity (N m^2)	Mo (N m)
1 segment	1.5	36.25	6.250	6	230	54	90	36	15	30.10^9	$1.1\ 10^{20}$
3 segments	1.415	36.18	6.5	5	228	54	90	12	15	30.10^9	$1.1\ 10^{20}$
	1.52	36.255	6.5	8	225	54	90	12	15	30.10^9	
	1.64	36.37	5.75	5	252	30	90	12	23	30.10^9	

Yielding *et al*. 1989, for example), assuming that the strike is nearly the same for each segment (Roger & Hébert 2008a). In this case of a unique fault plane, according to King & Vita-Finzi (1981) and Cisternas *et al*. (1982), a slip area of 40 km long and 15 km deep with a mean displacement of 6 m leads to an earthquake magnitude of $M_w = 7.3$ (i.e. $M_0 = 1.1 \times 10^{20}$). We will find the same orders for the parameters attributed to the multiple segments sources in the following (Table 1).

We will see further that this approach is rapidly limited since not enough deformation, according to the geodetic surveys (Yielding *et al*. 1981; Ruegg *et al*. 1982; Bezzeghoud *et al*. 1995), was then modelled in the central part of the segment. In fact, this single segment does not allow playing with the different parameters to best fit the observed data.

The advantage of using a multi-segments source is the possibility to vary the parameters of the part of the fault close to the sea, especially the slip value. The next subsection will debate the tsunami generation by both scenarios: such a unique fault plane is not able to generate enough sea deformation to match the Spanish tide gauge signals and to amplify in the same height range of the historical data.

2.2.2 *Second model: three-segment rupture*

After a more detailed study of the literature on this event, a source composed of three distinct segments has been tested (Roger *et al*. 2009; Fig. 4). Their locations have been based on the aftershocks' geographical location (Deschamps *et al*. 1982; Ouyed *et al*. 1983; King & Yielding 1984; Yielding *et al*. 1989; Bezzeghoud *et al*. 1995) and their depth distribution (Cisternas *et al*. 1982; Ouyed *et al*. 1983; Yielding *et al*. 1989).

The aftershocks' studies (Ouyed *et al*. 1983; King & Yielding 1984; Yielding 1985; Yielding *et al*. 1989) show that they are mostly located near the rupture surface features in terms of horizontal distribution along the two southern segments. However, there is a widespread location of aftershocks toward the sea when we look

© 2011 The Authors, *GJI*
Geophysical Journal International © 2011 RAS

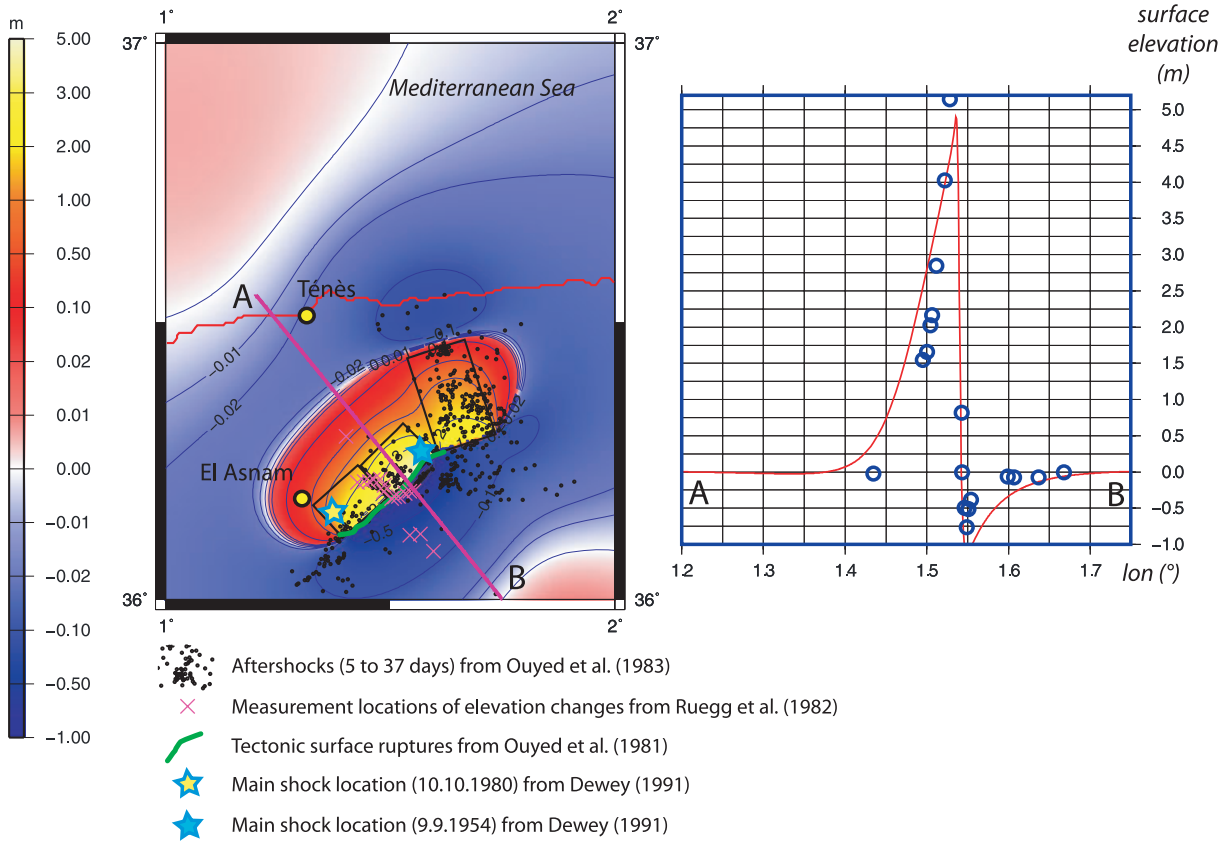

Figure 4. Coseismic deformation for a model composed of three fault segments matching the surface rupture segments exposed in the literature. The locations of the main shocks of 1954 and 1980, and aftershocks' epicentre from Ouyed *et al*. (1983) are indicated. A cross-section (A–B) in the middle of the rupture zone showing surface vertical displacement is represented (red curve) and superimposed to on-field post-seismic measurements of elevation changes projected on a profile from Ruegg *et al*. (1982) (blue dots).

to the northeast (until 40 km). This dispersion could have been associated to an unavoidable opening of the seismic network near the sea but most of the considered aftershocks have been re-located and show the same distribution (Yielding *et al*. 1989). In addition it could be attributed or correlated easily to the surface rupture features indicated by King & Yielding (1984) and linked to NW-dipping nodal planes with imbricated thrusting style as proposed by Yielding (1985). Ouyed *et al*. (1983) indicate that this could be due to the reactivation of a fan-like system of smaller reverse faults associated with surface folding. The depth distribution of the aftershocks is estimated between 2 and 10 km all along the rupture zone (Yielding *et al*. 1989). The mean depth of the fault planes is thereafter established around 6 km.

First, this aftershock distribution northwards allows us to propose a longer northeastern segment of about the same length than the two others (=12 km) and not simply 3–4 km as indicated by surface rupture features, leading to a total surface rupture length of 36 km. Then the aftershocks location between this northeastern segment and the sea, and their distribution in depth (King & Yielding 1984; Ouyed *et al*. 1983; Yielding *et al*. 1989), allow us to extend its width toward the north in our model, that is, closer to the sea. The proximity to the sea of the northeastern segment allows us to give more uncertainty for locating this one and to attribute to it realistic parameters.

As previously mentioned, the slip amplitude has been identified to be inconstant all along the rupture zone: all the studies conclude with a mean displacement (average value) of 3–4 m with maximum amplitude of about 6 m on the central segment (Cisternas *et al*. 1982; Nabelek 1985; Yielding 1985). Constraining of the faulting mechanism with geodetic measurements of vertical movements (Cisternas *et al*. 1982; Ruegg *et al*. 1982; Bezzeghoud *et al*. 1995) a specific slip value has been determined for each segment of the rupture fault. These values are in good agreement with the relations between the observed mean surface displacement and the subsurface slip on the fault plane proposed by Wells & Coppersmith (1994): a magnitude $M_w = 7.3$ earthquake leads to a ratio of 0.6–1.0 between the average subsurface displacement and the maximum surface displacement; thus a maximum surface displacement of 6 m corresponds to an average subsurface displacement on the fault plane of about 4–6 m. Our model fits as well as possible these previous results. This slip has been a bit exaggerated taking account of the other parameters. The related coseismic deformation is presented on Fig. 4.

All the corresponding parameters are summarized in Table 1.

2.3 Tsunami modelling

The initial bottom deformation is calculated based on elastic dislocation computed through Okada's formula (1985). Our method considers that the sea-bottom deformation is transmitted without losses to the entire water column, and solves the hydrodynamical equations of continuity (1) and motion (2) conservation. Non-linear terms are taken into account, and the resolution is carried out using a Crank Nicolson finite difference method centred in time and using an upwind scheme in space. This method has been widely used in the Pacific and Atlantic Oceans and the Mediterranean Sea and

© 2011 The Authors, *GJI*
Geophysical Journal International © 2011 RAS

contributes to tsunami hazard studies in several locations (Hébert *et al*. 2001; Roger & Hébert 2008; Sahal *et al*. 2009; Roger *et al*. 2010a,b):

$$\frac{\partial(\eta + h)}{\partial t} + \nabla \cdot [v(\eta + h)] = 0 \quad (1)$$

$$\frac{\partial v}{\partial t} + (v \cdot \nabla) \cdot v = -g\nabla\eta + \sum f \ . \quad (2)$$

The wave propagation is calculated on the entire Alboran Sea and the area between the Spanish east coast and the Balearic Islands. A special focus on Alicante Harbour (0°29′W, 38°20′N) where the largest usable tsunami signal has been reported and registered in 1980 is also presented with the use of four levels of imbricated grids (from 0 to 3) of increasing resolution. The larger (first level, grid 0) is built from an interpolation of the Gebco World Bathymetric Grid 1' (IOC, IHO & BODC 2003) at a space step of 500 m. Then the grid resolution increases close to the studied site, that is, when the water depth h decreases along with the tsunami propagation celerity equation $c = \sqrt{gh}$ which depends only on h, in the shallow water non-dispersive assumption.

Thus a high-resolution grid of Alicante Harbour, which is set up for the final grid level, is made from digitized, georeferenced and interpolated nautical bathymetric charts (SHOM 2001, 2005), in agreement with available harbour pictures, to complete the lack of bathymetric values near these structures. This grid has a resolution of 10 m (grid 3) and is able to reproduce the harbour major infrastructures such as docks or piers and coastal shallow water bathymetry (Fig. 3), which could have a significant influence on wave arrival times and amplitudes. Intermediate grids 1 and 2 are made with both datasets from grids 0 and 3. Grid 1 has been chosen to be at a 150 m resolution and grid 2 to be at a 50 m resolution in order to never have more than a factor of 4–5 between imbricated grids, in order to respect the Courant–Friedrichs–Lewy (CFL) criterion to ensure numerical stability (Courant *et al*. 1928) for each grid level, so that the shoaling effect is well reproduced and the wavelengths properly sampled. All these processes have been used in the case study of the Djijelli (Algeria) 1856 tsunami and its effects on the Balearic Islands (Roger & Hébert 2008) and the Algerian coast (Yelles *et al*. 2009).

3 RESULTS

3.1 Regional impact

First, the calculated initial deformation map presented in Figs 3 and 4 for both one- and three-segment sources shows that the initial coseismic deformation of an earthquake located at 45 km from the shore, with adequate parameters, is able to reach the sea. Thus the El Asnam earthquake itself could have been able to induce a small deformation of the sea surface and thus a tsunami. In fact, in each tested scenario, one of the major lobes of deformation (negative deformation) reaches the sea more or less and creates a deformation of the sea, that is, a tsunami, within a few centimetres (around 1–10 cm maximum; Figs 3 and 4).

Then this tsunami is able to propagate across the Mediterranean and the Alboran Sea.

It is worth noting that this coseismic deformation is able to induce submarine movements on the continental slope offshore Ténès as turbidity currents.

Fig. 5 represents the maximum wave heights reached at each point of the grids 0, 2 and 3 (Alicante Harbour) after 6 hr of tsunami propagation generated by the three-segment source scenario. We can see that some areas are more inclined to amplify the waves arriving from this part of the north African margin, offshore Ténès. The main sites showing noticeable amplification are, from the east to the west: the Spanish coast directly in front of the source area from the north east of Alicante to the neighbourhood of Cartagena (about 10 cm), including Alicante Harbour (40 cm) and the Balearic Islands; in fact the Balearic promontory seems to be particularly receptive to long wave amplification (as previously shown by Alasset *et al*. 2006; Roger & Hébert 2008; Sahal *et al*. 2009 in the case of the 1856 and 2003 northern Algeria events); the southern coasts of Ibiza and Formentera Islands (Fig. 5) show the most important wave heights about 15–20 cm (on this coarse grid 0; a better resolution would show most important wave heights in agreement with Green's Law (Synolakis 1991). Almeria Bay and the

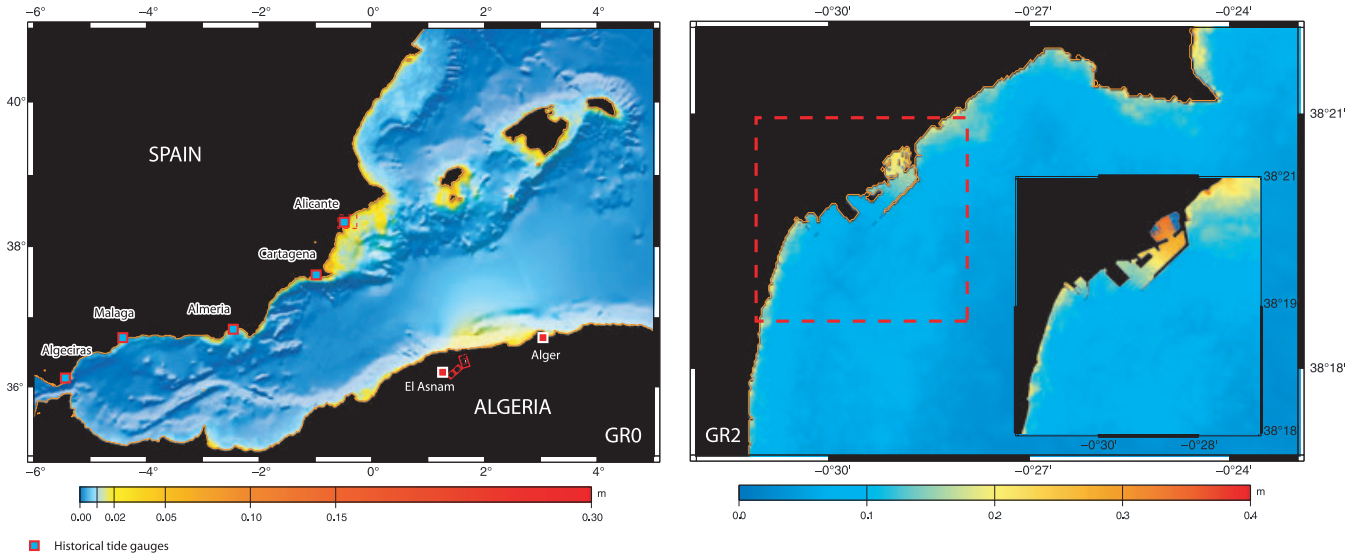

Figure 5. Maximum wave heights illuminated by bathymetric gradient on grid 0 (left-hand panel) after 6 h of tsunami propagation for a seismic source composed of three segments. Focus on Alicante Bay and Harbour are shown (right-hand panel). Historical tide gauge locations are also indicated (open red squares). Dashed boxes indicate the geographical location of GR2 and GR3, respectively.

© 2011 The Authors, *GJI*
Geophysical Journal International © 2011 RAS

neighbouring Malaga Bay (about 5–10 cm) are the most representative sites in the Alboran Sea.

The modelled maximum wave heights in coastal areas like Almeria or Malaga have been calculated on the 500 m resolution grid 0: this could result in a lack of coastal wave amplifications due to a shoaling effect or resonance phenomenon such as in Alicante Harbour. In fact we have not looked in detail into the other harbours where historical records have been found mainly because of the low tsunami amplitude (less than 10 cm) they show, which is hardly comparable to the modelling results.

The reader may notice that the wave heights in front of the peninsula northeast of Alicante could be related to submarine features such as canyons or low depths (as shown by Roger & Hébert 2008b in the case of the Minorca Canyon System in the Balearic Islands). Unfortunately, the lack of accurate bathymetric data in this area limits the use of modelling and thus does not allow us to conclude correctly.

In order to retrieve the tsunami waveform, a set of virtual tide gauges has been located everywhere on each grid. Some are located near the rupture area in order to control the initial sea surface deformation. Others are located in the maximum energy radiation zone (towards Alicante and the Balearic Islands) and in the Alboran Sea. We show the results of the two gauges of the Alicante inner and outer breakwater.

The two synthetic records in Alicante Harbour are shown on Fig. 6 concerning both the one- and three-segment rupture scenarios after 6 hr of tsunami propagation. The small initial coseismic deformation of about 10 cm offshore of Ténès (to the east, Fig. 4) has been able to induce sufficient sea surface deformation to propagate a tsunami towards the Spanish coast. The waves are composed of a first decrease of about 5 cm followed by an increase of about 5 cm of the sea level that is well reproduced by our model. The uncertainty in the arrival times indicated by Solovyev *et al*. (1992) allows us a range of possibilities for arrival times within several minutes. The period of the recorded signal is also well reproduced (around 15–20 min).

3.1.1 Note about arrival times in Alboran Sea (TTT)

The tsunami arrives in Malaga 1 hr 30 min after the seismic rupture and 2 hr in Algeciras (Fig. 1) which is in quite good agreement with the graphical estimation of arrival times from Solovyev *et al*. (1992) for Malaga, that is, more than 1 hr 10 min (Fig. 2). The 20 min difference could be related to wave slowing down when approaching the coast; due to the bad quality of bathymetric data along the coastline on this 500 m resolution grid, the synthetic gauge is not located at the exact location of the 1980 gauge, but farther from the coast, which could explain the 20 min delay. However there is a serious problem of arrival time for Algeciras that cannot be explained by the previous remark: in fact the amplitude of both signals is very small, about less than 1 cm peak to trough and maybe the tsunami arrival time has not been so well observed by Solovyev *et al*. (1991).

3.2 Impact in Alicante

The two historical records at Alicante Harbour are visible on Fig. 2. They are compared to the synthetic signals obtained with both scenarios (of one and three segments) in the harbour and outside (Fig. 6) corresponding to the outer and inner breakwater tide gauges indicated by Solovyev *et al*. (1992).

The only difference between the results of the simulations outside and inside the harbour concerns the tsunami amplitude showing a factor 2 between the one- segment scenario and the three-segment scenario.

This tide gauge signals underlines the arrival times but also the wave main period and the amplitude reached. We can see that a free oscillation mode is well reproduced inside Alicante Harbour (Fig. 6, upper panel) about 2 hr after the first wave arrival inside the harbour and could be related to resonance phenomenon inside the harbour. On the outer gauge the oscillation period of about 12–15 min is particularly well reproduced on the first peaks for both scenarios, despite the lack of amplitude in the synthetic signal compared to the real signal (factor 1/3 for the three-segment scenario, 1/6 for the one-segment scenario).

4 DISCUSSION

4.1 The harbour responses

In both 1954 and 1980, the best signal and highest amplitude is recorded on the Alicante instruments. Without considering the particular hypothesis of a sufficient submarine landslide or a tsunami directly triggered by the earthquake, this is in agreement with the fact that Alicante is located in the direction perpendicular to the fault azimuth, that is, the major direction of deformation (Figs 3 and 4) and in the main tsunami propagation path according to Okal (1988).

In 1980, we can note that it is the inner breakwater mareogram that shows the highest historical amplitude of oscillations (peak to trough) of 48 cm whereas the outer record shows only a maximum amplitude of 15 cm (Solovyev *et al*. 1991). This amplification on the inner gauge is probably due to a resonant harbour effect that could be initialized by long wave arrival in a semi-enclosed water body. This occurs when the period of these waves is similar to the period of free oscillations (eigenperiod) of the water surface of the harbour (Bellotti 2007; Sahal *et al*. 2009).

Notice that the locations of our virtual tide gauges are adapted from the locations indicated by Solovyev *et al*. (1992). This could be responsible for substantial differences observed between recorded signals and synthetic ones especially on the outer gauge: first the water depth under the gauge must be considered and then the tide gauge (real or virtual) can be located at a node of oscillation or not (Wüest & Farmer 2003; Rabinovich 2009). In fact, concerning the inner gauge, the resonant effect could be better reproduced and prevails on the other phenomenon.

Finally, the shape of the harbour has changed in 30 years, according to actual satellite views compared with historical maps of the harbour; new docks and piers have been built and this has probably had some noticeable impact on the global eigenperiod of the harbour (Bellotti 2007; Gonzales-Marco *et al*. 2008).

4.2 A possible contribution by the turbidity currents: comparison with the 1979 Nice event

On 1979 October 16, a submarine landslide occurred close to Nice (southern France). The initial destabilization volume has been estimated to be about 10 million cubic metres which rapidly increased to reach a total amount of 150 million cubic metres with sediments stripped from the slope (Assier-Rzadkiewicz *et al*. 2000). This was probably the origin of an important turbidity current (Piper & Savoye 1993) that cut two submarine cables located, respectively, 75 and 105 km from the coast. Assier-Rzadkiewicz *et al*. (2000) indicate that the bathymetric data revealed the substantial

© 2011 The Authors, *GJI*

Geophysical Journal International © 2011 RAS

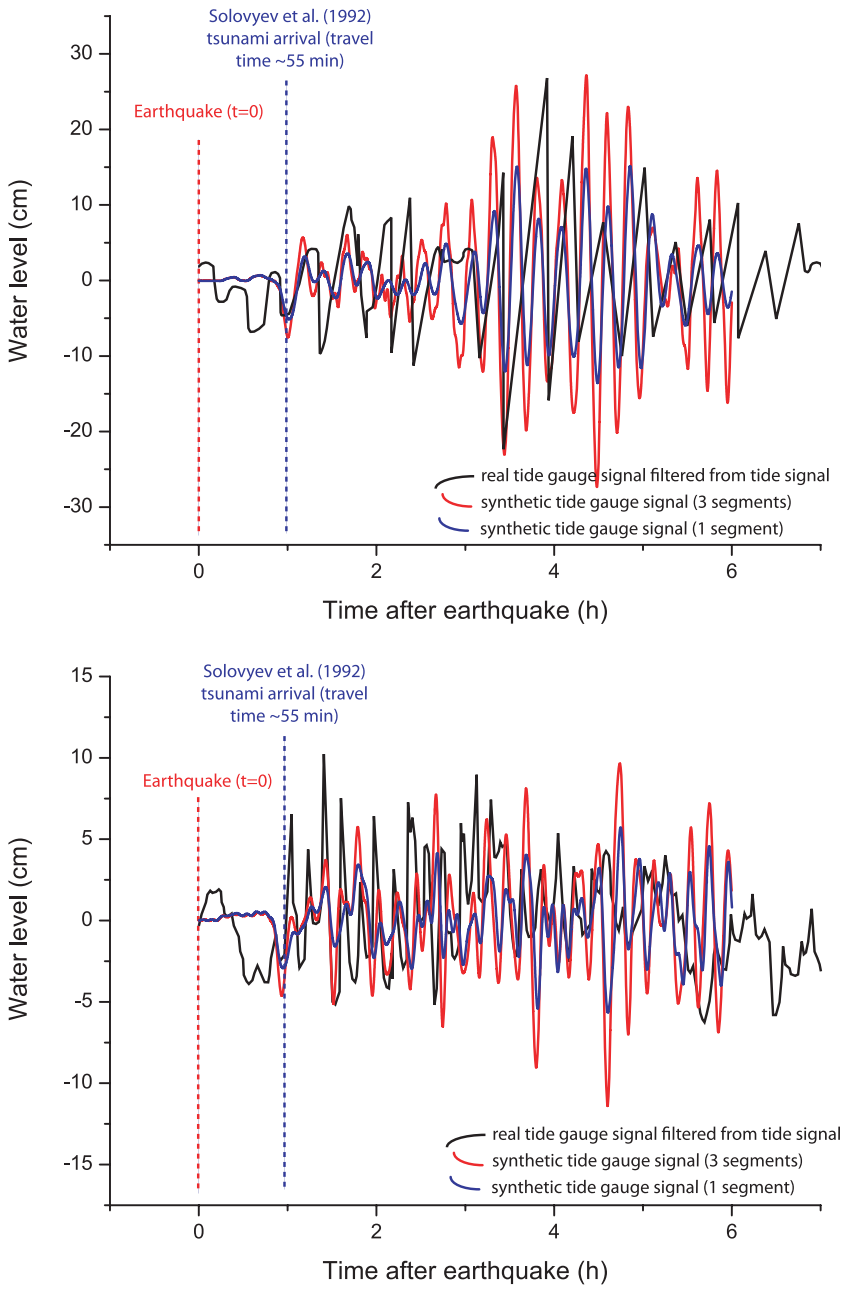

Figure 6. Synthetic signal registered on virtual tide gauges located in Alicante Harbour (see location of the gauges on Fig. 5 GR3): inner tide gauge (upper panel) and outer tide gauge (lower panel). The synthetic signal is superimposed on the real historical records (filtered from tide signal) at these two locations. Earthquake and tsunami times from Solovyev *et al*. (1992) are indicated.

modification of the sea-floor by this event and its path is indicated by a steeply incised chute.

A tsunami was induced by this submarine landslide with wave amplitude of about 3 m, 10 km away from the source at Antibes, in the Angel's Bay, and no more than a few dozen centimetres 30 km away (Mandelieu). This is due to the geometrical dispersion (frequency and amplitude dispersion) of waves on a sphere, explaining that the tsunami spectral amplitude decreases rapidly away from the source because of its multi-frequency composition typical of submarine landslide generated tsunamis (Okal 2003; Papadopoulos *et al*. 2007), and also because the observation site is not located within the main energy direction.

Assier-Rzadkiewicz *et al*. (2000) indicate that the period of each wave of the 1979 Nice event is estimated around 8 min, a value that is probably related to the considered harbour resonance. According to the recent study of Ioualalen *et al*. (2010), the period of those waves in the source area has been estimated as about 2–3 min for this event.

5 CONCLUSION

This study proposes an alternative hypothesis for the tsunami generation during the 1980 October 10 event. It shows that tsunamigenic seismic sources don't have to be located at sea (as in Djijelli, 1856 August) or partially at sea (as in Zemmouri, 2003 May) to generate a small tsunami, and this without considering underwater landslide triggering tsunamis. In fact an inland earthquake located as far from the sea as the El Asnam earthquake of 1980

© 2011 The Authors, *GJI*
Geophysical Journal International © 2011 RAS

October 10 is able to generate a tsunami due to the repartition of initial rupture deformation lobes, according to numerical modelling. Indeed, the proposed parameters of the rupture scenarios, chosen with the help of previous geological and geodetic measurements, are able to explain the observed tsunami. The comparison of synthetic tide gauge records and historical records highlights that the observed wave periods are well reproduced: only a tsunami generated by an earthquake could show eigenperiod of 15–25 min, as the one shown by the different historical records, a typical period of a tsunami generated by a landslide hanging around several minutes (2–10 min).

In addition, either a simple segment rupture scenario or a three-segment scenario are able to reproduce correctly the historical signals in terms of wave arrival, polarity, amplitude and period. This is well shown on the records at Alicante Harbour. The main reason for using a multiple-segment source is to reduce the energy in the southwestern side of the rupture and to increase it on the opposite side, that is, near the shore. In general the traveltimes indicated by Solovyev *et al*. (1992) are in good agreement with modelled TTTs.

Nevertheless, such important earthquakes ($M_w > 7.0$) could easily destabilize the unstable sediment cover along the margin and thus induce submarine mass movements and turbidity currents, which could also generate a local tsunami (one has been highlighted by a phone cable rupture in Algier's Bay on the same day). However several linked parameters should be considered in this case: the volume of the slide, the lack of wave observation along the Algerian coast, the period of the recorded signal along the Spanish southeastern coast and the dispersion phenomenon. A sediment movement able to produce a tsunami reaching Alicante and as far as Algeciras Harbour must be at least as important as the Nice 1979 event to produce a tsunami wave that would not disperse too fast. Bathymetric surveys offshore of the Algerian coast in this area have even not highlighted adequate scarps and no reports of huge coastal waves along the Algerian shore have been found.

The fact that the geodetic measurements led to a larger seismic moment value and that we use an artificial increase of seismic moment magnitude from 7.1 to 7.3 to reproduce the observations in terms of geodetic data but also tide gauge records allow us to indicate that tsunami data could help further investigation of seismic sources.

According to the modelling results and more particularly to the maximum wave height distribution maps, it could be interesting to investigate Ibiza and Formentera islands, which seem to be particularly inclined to wave amplification, in terms of harbour authority witnesses as well as on field proof, probably not for this recent event of 1980 but for potential older ones.

An accurate study of resonance phenomenon inside Alicante Harbour should be led in order to explain the origin of the 15–25 min oscillation period in 1980, using a coeval bathymetric map to produce the grid necessary for modelling. Then a comparison with the actual harbour shape could show whether the harbour still reacts or not to long wave arrival.

Tsunami modelling of the 1954 event could be done to show that this smaller rupture, in terms of energy, and in comparison to the 1980 event, is able to produce an even larger tsunami due to its geographical position closer to the shore (northeastward from the 1980 epicentre).

ACKNOWLEDGMENTS

This research was funded by the European project TRANSFER (Tsunami Risk ANd Strategies For the European Region) under the contract 0370 58, by the MAREMOTI project from the French ANR (Agence Nationale de la Recherche) under the contract ANR-08-RISKNAT-05–01c and by the LRC Yves Rocard (Laboratoire de Recherche Conventionné CEA-ENS). We are grateful to Eric Thauvin (CEA-DASE) for his precious help for bathymetric grids construction, Alain Rabaute (GeoSubSight company) and Pierpaolo Dubernet (ENS) for technical support, Carl Harbitz (Norwegian Geotechnical Institute) for constructive discussion about submarine landslides, Jocelyn Guilbert (CEA-DASE), Marc Nicolas (CEA-DASE), Mourad Bezzeghoud (Universidade de Evora), Raul Madariaga (ENS) and Paolo Marco De Martini (INGV) for constructive discussions about the earthquake of El Asnam in general and the source parameters. We would like to thank Wendy Austin-Giddings (BGS) for the proofreading of the manuscript and her interesting comments as well as the two anonymous referees.

REFERENCES

Alasset, P.-J., Hébert, H., Maouche, S., Calbini, V. & Meghraoui, M., 2006. The tsunami induced by the 2003 Zemmouri earthquake (M_w = 6.9, Algeria): modelling and results, *Geophys. J. Int.,* **166,** 213–226, doi:10.1111/j.1365-246X.2006.02912.x.

Ambraseys, N.N., 1981. The El Asnam (Algeria) earthquake of 10 October 1980; conclusions drawn from a field study, Technical note. *Q. J. Eng. Geol. Lond.,* **14,** 143–148.

Assier-Rzadkiewicz, S., Heinrich, P., Sabatier, P.C., Savoye, B. & Bourillet, J.F., 2000. Numerical Modelling of a Landslide-generated Tsunami: the 1979 nice event, *Pure appl.Geophys.,* **157,** 1707–1727.

Bellotti, G., 2007. Transient response of harbours to long waves under resonance conditions, *Coastal Eng.,* **54,** 680–693.

Bezzeghoud, M., Dimitrov, D., Ruegg, J.C. & Lammali, K., 1995. Faulting mechanism of the El Asnam (Algeria) 1954 and 1980 earthquakes from modelling of vertical movements, *Tectonophysics,* **249**(3–4), 249–266.

Bilek, S.L. & Lay, T., 1999. Rigidity variations with depth along interpolate megathrust faults in subduction zones, *Nature,* **400,** 443–446.

Boudiaf, A., Ritz, J.-F. & Philip, H., 1998. Drainage diversions as evidence of propagating active faults: example of the El Asnam and Thenia faults, Algeria, *Terra Nova,* **10,** 236–244.

Bourcart, J. & Glangeaud, L., 1956. Perturbations sous-marines et courants de turbidité du séisme d'Orléansville, *CR Acad. Sci.,* **T242,** 1504–1506.

Cattaneo, A. *et al*., 2010. Submarine landslides along the Algerian Margin: a review of their occurrence and potential link with tectonic structures, in Submarine mass movements and their consequences, *Adv. Nat. Technol. Hazards Res.,* **28,** III, 515–525, doi:10.1007/978-90-481-3071-9_42.

Cisternas, A., Dorel, J. & Gaulon, R. 1982. Models of the complex source of the El Asnam earthquake, *Bull. seism. Soc. Am.*, **72**(6), 2245–2266.

Courant, R., Friedrichs, K. & Lewy, H., 1928. Über die partiellen Differenzengleichungen der mathematischen Physik, *Mathematische Annalen,* **100**(1), 32–74.

Deschamps, A., Gaudemer, Y. & Cisternas, A., 1982. The El Asnam, Algeria, earthquake of 10 October 1980: multiple-source mechanism determined from long-period records, *Bull. seism. Soc. Am.,* **72**(4), 1111–1128.

Dewey, J.W., 1990. The 1954 and 1980 Algerian earthquakes: implications for the characteristic-displacement model of fault behaviour, *Bull. seism. Soc. Am.,* **81**(2), 446–467.

Domzig, A., Gaullier, V., Giresse, P., Pauc, H., Deverchere, J. & Yelles, K., 2009. Deposition processes from echo-character mapping along the western Algerian margin (Oran-Tenes), Western Mediterranean, *Mar. Petrol. Geology,* **26,** 673–694.

El-Robrini, M., Gennesseaux, M. & Mauffret, A., 1985. Consequences of the El-Asnam earthquakes: turbidity currents and slumps on the Algerian margin (Western Mediterranean), *Geo-Mar. Lett.,* **5,** 171–176.

© 2011 The Authors, *GJI*
Geophysical Journal International © 2011 RAS

Geist, E.L. & Bilek, S.L. 2001. Effect of depth-dependent shear modulus on tsunami generation along subduction zones, *Geophys. Res. Lett.,* **28**(7), 1315–1318.

Gonzales-Marco, D., Sierra, J.P., Fernandez de Ybarra, O. & Sanchez-Arcilla, A., 2008. Implications of long waves in harbor management: the Gijon port case study, *Ocean Coastal Manag.*, **51,** 180–201, doi:10.1016/j.ocecoaman.2007.04.001.

Hanks, T.C. & Kanamori, H., 1979. A moment magnitude scale, *J. Geophys. Res.,* **84**(B5), 2348–2350.

Harbitz, C.B., Lovholt, F., Pedersen, G. & Masson, D.G., 2006. Mechanisms of tsunami generation by submarine landslides: a short review, *Norwegian J. Geol.,* **86,** 255–264. ISSN 029–196X.

Hébert, H., Heinrich P., Schindelé F. & Piatanesi A., 2001. Far-field simulation of tsunami propagation in the Pacific Ocean: impact on the Marquesas Islands (French Polynesia), *J. geophys. Res.,* **106,** 9161–9177.

Heezen, B.C. & Ewing, M. (1955). Orléansville earthquake and turbidity currents, *Bull. Am. Assoc. Petrol. Geol.,* **39**(12), 2505–2514.

IOC, IHO & BODC, 2003. Centenary Edition of the GEBCO Digital Atlas, British Oceanographic Data Centre, Liverpool, (CD-ROM).

Ioualalen, M., Migeon, S. & Sardoux, O., 2010, Landslide tsunami vulnerability in the Ligurian Sea: case study of the 1979 October 16 Nice international airport submarine landslide and of identified geological mass failures, *Geophys. J. Int.,* **181**(2), 724–740.

Kasser, M., Ruegg, J.C. & Lepine, J.C., 1987. Deformations associated with the El Asnam earthquake of October 10, 1980 (Algeria), in: Recent Movements in Africa, eds Wassef, A.M., Boud, A., Vyskocil, P., *J. Geodyn.,* **7,** 215–219.

King, G. & Yielding, G., 1984. The evolution of a thrust fault system: processes of rupture initiation, propagation and termination in the 1980 El Asnam (Algeria) earthquake, *Geophys. J. R. astr. Soc.,* **77,** 915–933.

King, G.C.P. & Vita-Finzi, C., 1981. Active folding in the Algerian earthquake of 10 October 1980, *Nature,* **292,** 22–26.

Kulikov, E.A., Rabinovich, A.B., Thomson, R.E. & Bornhold, B.D., 1996. The landslide tsunami of November 3, 1994, Skagway Harbor, Alaska, *J. geophys. Res.,* **101**(C3), 6609–6615.

Lammali, K., Bezzeghoud, M., Oussadou, F., Dimitrov, D. & Benhallou, H., 1997. Postseismic deformation at El Asnam (Algeria) in the seismotectonic context of northwestern Algeria, *Geophys. J. Int.,* **129,** 597–612.

Nabelek, J., 1985. Geometry and mechanism of faulting of the 1980 El Asnam, Algeria, earthquake from inversion of teleseismic body waves and comparison with field observations, *J. geophys. Res.,* **90**(B14), 12 713–12 728.

Okada, Y., 1985. Surface deformation due to shear and tensile faults in a half-space, *Bull. seism. Soc. Am.,* **75,** 1135–1154.

Okal, E., 1988. Seismic parameters controlling far-field tsunami amplitudes: a review, *Nat. Hazards,* **1,** 67–96.

Okal, E.A., 2003. Normal mode energetic for far-field tsunamis generated by dislocations and landslides, *Pure appl. Geophys.,* **160**(10–11), 2189–2221.

Okal, E.A. & Synolakis, C.E., 2004. Source discriminants for near-field tsunamis, *Geophys. J . Int.,* **158,** 899–912.

Ouyed, M. *et al*., 1981. Seismotectonics of the El Asnam earthquake, *Nature,* **292,** 26–31.

Ouyed, M., Yielding, G., Hatzfeld, D. & King, G.C.P., 1983. An aftershock study of the El Asnam (Algeria) earthquake of 1980 October 10, *Geophys. J. R. astr. Soc.,* **73,** 605–639.

Papadopoulos, G.A., Daskalaki, E. & Fokaefs, A., 2007. Tsunamis generated by coastal and submarine landslides in the Mediterranean Sea, Submarine Mass Movements and Their Consequences 3rd International Symposium, *Adv. Nat. Technol. Hazards Res.,* **27,** 415–422, doi:10.1007/978-1-4020-6512-5.

Philip, H. & Meghraoui, M., 1983. Structural analysis and interpretation of the surface deformations of the El Asnam earthquake of October 10, 1980, *Tectonics,* **2**(1), 17–49.

Piper, D.J.W. & Savoye, B., 1993. Process of late Quaternary turbidity current flow and deposition on the Var Deep-sea Fan, Northwest Mediterranean Sea, *Sedimentology,* **40,** 557–582.

Rabinovich, A.B., 2009. Seiches and harbor oscillations, in: *Handbook of Coastal and Ocean Engineering,* pp. 193–236, eds Y.C. Kim, World Scientific Publ., Singapore.

Roger, J. & Hébert, H., 2008a. Results of the modelling of the El Asnam (Algeria) earthquake of 1980, *Geophys. Res. Abst.,* **10,** EGU2008-A-02131.

Roger, J. & Hébert, H., 2008b. The 1856 Djijelli (Algeria) earthquake and tsunami: source parameters and implications for tsunami hazard in the Balearic Islands, *Nat. Hazards Earth Syst. Sci.,* **8**(4), 721–731.

Roger, J., Hébert, H. & Briole, P., 2009. The tsunami triggered by the El Asnam (Algeria) earthquake of 1980: a new hypothesis of generation, *Am. Geophys. Un. Fall Meeting,* Abstract OS43A-1378.

Roger, J., Baptista, M.A., Sahal, A., Allgeyer, S. & Hébert, H., 2010b. The transoceanic 1755 Lisbon tsunami in Martinique, *Pure appl. Geophys.,* in press, doi:10.1007/s00024-010-0216-8.

Roger, J., Allgeyer, S., Hébert, H., Baptista, M.A., Loevenbruck, A. & Schindelé, F., 2010a. The 1755 Lisbon tsunami in Guadeloupe Archipelago: source sensitivity and investigation of resonance effects, *Open Oceanogr. J.,* **4,** 58–70.

Rothé, J.P., 1955. Le tremblement de terre d'Orléansville et la sismicité de l'Algérie, *La Nature,* **3237,** 1–9.

Ruegg, J.C., Kasser, M., Tarantola, A., Lepine, J.C. & Chouikrat, B., 1982. Deformations associated with the El Asnam earthquake of 10 October 1980: geodetic determination of vertical and horizontal movements, *Bull. seism. Soc. Am.,* **72**(6), 2227–2244.

Sahal, A., Roger, J., Allgeyer, S., Lemaire, B., Hébert, H., Schindelé, F. & Lavigne, F., 2009. The tsunami triggered by the 21 May 2003 Boumerdes-Zemmouri (Algeria) earthquake: field investigations on the French Mediterranean coast and tsunami modelling, *Nat. Hazards Earth Syst. Sci.,* **9,** 1823–1834.

SHOM (Service Hydrographique et Océanographique de la Marine), 2001. Ports d'Alicante et de Torrevieja, 1/10000^{e}. Publication 1969, 3rd edn, no. 6515.

SHOM (Service Hydrographique et Océanographique de la Marine), 2005. Abords d'Alicante, 1/25000^{e}. Publication 1991, 2nd edn, no. 7304 (INT 3167).

Shah, H.C. & Bertero, V., 1980. El-Asnam earthquake, Algeria, 10th October 1980. Preliminary reconnaissance report. USGS reconnaissance activities report, 56 pp, http://www.eeri.org/site/reconnaissance-activities/44-algeria/130-m73elasnam.

Solovyev, S.L., Campos-Romero, M.L. & Plink, N.L., 1992. Orleansville tsunami of 1954 and El Asnam tsunami of 1980 in Alboran sea (Southwestern Mediterranean sea), *Izvestiya, Phys. Solid Earth,* **28**(9), 739–760.

Stock, C. & Smith, E.G.C., 2000. Evidence for different scaling of earthquake source parameters for large earthquakes depending on faulting mechanism, *Geophys. J. Int.,* **143,** 157–162.

Synolakis, C.E., 1991. Green's law and the evolution of solitary waves, *Phys. Fluids A,* **3**(3), 490–491.

Tappin, D.R., Watts, P. & Grilli, S.T., 2008. The Papua New Guinea tsunami of 17 July 1998: anatomy of a catastrophic event, *Nat. Hazards Earth Syst. Sci.,* **8,** 243–266.

Tappin, D.R., Watts, P., McMurtry, G.M., Lafoy, Y. & Matsumoto, T., 2001. The Sissano, Papua New Guinea tsunami of July 1998—offshore evidence on the source mechanism, *Mar. Geol.,* **175,** 1–23.

Wells, D.L. & Coppersmith, K.J., 1994. New empirical relationships among magnitude, rupture length, rupture width, rupture area, and surface displacement, *Bull. seism. Soc. Am.,* **84**(4), 974–1002.

Wüest, A. & Farmer, D.M., 2003. Seiches, in: *Encyclopedia of Science & Technology,* 9th edn, McGraw-Hill, New York, NY.

Yelles Chaouche, K., 1991. Coastal Algerian earthquakes: a potential risk of tsunamis in Western Mediterranean? Preliminary investigation, *Sci. Tsunami Hazards, special issue,* **9**(1), 47–54.

Yelles-Chaouche, A., Roger, J., Déverchère, J., Bracène, R., Domzig, A., Hébert, H. & Kherroubi, A., 2009. The 1856 tsunami of Djidjelli (Eastern Algeria): Seismotectonics, modelling and hazard implications for the Algerian coast, *Pure appl. Geophys.,* **166,** 283–300, doi:10.1007/s00024-008-0433-6.

© 2011 The Authors, *GJI*
Geophysical Journal International © 2011 RAS

Yelles, K. *et al*., 2009. Plio-Quaternary reactivation of the Neogene margin off NW Algiers, Algeria: the Khayr-Al-Din bank, *Tectonophysics,* **475,** 98–116, doi:10.1016/j.tecto.2008.11.030.

Yielding, G., 1985. Control of rupture by fault geometry during the 1980 El Asnam (Algeria) earthquake, *Geophys. J. R. astr. Soc.,* **81,** 641–670.

Yielding, G., Jackson, J.A., King, G.C.P., Sinvhal, H., Vita-Finzi, C. & Wood, R.M., 1981. Relations between surface deformation, fault geometry, seismicity, and rupture characteristics during the El Asnam (Algeria) earthquake of 10 October 1980, *Earth planet. Sci. Lett.,* **56,** 287–304.

Yielding, G., Ouyed, M., King, G.C.P. & Hatzfeld, D., 1989. Active tectonics of the Algerian Atlas Mountains—evidence from aftershocks of the 1980 El Asnam earthquake, *Geophys. J. Int.,* **99,** 761–788.

© 2011 The Authors, *GJI*
Geophysical Journal International © 2011 RAS

Vulnerability of the Dover Strait to coseismic tsunami hazards: insights from numerical modelling

Journal:	*Geophysical Journal International*
Manuscript ID:	GJI-S-11-0091
Manuscript Type:	Research Paper
Date Submitted by the Author:	08-Feb-2011
Complete List of Authors:	Roger, Jean; ENS, Geologie Gunnell, Yanni; Université Lumière-Lyon 2, CNRS UMR 5600
Keywords:	Tsunamis < GENERAL SUBJECTS, Seismicity and tectonics < SEISMOLOGY, Fractures and faults < TECTONOPHYSICS, Europe < GEOGRAPHIC LOCATION

SCHOLARONE™
Manuscripts

Vulnerability of the Dover Strait to coseismic tsunami hazards: insights from numerical modelling

J. Roger[1,*], Y. Gunnell[2]

1 École normale supérieure, Laboratoire de Géologie, Paris, France

2 Université Lumière–Lyon 2, CNRS UMR 5600, Lyon, France

*corresponding author : jeanrog@hotmail.fr

For Peer Review

Abstract

On April 6, 1580, a large earthquake shook the eastern English Channel and its shores, with numerous casualties and significant destruction documented. Some reports suggest that it was followed by a tsunami. Meanwhile, earthquake magnitudes of $M_W = 7$ have been deemed possible on intraplate fault systems in neighbouring Benelux. This study aims to determine the possibility of a $M_W > 5.5$ magnitude earthquake generating a tsunami in the Dover Strait, one of the world's busiest seaways. In a series of numerical models focusing on sensitivity analysis, earthquake source parameters for the Dover Strait are constrained by palaeoseismological evidence and historical accounts, producing maps of wave heights and analysis of frequencies based on six strategically located virtual tide gauges. Of potential of concern to engineering geologists, a maximum credible scenario is also tested for $M_W = 6.9$. Sensitivity to parameter choice is emphasized but a pattern of densely inhabited coastal hotspots liable to tsunami-related damage because of bathymetric forcing factors is consistently obtained.

Keywords: tsunami hazard, palaeoseismology, intraplate seismicity, coastal vulnerability, Dover Strait, geology and society

1. Introduction

1.1. Historical accounts of seismicity in the Dover Strait

Earthquake catalogs and other studies available from France, Belgium and England show that the English Channel is seismically active (Alexandre 1990, Melville *et al*. 1996, Musson 2004). Three highly destructive events have been well documented because of the structural damages sustained at the time by castles and churches: the May 21, 1382, April 23, 1449, and April 6, 1580 earthquakes, all among the largest to have affected NW Europe. Overviews by Bungum et al. (2005) for Fennoscandia and Camelbeeck et al. (2007) for the lower Rhine region have shown that intraplate earthquakes of Mw = 6.9 or more either have occurred in the past or correspond potentially to the largest magnitudes for these regions. Although the Dover Strait has remained peripheral to most earthquake and tsunami hazard assessment reports relevant to the British Isles (e.g. Kerridge, 2005), this international shipping lane is connected to the continental fault systems of north-west continental Europe in addition to being situated within the geographical range of glacio-isostatic crustal stresses caused by the recession of the Scandinavian ice sheet during the late Pleistocene.

In the Dover Strait, an isoseismal map constructed by Neilson *et al*. (1984) (Fig. 1) indicates that the 1580 earthquake had a maximum epicentral intensity of IX (obtained using both the MSK, 1991, and the Modified Mercalli Scale) and a Richter magnitude of 6.2–6.9. These results were later revised to a maximum MSK palaeointensity to ~VIII in Calais and VII in Dover (Melville *et al*. 1996) but the pattern of isoseismals was nonetheless similar, with a rupture partially situated at sea (Fig. 1). These data are compatible with the mention in

For Peer Review

historical documents that the April 6, 1580 earthquake was soon followed (but without precise detail on how soon) by a series of huge sea waves (Neilson *et al*. 1984, Melville *et al*. 1996). Given the fine weather, calm seas (Neilson *et al*. 1984, Lamb 1991) and neap tides (Créach, pers. comm. 2010) at the time of the marine event, the waves could conceivably be attributed to a tsunami. This hypothesis has been ruled out without corroboration in a report by Kerridge (2005) on behalf of the former UK Department for the Environment, Food and Rural Affairs (DEFRA). Admittedly, no deposits attributable to a tsunami have so far been identified on the coastlines of northern France or south-eastern England. Absence of evidence, however, is not evidence of absence, and in a comprehensive synthesis of anomalous sea disturbances around British shores, Haslett and Bryant (2008) have cross-examined the detailed historical accounts available for both the UK and the continent. They concluded that the dismissal by DEFRA of some historical reporting by chroniclers of the time was misinformed and unjustified. Reports for 1580 of large waves reaching Kent and northern France at similar times are supported by French, English and Flemish sources (Melville *et al*. 1996). Flooding was more severe in Calais and Boulogne, with also 120 fatalities or more in Dover, additional deaths in France, and a minimum of 165 sunken ships reported.

In summary, what exactly happened in 1580 on the shores of the eastern English Channel remains unclear, some of the historical reports being unverifiably imprecise, inaccurate, or both. None the less, a recent tremor ($M_W = 4.0$), with an epicentre situated inland from Folkestone at a depth of 5.3 km, occurred on April 28, 2007 (Ottemöller *et al*. 2009). A magnitude $M_W = 3.0$ earthquake affected Folkestone again on March 3, 2009, confirming that the Strait is a recurring focus of intraplate seismicity involving ancient fault systems. In an attempt to unravel some of the confusion from a different angle, here we bring new resolution to the uncertainty surrounding tsunami hazards in the English Channel by testing the

For Peer Review

conditions and likelihood of tsunami generation through a series of numerical modelling experiments. We test the hypothesis of tsunami generation in the Dover Strait based on a range of rupture processes constrained by information on existing tectonic structures and the regional bathymetry, and by current knowledge of tsunami physics. We test for earthquake magnitudes that are consistent with the 1580 event on the one hand, and with more extreme magnitudes such as suggested by Camelbeeck et al. (2007) on the other.

1.2. Constraints on rupture mechanisms: evidence from the 1580 event

The Dover Strait is a sea passage 33 km wide at its narrowest point with a maximum water depth of ca. 60 m between Cap Gris-Nez and Dover. It is also cut by a NW–SE-striking fault network (Fig. 1). These Variscan tectonic structures have acted as en-échelon accommodation zones since Permian time in response to compression from the Pyrenean and Alpine collisions, to sea-floor spreading in the Atlantic Ocean (Lagarde *et al*. 2003), and to deglacial processes in northern Europe (Chadwick *et al*. 1983, Cazes *et al*. 1985, Pham *et al*. 2000, Mansy *et al*. 2003, Minguely *et al*. 2005).

The rupture processes appear to occur randomly on any of the numerous faults of the Weald–Artois shear zone complex, a situation reminiscent of North America and Fennoscandia where the local state of stress associated with recurrent intraplate seismicity is attributable to post-glacial rebound (Zoback and Grollimund 2001, Camelbeeck *et al*. 2007, Mazzotti and Townend 2010). Given that horizontal extension near the English Channel is ascribable to such processes (Bungum *et al*. 2010), the Dover Strait structures are thus potentially good candidates for rupture in response to variations in residual glacial loading stresses. The different earthquakes recorded in the study area could potentially occur on any of the identified fault planes and could exhibit normal, inverse or strike-slip palaeo-mechanisms

For Peer Review

with a maximum credible earthquake magnitude of 7.0 (Camelbeeck *et al*. 2007, Bungum *et al*. 2010). Our goal is not to validate the 1580 rupture source parameters, which would require unavailable palaeoseismic data, but to test the effectiveness and spatial distribution of waves generated in the Dover Strait as a consequence of an earthquake either similar to the 1580 event — or of greater magnitude given the seismic record of intraplate faults in the region (Camelbeeck *et al*. 2007). Given that any such thought experiment, or model, requires a maximum scenario of potential use to tsunami hazard assessment and mitigation plans typically required by governments, here we have opted for an absolute worst case scenario of $M_W = 6.9$, which presents the advantage of affording maximum confidence in formulating conclusions about the magnitude of risk to human installations on the affected shores. Whether the 1580 earthquake, or indeed any other, was caused by post-glacial rebound rather than by any other source of stress accumulation is of little relevance to the model, which addresses the impact of a single event and cannot provide insight into recurrence intervals or earthquake scaling laws for the area.

2. Modelling of an earthquake-generated tsunami

2.1. Coseismic deformation

2.1.1. Quantitative constraints

Given the limited data available, we propose three hypothetical rupture mechanisms: extensional, compressional, and strike-slip. Due to uncertainty in locating the 1580 epicentre, rupturing could occur on many of the identified faults, with preference for those capable of accommodating a magnitude ~6.0 earthquake. A $M_L = 6.2–6.9$ value for 1580 (Neilson *et al*. 1984) was revised to $M_L = 6.1$ (Melville *et al*. 1996) and later to $M_L = 5.8$ (Musson 2004).

For Peer Review

Grünthal and Wahlström (2003) have since empirically determined the relationship between Richter local magnitude M_L and seismic moment magnitude M_W for NW Europe (eq. 1):

$$M_W = 0.67(\pm0.11) + 0.56(\pm0.08)M_L + 0.046(\pm0.013)M_L^2 \quad (1)$$

This converts $M_L = 5.8$ to an equivalent M_W of ~5.5. According to available tsunami catalogues (e.g. http://tsun.sscc.ru/On_line_Cat.htm; http://www.ngdc.noaa.gov/nndc/struts/form?t=101650&s=70&d=7), any plausible scenario should apply a critical earthquake magnitude of at least $M_W = 6.3$, which is the empirically established lower physical limit of tsunami generation. The few tsunami observed after $M_W <$ 6.3 earthquakes are generated by coseismic landslides or, more unusually, by so-called tsunami earthquakes (Okal and Newman 2001, Bilek and Lay 2002). Based on eq. 2 (Hanks and Kanamori 1979), this corresponds to a critical seismic moment of $M_O = 3.35 \cdot 10^{18}$ N·m:

$$M_W = (2/3) \log M_O - 6.05 \quad (2)$$

with M_O in N·m ($M_W = 0.66 \cdot \log M_O - 10.7$ when M_O is in Dyn·cm).

A $M_W = 5.5$ earthquake corresponds to $M_O = 2.1 \cdot 10^{17}$ N·m of energy released, i.e. one order of magnitude below the critical value. For comparison, the $M_W = 6.9$ Zemmouri–Boumerdès (Algeria) earthquake of May 2003, leading to tsunami waves ca. 2 m high in the Balearic Islands (Alasset *et al*. 2006), corresponded to an energy release of $M_O = 2.01 \cdot 10^{19}$ N·m (Dziewonski *et al*. 1981, Ekström *et al*. 2005).

Following the widely used relationships presented by Wells and Coppersmith (1994) for strike-slip faults, a (sub)-surface rupture length (L) of 10–50 km and a rupture area of 100–300 km² can be inferred for the 1580 event, leading to a plane width (l) of 10–15 km (keeping the ratio $l/L = 1/3$). Such a rupture length value is in good agreement with the maximum epicentral zonation of ~50 km obtained by Neilson *et al*. (1984) and Melville *et al*. (1996)

For Peer Review

(Fig. 2). In our model, we located the ruptured fault zone based on the studies of Neilson *et al*. (1984), who show a NW–SE-oriented rupture situated mainly onshore in France and extending into the Dover Strait, and of Melville *et al*. (1996), who concluded on a rupture situated in the Dover Strait and lacking extensions onshore. An average coseismic fault displacement of ~0.1–0.5 m is estimated from Wells and Coppersmith (1994). A range of focal depths was tested in the model scenarios. A 50° dip angle has been proposed in agreement with several seismic studies that show the fault plane geometry (e.g. Cazes *et al.* 1985, Mansy *et al*. 2003).

2.1.2. Rupture scenarios

As earthquakes in this area are infrequent, it remains difficult to determine the focal mechanism precisely. We tested an array of credible scenarios under three different magnitudes (M_W = 5.5, 6.3 and 6.9), with the first batch involving thrust faulting, the second normal faulting, and the third simulating a strike-slip displacement on the Weald–Artois fault zone. All rupture parameters (Table 1) were determined in agreement with the regional geology and the empirical relationships of Wells and Coppersmith (1994). Initial sea-floor deformation was generated by calculating elastic dislocation with the Okada (1985) formula.

The energy distribution (deformation lobes) at constant depth from the surface (450 m) for constant fault dip and rake angles show that a M_W = 5.5 earthquake similar to the 1580 event, with its epicenter located in the central Strait (Fig. 2a), is unable to generate a tsunami. A M_W = 6.3 earthquake produces sufficiently large sea-floor displacement (ca. 20 cm) to generate a tsunami (Fig. 2b). A M_W = 6.9 earthquake (Fig. 2c), i.e. our worst case scenario for this region, affects both sides of the Channel and generates a tsunami. Scenarios 2d and 2e confirm that a deformation greater than 20 cm can affect both sides of the Channel provided the rupture zone is appropriately located (Fig. 2). A M_W = 6.9 scenario involving thrust

For Peer Review

faulting with a different fault plane geometry (Table 1, Fig. 2f) reveals even greater initial deformation (the coseismic slip increases from 1.25 to 2.5 m for the same magnitude). Experiment 2f emphasizes that coseismic slip magnitude is a major parameter and that precise knowledge of the fault rupture location is critical for assessing the related hazard.

2.2. Tsunami generation and propagation: method and model results

Based on the tsunami calculation code developed by the Commissariat à l'Énergie Atomique, our method considers that the initial sea-floor deformation, computed through Okada's elastic dislocation formula, is transmitted without loss to the entire water column and satisfies the hydrodynamic equations of continuity (1) and conservation of motion (2):

$$\frac{\partial(\eta + h)}{\partial t} + \nabla.[v(\eta + h)] = 0 \qquad (1)$$

$$\frac{\partial v}{\partial t} + (v.\nabla).v = -g\nabla\eta \qquad (2)$$

where η corresponds to water elevation, h to water depth, v to the horizontal speed vector, while g is the gravity constant.

Non-linear terms are taken into account, and the resolution is carried out using a Crank–Nicolson finite difference method centered in time and using an upwind scheme in space. This method has been successfully applied in case studies in the Mediterranean Sea and the Atlantic Ocean (Roger and Hébert 2008, Sahal *et al*. 2009, Roger *et al*. 2010). Wave propagation was calculated over the 100 m resolution bathymetric grid of the Strait (Fig. 1) obtained by interpolation (kriging) of a digitized and georeferenced 1:115,000 scale bathymetric chart (Imray 2007).

Figure 3 reveals that an earthquake with a magnitude $M_W < 6.3$ (Fig. 3a) will not produce a significant tsunami, nor will a pure strike-slip event (not shown). Whether compressional or extensional, the worst case scenario ($M_W = 6.9$) is, however, capable of generating a

For Peer Review

maximum wave height (H_{max}) of at least 1 m along the Strait coasts. Some specific coastal sites are also shown to be more vulnerable to long-wave arrival than others. H_{max} values exceeding 1.5 m can, for example, be expected at coastal hotspots (i.e. Boulogne, Calais, Cap Gris-Nez, Dover, Romney Bay, Pegwell Bay) apparent in Figure 3 panels b, c, and d. Normal faulting (Fig. 3d) leads to different wave heights because on this west-dipping fault plane energy radiation is propagated towards the south-east of the Strait (see Fig. 2d), whereas reverse faulting promotes energy propagation towards the north-east. Even when applying a different geometry (Fig. 3c), however, tsunami wave arrivals still converge on the same coastal hotspots.

The virtual tide gauge records in Fig. 3e show that the signal generated at the centre of the Dover Strait promotes different wave heights and periods at different coastal locations. The synthetic mareograms indicate that Dover could suffer the greatest impact, with first wave heights of ca. 1.5 m. Calais, where the tsunami would arrive approximately at the same time (< 5 min), receives considerably smaller waves (H_{max} < 0.5 m). Boulogne and Romney Bay receive the same wave (H_{max} ≈ 0.5 m) at the same time (~20 min). Pegwell Bay, to the north, receives an 80 cm high wave 45 min after the main shock. These arrival times are in good agreement with the TTT isopleths shown in Figure 1.

3. Discussion

Model results of earthquake-generated tsunami waves for a seismic source situated mainly in the Dover Strait (Melville *et al*. 1996) rather than onshore (Neilson *et al*. 1984) show that a M_W = 6.9 scenario can trigger a tsunami exceeding 1 m in height. The wave will amplify (>> 1 m) in some well identified coastal locations that are prone to amplification (shoaling effect due to local bathymetric configurations not resolved by the water-depth source data available

For Peer Review

for this study) and/or to resonance phenomena. The capacity for wave generation with amplitudes of less than 50 cm is none the less significant because even low-amplitude tsunami waves can have catastrophic consequences due to the resonance or wave trapping effects of long waves in semi-enclosed basins and harbours (Bellotti 2007, Sahal *et al*. 2009). This could occur in addition to the fact that the Channel is already known to present a risk of resonance-related hazards under storm forcing conditions (Wells *et al*. 2005), suggesting that the tsunami long waves could operate in the same way. Figures 3e and 3f show that bathymetric features have a sharp impact on wave propagation and frequency content. Four maximum energy peaks at $2.8 \cdot 10^{-4}$ to $4.4 \cdot 10^{-4}$ Hz (i.e. 60 to 38 min) and $6.1 \cdot 10^{-4}$ to $7.5 \cdot 10^{-4}$ Hz (i.e. 27 min to 22 min) are visible on the six spectra; two lower period peaks around 6 and 10 min are also visible. They correspond to the main periods of the signal and are directly linked to the geometry of the fault plane or are locally associated with specific bathymetric features. The 6 min peak (0.0026 Hz), visible on the Dover and Calais signals, could be associated with the eigenperiod of the English Channel. This value is in agreement with the relationship $T = 2l/\sqrt{gh}$, where T is the internal resonance of an elongated channel of length l exhibiting a parabolic shape (Rabinovich 2009) with a central depth h. In the same way, the 1 h-period peak at Pegwell Bay could be caused by the resonance of the wave between the Goodwin Sands (a shallow offshore sand bank) and the bay. Romney Bay and Boulogne are perfect examples of high frequency attenuation due to the very low slope and lack of bathymetric features separating these places from the source region. They show the same profile, which is slightly more energetic at Romney. Although the tide factor has not been considered here, identical tests could be proposed for neap and spring high tides, where a maximizing scenario would consider a centennial high tide in conjunction with a sea-level rise and a storm surge.

For Peer Review

Another modelling result is that the tsunami travel times to either side of the Channel (Fig. 1) are extremely short, and certainly much shorter than the 15 to 20 min time span normally required by warning systems for evacuating beach users. An early warning system, international or otherwise, would therefore be of little use, the only viable approach being to educate the general public to the idea of vacating the beach immediately in case of a felt tremor. Model results also emphasize the low risk of coseismic tsunami occurrence in the Dover Strait, certainly much lower than the occurrence of storm waves which, in this region, can reach much greater heights (e.g. Lamb, 1991). Fortunately, storm waves are more predictable because of the storm tracking capabilities of modern meteorological monitoring technology.

4. Conclusion

The model scenarios proposed in this study of the Dover Strait emphasize the importance of documenting historical seismicity (e.g. Haslett and Bryant, 2008) but also of numerical simulation as complementary tools in assessing the need for tsunami-related risk mitigation measures around the shallow shelf seas of intraplate regions that seem tectonically quiescent. Unless previously published calculations of $M_W = 5.5$ turn out to be underestimates of the true 1580 event magnitude, modelling results here cast doubt on the view that the 1580 event gave rise to a coseismic tsunami, or at least that the destruction reported in the historical records was directly tsunami-related. Although this may have intuitively been a foregone conclusion on the basis that tsunami are not known to be generated by earthquake magnitudes less than $M_W = 6.3$ (see Fig. 3a), the reconstructions of historical palaeoseismology are inevitably less precise than those of instrumental seismology. Accordingly, existing interpretations of the March 6, 1580 event continue to nurture uncertainty (compare Melville *et al*. 1996 with

For Peer Review

Neilson *et al*. 1984, or Haslett & Bryant 2008 with Kerridge 2005). The modelling tests thus provide an independent, though not necessarily a definitive, reality check on either the precision (i.e. destruction did occur, but was storm-related and intervened hours or days after the earthquake) or the authenticity of some historical accounts. This is perhaps the only way of validating historical data independently unless and until coseismic off-fault tsunami deposits can be positively identified and dated in these intensely urbanized coastal environments. Modelling results also reveal that even for an improbable maximum scenario of $M_W = 6.9$, the main impacts of a tsunami would be on cross-Channel navigation due to the resonance potential of some of the large modern harbours. Awareness is also raised to possible impacts due to shoaling on shallow underwater megadunes such as the Goodwin Sands and near more sensitive built-up locations such as in Romney Bay, Pegwell Bay, around Boulogne, and north of Calais (Fig. 3d).

Acknowledgments. This study was funded by the MAREMOTI project, ANR-08-RISKNAT-05-01c and the Laboratoire de Recherche Conventionné CEA-ENS (LRC Yves Rocard). We are grateful to R. Musson (British Geological Survey), to M. Rodriguez, A. Rabaute, N. Chamot-Rooke, F. Vivent and P. Dubernet (École Normale Supérieure), and to J. Luis (Universidade do Algarve, Portugal) for their informal comments and assistance.

For Peer Review

References cited

Alasset, P.-J., Hébert, H., Maouche, S., Calbini, V. & Meghraoui, M., 2006. The tsunami induced by the 2003 Zemmouri earthquake (M_W=6.9, Algeria): modelling and results. *Geophysical Journal International*, **166**, 213–226.

Alexandre, P., 1990. *Les séismes en Europe occidentale de 394 à 1259. Nouveau catalogue critique*. Observatoire Royal de Belgique, Série Géophysique, Hors-série, Bruxelles, 267 p.

Bellotti, G., 2007. Transient response of harbours to long waves under resonance conditions. *Coastal Engineering*, **54**, 680–693.

Bilek, S.L. & Lay, T., 2002. Tsunami earthquakes, possibly widespread manifestations of frictional conditional stability, *Geophysical Research Letters*, 29(14), 1673, doi:10.1029/2002GL015215.

Bungum, H., Olesen, O., Pascal, C., Gibons, S., Lindholm, C. & Vestol, O., 2010. To what extent is the present seismicity of Norway driven by post-glacial rebound? *Journal of the Geological Society, London*, **167**, 373–384.

Camelbeeck, T., Vanneste, K., Alexandre, P., Verbeeck, K., Petermans, T., Rosset, P., Everaerts, M., Warnant, R. & Van Camp, M., 2007. Relevance of active faulting and seismicity studies to assessments of long-term earthquake activity and maximum magnitude in intraplate northwest Europe, between the Lower Rhine Embayment and the North Sea. *In*: Stein, S., and Mazzotti, S. (eds.), *Continental intraplate earthquakes: science, hazard, and policy issues*: Geological Society of America Special Paper **425**, 193–224.

Cazes, M., Torreilles, G., Bois, C., Damotte, B., Galdeano, A., Hirn, A., Mascle, A., Matte, P., Pham, N.V. & Raoult, J.-P., 1985. Structure de la croûte hercynienne du nord de la

For Peer Review

France: premiers résultats du profil ECORS. *Bulletin de la Société Géologique de France*, **I**, 925–941.

Chadwick, R.A., Kenolty, N. & Whittaker, A., 1983. Crustal structures beneath southern England from deep seismic reflection profiles. *Journal of the Geological Society, London*, **140**, 893–911.

Dziewonski, A.M., Chou, T.-A. & Woodhouse, J.H., 1981. Determination of earthquake source parameters from waveform data for studies of global and regional seismicity. *Journal of Geophysical Research*, **86**, 2825–2852.

Ekström, G., Dziewonski, A.M., Maternovskaya, N.N. & Nettles, M., 2005. Global seismicity of 2003: centroid-moment-tensor solutions for 1087 earthquakes. *Physics of the Earth and Planetary Interiors*, **148**, 327–351.

Grünthal G., & Wahlström, R., 2003. An Mw-based earthquake catalogue for central, northern and northwestern Europe using a hierarchy of magnitude conversions. *Journal of Seismology*, **7**, 507–531.

Hanks, T.C. & Kanamori, H., 1979. A moment magnitude scale. *Journal of Geophysical Research*, **84**, 2348–2350.

Haslett, S.K. & Bryant, E.A., 2008. Historic tsunami in Britain since AD 1000: a review, *Natural Hazards and Earth System Science*, **8**, 587–601.

Imray Ltd, 2007. *England South Coast, Dover Strait, North Foreland to Beachy Head and Boulogne*. Map C8, scale 1:115 000, 1 sheet.

Kerridge, D., 2005. *The threat posed by tsunami to the UK*, Study commissioned by Defra Flood Management and produced by the British Geological Survey, Proudman Oceanographic Laboratory, Met Office and HR Wallingford, 167 p.

Lagarde, J.L., Amorese, D., Font, M., Laville, E. & Dugué, O., 2003. The structural evolution of the English Channel area. *Journal of Quaternary Science*, **18**, 201–213.

For Peer Review

Lamb, H.H., 1991. *Historic storms of the North Sea, British Isles and Northwest Europe*. Cambridge, Cambridge University Press, 207 p.

Luis, J.F., 2007. Mirone: a multi-purpose tool for exploring grid data. *Computers & Geosciences*, **33**, 31–41.

Mansy, J.-L., Manby, G.M., Averbuch, O., Everaerts, M., Bergerat, F., Van Vliet-Lanoe, B., Lamarche, J. & Vandycke, S., 2003. Dynamics and inversion of the Mezozoic Basin of the Weald-Boulonnais area: role of basement reactivation. *Tectonophysics*, **373**, 161–179.

Mazzotti, S. & Townend, J., 2010. State of stress in eastern and central North America seismic zones. *Lithosphere*, **2**, 76–83.

Melville, C.P., Levret, A., Alexandre, P., Lambert, J. & Vogt, J., 1996. Historical seismicity of the Strait of Dover–Pas de Calais. *Terra Nova*, **8**, 626–647.

Minguely, B., Mansy, J.-L., Everaerts, M., Manby, G.M. & Averbuch, O., 2005. Apport de la modélisation géophysique pour la comprehension de la structuration du Pas de Calais. *Compte Rendus de Geoscience*, **337**, 305–313.

Musson, R.M.W., 2004. A critical history of British earthquakes. *Annals of Geophysics*, **47**, 597–609.

Neilson, G., Musson, R.M.W. & Burton, P.W., 1984. The "London" earthquake of 1580, April 6, *Engineering Geology*, **20**, 113–141.

Okal, E.A. & Newman, A.V., 2001. Tsunami earthquakes: the quest for a regional signal. *Physics of the Earth and Planetary Interiors*, **124**, 45–70.

Ottemöller, L., Baptie, B. & Smith, N.J.P., 2009. Source parameters for the 28 April 2007 Mw 4.0 earthquake in Folkestone, United Kingdom. *Bulletin of the Seismological Society of America*, **99**, 1853–1867.

For Peer Review

Pham, N.V., Boyer, D. & Le Mouël, J.-L., 2000. Nouveaux arguments sur l'origine de l'anomalie magnétique du Bassin parisien (AMBP) d'après les propriétés électriques de la croûte. *Compte Rendus de l'Académie des Sciences, Paris, Earth and Planetary Sciences*, **331**, 443–449.

Rabinovich, A.B., 2009. Seiches and harbor oscillations. *In*: Kim, Y.C. (ed.), *Handbook of coastal and ocean engineering*. London, Imperial College Press, p. 193–235.

Roger, J., Allgeyer, S., Hébert, H., Baptista, M.A., Loevenbruck, A. & Schindelé, F., 2010. The 1755 Lisbon tsunami in Guadeloupe Archipelago: source sensitivity and resonance effects. *The Open Oceanography Journal*, **4**, 58–70.

Roger, J. & Hébert, H., 2008. The 1856 Djijelli (Algeria) earthquake and tsunami: source parameters and implications for tsunami hazard in the Balearic Islands, *Natural Hazards and Earth System Sciences*, **8**, 721–731.

Sahal, A., Roger, J., Allgeyer, S., Lemaire, B., Hébert, H., Schindelé, F. & Lavigne, F., 2009. The tsunami triggered by the 21 May 2003 Boumerdes–Zemmouri (Algeria) earthquake: field investigations on the French Mediterranean coast and tsunami modelling. *Natural Hazards and Earth System Sciences*, **9**, 1823–1834.

Wells, D.L. & Coppersmith, K.J., 1994. New empirical relationships among magnitude, rupture length, rupture width, rupture area, and surface displacement. *Bulletin of the Seismological Society of America*, **84**, 974–1002.

Wells, N.C., Baldwin, D. & Haigh, I., 2005. Seiches induced by storms in the English Channel. *Journal of Atmospheric and Ocean Science*, **10**, 1–14.

Zoback, M.D. & Grollimund, B., 2001. Impact of deglaciation on present-day intraplate seismicity in eastern North America and western Europe. *Compte Rendus de l'Académie des Sciences, Paris, Earth and Planetary Sciences*, **333**, 23–33.

For Peer Review

Figure and table captions

Figure 1. Location of the Dover Strait and its main coastal towns (projection: WGS 1984), with regional fault pattern, historical seismicity and isoseismals for the 1580 earthquake. The relief grid combines Shuttle Radar Topography Mission data on land and a digitized, georeferenced and interpolated 1:115,000 scale bathymetric chart (Imray 2007) of the Dover Strait. Blue dots are sites of seismicity recorded since 1973 (http://earthquake.usgs.gov/earthquakes/eqarchives/epic/). Tsunami travel times (TTT) of the first arrival are in minutes and are computed using the Mirone program (Luis 2007). They are generated by a point source located at the center of the Dover Strait. Coasts where continental elevations exceed 30 m are dominated by sea-cliffs.

Figure 2. Initial sea-floor deformation, in metres, computed for six different scenarios. a, b, c: compression for different indicated magnitudes; d: extensional mechanism; e: pure dextral strike-slip; f: compression with a different fault plane geometry and $M_W = 6.9$. Black dots indicate virtual tide gauge locations. Black rectangles show the fault plane geometries. Isoseismal line intensity VII according to Melville *et al*. (1996) is located in c.

Figure 3. Wave propagation models. a, b, c, d: maximum wave heights (H_{max}) for four scenarios after 90 minutes of tsunami propagation. Black areas represent shallow water, e.g. offshore sand banks or coastal beaches. Black circles indicate virtual tide gauge locations. e: synthetic mareograms at five virtual tide gauges for a $M_W = 6.9$ earthquake-generated tsunami. The virtual gauges are located in identical water depths of 1 m. f: amplitude spectra of the synthetic tide gauge signal computed for six coastal locations.

For Peer Review

TABLE 1. PARAMETERS FOR THE SIX MODELLED SCENARIOS

For Peer Review

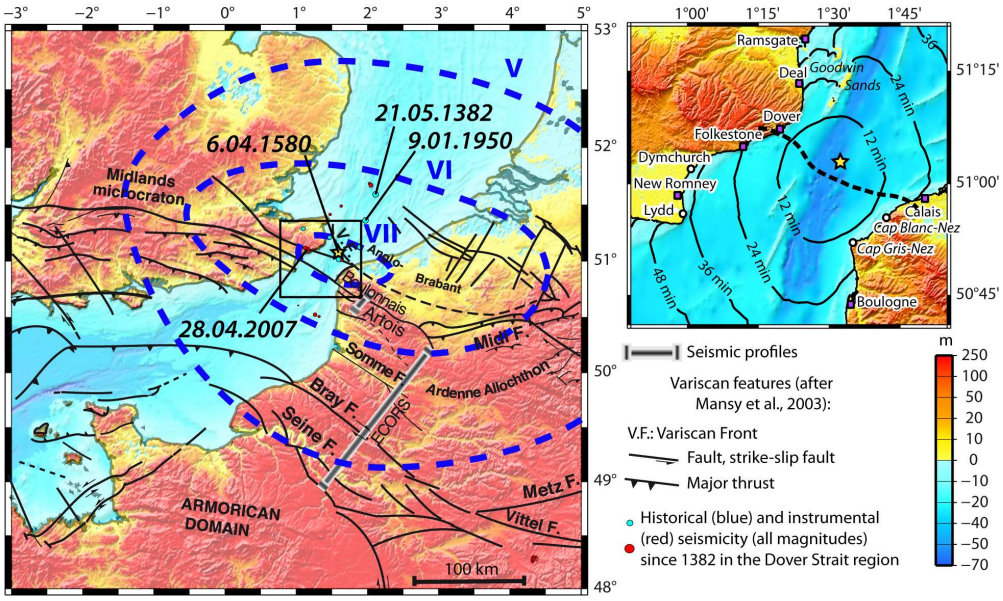

Figure 1. Location of the Dover Strait and its main coastal towns (projection: WGS 1984), with regional fault pattern, historical seismicity and isoseismals for the 1580 earthquake. The relief grid combines Shuttle Radar Topography Mission data on land and a digitized, georeferenced and interpolated 1:115,000 scale bathymetric chart (Imray 2007) of the Dover Strait. Blue dots are sites of seismicity recorded since 1973 (http://earthquake.usgs.gov/earthquakes/eqarchives/epic/). Tsunami travel times (TTT) of the first arrival are in minutes and are computed using the Mirone program (Luis 2007). They are generated by a point source located at the center of the Dover Strait. Coasts where continental elevations exceed 30 m are dominated by sea-cliffs.
166x98mm (300 x 300 DPI)

eview

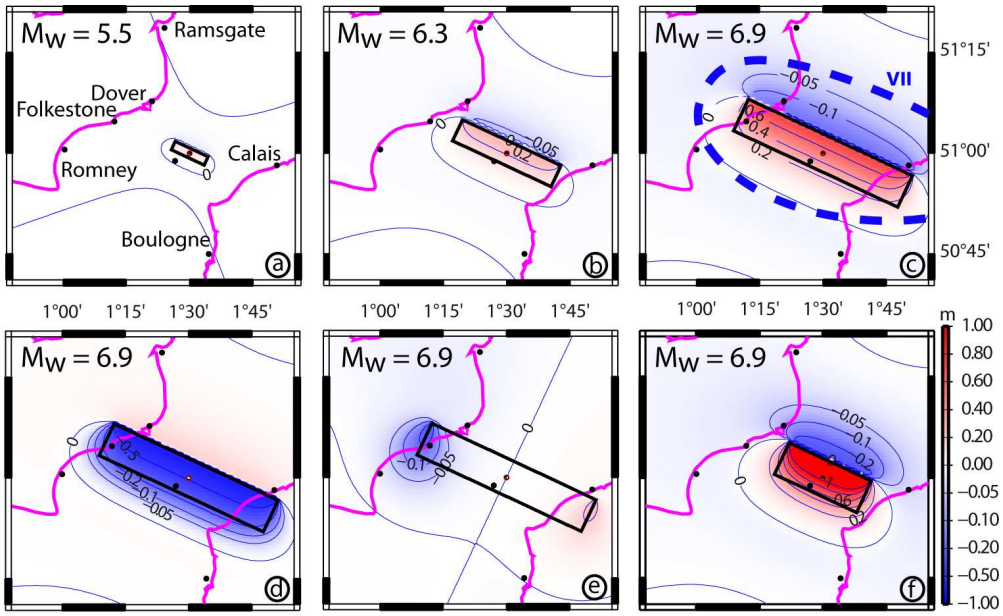

Figure 2. Initial sea-floor deformation, in metres, computed for six different scenarios. a, b, c: compression for different indicated magnitudes; d: extensional mechanism; e: pure dextral strike-slip; f: compression with a different fault plane geometry and MW = 6.9. Black dots indicate virtual tide gauge locations. Black rectangles show the fault plane geometries. Isoseismal line intensity VII according to Melville et al. (1996) is located in c.
128x78mm (300 x 300 DPI)

For Review

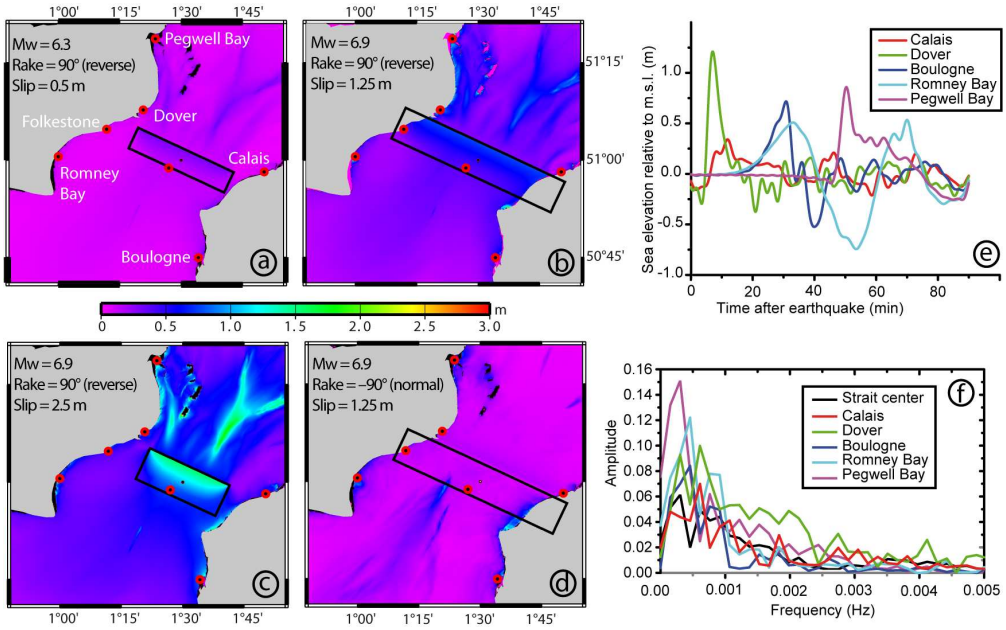

Figure 3. Wave propagation models. a, b, c, d: maximum wave heights (Hmax) for four scenarios after 90 minutes of tsunami propagation. Black areas represent shallow water, e.g. offshore sand banks or coastal beaches. Black circles indicate virtual tide gauge locations. e: synthetic mareograms at five virtual tide gauges for a MW = 6.9 earthquake-generated tsunami. The virtual gauges are located in identical water depths of 1 m. f: amplitude spectra of the synthetic tide gauge signal computed for six coastal locations.
147x92mm (300 x 300 DPI)

For Review

Scenario (see Fig. 2)		Depth of fault plane center* (km)	Fault plane dimensions** (km)		Coseismic slip (m)	Rake (°)	Seismic moment (M_O) (N·m)	Magnitude (M_W)
			L	W				
Compressional	a	2.0	10	4	0.2	90	2.4E+17	5.5
	b	4.3	30	10	0.5	90	4.5E+18	6.3
	c	6.2	50	15	1.25	90	2.8E+19	6.9
	f	6.2	25	15	2.5	90	2.8E+19	6.9
Strike-slip	e	6.2	50	15	1.25	0	2.8E+19	6.9
Extensional	d	6.2	5	15	1.25	–90	2.8E+19	6.9

* Fault-plane depths imply that the fault terminates 450 m beneath the sea floor, in accordance with existing seismic profile analyses.

** In each scenario, the fault plane center is situated at 51°N and 1.5°E with a N115° strike and a 50° dip.

For Peer Review

Partie 4

Conclusion générale

4) Conclusions et perspectives

4.1 Conclusions générales

Le travail présenté dans cette thèse représente un large panel des activités réalisées dans le domaine en plein essor de la recherche sur les tsunamis. Il comprend l'évaluation du risque tsunami, passant nécessairement par une connaissance de l'aléa, l'objectif final étant la mitigation (atténuation) de ce risque. La connaissance des évènements, associée à la recherche de documents historiques contemporains, aux enquêtes post-évènements ou à des campagnes de prospections sur le terrain à la recherche de dépôts sédimentaires, y est fortement soulignée. La reproductibilité des tsunamis observés par la modélisation numérique nécessite d'une part une bonne connaissance des mécanismes à l'origine des tsunamis, essentielle pour pouvoir évaluer correctement l'aléa. Pour cela, des données bathymétriques/topographiques reproduisant correctement les zones étudiées sont un éléments primordial comme le montrent principalement les études de l'impact du tsunami de Lisbonne de 1755 aux Antilles ou de celui de Zemmouri de 2003 dans le sud de la France : plus particulièrement, l'étude réalisée dans le cadre de cette thèse sur l'impact du tsunami de 1755 en Martinique (Roger et al., 2010b) montre pourquoi il est important de reproduire la bathymétrie ainsi que les formes des objets sous-marins (canyons, récifs submergés, etc.) le mieux possible dans les modèles numériques de terrain (MNT) utilisés pour modéliser la propagation d'un tsunami, aussi bien au large qu'à l'approche des côtes ('*shoaling*' et inondation).

Au travers de plusieurs évènements clés, les études menées au cours de cette thèse montrent que le risque associé à l'aléa tsunami en Méditerranée occidentale, bien qu'étant une réalité, comme dans tous les bassins en définitive, est très limité : d'une part parce que très peu d'évènements (origine sismique et glissements de terrains confondus) on été répertoriés (11 évènements) sur une période de temps très grande (700 ans) contrairement à la Méditerranée orientale ; d'autre part les amplitudes maximum de tsunami que l'on peut y observer atteignent une moyenne de 2 m en des points bien spécifiques qui réagissent particulièrement bien aux arrivées d'ondes longues du fait de phénomènes de focalisation d'onde (au niveau de canyons sous-marins par exemple) ou de '*wave trapping*', ou encore de phénomènes de résonance associés à la géométrie des ports, baies, lagons, etc. ; la majorité d'entre eux n'ont eu des conséquences en terme de pertes humaines et dégâts matériels que localement (mis à part les tsunamis de 1856 et 2003), ce qui est souvent attribuable à leur

origine due à un glissement de terrain. Ce mécanisme de génération pose par ailleurs un réel problème car, contrairement à un séisme qui peut faire office de sonnette d'alarme et prévenir qu'un tsunami peut avoir été généré par une secousse d'une certaine magnitude (estimée aux alentours de 6.0 mais dont on fixera le seuil plus bas dans la matrice de décision des systèmes d'alerte pour des raisons de sécurité), un glissement de terrain n'est à ce jour pas détectable en mer et donc aucune alerte ne peut être diffusée.

La mise en place d'un système d'alerte en Méditerranée occidentale est-elle alors bien justifiée à la vue de ces constatations et résultats d'études ?

De plus, le fonctionnement efficace d'un système d'alerte nécessite des moyens financiers conséquents et du personnel d'astreinte 24h/24, 7jours/7 ce qui n'est pas forcément raisonnable dans une zone ou la période de retour des tsunamis d'origine sismique potentiellement dangereux (impact moyen) est de plus de 50 ans. Enfin, sommes-nous prêt à gérer l'alerte descendante, c'est-à-dire l'évacuation des côtes en cas d'arrivée de tsunamis ?

Néanmoins, ces observations ne signifient pas que le risque est négligeable : en effet, les résultats des diverses simulations montrent que des études approfondies devraient être menées pour l'intégration du risque d'inondation associé à l'aléa tsunami dans les plans de prévention du risque submersion marine (PPR submersion) actuel, aussi bien en France que dans les pays du pourtour méditerranéen, et surtout dans les îles Baléares qui semblent être particulièrement exposées à l'aléa tsunami, faisant même office de bouclier protecteur pour le sud de la France dans la majeure partie des cas testés avec une source au niveau de la marge algérienne. De plus, les travaux concernant l'impact du tsunami de 2003 dans le sud de la France (Sahal et al., 2009, partie 3.1.1) montrent que des études approfondies de résonnance portuaire[1] devraient également être menées avec pour objectif de mesurer la période propre des bassins portuaires et de modifier leur géométrie afin de les rendre moins réactifs aux ondes longues de type tsunami (Bellotti, 2007 ; Gonzalez-Marco et al., 2008).

Pour ce qui concerne l'Atlantique nord, le golfe de Cadix reste un endroit problématique puisque d'un part on ne connait pas avec certitude la tectonique de la région, et que d'autre part, nous y trouvons l'origine d'un des 10 plus gros tsunamis jamais observés sur Terre : le tsunami de Lisbonne de 1755. Plusieurs autres tsunamis y ont été répertoriés mais

[1] Chaque port possède un mode oscillatoire auquel est associée une période de résonnance ou période propre (Jansa et al., 2007) qui est directement relié à sa géométrie et sa profondeur (Monso de Prat et Escartin Garcia, 1994 ; Woo et al., 2004).

sans qu'ils aient les mêmes caractéristiques dévastatrices de celui du 1er Novembre 1755 (excepté peut être ceux de 1722 de 1761, Baptista et al., 2006). En effet, les études menées en détail sur les îles de Guadeloupe et Martinique ont mis en évidence le fait qu'elles sont particulièrement exposées à un tsunami provenant de la péninsule ibérique. D'ailleurs, la réalisation d'un catalogue des tsunamis en Martinique au cours de cette thèse a permis de mettre en évidence le fait que, bien qu'ayant été généré à 6000 km de la source, le tsunami de 1755 reste l'évènement de référence pour cette île en terme d'évaluation des zones à risques associé à l'aléa tsunami. De la même façon, l'étude de ce même tsunami et de son impact sur les côtes canadiennes de Terre-Neuve a montré qu'une source localisée sur la marge est de l'Atlantique nord devrait être considérée dans les plans d'évaluation et de mitigation du risque tsunami sur les côtes canadiennes, au même titre que les tsunamis associés aux glissements de terrain géants du même type que celui de Grand Bank de 1929.

En marge de ces études d'impact de tsunami, je me suis aussi intéressé de manière détaillée aux sources sismiques à l'origine de certains de ces tsunamis.

Ainsi l'étude du séisme de El Asnam de 1580 montre qu'une source localisée entièrement à terre est néanmoins capable de générer un tsunami sans considérer de quelconques glissements de terrain annexes ou autres courants de turbidité mais seulement du fait de la répartition de la déformation initiale attribuée à la rupture et au relâchement des contraintes. Ce point est important à souligné car il a permis de réviser la matrice de décision pour le système d'alerte de Méditerranée occidentale (CRATANEM) quand à la distance maximum à la côte à partir de laquelle on ne déclenche plus d'alerte en cas de séisme d'une certaine magnitude.

Le détroit de Douvres reste également une zone très délicate en terme de risque tsunami, d'une part à cause de la proximité des côtes (la largeur du détroit mesure environ 32 km) et d'autre part du fait de sa fréquentation qui en fait une des zones les plus traversée au monde. L'estimation du risque dans cette région sismiquement active y est assez difficile puisque les mécanismes à l'origine du seul évènement connu répertorié en 1580 et présenté dans cette thèse sont finalement très mal connus. En effet, dans l'article soumis à la revue *Geology* (partie 3.2.5) nous proposons une origine sismique pour ce tsunami apparemment dévastateur des deux côtés du détroit, en justifiant un séisme de magnitude supérieur à 6.0 avec la réactivation des failles hercynienne sous le jeu des contraintes associé au rebond post-glaciaire du bouclier scandinave. Mais ce tsunami pourrait très bien avoir été généré par un glissement de terrain au niveau des falaises de Calais ou de Douvres ou des deux, sous l'effet

du séisme. Une étude de modélisation est en cours pour estimer le potentiel qu'aurait un tel évènement gravitaire à générer un tsunami capable d'avoir des conséquences significatives des deux côtés du détroit.

4.2 Perspectives

Je ne reviendrais pas plus ici sur l'étude sur le détroit de Douvres qui doit être finalisée sous peu.

En revanche, une étude est en cours concernant la source du séisme de 1755 dans le golfe de Cadix. Après avoir fait une synthèse de tous les travaux qui ont été menés dans la région au cours des dernières décennies, je me suis lancé, avec Alain Rabaute, dans la réalisation d'une carte morpho-tectonique (*en cours*) avec (in-)validation des interprétations préexistantes, sur la base des nombreux mécanismes au foyer disponibles, de la sismicité, des levés bathymétriques et des profils sismiques. En effet j'émets l'hypothèse que le séisme de 1755 peut avoir été initié suite à une rupture des contraintes accumulées au niveau du banc de Gorringe du fait de très gros séismes en décrochements (dont celui du 25 novembre 1941, d'une magnitude de 8.3, qui semble être le plus gros séisme en décrochement enregistré) sur la faille transformante de Gloria, reliant les Açores au détroit de Gibraltar. Une rupture simultanée sur la faille de Gloria (en décrochement) et le banc de Gorringe (en mouvement de compression sur une faille inverse) permettrait de proposer un scénario capable de générer un séisme de magnitude supérieure à 8.5 tout en restant en accord avec les lois empiriques de géologie reliant principalement la longueur de rupture à la magnitude et au glissement cosismique.

Concernant le séisme d'El Asnam de 1980, une seconde étude devrait être menée sur le séisme de 1954 localisé à proximité d'El Asnam afin de confirmer l'hypothèse d'une origine sismique du tsunami. En effet, nous disposons également de données d'enregistrements marégraphiques en 1954 mettant en évidence elles aussi l'arrivée d'un tsunami sur la côte espagnole. Du fait de ruptures de câbles sous-marins consécutives à la secousse, ce tsunami a été attribué à un glissement de terrain sous-marin. Or, au même titre que les enregistrements de 1980, les périodes de tsunami enregistrées ne sont pas du tout dans la gamme des glissements de terrain, mais bien dans celle des séismes.

Finalement, j'aimerais m'intéresser de plus près à la protection naturelle des côtes françaises par les barrières de corail principalement en Martinique mais aussi en Nouvelle-Calédonie, lieu également très touchés par les tsunamis (Sahal et al., 2010). En Martinique, il est important d'indiquer ici que depuis plusieurs années les coraux meurent progressivement. Ceci est apparemment la conséquence doublée de phénomènes naturels et anthropiques comme la pollution ou la surpêche dans ces zones très riches en biodiversité (Bouchon et al., 2008 ; Legrand et al., 2008). Des côtes jusque là à l'abri des vagues de tout type, vont se voir petit à petit exposées et probablement soumises à l'aléa tsunami ; quel sera alors l'impact d'un tsunami sur cette côte sans barrière de corail protectrice et constituée de nombreuses baies ?

Bibliographie

Références partie 1.1

Amara, R. (2010). Impact de l'anthropisation sur la biodiversité et le fonctionnement des écosystèmes marins. Exemple de la Manche-mer du nord. VertigO - la revue électronique en sciences de l'environnement, Hors-série 8 | octobre 2010. URL: http://vertigo.revues.org/10129.

Bogardi, J.J. (2004). Hazards, risks and vulnerabilities in a changing environment: the unexpected onslaught on human security ? Global Environmental Change, 14, 361-365.

Bryant, E.A. (2005). Natural Hazards. 2nd Edition, Cambridge University Press, Cambridge, 312 pp.

Bryant, E.A., Head, L., Morrison, J. (2005). Planning for natural hazards – How can we mitigate the impacts ? Faculty of Science – papers, 1-11. http://ro.uow.edu.au/scipapers/59

Dubois-Maury, J. (2005). Les risques naturels et technologiques. La documentation française, Problèmes politiques et sociaux, 908, 120 pp.

Intergovernmental Oceanographic Commission, 2005. Intergovernmental coordination group for the tsunami early warning and mitigation system in the North-Eastern Atlantic, the Mediterranean and connected seas. UNESCO, Resolution XXIII-14. http://www.ioc-tsunami.org/components/com_pdffarm/files/Resolution23_14.pdf

McBean, G., Ajibade, I. (2009). Climate change, related hazards and human settlements. Current Opinion in Environmental Sustainability, 1, 179-186.

Ministry for the Environment (2008). Coastal Hazards and Climate Change. A Guidance Manual for Local Government in New Zealand. 2nd edition. Revised by Ramsay, D, and Bell, R. (NIWA). Prepared for Ministry for the Environment. viii+127 pp. http://www.mfe.govt.nz/publications/climate/coastal-hazards-climate-change-guidance-manual/coastal-hazards-climate-change-guidance-manual.pdf

Rudloff, A., Lauterjung, J., Münch, U., Tinti, S. (2009). The GITEWS Project (German-Indonesian Tsunami Early Warning System). Natural Hazards and Earth System Sciences, 9, 1381-1382.

Stanchev, H., Palazov, A., Stancheva, M. (2009). 3D GIS model for flood risk assessment of Varna Bay due to extreme sea level rise. Journal of Coastal Research, SI 56 (Proceedings of the 10th International Coastal Symposium), 1597-1601. Lisbon, Portugal, ISSN 0749-0258.

Szlafsztein, C.F. (2005). Climate change, sea-level rise and coastal natural hazards: a GIS-based vulnerability assessment, state of Para, Brazil. International Workshop on Climate Change and Human Security, Oslo, Norway, 1-31.

Tinti, S. (2005). Tsunami research needs in Europe. Working document version 1, Outcome of the consultation meetings on Tsunami risk in Europe: status, gaps and needs related to

early warning systems. European Commission DG Research, Environment Programme, Unit: Environment and climate systems I.4, 12 pp.

Woods, R. (2008). Tsunami hazard for Otago. ORC Committee Report n°2008/002, File EN7010. www.orc.govt.nz

Références partie 1.2

Borrero, J.C., Synolakis, C.E., Fritz, H. (2006). Northern Sumatra field survey after the December 2004 great Sumatra earthquake and Indian Ocean tsunami. Earthquake Spectra, 22(S3), S93-S104.

Cartwright, J.H.E., Nakamura, H. (2008). Tsunami: a history of the term and of scientific understanding of the phenomenon in Japanese and Western culture. Notes and Records of the Royal Society, 62, 151-166. doi: 10.1098/rsnr.2007.0038

Cartwright, J.H.E., Nakamura, H. (2009). What kind of a wave is Hokusai's great wave off Kanagawa? Notes and Records of the Royal Society, 63, 119-135. doi: 10.1098/rsnr.2007.0039

Choi, B.H., Pelinovsky, E., Kim, K.O., Lee, J.S. (2003). Simulation of the trans-oceanic tsunami propagation due to the 1883 Krakatau volcanic eruption. Natural Hazards and Earth System Sciences, 3, 321-332.

Fine, I.V., Rabinovich, A.B., Bornhold, B.D., Thomson, R.E., Kulikov, E.A. (2005). The Grand Banks landslide-generated tsunami of November 18, 1929: preliminary analysis and numerical modeling. Marine Geology, 215, 45-57.

Fritz, H.M., Mohammed, F., Yoo, J. (2009). Lituya Bay landslide impact generated mega-tsunami 50th anniversary. Pure and Applied Geophysics, 166(1-2), 153-175.

Greenberg, D.A., Murty, T.S., Ruffman, A. (1993). A numerical model for the Halifax harbor tsunami due to the 1917 explosion. Marine Geodesy, 16(2), 153-167.

Harbitz, C.B., Lovholt, F., Pedersen, G., Masson, D.G. (2006). Mechanisms of tsunami generation by submarine landslides: a short review. Norwegian Journal of Geology, 86, 255-264.

Hills, J.G., Mader, C.L. (1997). Tsunami produced by the impacts of small asteroids. Annals of the New York Academy of Sciences, 822, 381-394. doi: 10.1111/j.1749-6632.1997.tb48352.x.

Intergovernmental Oceanographic Commission (2008). Tsunami Glossary, 2008. Paris, UNESCO. IOC Technical Series, 85, 36 pp. http://ioc3.unesco.org/itic/contents.php?id=328

Jansa, A., Monserrat, S., Gomis, D. (2007). The rissaga of 15 June 2006 in Ciutadella (Menorca), a meteorological tsunami. Advances in Geosciences, 12, 1-4.

Kowalik, Z., Proshutinsky, T., Proshutinsky, A. (2006). Tide-tsunami interactions. Science of Tsunami Hazards, 24(4), 242-256.

Kowalik, Z., Proshutinsky, A. (2010). Tsunami-tide interactions : a Cook inlet case study. Continental Shelf research, 30(6), 633-642.

Mattioli, G.S., Voight, B., Linde, A.T., Sacks, I.S., Watts, P., Widiwijayanti, C., Young, S.R., Hidayat, D., Elsworth, D., Malin, P.E., Shalev, E., Van Boskirk, E., Johnston, W., Sparks, R.S.J., Neuberg, J., Bass, V., Dunkley, P., Herd, R., Syers, T., Williams, P., Williams, D. (2007). Unique and remarkable dilatometer measurements of pyroclastic flow-generated tsunamis. Geology, 35(1), 25-28.

Monserrat, S., Vilibic, I., Rabinovich, A.B. (2006). Meteotsunamis: atmospherically induced destructive ocean waves in the tsunami frequency band. Natural Hazards and Earth System Sciences, 6, 1035-1051.

Murty, T.S., Loomis, H.G. (1980). A new objective tsunami magnitude scale. Marine Geodesy, 4(3), 267-282.

Murty, T.S., Stronach, J.A. (1989). State of tide and tsunami threat to the Pacific Coast of Canada. Natural Hazards, 2, 83-86.

Occhipinti, G. (2006). Observations multi-paramètres et modélisation de la signature ionosphérique du grand séisme de Sumatra. Thèse de doctorat de l'Institut de Physique du Globe de Paris, 229 pp.

Occhipinti, G., Lognonné, P., Kherani, A., Hébert, H. (2006). Three-dimensional waveform modeling of ionospheric signature induced by the 2004 Sumatra tsunami. Geophysical Research Letters, 33, L20104. doi:10.1029/2006GL026865.

Occhipinti, G., Komjathy, A., Lognonné, P. (2008a). Tsunami detection by GPS: how ionospheric observation might improve the Global Warning System. GPS World, 50-56.

Occhipinti, G., Kherani, E.A., Lognonné, P. (2008b). Geomagnetic dependence of ionospheric disturbances induced by tsunamigenic internal gravity waves. Geophysical Journal International, 173(3), 753-765.

Okal, E.A., Piatanesi, A., Heinrich, P. (1999). Tsunami detection by satellite altimetry. Journal of Geophysical Research, 104(B1), 599-615.

Paine, M.P. (1999). Asteroid impacts : the extra hazard due to tsunami. Science of Tsunami Hazards, 17(3), 155-166.

Papadopoulos, G.A. (2003). Quantification of tsunamis: a review. In: Submarine Landslides and Tsunamis (edited by A.C. Yalçiner, E.N. Pelinovsky, E. Okal and C.E. Synolakis). Proceedings of the NATO Advanced Research Workshop, Istanbul, Turkey, Kluwer Academic Publishers, Dordrecht, The Netherlands.

Paris, R., Roger, J., Wassmer, P., Loevenbruck, A. (2008). Témoignages et signature sédimentaire des tsunamis aux Baléares. Rapport d'études pour le CEA, 15 pp.

Paris, R., Wassmer, P., Sartohaldi, J., Lavigne, F., Barthomeuf, B., Desgages, E., Grancher, D., Baumert, P., Vautier, F., Brunstein, D., Gomez, C. (2009). Tsunamis as geomorphic crises: lessons from the December 26, 2004 tsunami in Lhok Nga, West Banda Aceh (Sumatra, Indonesia). Geomorphology, 104, 59-72.

Rabinovich, A.B., Monserrat, S. (1998). Generation of meteorological tsunamis (large amplitude seiches) near the Balearic and Kuril Islands. Natural Hazards, 18, 27-55.

Satake, K., Tanioka, Y. (1999). Sources of tsunami and tsunamigenic earthquakes in subduction zones. Pure and Applied Geophysics, 154, 467-483.

Sepic, J., Vilibic, I., Monserrat, S. (2009). Teleconnections between the Adriatic and the Balearic meteotsunamis. Physics and Chemistry of the Earth, Parts A/B/C, 34(17-18), 928-937.

Shuto, N. (1993). Tsunami intensity and disasters. Advances in Natural and Technological Hazards Research, Kluwer Academic Publishers, 1, 197-215.

Smith, W.H.F., Scharroo, R., Titov, V.V., Arcas, D., Arbic, B.K. (2005). Satellite altimeters measure tsunami. Oceanography, 18(2), 11-13.

Soloviev, S.L. (1970). Recurrence of tsunamis in the Pacific. In: Tsunamis in the Pacific Ocean (edited by W.M. Adams), East-West Center Press, Honolulu, 149-163.

Synolakis, C.E. (2004). Tsunami and Seiche. In: Earthquake Engineering Handbook, edited by Chen, W.F and Scawthorn, C., CRC Press, 9-1 to 9-90.

Tsuji, Y., Namegaya, Y., Matsumoto, H., Iwasaki, S.-I., Kanbua, W., Sriwichai, M., Meesuk, V. (2006). The 2004 Indian tsunami in Thailand: surveyed runup heights and tide gauge records. Earth Planets Space, 58, 223-232.

Van Dorn, W.G., LeMehaute, B., Hwang, L.-S. (1968). Handbook of explosion-generated water waves. Volume 1 – state of the art. Tetra Tech Report, TC-130, 174 pp.

Vilibic, I. (2005). Numerical study of the Middle Adriatic coastal waters' sensitivity to the various air pressure travelling disturbances. Annales Geophysicae, 23, 3569-3578.

Vilibic, I., Beg Paklar, G. (2006). High-frequency atmospherically-induced oscillations in the middle Adriatic coastal area. Annales Geophysicae., 24, 2759-2771.

Ward, S.N. (2001). Landslide tsunami. Journal of Geophysical Research, 106, 11201-11215.

Ward, S. N., Asphaug, E. (2000). Asteroid impact tsunami: A probabilistic hazard assessment. Icarus 145, 64-78.

Watts, P., Waythomas, C.F. (2003). Theoretical analysis of tsunami generation by pyroclastic flows. Journal of Geophysical Research, 108(B12), EPM4.1-EPM4.21.

Weisz, R., Winter, C. (2005). Tsunami, tides and run-up : a numerical study. Proceedings of the International Tsunami Symposium, Eds. : G.A. Papadopoulos and K. Satake, Cahnia, Greece, 27-29 June 2005, 322.

Références partie 1.3

Andrade, C., Broges, P., Freitas, M.C. (2006). Historical tsunami in the Azores archipelago (Portugal). Journal of Volcanology and Geothermal Research, 156(1-2), 172-185.

Baptista, M.A., Heitor, S., Miranda, J.M., Miranda, P., Mendes Victor, L. (1998a). The 1755 Lisbon tsunami; evaluation of the tsunami parameters. Journal of Geodynamics, 25(2), 143-157.

Baptista, M.A., Miranda P.M.A., Miranda, J.M., Mendes Victor, L. (1998b). Constraints on the source of the 1755 Lisbon tsunami inferred from numerical modelling of historical data. Journal of Geodynamics, 25(2), 159-174.

Baptista, M.A., Miranda, P.M.A., Miranda, J.M., Mendes Victor, L. (1996). Rupture extent of the 1755 Lisbon earthquake inferred from numerical modeling of tsunami data. Phys. Chem. Earth, 21(12), 65-70.

Baptista, M.A., Miranda, J.M., Chierici, F., Zitellini, N. (2003). New study of the 1755 earthquake source based on multi-channel seismic survey data and tsunami modeling. Natural Hazards and Earth System Sciences, 3, 333-340.

Barkan, R., Brink (ten), U., Lin, J. (2009). Far field tsunami simulations of the 1755 Lisbon earthquake: implications for tsunami hazard to the U.S. East Coast and the Caribbean. Marine Geology, 264, 109–122.

Bondevik, S., Lovholt, F., Harbitz, C., Mangerud, J., Dawson, A., Svendsen, J.I. (2005). The Storegga Slide tsunami: comparing field observations with numerical simulations. Marine and Petroleum Geology, 22(1-2), 195-208.

Brink (ten), U. (2009). Tsunami hazard along the U.S. Atlantic coast. Marine Geology, 264(1-2), 1-3.

Dawson, A.G., Long, D., Smith, D.E. (1988). The Storegga slides: evidence from eastern Scotland for a possible tsunami. Marine Geology, 82(3-4), 271-276.

Dawson, A.G., Lockett, P., Shi, S. (2004). Tsunami hazards in Europe. Environment International, 30, 577–585.

Gjevik, B., Pederson, G., Dybesland, E., Miranda, P. M., Baptista, M. A., Heinrich, P., and Massinon, B. (1997). Modelling tsunamis from earthquake sources near Gorringe Bank southwest of Portugal, J. Geophys. Res., 102, C13, 27 931–27 949.

Goodman-Tchernov, B.N., Dey, H.W., Reinhardt, E.G., McCoy, F., Mart, Y. (2009). Tsunami waves generated by the Santorini eruption reached Eastern Mediterranean shores. Geology, 37(10), 943-946. doi: 10.1130/G25704A.1

Gutscher, M.-A., Baptista, M.A., Miranda, J.M. (2006). The Gibraltar Arc seismogenic zone (part 2): Constraints on a shallow east dipping fault plane source for the 1755 Lisbon earthquake provided by tsunami modeling and seismic intensity. Tectonophysics, 426, 153-166.

Haslett, S.K., Bryant, E.A. (2007). Reconnaissance of historic (post-AD 1000) high-energy deposits along the Atlantic coasts of southwest Britain, Ireland and Brittany, France. Marine Geology, 242(1-3), 207-220.

Horsburgh, K.J., Wilson, C., Baptie, B.J., Cooper, A., Cresswell, D., Musson, R.M.W., Ottemöller, L., Richardson, S., Sargeant, S.L. (2008). Impact of a Lisbon-type tsunami on the U.K. coastline and the implications for tsunami propagation over broad continental shelves. Journal of Geophysical Research, 113, C04007. doi: 10.1029/2007JC004425.

Johnston, A. (1996). Seismic moment assessment of earthquakes in stable continental regions - III. New Madrid, 1811 – 1812, Charleston 1886 and Lisbon 1755. Geophysical Journal International, 126, 314– 344.

Kaabouben, F., Baptista, M.A., Iben Brahim, A., El Mouraouah, A., Toto, A. (2009). On the Moroccan tsunami catalogue. Natural Hazards and Earth System Sciences, 9, 1227-1236.

Levret, A. (1991). The effects of the November 1, 1755 Lisbon earthquake in Morocco. Tectonophysics, 193(1-3), 83-94.

Lima, V.V., Miranda, J.M., Baptista, M.A., Catalão, J., Gonzales, M., Otero, L., Olabarrieta, M., Alvarez-Gomez, J.A., Carreño, E. (2010). Impact of a 1755-like tsunami in Huelva, Spain. Natural Hazards and Earth System Sciences, 10, 139-148.

Mantovani, F., Vita-Finzi, C. (2003). Neotectonics of the Vajont dam site. Geomorphology, 54, 33-37.

Panizzo, A., De Girolamo, P., Di Risio, M., Maistri, A., Petaccia, A. (2005). Great landslide events in Italian artificial reservoirs. Natural Hazards and Earth System Sciences, 5, 733-740.

Pararas-Carayannis, G. (1973). The waves that destroyed the Minoan Empire (Atlantis). Sea Frontiers, 19(2), 94.

Pararas-Carayannis, G. (1992). The tsunami generated from the eruption of the volcano of Santorin in the Bronze Age. Natural Hazards, 5, 115-123.

Pareschi, M.T., Favalli, M., Boschi, E. (2006). Impact of the Minoan tsunami of Santorini : simulated scenarios in the Western Mediterranean. Geophysical Research Letters, 33(18), L18607.1-L18607.6.

Proenza, X.W., Maul, G.A. (2010). Tsunami hazard and total risk in the Caribbean Basin. Science of Tsunami Hazards, 29(2), 70-77.

Richardson, S., Musson, R., Horsburgh, K. (2007). Tsunami - assessing the hazard for the UK and Irish coast. In: Proceedings of the 41st Defra Flood and Coastal Management conference 2006, 4th July to 6th July 2006, University of York, London. London, Defra, 10.1.1-10.1.11.

Roger, J., Allgeyer, S., Daubord, C., Hébert, H. (soumis). L'aléa tsunami en France métropolitaine. Actes du colloque Risques Naturels en Méditerranée Occidentale, Carcassonne, France, Novembre 2009, *soumis*.

Roger, J., Baptista, M.A., Sahal, A., Allgeyer, S., Hébert, H. (2010c). The transoceanic 1755 Lisbon tsunami in the Martinique]. Pure and Applied Geophysics, Proceedings of the International Tsunami Symposium, Novosibirsk, Russia, July 2009, in press.

Roger, J., Baptista, M.A., Mosher, D., Hébert, H., Sahal, A. (2010b). Tsunami impact on Newfoundland, Canada, due to far-field generated tsunamis. Implications on hazard assessment]. Proceedings of the 9th U.S. National and 10th Canadian Conference on Earthquake Engineering, July 25-29, 2010, Toronto, Canada, n°1837.

Roger, J., Allgeyer, S., Hébert, H., Baptista, M.A., Loevenbruck, A., Schindelé, F. (2010a). The 1755 Lisbon tsunami in Guadeloupe Archipelago : source sensitivity and investigation of resonance effects . The Open Oceanography Journal, 4, 58-70.

Ruffman, A. (2006). Documentation of the farfield parameters of the November 1, 1755 "Lisbon" tsunami along the shores of the western Atlantic Ocean. Program and Abstracts, International Tsunami Society 3rd Tsunami Symposium, May 23-25, Honolulu, HI.

Smith, D.E., Shi, S., Cullingford, R.A., Dawson, A.G., Dawson, S., Firth, C.R., Foster, I.D.L., Fretwell, P.T., Haggart, B.A., Holloway, L.K., Long, D. (2004). The Holocene Storegga slide tsunami in the United Kingdom. Quaternary Science Reviews, 23(23-24), 2291-2321.

Thiebot, E., Gutscher, M.-A. (2006). The Gibraltar Arc seismogenic zone (part 1): Constraints on a shallow east dipping fault plane source for the 1755 Lisbon earthquake provided by seismic data, gravity and thermal modeling. Tectonophysics, 426, 135-152.

Tinti, S., Baptista, M.A., Harbitz, C.B. and Maramai, A. (1999). The unified European catalogue of tsunamis: a GITEC experience. Proc. International Conference on Tsunamis, Paris, 26-28 May 1998, 84-99.

Tinti, S., Maramai, A. and Graziani, L. (2001). A new version of the European tsunami catalogue: updating and revision. Natural Hazards and Earth System Sciences, 1, 255-262.

Tinti, S., Maramai, A. and Graziani, L. (2004). The new catalogue of the Italian tsunamis. Natural Hazards, 33, 439-465.

Udias, A., Lopez Arroyo, A., Mezcua, J. (1976). Seismotectonics of the Azores-Alboran region. Tectonophysics, 31, 259-289.

UNESCO-IOC. Tsunami glossary. IOC information document n°1221. Paris, UNESCO. http://ioc3.unesco.org/itic/files/tsunami_glossary_en_small.pdf

Weninger, B., Schulting, R., Bradtmöller, M., Clare, L., Collard, M., Edinborough, K., Hilpert, J., Jöris, O., Niekus, M., Rohling, E.J., Wagner, B. (2008). The catastrophic final flooding of Doggerland by the Storegga slide tsunami. Documenta Praehistorica XXXV, UDK 550.344.4(261.26)"633".

Zahibo, N., Pelinovsky, E. (2001). Evaluation of tsunami risk in the Lesser Antilles. Natural Hazards and Earth System Sciences, 1, 221-231.

Zitellini, N., Chierici, F., Sartori, R., Torelli, L. (1999). The tectonic source of the 1755 Lisbon earthquake and tsunami. Annali di Geofisica, 42(1), 49-55.

Zitellini, N., L. A. Mendes, D. Cordoba, J. Danobeitia, R. Nicolich, G. Pellis, A. Ribeiro, R. Sartori, L. Torelli, R. Bartolome, G. Bortoluzzi, A. Calafato, F. Carrilho, L. Casoni, F. Chierici, C. Corela, A. Corregiari, B. Della-Vedova, E. Garcia, P. Jornet, M. Landuzzi, M. Ligi, A. Magagnoli, G. Marozzi, L. Matias, D. Penitenti, R. Rodriguez, M. Rovere, P. Terrinha, L. Vigliotti, and A. Zahinos-Ruiz (2001). Source of 1755 Lisbon earthquake, tsunami investigated, EOS 82, no. 26, 285–291.

Références partie 1.4

Assier-Rzadkiewicz, S., Heinrich, P., Sabatier, P.C., Savoye, B., Bourillet, J.F. (2000). Numerical modelling of a landslide-generated tsunami : the 1979 Nice event. Pure and Applied Geophysics, 157(10), 1707-1727.

Anzidei, M., Baldi, P., Casula, G., Galvani, A., Kahlouche, S., Pesci, A., Riguzzi, F., Touam, S., Zanutta, A. (1999). First GPS measurements across the Central-Western Mediterranean area. Annali di Geofisica, 42(1), 115-120.

Bergman, E. A., Solomon, S.C. (1990). Earthquake Swarms on the Mid-Atlantic Ridge: Products of Magmatism or Extensional Tectonics?, J. Geophys. Res., 95(B4), 4943–4965, doi:10.1029/JB095iB04p04943.

Bird, D.E., Hall, S.A., Burke, K., Casey, J.F., Sawyer, D.S. (2007). Early Central Atlantic Ocean seafloor spreading history. Geosphere, 3(5), 282-298.

Biscontin, G., Pestana, J.M., Nadim, F. and Andersen, K. (2001). Seismic triggering of submarine landslides in soft cohesive soil deposits. Prediction of Underwater Landslide

Hazard, P. Watts, C.E. Synolakis and J.-P. Bardet (Eds.), Balkema, Rotterdam, The Netherlands.

Biscontin, G., Pestana, J.M., Nadim, F. (2004). Seismic triggering of submarine slides in soft cohesive soil deposits. Marine Geology, 203, 341-354.

Biscontin, G., Pestana, J.M. (2006). Factors affecting seismic response of submarine slopes. Natural Hazards and Earth System Sciences, 6, 97-107.

Cakir, Z., Meghraoui, M., Akoglu, A.M., Jabour, N., Belabbes, S., Ait-Brahim, L. (2006). Surface deformation associated with the Mw 6.4, 24 February 2004 AL Hoceima, Morocco, earthquake deduced from InSAR: implications for the active tectonics along North Africa. Bulletin of the Seismological Society of America, 96(1), 59-68.

Camerlenghi, A., Urgeles, R., Fantoni, L. (2010). A database on submarine landslides of the Mediterranean Sea. In: D.C. Mosher et al. (Eds.), Submarine Mass Movements and their Consequences, Advances in Natural and Technological Hazards Research, 28(III), 503-513. doi: 10.1007/978-90-481-3071-9_41

Cattaneo, A., Babonneau, N., Dan, G., Déverchère, J., Domzig, A., Gaullier, V., Lepillier, B., de Lépinay, B.M., Nouguès, A., Strzerzynsli, P., Sultan, N., Yelles, K. (2010). Submarine landslides along the Algerian Margin : a review of their occurrence and potential link with tectonic structures. In: D.C. Mosher et al. (Eds.), Submarine Mass Movements and their Consequences, Advances in Natural and Technological Hazards Research, 28, 515-525.

Chamot-Rooke, N., Rabaute, A. (2006). Plate tectonics from space. Map, CGMW, Paris.

DeMets, C., Gordon, R.G., Argus, D.F., Stein, S. (1990). Current plate motion. Geophysical Journal International, 101, 425-478.

Déverchère, J., Yelles, K., Domzig, A., Mercier de Lépinay, B., Bouillin, J.-P., Gaullier, V., Bracène, R., Calais, E., Savoye, B., Kherroubi, A., Le Roy, P., Pauc, H., Dan, G. (2005). Active thrust faulting offshore Boumerdes, Algeria, and its relations to the 2003 Mw 6.9 earthquake. Geophysical Research Letters, 32, L04311. doi:10.1029/2004GL021646

El-Robrini, M., Gennesseaux, M., Mauffret, A. (1985). Consequences of the El-Asnam earthquakes : turbidity currents and slumps on the Algerian Margin (Western Mediterranean). Geo-Marine Letters, 5, 171-176.

Eva, C., Rabinovich, A.B. (1997). The February 23, 1887 tsunami recorded on the Ligurian coast, western Mediterranean. Geophysical Research Letters, 24(17), 2211-2214.

Fine, I.V., Rabinovich, A.B., Bornhold, B.D., Thomson, R.E., Kulikov, E.A. (2005). The Grand Banks landslide-generated tsunami of November 18, 1929: preliminary analysis and numerical modeling. Marine Geology, 215, 45-57.

Gerardi, F., Barbano, M.S., De Martini, P.M., Pantosti, D. (2008). Discrimination of tsunami sources (earthquake versus landslide) on the basis of historical data in Eastern Sicily and Southern Calabria. Bulletin of the Seismological Society of America, 98(6), 2795-2805.

Gràcia, E., Pallàs, R., Soto, J.I., Comas, M., Moreno, X., Masana, E., Santanach, P., Diez, S., Garcia, M., Dañobeitia, J. (2006). Active faulting offshore SE Spain (Alboran Sea): implications for earthquake hazard assessment in the Southern Iberian Margin. Earth and Planetary Science Letters, 241, 734-749.

Grandin, R., Borges, J.F., Bezzeghoud, M., Caldeira, B., Carrilho, F. (2007). Simulations of strong ground motion in SW Iberia for the 1969 February 28 (Ms = 8.0) and the 1755 November 1 (M ~ 8.5) earthquakes – II. Strong ground motion simulations. Geophys. J. Int., 71, 1144-1161.

Grimison, N.L., Chen, W.P. (1986). The Azores-Gibraltar plate boundary: focal mechanisms, depths of earthquakes and their tectonic implications. Journal of Geophisical Research, 91, 2029-2047.

Hamdache, M., Pelaez, J.A., Talbi, A., Lopez Casado, C. (2010). A unified catalog of main earthquakes for Northern Algeria from A.D. 856 to 2008. Seismological Research Letters, 81(5), 732-739.

Harbi, A., Peresan, A., Panza, G.F. (2010). Seismicity of Eastern Algeria : a revised and extended earthquake catalogue. Natural Hazards, 54, 724-747.

Jiménez-Munt, I., Fernandez, M., Vergés, J., Afonso, J.C., Garcia-Castellanos, D., Fullea, J. (2010). Lithospehric structure of the Gorringe Bank : insights into its origin and tectonic evolution. Tectonics, 29, TC5019. doi:10.1029/2009TC002458.

Jolivet, L., Brun, J.-P., Meyer, B., Prouteau, G., Rouchy, J.-M., Scaillet, B. (2008). Géodynamique Méditerranéenne. Société Géologique de France, Ed. Vuibert, 216 pp.

Johnston, A.C. (1996). Seismic moment assessment of earthquakes in stable continental regions – III. New Madrid 1811-1812, Charleston 1886 and Lisbon 1755. Geophysical Journal International, 126, 314-344.

Kiratzi, A.A., Papazachos, C.B. (1995). Active crustal deformation from the Azores triple junction to the Middle East. Tectonophysics, 243, 1-24.

Lastras, G., Canals, M ; Hughes-Clarke, J.E., Moreno, A., De Batist, M., Masson, D.G., Cochonat, P. (2002). Seafloor imagery from the BIG'95 debris flow, western Mediterranean. Geology, 30(10), 871-874.

Lastras, G., Canals, M., Urgeles, R., De Batist, M., Calafat, A.M., Casamor, J.L. (2004). Characterisation of the recent BIG'95 debris flow deposit on the Ebro margin, Western Mediterranean Sea, after a variety of seismic reflection data. Marine Geology, 213(1-4), 235-255.

Lastras, G., Canals, M., Amblas, D., Frigola, J., Urgeles, R., Calafat, A.M., Acosta, J. (2007). Slope instability along the northeastern Iberian and Balearic continental margins. Geologica Acta, 5(1), 35-47. http://redalyc.uaemex.mx/pdf/505/50550103.pdf

Lee, C.-T., Huang, C.-C., Lee, J.-F., Pan, K.-L., Lin, M.-L., Dong, J.-J. (2008). Statistical approach to earthquake-induced landslide susceptibility. Engineering Geology, 100, 43-58.

Malamud, B.D., Turcotte, D.L., Guzzetti, F., Reichenbach, P. (2004). Landslides, earthquakes, and erosion. Earth and Planetary Science Letters, 229, 45-59.

Martin Davila, J., Pazos, A. (2003). Sismicidad del Golfo de Cadiz y zonas adyacentes. Seismicity of the Gulf of Cadiz and surrounding areas. Fisica de la Tierra, 15, 189-210.

Mazzotti, S., Adams, J. (2005). Rates and uncertainties on seismic moment and deformation in eastern Canada. Journal of Geophysical Research, 110, B09301. doi:10.1029/2004JB003510.

Mazzotti, S., Townend, J. (2010). State of stress in central and eastern North American seismic zones. Lithosphere, 2(2), 76-83. doi: 10.1130/L65.1.

Nocquet, J.-M., Calais, E. (2004). Geodetic measurements of crustal deformation in the Western Mediterranean and Europe. Pure and Applied Geophysics, 161(3), 661-681.

Nocquet, J.-M., Calais, E. (2003). Crustal velocity field of western Europe from permanent GPS array solutions, 1996-2001. Geophysical Journal International, 154, 72-88.

Okal, E.A., Synolakis, C.E. (2003). A theoretical comparison of tsunamis from dislocations and landslides. Pure and Applied Geophysics, 160, 2177-2188.

Papazachos, B., Papazachou, C. (2003). The most catastrophic events in Greece. The earthquakes of Greece, Ziti Publ., Thessaloniki, 286 pp., in Greek.

Reicherter, K., Becker-Heidmann, P. (2009). Tsunami deposits in the western Mediterranean: remains of the 1522 Almeria earthquake? Geological Society, London, Special Publications, 316, 217-235. doi:10.1144/SP316.14.

Reicherter, K., Hübscher, C. (2007). Evidence of a seafloor rupture of the Carboneras Fault Zone (southern Spain): relation to the 1522 Almeria earthquake? Journal of Seismology, 11, 15-26.

Ribeiro, A., Mendes-Victor, L., Cabral, J., Matias, L., Terrinha, P. (2006). The 1755 Lisbon earthquake and the beginning of closure of the Atlantic. European Review, 14(2), 193-205.

Roger, J., Baptista, M.A., Sahal, A., Allgeyer, S., Hébert, H. (2010c). The transoceanic 1755 Lisbon tsunami in the Martinique]. Pure and Applied Geophysics, Proceedings of the International Tsunami Symposium, Novosibirsk, Russia, July 2009. doi: 10.1007/s00024-010-0216-8.

Russo, R.M., Speed, R.C., Okal, E.A., Shepherd, J.B., Rowley, K.C. (1993). Seismicity and tectonics of the southeastern Caribbean. Journal of Geophysical Research, Solid Earth, 98(B8), 14299-14319.

Solovyev, S.L., Campos-Romero, M.L., Plink, N.L. (1992). Orleansville tsunami of 1954 and El Asnam tsunami of 1980 in Alboran Sea (Southwestern Mediterranean Sea). Izvestiya, Earth Physics, 28(9), 739-760.

Soloviev, S.L., Solovieva, O.N., Go, C.N., Kim, K.S., Shchetnikov, N.A. (2000). Tsunamis in the Mediterranean Sea 2000 B.C. – 2000 A.D. Kluwer Academic Publishers, Advances in Natural and Technological Hazards Research, 237 pp.

Stein, S., Sleep, N., Geller, R., Wang, S., Kroeger, G. (1979). Earthquakes along the passive margin of eastern Canada. Geophysical Research Letters, 6, 537-540.

Terrinha, P., Matias, L., Vicente, J., Duarte, J., Luis, J., Pinheiro, L., Lourenço, N., Diez, S., Rosas, F., Magalhães, V., Valadares, V., Zitellini, N., Roque, C., MendesVictor, L., MATESPRO Team (2009). Morphotectonics and strain partitioning at the Iberia-Africa plate boundary from multibeam and seismic reflection data. Marine Geology, 267, 156-174.

Udias, A., Lopez-Arroyo, A., Mezcua, J. (1976). Seismotectonic of the Azores-Alboran region. Tectonophysics, 31, 259-289.

Vannucci, G., Pondrelli, S., Argnani, A., Morelli, A., Gasperini, P., Boschi, E. (2004). An atlas of Mediterranean seismicity. Annals of Geophysics, supplement to n°47(1), 247-306.

Yelles-Chaouche, A., Boudiaf, A., Djellit, H., Bracene, R. (2006). La tectonique active de la région nord-algérienne. C. R. Géosciences, 338, 126-139.

Zitellini, N., Gràcia, E., Matias, L., Terrinha, P., Abreu, M.A., DeAlteriis, G., Henriet, J.P., Dañobeitia, J.J., Masson, D.G., Mulder, T., Ramella, R., Somoza, L., Diez, S. (2009). The quest for the Africa-Eurasia plate boundary west of the Strait of Gibraltar. Earth and Planetary Science Letters, 280, 13-50.

Zoback, M.D., Grollimund, B. (2001). Impact of deglaciation on present-day intraplate seismicity in eastern North America and western Europe. Compte Rendus de l'Académie des Sciences Paris, Earth and Planetary Sciences, 333, 23–33.

Références partie 2.1

Acosta, J., Canals, M., Lopez-Martinez, J., Muñoz, A., Herranz, P., Urgeles, R., Palomo, C., Casamor, J.L. (2002). The Balearic Promontory geomorphology (western Mediterranean) : morphostructure and active processes. Geomorphology, 49, 177-204.

Alasset, P.-J., Hébert, H., Maouche, S., Calbini, V., Meghraoui, M. (2006). The tsunami induced by the 2003 Zemmouri earthquake (Mw = 6.9, Algeria) : modelling and results. Geophysical Journal International, 166(1), 213-226.

Baptista, M.A., Heitor, S., Miranda, J.M., Miranda, P., Mendes Victor, L. (1998a). The 1755 Lisbon tsunami; evaluation of the tsunami parameters. Journal of Geodynamics, 25(2), 143-157.

Bishop, P., Sanderson, D., Hansom, J., Chaimanee, N. (2005). Age-dating of tsunami deposits: lessons from the 26 December 2004 tsunami in Thailand. In: The Indian Ocean tsunami: geographical commentaries One year on. The Geographical Journal, 171(4), 379-384.

Blanc, P.-L. (2008). The tsunami in Cadiz on 1 November 1755 : A critical analysis of reports by Antonio de Ulloa and by Louis Godin. C. R. Geoscience, 340, 251-261.

Blanc, P.-L. (2009). Earthquakes and tsunami in November 1755 in Morocco: a different reading of contemporaneous documentary sources. Natural Hazards and Earth System Sciences, 9, 725-738.

Borrero, J.C., Synolakis, C., Okal, E., Liu, P., Titov, V.V., Jaffe, B.E., Fritz, H.M. (2009). The past, present and future of tsunami field surveys post-Samoa, 2009. Abstract American geophysical Union, Fall Meeting 2009, #U23F-02.

Bussert, R., Aberhan, M. (2004). Storms and tsunamis: evidence of event sedimentation in the Late Jurassic Tendaguru beds of southeastern Tanzania. Journal of African Earth Sciences, 39, 549-555.

Cordier, S. (2010). Optically stimulated luminescence dating: procedures and applications to geomorphological research in France. Géomorphologie : relief, processus, environnement, 1, 21-40.

Cunha, P.P., Buylaert, J.P., Murray, A.S., Andrade, C., Freitas, M.C., Fatela, F., Munha, J.M., Martins, A.A., Sugisaki, S. (2010). Optical dating of clastic deposits generated by an extreme marine coastal flood: the 1755 tsunami deposits in the Algarve (Portugal). Quaternary Geochronology, 5, 329-335.

Dawson, A.G., Foster, I.D.L., Shi, S., Smith, D.E., Long, D. (1991). The identification of tsunami deposits in coastal sediment sequences. Science of Tsunami Hazards, 9(1), 73-82.

Dawson, A.G., Shi, S. (2000). Tsunami deposits. Pure and Applied Geophysics, 157, 875-897.

Dominey-Howes, D., Minos-Minopoulos, D. (2004). Perceptions of hazard and risk on Santorini. Journal of Volcanology and Geothermal Research, 137(4), 285-310.

EERI Special Earthquake Report (2010). Learning from Earthquakes: Samoa Earthquakes and Tsunami of September 29, 2009. EERI Newsletter 44(1), January 2010, 8p.

Fritz, H.M., Blount, C., Sokoloski, R., Singleton, J., Fuggle, A., McAdoo, B.G., Moore, A., Grass, C., Tate, B. (2007). Hurricane Katrina storm surge distribution and field observations on the Mississippi Barrier Islands. Estuarine, Coastal and Shelf Science, 74, 12-20.

Donahue, J., Olsen, M.J., Thio, H.K., Somerville, P. (2009). American Samoa tsunami reconnaissance report, September 29, 2009, NSF sponsored Geo-Engineering Extreme Events Reconnaissance (GEER) Report, Bray. J., Editor, 101p.

Dudley, W., Goff, J., Chagué-Goff, C., Johnston, J. (2009). Capturing the next generation of cultural memories – the process of video interviewing tsunami survivors. Science of Tsunami Hazards, 28(3), 154-170.

Fujino, S., Masuda, F., Tagomori, S., Matsumoto, D. (2006). Structure and depositional processes of a gravelly tsunami deposit in shallow marine setting: Lower Cretaceous Miyako Group, Japan. Sedimentary Geology, 187, 127-138.

Gonzalez, F.I., Milburn, H.M., Bernard, E.N., Newman, J.C. (1998). Deep-ocean Assessment and Reporting of Tsunamis (DART®): Brief Overview and Status Report. In Proceedings of the International Workshop on Tsunami Disaster Mitigation, 19-22 January 1998, Tokyo, Japan. http://www.ndbc.noaa.gov/dart/brief.shtml

Goto, K., Tada, R., Tajika, E., Bralower, T.J., Hasegawa, T., Matsui, T. (2004). Evidence for ocean water invasion into the Chicxulub crater at the Cretaceous/Tertiary boundary. Meteoritics & Planetary Science, 39(7), 1233-1247.

Goto, K., Tada, R., Tajika, E., Matsui, T. (2008). Chapter 15 – Deep-sea tsunami deposits in the Proto-Caribbean Sea at the Cretaceous/Tertiary boundary. Tsunamiites, 251-275. doi:10.1016/B978-0-444-51552-0.00015-1.

Goto, K., Miyagi, K., Kawamata, H., Imamura, F. (2010). Discrimination of boulders deposited by tsunamis and storm waves at Ishigaki Island, Japan. Marine Geology, 269, 34-45.

Gutscher, M.-A. (2005). Destruction of Atlantis by a great earthquake and tsunami? A geological analysis of the Spartel Bank hypothesis. Geology, 33(8), 685-688.

Gutscher, M.-A., Baptista, M.A., Miranda, J.M. (2006). The Gibraltar Arc seismogenic zone (part 2): Constraints on a shallow east dipping fault plane source for the 1755 Lisbon earthquake provided by tsunami modeling and seismic intensity. Tectonophysics, 426, 153-166.

Harbi, A., Benouar, D., Benhallou, H. (2003). Re-appraisal of seismicity and seismotectonics in the north-eastern Algeria. Part I: Review of historical seismicity. Journal of Seismology, 7, 115-136.

Harbi, A., Meghraoui, M., Maouche, S. (2010). The Djijelli (Algeria) earthquakes of 21 and 22 August 1856 (I_0 VIII, IX) and related tsunami effects Revisited. Journal of Seismology. doi: 10.1007/s10950-010-9212-9.

Haslett, S.K., Bryant, E.A. (2007). Reconnaissance of historic (post-AD 1000) high-energy deposits along the Atlantic coasts of southwest Britain, Ireland and Brittany, France. Marine Geology, 242(1-3), 207-220.

Hori, K., Kuzumoto, R., Hirouchi, D., Umitsu, M., Janjirawuttikul, N., Patanakanog, B. (2007). Horizontal and vertical variation of 2004 Indian tsunami deposits : an example of two transects along the western coast of Thailand. Marine Geology, 239(3-4), 163-172.

Humacoop (2005). Tsunami: les ONG au Coeur d'une tempête médiatique. Compte-rendu de l'intervention de Bruno David – Communication sans Frontières, *Tsunami : quels enjeux pour l'humanitaire de demain ?*, Humacoop Infos 1, 4-6. www.communicationsansfrontieres.net/documents/Humacoop_Tempete%20mediatique%20sur%20les%20ONG_Tsunami_juin2005_1.pdf .

Inoue, K. (2005). Massive tsunami in Indian Ocean Coasts. Disaster Management and Response, 3(2), 33.

Jaffe, B.E., Gelfenbaum, G. (2007). A simple model for calculating tsunami flow speed from tsunami deposits. Sedimentary Geology, 200, 347-361.

Joku, G.N., Davies, J.M., Davies, H.L. (2007). Eyewitness accounts of the impact of the 1998 Aitape tsunami, and of other tsunamis in living memory, in the region from Jayapura, Indonesia, to Vanimo, Papua New Guinea. Pure and Applied Geophysics, 164, 433-452.

Jovanelly, T.J., Moore, A.L. (2009). Sedimentological analysis of an ancient sand sheet of multiple origins at Lynch Cove, Puget Sound, Washington. Journal of Coastal Research, 25(2), 294-304.

Kortekaas, S., Dawson, A.G. (2007). Distinguishing tsunami and storm deposits: an example from Martinhal, SW Portugal. Sedimentary geology, 200, 208-221.

Lagos, M. , Arcas, D. , Ramirez, T. , Severino, R., Garcia, C. (2010) Alturas de tsunami modelas y observadas. Evento del 27 de Febrero de 2010, Chile. Resultados preliminaries, poster. ftp://146.155.48.6/geo/mlagoslo/Tsunami.../Poster_Mod_Obs_Tsunami.pdf .

Lian, O.B., Huntley, D.J. (2002). Luminescence dating. In: Tracking Environmental Change Using Lake Sediments. Volume 1: Basin Analysis, Coring, and Chronological Techniques. Eds: W.M. Last & J.P. Smol. Developments in Paleoenvironmental Research, 1(3), 261-282. doi: 10.1007/0-306-47669-X_12.

Luque, L., Lario, J., Zazo, C., Goy, J.L., Dabrio, C.J., Silva, P.G. (2001). Tsunami deposits as paleoseismic indicators: examples from the Spanish coast. Acta Geologica Hispanica, 36(3-4), 197-211.

Marshall, T. (2007). Hurricane Katrina damage survey, verification study. Report. Haag Engineering Co., 12 pp. www.haageducation.com/PDF/**Katrina**%20Verification%2012-06.pdf .

Martin Miguez, B., Le Roy, R., Wöppelmann, G. (2008). The use of radar tide gauges to measure variations in sea level along the French Coast. Journal of Coastal research, 24(4C), 61-68.

McAdoo, B.G., Dengler, L., Prasetya, G., Titov, V. (2006). Smong: How an oral history saved thousands on Indonesia's Simeulue Island during the December 2004 and March 2005 tsunamis. Earthquake Spectra, 22, S661−S669. doi:10.1193/1.2204966.

Melville, C.P., Levret, A., Alexandre, P., Lambert, J., Vogt, J. (1996). Historical seismicity of the Strait of Dover–Pas de Calais. Terra Nova, 8, 626–647.

Moore, A., Nishimura, Y., Gelfenbaum, G., Kamataki, T., Triyono, R. (2006). Sedimentary deposits of the 26 December 2004 tsunami on the northwest coast of Aceh, Indonesia. Earth Planets Space, 58, 253-258.

Morton, R.A., Gelfenbaum, G., Jaffe, B.E. (2007). Physical criteria for distinguishing sandy tsunami and storm deposits using modern examples. Sedimentary Geology, 200, 184-207.

Musson, R.M.W. (1994). A catalogue of British earthquakes. British Geological Survey technical Report, No. WL/94/04, pp.99.

Musson, R.M.W. (2004). A critical history of British earthquakes. Annals of Geophysics, 47, 597–609.

Neilson, G., Musson, R.M.W., Burton, P.W. (1984). The "London" earthquake of 1580, April 6. Engineering Geology, 20, 113–141.

Nott, J. (1997). Extremely high-energy wave deposits inside the Great Barrier Reef, Australia: determining the cause - tsunami or tropical cyclone. Marine Geology, 141, 193–207.

Nott, J. (2003). Waves, coastal boulder deposits and the importance of the pre-transport setting. Earth and Planetary Science Letters, 210, 269–276.

Okal, E.A., Fritz, H.M., Synolakis, C.E., Borrero, J.C., Weiss, R., Lynett, P.J., Titov, V.V., Foteinis, S., Jaffe, B.E., Liu, P.L.-F., Chan, I. (2010). Field survey of the Samoa tsunami of 29 september 2009. Seismological Research Letters, 81(4), 577-591.

Paris, R., Roger, J., Wassmer, P., Loevenbruck, A. (2008). Témoignages et signature sédimentaire des tsunamis aux Baléares. Rapport d'études pour le CEA, 15 pp.

Paris, R., Lavigne, F., Wassmer, P., Sartohaldi, J. (2007). Coastal sedimentation associated with the December 26, 2004 tsunami in Lhok Nga, west Banda Aceh (Sumatra, Indonesia). Marine Geology, 238, 93-106.

Pinegina, T.K., Bourgeois, J. (2001). Historical and paleo-tsunami deposits on Kamchatka, Russia: long-term chronologies and long-distance correlations. Natural Hazards and Earth System Sciences, 1(4), 177-185.

Platon (360 B.C.). Le Timée/ Le Critias. Dialogues.

Rabinovich, A.B. (2009). Seiches and harbour oscillations. Handbook of Coastal and Ocean Engineering (edited by Y.C. Kim), World Scientific Publ., Singapoure, chap. 9, 193-236.

Ramirez, M.T., Lagos, M., Arcas, D., Garcia, C., Severino, R. (2010). Geomorphological effects from the 27 February 2010 tsunami : a post-tsunami survey, central Chile. AGU Chapman Conference Abstract, Valparaiso, Viña del Mar, and Valdivia, Chile, 16-24 May 2010.

Roger, J., Gunnell, Y. (2010). Vulnerability of the Dover Strait to earthquake-generated tsunami hazards based on the coseismic marine event of April 6, 1580: insights from numerical modeling. *Submitted to* Geology.

Roger, J., Hébert, H. (2008). The 1856 Djijelli (Algeria) earthquake and tsunami: source parameters and implications for tsunami hazard in the Balearic Islands. Natural Hazards and Earth System Sciences, 8, 721-731.

Roger, J., Wassmer, P., Goett, H. (2010d). Mission TSUNORD 1. Rapport d'activité, projet ANR MAREMOTI, 17 pp.

Sahal, A. (2007). Effets des tsunamis en Méditerranée occidentale, constitution d'une base de données d'observation. Rapport de synthèse, financeur CEA, 30 pp., 4 annexes.

Sahal, A., Roger, J., Allgeyer, S., Lemaire, B., Hébert, H., Schindelé, F., Lavigne, F. (2009). The tsunami triggered by the 21 May 2003 Boumerdès-Zemmouri (Algeria) earthquake : field investigations on the French Mediterranean coast and tsunami modelling. Natural Hazards and earth System Sciences, 9, 1823-1834.

Scheffers, A. (2006). Ripple marks in coarse tsunami deposits. In A. Scheffers & D. Kelletat (eds), Tsunamis, hurricanes and neotectonics as driving mechanisms in coastal evolution (Proceedings of the Bonaire Field Symposium, March 2-6, 2006. A contribution to IGCP 495), E Schweizerbart, Stuttgart, Germany, Zeitschrift fur Geomorphologie Supplementband , 146, 221-233.

Soulsby, R.L., Smith, D.E., Ruffman, A. (2007). Reconstructing tsunami run-up from sedimentary characteristics – a simple mathematical model. Sixth International Symposium on Coastal Sediment Processes – Coastal Sediments '07. Coasts, Oceans, Ports and Rivers Institute (COPRI) of the American Society of Civil Engineers, May 13-17, New Orleans, Louisiana, 2, 1075-1088.

Srisutam, C., Wagner, J.-F. (2010). Reconstructing tsunami run-up from the characteristics of tsunami deposits on the Thai Andaman Coast. Coastal Engineering, 57, 493-499.

Tada, R., Iturralde-Vinent, M.A., Matsui, T., Tajika, E., Oji, T., Goto, K., Nakano, Y., Takayama, H., Yamamoto, S., Kiyokawa, S., Toyoda, K., Garcia-Delgado, D., Diaz-Otero, C., Rojas-Consuegra, R. (2003). K/T boundary deposits in the Paleo-western Caribbean basin, in C. Bartolini, R. T. Buffler, and J. Blickwede, eds., The Circum-Gulf of Mexico and the Caribbean: Hydrocarbon habitats, basin formation, and plate tectonics, AAPG Memoir, 79, 582–604.

UNESCO (2010). Tsunami and other coastal hazards warning system for the Caribbean and adjacent regions (CARIBE EWS) 12 January 2010 Haiti earthquake and tsunami event post-event assessment of CARIBE EWS performance. IOC Information Series, 90. http://www.ioc-unesco.org/components/com_oe/oe.php?task=download&id=8781&version=1.0&lang=1&format=1

UNESCO/IOC,NOAA, ITIC (2010). International Post-Tsunami Survey for the 25 October 2010 Mentawai, Indonesia Tsunami International Tsunami Survey Team - Mentawai (ITST-Mentawai). Framework and Protocols. Adapted from ITST-Samoa 2009.

Varley, P.M. (1996). Seismic risk assessment and analysis. In: Engineering geology of the Channel tunnel, published by T. Telford, Ltd, 520 pp., ISBN: 9780727720450.

Vött, A., Brückner, H., May, M., Lang, F., Brockmüller, S. (2007). Late Holocene tsunami imprint at the entrance of the Ambrakian gulf (NW Greece). Méditerranée, 108. URL : http://mediterranee.revues.org/index164.html.

Vries (de), D.H. (2010). Temporal vulnerability in hazardscapes: flood memory-networks and referentiality along the North Carolina Neuse River (USA). Global Environmental Change. doi: 10.1016/j.gloenvcha.2010.09.006.

Wassmer, P., Schneider, J.-L., Fonfrège, A.-V., Lavigne, F., Paris, R., Gomez C. (2010). Use of anisotropy of magnetic susceptibility (AMS) in the study of tsunami deposits : application to the 2004 deposits on the eastern coast of Banda Aceh, North Sumatra, Indonesia. Marine Geology, 275, 255-272.

Yamada, S., Gunatilake, R.P., Roytman, T.M., Gunatilake, S., Fernando, T., Fernando, L. (2006). The Sri Lanka tsunami experience. Disaster Management and response, 4(2), 38-48.

Références partie 2.2

Amsden, A.A. (1973). Numerical calculation of surface waves : a modified ZUNI code with surface particles and partial cells. Rept. LA-5146, Los Alamos Scientific Laboratory.

Baldock, T.E., Cox, D., Maddux, T., Killian, J., Fayler, L. (2009). Kinematics of breaking tsunami wavefronts: a data set from large scale laboratory experiments. Coastal Engineering, 56, 506-516.

Behrens, J., Bader, M. (2009). Efficiency considerations in triangular adaptative mesh refinement. Phil. Trans. R. Soc. A, 367, 4577-4589.

Bellotti, G. (2007). Transient response of harbours to long waves under resonance conditions. Coastal Engineering, 54, 680-693.

Carlier, G., Lachand-Robert, T., Maury, B. (2000). Une method numérique pour les problèmes variationnels sous contrainte de convexité. Comptes Rendus de l'Académie des Sciences – Series I – Mathematics, 330(5), 397-402.

Carrier, G.F., Wu, T.T., Yeh, H. (2003). Tsunami run-up and draw-down on a plane beach. J. Fluid Mech., 475, 79-99.

Chen, G., Zhou, J. (1992). Boundary element methods. Academic Press, London, 646 pp.

Courant, R., Friedrichs, K., Lewy, H. (1928). Über die partiellen Differenzengleichungen der mathematischen Physik, Mathematische Annalen, 100(1), 32–74. Version anglaise: URL : http://www.stanford.edu/class/cme324/classics/courant-friedrichs-lewy.pdf

Didenkulova, I., Parnell, K.E., Soomere, T., Pelinovsky, E., Kurennoy, D. (2009). Shoaling and runup of long waves induced by high-speed ferries in Tallinn Bay. Journal of Coastal Research, SI 56, 491-495.

Dutykh, D., Dias, F. (2009). Tsunami generation by dynamic displacement of sea bed due to dip-slip faulting. Mathematics and Computers in Simulation, 80(4), 837-848.

Eymard, R., Gallouët, T., Herbin, R. (2000). Finite volume methods. In Handbook of numerical analysis, Handb. Numer. Anal. VII, 713–1020, North-Holland, Amsterdam.

Gary, J. (1966). A generalization of the Lax-Richtmyer theorem on finite difference schemes. SIAM Journal on Numerical Analysis, 3(3), 467-473. URL: http://www.jstor.org/stable/2949642

George, D.L., Leveque, R.J. (2006). Finite volume methods and adaptive refinement for global tsunami propagation and local inundation. Science of Tsunami Hazards, 24, 319-328.

Grilli, S.T., Watts, P. (2005). Tsunami generation by submarine mass failure Part I : Modeling, experimental validation, and sensitivity analysis. Journal of Waterway, Port, Coastal, and Ocean Engineering, 131(6), 283-297.

Kowalik, Z., Murty, T.S. (1993). Numerical simulation of two-dimensional tsunami run-up. Marine Geodesy, 16, 87-100.

Liu, P.L.-F., Woo, S.-B., Cho, Y.-S. (1998). Computer programs for tsunami propagation and inundation. Cornell University, 104 pp.

Mader, C.L. (1973). Numerical simulation of tsunamis. Rept. HIG-73-3, Hawaii Institute of Geophysics, University of Hawaii.

Mader, C.L. (1988). Numerical modeling of water waves. University of California Press, Berkeley, California.

Mader, C.L., Gittings, M.L. (2002). Modeling the 1958 Lituya Bay mega-tsunami, II. Science of Tsunami Hazards, 20(5), 241-250.

Matsuyama, M., Tanaka, H. (2001). An experimental study of the highest run-up height in the 1993 Hokkaido Nansei-oki earthquake tsunami. ITS Proceedings, 7(7-21), 879-889.

Meinig, C., Stalin, S.E., Nakamura, A.I., González, F., Milburn, H.G. (2005). Technology Developments in Real-Time Tsunami Measuring, Monitoring and Forecasting. In Oceans 2005 MTS/IEEE, 19–23 September 2005, Washington, D.C. URL: http://nctr.pmel.noaa.gov/Dart/Pdf/mein2836_final.pdf

Mitchell, A.R., Griffiths, D.F. (1980). The finite difference method in partial differential equations. Wiley-Interscience Publication, Chichester, Wiley, 281 pp.

Murty, T.S., Rao, A.D., Nirupama, N., Nistor, I. (2006). Numerical modelling concepts for tsunami warning systems. Current Science, 90(8), 1073-1081.

Myers, E.P., Baptista, A.M. (1995). Finite element modeling of the July 12, 1993 Hokkaido Nansei-Oki tsunami. Pure and Applied Geophysics, 144(3-4), 769-801.

Nedelec, J.-C., Planchard, J. (1973). Une méthode variationnelle d'éléments finis pour la résolution numérique d'un problème extérieur dans R^3. Revue française d'automatique, informatique, recherche opérationnelle. Mathématique, 7(3), 105-129. URL : http://archive.numdam.org/article/M2AN_1973__7_3_105_0.pdf

O'Nions, K., Pitman, R., Marsh, C. (2002). Science of nuclear warheads. Nature, 415, 853-857. doi:10.1038/415853a.

Parnell, K., Delpeche, N., Didenkulova, I., Dolphin, T., Erm, A., Kask, A., Kelpsaite, L., Kurennoy, D., Quak, E., Räämet, A., Soomere, T., Terentjeva, A., Torsvik, T., Zaitseva-Pärnaste, I. (2008). Far-field vessel wakes in Tallinn Bay. Estonian Journal of Engineering, 14(4), 273-302. doi: 10.3176/eng.2008.4.01.

Patera, A. T. (1984). A spectral element method for fluid dynamics : laminar flow in a channel expansion. Journal of Computational Physics, 54, 468–488.

Peiro, J., Sherwin, S. (2005). Finite difference, finite element and finite volume methods for partial differential equations. In: Handbook of Materials Modeling. S. Yip (Ed.), Volume I: Methods and Models, 1-32.

Piatanesi, A. (1999). Caractérisation des sources sismiques par étude des tsunamis. Thèse de Doctorat, Institut de Physique du Globe de Paris, 185 pp. www.earth-prints.org/bitstream/2122/5284/1/PhD_thesis_**Piatanesi**.pdf

Setiyo Pranowo, W., Behrens, J.(2009). Unstructured finite element tsunami modeling and its application in/for Indonesia (Indian Ocean rim countries). International Symposium: Vision of Indonesian Intellectuals Overseas: Indonesian Development Strategy towards 2020 The Hague, 3-5 July 2009 Commission of Earth, Energy and Environment. URL: http://si-ppi-2009.com/index.php .

Settiyo Pranowo, W., Behrens, J., Schlicht, J., Ziemer, C. (2008). Adaptive mesh refinement applied to tsunami modeling: Tsunaflash. In: Proc. Int. Conf. Tsunami Warning (ICTW), ed: H. Adrianto, Jakarta, Indonesia.

Strikwerda, J.C. (2004). Finite difference schemes and partial differential equations. SIAM edition, Society for Industrial and Applied Mathematics, 2nd edition, 439 pp.

Tang, L., Titov, V.V., Chamberlin, C. D. (2009). Development, testing, and applications of site-specific tsunami inundation models for real-time forecasting. J. Geophys. Res., 114, C12025, doi:10.1029/2009JC005476.

Thompson, E.F., Hadley, L.L. (1995). Numerical modeling of harbor response to waves. Journal of Coastal Research, 11(3), 744-753.

Tinti, S., Gavagni, I., Piatanesi, A. (1994). A finite-element numerical approach for modeling tsunamis. Annali di geofisica, 5, 1009-1026.

Tinti, S., Gavagni, I. (1995). A smoothing algorithm to enhance finite-element tsunami modelling: an application to the 5 February 1783 Calabrian case, Italy. Natural Hazards, 12(2), 161-197.

Tinti, S., Piatanesi, A. (1996a). Numerical simulations of the tsunami induced by the 1627 earthquake affecting Gargano, southern Italy. Journal of Geodynamics, 21, 141-160.

Tinti, S., Piatanesi, A. (1996b). Finite-element simulations of the 5 February 1783 Calabrian tsunami. J. Phys. Chem. Earth, 21(12), 39-43.

Torsvik, T., Didenkulova, I., Soomere, T., Parnell, K.E. (2009). Variability in spatial pattern of long nonlinear waves from fast ferries in Tallinn Bay. Nonlin. Processes Geophys., 16, 351-363.

Titov, V.V., Gonzalez, F.I. (1997). Implementation and testing of the Method of Splitting Tsunami (MOST) model. NOAA Technical Memorandum ERL PMEL-112, 11 pp. URL: http://www.pmel.noaa.gov/pubs/PDF/tito1927/tito1927.pdf

Venturato, A.J., Arcas, D., Kanoglu, U. (2007). Modeling tsunami inundation from a Cascadia subduction zone earthquake for Long Beach and Ocean Shores, Washington. Pacific Marine Environmental Laboratory, NOAA Technical Memorandum OAR PMEL-137, 26 p.

Voller, V.R., Porté-Agel, F. (2002). Moore's Law and numerical modeling. Journal of Computational Physics, 179, 698-703.

Walsh, T.J., Caruthers, C.G., Heinitz, A.C., Myers III, E.P., Baptista, A.M., Erdakos, G.B., Kamphaus, R.A. (2000). Tsunami hazard map of the southern Washington Coast: Modeled tsunami inundation from a Cascadia subduction zone earthquake. Washington Division of Geology and Earth Resources, Geologic Map GM-49, 3–12.

Zeytounian, R.K. (2003). Joseph Boussinesq and his approximation : a contemporary view. C. R. Mecanique, 331(8), 575-586.

Zienkiewicz, O.C., Cheung, Y.K. (1967). The finite element method in continuum and structural mechanics. McGraw Hill, 272 pp.

Zienkiewicz, O.C., Taylor, R.L., Zhu, J.Z. (2005). The finite element method : its basis and fundamentals. Elsevier, 733 pp.

Références partie 2.3

Abadie, S., Butel, R., Mauriet, S., Morichon, D., Dupuis, H. (2006). Wave climate and longshore drift on the South Aquitaine coast. Continental Shelf Research, 26(16), 1924-1939.

Baba, T., Mleczko, R., Burbidge, D., Cummins, P.R., Thio, H.K. (2009). The Effect of the Great Barrier Reef on the Propagation of the 2007 Solomon Islands Tsunami Recorded in Northeastern Australia. Pure Appl. Geophys., 165, 2003–2018.

Basu, A., Saxena, N.K. (1993). Bathymetry computation from free-air anomaly data. Marine Geodesy, 16, 325-336.

Berry, M.V. (2007). Focused tsunami waves. Proceedings of the Royal Society A, 463, 3055-3071. doi:10.1098/rspa.2007.0051

Bilek, S.L., Lay, T. (1999). Rigidity variations with depth along interplate megathrust faults in subduction zones. Nature, 400, 443-446.

Borrero, J.C., Sieh, K., Chlieh, M., Synolakis, C.E. (2006). Tsunami inundation modeling for western Sumatra. PNAS, 103(52), 19673-19677. doi: 10.1073/pnas.0604069103

Bourillet, J.-F. (2007). Le canyon de Capbreton: carte bathymétrique, échelle 1/50000. IFREMER. ISBN 2-84433-158-0.

Chatenoux, B., Peduzzi, P. (2005), Analysis on the role of bathymetry and other environmental parameters in the impacts from the 2004 Indian Ocean Tsunami. A Scientific Report for the UNEP Asian Tsunami Disaster Task Force. UNEP/GRID-Europe. /http://www.grid.unep.ch/product/publication/download/environment_impacts_tsunami.pdfS.

Chatenoux, B., Peduzzi, P. (2007), Impacts from the 2004 Indian Ocean Tsunami: analyzing the potential protecting role of environmental features. Nat. Hazards. 40, 289–304. DOI 10.1007/s11069-006-0015-9.

Cirac, P., Bourillet, J.-F., Griboulard, R., Normand, A., Mulder, T. (2001). Le canyon de Capbreton : nouvelle approche géomorphologique. Actes du colloque international d'océanographie du Golfe de Gascogne, 31, 39-42. ISBN 2-84433-054-1.

Cochard, R., Ranamukhaarachchi, S.L., Shivakoti, G.P., Shipin, O.V., Edwards, P.J., Seeland, K.T., (2008), The 2004 tsunami in Aceh and Southern Thailand: A review on coastal ecosystems, wave hazards and vulnerability. Perspectives in Plant Ecology, Evolution and Systematics. 10, 3–40.

Dahlen, F.A. (1971). The elasticity theory of dislocations in real Earth models and changes in the rotation of the Earth. Geophysical Journal International, 23(3), 355-358.

Duong, N.A., Kimata, F., Meilano, I. (2008), Assessment of Bathymetry Effects on Tsunami Propagation in Viet Nam. Advances in Natural Sciences, 9(6).

Farr, T.G., Rosen, P.A., Caro, E., Crippen, R., Duren, R., Hensley, S., Kobrick, M., Paller, M., Rodriguez, E., Roth, L., Seal, D., Shaffer, S., Shimada, J., Umland, J., Werner, M., Oskin, M., Burbank, D., Alsdorf, D. (2007). The shuttle radar topogrpahy mission. Reviews of Geophysics, 45, RG2004. doi:10.1029/2005RG000183.

Geist, E.L., Bilek, S.L. (2001). Effect of depth-dependent shear modulus on tsunami generation along subduction zones. Geophysical Research Letters, 28(7), 1315-1318.

Gourlay, M.R. (1996), Wave set-up on coral reefs. 2. Set-up on reefs with various profiles. Coastal Engineering. 28, 17-55.

Gratton, Y. (2002). Le krigeage: la méthode optimale d'interpolation spatiale. Les articles de l'Institut d'Analyse Géographique, juin 2002, www.iag.asso.fr/pdf/krigeage_juillet2002.pdf .

Harbitz, C.B., Lovholt, F., Pedersen, G., Masson, D.G. (2006). Mechanisms of tsunami generation by submarine landslides: a short review. Norwegian Journal of Geology, 86, 255-264.

Haugen, K.B., Lovholt, F., Harbitz, C.B. (2005). Fundamental mechanisms for tsunami generation by submarine mass flows in idealised geometries. Marine and Petroleum Geology, 22, 209-217.

Hwang, C., Guo, J., Deng, X., Hsu, H.-Y., Liu, Y. (2006). Coastal gravity anomalies from retracked Geosat/GM altimetry: improvement, limitation and the role of airborne gravity data. Journal of Geodesy, 80, 204-216.

IOC, IHO and BODC, 2003. Centenary Edition of the GEBCO Digital Atlas, published on CD-ROM on behalf of the Intergovernmental Oceanographic Commission and the International Hydrographic Organization as part of the General Bathymetric Chart of the Oceans. British Oceanographic Data Centre, Liverpool, U.K.

Johanson, I.A., Fielding, E.J., Rolandone, F., Bürgmann, R. (2006). Coseismic and postseismic slip of the 2004 Parkfield earthquake from space-geodetic data. Bulletin of the Seismological Society of America, 96(4B), S269-S282.

Lebedev, S., Sirota, A., Medvedev, D., Khlebnikova, S., Vignudelli, S., Snaith, H.M., Cipollini, P., Venuti, F., Lyard, F., Bouffard, J., Cretaux, J.F., Birol, F., Roblou, L., Kostianov, A., Ginzburg, A., Sheremet, N., Kuzmina, E., Mamedov, R., Ismatova, K., Alyev, A., Mustafayev, B. (2008). Exploiting satellite altimetry in coastal ocean through the ALTICORE project. Russian Journal of Earth Sciences, 10, ES1002. doi:10.2205/2007ES000262

Lin, P., Liu, H.-W. (2007). Scattering and trapping of wave energy by a submerged truncated paraboloidal shoal. Journal of Waterway, Port, Coastal, and Ocean Engineering, March/April 2007, 94-103. doi: 10.1061/(ASCE)0733-950X(2007)133:2(94)

Llort-Pujol, G., Sintes, C., Gueriot, D. (2008). Analysis of Vernier interferometers for sonar bathymetry. Oceans 2008 proceedings, 15-18 sept. 2008, Québec City, 5 pp. doi: 10.1109/OCEANS.2008.5151958

Losada, I.J., Gonzalez-Ondina, J.M., Diaz-Hernandez, G., Gonzalez, E.M., (2008), Numerical modeling of nonlinear resonance of semienclosed water bodies: Description and experimental validation. Coastal Engineering, 55, 21-34.

Lurton, X. (2001). Précision de mesure des sonars bathymétriques en fonction du rapport signal/bruit. Measurement accuracy of bathymetric sonars as a function of signal/noise ratio. Traitement du Signal, 18(3), 179-194.

Mansinha, L., Smylie, D.E. (1971). Deformation of the ground around surface faults: Seismological Society of America Bulletin, 61, 1433-1440.

Okada, Y. (1985). Surface deformation due to shear and tensile faults in a half-space. Bull. Seismol. Soc. Am., 75, 1135-1154.

Okal, E.A., Synolakis, C.E. (2003). A theoretical comparison of tsunamis from dislocations and landslides. Pure and Applied Geophysics, 160, 2177-2188.

Quadros, N.D., Collier, P.A., Fraser, C.S. (2008). Integration of bathymetric and topographic LIDAR: a preliminary investigation. The International Archives of the Photogrammetry, Remote Sensing and Spatial Information Sciences. Vol. XXXVII. Part B8. Beijing 2008, 1299-1304.

Roger, J., Allgeyer, S., Hébert, H., Baptista, M.A., Loevenbruck, A., Schindelé, F. (2010a). The 1755 Lisbon tsunami in Guadeloupe Archipelago : source sensitivity and investigation of resonance effects . The Open Oceanography Journal, 4, 58-70.

Roger, J., Baptista, M.A., Sahal, A., Allgeyer, S., Hébert, H. (2010b). The transoceanic 1755 Lisbon tsunami in Martinique. Pure and Applied Geophysics, Proceedings of the International Tsunami Symposium, Novosibirsk, Russia, July 2009, in press. DOI: 10.1007/s00024-010-0216-8

Sahal, A., Roger, J., Allgeyer, S., Lemaire, B., Hébert, H., Schindelé, F., Lavigne, F. (2009). The tsunami triggered by the 21 May 2003 Boumerdès-Zemmouri (Algeria) earthquake : field investigations on the French Mediterranean coast and tsunami modelling. Natural Hazards and earth System Sciences, 9, 1823-1834.

Sandwell, D.T., Smith, W.H.F. (2009). Global marine gravity from retracked Geosat and ERS-1 altimetry: Ridge segmentation versus spreading rate. Journal of Geophysical Research, 114, B01411.

Satake, K. (1988), Effects of bathymetry on tsunami propagation: application of ray tracing to tsunamis. Pure and Applied Geophys. 126(1), 27-36.

Shen, Z.-K., Ge, B.X., Jackson, D.D., Potter, D., Cline, M., Sung, L.-Y. (1996). Northridge earthquake rupture models based on the Global Positioning System measurements. Bulletin of the Seismological Society of America, 86(1B), S37-S48.

Speranski, N., Calliari, L. (2001), Bathymetric lenses and localized coastal erosion in southern Brazil. Journal of Coastal Research. 34 (Special Issue), 209–215.

Tong, X., Sandwell, D.T., Fialko, Y. (2010). Coseismic slip model of the 2008 Wenchuan earthquake derived from joint inversion of interferometric synthetic aperture radar, GPS, and field data. Journal of Geophysical Research, 115, B04314.

Vignudelli, S., Berry, P., Roblou, L. (2008). Satellite altimetry near coasts – current practices and a look at the future, in 15 Years of Progress in Radar Altimetry, edited by J. Benveniste and Y. Menard, ESA, (in press).

Vignudelli, S., Cipollini, P., Roblou, L., Lyard, F., Gasparini, G.P., Manzella, G.,Astraldi, M. (2005). Improved satellite altimetry in coastal systems: Case study of the Corsica Channel (Mediterranean Sea). Geophysical Research Letters, 32, L07608. doi:10.1029/2005GL022602

Ward, S.N. (2001). Landslide tsunami. Journal of Geophysical Research, 106, 11201-11215.

Wells, D.L., Coppersmith, K.J. (1994). New empirical relationships among magnitude, rupture length, rupture width, rupture area, and surface displacement. Bull. Seismol. Soc. Am., 84(4), 974-1002.

Yeh, H., Liu, P., Briggs, M., Synolakis, C. (1994). Propagation and amplification of tsunamis at coastal boundaries. Nature, 372, 353-355.

Références partie 4

Baptista, M.A., Miranda, J.M., Luis, J.F. (2006). In search of the 31 March 1761 earthquake and tsunami source. Short notes, Bulletin of the Seismological Society of America, 96(2), 713-721.

Bellotti, G. (2007). Transient response of harbours to long waves under resonance conditions. Coastal Engineering, 54, 680-693.

Bouchon, C., Portillo, P., Bouchon-Navaro, Y., Louis, M., Hoetjes, P., De Meyer, K., Macrae, D., Armstrong, H., Datadin, V., Harding, S., Mallela, J., Parkinson, R., Van Bochove, J.-W., Wynne, S., Lirman, D., Herlan, J., Baker, A., Collado, L., Nimrod, S., Mitchell, J., Morrall, C., Isaac, C. (2008), Status of Coral Reefs ofthe Lesser Antilles: The French West Indies, The Netherlands Antilles, Anguilla, Antigua, Grenada, Trinidad and Tobago. In: Wilkinson C

et al (eds) Status of coral reefs of the world Vol. 3. Australian Institute of Marine Sciences, Australia, pp 265–280

Gonzales-Marco, D., Sierra, J.P., Fernandez de Ybarra, O., sanchez-Arcilla, A. (2008). Implications of long waves in harbor management : the Gijon port case study. Ocean & Coastal Management, 51, 180-201.

Legrand H., Rousseau Y., Pérès C., & Maréchal J.-P. (2008), Suivi écologique des récifs coralliens des stations IFRECOR en Martinique de 2001 à 2006. Revue d'Ecologie. 63(1-2), 67-84.

Sahal, A., Pelletier, B., Chatelier, J., Lavigne, F., Schindelé, F. (2010). A catalogue of tsunamis in New Caledonia from 28 March 1875 to 30 September 2009. Comptes Rendus Geoscience, 342, 434-447.

Woo, S.-B., Hong, S.-Y., Han, K.-N. (2004). Numerical study of nonlinear resonance in narrow bay. Oceans'04. MTTS/IEEE Techno-ocean'04, 3, 1512-1518. doi: 10.1109/OCEANS.2004.1406345

Annexes

Annexe 1

L'aléa tsunami en France métropolitaine

J. Roger[1], S. Allgeyer[1,2], C. Daubord[3], H. Hébert[2]

[1] *Ecole Normale Supérieure / Laboratoire de Géologie, 24, rue Lhomond, 75231 Paris CEDEX 5, France*

[2] *CEA, DAM, DIF, F-91297 Arpajon, France*

[3] *SHOM, CS 92803, 29228 Brest CEDEX 2*

Résumé

Depuis l'évènement du 26 décembre 2004 dans l'océan Indien, la communauté internationale a pris conscience des capacités dévastatrices des tsunamis. Face à l'augmentation exponentielle de la répartition de la population mondiale en zone littorale, la France a décidé d'évaluer le risque pesant sur ses côtes avec une attention particulière pour sa façade méditerranéenne. En effet, bien que ne se situant pas dans une zone où les tsunamis sont fréquents comme cela peut être le cas dans le Pacifique, le littoral français méditerranéen a tout de même été sujet, par le passé, à quelques tsunamis d'amplitude plus ou moins importante, générés soit à proximité de la côte (en mer Ligure par exemple en 1887) mais surtout au niveau de la marge nord-africaine et plus particulièrement, algérienne. Le tsunami le plus récent issu de la marge nord-africaine est celui associé au séisme de Zemmouri-Boumerdès (Algérie) de 2003 qui mit aux environs d'une heure pour atteindre la côte d'Azur, et le plus dramatique, celui associé au glissement de terrain de l'aéroport de Nice en 1979 qui fit 10 victimes.

La côte Atlantique française pourrait être impactée par les tsunamis initiés par les grands séismes au large du Portugal (par exemple : le tsunami de Lisbonne de 1755) ou par des glissements de terrain (Terre-Neuve, 1929). Mais ces types d'événements y restent globalement moins fréquents qu'en Méditerranée.

Pour ce qui concerne la Manche et la mer du Nord, quelques évènements historiques de plus ou moins grande ampleur ont été répertoriés.

Des études approfondies de modélisation numérique de tsunami sont menées conjointement avec des enquêtes de terrain (recherche d'archives et de dépôts de paléotsunamis). Elles permettent d'identifier quelles sont les zones les plus propices à générer des tsunamis et quelles sont celles qui vont les amplifier, rendant vulnérables certaines zones anthropisées.

Ces études menées au cours de divers projet nationaux et internationaux permettent de souligner l'évidence de l'aléa en Méditerranée occidentale et le risque sur la côte française ainsi que la nécessité de prévenir et de réduire ce risque, surtout en période estivale, ou vis-à-vis d'installations côtières vulnérables (ports, usines..).

Mots-clés : *tsunami, France, estimation de l'aléa, risque*

Abstract

Since the Indian Ocean event of the 26th December 2004, the international community has considered the destructive capacity of tsunamis. Facing the exponential rising of the world population in coastal areas, France has decided to estimate and mitigate the hazard on its coasts, with a special attention for the Mediterranean regions. In fact, although tsunamis are not as frequent as in the Pacific Ocean, some of the tsunamis having occurred in the Mediterranean Sea, either near the coast (Ligurian Sea event of 1887) or along the North-African Margin, have had more or less consequences, depending on the wave amplitude, in Southern France. The more recent tsunami generated on the North-African Margin has been induced by the 2003 Zemmouri-Boumerdès (Algeria) earthquake and travelled toward Southern France in about one hour. The more tragic is associated to the 1979 Nice Airport landslide that killed 10 people.

The French Atlantic Coast could be also impacted by tsunamis generated by big earthquakes offshore Portugal (for example: the 1755 Lisbon tsunami) or by submarine landslides (Newfoundland, 1929). But such events are still less frequent in the Atlantic Ocean than in the Mediterranean.

As far as the Channel and the North Sea are concerned, several historical events showing more or less impact have been listed.

Some detailed studies using numerical modelling of tsunami associated with field surveys (historical document investigations and paleotsunami deposits searches) allow to identify areas where tsunamis could be produced and regions that are able to amplify the waves, increasing the vulnerability of coastal inhabited areas.

Those studies led within the framework of national and international projects allow to underline the real tsunami hazard along the French coasts and the necessity to anticipate and to mitigate the hazard especially during the touristic season, or for vulnerable coastal installations (as harbors, factories, etc.).

Keywords : *tsunami, France, hazard assessment, risk*

1. Introduction et contexte général

La France métropolitaine, ou France continentale, présente 3 façades maritimes adjacentes : l'océan Atlantique à l'ouest, la mer Méditerranée au sud et la Manche (et la mer du Nord) au nord. Les tsunamis, au même titre que les séismes, ne font pas partie de la culture française du risque, au contraire des tempêtes, inondations, glissement de terrains, avalanches, etc. qui y sont relativement fréquents. Au contraire, il existe très peu d'observations de tsunamis en France métropolitaine, qui ne font pas non plus partie de la culture maritime métropolitaine. Probablement parce que, si certains ont pu être observés par le passé, il auraient été associés aux « raz-de-marée » ou surcotes liées au passage des dépressions atmosphériques (comme on en trouve beaucoup dans les rapports de marine aux Antilles), ou tout simplement parce que leur trop faible amplitude s'est toujours retrouvée masquée par le bruit de fond de la mer.

1.1. *Atlantique Nord*

D'un point de vue géologique et géodynamique, l'est de l'océan Atlantique, contrairement à l'océan Pacifique ou l'océan Indien, ne présente pas de grande zone de subduction au niveau de ses marges proches de la France. Ces marges, dites passives, ne sont pas propices à générer des grands tsunamis comme ceux de Sumatra ou du Chili. Toutefois, il présente deux zones actives : l'arc de subduction des Antilles à sa frontière avec la plaque Caraïbes qui n'a jusqu'à maintenant jamais généré de télé-tsunami enregistrés sur les côtes est de l'océan Atlantique, et surtout la zone de contact entres les plaques africaine et eurasienne au sud de la péninsule ibérique, présentant une paléo-zone de subduction (Gutscher et al., 2002, 2009) dont l'activité est encore discutée (Marques, 2010). Cette frontière de plaques, dont le fonctionnement est encore assujetti à de nombreux débats (Zitellini et al., 2009), est connue pour être à l'origine de plusieurs séismes et tsunamis associés dont le fameux, mais non moins dévastateur, séisme de Lisbonne du 1er novembre 1755, d'une magnitude estimée à 8.5-9.0 d'après les nombreuses descriptions et rapports historiques (Baptista et al., 1998). En plus des destructions directement infligées par la secousse sismique au Portugal, en Espagne et au Maroc, un tsunami trans-océanique s'est propagé dans tout l'océan Atlantique pour aller toucher des zones aussi éloignées que le Royaume-Uni (Horsburgh et al., 2008), les Açores, les Antilles (Roger et al., 2010(a)) ou encore Terre-Neuve (Roger et al., 2010(b)), où il fit de nombreux dégâts. De récents travaux ont mis en évidence l'impact possible de ce tsunami à la pointe de la Bretagne via l'étude de dépôts sédimentaires côtiers (Haslett et Bryant, 2007). L'enregistrement du tsunami de 1969 (lié à un séisme de magnitude 7.9 au large du Portugal) dans les données marégraphiques de la Rochelle vient d'être mis en évidence et confirme le fait qu'un tsunami généré dans le sud de la péninsule ibérique puisse toucher les côtes françaises.

Une autre source possible de tsunamis en Atlantique nord concerne les gros glissements de terrains sous-marins comme celui de Grand Banks (au large de Terre Neuve, Canada) du 18 novembre 1929 qui généra un tsunami qui se propagea dans l'Atlantique nord et qui fut enregistré sur des marégraphes de la côte portugaise (Fine et al., 2005).

1.2. *Méditerranée*

La Méditerranée, mer qui marque la frontière des plaques africaine et eurasiatique (Fig. 1) est plus complexe que l'océan Atlantique d'un point de vue géodynamique. Plusieurs jeux d'ouverture et de fermeture de bassins océaniques au cours des temps géologiques en ont fait une zone extrêmement

riche en systèmes de failles présentant tous types de mécanismes. Basé sur les différences de mécanismes, on peut facilement diviser la Méditerranée en deux parties distinctes : la Méditerranée orientale (qui s'étend de l'Italie à la Turquie), dans laquelle on trouve une forte sismicité associée à la subduction hellénique d'une part et à la subduction sous la Calabre d'autre part, zones où les séismes atteignent des magnitude supérieures à 7.5 et où plus de 350 tsunamis ont été répertoriés (parmi eux on trouve par exemple les grands séismes de Messine (1908) et de Catane (1693) pour l'Italie et ceux de Crête (365) et des Cyclades (1956) pour la Grèce, associés chacun à un tsunami destructeur) ; la Méditerranée occidentale, quant à elle, présente une sismicité faible à modérée (séismes de faible à moyenne intensité (M<7.3)) localisée essentiellement au niveau de la marge nord africaine (Algérie, mer d'Alboran) et en mer Ligure. La Méditerranée occidentale présente donc des marges passives et semi-passives (la marge nord africaine est considérée comme étant au stade d'initiation d'une zone de subduction). Ces marges ne présentent pas ou peu de plateau continental, zone « tampon » ou les éventuels tsunamis perdront de l'énergie et gagneront en amplitude par le jeu de divers mécanismes présentés par la suite, et ont des talus continentaux abruptes, propices aux instabilités gravitaires comme les courants de turbidités[1] et les glissement de terrains sous-marins.

En Méditerranée occidentale, les séismes et les glissements de terrain, principalement ont été à l'origine d'une poignée de tsunamis dont seulement quelques uns ont touché de manière certaine le sud de la France: le séisme de mer Ligure (1887), le glissement de terrain de l'aéroport de Nice (1979) et le séisme de Zemmouri-Boumerdès (2003). La localisation des sources des tsunamis les plus notables en Méditerranée occidentale est indiquée sur la figure 1.

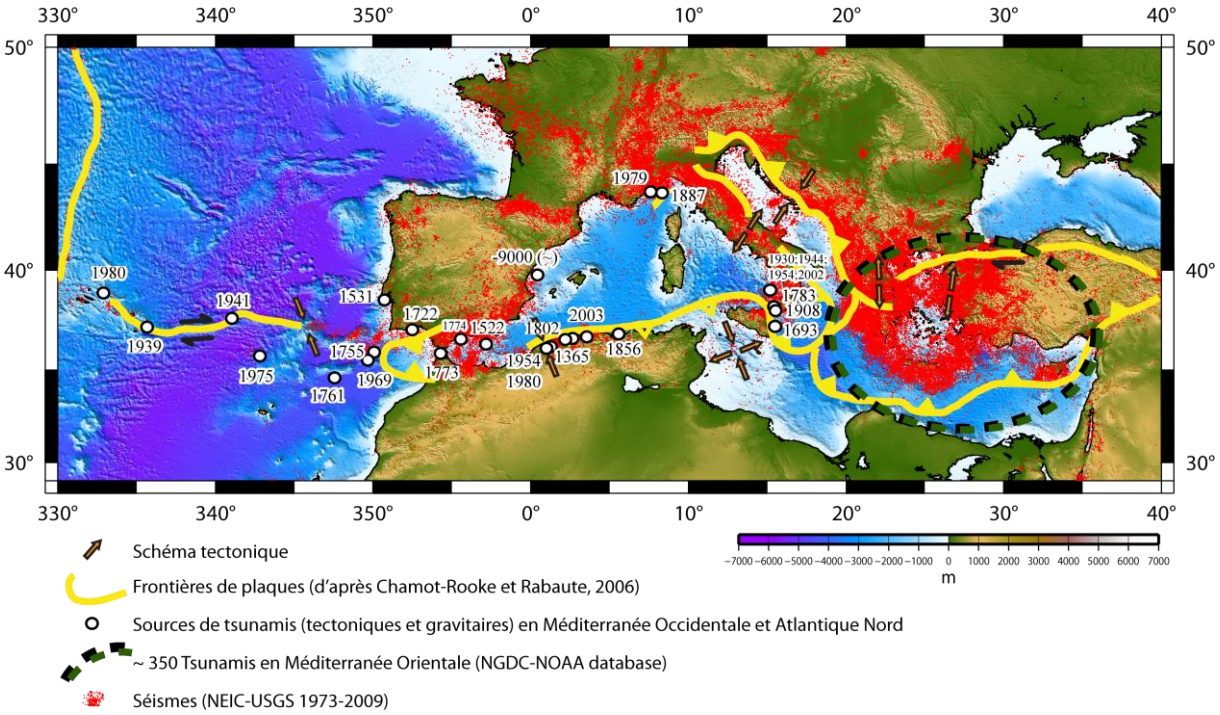

Figure 1 Localisation des sources des tsunamis significatifs connus en Méditerranée occidentale et au large de la péninsule ibérique.

[1] Courant dense en matériaux généré lors d'un glissement de terrain sous-marins.

1.3. *Manche et Mer du Nord*

La Manche et la mer du nord ne comprennent pas de limite de plaque, aussi bien active que passive. On peut y trouver seulement de la sismicité intraplaque associée à des paléo-réseaux de failles réactivés par divers mécanismes comme le rebond post-glaciaire[2] (Zoback et Grollimund, 2001). Mais en aucun cas on y trouvera de grands séismes de collision/subduction générateurs de tsunamis. Les tsunamis y ont donc une seule origine possible : les glissements de terrains.

De ce fait, la mer du Nord, beaucoup plus que la Manche du fait de sa profondeur moyenne et des pentes raides qu'elle peut avoir, peut être à l'origine de tsunamis associés à des glissements de terrains dans les fjord, comme l'événement de Storegga (Norvège), daté a environ 7000 ans, qui aurait mobilisé environ 3000 km^3 de matière (Lee, 2008 ; Løvholt et al., 2005), générant ainsi un tsunami de plusieurs dizaines de mètres d'amplitude d'après les modèles numériques calés avec les observations de dépôts réalisées in situ en Norvège, en Angleterre, en Ecosse et aux îles Shetland. Nous pouvons facilement imaginer qu'un tel tsunami pourrait avoir touché les côtes françaises.

Le cas particulier du séisme de Douvres (1580) a été rapporté dans plusieurs documents (Musson (1994, 1996) par exemple). Ce séisme, de magnitude estimée autour de 5.5 est connu pour avoir été suivi par 2 tsunamis, le second aurait atteint le Mont St Michel en coulant de nombreux bateaux dans la Manche (Baeteman, pers. comm.[3]). Un tel témoignage est à prendre en considération avec prudence mais néanmoins, l'hypothèse d'un glissement de terrain massif associé au séisme et capable de générer un tsunami dévastateur n'est pas à exclure (pour information, la bathymétrie de la Manche est très faible avec une profondeur moyenne de 120 m, remontant à 45 m entre Calais et Douvres et les fameuses falaises de craie de Douvres atteignent une centaine de mètres en altitude).

Le tableau 1 recense les tsunamis ayant touché ou ayant vraisemblablement touché les côtes françaises métropolitaines. On notera que la période connue s'étend sur à peine 500 ans.

[2] Rééquilibrage des masses terrestres consécutif à la fonte des calottes glaciaires (ajustement isostatique).

[3] http://www.sciencesnaturelles.be/active/sciencenews/archive2005/tsunami

Date	Origine		Tsunami		
	Séisme	Glissement de terrain	Local	Régional	Transocéanique
06/07-04-1580	Douvres, M5.3-5.9	*Voir discussion*	Inondation de la ville de Calais et des alentours, jusqu'à Boulogne (30 km) ; le lendemain une vague de 15 m ravage Douvres, 20-30 bateaux coulés		
01-11-1755	Plaine abyssale Horseshoe, au large du Portugal, M8.5-9.0				Témoignages dans tout l'Atlantique nord jusqu'aux Antilles, à Terre-Neuve, vagues de plusieurs mètres
21/22-08-1856	Jijel, marge algérienne, M7.2			La côte algérienne est touchée de Alger à Skikda (vague de 2-3m); on rapporte une vague anormale à Mahon (Baléares) (Roger et Hébert, 2008)	
23-02-1887	Mer Ligure, M6.2-6.5		1-2 m enregistrés à Gênes et Nice		
18-11-1929	Terre-Neuve (source gravitaire + séisme M7.2)	200 km^3			Enregistré par les marégraphes portugais (Lagos, Leixoes)
1931 (?)	Doggerbank, sud de la Mer du Nord, M6.1	*Voir discussion*	Un tsunami qui touche la Grande Bretagne principalement mais aussi le nord de la France		
28-02-1969	Plaine abyssal Horseshoe, off. Portugal, M7.9				Enregistré par le marégraphe de la Rochelle
16-10-1979	Nice (source gravitaire)	0.01 à 0.15 km^3	Vagues dans la baie des Anges (3 m à Antibes)		
21-05-2003	Zemmouri-Boumerdès, marge algérienne, M6.8			Le tsunami touche les Baléares (où il fait de nombreux dégâts) et la côte d'Azur	

Tableau 1 Les différents tsunamis ayant touché les côtes françaises.

2. Modélisation numérique

2.1. *Sources*

Dès lors que des tsunamis historiques ont été mis à jour, que ce soit via une connaissance de témoignages historiques ou via la découverte de dépôts sédimentaires associés, il faut parvenir à en déterminer la(les) source(s), tectonique, gravitaire, volcanique, ou voire cosmique (impact d'astéroïde ou de comète de dimension importante dans l'océan ; ce dernier cas concerne uniquement les tsunamis découverts via l'étude sédimentologique des paléo-dépôts, aucun n'est connu en France à ce jour). La modélisation permet de mieux comprendre des événements peu observés, ou de proposer des scénarios probables, et d'en étudier les effets à la côte.

Dans le cas d'un séisme, on recherchera les failles qui auront pu jouer suffisamment pour générer un tsunami ; cela correspond typiquement à des séismes ayant une magnitude supérieure à 6.0 d'après les

catalogues de tsunamis (par exemple voir le catalogue en ligne du Laboratoire Tsunami de Novosibirsk, Russie : http://tsun.sscc.ru/nh/tsunami.php) et en accord avec les travaux de Wells et Coppersmith (1994). Pour cela de nombreuses méthodes existent comme par exemple la sismique réflexion associée à des sondages bathymétriques et des analyses néotectoniques. L'exercice s'avère moins difficile lorsqu'une partie ou même la totalité de la rupture de surface se situe à terre (voir le cas du séisme de Zemmouri-Boumerdès de 2003, présentant une rupture partiellement à terre ou celui, plus controversé, de El Asnam de 1980, présentant une rupture entièrement à terre cette fois, et qui ont tous les deux été suivis d'un tsunami).

De la même façon dans le cas d'un glissement de terrain, on recherchera une zone « fraîchement » décapée de sa couverture sédimentaire, que ce soit à terre (dans les fjord par exemple) ou sous la mer (par exemple les prospections bathymétriques menées le long de la marge nord algérienne lors des campagnes Maradja 1 et 2 (Domzig et al., 2009)).

Une fois la source connue, nous allons lui attribuer des paramètres (taille, volume de matière mobilisé, rigidité du milieu considéré, déplacement, etc.) qui seront les premières données de base introduites dans un modèle numérique et/ou analogique ; les secondes données correspondent à la bathymétrie (et à la topographie dans le cas ou l'on souhaite simuler les inondations). Pour bien faire comprendre le processus nous nous proposons de traiter dans la suite le cas du tsunami généré par le séisme Zemmouri-Boumerdès du 21 mai 2003.

2.2. *Etude de cas : le tsunami de Zemmouri, Algérie (2003)*

Le 21 mai 2003, un séisme de magnitude 6.8 frappe la côte algérienne dans la région de Zemmouri-Boumerdès. Près de 2300 victimes, plus de 10000 blessés et d'importantes destructions sont à déplorer. Outre la violence du choc, ce séisme généra un tsunami qui sera enregistré en de nombreux endroits de Méditerranée occidentale, sur la côte Algérienne, mais aussi aux Baléares (marégraphes de Palma et San Antoni) où il fera également de nombreux dégâts avec des amplitudes de plus de 2 m en certains endroits et d'importantes vidanges de ports/inondations de zones basses (Alasset et al., 2006 ; Paris, pers. comm.). Une enquête révèlera par la suite que le sud de la France n'a pas été épargné, plus particulièrement la Côte d'Azur ou d'importantes amplifications de vagues et des tourbillons furent enregistrés dans quelques ports (Sahal et al., 2009).

2.2.1. *La physique derrière les modèles*

Dans le cadre de ce document, toutes les méthodes de modélisation ne sont pas explicitées. L'objectif étant de donner au lecteur une idée générale.

Afin de modéliser le tsunami, il faut avant toute chose fournir au modèle une information primordiale qui va ensuite gouverner le comportement du tsunami, de la source aux zones impactées : il s'agit de la déformation initiale, i.e. ce qui est nécessaire pour générer un tsunami. Il existe plusieurs modèles de calcul de déformation initiale ou déformation cosismique. Dans le cas présenté ici, il s'agit d'un modèle de dislocation élastique calculée à partir de la formule d'Okada (1985) qui utilise des paramètres simples tels que la position dans les trois dimensions de la faille, ses dimensions, les angles de glissement et quelques paramètres qualifiant la solidité des couches géologiques pour calculer une déformation du sol (coefficient de rigidité des roches principalement). Cette méthode, qui considère que la déformation du fond de la mer est transmise intégralement (sans pertes) à la colonne d'eau sus-jacente (par effet piston), résout les équations d'hydrodynamique de conservation de continuité (1) et de quantité de mouvement (2), (reliant la déformation de la surface de l'eau (η) , à la hauteur de la colonne d'eau (h) et à la vitesse de déplacement horizontale (v)) selon l'approximation des ondes

longues. Les termes non linéaires comme la force de Coriolis sont pris en compte, et la résolution de ces équations est effectuées selon la méthode des différences finies. Cette méthode a été largement testée dans le cadre des études dans le Pacifique, aux Antilles et en mer Méditerranée (Hébert et al., 2007; Roger et Hébert, 2008; Sahal et al., 2009, Roger et al., 2010(a,b)).

$$\frac{\partial(\eta + h)}{\partial t} + \nabla.[v(\eta + h)] = 0 \qquad (1)$$

$$\frac{\partial v}{\partial t} + (v.\nabla).v = -g\nabla\eta + \sum f \qquad (2)$$

2.2.2. *Les grilles bathymétriques*

Les grilles bathymétriques sont réalisées à partir de données acquises lors de campagnes en mer par le biais de sondeur multifaisceaux, de points de sondage indiqués sur des cartes marines (parfois anciennes), etc. Elles doivent représenter au mieux la morphologie des fonds marins à la résolution que l'on souhaite : par exemple, si l'étude vise à reproduire un phénomène de résonance portuaire, il faudra que la grille bathymétrique utilisée dans la modélisation reproduisent les structures pouvant avoir une influence sur les ondes, c'est à dire des structures de l'ordre de quelques mètres (i.e. les digues, les jetées, etc.). Au contraire, si on ne considère que la propagation du tsunami en haute mer, une résolution large de plusieurs centaines de mètres, voir plusieurs kilomètres sera suffisante.

2.2.3. *Résultats de modélisation*

Les résultats de modélisation de tsunami vont apporter principalement des informations concernant le temps de trajet du tsunami depuis son initiation (par séisme, glissement de terrain, éruption volcanique, etc.), sa polarité (élévation ou baisse du niveau marin en premier), sa période et son amplitude maximale.

Ils peuvent être présentés sous plusieurs formes en fonction de la finalité des résultats : soit sous forme de marégrammes synthétiques qui pourront être comparés à des marégrammes réels que l'on aura au préalable, et en fonction des besoins, filtrés de la marée et des hautes fréquences parasites (Fig. 2); soit sous forme de carte de hauteurs de vague maximums (Fig. 3) et par extension, sous forme de carte d'inondation si on a décidé de calculer la propagation à terre.

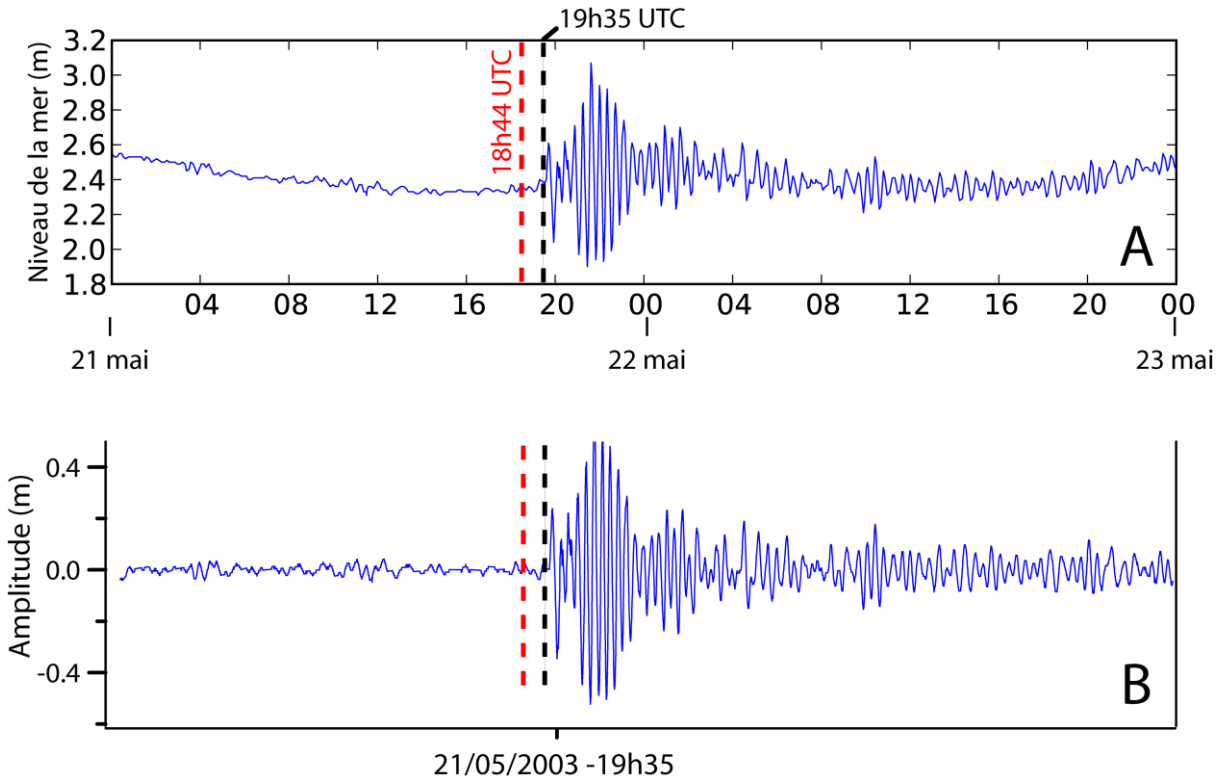

Figure 2 Marégramme enregistré dans le port de Palma (Baléares) les 21 et 22 mai 2003 : A) signal brut ; B) signal brut filtré de la marée. L'heure du séisme et l'heure d'arrivée du tsunami sont indiqués respectivement par les lignes discontinues rouge et noir.

Dans le cas du tsunami de Zemmouri-Boumerdès de 2003, plusieurs hypothèses de source ont été proposées (Alasset et al., 2006). La figure 3A montre la directivité du tsunami depuis la côte algérienne : il est essentiellement orienté vers les îles Baléares. Cette directivité dépend essentiellement de l'azimuth du plan de faille considéré (Okal, 1988). On y voit clairement le rôle de bouclier exercé par le promontoire des Baléares protégeant ainsi la côte espagnole et le golfe du Lion (France). On notera ici qu'une source située plus à l'est sur la marge algérienne, comme par exemple le séisme de Jijel de 1856 aurait certainement un impact beaucoup plus important sur les côtes françaises (Roger et Hébert, 2008). Toutefois, l'amplitude des vagues modélisée ne dépasse pas les 40 cm sur cette première grille de résolution spatiale d'un kilomètre. Il est alors intéressant d'augmenter la résolution pour regarder plus en détail ce qui se passe à la côte (on parlera de l'effet de « shoaling », i.e. la variation de la hauteur des vagues due à une variation de profondeur). Pour modéliser plus correctement l'amplification des vagues dont la longueur d'onde raccourcit lorsque la profondeur d'eau décroît (et pour réduire les temps de calcul), plusieurs niveaux de grilles sont alors réalisés en se rapprochant de la zone d'intérêt ; ainsi la grille du golfe de la Napoule atteint une résolution de 40 m et les ports considérés (Cannes et la Figueirette) une résolution de 3 m. Ces zooms permettent de distinguer des zones favorisant l'amplification du tsunami comme par exemple au large des îles des Lérins (Fig. 3B) ou dans les ports (Fig. 3C).

Les enregistrements marégraphiques de stations algérienne (Alger), espagnoles (Palma, Ibiza, San Antoni, Malaga, Valencia, etc.) et françaises (Sète, Marseille, Toulon, Nice, etc.) de plus ou moins bonne qualité (du fait de l'échantillonnage qui est souvent trop large, jusqu'à un point toutes les 15 minutes pour le marégraphe d'Alger) ont permis de discuter les résultats obtenus avec les modèles (Alasset et al., 2006 ; Sahal et al., 2009) : certains temps d'arrivée sont à ce jour encore difficiles à ajuster pour faire caler les modèles de rupture du séisme de 2003 avec la réalité. La comparaison des

données marégraphiques réelles et virtuelles permet donc également de discuter de la viabilité des sources proposées.

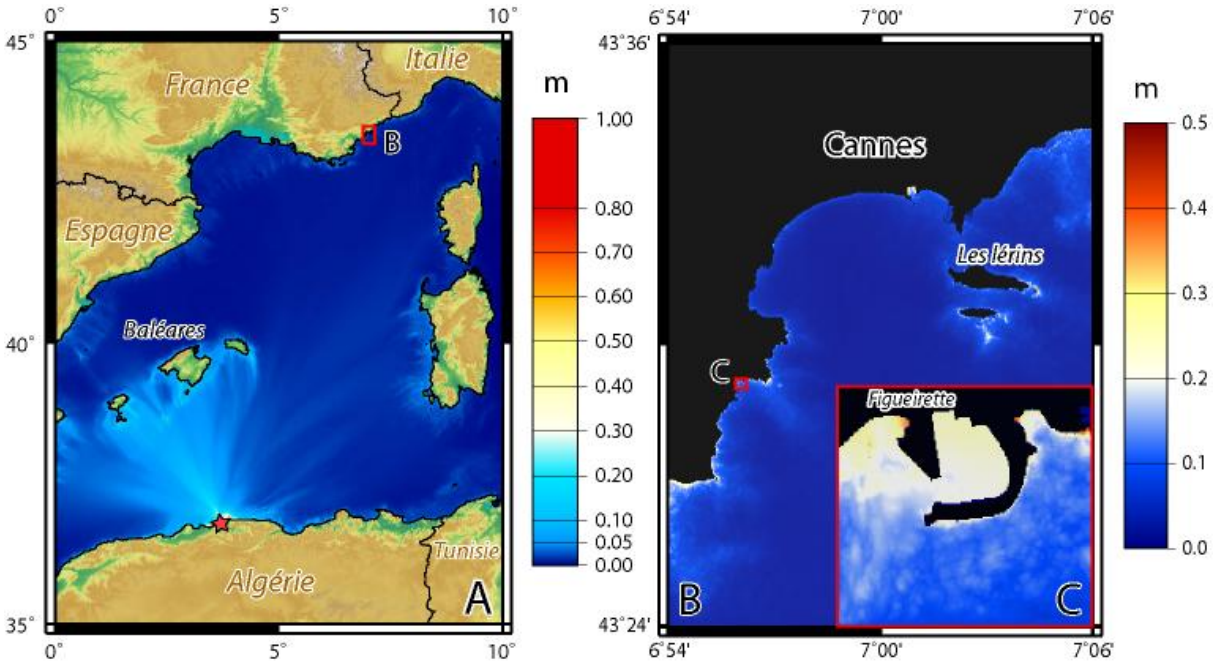

Figure 3 Hauteurs de vague maximums après 4h de propagation d'un tsunami généré par le séisme de Zemmouri avec la source de Yelles et al. (2004) sur des grilles de différentes échelles: Méditerranée occidentale (A) ; golfe de la Napoule (B) ; port de la Figueirette (C).

Note sur la résonance

La résonance est un phénomène naturel selon lequel, lorsqu'un objet physique est soumis à des vibrations proches de sa période propre ou période de résonance, il va se mettre à osciller jusqu'à atteindre un régime d'oscillation d'équilibre qui dépend des autres forces mises en jeu. Plus pratiquement, les modes de résonance d'un bassin rectangulaire sont les plus simples à trouver. Ils consistent à rechercher des figures qui permettent de découper la surface en plusieurs parties de même dimension dans un sens et dans l'autre (Fig. 4). Ainsi nous pouvons numéroter ces modes de résonance par deux indices (n et m) symbolisant le nombre de « zéros » (appelés aussi nœuds de résonance, i.e. zones qui n'oscillent pas) que l'on peut trouver selon les deux axes.

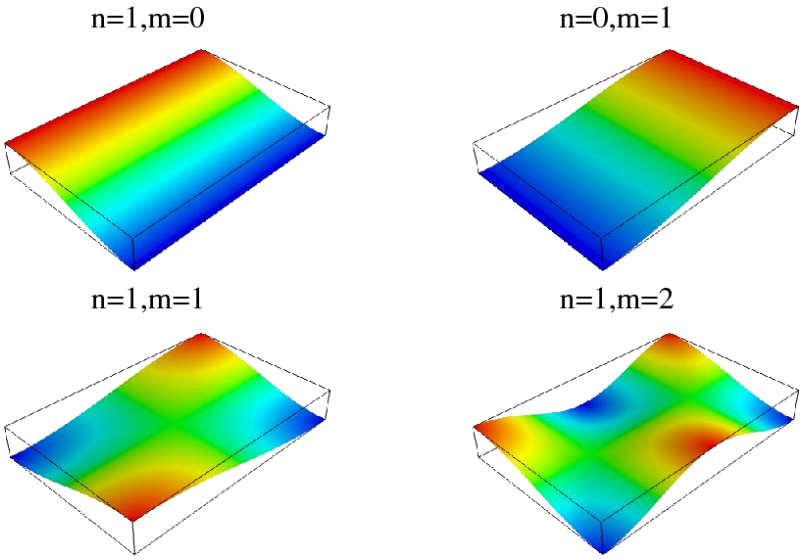

Figure 4 Découpage de la surface d'un bassin rectangulaire en parties de même dimensions, symbolisant les différents modes de résonance.

Dans le cas de système physique plus complexe (tel que les ports, les baies, les lagons) les résonances ne peuvent que se retrouver par des méthodes mathématiques plus complexes et l'utilisation du modèle numérique de terrain (MNT) est indispensable. De manière générale, ce type d'étude est réalisé pour connaître les effets des vagues de vents et de la houle sur les infrastructures portuaires et les bateaux qu'elles abritent. Ainsi, pour revenir au cas du tsunami de 2003, nous pouvons observer plusieurs mode de résonances pour chaque port et plus particulièrement pour le port de la Figueirette (Fig. 5) dont le mode principal est à 3.84 min. Autre exemple, le marégraphe du port de Palma (Baléares) semble avoir enregistré une oscillation basse fréquence d'une période de l'ordre de 20 min, typique d'une résonance (Fig. 2).

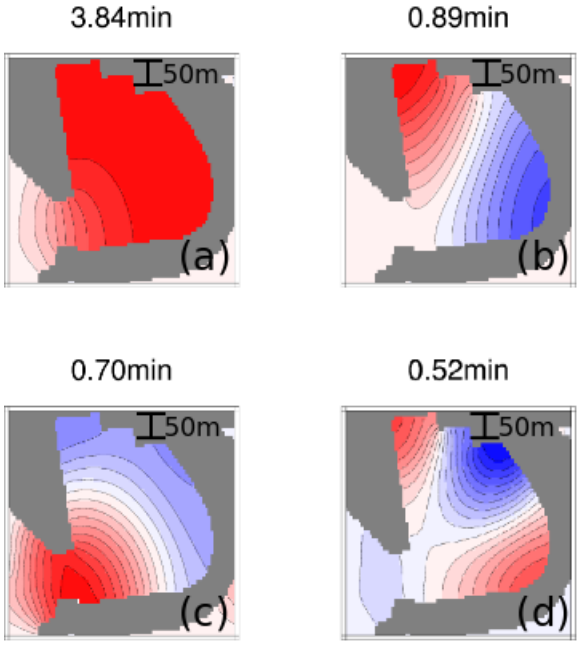

Figure 5 Présentation de différents modes de résonance du port de la Figueirette.

4. Discussion générale

4.1. *Evaluation du risque – notion de vulnérabilité*

Les différents résultats de modélisation, que ce soit les cartes de hauteur maximale de vagues (Fig. 2), les cartes d'inondation, les spectres de résonance dans les baies ou les ports, permettent de souligner les zones où l'onde du tsunami aura a priori plus tendance à s'amplifier de manière à mettre en péril les intérêts humains ou économiques. Après une estimation de l'aléa tsunami dans une zone bien déterminée, une étude de vulnérabilité sera donc menée pour estimer quels sont les enjeux humains, sociaux, financiers, économiques et touristiques. Les deux études couplées constitue une étude du risque qui par définition représente la convolution d'un aléa et des vulnérabilités. Cette étude permettra ensuite de faire ressortir des zones dites « à risque ».

4.2. *La recherche de paléo-tsunamis*

La recherche de paléo-tsunamis ou plutôt de paléo-dépôts de tsunamis qui auraient été enregistrés dans les dépôts sédimentaires d'une région (couches sédimentaires ou blocs déposés) nous apporte beaucoup d'informations concernant l'aléa tsunami dans cette région (Bourrouilh-Le Jan et al., 2007 ; Pignatelli et al., 2009). Pour savoir où chercher, la modélisation numérique est un outil crucial puisqu'elle aide à définir des zones où les tsunamis auront atteint une amplitude suffisante pour, par exemple, dépasser un cordon dunaire pour déposer ensuite le sable dans une zone lagunaire d'arrière-dune. Les zones lagunaires sont des milieux favorables à une bonne conservation de dépôts associés à un tel événement principalement du fait des forts taux de sédimentation qui y règnent, recouvrant ainsi rapidement par des dépôts terrigènes, les dépôts d'origine marine apportés par le tsunami (par exemple voir Morales et al., 2008).

Un problème majeur reste toutefois à souligner : les dépôts de tsunami peuvent se mélanger avec les dépôts de tempêtes, beaucoup plus nombreuses, surtout en France métropolitaine, et la distinction peut s'avérer ainsi difficile (Kortekaas et Dawson, 2007). Par exemple vers la Rochelle, s'il y avait des dépôts de tsunami conservés dans les sédiments, ils doivent être complètement « noyés » dans les dépôts de tempête, qui inondent souvent les zones basses dans ces régions (voir par exemple les inondations générées par la tempête Xynthia de février 2010).

4.3. *Les limites de la modélisation*

La résolution des données bathymétriques et topographiques utilisées pour modéliser la propagation d'un tsunami est un facteur limitant à la reproduction du phénomène à son approche à la côte à partir du moment où l'on ne reproduit pas les structures sous-marines capables d'avoir une influence parfois considérable sur le tsunami (sur sa forme, sur son amplification, sa perte d'énergie par réflexion, sur son éventuel déferlement, etc.) comme les canyons sous-marins, les infrastructures portuaires, etc.

5. Conclusion

Les recherches historiques montrent que l'aléa tsunami est bien présent en France métropolitaine, que ce soit en Méditerranée mais aussi sur les côtes Atlantique et de la Manche. Néanmoins les évènements les plus marquants pour les côtes françaises voient leur origine en Méditerranée occidentale. Le peu d'évènements tsunamigéniques (séismes et glissements de terrain réunis) à notre disposition ne permet pas malgré tout de réaliser une étude approfondie du risque existant pour les côtes françaises. L'outil modélisation numérique (et parfois analogique) autorise alors à spéculer sur les potentiels effets qu'aurait un tsunami généré par des sources identifiées clairement ou non et à pallier le manque de données historiques.

La finalité de toutes ces études sur les tsunamis est donc de parvenir à bien comprendre l'aléa pour ainsi réduire le risque au maximum en passant par la prévention et l'installation de systèmes d'alerte aux tsunamis viables. C'est dans ce cadre, et suite à la catastrophe de 2004 dans l'Océan Indien, que la communauté internationale, par le biais de l'UNESCO (Intergovernmental Oceanographic Commission, 2005), a décidé de doter chaque bassin océanique, Méditerranée comprise, de systèmes d'alerte aux tsunamis.

Ces systèmes d'alerte sont en cours de préparation et/ou d'installation. Pour l'instant uniquement capable de prévenir le risque de tsunami d'origine sismique, ils sont couplés aux réseaux de surveillance sismique, c'est à dire qu'une magnitude de base (typiquement M6.0-6.5) a été définie comme étant la limite inférieure à partir de laquelle un séisme peut être générateur d'un tsunami. Il faut noter ici qu'un tsunami d'une magnitude inférieure peut bien évidemment déstabiliser des sédiments, générant ainsi un glissement de terrain apte à induire un tsunami. Dans ce cas, l'alerte sera donnée si et seulement si des capteurs de pression (comme ceux associés aux bouées DART) enregistrent le passage du tsunami.

Dans tous les cas, l'alerte lancée est surtout un moyen de prévention pour les populations éloignées. Pour les zones proches de la source, seule l'éducation permet de sauver des vies (connaissance des réflexes à avoir en cas de séisme, en cas de retrait soudain de la mer, etc.).

6. Remerciements

Les auteurs remercient toute l'équipe du « Colloque Risques naturels en Méditerranée Occidentale » (16-21 novembre 2009, Carcassonne) et tout particulièrement Frédéric Ogé (CNRS) pour l'organisation et l'invitation à présenter les travaux détaillés dans ce manuscrit. Ils remercient également Jean-Michel Bragard et Cecile Baeteman (Institut royal des sciences naturelles de Belgique) pour les informations concernant les tsunamis en Manche et mer du Nord, ainsi que Raphael Paris (GEOLAB, CNRS) pour sa disponibilité pour discuter des dépôts de tsunami.

Ce travail a été financé par l'ANR RiskNat MAREMOTI sous le contrat ANR-08-RISKNAT-05-01c.

Références

Alasset P.-J., Hébert H., Maouche S., Calbini V., Meghraoui M., 2006: The tsunami induced by the 2003 Zemmouri earthquake (Mw=6.9, Algeria): modelling and results. *Geophys. J. Int.*, 166, 213–226.

Baptista M.A., Heitor S., Miranda J.M., Miranda P., Mendes V.L., 1998a : The 1755 Lisbon tsunami; evaluation of the tsunami parameters. *J Geodyn*, 25(**2**): 143-57.

Bourrouilh-Le Jan, F.G., Beck, C., Gorsline, D.S., 2007 : Catastrophic events (hurricanes, tsunami and others) and their sedimentary records: Introductory notes and new concepts for shallow water deposits. *Sedimentary Geology*, 199, 1–11.

Domzig A., Gaullier V., Giresse P., Pauc H., Déverchère J., Yelles K., 2009 : Deposition processes from echo-character mapping along the western ALgerian margin (Oran-Tenes), Western Mediterranean. *Marine and Petroleum Geology*, 26, 673-694.

Fine I.V., Rabinovich A.B., Bornhold B.D., Thomson R.E., Kulikov E.A., 2005: The Grand Banks landslide-generated tsunami of November 18, 1929: preliminary analysis and numerical modeling. *Marine Geology*, 215, 45–57.

Gutscher, M.-A., Dominguez, S., Westbrook, G.K., Leroy, P., 2009: Deep structure, recent deformation and analog modeling of the Gulf of Cadiz accretionary wedge: implications for the 1755 Lisbon earthquake. *Tectonophysics*, 475, 85–97.

Gutscher, M.-A., malod, J., Rehault, J.-P., Contrucci, I., Klingelhoefer, F., Mendes-Victor, L., Spakman, W., 2002: Evidence for active subduction beneath Gibraltar. *Geology*, 30, **12**, 1071-1074.

Haslett, S.K., Bryant, E.A., 2007: Reconnaissance of historic (post-AD 1000) high-energy deposits along the Atlantic coasts of southwest Britain, Ireland and Brittany, France. *Marine Geology*, 242, 207-220.

Hébert H., Sladen A., Schindelé F., 2007: The great 2004 Indian Ocean tsunami: numerical modeling of the impact in the Mascarene Islands. *B. Seismol. Soc. Am.*, 97, **1A**, S208-S222.

Horsburgh K.J., Wilson C., Baptie B.J., Cooper A., Cresswell D., Musson R.M.W., Ottemöller L., Richardson S., Sargeant S.L., 2008: Impact of a Lisbon-type tsunami on the U.K coastline and the implications for tsunami propagation over broad continental shelves. *Journal of Geophysical Research*, 113, **C04007**, doi:10.1029/2007JC004425.

Intergovernmental Oceanographic Commission, 2005. Intergovernmental coordination group for the tsunami early warning and mitigation system in the North-Eastern Atlantic, the Mediterranean and connected seas. UNESCO, Resolution XXIII-14. http://www.ioc-tsunami.org/components/com_pdffarm/files/Resolution23_14.pdf

Kortekaas, S., Dawson, A.G., 2007: Distinguishing between tsunami and storm deposits: An example from Martinhal, SW Portugal. *Sedimentary Geology*, 200, **3-4**, 208-221.

Løvholt F., Harbitz C.B., Haugen K.B., 2005: A parametric study of tsunamis generated by submarine slides in the Ormen Lange/Storegga area off western Norway. *Marine and Petroleum Geology*, 22, 219–231.

Marques, F.O., 2010: Comment on "Deep structure, recent deformation and analog modeling of the Gulf of Cadiz accretionary wedge: Implications for the 1755 Lisbon earthquake", by Gutscher et al. 2009. *Tectonophysics*, 485, 327-329.

Morales, J.A., Borrego, J., San Miguel, E.G., Lopez-Gonzalez, N., Carro, B., 2008: Sedimentary record of recent tsunamis in the Huelva Estuary (southwestern Spain). *Quaternary Science Reviews*, 27, 734–746.

Musson, R.M.W., 1994: A catalogue of British Earthquakes. *British Geological Survey technical Report*, No. WL/94/04, pp.99.

Musson, R.M.W., 1996: The seismicity of the British Isles. *Annali di Geofisica*, 39, **3**, 463-469.

Okada Y., 1985. Surface deformation due to shear and tensile faults in a half-space. *Bull. Seismol. Soc. Am.*, 75, 1135-1154.

Okal, E.A., 1988: Seismic parameters controlling far-field tsunami amplitudes: a review. *Natural Hazards*, 1, 67-96.

Pignatelli C., Sansò P., Mastronuzzi G., 2009: Evaluation of tsunami flooding using geomorphological evidence. *Marine Geology*, 260, 6–18.

Roger J., Allgeyer S., Hébert H., Baptista M.A., Loevenbruck A., Schindelé F., 2010(a): The 1755 Lisbon tsunami in Guadeloupe Archipelago : contribution of numerical modelling. *The Open Oceanography Journal*, in press.

Roger J., Baptista M.A., Mosher D., Hébert H., Sahal A., 2010(b): Tsunami impact on Newfoundland, Canada, due to far-field generated tsunamis. Implications on hazard assessment. *Proceedings of the 9th U.S. National and 10th Canadian Conference on Earthquake Engineering*, July 25-29, 2010, Vancouver, Canada (accepted).

Roger J., Hébert H., 2008: The 1856 Djijelli (Algeria) earthquake and tsunami: source parameters and implications for tsunami hazard in the Balearic Islands. *Natural Hazards and Earth System Sciences*, 8(**4**), 721-731.

Sahal A., Roger J., Allgeyer S., Lemaire, B., Hébert H., Schindelé F., Lavigne F., 2009: The tsunami triggered by the 21 May 2003 Boumerdes-Zemmouri (Algeria) earthquake: field investigations on the French Mediterranean coast and tsunami modelling. *Natural Hazards and Earth System Sciences*. 9, 1823-1834.

Zitellini, N., Gracia, E., Matias, L., Terrinha, P., Abreu, M.A., DeAlteriis, G., Henriet, J.P., Danobeitia, J.J., Masson, D.G., Mulder, T., Ramella, R., Somoza, L., Diez, S., 2009: The quest for the Africa-Eurasia plate boundary west of the Strait of Gibraltar. *Earth and Planetary Science Letters*, 280, 13-50.

Zoback, M.D., Grollimund, B., 2001: Impact of deglaciation on present-day intraplate seismicity in eastern North America and western Europe. *C. R. Acad. Sci. Paris, Sciences de la Terre et des planètes / Earth and Planetary Sciences*, 333, 23–33.

Annexe 2

Ce document présente une synthèse des travaux de recherche préliminaires sur le séisme et le tsunami du 6 avril 1580 dans le détroit de Calais-Douvres a l'issue de la mission de terrain TSUNORD des 11 et 12 mai 2010. Cette étude, qui entre dans le cadre du projet MAREMOTI-WP2 (observations géologiques et historiques) pour l'estimation de l'aléa tsunami dans la Manche, est coordonnée par le laboratoire de géologie de l'Ecole normale supérieure (Paris) et réalisé conjointement avec GEOLAB (Université Blaise Pascal, Clermont-Ferrand) et le LGP (Université Paris 1).

J. ROGER[(1)], P. WASSMER[(2)], H. GOETT[(3)]

1 Ecole normale supérieure, Laboratoire de Géologie
2 Université de Paris 1 Panthéon-Sorbonne, Laboratoire de Géographie Physique
3 Université Louis Pasteur, Faculté de Géographie, Strasbourg

1) Cadre général

Il a été rapporté dans plusieurs catalogues de séismes tels que ceux de Vogt (1979) (Fig. 1) ou Musson (1994, 1996) par exemple ou celui du BRGM (http://www.sisfrance.net/donnees_dates.asp) qu'un évènement de magnitude estimée à 6.2-6.9 (Neilson et al., 1984) a eu lieu le 6 avril 1580 et a affecté une vaste région incluant le nord de la France avec des villes touchées (maisons et églises détruites) comme Calais, Boulogne et même Rouen dans la vallée de la Seine (où il est mentionné que des clochers sont tombés), l'Angleterre (on parle du « séisme de Londres » dans de nombreux écrits puisqu'il est aussi un des deux plus gros séismes ressentis dans cette ville d'après le catalogue des séismes anglais de Musson (1994)), la Belgique et les Pays-Bas. L'épicentre a été localisé dans le détroit de Calais-Douvres grâce aux études macrosismiques basées sur les rapports et autres documents historiques (Fig. 2). La carte ainsi obtenue montre une orientation de la zone de rupture selon un azimut en accord avec l'orientation des failles hercyniennes (Fig. 3 et 4).

B. Tableaux régionaux

TABL. 1. — *Picardie - Artois - Flandres - Ardennes* (J. Delaunay).

Date		Epicentre macrosismique		Séisme régional	Séisme lointain	Effets régionaux	Intensité (échelle MSK)	Nature des sources	Anthologie	Degré de connaissance du séisme
Séisme régional	Séisme lointain	Régional	Lointain	Lieux et aires affectés dans la région et hors d'elle	dans la seule région					
854		?		-Tournai -Cambrai -Mayence		Dégâts immobiliers à Cambrai	Cambrai : VII-VIII	Compilateurs	"... à Cambrai la Tour de l'Eglise Saint Pierre en s'écroulant écrasa plusieurs maisons voisines ..." (H. DOUXAMI d'après LECARRENTIER et HAVERLANDT,1912, in : Bull. soc. géog. Lille, t58).	Médiocre
	6-04-1580		Mer du Nord		Ensemble de la région	Raz de marée .Dégâts à Calais Douai . Arras .Victimes à Calais ?	Calais:VII Douai: VI-VII Arras:VI-VII	Archives Chroniques Travaux savants Compilateurs	Calais : "... de terribles secousses et pertes au démolissement et entière submersion de quelques bâtiments ..." (Anonyme 1580, Horrible tremblement de terre advenu en plusieurs endroits de ce royaume, Paris). Douai :"... espouvantable tramblement de terre ayant causé cheute de pierres d'aucunes maison de ladite ville ..." (Arch. Mun. Douai BB 13). Arras : "... plusieurs couvertures de cheminées vielles et caduques seraient tombées ...(Arch. com. Arras, Mémoriaux du Magistrat, cote XV f° 103,in HIRSCHAUER, 1909, Météorologie rétrospective, Arras).	Moyen
	4-04-1640		Région de : Cologne - Düren		-Cambrai -Lille -Douai -Orchies -Vendresses -Mouzon	Dégâts à : -Lille -Douai -Orchies ?	?	Compilateurs	"... dans les villes de Lille, Douay, Orchies et à l'environ ... tremblement de terre qui causa bien du dommage ..." (H. DOUXAMI 1912 in Bull. soc. géog. Lille t58 d'après Manuscrit 636 Arch. munic. Lille). "... Lille et en autres lieux icy à l'entour laquelle elle fit grand dommage en Europe ..." (H. DOUXAMI 1912 in Bull. soc. géog. Lille, t58 , d'après chronique lilloise de Chavatte).	Médiocre
	18-09-1692		Pays-Bas ?		-Dunkerque -St Mard -Lille -Amiens -Rumegies -Roubaix -Cambrai -Coucy -Aire -Beaucamp -Manicamp -Laon -Château-Porcien -Damouzy -La Neuville -Les Wassigny	Dégâts à Lille : .Tremblement des constructions	Lille:VII ? Coucy:VII ? Linselles:VI St Amand: VI Roubaix : V ? Houplin: V	Archives Registres paroissiaux Chroniques Compilateurs	"... Lille et icy à l'entour ... lesquelles eurent beaucoup de cheminées abbatues en la ville de Lille ... aucun dire que les cloches ont batelé ..." (copie de la chronique de Chavatte, reprenant elle-même le livre de MANTEAU, XVIIIème, Bibl. mun. Lille). "... à l'abbaye de St Amand la voute de la bibliothèque... a foncé" (Journal d'un curé de campagne au XVIIème siècle publié par H. PLATELLE 1965). Liry : "... l'église fut si éprouvée ... que les voutes menaçaient ruine ..."(J. VILLETTE, 1905, Arch. dép. Marne G. 283 n°4 Ardennes et Argonne, t12).	Moyen

Figure 1 Extrait du catalogue de Vogt (1979).

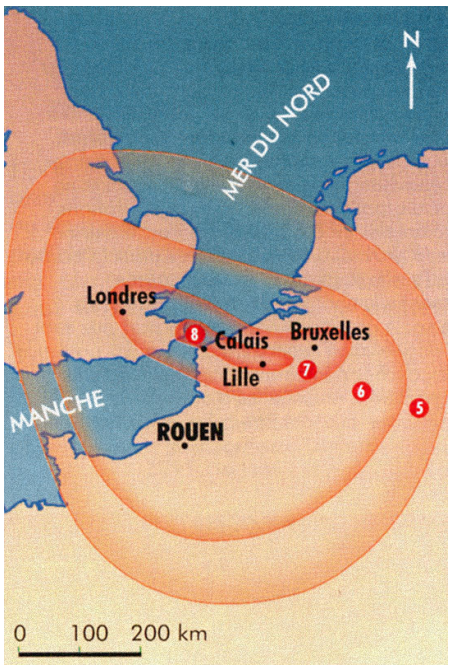

Figure 2 Carte des isoséistes du séisme du 6 avril 1580 (Nicolas et Berthoux, 1995).

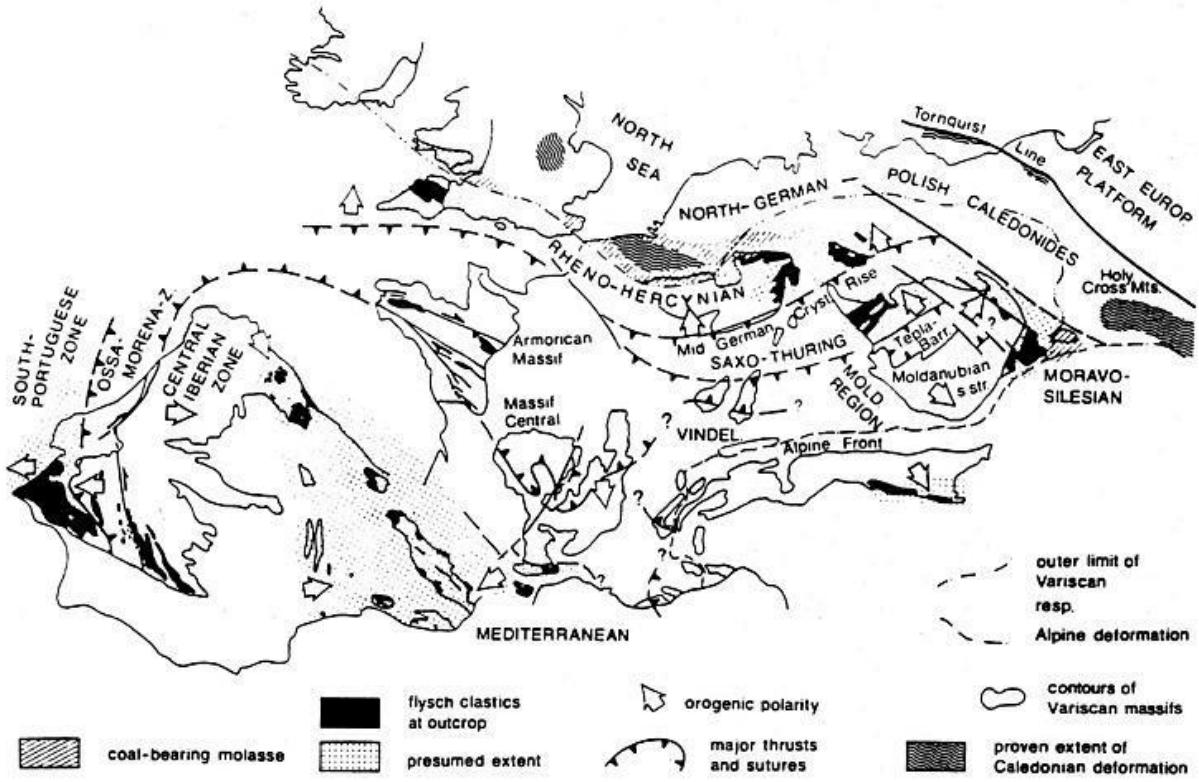

Figure 3 Eléments structuraux principaux de la ceinture hercynienne européenne pendant le Carbonifère inférieur (Franke, 1989).

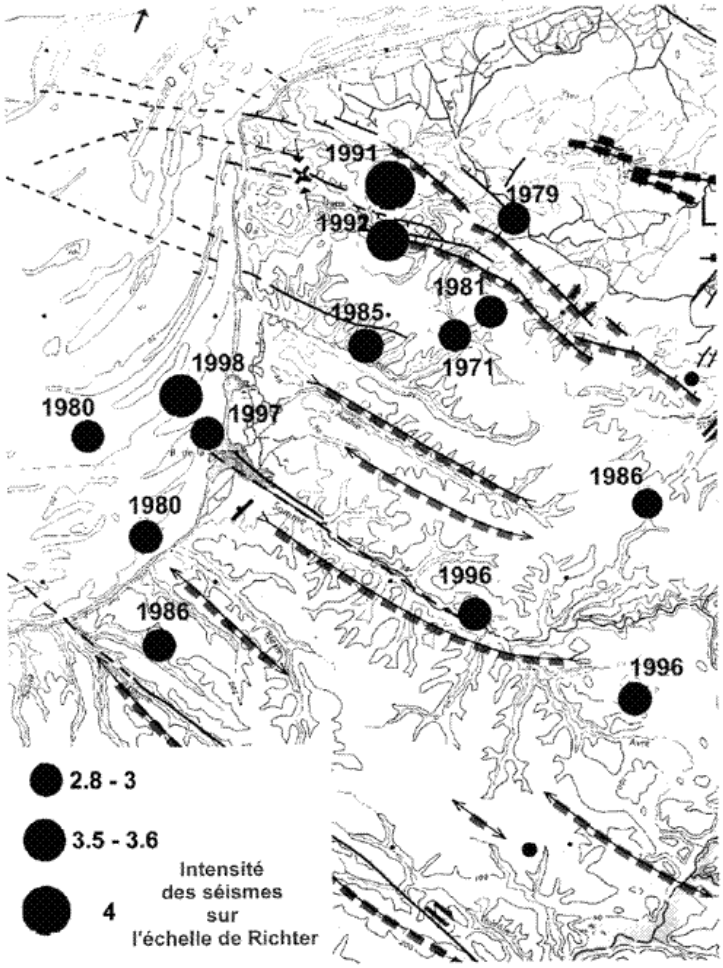

Figure 4 Localisation, intensités et dates des séismes instrumentaux (IPGS) de 1962 à 1998 sur la carte tectonique du nord de la France (CNDP-CRDP de l'Académie d'Amiens, 2006).

Pour information, la région Nord-pas de Calais, affectée par ce séisme, a été classée en aléa sismique de faible à modérée sur la nouvelle carte de l'aléa sismique pour la France métropolitaine et les communautés d'outre-mer du 21 novembre 2005 (DDRM, 2009). En effet, comme le montre la figure 4, quelques séismes de magnitude supérieure à 3 y ont été enregistrés depuis les années 70.

Le tsunami

Le séisme de 1580 est connu pour avoir été suivi par 1, voir 2 tsunamis, qui auraient inondés les villes de Douvres, Calais et Boulogne. Le second tsunami aurait atteint le Mont St Michel en coulant de nombreux bateaux dans la Manche (Discourse, 1580 in Haslett et

Bryant, 2008)). Un tel témoignage est à prendre en considération avec prudence, sachant que Musson (1994) indique que les effets marins du séisme (vagues) auraient pu être causés en fait par une tempête ayant eu lieu quelques jours plus tard, hypothèse repoussée par Haslett et Bryant (2008) qui indiquent que la tempête a eu lieu du côté du Mont Saint Michel à la même époque. Mais néanmoins, l'hypothèse d'un glissement de terrain massif associé au séisme et capable de générer un tsunami dévastateur n'est pas à exclure surtout quand on sait que le mur du château de Douvres et la falaise sous-jacente se sont effondrés lors du séisme (Haslett et Bryant, 2008). Pour information, la bathymétrie de la Manche est très faible avec une profondeur moyenne de 120 m, remontant à une soixantaine de mètres seulement entre Calais et Douvres (Fig. 5); les fameuses falaises de craie de Douvres atteignent une centaine de mètres en altitude (Roger et al., 2010). L'hypothèse d'un tsunami générer directement par le séisme semble moins probable du fait des mécanismes de ces failles hercyniennes mais toutefois possible, du fait 1) de la magnitude et de la profondeur (superficielle) estimées du séisme (qui représente une libération d'énergie suffisante pour généré un tsunami) et 2) de l'association à des phénomènes locaux d'amplification des ondes (résonance, wave trapping, réflexion, réfraction, etc) comme cela a pu être le cas dans l'estuaire de la rivière de Boulogne; ainsi des simulations de tsunamis seront effectuées avec différents scénarii de rupture afin de valider ou invalider cette hypothèse d'origine sismique du tsunami dans cette zone. Des simulations de glissement de terrain (submarine landslides) ou de chute de roches (aerial rock slides) pourront également être effectuées.

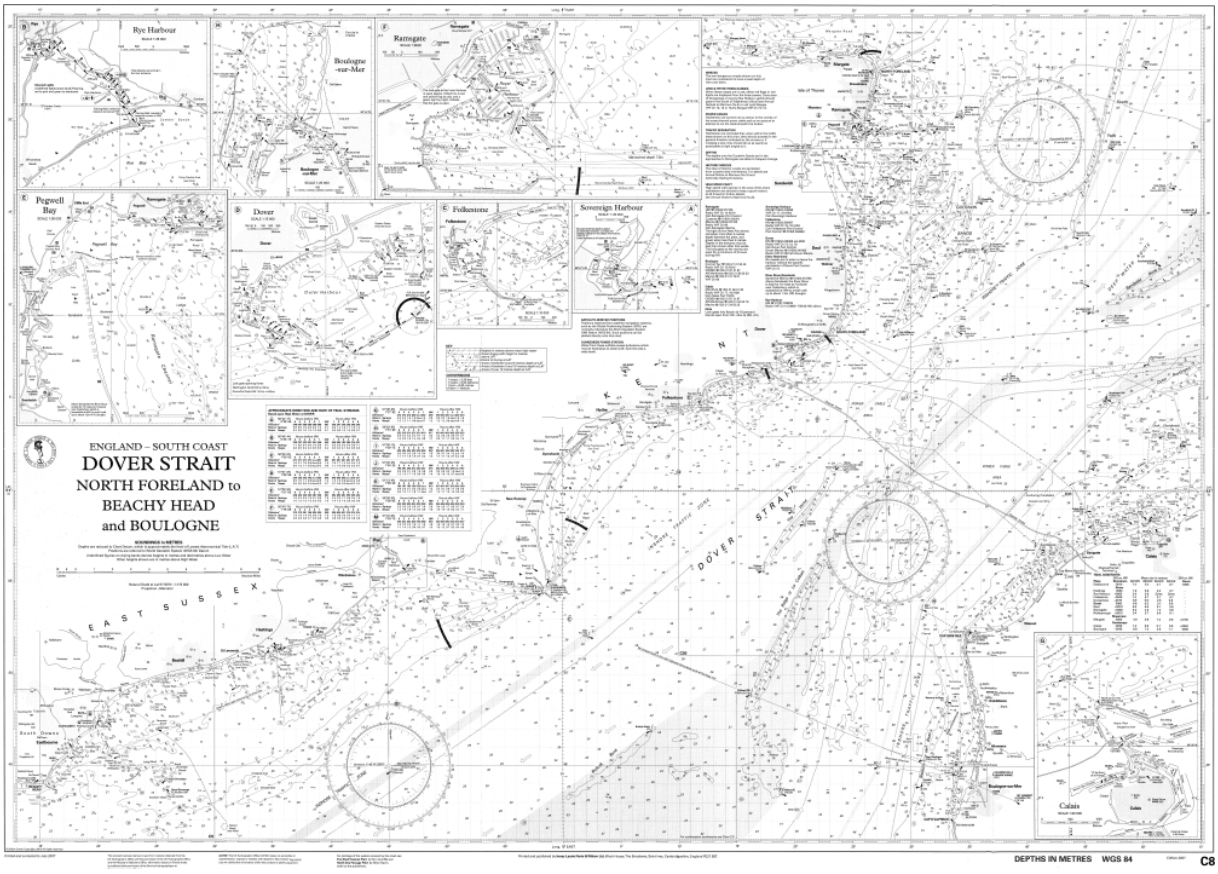

Figure 5 Carte bathymétrique du canal de Calais-Douvres (Imray - Dover Strait, 2007).

Ces falaises sont sujettes à l'érosion qui entraine un recul du trait de côte progressivement comme on peut le voir sur la figure 6 (Dornbusch, 2006). Ce recul est ponctué par des évènements de type glissements de terrain ou plus exactement « flow chalks » (Dornbusch et al., 2008) du à des variations de pression de pores dans ces roches calcaires très poreuses (> 40%) proches de la saturation en eau, leur donnant un caractère liquide ou « flow » au moment du glissement (i.e. peu de cohésion) (Hutchinson, 1969, 2002). Nous n'approfondirons pas l'analyse de ces glissements de terrain ici ; seuls les volumes maximum recensés et les zones touchées par des évènements plus récents nous intéressent dans le cadre de cette étude préliminaire.

Ainsi, les travaux de Hutchinson (2002) indiquent des volumes maximums de débris mobilisés de l'ordre de 1-1.25 10^6 m^3 (glissement de Great Fall du 19.12.1915) et plus (Steady Hole, 19.12.1915). Par comparaison avec l'évènement de Nice (16.10.1979), on se trouve ici dans un cas d'effondrement aérien avec un volume de débris environ 10 fois moindre ; d'après Assier-Rzadkiewicz et al. (2000), un effondrement de moins de 10 millions de m^3 semble insuffisant pour engendrer un tsunami dévastateur. Néanmoins les

mécanismes de glissement sont très différents pour ces « chalk flows » ; cela fait partie des points à investiguer par la suite.

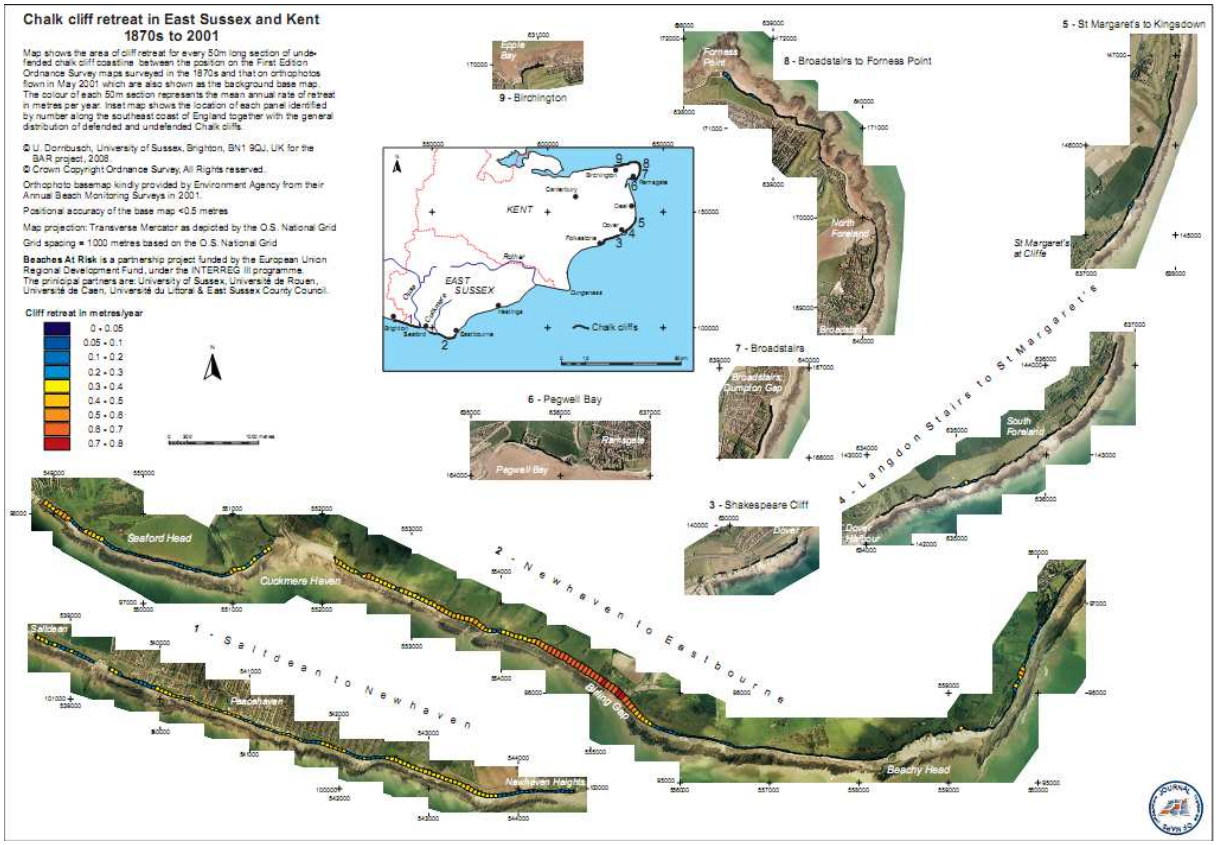

Figure 6 Le recul des falaises dans le Sussex et le Kent (Angleterre) des années 1870 à 2001 (Dornbusch, 2006).

Note sur la marée

Pour Melville et al. (1994), le fait que l'inondation ait eu lieu 2 jours consécutifs réfute l'hypothèse d'un tsunami mais correspondrait plutôt à une marée extrême. En revanche, Haslett et Bryant (2008) indiquent les heures de la grande marée haute la plus proche, c'est-à-dire respectivement à 15h25 le 16 avril (tsunami à 16h30 (heure locale) le 6 avril 1580) et à 4h12 le lendemain (tsunami à 4h30 (heure locale)), mais malheureusement sans pousser l'analyse : on peut remarquer la similarité des dates et des heures.

Objectifs de l'étude

Cette région, bien que peu soumise aux séismes et aux tsunamis, doit être considérée comme partie intégrante du littoral français dans le cadre de ce projet. Du fait de la méconnaissance de cet évènement d'avril 1580, avec beaucoup d'incertitude quant aux informations citées par-ci par-là dans les revues scientifiques, journaux et autres sites web, la première étape de l'étude concerne la recherche de documents historiques originaux relatifs à cet évènement ainsi que la mise en évidence de traces sédimentaires in-situ.

2) Mission TSUNORD

Les premières prospections bibliographiques nous ont permis de mettre en place une mission sur le terrain que nous avons nommé TSUNORD (pour Tsunami du Nord).

Cette mission, qui a permis de recenser un certain nombre d'informations et de prendre des contacts auprès de différents organismes locaux du nord de la France, s'est déroulée en deux temps :

Les recherches de documents historiques

Les analyses sédimentaires

Les villes visitées lors de cette étude sont Boulogne, Calais, Bray-dunes et De Panne (Belgique).

Figure 6 Carte IGN du littoral du nord de la France, de Wimereux (voisine de Boulogne-sur-mer, 2 km au nord) à De Panne (en Belgique) (www.geoportail.fr).

a) Les documents historiques

Les recherches de documents historiques ont été réalisées dans les archives municipales des villes de Boulogne et Calais, villes mentionnées dans l'unique document historique contemporain connu (Discourse, 1580).

Peu de documents sur l'histoire de Calais ou de Boulogne nous renseignent sur ce séisme d'avril 1580 et pour cause, l'information la plus importante que l'on retire de cette prospection est la suivante : les anglais, les espagnols et les français se sont « échangé » Calais pendant une longue période, avec toutes les pertes et destructions de documents qui peuvent en découler, en 1595 (ou 1596) la ville, redevenue française en 1598, est de nouveau perdue par les espagnols : d'après les différents services de documentation interrogés dans la région, les anglais puis les espagnols l'auraient quittée en emportant apparemment toutes les archives et autres documents avec eux. D'après eux elles seraient stockées à Douvres et d'autres villes anglaises et espagnoles, et ne sont pas en mesure d'être restituées à la France. Une prise de contact avec les archives et bibliothèques de Douvres (Kim Norton, Dover Museum), et Londres (Hellen Pethers, Library of the Natural History Museum ; Shelah Duncan et Katrina Dean, The British Library) nous renvoit en général à la recherche de ces documents anciens dans les archives françaises, à Strasbourg et à la bibliothèque nationale à Paris.

En revanche, des documents non mentionnés dans les précédentes études ont pu être mis à jour : ce sont les notes d'un séisme 6 avril 1580 (Twysden, 1580?) ou le rapport sur le séisme du 22 avril 1580 (Bishop of London, 1580) (tous deux disponibles à la British Library).

b) Les analyses sédimentaires

Description géomorphologique du territoire considéré

Entre Equihen et Sangatte, les falaises du Boulonnais alternent avec de grands massifs dunaires qui cèdent ensuite la place a un cordon dunaire qui s'étire jusque Bray-Dunes, protégeant la plaine maritime flammande dont l'altitude moyenne n'est que de 2 à 5 m au dessus du niveau marin. Les dunes du Boulonnais sont relativement hautes et sont représentées par deux ensembles principaux, les dunes de la Slack et les dunes de la baie de Wissant. Les premières, hautes de 15 à 20m sont larges et végétalisées, souvent taillées côté mer en falaises sableuses ; les secondes sont de hauteur plus réduites mais également larges et végétalisées. Les dunes entre Sangatte et la frontière belge sont constituées par un cordon sableux plus étroit dont l'altitude n'excède pas 5 à 10m. Elles sont couvertes d'une

végétation dense et souvent entaillé par des formes de déflation. A l'arrière de ces dunes, la plaine maritime s'étend jusqu'au pied des collines de l'Artois.

Gain de terrains sur la mer

Cette région a de tous temps été un lieu privilégié d'affrontements entre le domaine maritime et le domaine continental.

Dans son article sur l'évolution d'un écosystème dunaire dans les Flandres au cours du Moyen Age, Augustyn (1995) montre que les dunes ont été régulièrement arasées et la plaine maritime inondée au cours d'invasions marines de courte (tempêtes, raz de marées = surcotes) ou de longue durée (transgression marine).

Pour les invasions de courte durée, elle parle notamment de la ville d'Ostende qui, un siècle après sa fondation, a subi une inondation catastrophique. L'inondation de Saint Clemens en 1334 a vu les dunes côtières intégralement arasées. A la suite de cet événement, l'église qui se trouvait sur le front de mer a été déplacée au centre de la ville et les quartiers qui avaient durement subi l'inondation ont été abandonnés aux vagues. Moins de soixante années plus tard, au cours de l'inondation de la Saint Vincent, la ville fut à nouveau inondée. Le 19 novembre 1404, une tempête de nord-ouest connue comme la première inondation de la Saint Elisabeth détruisit quasiment l'ensemble du cordon dunaire qui s'était reconstitué. Au cours de l'inondation de la Saint Elisabeth de 1424. La ville fut à nouveau submergée.

Outre ces invasions de courtes durées aux effets géomorphologiques importants, cette région a subi des variations régulières de niveau marin qui ont conduit à des inondations régulières de la plaine maritime. La transgression Dunkerque II se place entre le IIIème et le VIIIème siècle de l'ère chrétienne. Les plaines côtières sont envahies par la mer qui pénètre jusqu'à 10 km vers l'intérieur des terres par rapport au trait de côte précédent. Les implantations celtiques qui occupaient ces basses terres auraient été abandonnées à cette époque.

La mer se retire lentement pendant la phase de régression carolingienne (VIIIème siècle). Les prés salés qui se forment d'abord sur les terres émergées permettent l'élevage de moutons. Au fur et à mesure du retrait de la mer des herbages apparaissent, servant de pâture au bétail. L'élevage et plus tard l'exploitation agricole est encouragée et dirigée par les moines Cisterciens de Gand. Les exploitants se groupent et sont à l'origine des premières communautés villageoises. C'est de cette époque que datent les premières tentatives d'assèchement des terres au moyen de fossés et de petites digues.

Mais le sort s'abat à nouveau sur la plaine flamande: lors de la transgression Dunkerque III aux alentours de l'an mil la mer s'engouffre dans l'estuaire de l'Yser et une grande partie des basses terres est à nouveau inondée.

Beun et Broquet, (1980) ont retracé les variations marines de longue durée qui se sont succédées au cours de l'Holocène dans cette région sur le diagramme ci-dessous (Fig. 7).

Les sondages que nous avons réalisés dans la plaine maritime à l'aide d'une tarrière montrent que le sol de surface, limono-sableux recouvre un niveau limoneux quelquefois limono-argileux plus collant sous lequel apparaissent des passées sableuses grises reposant sur une couche de tourbe noire plus ou moins épaisse qui constitue le sous bassement général de la plaine côtière et qui aurait été mise en place au cours de la transgression Dunkerque II.

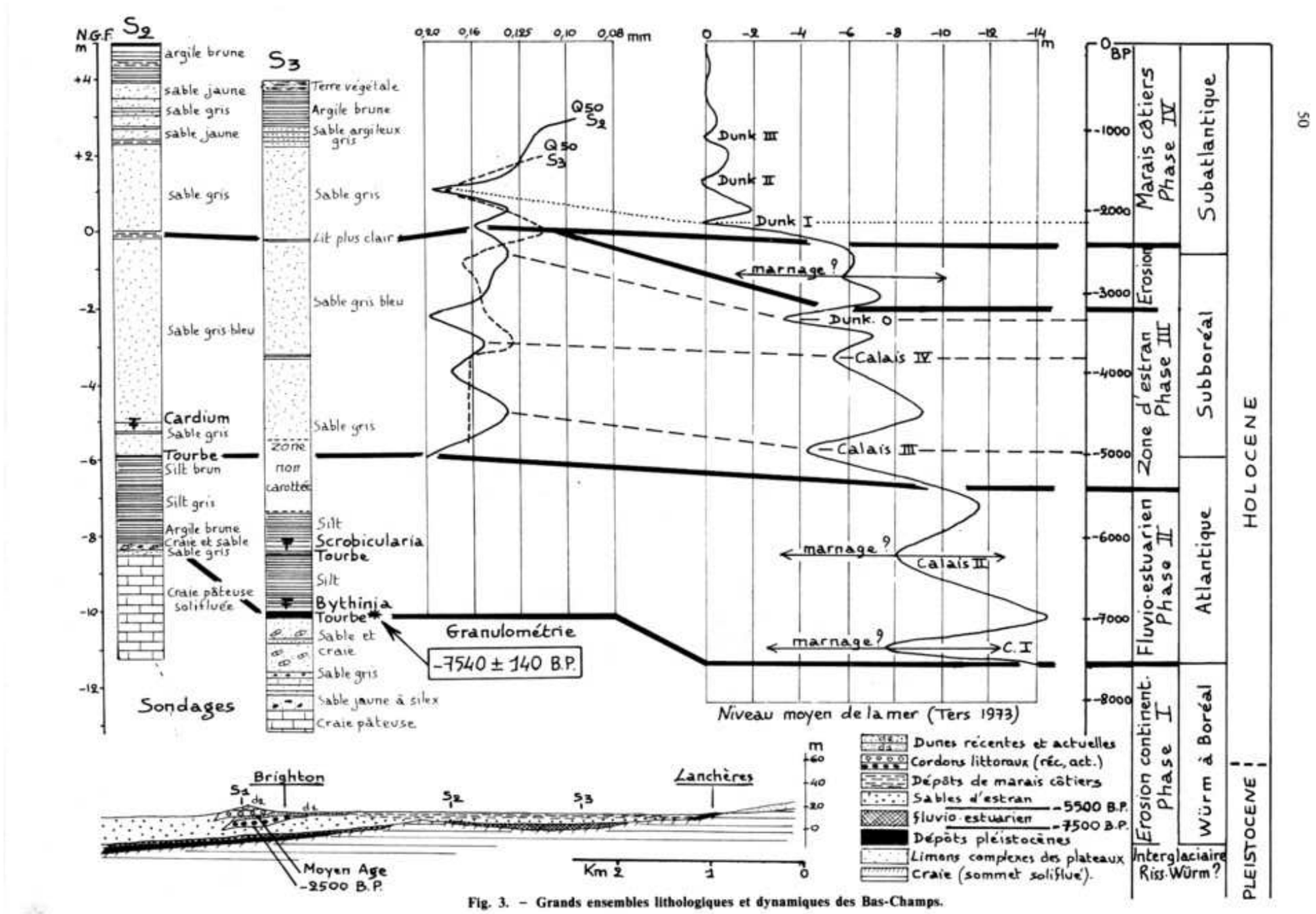

Fig. 3. – Grands ensembles lithologiques et dynamiques des Bas-Champs.

Fig. 3. – General sketch of the dynamic environment in the « Bas-Champs ».
Recent dunes – Pebble bars – Marshes deposits – Beach sands – Fluvio-estuarian deposits – Pleistocene deposits – Plateaus'

Figure 7 Variations marines au cours de l'Holocène dans la région de Dunkerque (Beun et Broquet, 1980).

Conclusions et perspectives

L'étude préliminaire de cet évènement du 6 avril 1580 révèle bien la difficulté que représente l'étude d'un évènement aussi ancien, aussi bien d'un point de vue historique que géologique. En effet, cette région a été soumise aux guerres de possessions entrainant probablement la perte de documents relatant le phénomène ; elle est également soumise à l'érosion littorale importante dans cette région calcaire (Boulonnais) et au multiples transgressions marines et/ou assèchement anthropique : on se retrouve avec un trait de côte variable au cours du temps, ce qui ne facilite pas la tâche de recherche de marqueurs de tsunami in situ (dépôts de tsunami).

Les enquêtes dans les archives, bibliothèques (municipales, départementales) et services techniques des mairies des différentes communes visitées, mais aussi en Angleterre, n'ont rien apporté de concret à cette étude. Le seul document historique (Discourse, 1580) qui a pu être retrouvé lors de précédente études (et que nous nous efforçons d'acquérir dans le cadre de cette étude) mentionne les villes de Calais, Boulogne et Douvres, les autres villes n'existant tout simplement pas à l'époque (c'est le cas de Bray-dunes) : ceci limite encore une fois les recherches de documents historiques. En revanche cette étude a permis d'identifier un second document de Coquerel (1580) traitant a priori également du séisme de 1580, et disponible sur commande à la bibliothèque de l'Arsenal (BNF, Paris).

Les prospections effectuées en différents endroits du littoral entre Boulogne et De Panne dans des milieux a priori favorables à la conservation d'éventuels dépôts n'ont pas abouti, principalement du fait de la présence de remblais plus ou moins récents sur quasiment tous ces sites (zones fortement agricoles, nombreux travaux liés à l'entretien des canaux).

Perspectives :

La première perspective serait de parvenir à identifier des zones non anthropisées et non remodelées depuis 1580 afin de pouvoir y effectuer des forages plus profonds. Cécile Baeteman (Service géologique de Belgique, e-mail : Cecile.Baeteman@vub.ac.be) mentionne des travaux de terrassement qui auraient permis de mettre à jour un amoncellement de coquillages (frontière franco-belge) qui aurait été attribué à une autre cause qu'une tempête (http://www.sciencesnaturelles.be/active/sciencenews/archive2005/tsunami).

Malheureusement, l'intéressée ne semble pas motivée pour nous en dire davantage d'après les échanges de mails.

En parallèle, des modélisations de tsunami seront menées à partir de scénarii de rupture simples après identification de failles potentiellement aptes à générer un séisme de magnitude supérieure à 6.0. Les recherches sur les glissements de terrain au niveau des falaises de craie du Boulonnais seront également approfondies.

La modélisation de l'évènement sismique ou même gravitaire sera faite après digitalisation des cartes marines acquises lors de cette étude.

Remerciements :

Nous remercions toutes les personnes qui ont pu nous aider de près comme de loin pour la bonne réalisation de cette étude (personnel des bibliothèques, services techniques, chercheurs français, belges et anglais, etc.). Nous tenons à remercier particulièrement Yanni Gunnell (LGP, Paris 1) pour la mise à disposition des cartes marines et documents sur les glissements de terrain côtiers en Angleterre.

Bibliographie

Augustyn, B., 1995. De evolutie van het duinecosysteem in Vlaanderen in de Middeleeuwen: antropogene factoren versus zeespiegelrijzingstheorie , Historisch-Geografisch Tijdschrift, 13 (1), p. 9-19.

Beun, N., Broquet, P., 1980. Tectonique quaternaire (Holocène ?) dans la plaine littorale picarde des bas champs de Cayeux et leurs abord orientaux. Incidences possibles sur le réseau hydrographique régional. Bulletin de l'association Française pour l'Etude du Quaternaire, Vol. 17 1-2, 47-52.

Bishop of London (1580). Bishop of London to Lord Burghley; of a Form of Prayer for a public fast, on account of a late earthquake, April 22, 1580.

CNDP-CRDP de l'académie d'Amiens (2006). Les séismes. Thém@doc. (http://crdp.ac-amiens.fr/seismes/014.htm)

DDRM - Dossier Départemental sur les Risques Majeurs (2009). Le risque sismique. Dossier Thématique, 9 pp. (www.nord.pref.gouv.fr)

Discourse (1580). Discours d'une merveilleuse et veritable copie du grand deluge, 1580, J. Coquerel, Paris.

Dornbusch, U. (2006). Chalk cliff retreat in East Sussex and Kent 1870s to 2001.

Dornbusch, U., Robinson, D.A., Moses, C.A., Williams, R.B.G. (2008). Temporal and spatial variations of chalk cliff retreat in East Sussex, 1873 to 2001. Marine Geology, 249(3-4), 271-282.

Franke, W. (1989). Variscan plate tectonics in Central Europe - current ideas and open questions. Tectonophysics, 169, 221–228.

Haslett, S.K., Bryant, E.A. (2008). Historic tsunami in Britain since AD 1000: a review. Nat. Hazards Earth Syst. Sci., 8, 587-601.

Hutchinson, J.N. (1969). A reconsideration of the coastal landslides at FolkestoneWarren, Kent. Géotechnique, 19(1), 6-38.

Hutchinson, J.N. (2002). Chalk flows from the coastal cliffs of northwest Europe. Geologicazl Socity of America, review in Engineering Geology, 15, 257-302.

Imray (2007). Dover Strait, North Foreland and Beachy Head. Imray Laurie Norie and Wilson Ltd.

Musson, R.M.W. (1994). A catalogue of British Earthquakes. British Geological Survey technical Report, No. WL/94/04, pp.99.

Musson, R.M.W. (1996). The seismicity of the British Isles. Annali di Geofisica, 39, 3, 463-469.

Neilson, G., Musson, R.M.W., Burton, P.W. (1984). The "London" earthquake of 1580, April 6. Engineering Geology, 20, 113-141.

Nicolas, M., Berthoux, N. (1995). Prévoir les séismes; Le séisme du Pas-de-Calais, 6 avril 1580. La Recherche, Dossier thématique, 279.

Roger, J., Allgeyer, S., Daubord, C., Hébert, H. (2010). L'aléa tsunami en France métropolitaine. Actes du colloque Risques naturels en Méditerranée occidentale, Carcassonne, France, Novembre 2009 (soumis).

Twysden, R. (?).Additional Manuscript 34,177. MISCELLANEOUS PAPERS relating to the Twysden family. Amongst them are: (c) Similar notes [by himself] of the family of Roger Twysden and his wife Anne, dau. of Sir Thomas Wyat, 1542-1592; with notes of a great snow-storm 4 Feb. 1578 [9], and of an earthquake 6 Apr. 1580. ff. 18, l9; Paper; ff. 88. xvith-xixth centt. Folio.

Vogt, J., 1979. Les tremblements de terre en France. Mémoires du BRGM N°96.

Personnes intéressés par l'étude

Thierry Camelbeeck

e-mail : cam@oma.be
Téléphone : +32(0)23730252
Observatoire Royale de Belgique, section de seismologie, Avenue Circulaire, 3 - 1180 Bruxelles

Simon Haslett (Prof.)

e-mail : Simon.Haslett@newport.ac.uk
Téléphone : +44(0)1633432016
Centre for Excellence in Learning and Teaching (CELT); University of Wales, Newport.

Roger musson

e-mail : rmwm@bgs.ac.uk
Téléphone : +44(0)1316671000 (standard)
British geological Survey, Murchinson House, West mains road, Edinburgh, EH9 3LA, Scotland

Annexe 3

Procédure de réalisation des grilles bathymétriques

J. ROGER, B. LEMAIRE, CEA/DASE/LDG/RSG
E. THAUVIN, CEA/DASE/LDG/TSE

Fichier créé le 19/03/2008, modifié le 15/09/2008

AVANT-PROPOS

Le calcul de la déformation initiale du sol générant un tsunami et la propagation des ondes de ce tsunami se fait via l'utilisation de données de profondeur d'eau sous la forme de grilles dîtes bathymétriques. Lorsque le calcul de la propagation se fait par la méthode des différences finies les grilles en question doivent être régulières (pas spatiaux ∂x et ∂y constants). Pour des calculs simples et rapides on utilisera la bathymétrie GEBCO[1] 1' (BODC[2], 1997) que l'on pourra dégrader (à 5' par exemple) ou affiner par interpolation (à 30'' par exemple). Pour des calculs plus précis, par exemple dans le cadre de l'étude des effets d'un tsunamis sur un port, et du fait de l'importance croissante de la bathymétrie sur l'amplitude et la forme des vagues à l'approche des côtes (quand la profondeur d'eau diminue) il sera intéressant de réaliser des grilles plus fines en résolution prenant en compte les structures portuaires et la bathymétrie locale. Concernant le calcul de l'inondation (run-up) à terre on pourra rajouter des données de topographie à ces grilles. Ensuite, pour des raisons de temps de calcul, il sera intéressant de réaliser plusieurs niveaux de grilles de résolution croissante du large vers le port considéré ou inversement en faisant bien attention à leur imbrication possible lors du calcul.

Dans ce document, je vais donc présenter la procédure de réalisation de ces grilles que nous appellerons grilles haute résolution et nous nous assurerons de l'imbrication des différents niveaux.

1) Récupération des données
2) Géoréférencement
3) Numérisation
4) Création des grilles
5) Imbrication

[1] General Bathymetric Chart of the Oceans, http://www.bodc.ac.uk/data/online_delivery/gebco/
[2] British Oceanographie Data Centre, http://www.bodc.ac.uk/

1) Récupération des données

Les données peuvent avoir différentes origines et formats. Le tout est de pouvoir les ouvrir dans ArcGIS pour continuer la manipulation. Le plus souvent les données haute résolution seront récupérées de cartes marines scannées en format TIFF (*.tif) par exemple (Fig. 1).

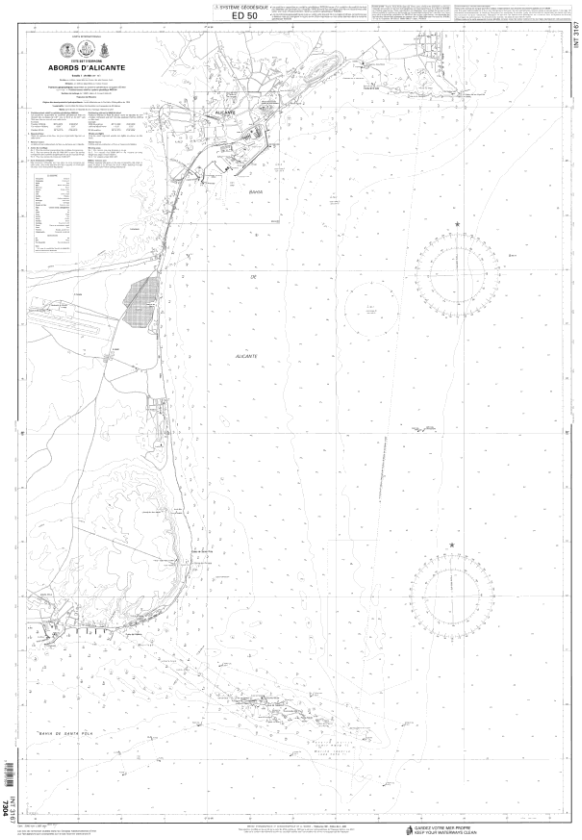

Figure 1 Carte marine des abords d'Alicante (Esp.) dans le système géodésique ED50 - Carte SHOM n°7304

2) Géoréférencement

La carte scannée ou les autres types de données (données GEBCO, SHOM, sondeur multifaisceaux, etc.) sont ouverts dans ArcGIS pour être géoréférencée.
Avant tout s'assurer d'avoir les barres d'outils « éditeur », « géoréférencement »… utiles pour la suite.
Il est également nécessaire de s'assurer que les nombres décimales sont notés avec un « . » au lieu d'une « , ». Pour cela, se placer dans …

Le géoréférencement consiste en l'attribution de coordonnées géographiques (d'un système que l'on définira au préalable, souvent le WGS84) aux points d'une image ou d'un ensemble de données. Cette manipulation va permettre par la suite de connaître les coordonnées de tous points visualisés.

N.B. : les options à sélectionner sont surlignées en jaune

Nouveau document → Nouvelle couche → ajouter données

Clic droit sur couche → propriétés → systèmes coordonnées → importer (WGS84 etc…)

Pyramide : oui

Couche → Propriété WGS84 (vérification de la couche en cours : nom image en cours)

(zoom sur la couche pour visualiser)

Dans la barre d'outils géoréférencement, mise en place de points d'accroche : on positionne sur l'image des points dont les coordonnées sont connues (les croisements des parallèles/méridiens sur la carte par exemple) en leur attribuant les coordonnées indiquées ; ces points vont servir de base au positionnement de l'image dans le système géographique considéré. Pour cela, il suffit de cliquer droit sur les points en question → ajouter x et y

géoréférencement → mettre à jour le fichier *.tfw créé

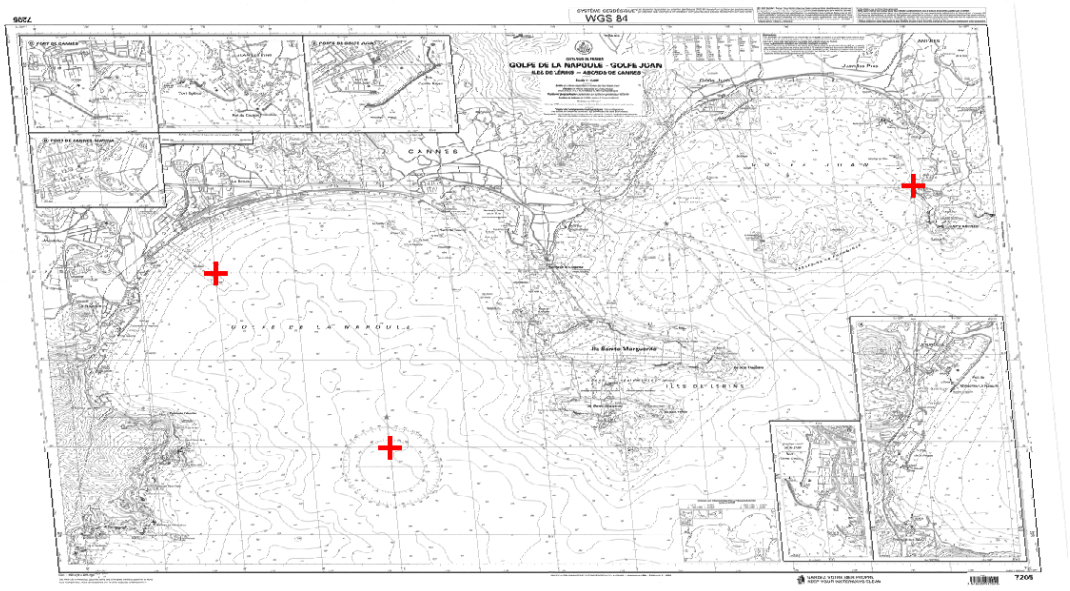

Figure 2 Carte marine du Golfe de la Napoule dans le système géodésique WGS84 - Carte SHOM n°7205
En rouge sont représentés les points de géoréférencement

3) Numérisation des données

a) Couche de points :

Les points sont le plus souvent positionnés sur les points de sonde indiqués sur les cartes ou en des endroits où l'interpolation qui va suivre risque de créer des artefacts.

Ouverture de ArcCatalog → [créer shapefile] (le shapefile, ou fichier de formes, correspond au fichier dans lequel vont être stockés les points rajoutés)

Clic droit dans le répertoire de travail → nouveau fichier de forme

Modifier le système de coordonnées → sélection (WGS84)

⚠ Les différents systèmes de coordonnées se trouvent :

Couches → propriétés → système coordonnées → prédéfini → geographic CS → world → WGS 1984

Retour dans ArcMap : ajouter données → ouvrir le fichier shapefile précédemment créé (*.shp), alicante_points.shp par exemple

Définition des champs→ ouvrir la table attributaire
Options : ajouter un champ que l'on nommera X auquel on attribue une valeur en réel double (et ré-itérer pour Y et Z)

Barre d'outils Editeur → ouvrir une session de mise à jour (attention à choisir le bon shapefile)
→ créer une nouvelle entité
→ avec le crayon positionner cette nouvelle entité (un point dans notre cas)
cliquer sur chiffre et attributs (donner la valeur Z que l'on veut attribuer à ce point)

⚠ D'abord sauvegarder les mises à jour puis le fichier

Après avoir positionné tous nos points et leur avoir attribué une valeur Z, on ouvre la table attributaire (en cliquant à droite sur la couche considérée). Les champs X et Y sont tous vides. On va alors demander à la machine de récupérer les valeurs X et Y pour tous nos points de manière automatique. Pour cela on sélectionne la colonne des X (en bleu), on clique droit, calculer les valeurs → charger → point_get_X.cal → OK, et on vérifie la colonne pour voir si on n'a pas fait d'erreur. Et de même pour la colonne des Y.

⚠ Les fonctions point_get_X.cal et point_get_Y.cal de trouvent dans le répertoire:

Trs_proj sur Pariou → geotheque → traitement → geo-traitement → ArcGIS → expression→ calculate

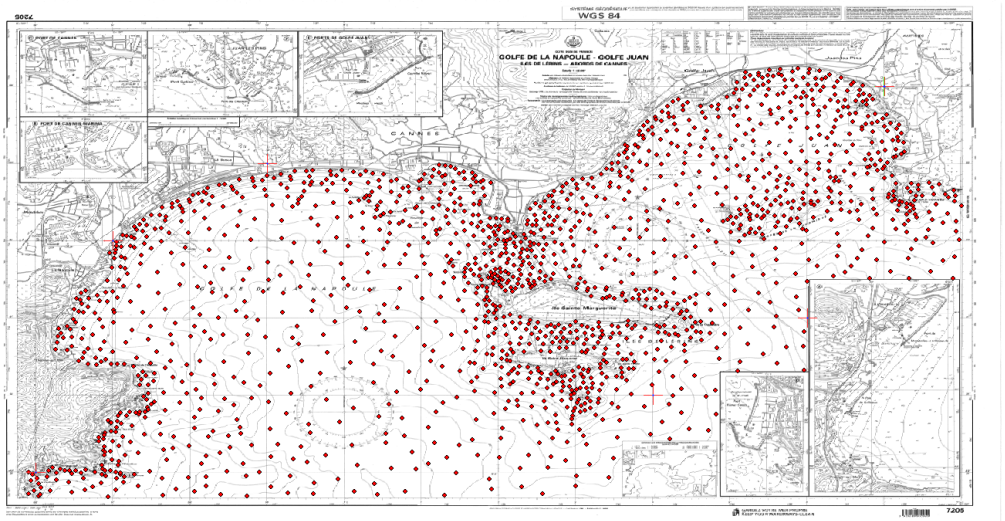

Figure 3 Carte marine du Golfe de la Napoule dans le système géodésique WGS84 - Carte SHOM n°7205 En rouge est représentée la couche de points

Les valeurs x, y et z de ces points vont ensuite devoir être exportées sous forme d'un fichier texte par exemple (en comprenant 3 colonnes correspondant aux 3 champs).
On sélectionne les lignes à exporter puis :
Table attributaire → options → exporter (*.txt)

b) Couches de polylignes :

Les polylignes sont utilisées pour reproduire les lignes de niveaux des cartes marines mais aussi les structures de port comme les digues et pontons et le trait de côte.
Même procédure que dans le cas des points sauf qu'il faut choisir l'option polyligne lors de la création du shapefile (alicante_ligne.shp par exemple).

⚠ Pour créer le champ Z, quitter le mode mise à jour.

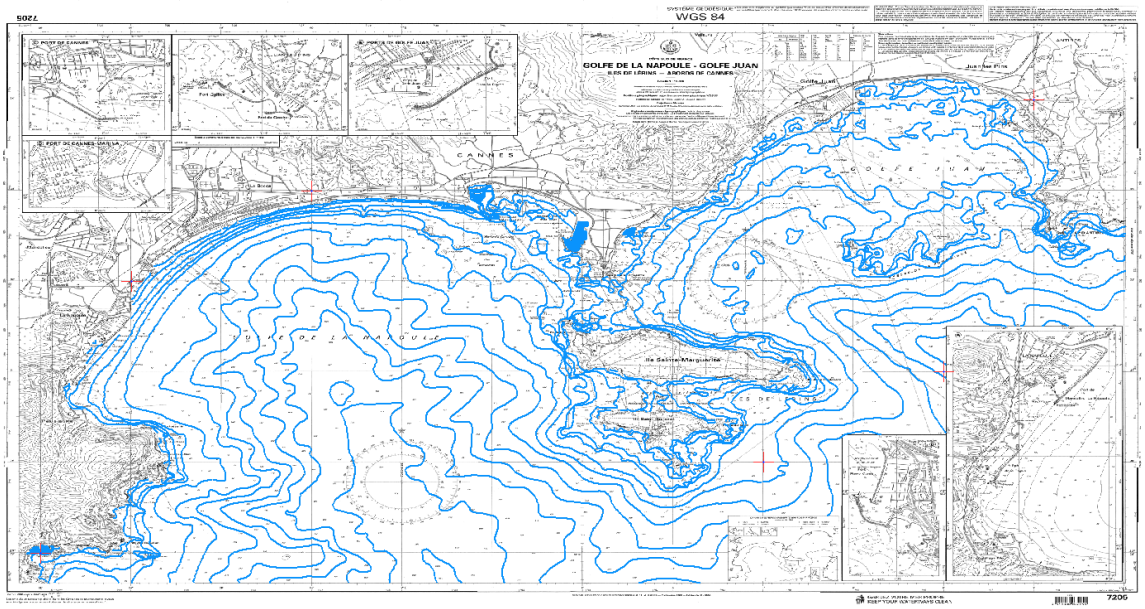

Figure 4 Carte marine du Golfe de la Napoule dans le système géodésique WGS84 - Carte SHOM n°7205
En bleu est représentée la couche de polylignes

Par contre la procédure d'exportation est différente.
Il va falloir transformer les lignes en points pour pouvoir ensuite concaténer les fichiers points et lignes (au même format). Pour cela on se sert d'Arcview 3.3 :
Charger le fichier ligne.shp
Fichier → extensions → cocher « poly conversion to spaced points »

⚠ Si l'erreur « violation of segmentation » s'affiche, faire une sélection des entités

Clic sur shapefile → thème « convert to points »
De la même façon que pour les points il faut récupérer les valeurs x et y ; pour cela on entre en mise à jour → calculer → [Shape].getx
[Shape].gety

Table attributaire → option → exporter → *.txt

La manipulation finale consiste à « sommer » les 2 fichiers (ou plus) contenant les 3 colonnes x, y et z pour les points et les points provenant des lignes :
La méthode la plus simple est de procéder sous Unix (terminal de commande) :

⚠ Pour utiliser les fichiers .txt, créés avec ArcGIS, sous Unix, penser à utiliser la commande : **dos2unix ↔ unix2dos**

Tout d'abord ouvrir chacun des 2 fichiers pour vérifier qu'ils sont corrects (supprimer les en-têtes par exemple. S'il y a une colonne en trop on pourra utiliser la fonction awk :

awk '{print $2,$3,$4**}'** points_exp.txt > points.txt → si on souhaite supprimer la colonne 1

Si l'on souhaite changer les ' ;' en espace → **sed** 's/ ;/ /g' old.txt > new.txt

De même pour l(es)'autre(s) fichier(s) puis on peut concaténer :

cat points.txt lignes2points.txt > output_xyz.txt

c) Importation des données GEBCO :

En ce qui concerne les données GEBCO, elles sont fournies en grilles régulières avec une résolution de 1' (~1.8km) et seront utilisées pour les zones de grande profondeur. Pour récupérer les données sous ArcGIS, on transforme tout d'abord le fichier du format .grd au format .txt :

grd2xyz gebco.grd > gebco.txt

dos2unix gebco.txt

Puis, rajouter dans le fichier .txt ainsi obtenu, les noms des champs en en-tête :

«X » « Y » « Z »

outils → Ajouter données XY… → gebco.txt (renseigner les champs et système coordonnées)

→ attention à sortir le fichier en format UNIX (pour des raisons de symboles invisibles) et de bien spécifier les « délimiteurs » dans le schema.ini (ex : Delimited(;))

Cela crée une couche « événements gebco.txt ». Pour en tirer un fichier de formes :

Evénements gebco.txt → Données → exporter les données

3) Interpolation

Les points que nous avons numérisés ne sont pas répartis de manière uniforme sur une aire rectangulaire. L'interpolation va permettre de générer une grille régulière à partir de ces points (pas spatiaux ∂x et ∂y constants).

On se servira pour l'interpolation du logiciel Surfer®. Le mode d'interpolation choisi est le krigeage (kriging en anglais).
Pour cela on va dans le menu Grid → data
On choisi le nom du fichier à interpoler (output_xyz.txt) ainsi que le pas d'interpolation voulu : si on souhaite avoir une grille de sortie avec une résolution spatiale de 10m, on lui demandera d'utiliser un pas d'interpolation de 0.00009° en x et y.

Mètres	Minutes	Degrés
10	0.0054054	0.00009009
20	0.0108108	0.000180180
50	0.027027	0.00045045
100	0.054054	0.0009009
200	0.108108	0.00180180
500	0.27027	0.0045045
1000	0.54054	0.009009

Tableau 1 Correspondances mètres/minutes/degrés pour plusieurs valeurs de résolution

Le fichier obtenu après interpolation est une grille *.grd de type Surfer® inexploitable sous GMT; on va alors devoir exporter les données :

Grid → Convert

En donnant le nom du fichier de départ (le *.grd Surfer®) et le nom du fichier de sortie en *.DAT (fichier de type xyz)

Insertion de la grille de données obtenues par interpolation dans la grille de données Gebco :
Pour que l'imbrication d'une grille à l'autre se fasse sans problème il est nécessaire de réaliser un jeu de données unique comprenant toutes les données qui vont servir pour réaliser les différentes grilles.
Pour cela on utilisera un script *.csh (ou *.sh ou programme fortran, exemple en annexe) pour sélectionner les données à garder ou non et associer les différents jeux en prenant soin de laisser des espaces entre chaque type de données pour que la jonction par interpolation (à nouveau sous Surfer®) se fasse correctement.

Une fois que les fichiers *.DAT de différentes résolutions sont générés, il faut créer les grilles GMT qui seront lisibles par le code.

Le fichier obtenu va servir à générer une grille GMT (*.grd aussi) cette fois en utilisant la commande suivante :

xyz2grd fichier.dat **–R**Xmin/Xmax/Ymin/Ymax **–I**∂x/∂y **–G**fichierGMT.grd

Qui sera à son tour convertit en fichier lisible par le code contenant uniquement la colonne des Z classés de manière régulière en partant du bas à gauche de la grille.

grd2xyz –ZBLa fichierGMT.grd > depth.gr0x

Il est nécessaire de garder les noms de fichiers des grilles tels que ‘depth.gr0x’.
Pour plus de détail sur les fonctions GMT voir l’ouvrage de Wessel et Smith (2007).

REFERENCES :

British Oceanographic Data Centre - The Centenary Edition of the GEBCO Digital Atlas, Liverpool, U. K, 1997. → *disponible à l’adresse suivante:*

http://www.ngdc.noaa.gov/mgg/gebco/grid/1mingrid.html

Wessel, P., Smith, W.H.F., 2007 – The Generic Mapping Tools GMT, a map-making tutorial, version 4.2.0.

Exemple de programme faisant le tri entre les données SHOM et GEBCO.

```
program tri
implicit none

integer i,j
real, dimension(361201) :: xG,yG,zG              !GEBCO
real, dimension(1904889) :: xS,yS,zS             !SHOM
real distance, min


OPEN(  UNIT = 1 ,                    &
       FILE = '45n35n0w10e.txt',     &
       FORM = 'formatted',           &
       ACTION = 'read',              &
       STATUS = 'old')

OPEN(  UNIT = 2,                     &
       FILE = 'SHOM2.txt',           &
       FORM = 'formatted',           &
       ACTION = 'read',              &
       STATUS = 'old')

OPEN(  UNIT = 3,                     &
       FILE = 'TMP.txt',             &
       FORM = 'formatted',           &
       ACTION = 'readwrite',         &
       STATUS = 'unknown')

min = 100.

do i=0,1904888
       READ(2,*) xS(i),yS(i),zS(i)
end do

do i=0,361200
       READ(1,*) xG(i),yG(i),zG(i)
       print *, 'goto :', i*100./361200, '%'
```

```
        if (xG(i)<2.98.or.xG(i)>10.04.or.yG(i)<40.96.or.yG(i)>43.866) then
                WRITE(3,*) xG(i),yG(i),zG(i)
        else if(xG(i)>=2.98.and.xG(i)<=10.04.and.yG(i)>=40.96.and.yG(i)<=43.866) then
                if(zG(i)>=0.) then
                        WRITE(3,*) xG(i),yG(i),zG(i)
                else if(zG(i)<0.) then
                        do j=0,1904888
                                distance = sqrt((((xS(j)-xG(i))**2)+(yS(j)-yG(i))**2))
                                !print *, 'distance=',distance
                                if(distance <= min) then
                                        min=distance
                                else if(distance < 0.016) then
                                        min=distance
                                        exit
                                end if
                                distance=0.
                        end do
                if(min>0.016) WRITE(3,*) xG(i),yG(i),zG(i)
                end if
                min=100.
        end if
end do

        CLOSE(1)
        CLOSE(2)
        CLOSE(3)

end program
```